

AD619695

AFCRL-65-486  
JULY 1965  
AIR FORCE SURVEYS IN GEOPHYSICS, NO. 167



## AIR FORCE CAMBRIDGE RESEARCH LABORATORIES

L. G. HANSCOM FIELD, BEDFORD, MASSACHUSETTS

### Proceedings, 1964 AFCRL Scientific Balloon Symposium

ARTHUR O. KORN, JR.

EDITOR

1 COPY	2 OF	3	4	5
HARD COPY		\$.	7.20	429P
MICROFICHE		\$.	2.00	
429P				

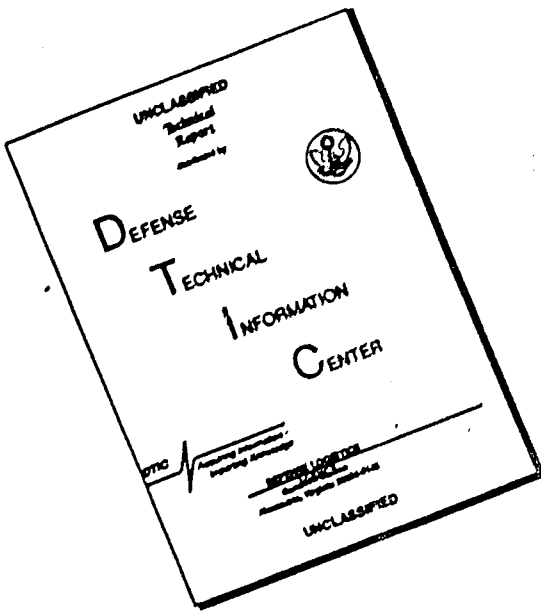
DDC  
REF AUG 30 1965  
RUBBER V LD  
DDC-IRA E

OFFICE OF AEROSPACE RESEARCH  
United States Air Force



ARCHIVE COPY

# DISCLAIMER NOTICE



THIS DOCUMENT IS BEST  
QUALITY AVAILABLE. THE COPY  
FURNISHED TO DTIC CONTAINED  
A SIGNIFICANT NUMBER OF  
PAGES WHICH DO NOT  
REPRODUCE LEGIBLY.

**BLANK PAGES  
IN THIS  
DOCUMENT  
WERE NOT  
FILMED**

AFCRL-65-486  
JULY 1965  
AIR FORCE SURVEYS IN GEOPHYSICS, NO. 167



AEROSPACE INSTRUMENTATION LABORATORY PROJECT 6665

## AIR FORCE CAMBRIDGE RESEARCH LABORATORIES

L. G. HANSCOM FIELD, BEDFORD, MASSACHUSETTS

# Proceedings, 1964 AFCRL Scientific Balloon Symposium

ARTHUR O. KORN , JR.

EDITOR

OFFICE OF AEROSPACE RESEARCH  
United States Air Force



## **Abstract**

Published herein are the papers presented at the second annual AFCRL Scientific Balloon Symposium covering the advances shown in balloon design, materials, instrumentation, meteorology, and scientific applications since the last symposium held in Boston on 25, 26 and 27 September 1963. Balloon technology presentations include stress studies, new balloon films, sensing elements, telemetry systems and a new balloon locating system. Applications and experience in working with tethered, meteorological and sounding balloons are discussed. In addition, information is presented on such existing programs as BAL-AST, and Surveyor and such proposed projects as the "AFCRL Stratospheric Humidity Program" and "The Mars Balloon".

## **Contents**

I.	TETHERED AEROLOGICAL BALLOON SYSTEM by S. D. Elliott, Jr.	1
II.	IMPROVEMENT IN BALLOON DESIGN THROUGH SCALE MODEL ANALYSIS by J. A. Winker	27
III.	POLYETHYLENE FILM WITH HI-SLIP ADDITIVE AS A BALLOON BARRIER MATERIAL by J. A. Haueter	41
IV.	STATISTICAL IMPLICATIONS OF BALLOON MATERIALS by R. L. Hauser	47
V.	BEHAVIOR OF POLYETHYLENE IN SIMULATED BALLOON ENVIRONMENT by W. B. Parsons	55
VI.	A NEW HIGH-ALTITUDE PLASTIC BALLOON LAUNCH METHOD by F. X. Doherty	73
VII.	A NEW POLYOLEFIN-FILM BALLOON MATERIAL by D. R. Williams	81
VIII.	BALLOON BURST DISCUSSION by N. Sissenwine	85
IX.	BALLOON LAUNCHING FROM AIRPLANES AND HELICOPTERS by L. Slaughter	95
X.	ULTRA THIN FILM BALLOONS by D. W. Cox, Jr.	115
XI.	HEAT TRANSFER CONSIDERATIONS OF INSTRUMENTATION PACKAGES AT HIGH ALTITUDES by A. Piacentini, K. Lindenfelser and D. Dube	121
XII.	A NEW MATERIAL CAPABILITY FOR THE BALLOON FIELD by R. S. Ross	123
XIII.	APPLICATION OF A TETHERING SYSTEM TO A SPECIFIC REQUIREMENT by M. S. Kretow	135

XIV. DESIGN CONSIDERATIONS FOR SOFT LANDING OF BALLOON PAYLOADS by J. P. Jackson	139
XV. TEMPERATURE MEASUREMENTS FROM FLOATING BALLOONS by W. C. Wagner	157
XVI. BALLOON LOCATING SYSTEM by R. J. Cowie, Jr.	169
XVII. TWO NEW SPECIAL-PURPOSE METEOROLOGICAL BALLOONS by E. Nelson and M. Sharenow	187
XVIII. SUPERPRESSURE BALLOON FLIGHTS FROM JAPAN by V. E. Lally	205
XIX. INSTABILITY OF SPHERICAL WIND-SENSING BALLOONS by D. F. Reid, USAF	213
XX. A PRELIMINARY INVESTIGATION OF HIGH ALTITUDE MINIMUM WIND FIELDS by G. F. Nolan	229
XXI. TOWARD IMPROVED MEASUREMENTS OF STRATOSPHERIC HUMIDITY WITH BALLOON-BORNE FROST-POINT HYGROMETERS by J. G. Ballinger, L. E. Koehler, M. P. Fricke and R. D. Murphy	231
XXII. AFCRL STRATOSPHERIC HUMIDITY PROGRAM by D. Grantham, N. Sissenwine and H. Salmela	261
XXIII. BALLOON-SUPPORTED PLATFORMS IN COMMUNICATIONS by C. A. Strom, Jr. and C. N. Lawrence	273
XXIV. THE ROTATION OF BALLOONS AT FLOATING ALTITUDE by A. E. Germeles	279
XXV. A BALLOON-BORNE MICROPHONE SYSTEM by J. W. Coffman	281
XXVI. ACOUSTIC DETECTION OF HIGH-ALTITUDE TURBULENCE by J. W. Wescott	295
XXVII. QUALITY ENGINEERING OF SCRIM-REINFORCED BALLOONS by T. W. Kelly, A. O. Korn, L. Curtis and R. Moroney	317
XXVIII. WATER IN THE ATMOSPHERES OF PLANETS by J. Strong	337
XXIX. THE MARS BALLOON -FEASIBILITY AND DESIGN by M. H. Davis and S. M. Greenfield	341
XXX. BALLOONS FOR THE SCIENTIFIC EXPLORATION OF MARS by S. M. Greenfield and M. H. Davis	353
XXXI. THE BALLOON AS A STEPPING-STONE TO SPACE FLIGHT by O. C. Winzen	365
XXXII. COSMIC RAY BALLOON EXPEDITION TO INDIA, IQSY-EQEX by R. Kubara and B. Stiller	393
XXXIII. THE TECHNIQUE OF CLUSTERS OF SOUNDING BALLOONS by A. Dollfus	399
XXXIV. DETECTION OF WATER VAPOR IN THE ATMOSPHERES OF VENUS AND MARS by A. Dollfus	409
XXXV. THE PARAVULCOON RECOVERY SYSTEM--AERIAL DEPLOYMENT FEASIBILITY STUDIES by A. J. Oberg, R. A. Pohl and C. L. Pritchard	419

## Welcome to the Symposium

Leo A. Kiley, Col. USAF  
Vice Commander (now Commander)  
Air Force Cambridge Research Laboratories  
Bedford, Massachusetts

On behalf of the AFCRL Commander, Brigadier General B. G. Holzman, I would like to welcome you to this, the second AFCRL Scientific Balloon Symposium. I am sure that many of you attended the very fine symposium that we held here in Boston last year. I am grateful for this opportunity to welcome you back this year.

As many of you know, the Air Force Cambridge Research Laboratories are the leading Air Force laboratories in the field of environmental research. A basic requirement for conducting this research is for vehicles to transport instrument packages - sensors - into and well above most of the earth's atmosphere. The wide scope of our environmental research program demands the use of a variety of vehicles; aircraft, of which we have six assigned to the laboratories, including a U-2 aircraft; and satellites, two of which within the past year we designed and fabricated completely at AFCRL. In addition, we use Air Force and NASA satellites on which each year we place some 15 to 20 piggyback packages. We use rockets extensively, about 30 each year, which we launch from sites literally all over the world. Last, and in many ways more important than vehicles of other types, is our extensive scientific balloon program.

In many ways, our balloon program covers a much broader scope than our programs involving other vehicles. In the case of other vehicles, we simply use

those developed by others. But with respect to balloons, we are intimately involved in new design and new ballooning techniques, as well as the use of balloons to carry our instrument packages well above all but a fraction of the earth's atmosphere. Moreover, we have the responsibility for providing our balloon launch capability to other Air Force agencies using balloons in their research programs.

There is no need for me here today to recount for you the many advantages that balloons afford us over other types of environmental research vehicles. I would like to stress the fact, a fact implied in the very sponsorship of this symposium, of the strong role that balloons have in our program here at AFCRL, and the fact that our program will involve the use of balloons well into the foreseeable future.

Judging from the very fine program that your Chairman, Mr. Thomas Kelly, has organized, I believe that you will have an extremely interesting and worthwhile symposium here. I only regret, after looking over the titles of many of the fine papers, that I will not be able to attend all of your sessions. I hope that as a result of this symposium, those of you who are not associated with AFCRL will find that you have obtained a broader knowledge of our research program, and that from this symposium you will achieve a closer and more profitable work relationship with our scientists.

Thank you.

## **Introductory Remarks**

**Robert M. Slavin**

**Chief, Aerospace Instrumentation Laboratory  
Air Force Cambridge Research Laboratories  
Bedford, Massachusetts**

### **I. INTRODUCTION**

One objective of the AFCRL Scientific Balloon Symposium held last year was to create an opportunity for scientific users of balloons to become acquainted with existing and projected flight capabilities. We also wished to present a balanced exchange of information so that the same scientific users of balloons would have an equal opportunity to discuss their balloon-borne experiments and thus provide background information for the persons or groups involved in designing, developing, and attempting to launch and fly these systems. Our desire was to cover a broad spectrum of balloon activities with a group of representative individuals so as to stimulate advances not only in balloon technology but also in the creative use of balloons in research.

Until the advent of the so-called space-age, development of balloon technology had not been so rapid that new and abundant technical improvements were made each year. With the ever-increasing attention focussed on man's efforts to thrust larger payloads higher into the atmosphere and space, developments of many aspects of ballooning, while rapid, were unfortunately relegated to a position of relative obscurity. In the rush to apply the rapidly burgeoning capabilities of

powered flight to the solution of space oriented problems the simpler, less expensive, and proven techniques were sometimes overlooked. In an effort to correct this situation, as well as to promote the cause of ballooning, we at AFCRL felt that a Balloon Symposium would provide the opportunity for the scientific community to be reintroduced to the existing and potential capabilities of balloons. At the same time, such a symposium would provide an opening for those concerned with advancing balloon technology to set their goals toward those of the user.

Reactions of participants to the Symposium held last year were most favorable, an indication to us that our objectives were substantially met. We feel now that the objectives of that year are still valid and hope that this Symposium will prove to be even more successful in providing a mechanism for a free exchange of information and ideas related to balloons and their use.

Before beginning the activities of the first day, I would like to take a moment to summarize the interests of the AFCRL Balloon Groups for those of you not yet acquainted with us. As a part of the Aerospace Instrumentation Laboratory of AFCRL, the Balloon Group has been in existence for approximately fourteen years. The overall responsibility of this group has been the design and development of balloons, companion instrumentation, and launch procedures to meet the operational requirements of several elements of the Department of Defense. We therefore support scientific activity within the Air Force as well as other scientific work which may be of interest to the Air Force. The Holloman launch site and the adjacent White Sands Missile Range complex when combined with our Chico, California, launch site can be utilized to launch balloon payloads year round with tracking, control, and recovery capability. Therefore we, with a more than nominal interest in balloon activities, are pleased to sponsor this Symposium and anticipate that the results will ultimately benefit all of us.

The Symposium calendar has been organized with the intent of grouping presentations which are related. The speakers have been selected on the basis of their contributions to balloon technology or their contribution to the advancement of science through research using balloons. In addition to the formal presentations I would expect that the opportunity for many of you to exchange ideas informally will be of great value.

As a final comment, I hope that this Symposium will meet the needs outlined and that a proper balance between presentations relating to balloon borne experiments and those pertaining to balloon technology will be maintained. We feel that the facilities here are quite suited to the proceedings of this Symposium and hope that each of you will find the time spent here stimulating and worthwhile.

# **PROCEEDINGS OF 1964 AFCRL SCIENTIFIC BALLOON SYMPOSIUM**

## **I. Tethered Aerological Balloon System**

**Shelden D. Elliott, Jr.  
U. S. Naval Ordnance Test Station  
China Lake, California**

### **Abstract**

The Tethered Aerological Balloon System (TABS) currently under development at NOTS is designed to maintain a captive balloon and payload at stratospheric altitudes for an indefinite period of time, taking advantage of the region of minimum wind velocity nearly always present at some level in the lower stratosphere. The system consists of: (1) a conventional polyethylene balloon fitted with a self-deploying reefing system to reduce lateral drag; (2) an airborne telemetry/command package capable of monitoring up to six aerological or other parameters concurrently; additional packages may be distributed along the tether as needed; (3) a NOTS-developed glass fiber tether having a tensile strength comparable to that of steel, at one-fourth the weight of steel, fabricated in splice-free lengths exceeding 100,000 feet, and (4) a mobile ground vehicle from which all functions subsequent to launch can be performed, carrying a crew, control winch, and equipment to communicate with a ground telemetry and command station; the vehicle can run with the wind to reduce lateral drag loads on ascent or descent. The system is expected to become operational this fall (1964). Various uses and possible further developments of such a stratospheric moored platform will be discussed, including applications to manned systems.

---

(Received for publication 23 March 1965)

## I. INTRODUCTION

In June of 1962, our attention was drawn to a proposal by Mr. Charles A. Smith, of Aerological Laboratories, Encino, California, in which the possibility of mooring a balloon at stratospheric altitudes for extended periods of time was discussed. The system was originally intended to support a vertical chain of sensors to monitor meteorological parameters continuously, at a single location, over a range of altitudes--hence the acronym TABS: Tethered Aerological Balloon System. The utility of such a system, if feasible, in providing a relatively fixed high-altitude long-duration platform for a wide range of geo-physical observations was immediately evident, and Mr. Smith was invited to NOTS for further discussion of his proposal.

The feasibility of such a system rests upon the observation that profiles of wind velocity as a function of altitude, such as those illustrated in Figure 1, almost invariably show a maximum in the troposphere, followed by a minimum in the lower stratosphere. In the region of the maximum, generally between 30,000 and 50,000 feet, the wind velocity exceeds 50 knots nearly half the time and not infrequently reaches 100 knots. At the minimum, however, which usually lies between 55,000 and 75,000 feet, the wind velocity exceeds 20 knots in less than five percent of the profiles studied, and is generally below 10 knots. The wind direction is, as a rule, reasonably constant through the troposphere, but often changes sharply just below the minimum. The altitude of the minimum shows considerable day-to-day variation, and this, coupled with its often rather limited vertical extent, renders its existence much less evident when profiles are averaged over periods of several days, or over successive years at the same date.

Attempts to moor conventional balloons in the troposphere under any but the lightest wind conditions are frustrated by the excessive drag loads imposed, and flights of any significant duration are impractical. The use of high lift-to-drag, aerodynamically shaped lifting vehicles alleviates the situation somewhat, but such systems have nevertheless proven unsuitable for flights to altitudes much in excess of 20,000 feet. If, however, one can place the balloon in the region of minimum winds the drag on the balloon will be much lower; only the relatively small cross-section tether will be exposed to the high velocity tropospheric winds, and a minimum total system drag can be maintained by slight adjustments in balloon altitude. It should, therefore, be possible to maintain the system aloft for a considerable period of time, provided that the wind velocity at the balloon remains relatively low, and does not become unreasonably great at lower altitudes.

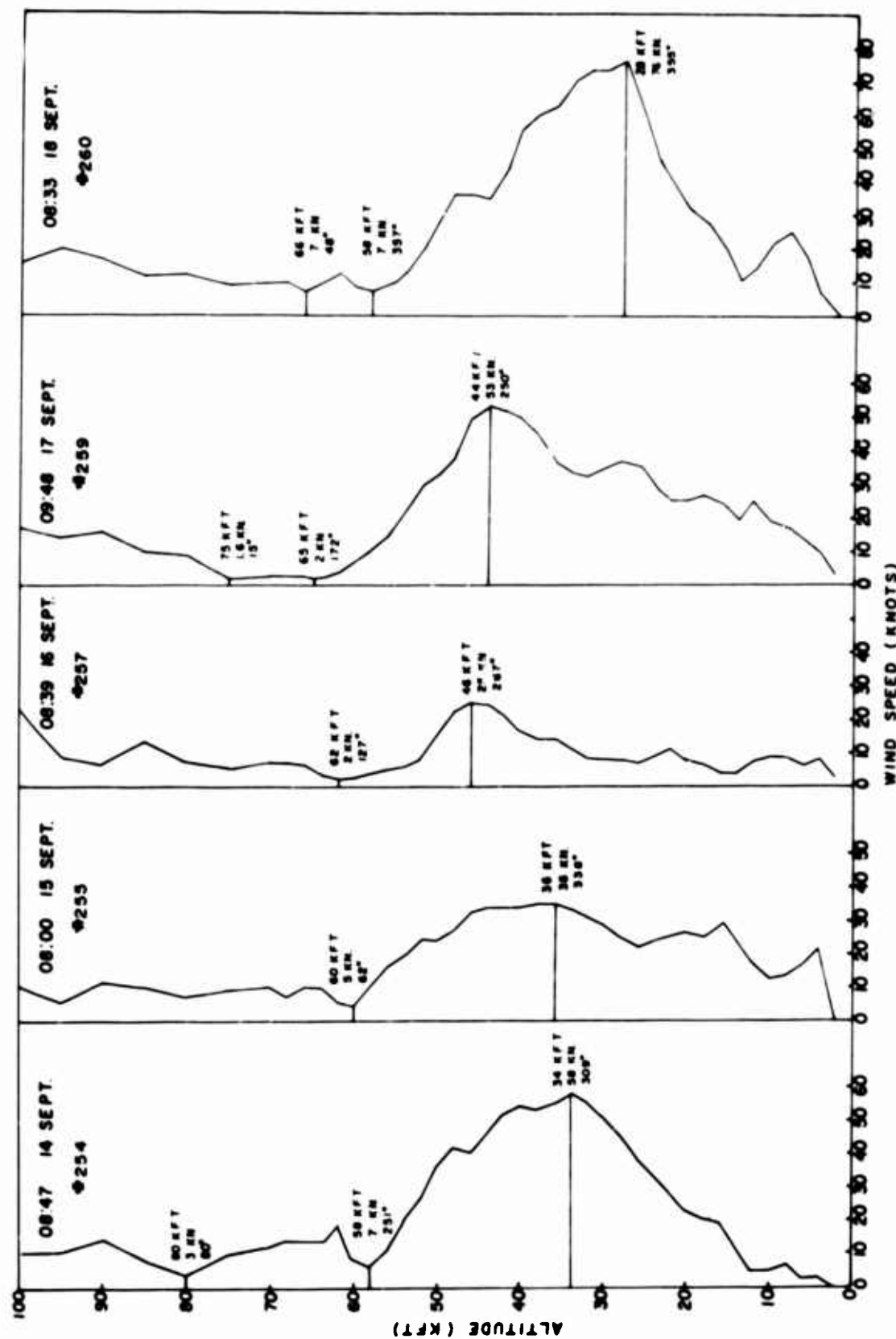


Figure 1. NOTS Wind Profiles (Rawinsonde) - Week of 14 Sept., 1964

Such a system of course requires balloons of suitable design and construction to support the vertical and horizontal loads involved, made of materials providing sufficient gas retention and resistance to deterioration under stratospheric conditions to remain aloft for days or weeks at a time. The former requirements appeared to be satisfactorily met by existing natural-shape taped polyethylene balloons, and while information on the latter problems was as yet relatively sparse, it appeared probable that current and projected developments in balloon technology would provide vehicles suitable for flights of at least moderate duration.

It is also necessary to consider the properties of the tether employed. The "classical" material, music wire, has great tensile strength--up to 280,000 pounds per square inch in diameters near 1/10 inch--and more modern steels are available which are up to fifteen percent stronger. Steel, with a specific gravity of 7.8, is, however, also very heavy, and it is found that even the best alloys will support their own weight in lengths only up to approximately 110,000 feet. The total tether length required for a balloon moored at 75,000 feet can easily approach this value, leaving no margin of strength to meet the additional loads imposed by aerodynamic drag and the excess balloon lift required to hold the system erect. One possible solution, that of tapering the tether downward from the balloon, also fails because with high tropospheric winds the tension in the tether at the ground may become comparable to that at the balloon.

Since it thus appears that the strength-to-weight ratio of the tether material is a critical parameter, it becomes evident that the solution is to be sought in the direction of the light-weight, high-tensile-strength materials have resulted from recent technological advances. It was found from preliminary analyses that if a material having a tensile strength of 150,000-200,000 psi and a specific gravity of 1.5 to 2.0 could be procured, the stratosphere-moored system would become feasible. It appeared that several candidate materials were or would soon become available which might fall within this range.

In order to assess the feasibility of a stratospheric moored balloon system in general, and to ascertain the balloon and tether parameters required to meet specific wind conditions, an approximate method of analysis was worked out (see Section 4 of this paper) which involves the balancing of the vector forces acting at successive points from the balloon down along the tether to the ground, the entire system being presumed in equilibrium. The analytical process yields, for a particular wind profile, a balloon of specified lift and weight, an assumed payload, a tether of given diameter, density, and tensile strength, and a set of figures for tether tension and angle to the vertical at successive uniform intervals of

altitude. Failure of the system is indicated by an increase in tension beyond the specified breaking strength of the tether or an increase in the tether angle beyond the horizontal (in which case, of course, the tether cannot reach the ground). It is then necessary to increase either the balloon lift (and drag) or the tether strength (and hence tether drag and weight) and repeat the calculation, until either an equilibrium configuration is found or the ultimate capacities of the balloon or tether material are exceeded. In the former case, the given wind profile can be tolerated; in the latter it cannot, and such winds must either be avoided, or countered by improvements in balloon design or tether material.

The ground station from which the system is to be flown must incorporate a winch capable of deploying the system, adjusting its flight altitude as necessary in order to maintain the system aloft, and retrieving the payload (with tether and balloon, if possible) at the end of the flight. The ground station must be provided with data concerning the wind velocity as a function of altitude. These might be obtained from periodic free-balloon soundings during the flight; a much more satisfactory solution, however, would be to equip the airborne system with instruments capable of measuring the wind velocity at the balloon and at various points along the tether, and continuously telemetering this information to the ground station.

There is a further requirement for the ground station, if the system is to be truly operational. Provided that the balloon can be maintained aloft under a given wind profile, the question now arises: is it possible to launch the system in the first place under such conditions? Analysis, and subsequent experience, suggest that the system envisioned cannot be maintained erect if the relative wind at the balloon exceeds approximately 20 knots, at any altitude. If we wish to have the balloon rise slowly, under the control of the winch operator, we obviously cannot launch the system except when the wind is below 20 knots at all altitudes; such days are relatively rare, occurring less than ten percent of the time. If we wish to fly the system under less ideal conditions, we must resort to other methods.

One possibility is to allow the balloon to rise and move with the wind as if it were free, paying out the tether as fast as it is needed. This has two serious drawbacks: first, the tether reel-out rate may become excessive for any reasonable winch system; and, second, the balloon may be carried so far downwind by the time it comes to altitude that the weight of tether to be supported may exceed the balloon's lifting capacity.

A more attractive solution would be to mount the winch on a mobile land vehicle (or a ship at sea). If the vehicle can then move more or less parallel to the existing winds at speeds up to, say, 40 knots, it should be possible to launch the balloon and allow it to rise under control to altitude through winds up to 60 knots, provided

sufficient maneuvering space is available. Even higher winds at specific altitudes might be tolerated by allowing the balloon to rise "free" through the regions in which they occur.

The system thus proposed appeared to offer sufficient promise to warrant further study by our group at NOTS. A large stock of miscellaneous balloons, acquired in connection with other projects, was on hand; other necessary materials and equipment were readily available; several areas on base offered airspace closed to civil traffic, lying above relatively flat and accessible desert terrain; and several of our personnel were experienced in the handling and launching of balloons. A series of tests was therefore undertaken, using small (18-and 23-foot) balloons, nylon line, and a surplus aerial tow-target winch mounted aboard a pickup truck.

No records were established during these tests, although successful flights to relatively low altitudes (~ 5000 feet) were made, but a great deal was learned about the handling and rigging of balloons for this type of operation. The mobile-winch technique was tested and found feasible, and the design parameters for the ground vehicle and its equipment were established. A considerable amount was learned about the properties required for the tether, and possible methods for its deployment; and finally a great deal of data was received against which the analytical technique outlined above could be checked, and from which aerodynamic parameters such as drag coefficients, pertinent to the analysis, could be derived empirically.

On the basis of these results, it was decided to proceed with a program directed toward the development of an operational system capable of supporting a payload of a few tens of pounds in the lower stratosphere for as much as a week at a time. Funds were solicited and procured from the Atomic Energy Commission and subsequently from the Department of Defense, a contract was drawn up with Aerological Laboratories, and a full-scale developmental program was undertaken. During the past two years this program has led to a system which is on the verge of becoming operational. The components of the system and some of the developments leading to their present configuration will be described in the next section.

## 2. SYSTEM CONFIGURATION

During the early stages of project TABS, a number of possible operational sites were considered. The requirement of extensive restricted airspace and terrain permitting considerable mobility limited serious consideration to a few large military reservations in the West, and none of these offered sufficient advantages over NOTS to warrant the more complex logistics involved. The use of a Navy vessel at sea was explored and found both feasible and attractive; again, however, the amount of planning and scheduling involved suggest that such operations should be postponed until a working system has been developed and tested.

Of the areas available at NOTS, the most suitable was found to be the Randsburg Wash Test Range, an annex to the southeast of the main body of the Station, adjoining and sharing airspace with Edwards Air Force Base and the Army's Camp Irwin reservation. Ground usage of this range is limited and the airspace is generally available on weekends, and by arrangement at other times.

An existing road, extending for fourteen miles in the general direction ( $260^{\circ} \rightarrow 80^{\circ}$ ) of the summer tropospheric winds, and free of sharp bends or overhead wires, was graded and realigned to permit smooth travel of the winch vehicle at speeds up to forty-five miles per hour (see Figure 2). While other more convenient areas of the Station have been employed for small-scale tests, Randsburg Wash has been and will continue to be the site of our major operations.



Figure 2. Balloon Flight Area at Randsburg Wash Test Range, U. S. NOTS. The mobile launch road extends generally eastward (azimuth  $\sim 80^{\circ}$ ) for fourteen miles from the balloon inflation site 1 to its terminus at 2

One of the problems familiar to every balloonist--that of preventing a partially-inflated balloon from converting itself into a spinnaker under the influence of a gust of wind--is doubly serious in the case of the tethered balloon. This is so because, while a free balloon once launched, moves with the wind and thus no longer requires restraint, the tethered balloon may be subjected to appreciable lateral winds all the way to altitude. A surprisingly simple solution to this problem has been found, however: a close-fitting sleeve of polyethylene is slid over the lower three-quarters of the length of the uninflated balloon. Upon inflation, the balloon then assumes an ideal "ball-on-a-stick" configuration with a taut bubble which resists deformation under a lateral wind loading and exhibits drag characteristics not greatly inferior to those of a smooth sphere. As the balloon rises to altitude and the bubble expands, the sleeve is forced down accordion-wise, offering sufficient resistance to maintain the desired configuration.

This system has been tested with static inflations of the 18-foot, 23-foot and 75-foot balloons employed in our program, with entirely satisfactory results. Figure 3 shows the static inflation of a 75-foot balloon in an airship hangar at Santa Ana, California. The 18-foot and 23-foot sizes have also been flown, tethered, to altitudes as high as 15,000 feet with success using this method; (Figure 7 illustrates a 23-foot balloon so rigged for a low-altitude test flight, with the balloon more than half expanded at ground level). In installing the sleeve clutch it is essential to refold the balloon in such a way that the portion within the sleeve has the form of a fluted column with the load tapes on the outside and the gore panels tucked inward, to avoid pinching the envelope material as it emerges from the sleeve.

A further advantage of this technique is that it provides an appreciable enhancement of the vertical ascent rate. With the large free lifts (often exceeding 60 percent of the balloon gross lift at ground level) which must be provided in order to support the tether weight as well as wind-drag forces when the balloon comes to altitude, the rising balloon, if unrestrained, assumes a variety of extremely unstable configurations which greatly increase its drag and reduce its ascent rate. The sleeve-clutched balloon, on the other hand, takes on a stable, somewhat flattened "mushroom" shape and ascends considerably more rapidly, with a minimum of billowing and pendulation. This has been verified by radar and phototheodolite observations of pairs, clutched and unclutched, of 18-foot balloons inflated to large free lifts and allowed to ascend together from adjacent release points. The clutched balloons ascended at a rate up to 15 percent greater than the unclutched ones, and exhibited vertical drag coefficients of 1.2-1.6.



Figure 3. Static Inflation of 75-Foot Taped Polyethylene Balloon to Test Deployment of Sleeve Clutch

As noted in Section 1 of this paper, it is desirable to provide airborne wind-speed sensors and telemetry to relay wind-velocity data to the ground. An altitude sensor is also of considerable utility, especially during the ascent phase. If instrumented payloads are ultimately to be carried, telemetry channels are also desirable for relaying their data to the ground. A ground-to-air command system should also be provided, both to permit voluntary separation of the payload and tether from the balloon if necessary at the termination of the flight, and to allow switching of modes of operation of the airborne instruments to conform to observational requirements.

The package represented by the block diagram of Figure 4 has been developed to fit these requirements. Powered by silver-zinc alkaline batteries, it provides up to six channels of FM telemetry on a single VHF carrier (only two channels are currently utilized, for pressure altitude and wind-speed data) as well as a UHF command receiver for mode selection and balloon cut-down. This apparatus is housed in a glass-resin-covered foam plastic case eight and one-half inches square and 56 inches high, and is carried in the balloon train, the load being transmitted through a pair of steel stays straddling the package. No particular effort was made to avoid weight; the entire package, with two turnstile antennas, weighs somewhat less than fifty pounds. Two identical packages have been constructed and tested and are shown in Figure 5.

The ground station, incorporating a pair of helical antennas, a command transmitter, telemetry receiver, discriminators for the data channels, paper chart and magnetic tape recorders, and meters for pressure and velocity read-out, was originally housed aboard the winch vehicle. It has since been found more practical to remove the ground apparatus to a separate location, and it is presently housed either in a fixed instrumentation site, for operations at Randsburg Wash, or in an air-conditioned mobile van, for use elsewhere. Communication with the winch vehicle is maintained by a radio link.

A wide variety of possible tether materials was investigated and tested. Of these materials, the most promising was a collimated bundle of glass fibers embedded in epoxy resin, but commercially available specimens suffered from limited flexibility and brittleness and could not be procured in sufficiently great lengths. Personnel of the Materials Engineering Branch at NOTS felt that these limitations could be overcome, and offered to undertake the development of a suitable tether.

A pilot production line was set up and experiments were carried out using various combinations of glass tether and resin, with highly satisfactory results. Specimens were made in diameters ranging from 0.060 inch to 0.095 inch, with breaking strengths of 800 to 1800 pounds. Tensile strengths in excess of 225,000 psi could be achieved consistently with occasional specimens running over 300,000 psi. With a resin content of approximately 20 percent by weight, the samples displayed a specific gravity of 1.6 to 1.7, yielding strength-to-weight ratios and breaking strengths exceeding those of music wire by a factor of four. All of these results could be achieved while retaining a high degree of flexibility comparable to that possessed by steel wire in similar sizes. This portion of the tether development culminated with the production of a continuous splice-free length of material 0.065 inch in diameter and 8500 feet long with a minimum break strength of approximately 750 pounds. This specimen was used successfully throughout a series of trial flights and performed in highly satisfactory fashion.

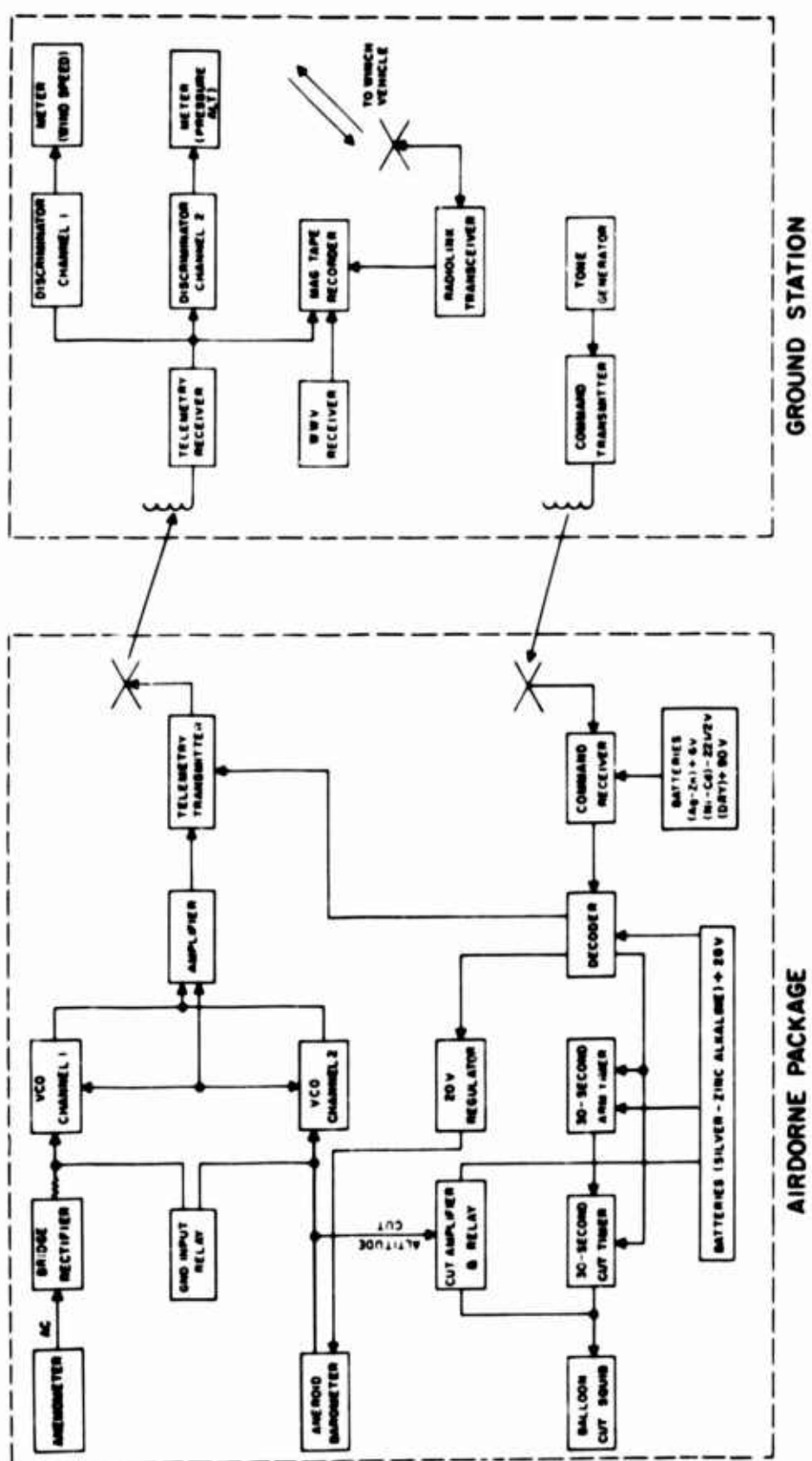


Figure 4. TABS Telemetry & Command System



Figure 5. TABS Airborne Telemetry/Command Packages, Closed and with Cover Removed. The cylindrical-vane anemometer plugs into the large fitting at the top, next to the cut-down squib connector. The aneroid barometer assembly is mounted on the fifth shelf from the top inside the package. The lower six trays carry the silver-zinc and nickel-cadmium batteries. The antenna leads extend through the bottom of the package.

In view of these results, it was decided to set up a full-scale production line capable of manufacturing the tether in lengths up to 150,000 feet. A 20-foot by 200-foot area in an existing building was partitioned off and partially enclosed with dust-excluding screening and positive-pressure air conditioning, and the pilot production line was reconstructed on a larger and more permanent scale. This facility is illustrated in Figure 6. In the background may be seen the racks which carry up to 150 bobbins, each wound with approximately 160,000 feet of "single-end" (208 filament) glass roving. The "ends" are drawn off the bobbins under controlled tension, gathered loosely together in a resin pre-wetting chamber, and pass through a resin impregnation bath. Emerging from the bath through an initial sizing die, the cylindrical bundle is partially cured in a tubular oven, drawn through a final sizing die, and thence through a series of finish curing ovens to emerge in finished form in the right foreground. The cured tether is then allowed to cool as it travels some 100 feet further through open air, to be wound onto a variable speed take-up drum. Continuous production rates of up to 40 feet per minute have been achieved. It has also been found possible to introduce individual ends into the line during production, in the event of breakage or exhaustion of a bobbin; in principle, at least, this would permit production of unlimited continuous lengths of tether. The new production line has been completed, and pilot specimens have been manufactured; preparations are currently being made to produce a full-length tether during the next few weeks.

While the new facility was being constructed, Owens-Corning Fiberglas, Inc., who had been supplying our glass roving, offered to manufacture for us approximately 50,000 feet of 1500-pound break strength material of basically similar construction. This proposal was accepted, as providing a possibility for conducting intermediate-altitude tests; Owens-Corning were able, however, to produce a total length of 81,000 feet of material of 0.093 inch diameter testing to 1650 pounds, and the entire quantity was purchased. It has been wound onto the winch drum and is presently ready for use in a full-scale stratospheric flight, as soon as suitable conditions of weather and range clearance are encountered.

A number of problems remain to be explored with regard to the glass-resin tether. One of the most important concerns the making of attachments to the ends of the tether, which of course, cannot be knotted. For tensile tests, hollow metal ferrules are potted with epoxy resin to the ends of the test specimens, but the curing process is slow, unless heat is used, while careless handling will allow the sample to break if kinked near the mouth of the holder; a new approach providing a rapid, secure connection is needed here. For attachment to the winch drum or the balloon load line, a few turns about a reasonably large-diameter cylindrical surface provide adequate friction to hold the tether end securely, without excessive local stresses (for the attachment to the balloon load line, a large, lightweight but

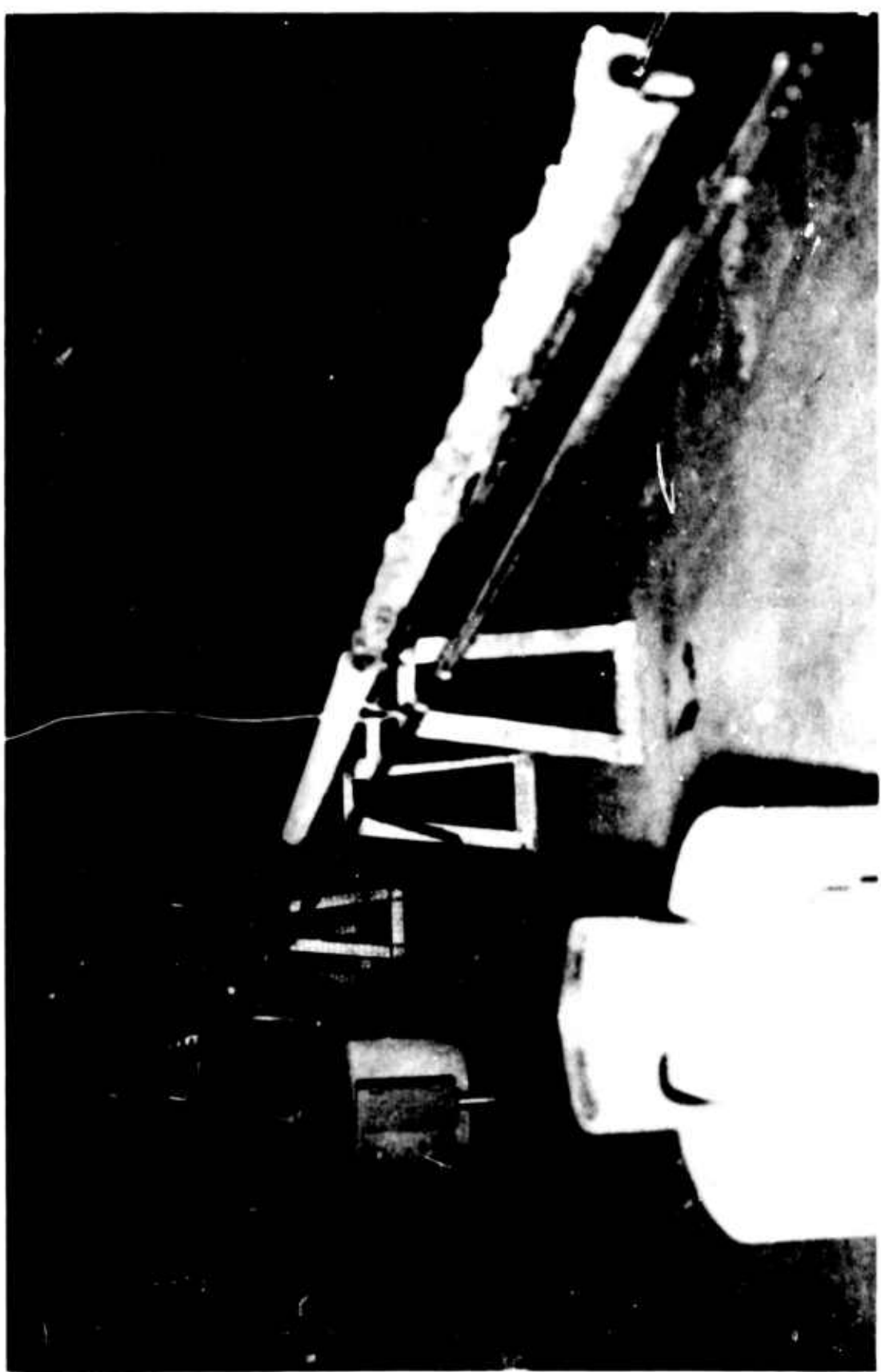


Figure 6. Single-End Glass-Resin Tether Production Line. The impregnating and curing area is enclosed in dust-excluding plastic screening, maintained under positive air pressure by the air conditioner at extreme left rear. The glass roving is drawn from bobbins on the racks at the rear of the room, gathered together and resin-impregnated, and passed through a series of sizing dies and tubular curing ovens to emerge as finished tether at lower right.

rigid flanged hoop some 24 inches in diameter and one inch broad is used, with the flanges extended on one side to hold a shackle pin to which the load line is tied). What is needed, however, is a simple, rapid field technique for making splices in the middle of the line without degrading either its strength or its flexibility to any significant degree. Efforts are currently being made to solve both of these problems.

It has been found entirely feasible to imbed one or more copper wires into the tether as it is being fabricated, at only a slight penalty in weight and tensile strength. The possibility of also depositing a conducting outer layer over the tether, to provide a coaxial conductor, is being considered; such techniques would, of course, be of great usefulness for supplying power to and communicating with an airborne system.

Initial experiments involving a pickup truck with a hand- or electric-powered tow-target winch as a mobile launch platform indicated that a somewhat more sophisticated system would be required. An effective, if unlikely, solution was provided by the acquisition of the surplus amphibious truck illustrated in Figures 7 and 8. Six-wheel drive and large diameter tires permit traversal of dirt roads and open desert terrain at adequate speeds with excellent stability; extensive and relatively unobstructed deck space, coupled with a variety of power take-off points provided an ideal base for the winch and tether rigging required. The main winch, of 18-inch core and 36-inch flange diameter, 32 inches between flanges, with a capacity of 100,000 feet of 0.125-inch cable, was specially fabricated and mounted on a framework at the stern of the truck. The winch is driven through a four-speed automotive transmission and multiple V-belt by a hydraulic motor. This motor is in turn connected to a variable displacement hydraulic pump driven by the power take-off originally used for the vehicle's propeller shaft. Reel-in under power, and hydraulic braking of the winch on reel-out may be controlled independently of the truck's road speed by valves at the hydraulic control operator's position amidships. The tether passes off the winch through a level-wind guide pulley, forward to a second pulley at the bow, and then back to a final fairlead pulley mounted on a welded superstructure over the truck's center of gravity. The bow pulley is supported by a framework incorporating an electromechanical load cell providing continuous monitoring of tether tension, and is equipped with a footage counter; the fairlead pulley is universally mounted and fitted with a Teflon-bushed lead-out sleeve, permitting the tether to emerge unobstructed in any direction in the upward hemisphere. All pulleys, as well as the drum core and the lead-out shoe have a minimum radius of nine inches. Maximum reel-in and reel-out rates under light loads are in excess of 2000 feet per minute, and reel-in can be accomplished at low speeds against a tether tension of up to 2000 pounds.

Adjacent to the hydraulic control position are a second seat and a console, originally carrying the ground-based components of the TM/command system, but at present fitted with the transceivers for the ground-station radio link and a

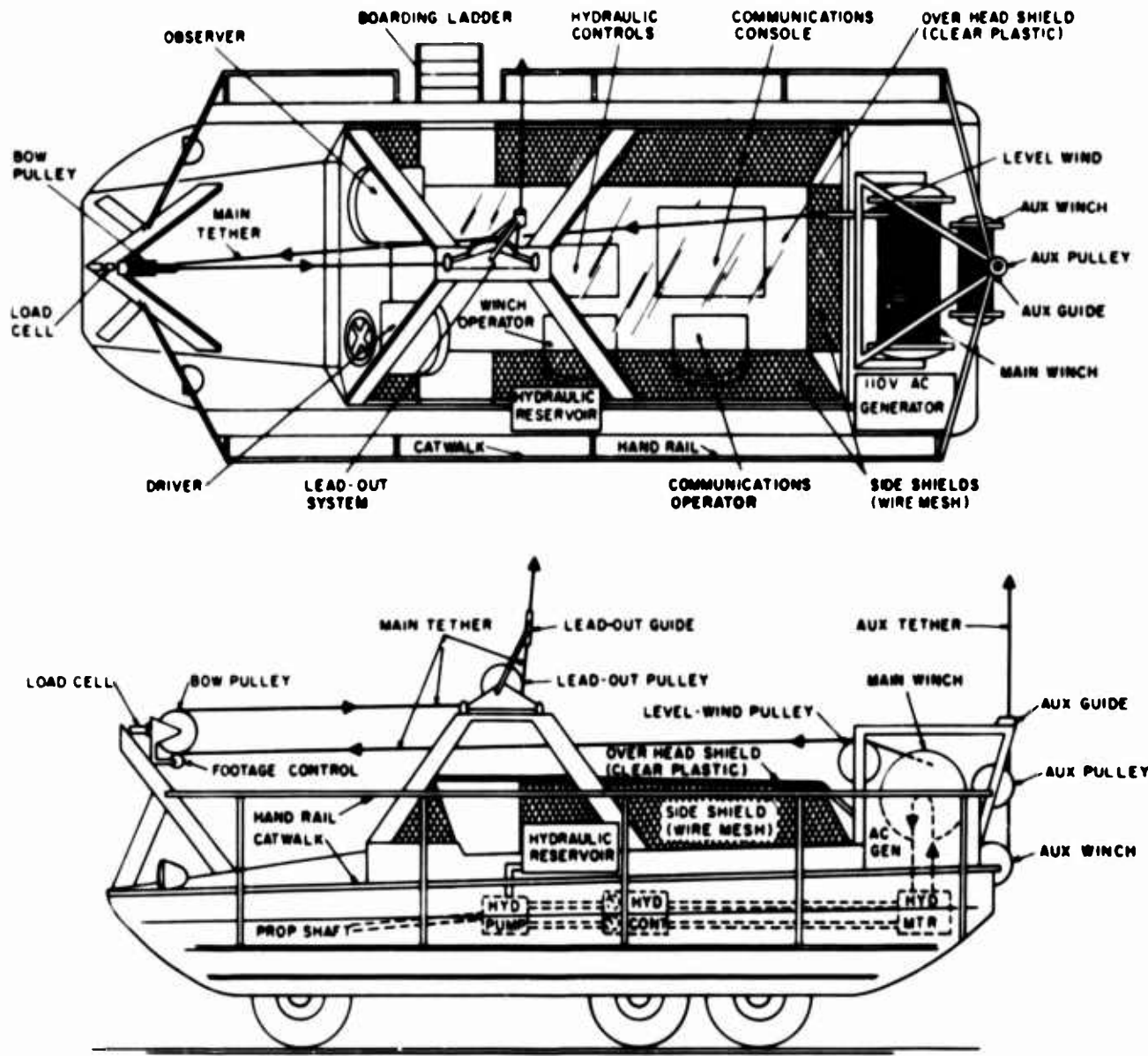


Figure 7. Tabs-Mobile Winch Vehicle

control panel for the intercom system used by the personnel aboard the truck. The personnel includes the hydraulic and communications operators, the vehicle driver and one observer, seated facing backwards and upwards in the driver's compartment. All personnel are shielded from possible injury in the event of tether breakage by side and overhead screens of wire mesh or clear plastic.

A small auxiliary winch at the extreme stern of the vehicle, together with a guide pulley and lead-out grommet provide a means for initial erection of the balloon and load train, and for transfer of the load to the main tether. A gasoline-driven 110-volt a-c generator is also mounted at the stern, to provide power for flood lights during night operations, and any additional instrumentation which may

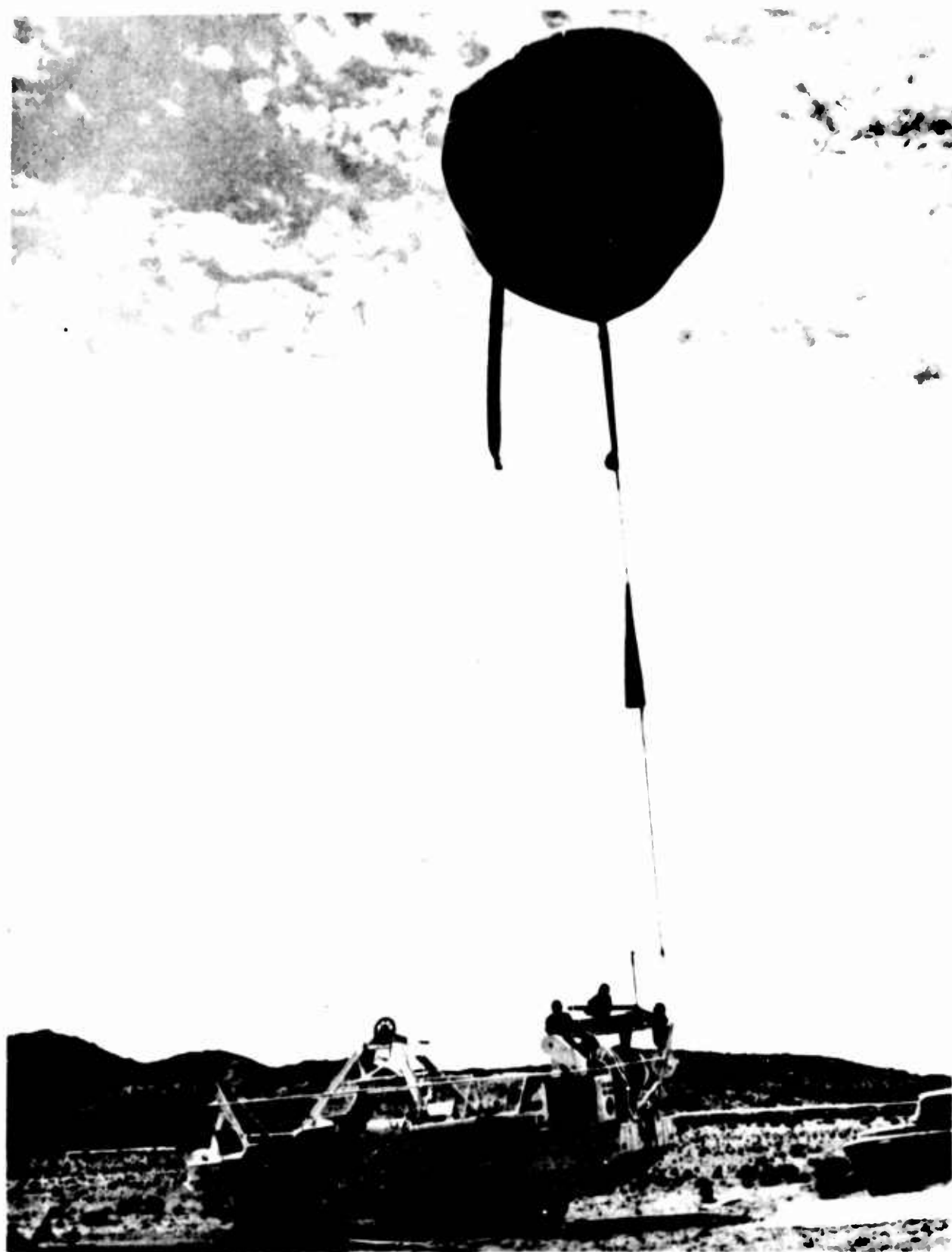


Figure 8. Final Preparations for 5000-Foot Telemetry Check-Out Flight Using 23-Foot Sleeve-Clutched Balloon, Glass Tether, and Mobile Launch Vehicle. The balloon is attached to the auxiliary winch by a secondary handling line

be used for a specific operation (all of the basic instrumentation for the flight system being battery-powered). An emergency mechanical braking system for the main winch has controls accessible from several points aboard the vehicle. A catwalk and handrail extend along both sides of the truck, permitting free access to all stations.

The present configuration of TABS is the result of a large number of small- and medium-scale flight operations, one of the most recent of which--a telemetry test flight to 5000 feet using the glass tether and a 23-foot balloon--is shown in Figure 7. Continuous refinements in components and techniques have been made as their need was indicated by practical experience. Flights with the system under full control have been made to 15,000 feet altitude (18,000 MSL) using music wire tether, and the original sample of glass tether was used for three flights to 3000, 5000 and 6000 feet, with full recovery of balloon and payload in each case. Analysis of these flights has provided hitherto unavailable data on the aerodynamics of the system, which permit the original analytical technique to be extended with considerable confidence to the full-scale stratospheric flights planned for the immediate future.

The development program is expected to culminate in a series of three flights to stratospheric altitudes using the present TABS components and Winzen 225,000-cubic-foot, 75-foot diameter taped polyethylene balloons. The first flight will be performed under optimum wind conditions permitting, if possible, a static launch, and will carry instrumentation solely to test the performance of the system itself. The first flight will be limited to a few hours' duration.

Two subsequent flights will be conducted, primarily to test the system under more severe wind conditions requiring a mobile launch, and it is hoped that at least one of these will be of several days' duration. A few tens of pounds of scientific apparatus may be included in the payload for these later flights.

The first flight will be conducted as soon as feasible, using the Owens-Corning tether on hand. The two later flights will require tether lengths in excess of 100,000 feet, and will probably use NOTS-manufactured tether.

### 3. FUTURE PLANS

Our plans for the future use of TABS fall into two categories: those utilizing the present system for various geophysical research projects, and those directed toward further development of tethered high-altitude systems.

The original concept of TABS involved its use as a moored, permanent meteorological station. This still represents one of the most important functions which such a system could fulfill, namely, to provide a continuous record of

aerological parameters at a fixed point (or series of points, with sensor packages attached to the tether at various altitudes) in the atmosphere. In addition, TABS would make possible the direct measurement of such quantities as vertical wind velocities and precipitation nuclei concentrations which are of interest to our weather modification program at NOTS.

A somewhat related problem is that of atmospheric electricity. Measurements of the atmospheric potential gradient have hitherto relied upon summation or integration of a sequence of short vertical base-line observations, and have yielded contradictory and non-reproducible results. A tethered system using the glass-resin line with one or more imbedded conductors, as mentioned above, would make possible direct measurement of the atmospheric potential as well as its variation with time. Efforts are being made to develop suitable collectors and measuring instruments, and to test various conducting-tether configurations. The interesting possibility of using the atmospheric electrostatic charge as a source of continuous power is also to be investigated.

TABS could also be used as a platform for photographic, photoelectric, and ultimately television observations, both of the ground and clouds below and of astronomical objects above the balloon. The possibility of using wind-vector forces as a simple source of first-order azimuthal stabilization for such instrumentation is of great interest, especially insofar as a stabilized platform would permit relatively long exposures at high resolutions and narrow bandwidths.

The tethered system also provides an ideal vehicle for long-term detection and collection of various atmospheric constituents and contaminants. With a moderate horizontal wind at the instrument, contamination by material associated with the balloon, payload and tether could be avoided. Suitable collectors and detectors of sufficiently light weight already exist, and will be employed with TABS for study of atmospheric moisture, precipitation nuclei, micrometeorites, organic material, and so forth.

Since the lift of a balloon increases as the cube of its dimensions, and its projected area, and hence drag, varies as the square (similar considerations applying, of course, to tether strength and drag), the efficiency of the system will increase with size. On the other hand, greater size will increase the problems associated with inflating and launching the system, especially under adverse conditions.

Two approaches to these problems are available. The first, and simplest is to operate from a vessel at sea permitting movement in any direction at reasonable speeds. Matching of vessel speed with wind velocity will permit vertical inflation of the balloon from a limited deck space, so that a small, fast ship such as a destroyer could be used. It is hoped that this approach, using the present system, can be tested in the near future.

To operate a larger, all-weather system on land, however, it will probably be necessary to abandon the mobile technique, since the extensive airspace and ground access required will not be generally available, and the larger capacity winching system needed would become somewhat unwieldy. The most direct approach would involve: first, some method of protecting the balloon during inflation and prior to launch (several such methods have been proposed in recent years); and, second, a substantial increase in balloon ascent rate, best achieved by use of a low-drag aerodynamic configuration. If ascent rates of 2500 to 3000 feet per minute could be achieved, a static launch technique would become entirely feasible, even in the presence of relatively high tropospheric wind velocities. Experiments are to be conducted at NOTS with small streamlined balloon shapes to determine whether stable ascent can be achieved at such rates, and to develop means for maintaining efficient aerodynamic configurations over the large balloon expansion range needed.

The possibility of mooring balloons at altitudes above that of the wind minimum has also been given extensive consideration. While the strength-to-weight ratio of the glass-resin tether is certainly adequate for flights to the highest altitudes which can be reached by conventional balloons, it is felt that the most efficient system would involve deployment of a high-altitude second stage from a balloon moored at the wind minimum. The upper stage should combine sufficient buoyant lift to support itself and its tether in low winds with aerodynamic lift and control for station-keeping in higher winds. Model studies leading toward such a system could be conducted using the present TABS.

Finally, the tethered balloon system offers an attractive solution to many of the problems hitherto encountered in manned high-altitude balloon operations, especially those involving flights of long duration. The balloon can be confined to a relatively limited region of airspace, line-of-sight communications can be maintained, and it might even prove feasible to conduct resupply operations by "flying" a small balloon and payload up along the tether.

#### 4. ANALYTICAL PROCEDURE

As noted in Section 1 of this paper, an analytical program has been worked out and refined by experience, which permits determination either of the balloon and tether parameters required to adapt the system to a general class of wind conditions, or of the feasibility of flying a given system under a specific wind profile. The procedure has been simplified to the point where it can be performed in a relatively short time immediately prior to a flight by manual computation following a pibal or rawinsonde sounding. The vehicle rate profile for a mobile launch can likewise be readily computed on the basis of a last-minute sounding. Examples

of such computations are presented in the following paragraphs for the existing system in a recent, typical wind profile.

Figure 9 illustrates the configuration which will be assumed by a tethered system having the parameters indicated on the right in the figure, under the wind profile of 17 September 1964 (see also Figure 1, where the wind velocity is plotted in knots rather than feet per second). The procedure is as follows:

- a. Select balloon flight altitude:  $h_o = 64,000 \text{ ft}$
- b. Select balloon net lift:  $L_b = 750 \text{ lbs}$
- c. Determine balloon projected area at the given  $h_o$ ,  $L_b$  from balloon inflation tables:  $A_b = 4000 \text{ ft}^2$  (balloon assumed spherical)
- d. Determine wind drag on balloon:  $D_b = C_{Db} (\rho_o V_o^2 / 2) A_b = 3.5 \text{ lbs}$

( $C_{Db}$  = balloon drag coefficient = 0.8

$$\rho_o = (\text{atmos. density at } h_o) = 20 \times 10^{-4} \text{ slugs/ft}^3$$

$$V_o = 3.3 \text{ ft/sec, both from rawinsonde reduction})$$

- e. Specify payload weight (including TM/command package, antennas, load line, load ring, parachute, squib cannons):  $W_p = 88 \text{ lbs}$
- f. Compute tether angle at balloon by vector resolution:

$$\theta_o = \tan^{-1} D_b / (L_b - W_p) = \tan^{-1} 49.4 \times 10^{-3} = 0^\circ 17'$$

- g. Compute tether tension at balloon:

$$T_o = D_b / \sin \theta_o = (L_b - W_p) / \cos \theta_o = 662 \text{ lbs}$$

- h. Select first altitude increment:  $\Delta h_1 = 4,000 \text{ ft}$
- i. Compute tether length in  $h_1$ :  $\ell_1 = \Delta h_1 / \cos \theta_o = 4,000 \text{ ft}$
- j. Compute tether flat-plate area:  $A_1 = 7.85 \ell_1 / 1000 = 31.4 \text{ ft}^2$
- k. Compute tether drag force:  $D_1 = C_{Dt} (\rho_1 V_1^2 / 2) A_1 = 0.30 \text{ lbs}$

( $C_{Dt}$  = tether drag coefficient = 1.2 (mean value from experiment + theory)

$\rho_1 = 2.25 \times 10^{-4} \text{ slugs/ft}^3$ ,  $V_1 = 8.35 \text{ ft/sec, both from rawinsonde data at increment midpoint, 62,000 ft}$ )

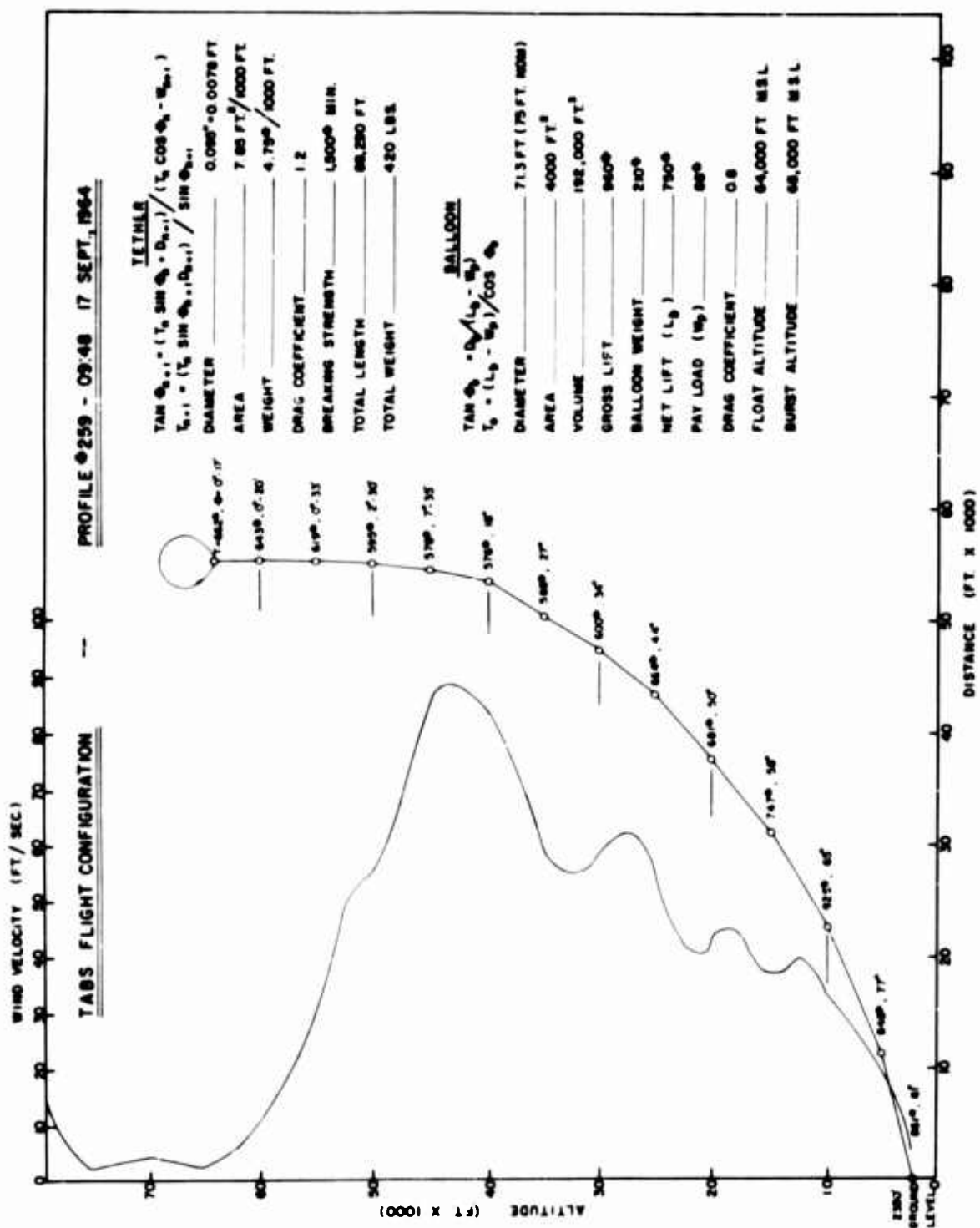


Figure 9. TABS Flight Configuration

1. Compute tether increment weight:  $W_1 = 4.75 \ell_1 / 1000 = 19.0$  lbs

m. Compute tether angle at  $h_1 = h_o - \Delta h_1 = 60,000$  ft:

$$\theta_1 = \tan^{-1} (T_o \sin \theta_o + D_1) / (T_o \cos \theta_o - W_1) = 0^{\circ} 20'$$

n. Compute tether tension at  $h_1$ :

$$T_1 = (T_o \sin \theta_1 + D_1) / \sin \theta_1 = 643$$
 lbs

o. Repeat steps h - n for successive increments in altitudes of 5000 ft, from 60,000 ft to 5000 ft, final increment 2650 ft from 5000 ft to ground (2350 ft)

From the values of  $\theta_n$  and  $T_n$  thus obtained at each altitude  $h_n$ , a flight configuration such as that in the center of Figure 9 can be plotted. If at any point  $\theta_n$  exceeds  $90^{\circ}$ , or  $T_n$  exceeds the tether breaking strength (1500 lbs), the system cannot be flown. For the procedure outlined above, a previous computation with  $L_b = 650$  lbs showing  $\theta = 90^{\circ}$  at approximately 4000 ft altitude was redetermined for  $L_b = 750$  lbs, with the acceptable results shown in the figure. This profile is, however, close to the maximum which the present system could tolerate; the balloon is very near its maximum inflation, while the tether angle at the ground is dangerously large. The tether tension, however, is at all points well below the specified minimum breaking strength. The total length of tether out is somewhat greater than that presently on hand, but well within the length scheduled for production at NOTS.

Referring to the remaining profiles illustrated in Figure 1, a flight would have been marginally possible on the 14th because, although the velocity at the maximum is somewhat greater than on the 17th, it is relatively less below 20,000 feet, and the altitude of the minimum is considerably lower. The system would encounter no difficulty on the 15th or 16th, and the vertical extent of the low-velocity region could permit flights to considerably greater altitudes. It is unlikely that the present system could have been maintained aloft on the 18th.

In all such calculations the winds are assumed to be constant in direction. In most cases, this is in fact a reasonably good assumption over the region of moderate-to-high wind velocities; moreover it makes the calculations somewhat conservative because a variation in wind direction with altitude will reduce tether angle to some extent.

Application of the mobile launch technique to the profile of the 17th is illustrated in Figure 10. If the balloon were to rise freely, with the wind, at a rate of 1200 ft/min (which should be achieved by a well-clutched balloon having a vertical

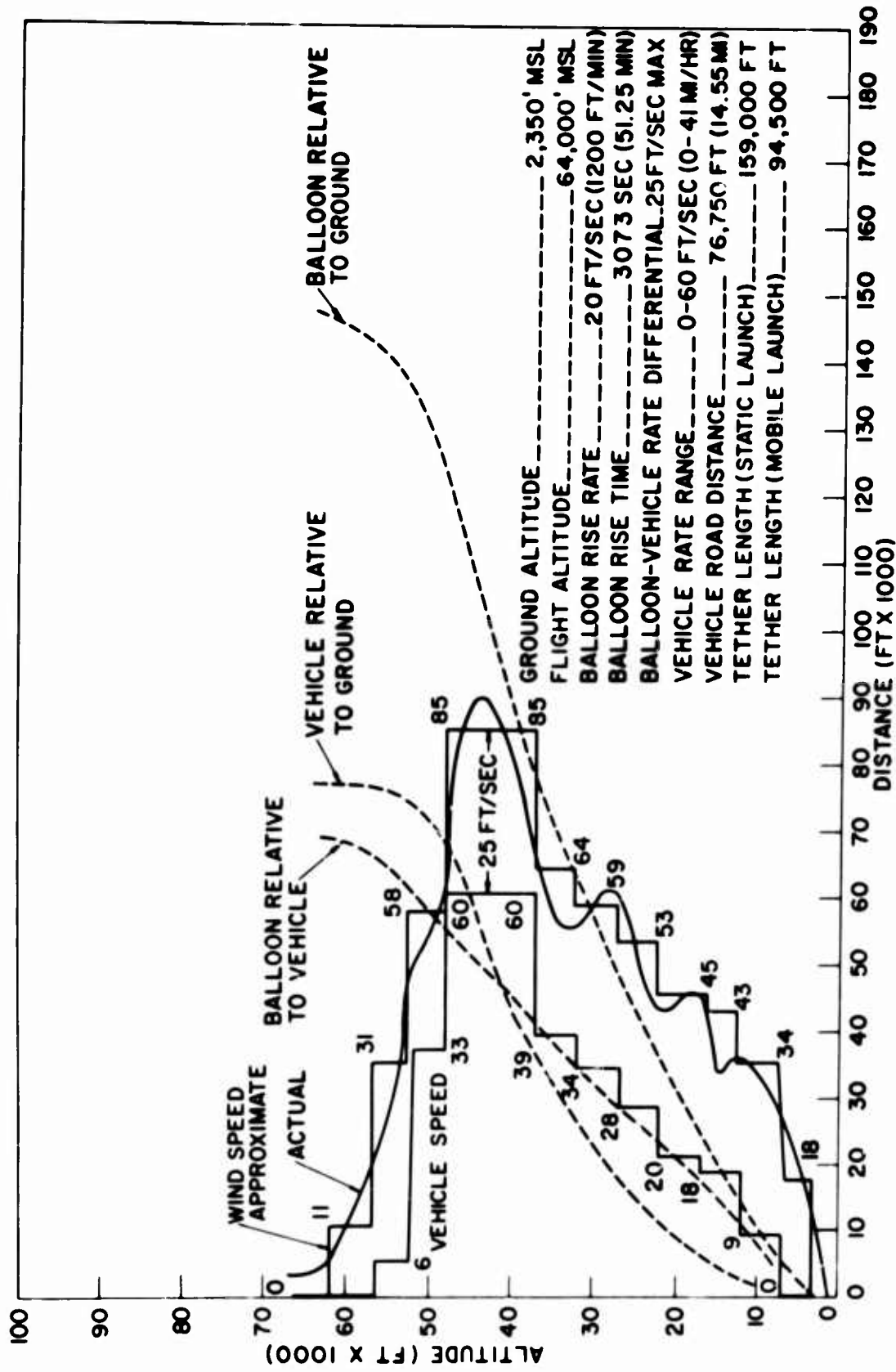


Figure 10. TABS Mobile Launch - Profile Matching Technique Profile #259 - 09:48  
17 September 1964 Randsburg Wash Road

drag coefficient of 1.5-1.6) it would follow the right-hand dashed curve, coming to altitude some 28 miles downwind, and requiring slightly over 30 miles ( $\sim 160,000$  feet) of tether. The weight (760 lbs) of this amount of tether exceeds the lift available, and this launch mode is obviously not feasible.

If one approximates the actual wind profile by the 5000-foot-interval stepped profile which overlies it in the figure, and then assumes a conservative vehicle-balloon rate differential of 25 ft/sec ( $\sim 15$  knots), the vehicle rate profile indicated by the left-hand stepped curve is obtained. The vehicle is then driven for periods of 4 min 10 sec ( $= 5000 \text{ ft} + 1200 \text{ ft/min}$ ) at each of the various speeds indicated in the figure, attaining a maximum speed of 60 ft/sec = 41 mph and following the central dashed curve. The total road distance covered is 14.6 miles, which is just feasible, utilizing a section of available road lying to the west of point 1 in Figure 2. The balloon, following the left-hand dashed curve relative to the vehicle, now comes to altitude 13 miles downwind of the end of the road (2, Figure 2), with 18 miles ( $\sim 95,000$  ft) of tether deployed, for a total weight of 450 pounds. This is quite acceptable, and the balloon would gradually drift back upwind, with the tether being retrieved under light tension, until the configuration of Figure 9 was reached.

Of the profiles in Figure 1, that of the 14th is too severe; the tropospheric winds are blowing at some  $50^\circ$  to the road direction, giving a cross-wind component of some 40 knots. Even if the wind were blowing along the road, the 58-knot maximum would require excessive vehicle speeds, unless the rate differential were allowed to approach 20 knots. On the 15th the winds, although relatively low, are at some  $80^\circ$  to the road direction, making a mobile launch impractical. Free ascent of the balloon from a static ground point would, however, consume less than 100,000 feet of tether, and would be feasible.

The profile of the 16th offers some choice: the balloon could be let out under control from a static position to 40,000 feet, and then allowed to rise free to approximately 50,000 feet; or the mobile launch method could be used, with the vehicle rate profile matched to that of the wind velocity, the vehicle remaining more or less directly below the balloon during the entire ascent. On the 18th, again, launching would prove impossible.

We thus see that, during the week under consideration, the system could be launched and maintained aloft over a full three days, from the 15th through the 17th. The following is a fairly typical pattern: a recent study indicated that of some 83 days during June-September 1964 on which soundings were made, static launches could be made on six, and free-rise or mobile launches on 22, for a total of 34% of the days considered. Similarly, the system could be maintained aloft on 58, or 70%, of the days studied, many of these falling into groups of a week or more.

The various drag coefficients used in these calculations have been derived from analysis of flights to altitudes of up to 15,000 feet (and to 50,000 feet for the ascent rate observations with free balloons). They are at least plausible when compared with theoretical calculations and the limited experimental data obtained elsewhere, and there is no evident reason for doubting their applicability at higher altitudes. The empirical drag coefficients for the balloon, 0.7 to 0.8 lateral and 1.2 to 1.6 vertical, lie between the values for a smooth sphere (0.5) and a circular flat plate (2.0); the higher figure for vertical drag evidently results from the observed flattening of the balloon crown at high ascent rates.

The assumed tether drag coefficient of 1.2 is somewhat more complex. Strictly speaking, one should consider an element of the tether as an inclined cylinder subject to normal and parallel drag forces as well as lift, and three coefficients should be employed. It appears, however, that by using a single drag coefficient and utilizing the total flat plate area (not just the component normal to the wind) of the tether, a reasonable approximation to the actual forces on the tether can be obtained, permitting a great simplification of the calculations. The drag coefficient thus determined falls in the range 1.1 - 1.3. Parallel (skin) drag is found to be negligible except at high tether inclination angles, which in the normal TABS configuration occur only near the ground. Lift forces, which will be negative and thus equivalent to an excess tether weight, are significant principally at intermediate angles. These also are encountered at relatively low altitudes. Normal drag coefficients, based on Reynolds' number calculations for the prevailing velocities and tether dimensions, range from 2.0 at 10 ft/sec at 80,000 feet, to 1.1 at 10 ft/sec and 0.8 at 50 ft/sec at the ground (at 1 ft/sec at 80,000 ft the coefficient can reach a value of 6, but the drag force at such a low velocity and atmospheric density is negligible). The assumption of a drag coefficient of 1.2 applied to the total projected area of the tether results generally in a moderate overestimation of the tether drag force. This offsets the effect of neglecting lift forces upon the derived values of  $\theta$  at intermediate altitudes, and somewhat overestimates the tether tension. Similarly, near the ground the calculated drag is considerably in excess of the actual normal drag, which probably overcompensates for neglect of parallel drag. The result is a relatively conservative assessment of system capabilities which should suffice for the present; actual high-altitude flight data will ultimately provide more precise information on which a more detailed and accurate analysis can be based.

## II. Improvement in Balloon Design Through Scale Model Analysis

J. A. Winker  
Raven Industries, Inc.  
Sioux Falls, South Dakota

### Abstract

The history of plastic ballooning has been one of ever-increasing demand for payload and altitude capability. To meet this challenge, improvements must be made either in balloon materials or in design. In recent years much effort has been applied to the materials aspect of the problem with gratifying but expensive results.

New design concepts are called for which will extend the capability of less expensive balloons. Since most balloon failures occur at midaltitudes on ascent, more must be learned about the stresses on partially inflated balloons. A scale model study has been instituted to investigate the configurations and stresses for this condition. Initial work has been aimed at establishing model laws and at comparing different standard balloon designs. A new balloon design has been explored by this technique and preliminary verification of the model data has been made in full-scale flights.

### I. INTRODUCTION

Only fifteen years ago it was considered a rather significant achievement to carry loads of 100 pounds or more to an altitude of 100,000 feet. Since

then, we have seen a considerable advance in capability with such accomplishments as lifting payloads of 150 pounds to 150,000 feet and some 15,000 pounds to medium altitudes. Along with this has come some improvement in reliability, but not as much as could be desired. The advances which have been attained were made possible by the development of better designs and better materials. Since balloon users are continually seeking greater lift and altitude capability, this process of betterment must be continued.

Much effort has been expended in recent years developing sophisticated, reinforced balloon materials. These are very excellent materials in their proper application, but there is no evidence that they can or should be used in the general area of "workhorse" balloons. Current work on improved low-cost films is more apropos to the majority of balloon experimentation and should lead to a worthwhile advance in the state-of-the-art.

In spite of improved materials that may be available now or in the future, some capability limit exists with the designs now in use. Therefore, if we are to obtain the maximum growth in the technology, the design aspect of the problem must not be neglected. The work reported on here aims at learning more about stresses in partially-inflated balloons. The results of these studies should permit the formulation of designs superior to contemporary types.

## 2. MODEL TESTING

The greatest hazard to the polyethylene balloon is ascent through the tropopause and the lower stratosphere regions. It is here, where the balloon has expanded to only a small fraction of its full volume, that a large majority of balloon failures occur. Thus, if designs are to be improved, it appears essential that more information be gained on stress patterns in partially inflated balloons.

A certain amount of this information has, and can, be obtained by photography -- up cameras, internal cameras, telescopic cameras, and so on -- or by personal observation from manned flights or escort aircraft. Such data, while useful, present only a small part of the information necessary. Also, the occasions are infrequent when such techniques of observation may be employed.

To obtain a large amount of information inexpensively, the Air Force Cambridge Research Laboratories has sponsored a scale-model investigation program utilizing "water models". Sporadic water-model tests had been conducted

by various groups in the past, but no specific effort was known which tried to establish meaningful model laws. It is expected that eventually, as a result of the current program, many facets of balloon performance will be predictable through model testing.

To provide the greatest realism in the test method, a large water tank was constructed so that the buoyant envelope would act in its denser "atmosphere" much as a real balloon does. This facility eliminates the typical problem of air-water intermix usually present in suspended, water-inflated models and it also allows for eventual testing with other combinations of atmosphere and buoyancy media.

The water tank is an octagonal structure seven feet across the flats and eight feet deep (Figure 1). Each inflation test is recorded photographically with still and time-lapse cameras. The degree of inflation is determined by measuring the lift with a load cell whose output is recorded during the test run.

The work which has been completed to date was primarily for comparisons and background information and to establish a foundation for future analyses. In this effort, a large number of scale-model balloons have been inflated to rupture. The data collected include ultimate lift at failure, shapes at various degrees of inflation, and the location and nature of the rupture. A comparison was made between six different balloon designs, three of which were taped and three tapeless. The burst values correlate quite well with known or derived values for full-scale balloons. A good deal of additional numerical data will be required, however, before quantitative analytical steps can be taken to make accurate predictions of the performance of new balloon designs. While these data are being acquired, we can still make very good use of the qualitative results of the tests which have been run.

### 3. BURST MODE HYPOTHESIS

It appeared significant in the model failures that rupture almost invariably occurred on the top, nearly-flat region of the bubble. A search through eye-witness accounts and photographic records of actual balloon failures reveals that the little tangible evidence available seems to indicate that these also occur near the very top. No evidence was uncovered which would point to any other area as being the initiation point for failures.

In the models, the failure was predominantly the result of transverse stressing. This seems incongruous at first since a natural shape balloon by definition cannot have transverse stresses. Also, there is obviously surplus material in the bubble which should be available to relieve the stressed area. The answer to the first statement is, of course, that the shape of a typical balloon at launch is not like that of a theoretical sub-pressure balloon. The vast excess of material tends to form

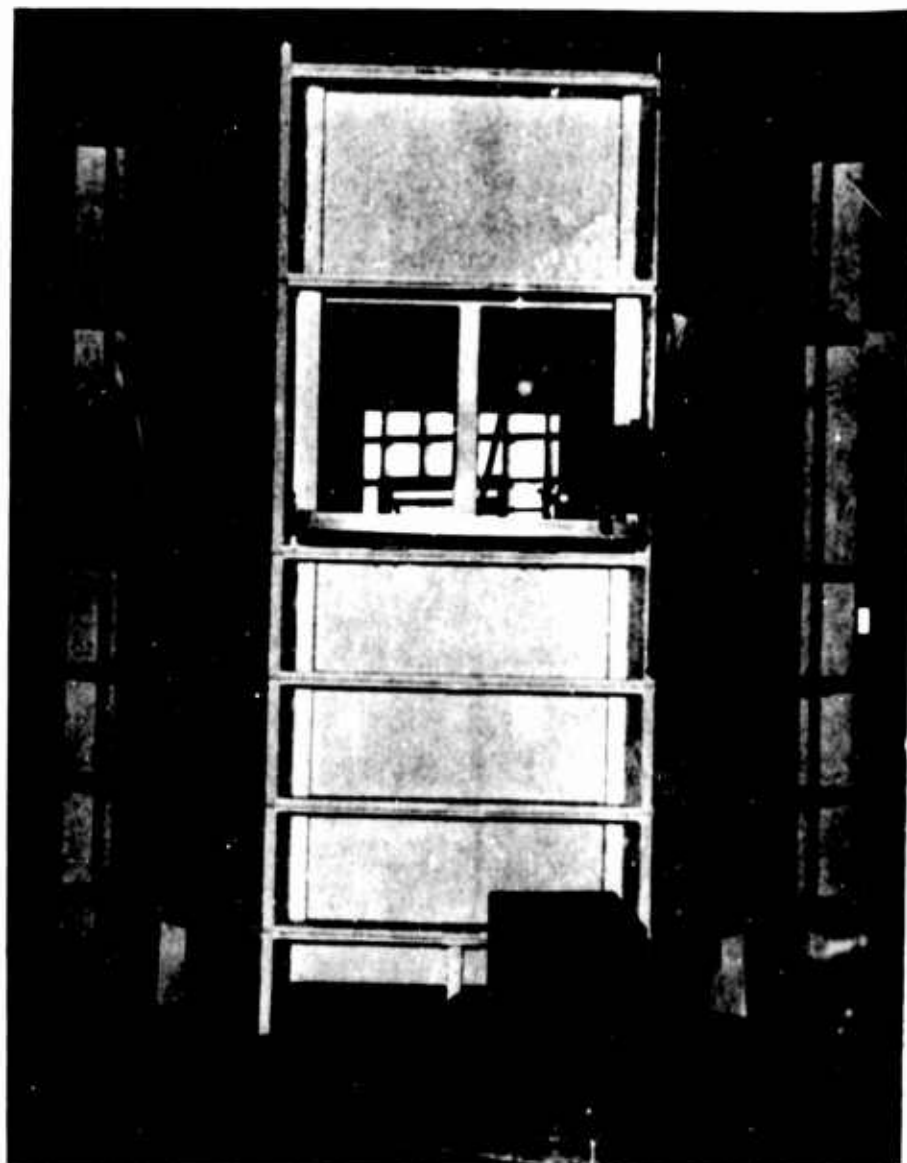


Figure 1. Water Tank Test Facility

a large cavity under the gas bubble causing it to deviate substantially from a theoretical shape. It is this same nonsymmetrical arrangement of material which can set up the transverse stresses in the top region.

Figures 2 through 5 show various aspects of a full-scale static balloon inflation. Note in Figure 2 that while the stress lines on the outer portions of the bubble (left side) are reasonably meridional, those in the sub-pressure cavity cross the gore seams at distinct angles. Note also that these stress lines are essentially two-dimensional curves and may be imagined to lie on a vertical plane. In Figure 3, a hypothetical "stress plane" has been superimposed over the bubble to better illustrate the path of the stress line. It may be seen that the angle between the stress line and the gore seams increases from approximately zero to 60° in the visible field of this photograph.



Figure 2. Stress Pattern in Partially Inflated Bubble

Figure 4 shows the same bubble and the same stress plane from above. This area of the balloon is largely under biaxial load and the stress lines cannot be seen, but it is not difficult to imagine the stress lying on the surface of the plane until it crosses a gore at a 90-degree angle resulting in a perfectly transverse load. At this point the stress line leaves the planar surface and follows an imaginary circumferential path to a matching stress line in the opposite side of the cavity.

This type of stress pattern is not inevitable in all bubbles and its severity seems to be directly related to the configuration of the sub-pressure cavity. The effect will be most prominent at low altitudes and low levels of inflation. In the

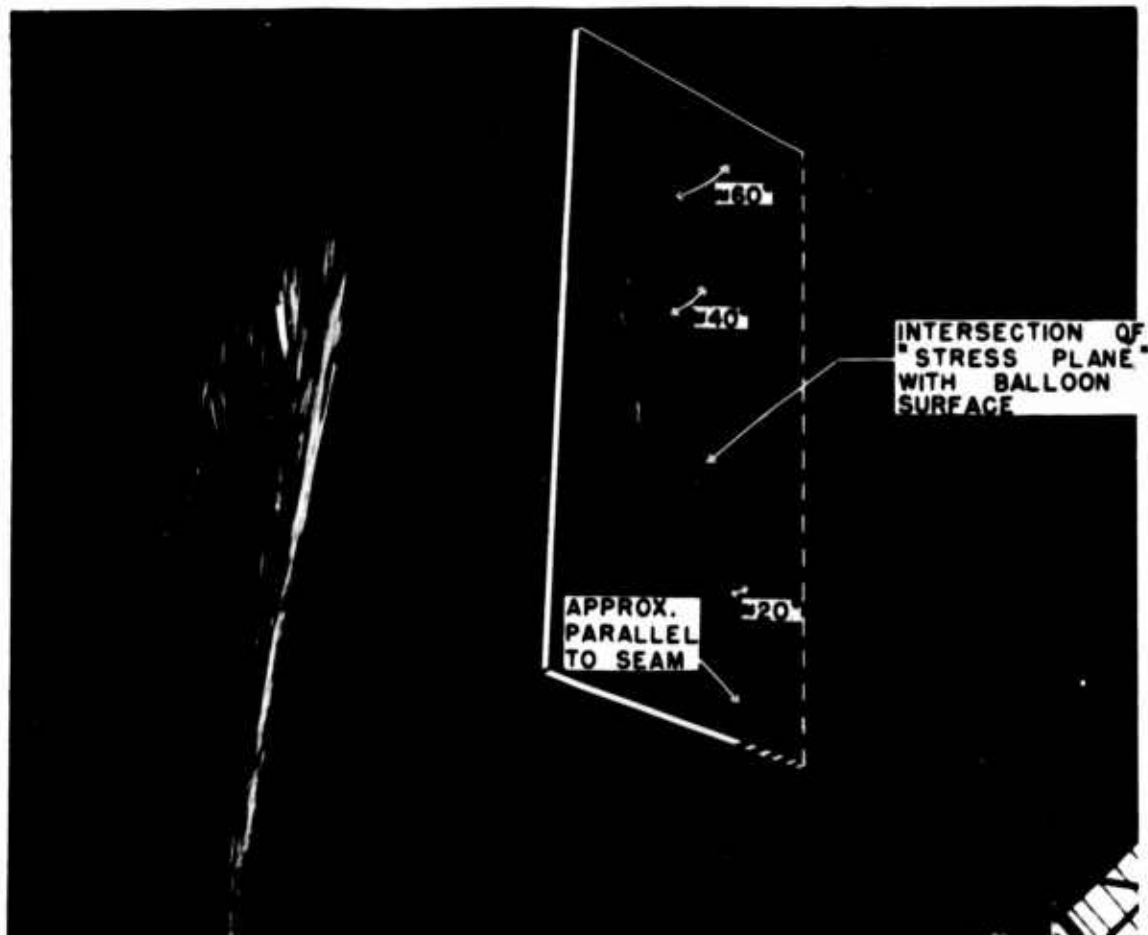


Figure 3. Representation of Hypothetical Stress Plane

example shown, the balloon is approximately 5 percent inflated. Figure 5 is a later view of the inflation test showing the balloon when it is almost 14 percent full. At this stage the sub-pressure cavity is greatly diminished and the resulting angles between the stress lines and the seams are more moderate. It may be presumed that the transverse stressing on the top of the bubble is considerably relieved.

The effects of the sub-pressure cavity appear to be drastically reduced in any balloon by the time it is 8 to 12 percent full. After this stage, there is comparatively little likelihood of failure. It is unfortunate that the occurrence of the critical shape coincides with the balloon's presence in the coldest, most turbulent part of the atmosphere. This double effect surely results in more failures than would be caused by either factor alone. It is important to note here that development of low-cold-brittleness films will probably not completely eliminate ascent failures; severe unsymmetrical loading must also be eliminated.

If the stress-generation hypothesis is correct, then how can the problem be circumvented? There are two basic means of controlling the stress situation in the balloon top. First, if the bubble configuration can be made more nearly symmetrical,



Figure 4. Development of Circumferential Stress

the problem is minimized or eliminated. Second, the shape could be ignored and the top reinforced to accommodate the stresses. The highly successful scrim balloons are the brute-force application of the second approach, but except for selected cases this solution is too expensive. A more widely applicable method of reinforcement is to place a cap just over the critical top region. Such a cap may take any of several physical forms and be installed by a variety of procedures.

Reinforcement may be a satisfactory solution for some circumstances, but a general solution to the problem would be more desirable. A symmetrical bubble would answer this criterion, and while complete symmetry may be impractical to achieve, close approximations should be possible. The simple expedient of full



Figure 5. Moderation of Transverse Loading as Inflation Increases

tailoring (which is hardly new) will go far toward attaining this goal. Alternatively, there are numerous possible methods of manipulating the excess material to distribute it around the bubble. Consideration of these methods leads to many ramifications, one of which will be treated in detail in the remainder of this paper.

#### .4. SVT BALLOON DESIGN

It has long been our belief that tapes on balloons are a necessary evil. The familiar tapeless balloon is perfectly capable of supporting enormous loads when fully inflated at ceiling. It is severely limited, however, in what it can lift at low altitudes in a partially inflated state. Therefore, tapes have been used as a necessary expedient to increase lift capabilities. The presence of comparatively rigid strips acting as strength members seems somehow incompatible with the light, flexible somewhat elastic films to which they are attached. This is especially so with the lighter gauges of film now being used predominantly in the higher altitude work.

These feelings, coupled with the germs of the ideas expressed in the foregoing hypothesis, led to investigations and design concepts for "heavy load" tapeless polyethylene balloons, that is, a tapeless balloon which can safely carry loads equal to those of taped balloons. The culmination of this investigation was a design which employed a fully-tailored gas-seal contour to achieve a bubble as uniform as possible, but the gore pattern was that of a semi-cylinder balloon to provide the requisite strength (Figure 6). The design was termed SVT, for Simulated Variable Thickness, because if the design is considered as fully tailored, the extra gore material distributed around the surface of the balloon would provide additional meridional strength equivalent to a film of increasingly greater thickness. This additional material allows the tapeless balloon to carry large loads while the lift is concentrated in a small bubble.

Preliminary tests of the design were conducted under a company-sponsored effort. The results were sufficiently encouraging that the design was selected for evaluation in the AFCRL water-model program. This work substantiated the theory involved, and subsequently the concept was verified with full-scale vehicles under a development contract with the Office of Naval Research. The first effort under this contract was the static inflation of the crown section of a 1/2 mil, 9 million cubic foot balloon. This bubble constrained a lift of 3,620 pounds (Figure 7) before it failed because of creep in the material. The lift was over four times any lift previously contained in a half-mil polyethylene tapeless balloon and was even beyond the predicted capacity.

Since static inflations are not flights, it was still necessary to obtain flight experience with the SVT. A 1/2 mil, 3 million cubic foot balloon was constructed for this purpose and flown with a gross inflation of 1080 pounds (Figures 8 and 9) or some 50 percent more than is recommended with the equivalent conventional tapeless design. This balloon performed ideally in all respects. Figure 9 shows the balloon at 41,000 feet when it is 2 1/2 percent full. Despite the fact that this should be in the region of critical shape, the sub-pressure cavity is not severe. While the stress lines cannot actually be seen in this photograph, it is apparent that the angle they form with the gores will not cause serious trouble.

Like any new design, this one has not been 100 percent successful. The problems which have been encountered are probably related to manufacturing procedures, but the presence of even a moderate sub-pressure cavity is suspect. Therefore, in current SVT balloons a belt-and-suspender approach is being taken. To augment the shape advantage of SVT over semi-cylinder configurations, the external flaps are being anchored one to another to provide a positive cap, reinforcing the top of the bubble. The first of this variation of SVT design (a 1/2 mil, 6 million cubic footer) has recently been flown in a completely successful flight with a gross inflation of some 950 pounds.

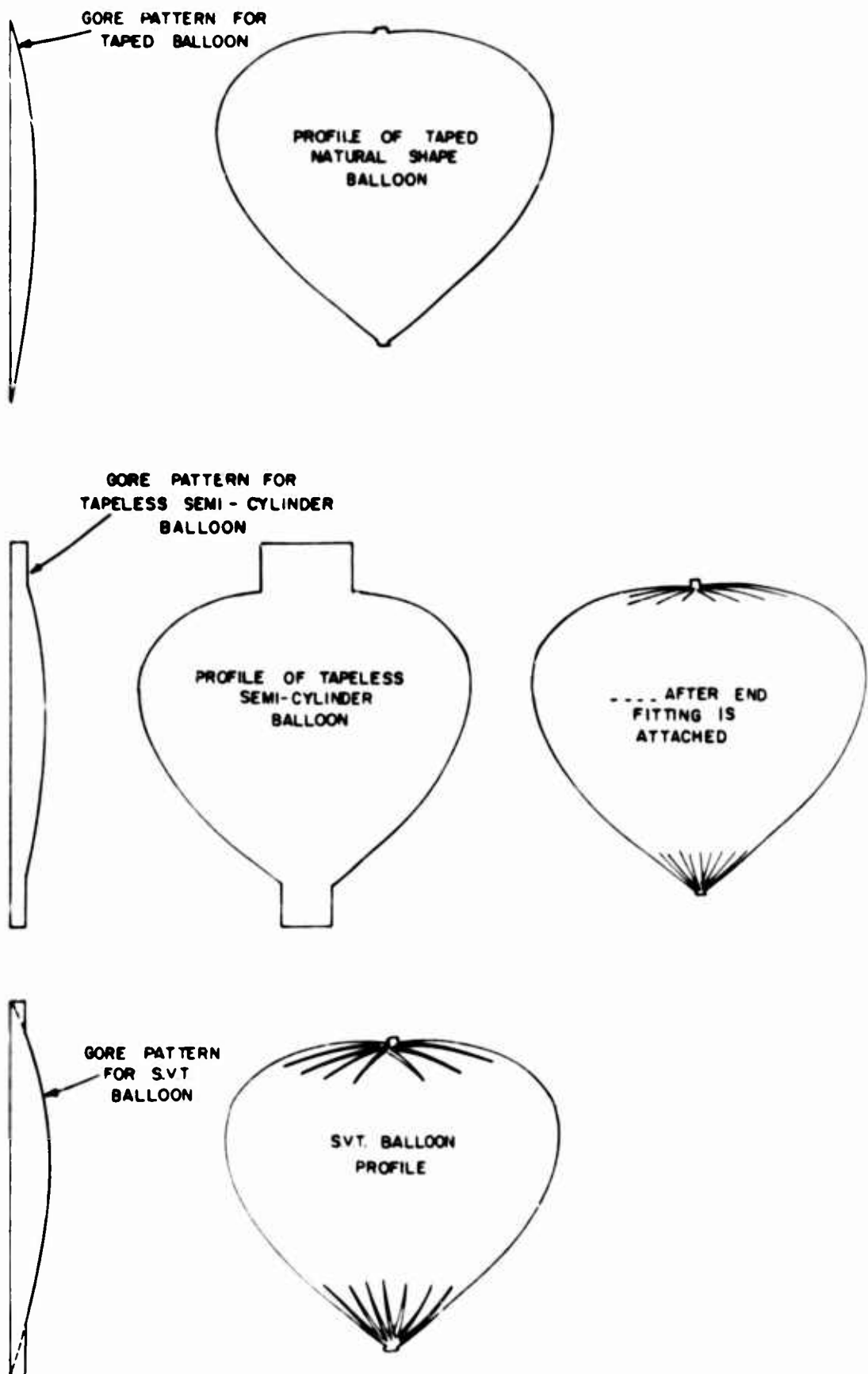


Figure 6

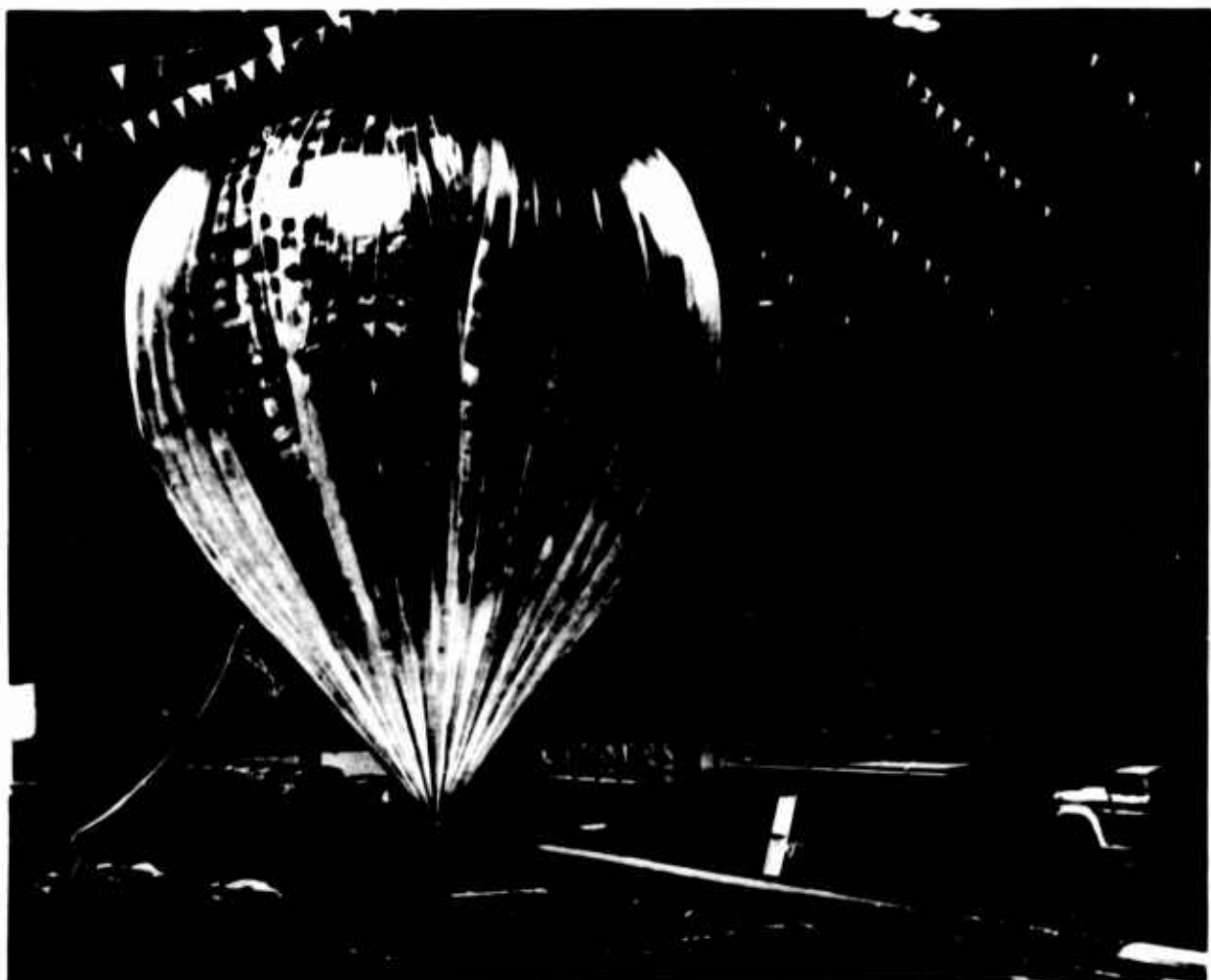


Figure 7. 1/2 MIL SVT Bubble Lift: 3620 Pounds

The SVT design is equally applicable to thin and heavy films and to reinforced materials. Initially, its greatest use will be in thin-film balloons when maximum altitudes must be reached. All flights to date have utilized films of 0.55 and 0.75 mil polyethylene and successful performance has been demonstrated in balloon sizes from 3,000,000 to 9,000,000 cubic feet. Figure 10 shows a comparison of the potential lift capabilities of SVT balloons as compared to semi-cylinder designs. The gross lifts involved in the flights which have been made fall midway between the limit profiles. There is no reason to expect that the designated SVT limit is not attainable.

When manufacturing techniques are fully worked out and the SVT concept reaches full fruition, it will have the advantage of the load capabilities of present taped balloons at a cost only slightly higher than that of conventional tapeless balloons. It is very possible that, in combination with some of the new promising films, this design will attain a degree of reliability which is unheard of short of scrim construction.



Figure 8. 3 Million Cu. Ft. SVT Balloon 1080 Lb. Gross Lift

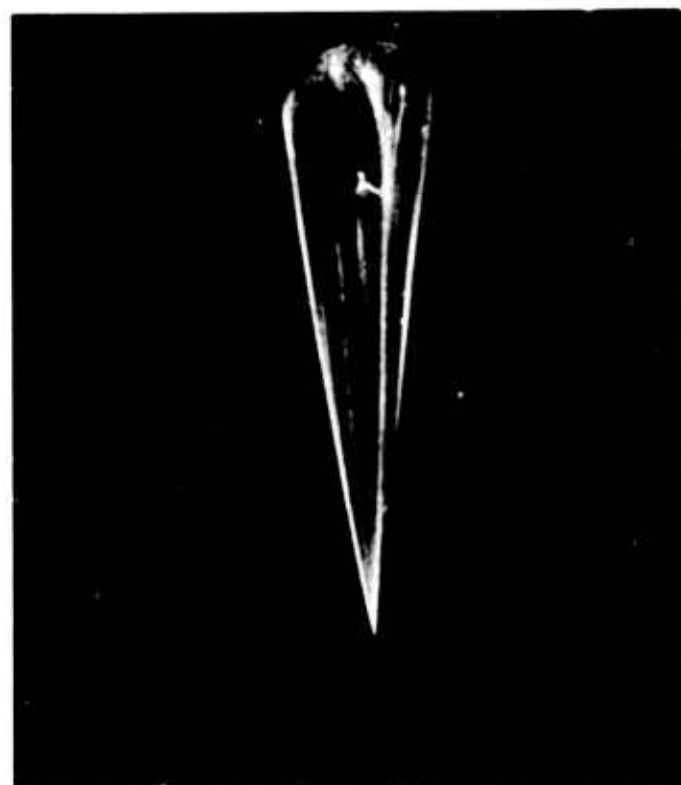


Figure 9. 3 Million Cu. Ft. SVT Balloon at 41,000 Ft

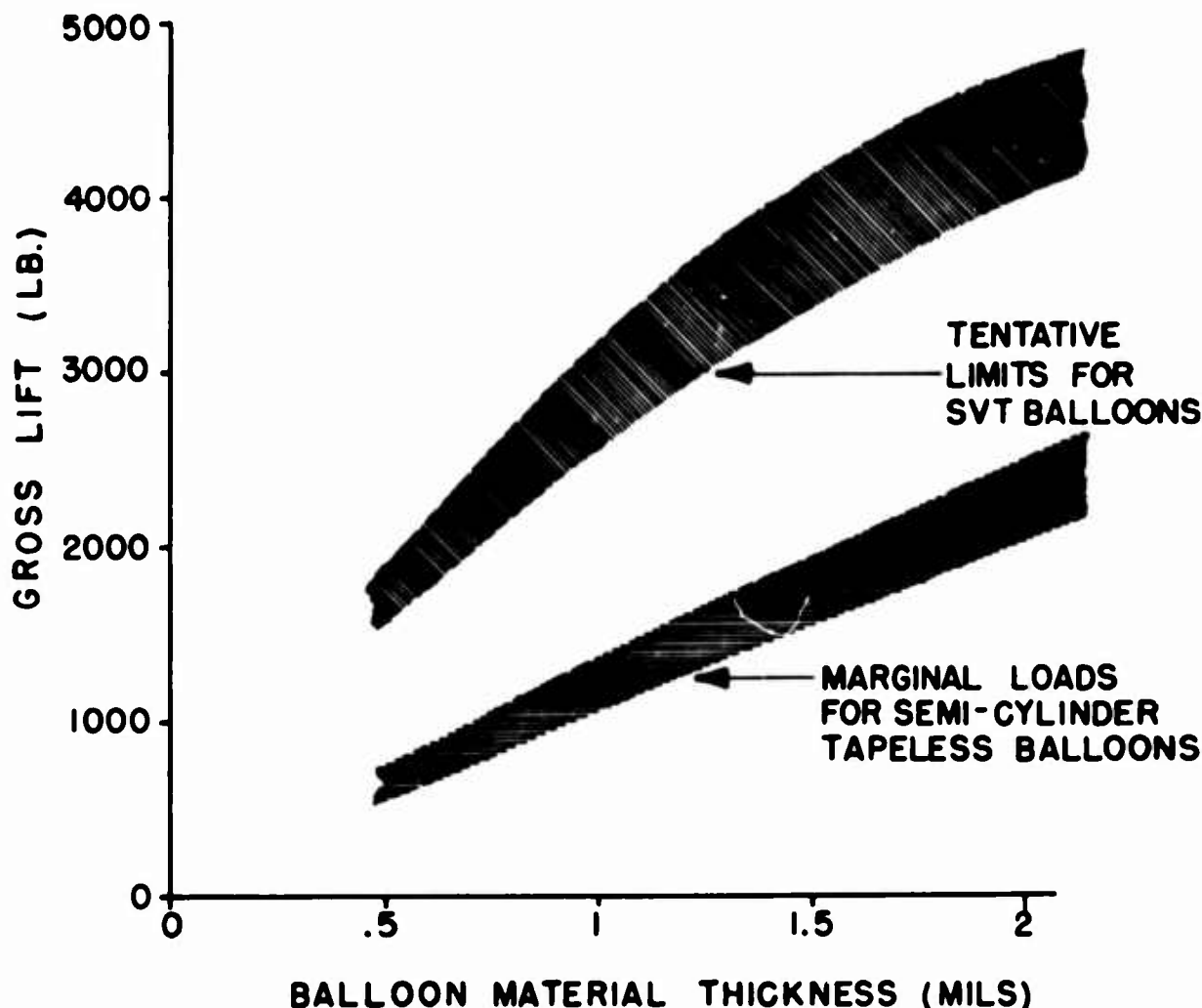


Figure 10. Lift Capabilities of Tapeless Balloon Designs

### 5. SUMMARY

No matter what improvements or advances are made in materials, new designs are necessary for maximum expansion of balloon capability and utilization of those materials. In order to develop new designs, it is necessary to establish the shortcomings and limitations of existing configurations. Scale model analysis is proving to be a valid and inexpensive method of obtaining this knowledge.

Preliminary observations have led to the conclusion that most ascent failures originate on the top of the bubble. The probable reason for this is the presence of a circumferential stress induced by bubble asymmetry. This hypothesis leads to the suggestion that design improvement may be achieved by restoring a degree of symmetry and/or reinforcing the top region.

The SVT design is the first of a family of designs making use of these thoughts. It shows strong promise as an improved balloon design.

### **III. Polyethylene Film with a Hi-Slip Additive as a Balloon Barrier Material**

**J. A. Haueter**  
**Viron Division of**  
**Geophysics Corporation of America**  
**Minneapolis, Minnesota**

#### **Abstract**

One of the factors blamed for polyethylene-balloon ascent failures is blocking between layers of film as the balloons expand and unfold during ascent. This blocking could prevent the balloon from unfolding and cause an internal buildup of superpressure until the balloon ruptures. The use of a slip additive in polyethylene film to decrease the film coefficient of friction was studied as one of the solutions to this blocking problem.

Polyethylene suppliers have long used slip additives in their commercial film. Air Force Cambridge Research Laboratories funded a program with Viron to test the use of a hi-slip additive in the balloon-grade polyethylene to determine its acceptability for use as a balloon barrier material. Viron has laboratory-tested the film and has used it to build three 2.94-million-cubic-foot balloons. This report describes the characteristics of the film, summarizes the test results and the production problems involved, and presents the limited flight history of balloons flown.

## 1. INTRODUCTION

One of the factors suspected of being the cause of polyethylene-balloon ascent failures is blocking between layers of film as the balloon expands and unfolds during ascent. This blocking could prevent the balloons from maintaining a natural shape as they expand, resulting in circumferential stress buildup and perhaps isolated stress concentrations which could lead to balloon rupture. This blocking theory is substantiated by pictures taken from balloon-borne cameras. These pictures show material deployment as being intermittent and jerky rather than a smooth, continuous process.

Consider, for example, the ascent of a standard 3-million-cubic-foot, 1.5-mil polyethylene balloon with a gore length of 270 feet. Assuming this balloon to ascend at 1000 ft/minute, the balloon expansion in the critical 40,000 to 60,000-foot area would theoretically require 4 to 5 ft/minute of circumferential unfurling. At this rate stresses could build up rapidly if the balloon were restrained.

In an effort to relieve the blocking problem and facilitate more uniform deployment of expanding-ascending balloons, methods of decreasing the coefficient of friction of the balloon barrier material to reduce blocking were investigated. Presently this is done by dusting with cornstarch or polyethylene powder. Discussions with polyethylene film manufacturers led to testing of polyethylene film with a "slip" agent added. I will outline this program in terms of the slip additive, test program and results, manufacturing problems, and flight results.

## 2. SLIP ADDITIVES

Slip additives have been used in polyethylene films for some time. The additive used in the film we tested is a saturated fatty acid amid. This substance is thoroughly mixed with the melted polyethylene resin before extrusion. The additive mixes well with the resin at extruding temperatures but does not react chemically with it. Upon cooling and crystallizing of the extruded film, the additive exudes to the surface, coating both sides of the polyethylene with a thin film.

The final result, then, is basically the standard polyethylene with very thin layers of the slip additive on both sides. These layers of the slip agent impart the slipperiness to the polyethylene, the polyethylene's apparent coefficient of friction being determined by the percentage of additive used in the film resin. It should be noted, however, that the slip agent can be worn off by friction.

Polyethylene films using this type of additive are presently marketed in five grades of slipperiness - no slip, low slip, medium slip, high slip, and extra high slip. "No slip" has no additive and the others have increasingly higher percentages of additive. Present balloon films as purchased per MIL-P-4640A contain no slip additives.

### 3. TESTING PROGRAM

The film tested in this program was 1.5-mil polyethylene with the "hi-slip" amount of slip additive. This film will be referred to as hi-slip polyethylene from here on. The film was supplied to Viron certified to conform to MIL-P-4640A.

The purpose of the testing program was to determine if hi-slip polyethylene offered any advantages over standard polyethylene for use in high-altitude balloons. The program was conducted in two steps. First, a series of tests was conducted to determine the film's physical properties and fabrication capabilities; and second, two model balloons were constructed and tensile-tested to compare the holding ability of two types of commonly used end fittings.

The physical material evaluation consisted of testing the film for coefficient of friction; material tensile strength, both longitudinal and transverse; seal strength; peel adhesion of pressure-sensitive tapes; and tear initiation. All tests were conducted at room temperature and at -60°C, per ASTM test standards. Graphs were made of Instron test results. Tests were conducted on both standard and hi-slip polyethylene.

The particulars of these test results will not be covered. Rather, a general comparison of the two films as they performed in each test will be presented.

Standard tensile tests were conducted on both the films with no apparent difference between the two. The hi-slip film acted quite similarly to standard polyethylene, both in elongation and in ultimate tensile strength.

Seal tests of both hot jet and vertrod seals of hi-slip to hi-slip, and hi-slip to standard polyethylene were made. No significant difference in seal strengths as compared to seals of standard polyethylene was noted.

Tape-peel adhesion tests were conducted on both films utilizing Minnesota Mining No. 480 polyethylene tape and No. 890 glass filament tape. Peel was 180° at a stripping rate of 2 and 5 inches per minute. Adhesion to the hi-slip film was slightly better than to standard film at room temperature, but cold-temperature adhesions were equally poor for both films. It is significant for all polyethylene balloons, that as temperature decreases from +25°C to -60°C, material and seal strength of polyethylene double, whereas tape-peel adhesion is reduced to 1/10 its normal value.

Tear resistance of both films was nearly equal.

Coefficient of friction of films varied as would be expected. Both static and sliding coefficients were measured at 2- and 5-inch-per-minute pull rates.

Figure 1 shows schematically the friction-testing apparatus used with the Instron tensile tester. At room temperature the coefficient of friction of hi-slip polyethylene was only about 25 to 40 percent of that of standard polyethylene. At -60°C, the

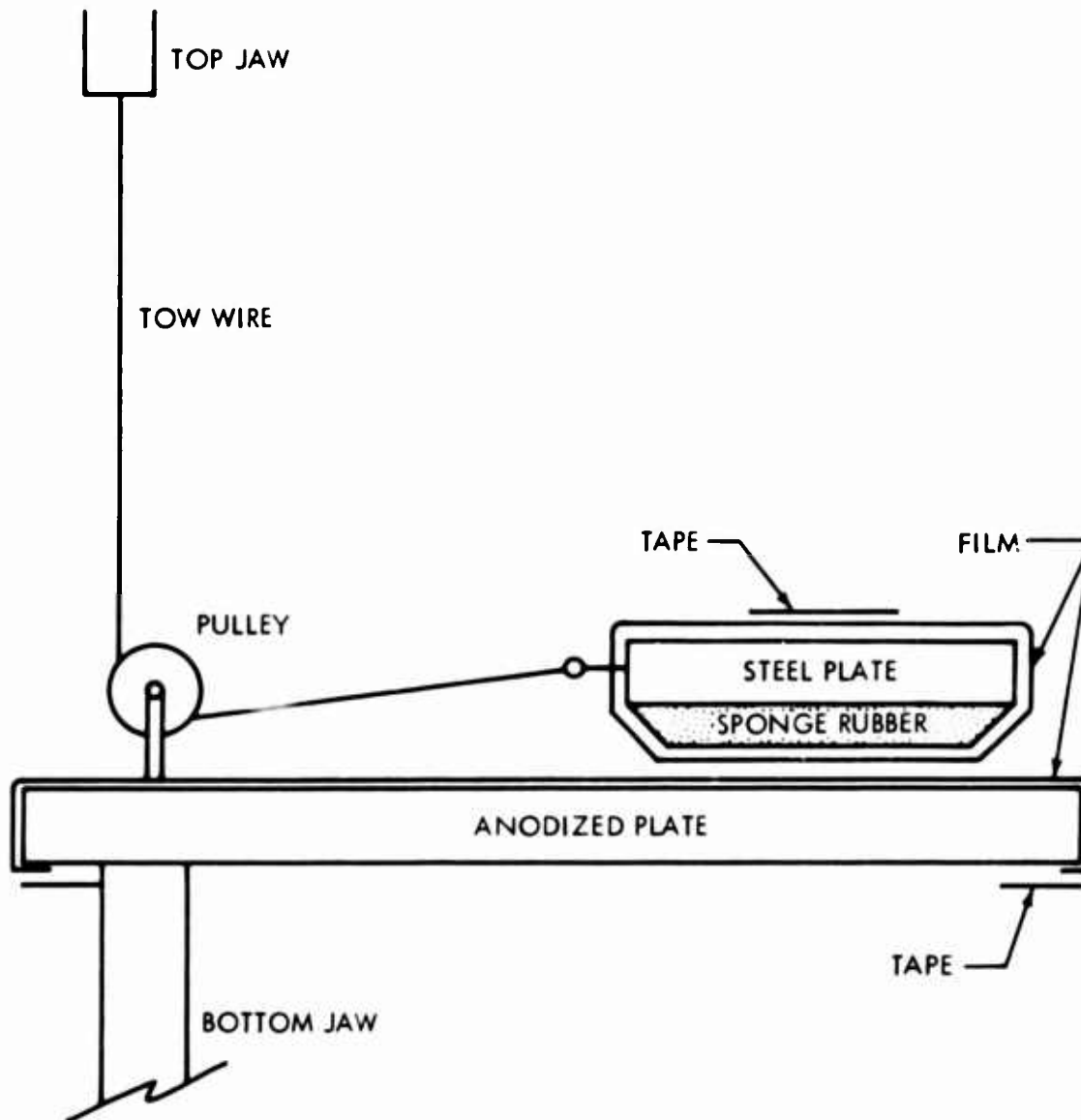


Figure 1. Coefficient of Friction Testing Apparatus

hi-slip coefficient was about 66 percent of that of standard polyethylene. Decreasing the temperature decreased the friction coefficient in both cases. Some tests were conducted with no effort made to reduce the humidity at -60°C. Results indicated no significant difference in the coefficient of friction between the two films.

In summary of these tests, the only significant difference in the two films is in the coefficient of friction, as pointed out above.

In the second step of testing, two four-foot-long model balloons were constructed to duplicate the 128-TT end fitting configuration and tested to destruction. One balloon was made with standard polyethylene, the other with hi-slip. Banded EV-13 type fittings were put in the top of these balloons and 5-inch fused wedge and collar

fittings were put in the bottom. Both balloons failed after the polyethylene yield point had been exceeded. The hi-slip polyethylene held well in both end fittings.

#### 4. MANUFACTURING PROBLEMS

Fabrication of hi-slip balloons did present some problems. Viron has fabricated three balloons of hi-slip polyethylene. These balloons were made for NCAR of 1.5-mil polyethylene. They were standard 2.94-million-cubic-foot tailored-taped balloons designed to lift a nominal payload of 1500 pounds to 100,000 feet.

The handling of the material on the rolls was difficult, as the core would "telescope" out of the roll if not secured or if the roll was not held perfectly level. On the sealing table, each gore had to be taped individually to the table at 2-foot intervals to prevent the gores from slipping from the pressure of the weight of those on top of them. Tape adhesion and sealing were the same as is usual. Uniform deploying of material in the end fittings during end-fitting assembly was much easier than usual due to the slipperiness of the film.

In summary, the slipperiness of the film does make the fabrication job more difficult and time-consuming but it is not detrimental to the quality of the final balloon if proper precautions are exercised. The cost is increased by about 10 percent over that of a standard balloon because of the increased handling involved.

#### 5. FLIGHT RESULTS

Three balloons have been made of hi-slip polyethylene. These three were the 2.94-million-cubic-foot balloons mentioned above. To this date, only one of these balloons has been flown. This balloon was flown from Palestine, Texas, and failed on ascent at about 48,000 feet.

Some of the balloon film was recovered after descent. Examination of the material showed it to have a slipperiness comparable to that of standard polyethylene. Apparently the slip additive had worn off the polyethylene during the fast, violent descent, verifying the prediction that it will come off with friction. As is usually the case, no other information could be gained concerning the failure either from the flight history and conditions, or from an examination of the recovered material.

## 6. CONCLUSIONS

A few conclusions can be made as a result of the testing program and fabrication. First, the addition of the slip additive to the basic polyethylene resin does not significantly change the physical properties of the film other than the coefficient of friction, nor does it affect the use of tapes, seals, or other materials or processes used on the film in connection with balloon fabrication. Second, the slip additive reduces the coefficient of friction of the film appreciably, especially at room temperature. As the film temperature is decreased, however, the difference in coefficient of friction of the two films decreases considerably. The difference in the hi-slip friction coefficient of 33 percent over standard polyethylene at low temperature, however, leaves some doubt that it will be a significant aid in minimizing blocking at low temperatures.

Although hi-slip polyethylene as described above is not considerably better than standard polyethylene for balloon use, the concept of using slip additives in polyethylene films should not be abandoned. A lower degree of additive, for example, might be used with thin polyethylene films to decrease blocking problems both in fabrication and in flight.

The fact that polyethylene with a slip additive has been produced to MIL-P-4640A and has proven adequate for balloon construction opens this film configuration up for any balloon use in which it might prove better than standard polyethylene.

## IV. Statistical Implications of Balloon Materials

R. L. Hauser  
National Center for Atmospheric Research  
Boulder, Colorado

### Abstract

The author has been working the last two years with the scientific balloon group of the National Center for Atmospheric Research.

Our concern in the NCAR work has been directed toward improvement of balloon materials for better flight reliability. In this program we have tested a large number of candidate materials -- films and scrims -- and have been concerned with both character and quality.

The quality of polyethylene balloon film is the basis for this paper, since we must recognize that variation of quality is an unavoidable reality in all materials. The strength properties of balloon films will vary from sample to sample in a manner that might be either the normal or the Poisson distribution, as shown in Figure 1. These are the more probable distributions, but others are certainly very possible.

### I. DESIGN CRITERIA

Balloons are designed principally for axial tensile loads on the basis of strength per unit width of material. The weight concern is expressed in terms of weight per area, usually as pounds per thousand square feet.

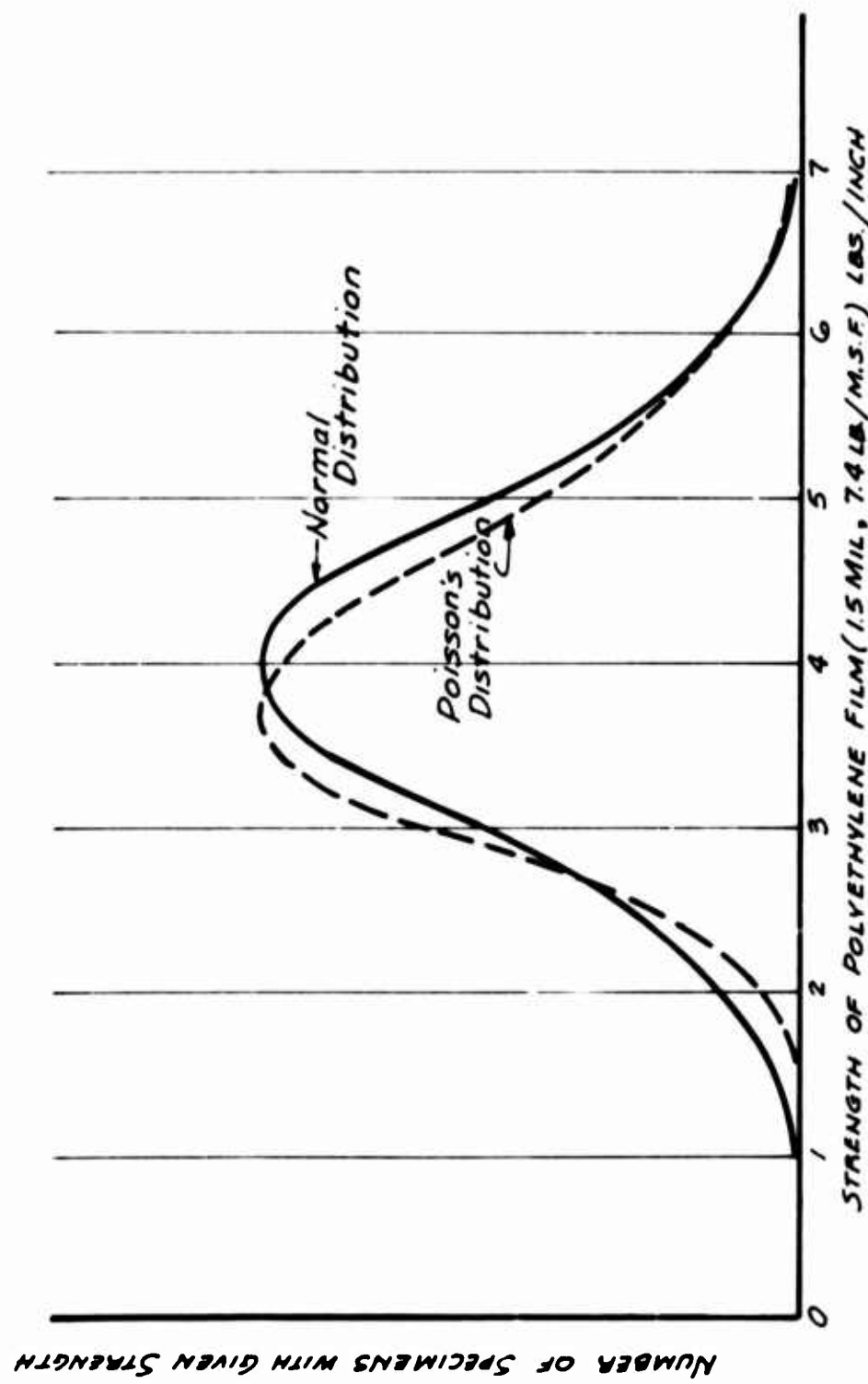


Figure 1. Most Common Property Distributions of Materials

Balloon films are most often compared on the basis of calculated tensile strength and measured thickness. Thickness measurements can seldom be made to a precision better than  $\pm$  5 percent. Where tensile strength (psi units) is calculated from measured thickness, the strength data are subject to inaccuracies of thickness.

More meaningful and more accurate design data are obtained when film strength is calculated on the basis of strength per width and when film thickness is identified merely as weight per area. These criteria are better for specification purposes as well as for design.

For example, where specifications may now call for 1.5-mil polyethylene ( $\pm$  0.3 mil) of tensile strength greater than 2000 psi, a better equivalent specification would be:

weight not to exceed 8.65 lb/1000 sq ft  
strength, not less than 2.4 lb/inch.

## 2. SAMPLING PLANS

Recognizing the variability of strength and/or thickness, our next concern is to sample the product in such a manner that we learn this variability. The criteria for acceptance of purchased balloon films as well as for design, should be based upon the realities of variation. Statistics provide an identification of these realities.

In the polyethylene specification, MIL-P-4640A, each lot of material is sampled for property evaluation by taking test specimens each 10,000 feet or at each end of the rolls. This is not a random sampling, as is desired, and there should be opportunities for increasing the number and locations of samples. Four tensile tests per lot are now required (two each in machine and transverse direction) and five thickness measurements are made per roll of film. These represent less than one part per million of product, and insure at best that no more than about five percent of the product will be outside of specification values.

The operating characteristic curves for these samplings are presented in Figure 2. If strength per width is calculated from thickness data, there is an 80-percent probability of accepting material containing 10 percent defective area (below specification minimum). We suggest that the sampling plan of MIL-P-4640A is inadequate to assure delivery and acceptance of satisfactory product. The

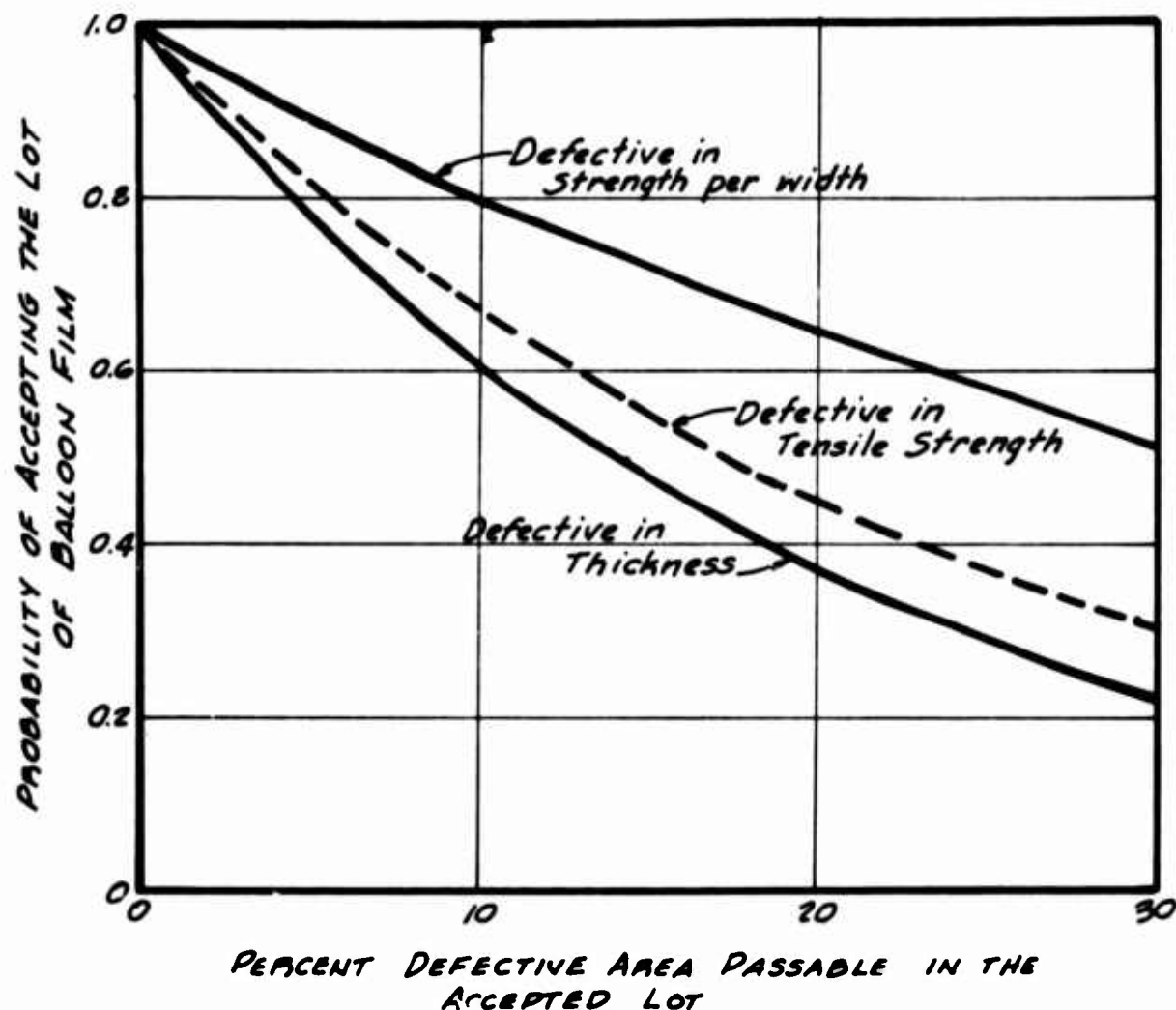


Figure 2. The Acceptance Probability of Defective Polyethylene Balloon Film by the Sampling Plan of MIL-P-4640A

accept/reject criteria are based upon insufficient samples and nonrandom sample selection.

A better plan would be to evaluate the strength per width and the weight per area for at least 15 samples per lot, to give an Acceptance Quality Level of 0.04 percent defective. This follows code G normal inspection, outlined in MIL-STD-414, "Sampling Procedures and Tables for Inspection by Variables for Percent Defective." In this method, the average value and the standard deviation are calculated, and the sample is accepted or rejected on the basis of a presumed normal distribution of properties.

For example, if 3.0 lb/inch is the minimum acceptable strength of polyethylene film weighing less than 8.7 lb/1000 sq ft, material A of Figure 3 is not acceptable, but material B is satisfactory. Sample A has a higher average strength, but it shows greater variation than Sample B.

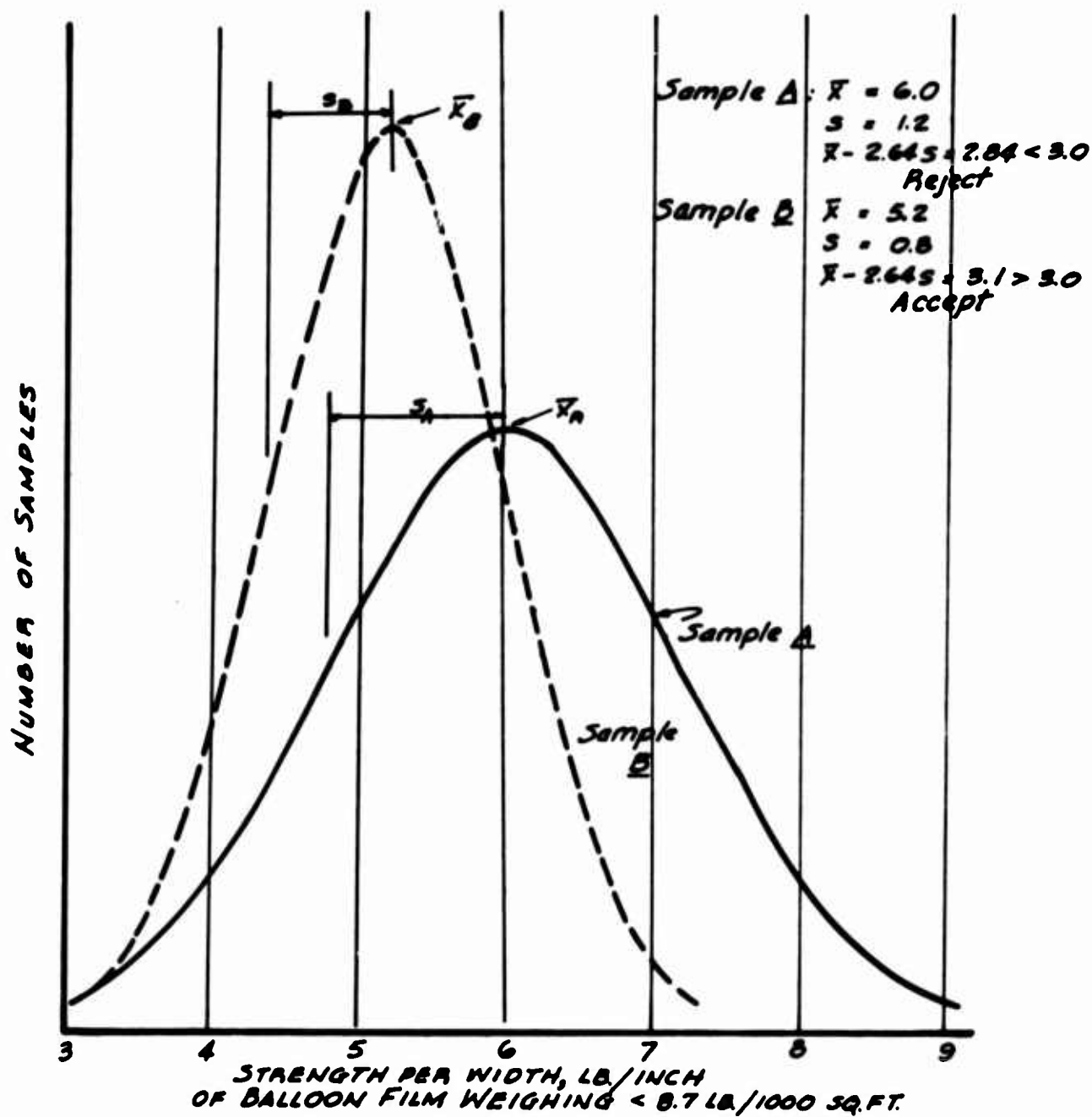


Figure 3. Effect of Material Variation in Acceptability

### 3. DESIGN ALLOWABLES

The design allowable for a material is usually below its yield strength and far enough below ultimate strength to provide a good safety factor. The design allowable should be at a sufficient increment below ultimate strength so that even extreme material variations do not cause failure.

After accepting material B of Figure 3, we now proceed to manufacture a balloon of  $3 \times 10^6$  cubic feet volume. During gore assembly we take additional tensile strength samples and find that the material has an average strength  $\bar{x}$  and standard deviation  $\sigma$  which may differ slightly from the acceptance results which were based upon a smaller number of samples (and perhaps upon more than one lot of material). If we find that the material has a normal variation, then the number of material defects expected in the balloon can be learned from Figure 4. In this case, a defect represents an area 1 inch wide with strength less than the design allowable. This graph points out the importance of using more conservative design allowables (or better material) for larger balloons in order to minimize the presence of defects. In our design example with a design allowable of 1.6 lb/inch, we would expect to have 12 defect areas in the balloon. The same statistical procedures that were used to prepare Figure 4 could be used to indicate the probable number of defects in balloon gore seals of a complete balloon.

#### 4. CONCLUSIONS

As the supply of balloon materials is becoming more plentiful, there is opportunity and need to revise procurement specifications to reflect more reliable inspection procedures. Design and performance criteria should be used as the basis for specification requirements.

The greater probability of material and fabrication defects in larger balloons should be recognized by the industry, and more conservative design allowables or better quality materials should be used to maintain equal material reliability.

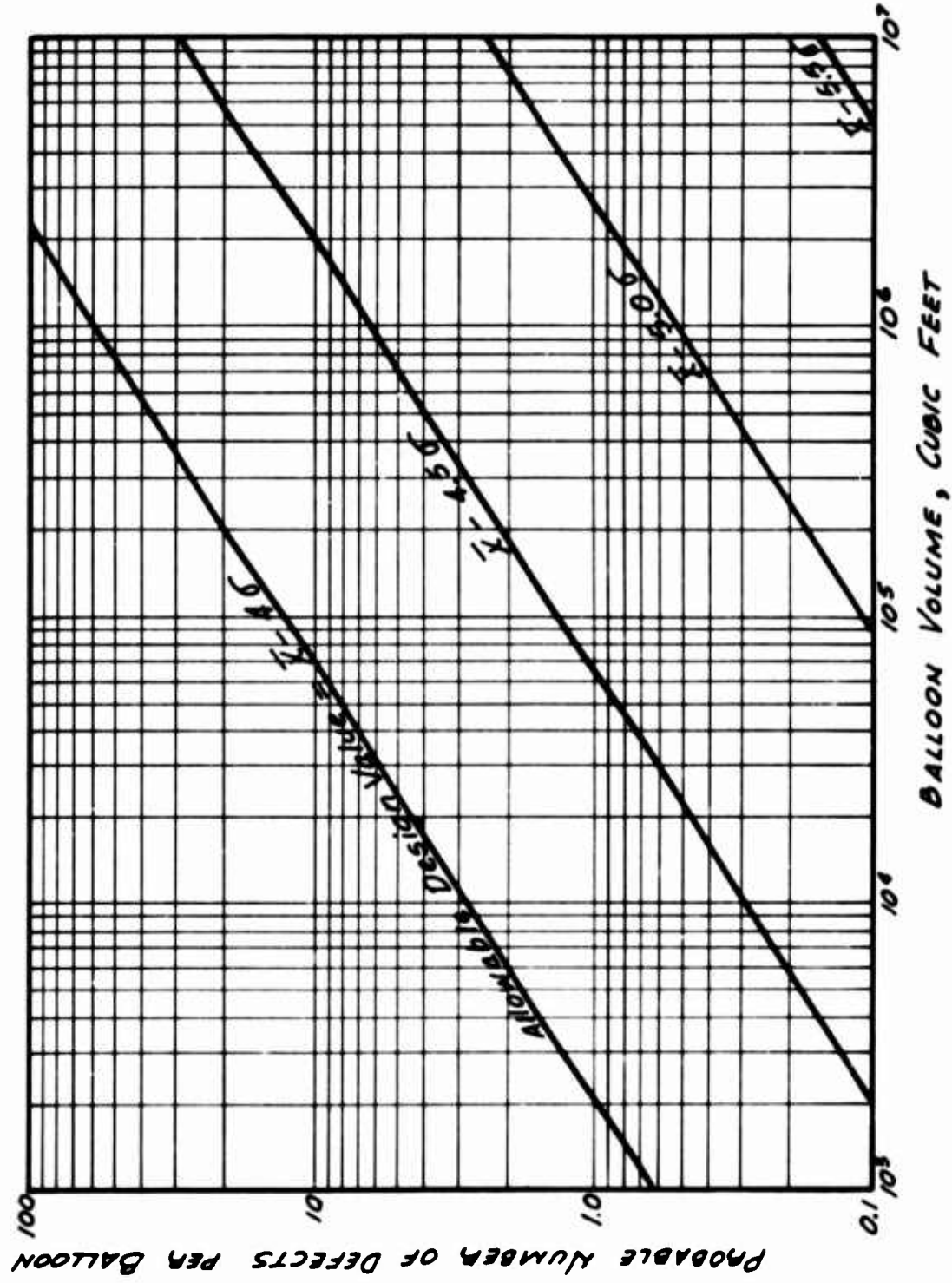


Figure 4. Probable Defects in a Natural Shape Balloon (Shape Factor = 0.30)  
as a Function of Safety Increment in Design

## V. Behavior of Polyethylene in Simulated Balloon Environment\*

W. B. Parsons  
Litter Systems, Inc.  
St. Paul, Minnesota

### Abstract

In our research to evaluate potential balloon materials,\* we have conducted a survey of available plastic films to find those most promising for balloon manufacture. These will be compared with polyethylene and Mylar--the most predominant materials in balloons at present. There is no assurance, of course, that either will be replaced as the materials of choice; consequently, some of our studies are designed to permit a broader understanding of the characteristics of polyethylene and Mylar.

This paper is limited to our initial studies of polyethylene--with particular emphasis on influence of temperature, high-frequency stressing, comparison of lubricants, and cold brittleness. We shall describe some of the equipment that we have developed for these and future studies. While some results are available for presentation here, we are not as yet in a position to draw conclusions as to where these data may lead in relation to balloon performance or to the design of better balloons.

---

\*Contract AF 19(628)-2944 - "Evaluation of Potential Balloon Materials" for Electronic Systems Division, Air Force Cambridge Research Laboratories.

## I. TEST MATERIAL

The material on which tests were performed is described in Table 1.

Table 1. Test Material

Source	- VisKing Corporation, Division of Union Carbide (now Ethyl VisQueen Film Division, Ethyl Corporation)
Type	- Polyethylene
Resin	- Union Carbide DFD 5500
Identification	- Reference 01-24153, ARL 511
Width	- 33 inches center fold
Thickness	- 2 mil nominal, 1.98 mil (average of 4 measurements)
	<u>Machine Direction</u> <u>Transverse</u>
Tensile Strength (psi)	2349      3260
Elongation, ultimate (%)	606      788
Toughness (milliseconds) Falling Ball - flat 39.6, crease 36.9	
Melt	- 0.649 gram/10 min
Cold Brittleness	- 4 ductile at -68°C

## 2. INFLUENCE OF TEMPERATURE ON CERTAIN PROPERTIES OF POLYETHYLENE

Figure 1 portrays equipment which was used to carry out the first phase of this work. Environment was supplied to the test chamber by a Tenney TSU 150 Servo supply which circulates 40 cfm through various test chambers to which it may be attached. Either dry ice, liquid CO<sub>2</sub>, or both may be used as coolant. The temperature control is adjusted manually and the thermostatically controlled damper provides a bypass so that chamber air is recirculated without passing through the dry ice bed. If necessary, heat can be added during the recirculation process.

The test chamber is a multipurpose unit fabricated for use on this specific program. A door opens at the back, while the front is a triple-pane window. When completely outfitted the chamber can accommodate up to 40 specimens (film or seals). Bottom clamps are rigidly attached, while upper clamps are attached to air cylinder shafts. Pressure regulators, gages, and manifolding are so arranged that up to five different infinitely variable pressures can be maintained at a given time,

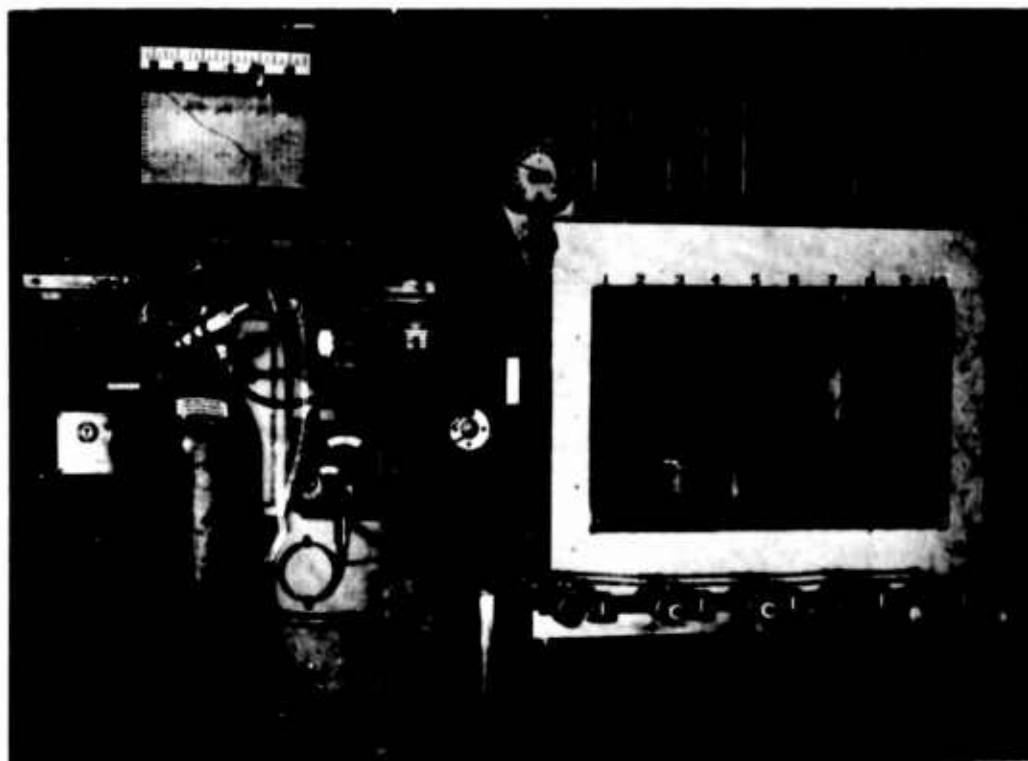


Figure 1. Apparatus for Conduct of Dead Load Tests at Low Temperatures

making it possible to conduct prolonged seal tests using a number of different dead loads at the same time. Load tapes can also be tested with this apparatus since its pressure capability and strength have been designed with this requirement in mind. The pressure cylinder approach was adopted to provide a convenient means of loading after the specimens had been cooled to the desired temperature--a means, unlike weights, that will not subject remaining specimens to shock and vibration when one specimen fails.

#### 2.1 Length vs Temperature (Nonloaded Specimens)

Creep tests under very light loads can be made by pinning the shafts to fix the position of the upper clamps and suspending desired loads in the form of weights. Figure 2 indicates the change in length of nonloaded polyethylene specimens. Length measurements were made by cathetometer. The contraction experienced is plotted against the various points at which the temperature was stabilized. Five specimens in which the long axis paralleled machine direction were used, as well as five transverse direction samples. To illustrate the range of values, all points are plotted; for any given temperature, the cluster to the right represents machine direction values, while the cluster on the left represents values for transverse direction. Averages for both were so nearly the same as to make a graph of the

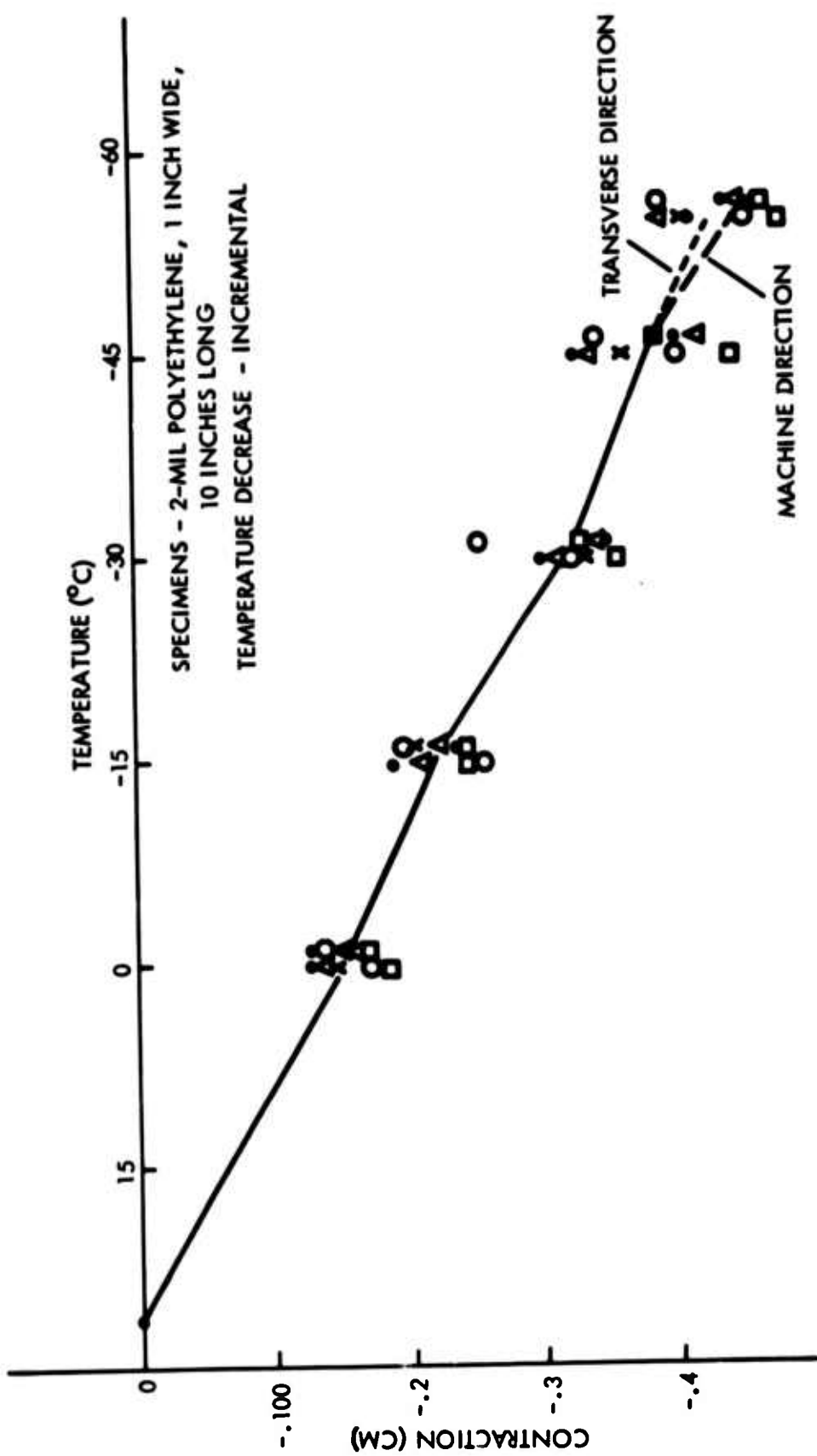


Figure 2. Influence of Temperature Change on Polyethylene Dimensions

two indistinguishable except below -45°C, at which the machine direction contraction was somewhat more pronounced. The total contraction of 0.44 cm represents 1.7 percent based on the average nominal length of 25.4 cm. Initial specimen lengths varied 0.45 percent. For a check on accuracy, two readings were taken on each of the ten clamps. The average difference was 0.012 cm which represents from one-third to one-seventh the range of values at a given temperature, or a trifle more than two of the smallest divisions in the graph grid.

## 2.2 Length vs Temperature (Loaded Specimens)

A second test series utilized the same equipment with minor exceptions. Weights of 0.6 and 1.0 pound were suspended from specimens (four each for machine and transverse direction). The period of preloading at room temperature varied from 42 min to 1 hr and 50 minutes. Occasional measurements were made to monitor the elongation, although emphasis was not placed on this effort because it will be performed with greater sophistication in another portion of the program.

Figure 3 illustrates the contraction of these loaded polyethylene specimens as they were cooled. The axis intersection represents room temperature and the established "zero" point with respect to increments in specimen length, that is, the length under load immediately before the temperature reduction was begun. Machine and transverse direction specimens were subjected to temperature reduction rates of both 1 and 2°C/min (simulating ascent rates of 500 and 1,000 ft/min respectively) while under both 300 and 500 psi stress. Primary control of temperature decrease rate was by positioning of a slide in the inlet orifice. Temperature vs time was monitored by means of a Brown recorder. Figure 3 is typical of the results of all eight combinations. It represents machine direction polyethylene cooled at 2°C/min while under load of 300 psi. The contraction at the lowest temperature reached (-64°C) was about 0.43 cm from the most stretched condition reached prior to cooling. Those points to the left of the vertical axis are plotted with the time sequence from left to right (no scale). These data represent the length changes under preload without regard to temperature (that is, at room temperature and before temperature reduction was started); however, the original length is not shown here.

Table 2 provides some opportunity to compare results illustrated in Figure 3 with those obtained in other tests of this type. From the table we note that the amount of contraction experienced is slightly less for the runs conducted at 2°C/min than for the slower 1°C/min runs. Also of note is the fact that elongations (calculated from nominal initial lengths) experienced at room temperature are greater for 500-psi loaded specimens than for 300-psi. Even for 300-psi loadings, the contraction does not quite bring the specimen back to its original length. In other

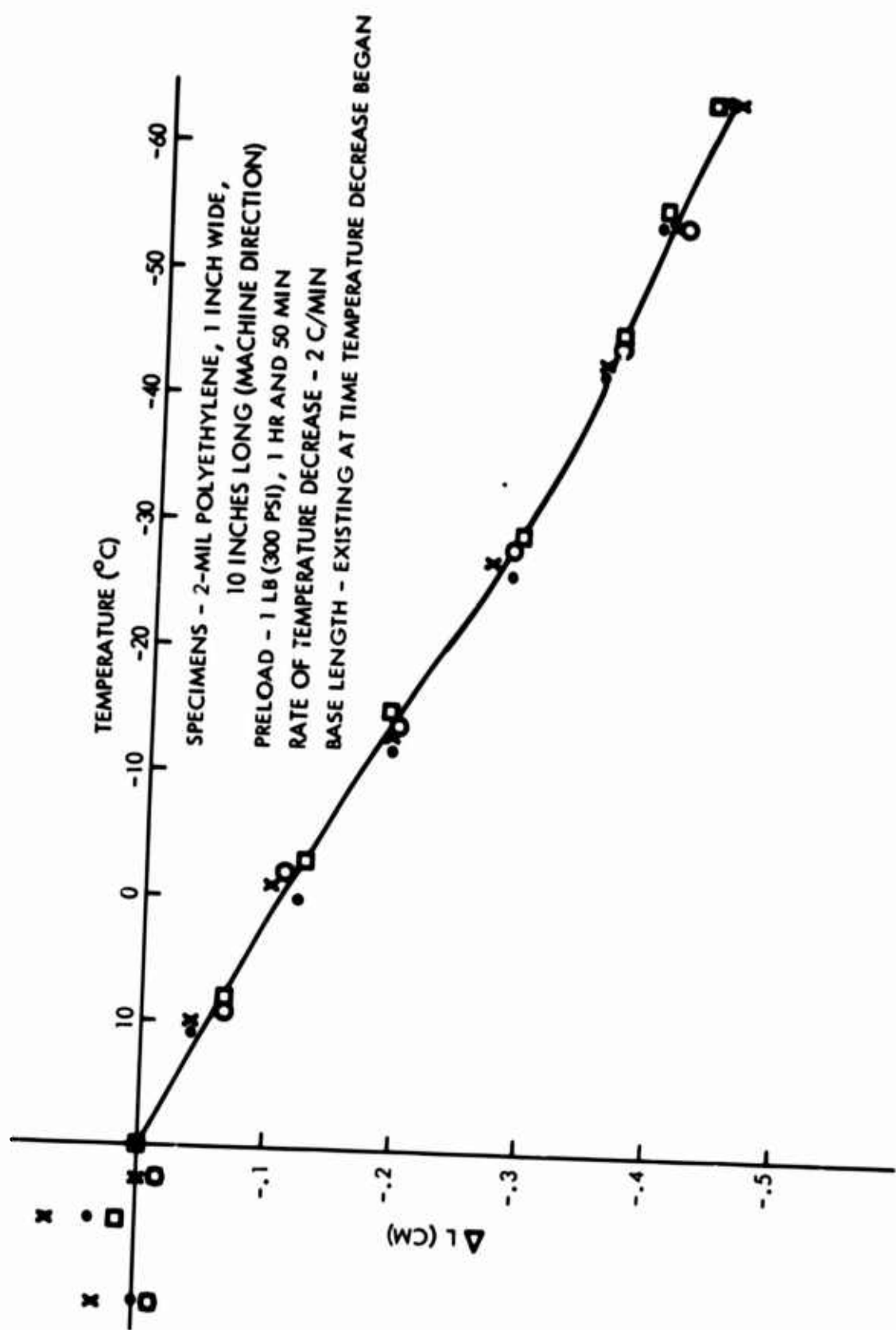


Figure 3. Influence of Temperature Change on Preloaded Polyethylene Specimens

Table 2. Length Changes in Loaded Polyethylene

Type Run	Preload Period	Elongation at Room Temperature (cm)		Maximum Contraction (cm)		Comments
		300 psi	500 psi	300 psi	500 psi	
MD 1°/min	1 hr 24 min	0.689	1.167	~0.45	~0.45	Contraction of 300 and 500 psi loaded specimens about the same at all temperatures
MD 2°/min	1 hr 50 min	0.487	0.939	~0.40	~0.40	500 psi specimens showed most contraction at intermediate temperatures
TD 1°/min	1 hr 40 min	0.584	1.120	~0.50	~0.50	As above
TD 2°/min	42 min	0.451	0.851	~0.36	~0.32	300 and 500 psi specimens about equal in contraction at intermediate temperatures

words, the elongation imparted by the load is greater than the contraction attributable to temperature reduction. It is also interesting to observe that the amount of contraction in cooling from room temperature to approximately -60°C is about the same for both loaded and nonloaded specimens.

### 2.3 Stress vs Temperature (Fixed-Length Specimens)

A third series of tests were designed to study thermal influence on polyethylene in relation to stress. Specimens were rigidly clamped in jaws of the Instron Tensile Tester. The Tenney Servo unit was used to supply our specially-designed test chamber constructed by Custom Scientific Instruments, Inc. Temperature was monitored by the Brown recorder. Rate of temperature decrease was controlled in most test runs by varying the inlet duct orifice, although variation in blower speed by means of a Variac was also found effective. As with the previous series, both machine and transverse direction specimens were tested at rates of 1 and 2°C/min. Four specimens were tested under each condition, although one of each was pre-loaded to 500 psi. With two specimens the temperature was decreased to a much lower level although close control over rate of temperature decrease could not be maintained when the liquid nitrogen booster was added at approximately -60°C.

Figure 4 depicts raw data recordings of stress vs time and temperature vs time for a run made with transverse direction material at a temperature decrease rate of 1°C/min. Also indicated at the base of the stress vs time curve are the corresponding temperatures. Figure 5 is similar to Figure 4 except that in this test the inlet orifice opening was not varied to control temperature during the test. Note that both curves are much more smooth. Figure 6 is a plot of stress vs temperature obtained by analysis of the curves (such as Figure 4) applicable to all the transverse direction specimens cooled at 1°C/min. The lower curve represents three specimens which were initially loaded only sufficiently to provide slight stress indication, assuring that there was no slack. The upper curve represents two specimens preloaded to 500 psi immediately before beginning the temperature decrease. Once the minimum temperature was reached the inlet orifice was closed and the specimen allowed to warm. Figures 4 and 5 illustrated the abrupt warm-up which was accompanied immediately by a corresponding reduction in stress. In Figure 6 we note that the stress at -45°C during the warm-up is higher than during the cool-down, confirming the observation made earlier that there is at least a slight lag in the response of film to temperature change.

Although we have shown only the stress-temperature relationship for transverse direction material cooled at the 1°C/min rate, curves for the other three conditions (machine direction 1° and 2°, and transverse direction 2°) are essentially identical. Likewise, all curves for preloaded specimens are essentially identical.

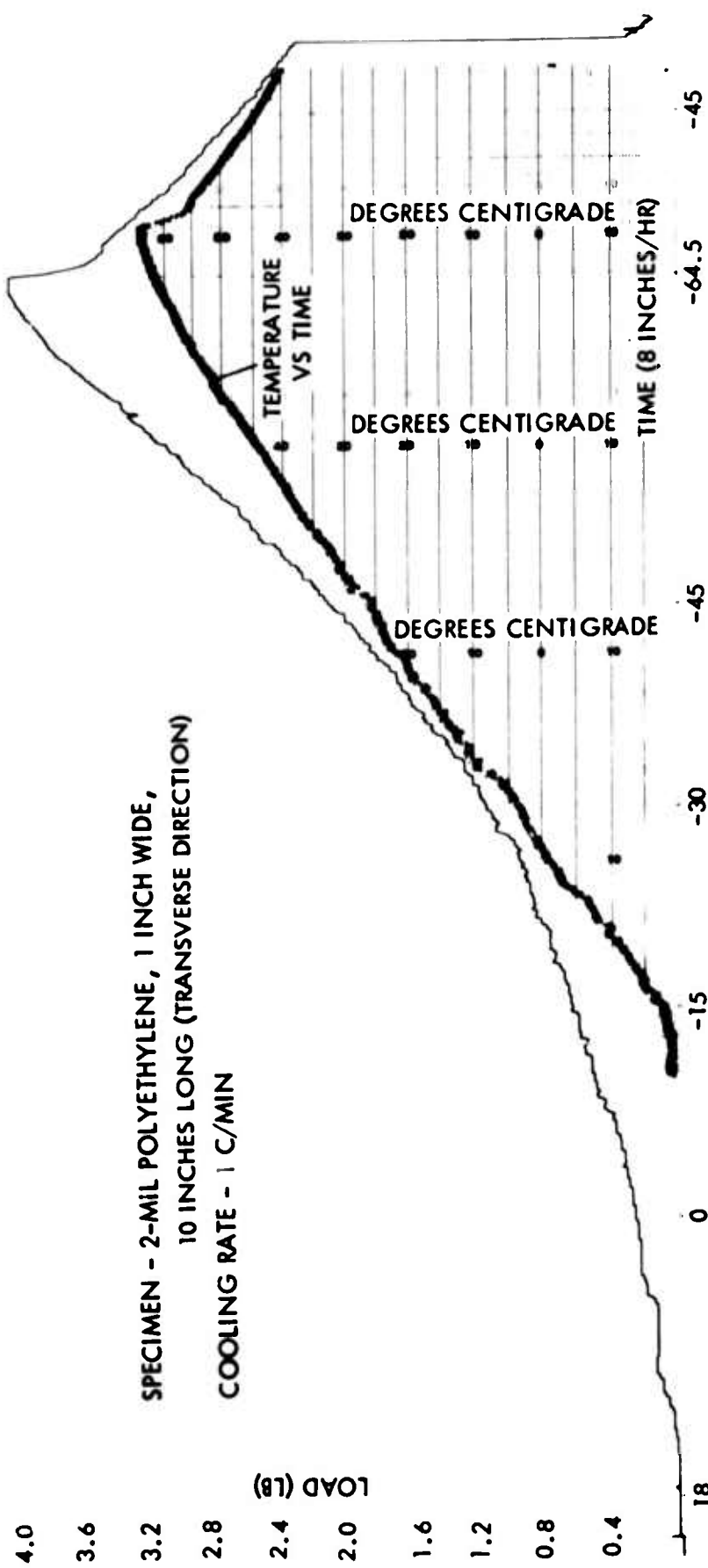


Figure 4. Influence of Temperature Change on Stress in Rigidly Clamped Polyethylene

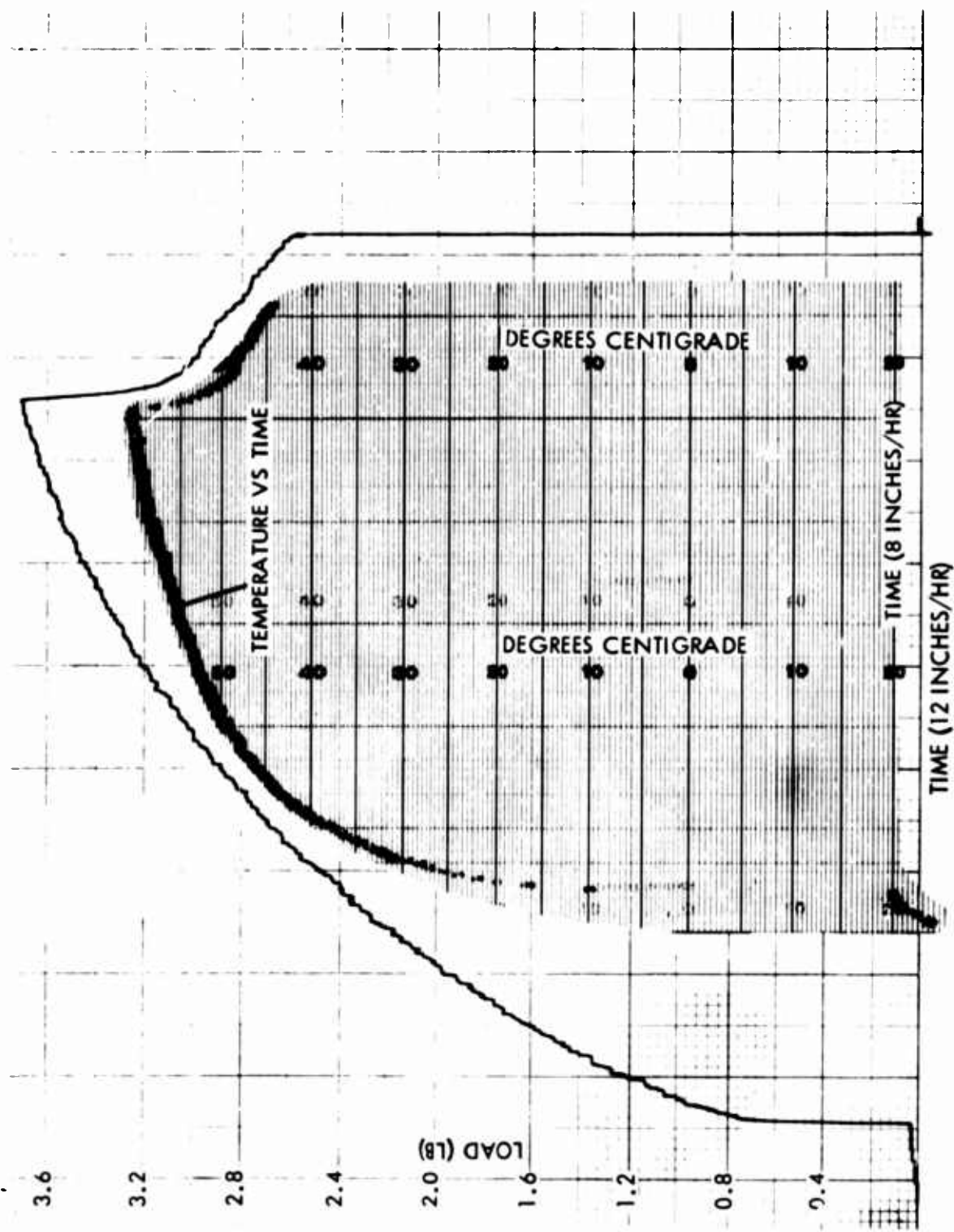


Figure 5. Influence of Temperature Change on Stress in Rigidly Clamped Polyethylene

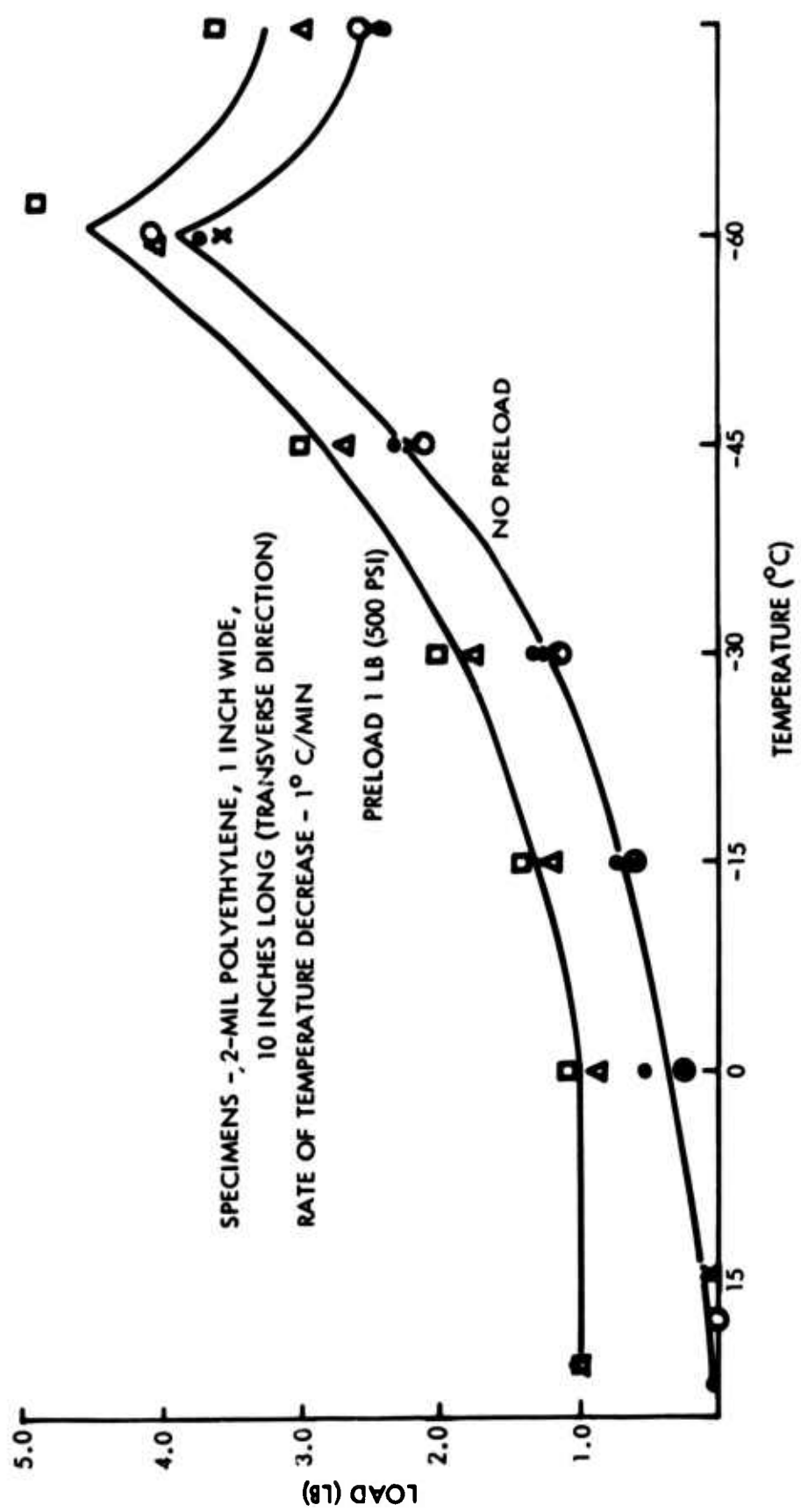


Figure 6. Stress Developed in Rigidly Clamped Polyethylene as Temperature is Decreased

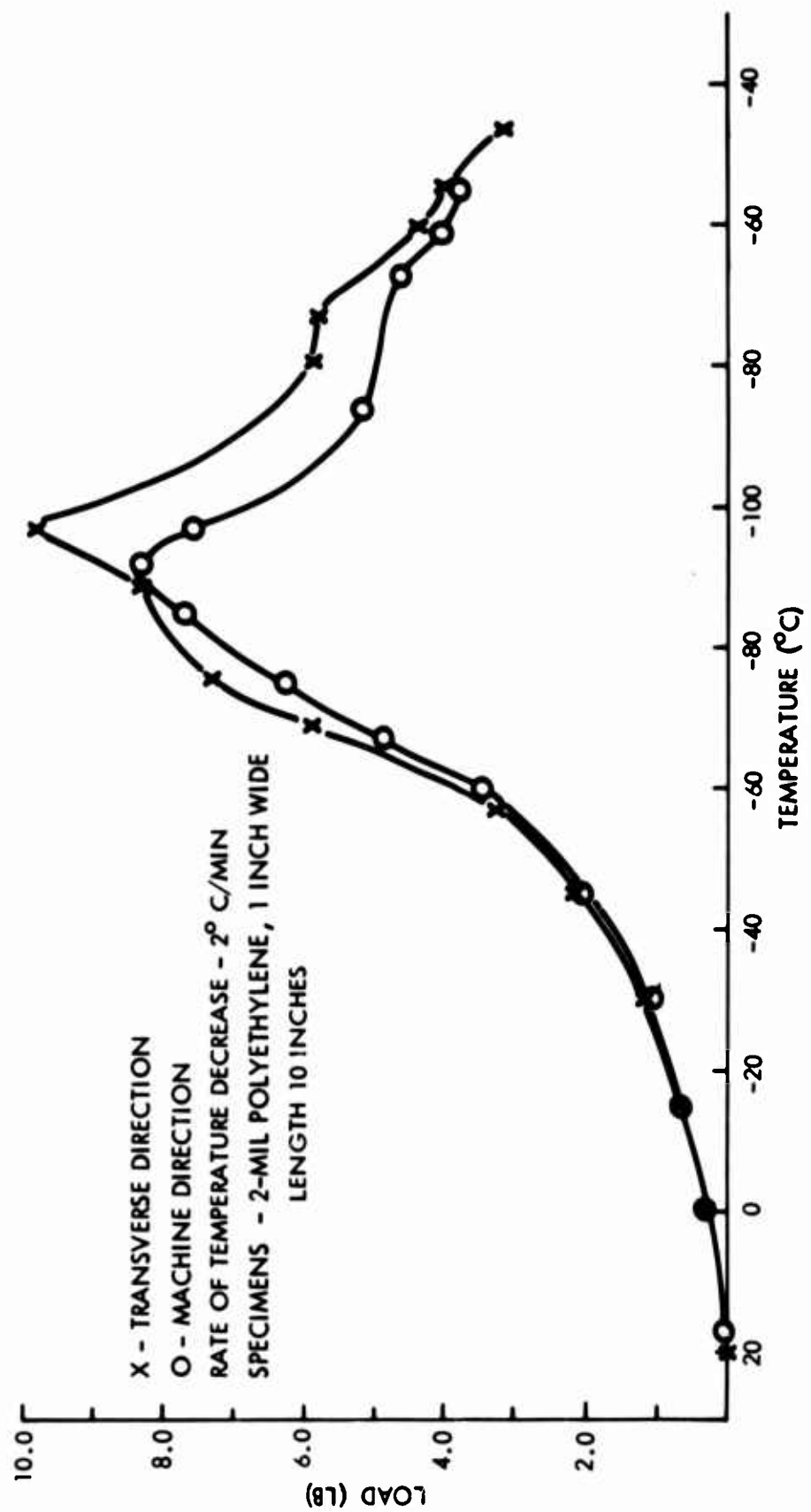


Figure 7. Stress Developed in Rigidly Clamped Polyethylene Specimens at Very Low Temperature

The curves presented in Figure 7 were obtained in the same manner as those in Figure 6 except that they represent individual specimens--one machine and one transverse--rather than several. The transverse direction specimen (X) was cooled to a slightly lower temperature than was the machine direction sample (0). Below -60°C the temperature was recorded manually by reading a thermometer since the Brown recorder range terminated at -65°C. The thermometer appeared to have more lag than the thermocouple/recorder combination. The most puzzling disclosure of this test was that the machine direction specimen actually appeared to experience a decrease in stress during the final period of cooling. It is considered possible, however, that there may have been a previous rapid cooling not sensed by the thermometer that could have caused the peak stress indication. If this is the case, there is an even more pronounced difference in the maximum stresses obtained with machine vs transverse direction materials at extremely low temperatures.

### 3. HIGH-FREQUENCY STRESSING

A special test apparatus has been designed and constructed to investigate the performance of polyethylene under high-frequency stressing. Figure 8 is a photograph of this equipment. Its characteristics are described in Table 3.



Figure 8. Device for Conduct of High Frequency Cyclic Load Testing

Table 3. Cyclic Tensile Tester

Power - 1/3 hp, 1725 rpm motor
Rate Control - Graham Model BD4 Variable Speed Drive infinitely variable from 0 to 1725 rpm
Conversion from rotary to oscillatory motion - eccentric head from vertical milling machine
Offset Range - 0 to 0.6 inch providing maximum amplitude of 1.2 inches
Bearing Block - Thompson linear ball bearings
Counter - General Controls Model CM5A mechanical type
Linear Variable Differential Transformer - Columbia Model 5-1000-53R
Strain Gage - Full bridge circuit composed of Budd model 341-500 gages
Gage Mounting - 0.005 inch beam of spring steel the end of which is clamped to a post suspended between two diaphragms of 0.025 inch spring steel - provide linear displacement with force
Recorder - X-Y. LVDT output, matched and amplified is plotted on the X axis, strain gage output, amplified is plotted on the Y axis

This tester will be modified for use in performance of other phases of our experiments. A modification in the linkage to produce simultaneous rotation and reciprocation plus addition of different clamps will permit twisting and squashing of cylindrical specimens. When tests are carried out at low temperatures (as a conditioning process) and samples are studied for such parameters as tensile, tear, and permeability, the ability to withstand low temperature flexing can be evaluated. Another modification will involve use of an electromagnet to impart a transient load at controlled fixed or variable rates. Equipment will be oriented so that specimens are vertical for this test.

#### 4. COMPARISON OF LUBRICANTS

Still another phase of our work has been an evaluation of polyethylene powder\* against the present lubricant, cornstarch. One portion of the effort involved effectiveness in preventing undesired film adhesion due to bleeding by adhesive tapes. Although this work is not complete, results to date are summarized in Table 4.

---

\*U. S. Industrial Chemical Co. Microthene 711-939 (mass mean diameter of 9 microns).

Table 4. Effectiveness in Combatting Adhesive Bleeding  
Powdered Polyethylene vs Cornstarch

Powder	Tape Surface Exposed	Tape	Room Temperature Performance
Starch	Nonadherent	890	Effective
Poly	Nonadherent	890	6 or 10 showed slight adhesion
Starch	Adhesive	890	10 adhered somewhat
Poly	Adhesive	890	10 adhered severely
None	Nonadherent	480	no adhesion
Starch	Nonadherent	480	not checked since control not adhered
Poly	Nonadherent	480	not checked since control not adhered
Starch	Adhesive	480	adhered
Poly	Adhesive	480	adhered

These examinations were made following room temperature storage for several weeks. They indicate that polyethylene powder is less effective than cornstarch to prevent adhesive bleeding of load tapes. In addition, much greater effort is required in application of the polyethylene powder because it does not adhere as well as cornstarch to the edges of the tape. Addition of Cab-O-Sil®\* or Santocel®\*\* is reported to improve flowability and might prove to be effective in eliminating this disadvantage.

The next phase of this work involved comparing strength obtainable in seals of polyethylene contaminated by poly powder as opposed to those contaminated by cornstarch. All seals were made with the hot jet sealer using materials dusted with contaminant, shaken to remove excess, but not rubbed or wiped. Specimens were cut to 1-inch width and initial jaw separation was 3 inches. The jaw separation rate was 20 inches per minute. The following results were obtained and represent averages of five determinations:

Control (uncontaminated)	5.15 lb	(all root breaks)
Polyethylene powder contaminated	5.81 lb	(all root breaks)
Cornstarch contaminated	2.47 lb	(all but one peeled)

Thus, on the basis of tests conducted so far, polyethylene powder can be said to be less effective in preventing ill effects from adhesive bleeding, more difficult to apply, but much less detrimental to seal strength than the conventional cornstarch.

\*A product of Cabot Corporation, Oxides Division.

\*\*Monsanto Chemical Company.

### 5. COLD BRITTLENESS

The final item to be mentioned has been a preliminary evaluation of the Society of Plastics Industry Cold Brittleness Tester (ASTM D1790-62). American Society for Testing and Materials advises in the 1962 revision that the tester was developed for use with pigmented vinyl, and that its effectiveness with other films must be determined by the user. Figure 9 pictures this tester in our environmental chamber. In the test, specimens 2 x 5-3/4 inches are formed into loops and stapled to cards. The hammer/anvil tester, proper, was purchased from U. S. Testing, but the rotating, indexing disc--as well as the means for remotely elevating the hammer and initiating its fall--was designed and constructed by Litton. This modification provides a convenient means of testing ten specimens without necessity of opening the box. Several different polyethylenes have been tested at temperatures as low as -95°C without eliciting brittleness. We have found the unit very discriminating with vinyl, for example, all good at -35°C; all bad at -40°C, and mixed results at -37°C. The fact that the first unit purchased would not operate in the cold and the replacement unit bound up before -68°C was reached provided some tip-off that routine usage of this tester must not be in the temperature range of interest for balloons. While we have a few more ideas as to how we may obtain useful information with this equipment, we believe that it is almost hopeless.

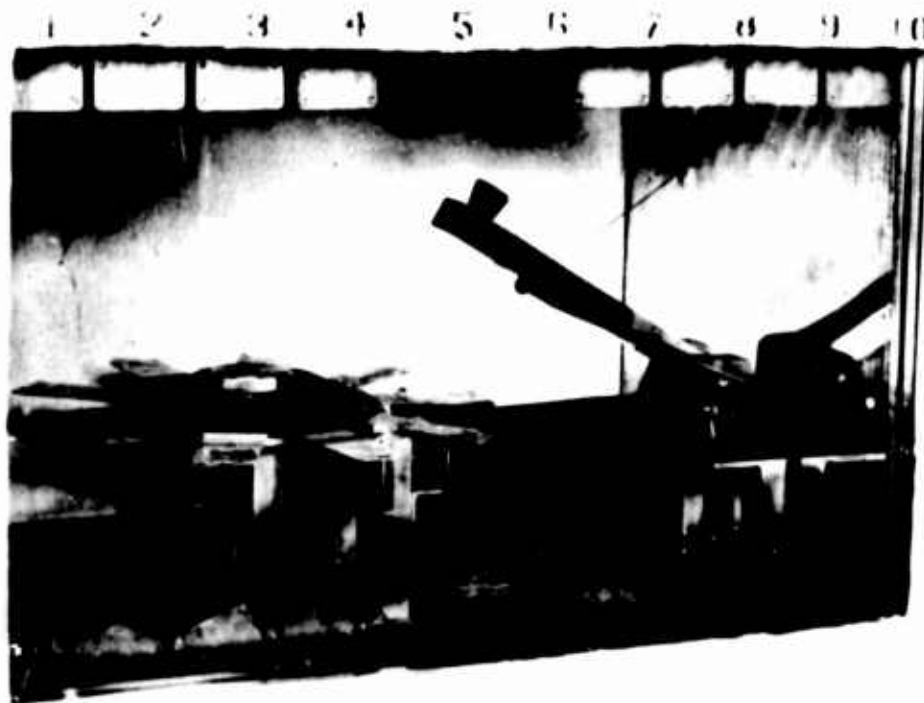


Figure 9. Device for Conduct of Cold Brittleness Temperature Determinations

## 6. SUMMARY

A brief review of preliminary studies on polyethylene has been presented. This work is a part of a larger program designed to find the optimal materials for the fabrication of balloons and to accumulate information which will enable most intelligent use of that material for the application.

## VI. A New High-Altitude Plastic Balloon Launch Method

Francis X. Doherty  
Air Force Cambridge Research Laboratories  
Bedford, Massachusetts

The ability to launch large balloon systems on land increases in difficulty as a function of surface wind velocity.

My association with balloon launchings over the last 10 years, until recently, that is, has been limited to those in which the conventional or "dynamic" launch method was used. Briefly, for those of you not acquainted with the "dynamic" method, the full length of a balloon is laid out on an aircraft runway or some other suitable launch pad -- depending on the balloon size, the length required for this layout can exceed 300 feet -- the bottom end fitting is tied into the top apex of a safety parachute and the parachute risers are tied into the payload, usually suspended on a suitable motor vehicle. About 70 feet down from the top of the balloon, we run the balloon under the roller arm of a vehicle we call the launch arm vehicle. Lifting gas, helium or hydrogen, is then transferred to this top section of the balloon. When the proper amount of gas has been transferred to the balloon, the balloon is released at the launch arm vehicle and the plan is that it erect itself vertically over the vehicle carrying the payload. This vehicle then either maneuvers or stands still, depending on the surface wind, to keep the balloon directly over the payload for the final release and system launch.

I am sure that those of you who have launched balloons this way are aware of the possible limitations and hazards. And those of you who have not need not tax your imaginations too much to appreciate some of the embarrassing situations you might find yourself in when using the dynamic method if you experience a variable surface wind situation.

Usually, you find yourself running off the runway trying to catch the balloon to get under it. While doing this, you can expect to find a wire fence staring you in the face -- or a building, usually a large aircraft hangar -- or as we have experienced on more than one occasion, a row of parked aircraft. The least that usually can happen to you is that you have to accelerate over rough terrain and your payload is exposed to considerable shock. The results in a launch effected this way can be tragic.

During the years 1960, 1961 and 1962, AFCRL, along with several other Government agencies and contractors, participated in a program called Project BANSHEE. The program was sponsored by the DASA and was described during last year's symposium by Mr. Jack Kelso of DASA. Its basic objective was to investigate the blast effects of HE detonations at several high altitudes. Some 20 "hot" launches were conducted during BANSHEE -- by "hot" I mean the system was launched carrying a 500-pound, 24-inch sphere of raw HE -- Pentolite. All BANSHEE launches were "dynamic" and we had our share of exciting runs, particularly since we were deploying a 200-foot instrument train during the launch run.

It was during BANSHEE that it became apparent to several people that a higher degree of efficiency, effectiveness and safety could be realized by operating at sea. With a vessel of suitable speed and maneuverability and while running with the wind, launchings of systems carrying sensitive payloads, for example HE as in BANSHEE, could be regularly conducted in calm surface conditions. Overflight of populated areas with a potentially dangerous payload, although never a problem in BANSHEE, but always to be considered and provided for in safety circuitry, could be completely eliminated.

Over a period of years, several balloon programs have been conducted at sea aboard ships by AFCRL and by other agencies, and in most instances the ship was found to be the ideal launch platform. I say "in most instances" because it is vital that the vessel have sufficient speed to counteract any wind, and that it be able to sustain this speed. Several times the ship was found limited in speed and not able to neutralize the wind. However, highly successful as shipboard launching has been, the requirement to lay the full length of the balloon out on deck for the conventional inflation and release procedure -- "the dynamic method" -- has in most cases limited the selection of ships to the various classes of aircraft carriers. I think you can appreciate that the limitations of availability and extremely high operating cost of a vessel of this type are prohibitive except in extreme cases.

The DASA, therefore, requested that AFCRL develop a shipboard launch technique which would circumvent the restrictions of the aircraft carrier and still retain the highly desirable properties of a shipboard launch. In accordance with this request, we at AFCRL have developed a shipboard launch method which is designed for operational use aboard small vessels. The need for expansive deck space is eliminated by inflating and deploying the balloon directly from its shipping crate. A tethering technique is then used to position the balloon directly over the payload, at which time the launch is made.

The realization of this method required the development of a special "launcher" device which you see in Figure 1. Briefly, it is an electro-hydraulic device consisting of a system of rollers through which the balloon is deployed and controlled. Additionally, it has a balloon bottom end fitting tie down and release device, in which is incorporated a free lift sensor and indicator, and a balloon transfer-deployment winch (Figures 2 and 3). The model shown measures approximately 7' x 7' x 7' and weighs approximately 2000 pounds.

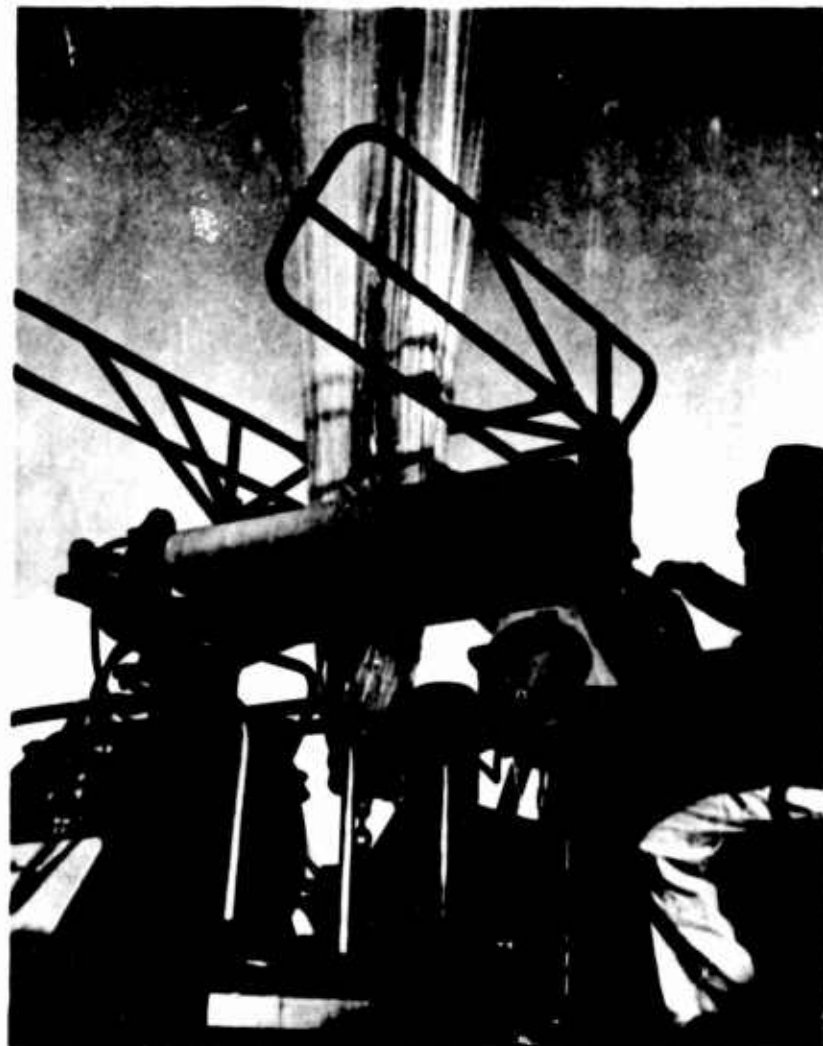


Figure 1



Figure 2

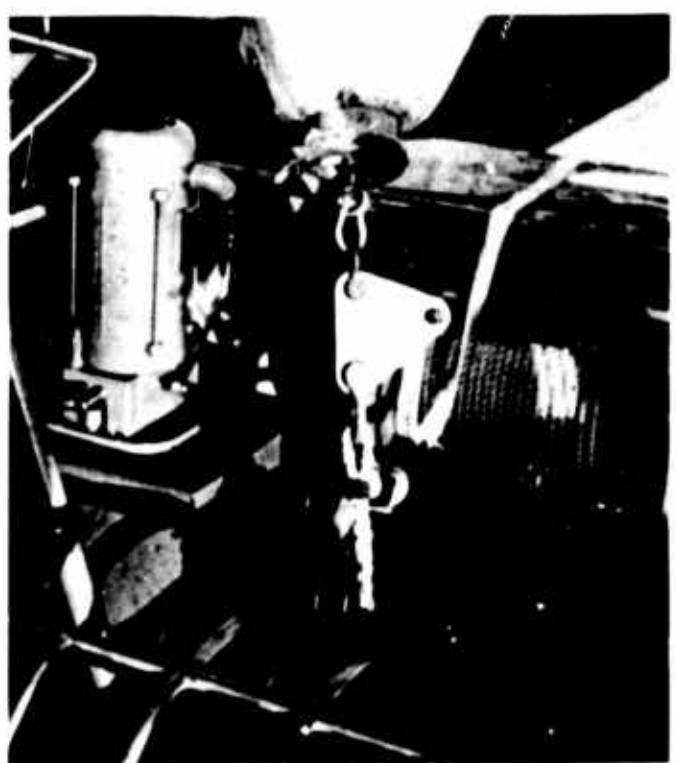


Figure 3

To date, this launch method has been successfully tested during three individual test series. The first two of these, consisting of 18 exercises, were conducted at the AFCRL Chico, California Operating Location. Natural calm surface winds were required for these exercises to simulate the shipboard conditions.

As you can see from Figures 4 and 5, in accordance with our concept of operating within a minimum space, all activities except the helium trailer operations were confined to the launch area, a 40 foot by 8 foot flatbed trailer vehicle.

The third series, of which I would now like to show you a short film (in this paper still photographs from the film appear as Figures 6, 7, 8 and 9), was conducted during the period 24 through 27 August 1964 aboard the USS Wood County, LST-1178, in the U. S. Navy VACAPES Control Area. Four complete balloon systems were successfully launched without incident in true surface wind conditions up to 17.0 knots.

In addition to concentrating heavily on the launch technique, we imposed certain other requirements on ourselves. In order to trouble the Navy as little as possible, we worked for minimum loading and unloading times. The result was that within 18 hours all the equipment, from helium trailers and instrument van to balloons, was fully loaded and prepared for sea. Within 24 hours of returning to port the same equipment was unloaded. Another aim was to operate without requiring any permanent modification to the ship. Electrical grounding straps on our major items of equipment were the only requirements and these were imposed by the ship itself.

As you can see, WOOD COUNTY is not an extremely small vessel but it is considerably smaller than a carrier and much less costly to operate. Our need for this class vessel was governed by our speed requirement plus our self-imposed requirement for sufficient helium storage space for at least three flights. As you can see, vehicle storage space is plentiful and it is possible to carry 16 helium trailers on the tank deck alone.

We believe this new launch technique substantially simplifies currently-employed methods of land-based launchings and will have definite application in remote-area operation. Balloons carrying payloads up to 1800 pounds can now be launched from a very small deck area under wind speeds as high as the sustained maximum speed capabilities of the ship. We are presently modifying and refining the launch system to accommodate payloads up to 4000 pounds.



Figure 4

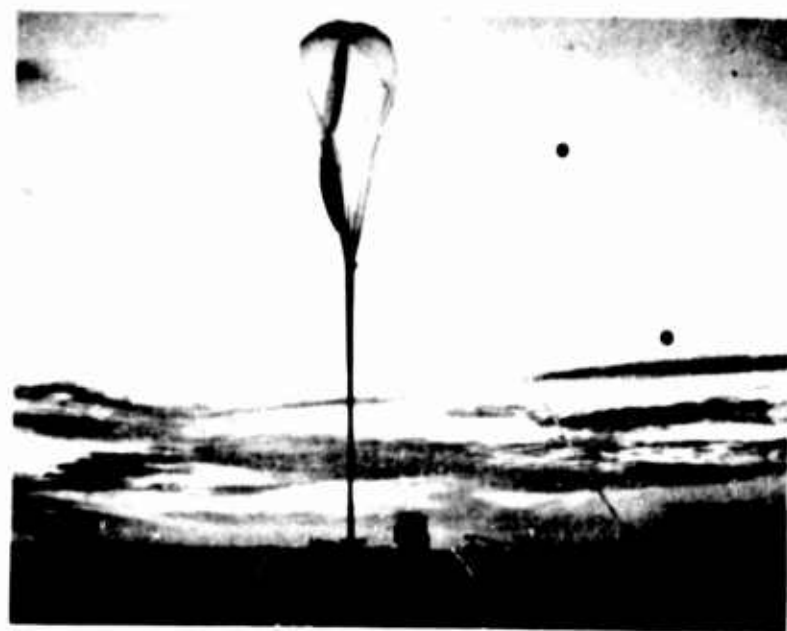


Figure 5



Figure 6

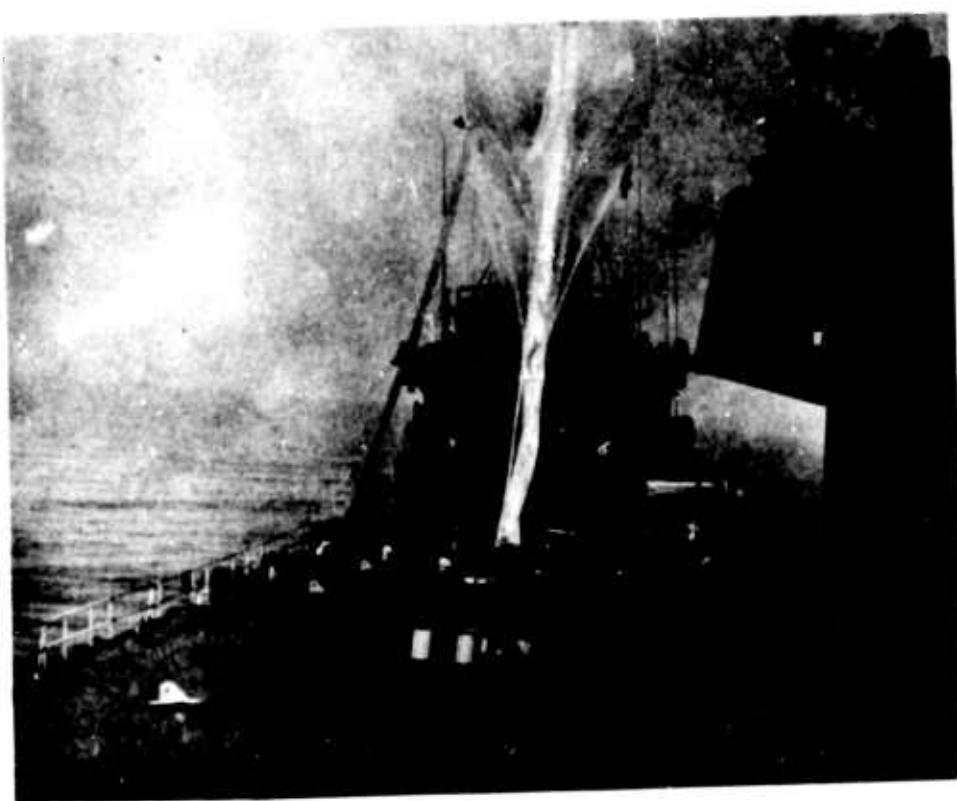


Figure 7

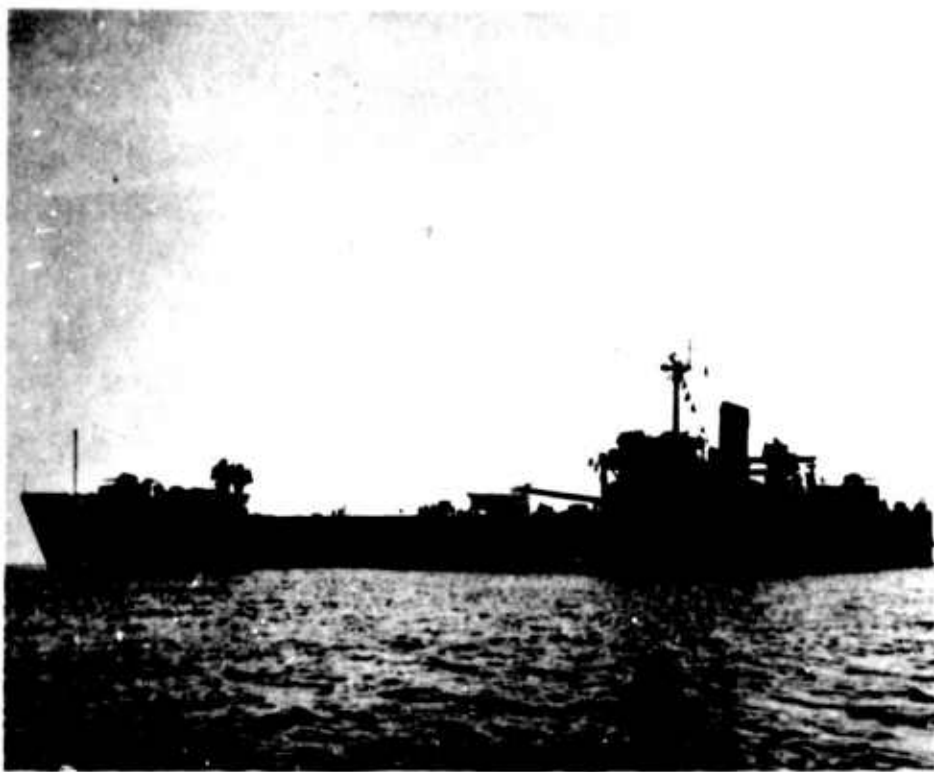


Figure 8



Figure 9

## VII. A New Polyolefin-Film Balloon Material

Donald R. Williams  
Winzen Research Inc.  
Minneapolis, Minnesota

Most polyolefin balloon film for stratospheric research activity has for many years been of the type specified in Military Specification MIL-P-4640A (USAF) dated 17 June 1957. Amendment I to this specification was issued 26 May 1958 and since that time no changes have been made. The original date of issue of the basic specification, numbered MIL F 4640 (USAF) was 5 September 1956. Thus we see that for at least eight years there has been little change in polyethylene type balloon materials. The only significant change in the amendment referred to above was the reduction in tensile strength requirements in the machine direction from 2500 psi to 2000, and in the transverse direction from 2000 to 1600. To people familiar with the film industry, the lack of progress can be explained by a combination of circumstances. One of the major reasons is the small size of the market compared to other markets for polyethylene film which have developed during this period.

During the last year or two the failure rate of polyethylene balloons has been very distressing to the entire industry. While we at Winzen Research feel that many failures are due to poor workmanship and manufacturing techniques, we feel that we have minimized failures of this type by adopting certain philosophies of manufacturing. We select our manufacturing methods and techniques not to give the fastest rates of production and lowest costs but rather to give the highest possible

reliability. We feel that this is most important in a vehicle of this type for fairly obvious reasons.

An analysis of failure of balloons manufactured by us reveals that the one factor that always seems to be present during failure is a cold tropopause temperature. Certainly not all of our balloons have failed in the presence of a cold trop, but whenever a failure does occur, a cold trop has almost invariably been present. This would indicate that a cold trop temperature has been a critical environment for polyethylene balloons. We feel that under optimum conditions of balloon unfolding and in the absence of other defects, the balloon will go through a cold trop and fly successfully. Unfortunately, these ideal conditions are not easily achieved as it is almost impossible to control the unfolding, the aerodynamic flutter, particularly at higher ascent rates, wind shears, and so forth.

The polyethylene material manufactured to the requirements of Specification MIL-P-4640A is tested for brittleness at -68°C by dropping a two inch diameter steel ball through a sample normalized at this temperature. If a fractured tear results the sample does not pass the test but if the tear is a ductile tear the sample is accepted. A fractured tear resembles the fracture seen when a pane of glass is broken while a ductile tear is a more or less straight line with usually no more than one branch if any. The type of tear is quite easy to distinguish and the results are reasonably consistent. Eight specimens are tested from a roll and, in order to be acceptable, no more than one specimen shall exhibit a shattered tear. Efforts have been made by some procuring activities in recent months to tighten this specification by requiring cold brittleness testing of samples from each roll of polyethylene film used. This is in contrast to the selective sampling of lots as called for in the MIL Specification. Two samples from each roll are taken and if either sample fails the roll is rejected. Our philosophy of testing at Winzen Research does not agree with this method of sampling and rejection. Film is made in continuous lengths so the top of one roll is immediately adjacent in production to the bottom of the following roll. We feel it does not buy one anything to reject the one roll and keep the other if the first roll does not pass and the next one does. Sampling from the ends of rolls statistically gives a very low sampling rate to begin with so we reject the entire lot if one sample fails. All of this indicates that balloon film produced in the past has been very marginal in passing a requirement of a brittle point test at -68°C. Our testing over a considerable period of time certainly bears this out.

Winzen Research has recognized these problems and on their own initiative and entirely with their own funds undertook a research and development program to come up with an improved material. The first results are a new polyolefin film material called StratoFilm\*. A facility was set up at Mt. Vernon, Texas to produce

---

\*Trade Mark Applied For

this material commercially. While all properties surpass the requirements of MIL P4640 A by substantial margins, the most significant improvement is in cold brittleness. By the MIL P4640A test the brittleness temperature must be at least as low as -84°C (-119°F) or lower. This temperature is lower than the more commonly encountered tropical tropopause temperatures and so, we feel, gets one out of the critical environment area. Generally the films produced are well below this temperature limit. StratoFilm is produced under Winzen Research Inc., Specification No. 340. There are several significant differences between this specification and the MIL Specification in addition to the cold brittleness test limits. In contrast to checking five points across the web for thickness variation and averaging them for nominal thickness and setting a maximum variation of -0.3 mil, +0.4 mil, the WRI Specification calls for a continuous reading across the web with a maximum variation of  $\pm$  0.3 mil. While it is not called out in WRI Specification No. 340, production specifications call for accurate control of average thickness, usually referred to as yield, by weighing a lineal yard of material and insuring that the weight is within acceptable limits. By this method average weight is held to about 2 percent variation, although on small runs it may run as high as 5 percent. Any sample falling outside the thickness tolerance limits will reject the entire lot from which the sample is taken.

Width is not considered an important parameter in the WRI Specification. WRI Specification No. 340 calls for a minimum tensile strength in both directions of 2400 psi. MIL 4640 requires only 2000 in the machine direction and 1600 in the transverse direction. We feel it important to balance the tensile strength in both directions as closely as possible. We call for a minimum elongation in both directions of 400 percent. The MIL Specification calls for 400 in the transverse direction but only 250 in the machine direction. We have found so many variables and so many inconsistencies in the toughness test as given in MIL 4640A that we do not include it in our specification. We do include a tensile test across the fold in the material if the fold is to end up in the balloon wall. Specification No. 340 calls for this test to yield a strength at least 90 percent of the average transverse tensile strength. To repeat, the cold brittleness test in MIL 4640A is run at -68°C and in WRI No. 340 at -84°C. Failure of any sample in a lot in the WRI Specification rejects the whole lot. In 4640 one failure out of 8 is allowed and a lot can be resampled under certain conditions. In the modification of 4640 calling for auxiliary testing, if a sample fails it rejects that particular roll. Representative results on tests of recent lots of StratoFilm show brittlepoint temperatures as low as -150°F (-101°C). Generally, properties have been very gratifying.

The flight history of balloons made from StratoFilm is of course limited as yet. However, so far there have been no failures to our knowledge on balloons that have got off the ground. The first balloons made from StratoFilm were on a crash program to test their reliability for use on the NCAR-managed IQSY-EQEX Cosmic Ray Balloon Expedition to India early in 1965. Cold tropopause temperature is, of course, expected. We understand this program will be covered in detail in another paper later in this symposium. Suffice to say that because of the urgency of the test, two of the four balloons were made in our Minneapolis Facility and they flew normally. Two were made in our, at that time new, facility in Texas. Neither of these got off the ground, one we feel because of wind and launch problems and the other because of a poorly installed apex end fitting. This balloon was replaced at no charge and has subsequently flown satisfactorily at Palestine. These were 2.94 mm-cubic-foot capacity, 3/4-mil balloons. Tropopause temperatures in Panama were -78° and -76°C and during the Palestine flight -68°C. Three of the same size and weight balloons were flown successfully by the Schjeldahl Company. The first of their flights was launched under conditions where the wind came up during inflation and was reported as gusting to 20 knots. At least one 2.94 mm-cubic-foot, 1-1/2-mil balloon has been flown by Goodfellow Air Force Base with normally expected results. At least one 128-foot diameter tailored, tapeless 2-mil balloon has been flown very satisfactorily at Holloman Air Force Base. Tropopause temperature was -68°C. More flight reports will be coming in regularly and we have high hopes of a high degree of success.

We feel that the polyethylene balloon industry was getting in a precarious position due to the high percentage of unsuccessful flights. We hope that the development of StratoFilm by Winzen Research will bring this type of balloon to a high degree of reliability and extend its usefulness to heavier loads and higher altitudes at a comparatively low cost.

## VIII. Balloon Burst Discussion

N. Sissenwine  
Air Force Cambridge Research Laboratories  
Bedford, Massachusetts

### I. INTRODUCTION

Strong wind and associated turbulence, especially near the tropopause (which varies from 30,000 to 50,000 feet) have been suspected as a major factor in the tearing and bursting of large balloons. It appears that interaction of the upper wind flow on balloon systems, which could lead to damage, can be considered as the sum of two separate forces:

- a. The resultant force of the components mounted on the film and of the load as they oppose horizontal acceleration of the balloon due to general change of wind velocity with altitude, the shear;
- b. Differential tearing forces on the balloon film due to turbulence or gusts.

A truer picture of wind forces would, no doubt, reveal a combination of shear and gust effects, perhaps supplemented by acceleration forces due to changes in buoyancy as the balloon passes from the troposphere into the stratosphere. Whether such wind forces can actually damage balloon vehicles will depend upon their magnitude as related to the balloon geometry and strength. This note presents some related data on the wind, from which preliminary determinations of their importance in balloon failure can be made.

## 2. SHEAR FORCES

The simplest approach to the shear portion of the problem would be to examine the shear each time there is a balloon failure, utilizing the upper wind sounding, currently obtained with the AN/GMD-1 equipment, which was used to support the flight. Unfortunately, as can be seen from Figure 1, reliability of GMD-1 shears through layers of a few thousand feet at tropopause altitudes when the flow is strong, is not great. For the case illustrated, the shear three thousand feet or so above the peak of the wind profile which would have been indicated by the GMD-1, is two to three times that detected by the more accurate follow-on sounding system, the AN/GMD-2, which is just coming into the inventory.

Another approach to this problem is to examine the statistics of reliably-obtained wind shears in order to arrive at realistic extremes which can be utilized in examining the possible forces on the balloons. Such a study could lead to realistic criteria for wind shear against which balloon configurations should be designed. Unfortunately, only a limited amount of applicable data is available.

Figure 2 shows shear versus altitude for probabilities of 1, 5, 10, and 20 percent from 49 AN/GMD-2 soundings obtained in the Boston area in 1957. Analogous presentations for 3,000- and 5,000-foot-thick layers are also available. Shear magnitude falls off with thickness so that the 1-percent value at 35,000 feet, averaged through a 5,000-foot layer, is only half the value shown in Figure 2 for 1,000-foot layers.

New England is subjected to stronger upper-air flow than that over the usual locations for balloon launches in New Mexico, California, Minnesota and Texas. Consequently the likelihood of shears as great as those in Figures 1 and 2 over those locations will be somewhat lower. Also, these shears may not be exactly representative of the probabilities depicted for the Boston area since there was quite strong jet-stream activity during 1957. However, the values portrayed in Figure 2 may be somewhat of an under-estimate of the actual shear. These thousand-foot shears are the difference between wind vectors a thousand feet apart in altitude but each wind vector was obtained from the average movement of the balloon over a two-minute time period while rising through a 2,000-foot layer, a smoothing process. Also, somewhat greater shears than the general wind profile would be encountered for layers thinner than a thousand feet but the limitations in the AN/GMD-2 equipment system prevent obtaining such detailed information.

From the balloon's viewpoint, the worst condition depicted by this figure is at an altitude of 35,000 feet where there is a 1% probability that a balloon will change horizontal velocity by nearly 80 fps (55 mph) while rising only a thousand feet if it were to respond completely to the wind, a fair approximation. At a rate of ascent of 1,000 fpm it would be subjected to a horizontal acceleration of  $1.3 \text{ ft/sec}^2$  or about  $0.04g$ .

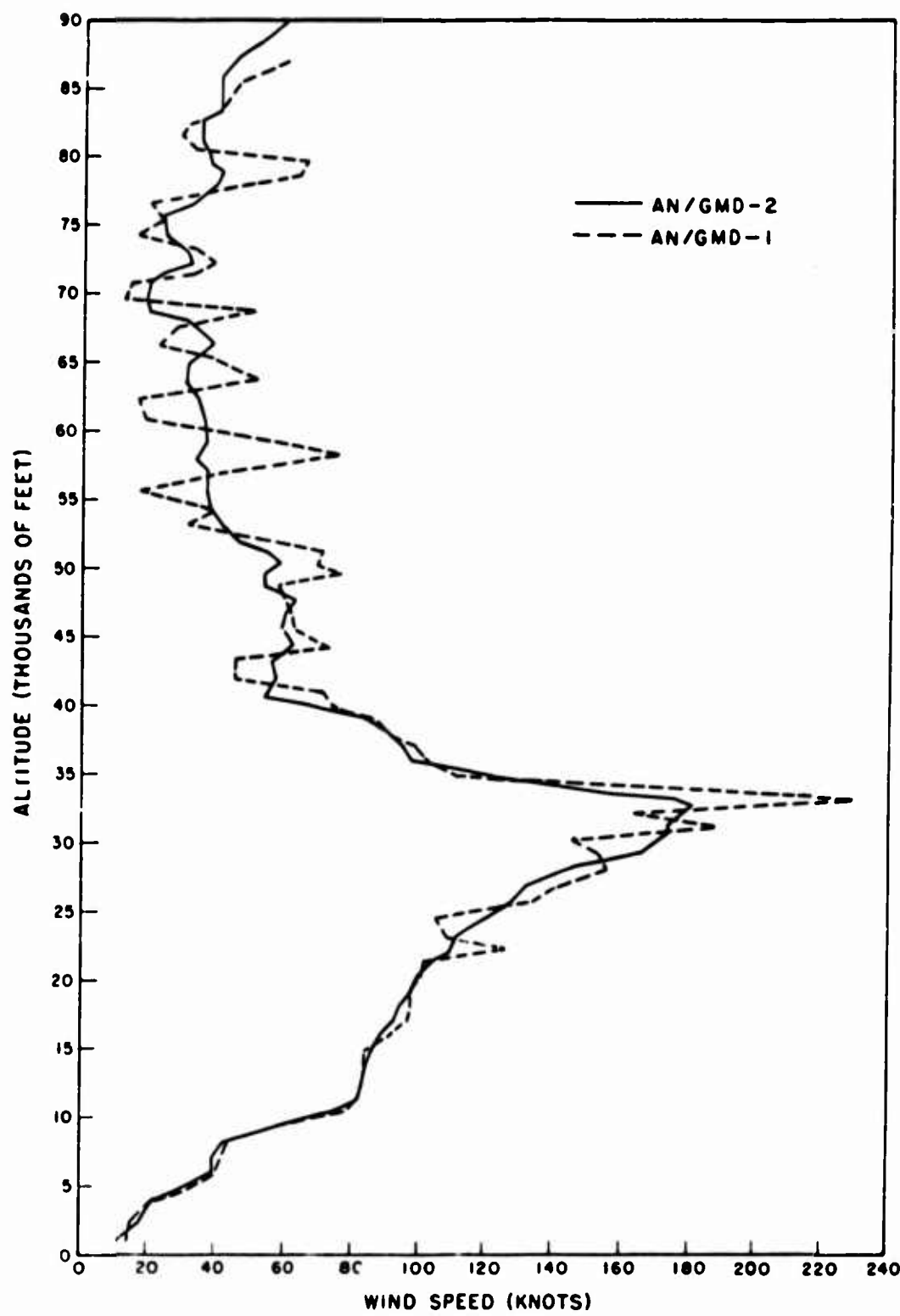


Figure 1. Wind Speed Profile for AN/GMD-2 Versus Graphically Derived AN/GMD-1 - L. G. Hanscom AFB, 3 April 1957

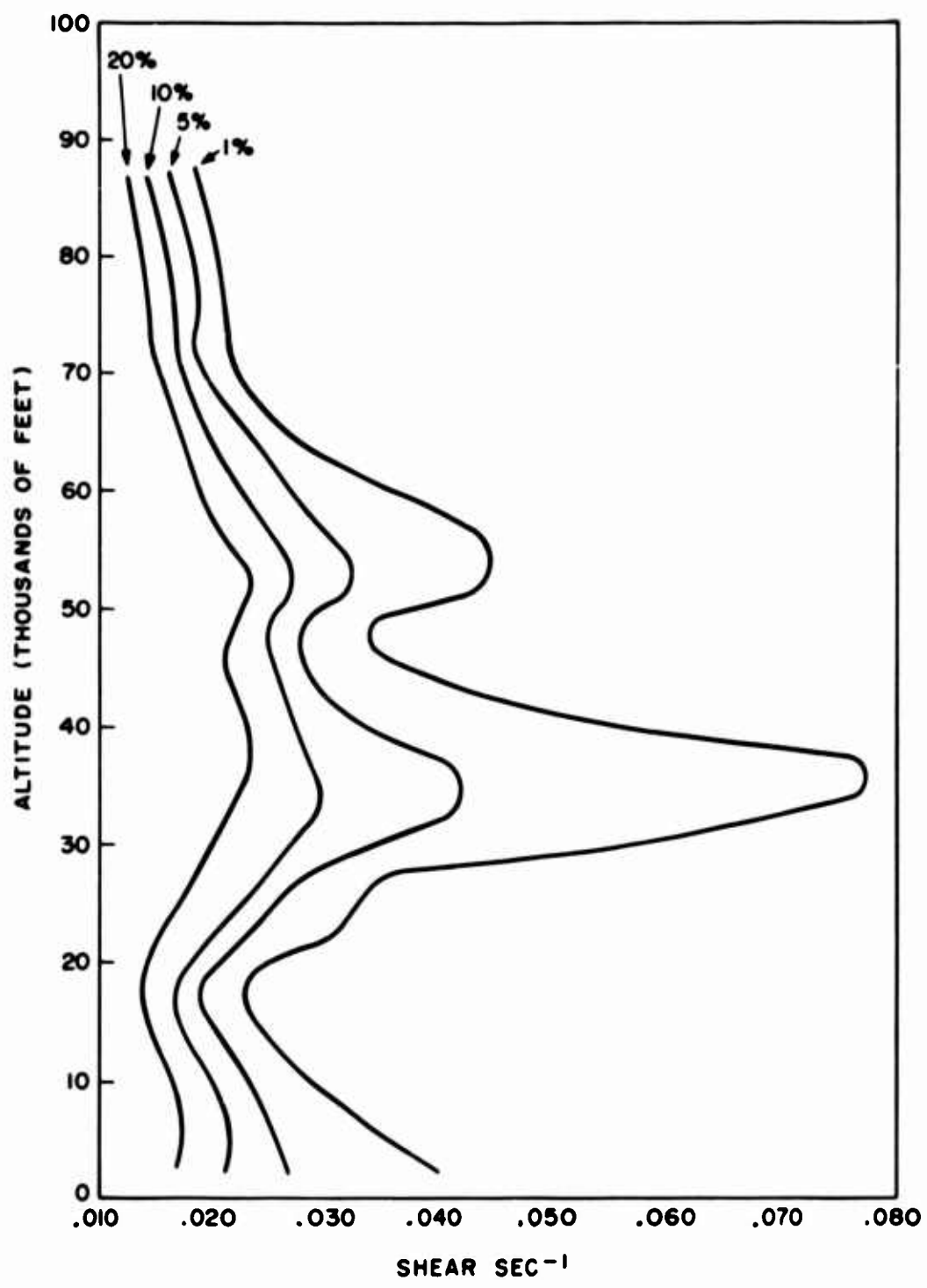


Figure 2. Probability Occurrence of Extreme 1000-Ft Shears with Height

I doubt that such accelerations are sufficiently great to be responsible for balloon bursts but I believe that these values should be looked into more deeply by knowledgeable balloon systems designers especially if faster ascent rates are planned.

### 3. TURBULENCE FORCES

To the rising balloon a gust may be considered as the small-scale fluctuation of wind velocity with altitude while the balloon moves with the velocity of the generalized wind profile which includes wind shear discussed in the previous section. However, these gusts in turn have their own shear profiles. As will be seen, the shear in these gusts will be nearly an order of magnitude higher than the shear in the generalized wind flow as portrayed by weather balloon soundings which average out gustiness during the two minutes of rise required to obtain a wind vector.

One reasonable assumption in examining the criticality of such gusts is to assume that they are made up of eddies which are rotating around a horizontal axis in the strong shear above and beneath jet stream wind profiles of the type portrayed in Figure 1. If such a vortex with, say, a 100-foot radius were penetrated by a 100-foot-diameter balloon, a reasonable size for a large vehicle ascending through the tropopause, it is conceivable that the full horizontal component force of the gusts would be imparted to the upper or lower part of the balloon whereas the part diametrically opposite would not be subjected to it. This would result in a tearing force.

A direct attack on this problem would be to investigate turbulence existing during the passage of balloons which had burst. However, applicable turbulence data are even more difficult to obtain operationally than accurate wind shear. I understand that there are current efforts to obtain such information from accelerometer-instrumented balloons. From these accelerations it is hoped that details of wind changes can be deduced to provide gust data analogous to aircraft-obtained gust statistics shown in Figure 3. My hope, however, for obtaining the volume of turbulence data necessary for thorough consideration of this problem is a new sounding system, the ROSE. Lt. Reid will discuss this system in a later paper. I will only note that wind profile details averaged through a hundred feet or less, with an accuracy of a few feet per second, are promised.

Since we cannot perform adequate post-mortem analysis on balloon bursts, let us examine the gust data depicted in this NACA graph (Figure 3) for applicability to the problem. The 610 gusts shown in this figure are the peak speeds and the distances over which the airplane traveled while this peak was being attained. Instrumentation included both accelerometers and refined pressure anemometry. Altitudes of the aircraft, which were all flown in the mid to late 1940's, did not exceed

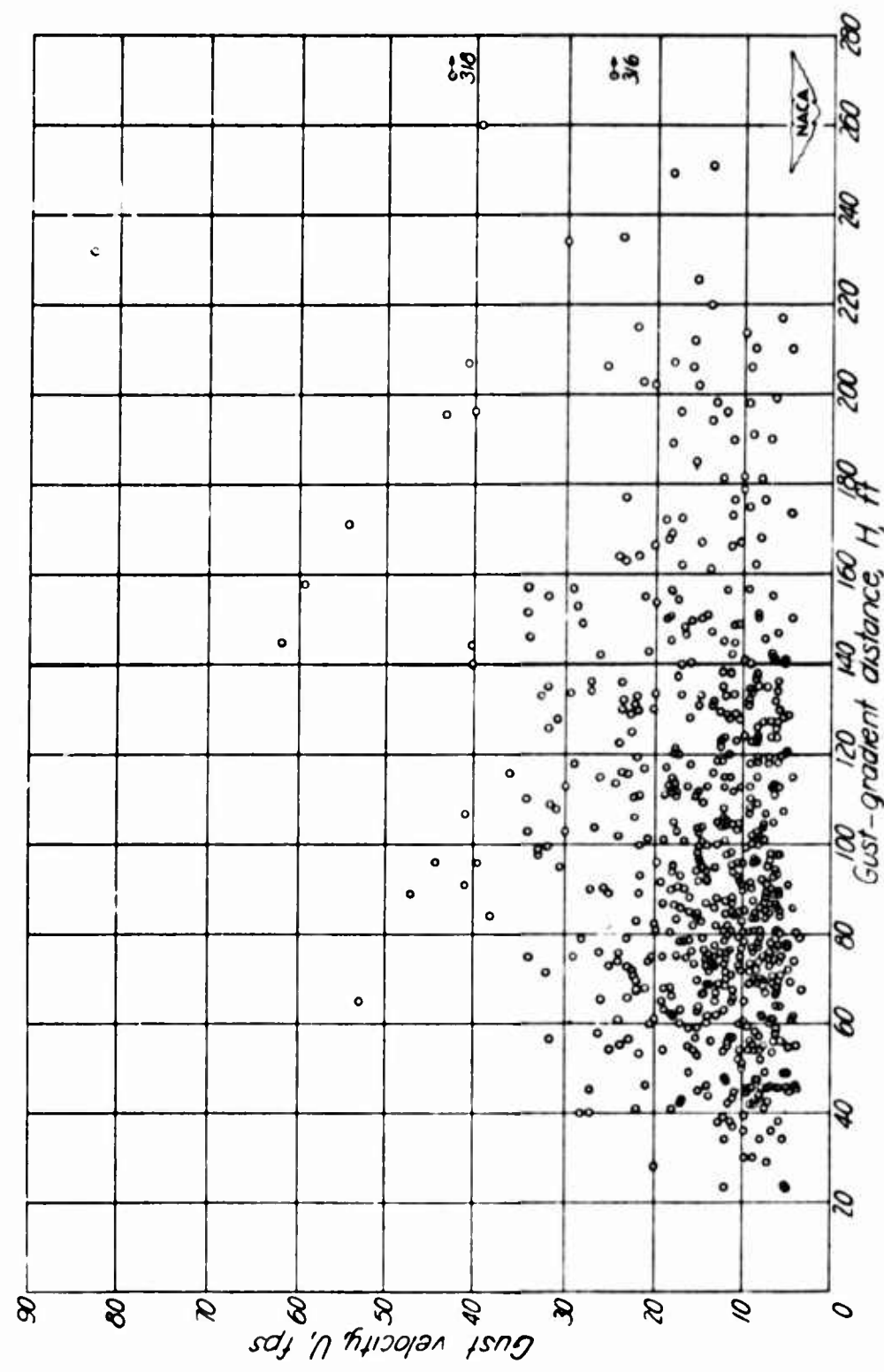


Figure 3. Gust Velocity  $U$  as a Function of Gust-Gradient Distance  $H$

40,000 feet. It may be seen that a nominal gust gradient distance to use for some preliminary investigations is 100 feet. Also, a reasonably strong gust speed to be used with this gust length is 50 fps. Values as high as 83 fps are indicated on the graph. In an AFCRL glider investigation of the mountain wave, a true gust speed of 70 fps was encountered at 40,000 feet.

A question as to the applicability of these gusts to vertically-rising balloons can be raised since these were observed by horizontally-moving aircraft. However, other studies indicate that gustiness in the free atmosphere is essentially isotropic, that is, has no favorite direction. In fact, if one can visualize gusts associated with the shear in the jet stream as rotating cylinders, the force to both horizontal and vertical penetrating vehicles would be the same.

In order to provide more of a "handle" of what might be encountered specifically at tropopause altitude, I have included Figure 4, in which the magnitude of accelerometer-deduced gusts is related to the general wind shear through 2,000-foot-thick layers above and below the jet stream. These data were obtained at tropopause altitudes with highly-precise radar-navigation wind equipment and VGH turbulence recorders during AFCRL's B-47 jet stream research in the late 1950's. You will note that there are some correlations between gust and shear intensity although it is far from as high as expected. This is one of the reasons why it is difficult to forecast clear-air turbulence, a very important problem in today's jet-aircraft travel. Even in this very limited sample, a true gust of 35 fps was observed. One can see that much higher values could be expected with the stronger wind shear of the 1-percent magnitude presented in the upper curve of Figure 2. The size of these gusts was not available but it is quite likely that they, too, would be somewhere around a hundred fps.

Let us take as an example an ascending balloon, which is moving with the general wind flow so that there is no relative wind over it, suddenly penetrating a layer of turbulent vortices which have a radius of 100 feet and an amplitude of 50 fps. Almost any geometric arrangement of the force of these gusts on the balloon is possible, especially since there is likely to be a couple of thousand feet of such vortices. A quick calculation would reveal that at 40,000 feet, the peak dynamic pressure of such a gust will be about 3/4 pound/square foot. Let us use an extremely naive simplification, that the average pressure is half a pound/square foot and that it is applied uniformly to the upper half of the balloon, an area of 4,000 square feet; whereas there is no gust force on the lower half of the balloon. An unbalanced force of 2,000 pounds is obtained. It is centered somewhat between the top of the balloon and the equator. It tries to tear the upper portion of the film from the rest of the balloon and the train which are not subjected to it.

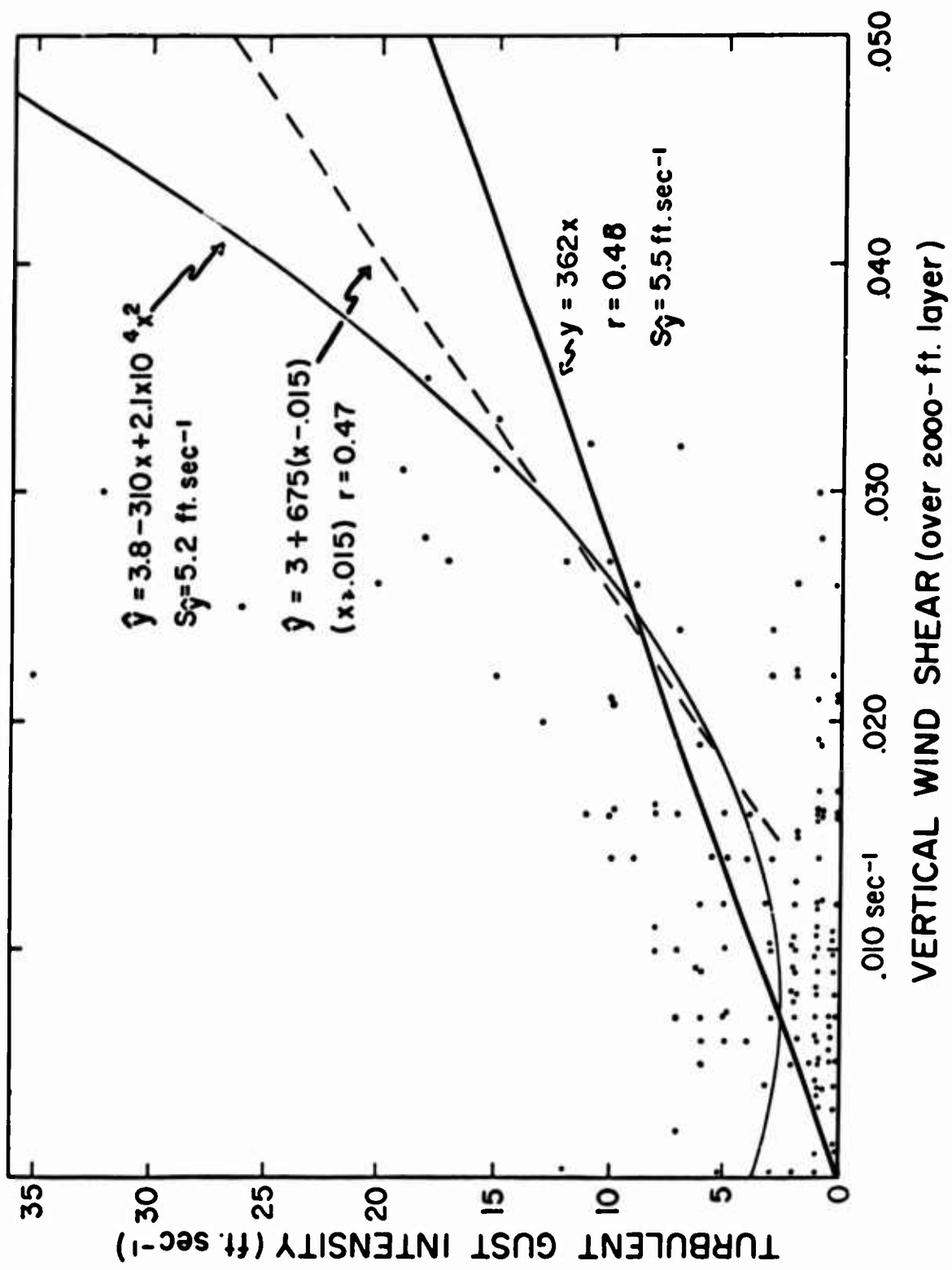


Figure 4

A realistic geometric distribution of this gust force would have to be developed and related to the balloon configuration before any firm conclusions as to the importance of this gustiness can be reached. However, I believe these extremely preliminary quantities warrant a deeper investigation.

## IX. Balloon Launching from Airplanes and Helicopters

Lomis Slaughter  
Anderson, Greenwood & Co.  
Houston, Texas

### Abstract

The purpose of this report is to advise balloon users and potential balloon users that, through work sponsored by AFCRL, techniques have been developed for launching balloons and balloon-supported payloads from high speed airplanes. Additionally, a sound start has been made on a technology for the launching of balloons from helicopters. To make these minimum statements more meaningful, this report sketches the state-of-the-art in these two areas discussing the techniques, the current experience level as to payload weights, balloon sizes, and aircraft speeds, and touches on the basic economics of pounds and dollars.

#### I. LAUNCHING FROM CONVENTIONAL AIRCRAFT

The balloon-launching unit, with the appearance of a bomb, is carried on external or internal stores positions on fighter-type aircraft. (See Figure 1.)

Arrangements for release from transport aircraft can also be made and are of interest for the larger launcher units. The step-by-step process of launching is shown in the following series of illustrations.

**Figure 2** - Balloon unit is dropped or ejected from the launching aircraft which may be of any type including the latest high-performance fighter airplanes.

**Figure 3** - Drag parachute is deployed to slow the unit and reduce the main canopy opening shock. The drag parachute is then released and deploys the main canopy.

**Figure 4** - Main parachute opens and quickly establishes stable descent. Payload and balloon are supported on top of main canopy.

**Figure 5** - Balloon protective cover is released and balloon inflation begins atop main parachute.

**Figure 6** - Balloon inflation is completed and balloon and payload separate from parachute.

**Figure 7** - Actual hardware in test drop near completion of inflation.

**Figure 8** - Balloon and payload ascend to design altitude. Parachute and gas bottle descend.

This, then, is the general scheme of launching balloon-borne payloads from conventional airplanes which has evolved in AFCRL development carried out at Anderson, Greenwood & Co. Over 200 launches from airplanes have been made by this group, or under its supervision. Many of these launches were developmental tests involving less than a complete system or with the balloon tethered to the parachute, but 100 complete, free-balloon launches have been carried out and of the last 32, 26 were completely successful in launching undamaged balloons; 26/32 = 81 percent. Thus 80 percent is the current experienced reliability.

Figure 9 is a tabulated record of these Anderson, Greenwood & Co. - conducted air launches. The tabulation covers six basic units which have been engineered and developed and gives an indication of the overall quantity of experience which has been accumulated.

From the tabulation several additional facts about air-launching experience may be noted:

Maximum payload size is given somewhat indirectly by maximum lift (a term indicating the sum of balloon and payload weight). Largest units air launched to date have a lift of 78 pounds - actual payload flown on this unit was 57 pounds.

Maximum launching speeds - a number of launches have started with separation from the airplane at Mach 0.95. Slower aircraft speeds at launch minimize unit separation and deceleration problems.

Maximum launch altitude - aircraft release at 45,000 feet and balloon deployment in that vicinity is proved possible by a number of flights. Lower altitudes afford a milder environment as regards temperature and parachute-opening shock.

In addition to payload-carrying balloons, Series 106 and Series 110 units launch metalized mylar balloon spheres of 6-foot diameter and 10-foot diameter, respectively. These units have been employed in armament development as high-altitude radar targets. Figure 10 shows the Series 110 unit on the ejector bomb rack of a Navy fighter airplane.

A cross sectional schematic of this unit, Figure 11, is typical.

1. Pressure bottle for helium storage.
2. Explosively-actuated charge valve.
3. Balloon inflation hose.
4. Header (a platform at parachute apex for payload, balloon, balloon release and helium connection).
5. Balloon-release fitting.
6. Payload pack.
7. Balloon.
8. Drag parachute.
9. Squib-operated tail lid ejector and drag chute release.
10. Main parachute.
11. Programmer timer.
12. Batteries.
13. Canister.
14. Bomb rack lugs.

Figure 12 illustrates the major elements of the system after parachute deployment to show the fill line going around the parachute canopy to the header on the parachute canopy apex, and then through the balloon-release fitting to the balloon. In this illustration the drag chute has performed its function of preliminary slow-down and main-chute deployment. The balloon is still under its deployment protective cover provided to relieve the balloon of parachute whiplash loads and aerodynamic forces during parachute deployment.

In Figure 13 the balloon inflation has been accomplished and the balloon and payload have separated from the header on the parachute canopy.

Figure 14 is an incompletely-assembled Series 106 unit, allowing the examination of some of the sub-components.

- A. Payload. The payloads for air-launched balloon systems cover a broad spectrum ranging from relatively simple radar-reflective metalized coating on the balloon film itself to complex instrument packages capable of gathering and transmitting several items of scientific or military data. These packages have included a ballasting system to maintain balloon altitude for long duration flights, although a superpressure balloon could now be recommended in many applications. The usual design requirements for airborne payloads apply;

- lowest possible weight, high density packaging, and resistance to mechanical shock. Payload weight and flotation altitude are the parameters on which the remainder of the package is based and from these the following are successively selected; balloon gas storage bottle, parachute system, and canister.
- B. Balloon. Balloon design is an evolving complex technology and a large variety of balloon materials and designs are currently in use, each offering special advantages in its area of employment. Since the specific application is of prime importance in the design of the balloon, no definitive statement can be made here. A variety of balloon configurations may be used, including streamlined shapes for high ascent rates (say 1000 fpm), cylindrical or tetroon shapes for economical manufacture, or spherical or sphere-cone configurations for the most efficient lifting characteristics. Radar reflectivity may be built into the balloon itself by the use of metalized fabric corner reflectors within the envelope, metalized balloon film, or the use of metallic dipoles attached to the balloon film.
- C. Gas Storage Bottle and Charging System Components. As will later be shown, the volume and weight of the helium gas storage component of the unit is a major factor in determining package weight and size, and therefore in selecting the required parachute system. Highly-developed, high-strength steel and fiberglass bottles are available and provide for minimum air-launched device size. Where cost factors greatly outweigh size and weight consideration, a low-stressed steel bottle of one of a number of nearly standard sizes can be utilized with an attendant increase in the overall size and weight of the package.
- D. Fill Valve. A twin-squib explosive valve mounted on, or near, the storage bottle is used to admit the lifting gas to the fill hose at the proper time. This valve is absolutely leak-tight in the closed position permitting the package to be stored for extended periods in the pressurized condition.
- E. Fill Hose. This hose, which transmits the lifting gas from the storage bottle to the balloon, is attached to a parachute shroud line and continues along the top side of the canopy to the "header" at the apex of the parachute. The gas passes through the header, around or through a cloth diffuser, which disperses the jet, preventing damage to the balloon.
- F. Canister. Generally, the canister is a fairing and carrying structure for the other components. Its aerodynamic shape must be compatible with the launching airplane while providing for minimum shock loading and maximum stability during separation from the aircraft. In cases where force ejection is required for high speed launching of the package, the canister must be designed to withstand and distribute the high loads exerted by the ejection system.

For high altitude devices the canister may also include provisions for insulation, or heaters, to protect the payload, balloon, and programmer. The canister is equipped with access doors for service and checkout of the balloon device and payload.

- G. Programmer. A mechanically-driven system of electrical sequencing is employed on almost all of the packages currently in use, although in very minimum systems powder-train timing is envisioned. The programmer power pack consists of the batteries required to operate the various squibs through the programmer circuits. The type of battery employed depends on such factors as launch altitude, time in low temperature environment before launch, shelf life required, and overall electrical requirements.
- H. Header. The assembly of balloon attachment and release mechanisms is referred to as the header. This mechanical assembly is secured to the apex of the parachute where it performs a number of launching functions as follows:
1. It serves as attach point and release mechanism for the payload.
  2. It serves as attach point for the helium fill line.
  3. It serves as attach point for the balloon protective cover and releases the cover just prior to balloon inflation.
  4. It serves as disconnect point between fill line and balloon.
- I. Parachute System. Launch speed and altitude, together with package size and weight, are the basis of parachute system design. Parachute experience formalized in the services' parachute handbook covers the requirements in practically all instances, and in most cases existing drag parachutes and main canopies can be used thereby avoiding developmental costs.

#### 1.1 Weight and Cost Considerations

Due to the high costs of very lightweight gas storage bottles (particularly high when special tooling and qualification tests are required), there is a strong inverse relation between balloon air launcher cost and launcher weight for a particular payload-altitude requirement. To place a few pounds of payload on a balloon which will rise to an altitude of "h" feet by air launching is more expensive if the launching unit must also be as light as possible. In many, if not most situations, the balloon launcher device in weight and size is much smaller than the loads for which the aircraft is normally used and thus, size and weight are clearly secondary to project cost. In this case gas storage bottles of minimum sophistication can be employed resulting in the most economical unit possible. However, in those cases where project or mission success is sensitive to weight and size, true economy may demand the ultimate that current technology offers. Let us take an example:

Assume the requirement of air launching a sixteen-pound payload at 5,000 feet to rise to 25,000 feet at 600-800 fpm rate of rise, and flotation at 25,000 feet for one hour minimum (no sunset requirement).

Figure 15 analyses three units all designed to this requirement. Unit 1 is the most sophisticated, consisting of fiberglass or composite material special bottles. Unit 2 is a high-strength steel bottle, and Unit 3 is an economical mild steel bottle. As we scan the weights column we can see that bottle weight increases significantly and that there is an important effect on the parachute size and weight as well as on the weight of the fairing. Most other items are substantially unaffected. The gross weights of the three units vary; 90 pounds for the most sophisticated unit, 140 pounds for the high-strength steel bottle unit, and 266 pounds for the most economical unit. The remainder of the tabulation shows a variation in the cost per unit for these three units with quantities of 10, 100, and 1000. It can be seen that the cost is sensitive to bottle selection in all categories, although it is most important in low quantities, where the cost of \$16,000 for the most sophisticated unit can be compared with \$2,900 for the most economical, whereas at the quantity level of 1000 units the sophisticated unit costs \$3,480 compared to \$1,414 for the most economical unit.

Figure 16 may be used to estimate balloon size and device weight for units built around high-strength steel bottles. An example of use of the chart is traced out on its face; a 50 pound payload to float at 65,000 feet, carried by a rugged balloon equivalent in weight to 1.5 mil polyethylene is indicated to require a 34-foot-diameter natural-shaped balloon. The overall device weight is indicated as 450 pounds.

This, then, is the air-launched balloon. The purpose of the device is to place scientific or military payloads at a desired location at a preselected time with the maximum independence from wind, terrain, or enemy control. A satisfactory technique has been developed and substantial experience has been acquired. System elements such as timer, explosive valves, releases, fill lines, balloon- and payload-separation devices for application to any detailed requirement are available. Figure 17 shows a proposed design freeing the payload from involvement with balloon and parachute and thus facilitating payload checkout or alternate payload substitution.

## 2. BALLOON LAUNCHING FROM HELICOPTERS

If the distance of the most desirable launch point is less than 100 miles from a ground operating base and if larger payloads are required, or if the cost of the expended air-launching hardware is prohibitive, helicopter air launching may have advantages over both ground launch and launching from airplanes.

Under some circumstances it may be very desirable to be able to launch load-carrying balloons at a given place under wind conditions that make ground launching unreliable. In other instances it is desirable to launch with a minimum lapse of time between choice of launch point and launch.

Relative to ground launching, the following advantages appear attainable by helicopter launching:

1. Elimination of dependence on wind.
2. Attainment of more reliable placement on course, or over range.
3. Attainment of higher launching reliability due to reduction of wind force across balloon envelope.
4. Reduction of size of launching crew.
5. Elimination of dependence on terrain or surface roads.
6. Selection of launch point based on current and short lead-time forecasts.
7. Execution of over-water, rough terrain, or forest-area launches.
8. Launches where ground launch would leave undesirable evidence.

While these same desirable features accrue to airplane launching, helicopter launching has the further advantage that very little equipment is expended, so that for large loads it will prove more economical than launching from airplanes.

A preliminary series of tests to evolve the technique and equipment for helicopter balloon launching has been carried out under the sponsorship of AFCRL. The indications from these tests are positive in that a number of successful launchings were carried out.

While we won't win an Oscar for the accompanying film, it affords an easy way of explaining the most successful of several experimental launching techniques tried. (Still photographs from the film appear in this paper as Figures 18 through 24.)

Film: Helicopter Launch Sequence:

Launching sequence:

1. Package consisting of the balloon and payload is lowered to the full extension of the fill line using a winch with a brake. Helicopter is flown with 3 to 5 knots of forward velocity.
2. The balloon package cover is released and helium from the bottle complex in the helicopter is flowed through the fill line to inflate the balloon.
3. Filling is nearly complete - helicopter still at 3 to 5 knots forward - fill line is still connected.
4. Filling having been completed, balloon and payload are released from suspending and towing fill hose. Load swings under balloon and free-balloon flight begins.

The rest of this film shows an actual test at Ft. Sill, Oklahoma.

This balloon, payload, fill line arrangement is not the first approach, but is the end point of an evolutionary process. In our opinion, this is the way to accomplish a balloon launch from a helicopter, with detailed improvements, of course.

The winch developed for this project is seen in Figure 18. Its function is to pay out the payload and balloon-carrying fill hose, and to rewind the fill hose after the balloon and payload have been released. Helium gas from the fill bottles in the helicopter pass through a rotative fitting in the winch and through the 400 feet of fill line to the balloon.

In addition to giving the pilot peace of mind, the 400-foot fill line also allows the balloon to fill in the quiet air outside of the helicopter downwash pattern.

Figure 19 summarizes the technique shown in the moving picture sequence. Figure 20 shows the details of the balloon to load and fill line arrangements. Only three tests have been carried out with this configuration, but all were successful.

The method is thought to have the following advantages:

1. Factory-packaged balloon is never thereafter touched, eliminating handling by inexperienced personnel, and balloon handling in difficult circumstances. This should make for good reliability.
2. Balloon buffeting is minimized with low-velocity forward tow.
3. Helicopter-piloting problems are minimized by avoiding a hover requirement which allows easier pilot technique and usable flight instrument readings.
4. Since the balloon does not store on or feed off the winch, winch size is a minimum and hose level-winding is possible.
5. Balloon at end of line supplies aerodynamic damping forces required to minimize any whip action.

Equipment for helicopter balloon launches consists of:

1. Gas storage bottles secured within the helicopter.
2. Gas manifolding, valving, and plumbing.
3. Fill hose (400 feet made for a happy helicopter pilot). Fill hose carries electrical leads for all launching functions.
4. Balloon package release means.
5. Fill hose disconnect means.
6. A winch storing the 400-foot fill hose in the helicopter and capable of lowering the balloon and payload on the fill hose and capable of retracting the fill hose after balloon release.

To show the size of payloads which may be launched with helicopter equipment currently in the inventory, let us take a hypothetical problem of helicopter launching balloon units designed to carry payloads to 100,000 feet.

Figure 21 plots balloon payload against project load in the helicopter composed of the following item weights:

1. Payload
2. Balloon
3. Helium
4. Helium Bottles
5. Winch
6. Balloon crew of two.

On this same curve the payload available from helicopters with approximately two hours' duration of fuel shows that the HU-1 series, Figure 22, is suitable for launching balloon systems with 100K altitude capability and payloads up to 200 pounds. The CH47A, Figure 23, can carry a project load of 6000 pounds, theoretically sufficient for 1000 pound payloads to 100K ("theoretically", because helicopter cargo volume has not been studied in detail). Rough calculations based on known loads indicate the one hundred 18-inch spherical fiberglass bottles can be accommodated in the cargo space of the CH47A.

Figure 24 shows the start of a launch test and Figure 25 shows a balloon after release from the fill line. In the two techniques just described some improvements in the balloon system as a vehicle are offered. The tools are available for your use in geophysical research, in communications, in surveillance, or in weaponry.



Figure 1. Launching Unit on Fighter Aircraft



**Figure 2.** Balloon Unit is Dropped or Ejected from the Launching Aircraft Which May Include the Latest Types of High Performance Fighter Airplanes



**Figure 3.** Drag Parachute is Deployed to Slow the Unit and Reduce the Main Canopy Opening Shock. The drag parachute is then released and deploys the main canopy



**Figure 4.** Main Parachute Opens and Quickly Establishes Stable Descent. Payload and balloon are supported on top of main canopy



**Figure 5. Balloon Protective Cover is Released and Balloon Inflation Begins Atop Main Parachute**

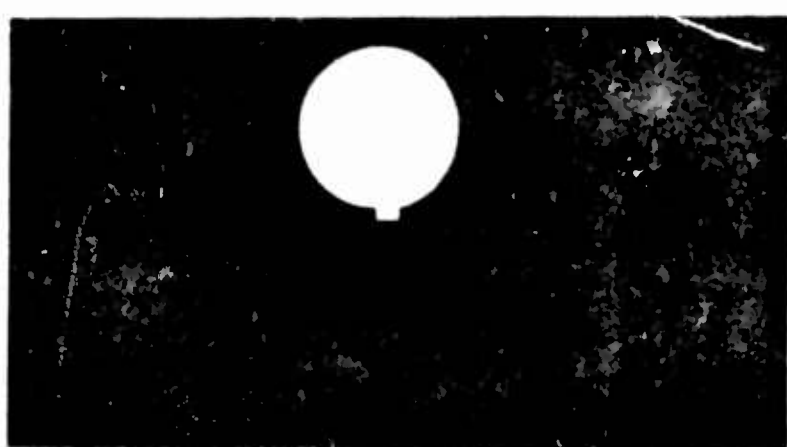


**Figure 6. Balloon Inflation is Completed and Balloon and Payload Separate From Parachute**



Figure 7. Completion of Inflation

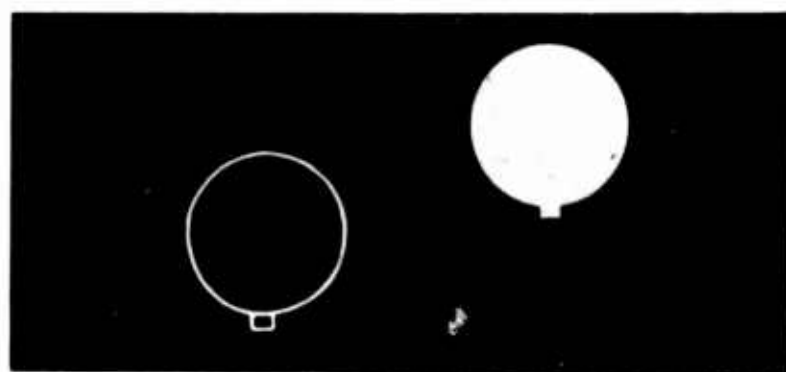


Figure 8. Balloon and Payload Ascend to Design Altitude. Parachute and gas bottle descend.

SUMMARY OF AIR LAUNCHED BALLOON TESTING BY ANDERSON, GREENWOOD & CO.								
Device Nomenclature	Use	Max. Lift (lbs.)	Launch Speed	Launch Altitude (ft.)	Developmental Launchings	Launches with Balloons	Successful Balloons	Total Air Launches
Experimental Unit	Develop concept	1.0	200K	10,000	56	30	10	86
Series 1A	Advance State of the Art	16.6	.95M	45,000	10	21	9	31
Series 1B	" "	16.6	.95M	45,000	9	17	10	26
Series 11	Hurricane Marker	39.0	250K	15,000	39	17	15	56
Series 37-1	"	78.0	250K	15,000	--	10	9	10
Series 110	Radar Target	1.4	.95M	45,000	15	5*	4*	20

Figure 9. Summary of Units Tested



Figure 10. Series #110 Unit on Navy Fighter Aircraft

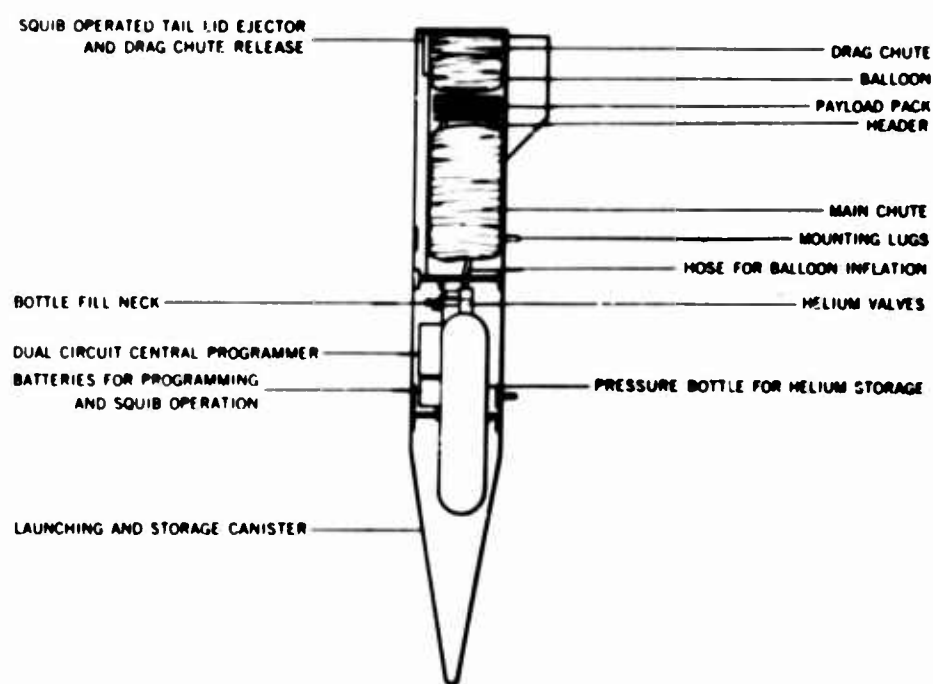


Figure 11. Cross Section of Series #110 Unit

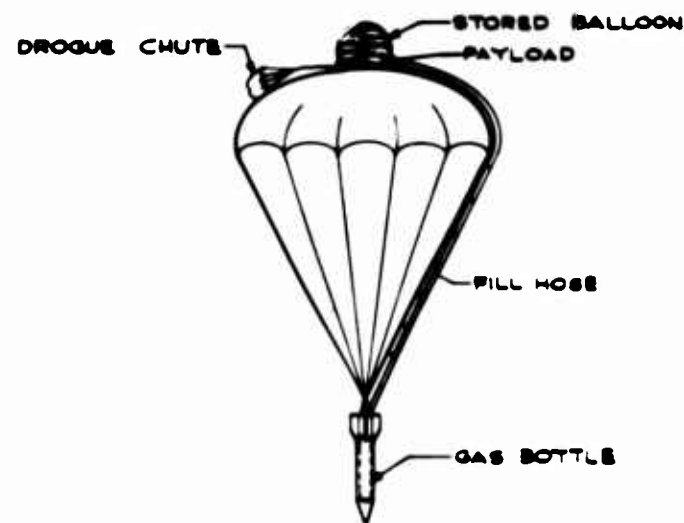


Figure 12. Launching Unit After Parachute Deployment

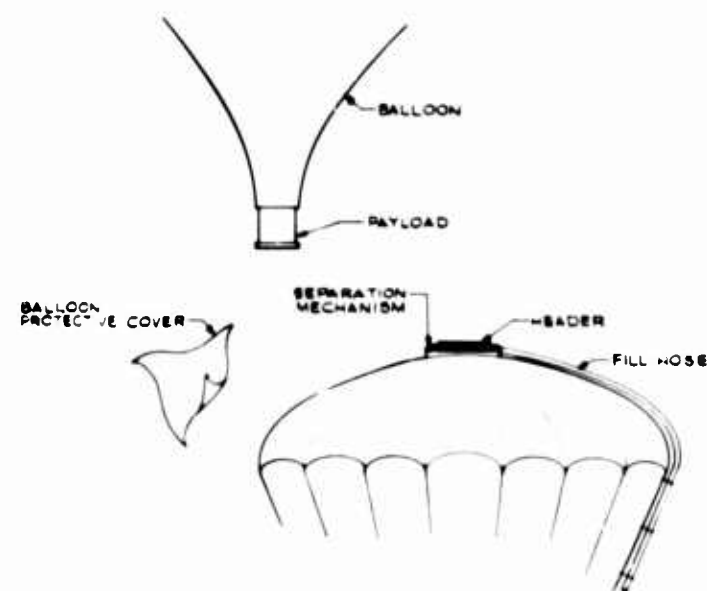


Figure 13. Parachute and Balloon at Separation



Figure 14. Partially Disassembled Series #106 Unit

WEIGHT COMPARISON			
	Most Sophisticated Glass, Composite or Spec. Steel Bottle	High Strength Steel Bottle	Economical Mild Steel Bottle
Payload	16.0	16.0	16.0
Balloon	1.5	1.5	1.5
Helium	1.7	1.7	1.7
Bottle	52.7	98.9	208.5
Parachute	3.9	6.5	10.5
Drague	.8	1.0	1.9
Fairing	8.5	9.0	20.0
Hose	1.5	1.5	1.5
Plumbing, Fittings & Misc.	<u>3.4</u>	<u>3.9</u>	<u>4.4</u>
	90.0	140.0	266.0
<u>10 Units</u>			
Estimated Hardware Cost	\$ 6,000	\$ 4,800	\$ 2,500
Allocated Engineering Cost	<u>10,000</u>	<u>10,000</u>	<u>400</u>
Unit Total	\$16,000	\$14,800	\$ 2,900
<u>100 Units</u>			
Estimated Hardware Cost	\$ 4,500	\$ 3,600	\$ 1,880
Allocated Engineering Cost	<u>1,000</u>	<u>1,000</u>	<u>40</u>
Unit Total	\$ 5,500	\$ 4,600	\$ 1,920
<u>1000 Units</u>			
Estimated Hardware Cost	\$ 3,380	\$ 2,700	\$ 1,410
Allocated Engineering Cost	<u>100</u>	<u>100</u>	<u>4</u>
Unit Total	\$ 3,480	\$ 2,800	\$ 1,414

Figure 15. Comparison of Three Units

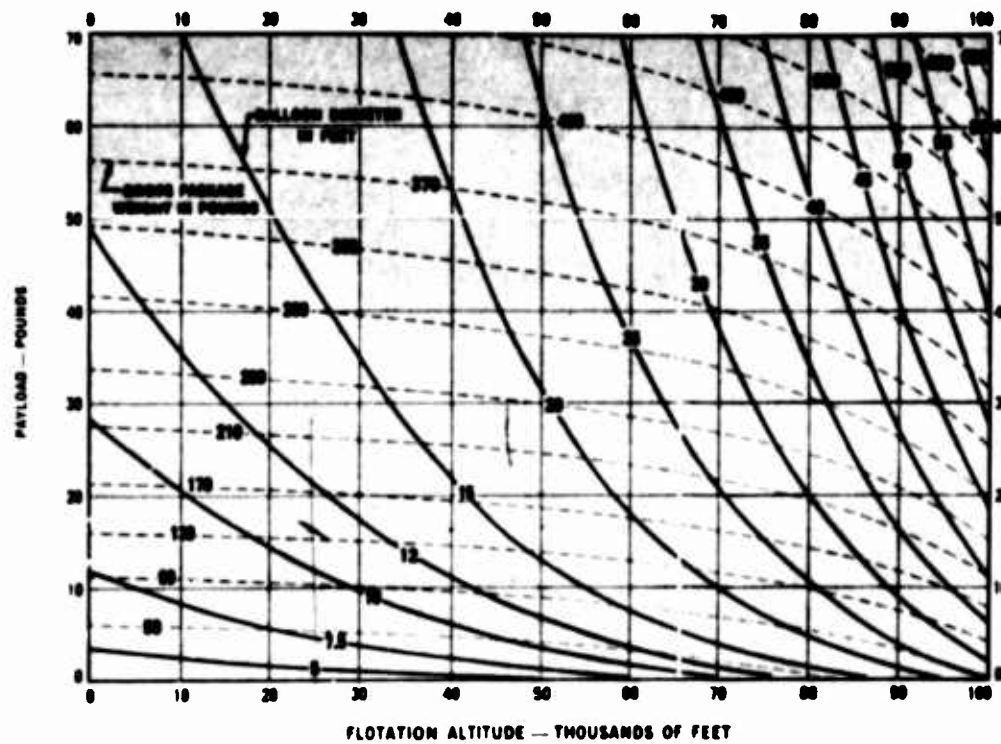


Figure 16. Payload vs Flotation Altitude for Various Diameters of Balloons and Gross Air Launched Package Weights

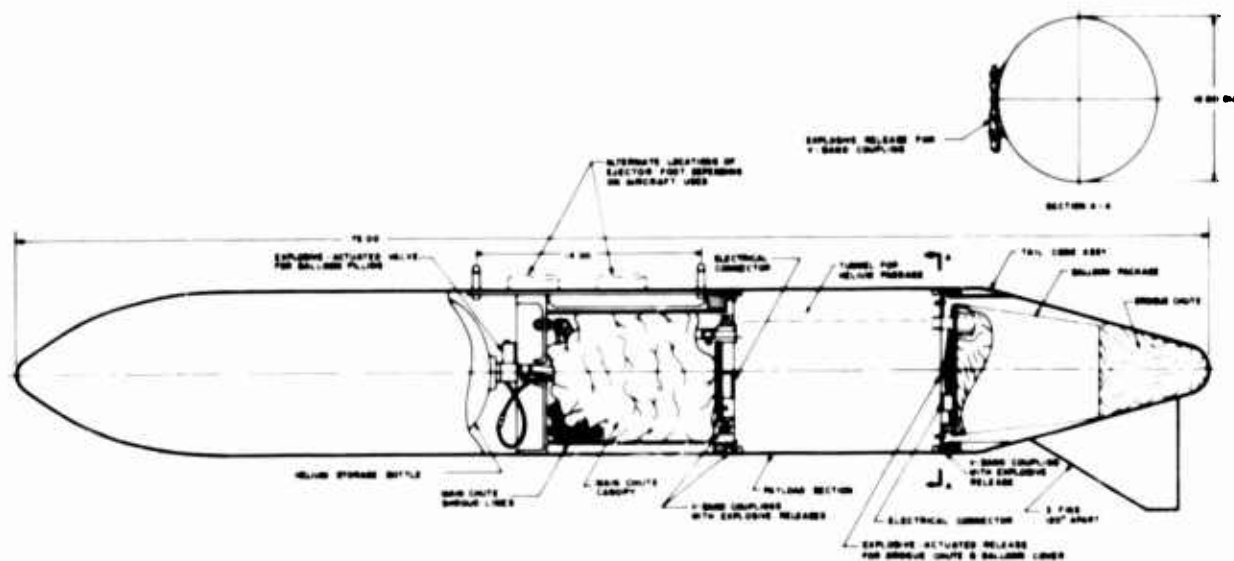


Figure 17. A Proposed Design

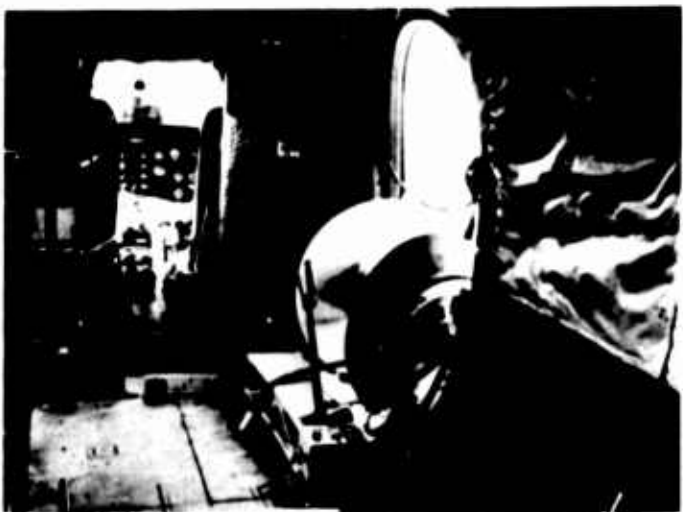


Figure 18. Lowering Winch in H-21 Helicopter

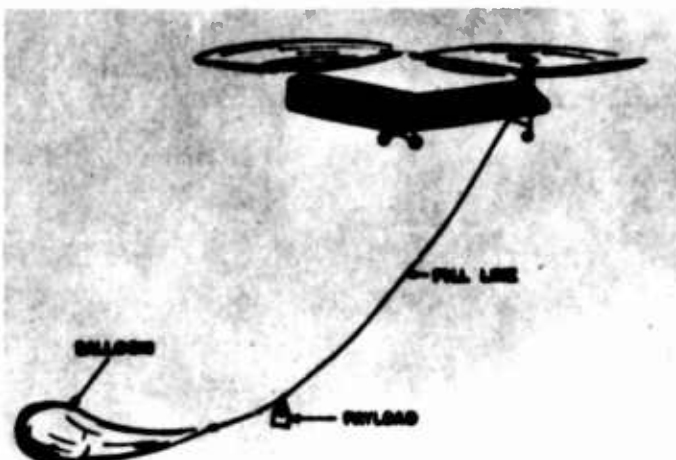


Figure 19. Deployment Technique

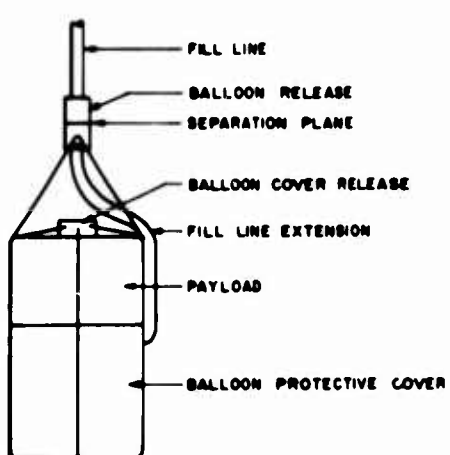


Figure 20. Balloon, Payload and Fill Line Arrangement

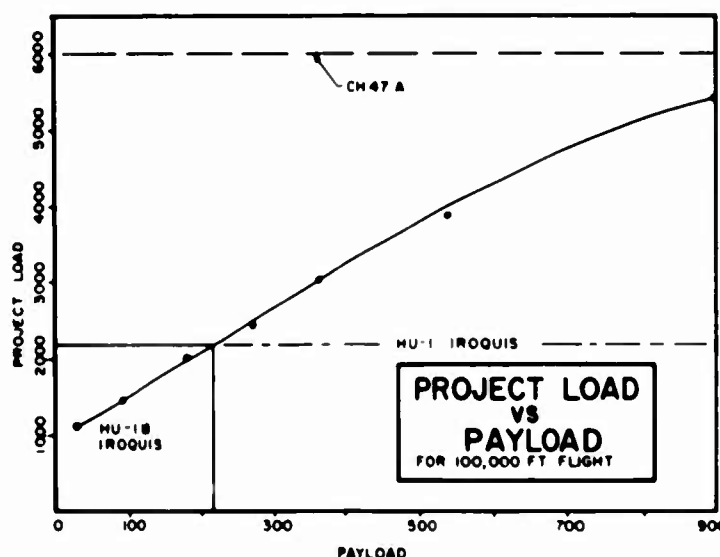


Figure 21. Project Load vs Payload for 100,000-Foot Flight



Figure 22. HU-1 Series Helicopters



Figure 23. CH47A Series Helicopter



Figure 24. Start of a Launch Test



Figure 25. Balloon After Release From Fill Line

## X. Ultra Thin Film Balloons

Dale W. Cox, Jr.  
Sea-Space Systems, Inc.  
Torrance, California

Achieving float altitudes in excess of 150,000 feet has always been a balloon performance goal at Sea-Space Systems. To realize such performance, lightweight fabrics are mandatory. Our thin-film philosophy at Sea-Space, since the start of the Corporation three years ago, started from the premise that 1/2-mil polyethylene is a heavy-gauge material. Last year at this Symposium some eyebrows were raised when Dewey Struble announced that polyethylene derivative films of 1/7-mil gauge had been extruded by our company. Films of such thin gauges are used in the fabrication of SSS composite balloon film -- MERFAB. This year we are happy to report that further improvements have been made. Using special experimental resins, good quality films have been extruded with a gauge of 1/10 mil ( $5 \times 10^{-4}$  lb/ft<sup>2</sup>). Such materials are part of a program leading toward an advanced passive satellite, one example of the need for such ultra-light-gauge films.

For balloon applications, Sea-Space uses these lightweight plastics as the raw materials to fabricate the MERFAB family of fiber-reinforced, composite polyethylene-derivative balloon films. MERFAB is produced in widths up to 12 feet and can be programmed for strength to 40 lbs/inch. The strength of the composite film is a straightforward manufacturing problem dependent upon the type of reinforcing fibers and the fiber spacing. With such lightweight materials, float

altitudes in excess of 150,000 feet are a definite capability. Figure 1 shows a MERFAB balloon inflated in its launcher. With balloons capable of such high float altitudes, many scientific experiments waiting to hitchhike on somebody else's rocket launch, or which are being shelved because of the high costs of a booster, can be executed at a fraction of the cost of a rocket. These are the payloads Sea-Space Systems is interested in flying. Recently two successful MER N balloons of  $1.25 \times 10^6 \text{ ft}^3$  were flown by Mr. Al Shipley of NCAR from Page, Arizona. Two launching methods were used for these balloons, one the Sea-Space approach with a covered shroud as shown in Figure 1, and the second a conventional launch with a clutch.



Figure 1. MERFAB 1-1/2 Million-Cubic-Foot Balloon Inflated in SSS Launcher

Both of these two flights were successful, each carrying a 25-pound instrumentation payload. The first balloon reached an estimated 150,000 feet;

the precise altitude was not verified due to instrumentation problems. The float time was approximately 7 hours. The recent MER N flight launched last Thursday reached an altitude in excess of 150,000 feet verified by extrapolated data from a hypsometer. Flight time was approximately three hours when the balloon, still at float altitude, was lost both optically and by telemetry.

Examining these balloons in greater detail: the MER N design was a natural shape,  $1.25 \times 10^6 \text{ ft}^3$  balloon weighing approximately 91 pounds. Gore length was 200 feet and maximum diameter was 138 feet. Theoretical altitude with a 25-pound payload was slightly greater than 150,000 feet. By way of comparison, a  $6 \times 10^6 \text{ ft}^3$ , 1/2 mil conventional PE balloon could also carry 25 pounds to 150,000 feet; or a  $9 \times 10^6 \text{ ft}^3$ , 3/4 mil conventional balloon would have the same performance as the MER N  $1.25 \times 10^6 \text{ ft}^3$  balloon.

I would like to mention one unusual fact about MERFAB as a balloon film, specifically its cold-brittleness characteristics. This material in light gauges has been tested in a NASA twistflex machine in liquid nitrogen. After 300 severe twisting and flexing cycles at  $-323^\circ\text{F}$ , when the tests were stopped, the material had not failed and showed no apparent damage. Tests in liquid hydrogen are in process by NASA at present. In addition, on one flight a MERFAB balloon ascended with no difficulty through a  $-97^\circ\text{F}$  tropopause with a wind shear of approximately 56 knots in 7,000 feet of altitude. So we at Sea-Space feel rather confident that MERFAB balloons do not have any cold-brittleness problems.

Over the past several years, Mr. Tom Kelly of CRL has supported the development of MERFAB and is presently sponsoring work leading to the next generation of large MERFAB balloons. In this program will be a  $3.5 \times 10^6 \text{ ft}^3$  balloon capable of lofting a 100-pound payload to 150,000 feet or a 35-pound payload to 154,000 feet. A new  $4.5 \times 10^6 \text{ ft}^3$  balloon will loft a 25-pound payload to an altitude of 158,000 feet or a pressure less than 1 mb. Flight testing balloons with these capabilities is forecast.

Two subjects that always come up about balloons are the cost and the reliability. Of the large (over a million cubic feet) MERFAB balloons which have been successfully launched, two out of the three achieved their performance objective and reached 150,000-foot altitude with the specified payload. Further reliability data will be a subject of keen interest to us all. As for costs, on the basis of carrying a specified payload to an altitude in excess of 135,000 feet, a MERFAB balloon is no more expensive than a conventional taped polyethylene balloon. As a matter of fact, it might be cheaper when you put the cost of helium, transportation, and so forth, into the dollar equation.

I would now like to show you two MERFAB balloon flights, one sponsored by Mr. Vin Lally of NCAR and the other by Mr. Henry Demboski of the Office of Naval Research. (A movie of MER N and MER P launches followed.)

In addition to ground launch of such conventional-vented balloon systems as we saw in the movie, Sea-Space has air-launched from a Cessna 195 airplane a MERFAB balloon with a train over 200 feet long as a part of an SSS research effort. The inflation equipment and launch technique are capable of the air launching of a number of kinds of balloons as well as rather substantial size systems. Other type balloons air launched with this unit have been neoprene, nylon and conventional polyethylene. A balloon fabricated with Sea-Space's new composite polypropylene balloon film, S-FAB, was also designed to be used with this unit and has been flown several times. Figure 2 shows an S-FAB research balloon. Patent applications covering this system are in process.



Figure 2. S-FAB Research Balloon

Dr. Elliott, our neighbor at China Lake, has covered the advances in tethered-balloon technology at NOTS. Sea-Space has also been involved in

tethered-balloon work, and is very much interested in programs of this nature. As far as we know, Sea-Space is the only corporation that has fabricated and successfully flown a tethered instrumentation balloon in a nuclear event. The balloon lofted an instrument array weighing 800 pounds to 1200 feet. Our recent tethered-balloon work has been associated with designing lift vehicles for long-term tether at altitudes of 100,000 feet and above. Again MERFAB gives us a very competitive performance advantage. SSS Fiberglass SPACECABLE, developed for balloon tethering, is currently being used on spacecraft being prepared for earth-orbital launch during the next year.

In conclusion, the balloon industry has a real challenge in meeting the needs of the Space Age. Free balloon float altitudes in excess of 150,000 feet will allow scientists to gather much astrophysical data at a fraction of the cost of a rocket launch, with far less complexity than that of a Cape Kennedy launch operation, and in the future, it is hoped, with greater reliability than with any satellite systems. MERFAB balloons have the potential of lofting significant payloads to altitudes in excess of 160,000 feet. MERFAB balloon flights to date have demonstrated their capability of high-altitude flight. Hopefully, this capability can be a building block in the science of ballooning and create a tool useful for scientists in extending man's knowledge of the universe.

## XI. Heat Transfer Considerations of Instrumentation Packages at High Altitudes \*

A. Piacentini  
Lehigh University  
Bethlehem, Pennsylvania

K. Lindenfelser  
Air Force Cambridge Research Laboratories  
Bedford, Massachusetts

D. Dube  
The B. F. Goodrich Company  
Akron, Ohio

### Abstract

A theoretical method for designing thermal packages used to house instrumentation carried aloft by high altitude balloon vehicles was developed. Because of the odd package shapes and the constantly varying boundary conditions, a numerical method of analysis was employed for the solution of the heat transfer equations. This approach allows the consideration of all pertinent variables, but its complexity requires a large number of computations. Accordingly, the problem was programmed for solution on a high-speed electronic digital computer. The computer program was initially written for a rectangular parallel package. Temperature distributions calculated from the flight simulation program were compared to temperature distributions measured on actual balloon flights. It was concluded that the method developed is a reliable one.

---

\*This talk was based on material contained in an AFCRL in-house report to be published June 1965.

## XII. A New Material Capability for the Balloon Field

R. S. Ross  
Goodyear Aerospace Corporation  
Akron, Ohio

### Abstract

It is quite readily recognized and understood that in the development field, each new advance in hardware is closely related to the material from which the component is fabricated. As improvements in materials are found, even further advances in performance are possible.

This has been particularly true in the balloon field where material improvements have resulted in new gas tightness for longer endurance flights and lighter weight for higher altitude capabilities. The material development to be discussed here consists of a means for obtaining balloon components in predetermined shapes so as to permit relative movement between the balloon and the surrounding air. The performance improvement could, therefore, be in stability, drag reduction or increased lift. The specific application will determine how this material can best be used and the amount of improvement in performance that can be expected.

Manufacturing machinery and fabricating techniques are now being evaluated that will permit greater rate of climb for free balloons and increased lift and stability for tethered balloons, which could result in altitude capabilities above those possible by static lift alone.

**PRECEDING PAGE BLANK**

## 1. INTRODUCTION

In engineering circles, it is common knowledge that there is often a close relationship between advanced developments and improvements in materials. However, it is not definitely established which must come first, the new material that makes the application practical, or the solution to the problem, which necessitates the development of better material properties. In any event, a material improvement always opens up problem-solution possibilities whether or not they are immediately apparent. This paper discusses a new fabrication technique, which can be the basis for a new material development. A few possible applications for such a material are illustrated as a stimulus for even further problem solving.

Originally, the machinery to be discussed here was developed with a space application in mind. This material was to encounter high loads and high temperatures. These properties are not needed for balloon applications, so it will be important to understand the basic fundamentals of the material construction itself and how it evolved. This paper, therefore, includes the development of the basic material, a brief description of possible future material, and a few examples of how these materials might be used in applications for increased performance. The engineer dealing in advanced developments will readily see the potential of this new technique.

## 2. BASIC FUNDAMENTALS

This particular paper will concentrate on pressurized structures since they are most applicable to balloon problems. However, rigidized variations of the techniques are also possible. Originally the balloon designer was limited to using shapes which are of conventional pressure-vessel contour, such as spheres, spheroids (oblate or prolate), ellipsoids, toroids, cylinders, cones, and so forth, and combinations of these. In order to simulate a flat surface, several cylinders were joined together making a multilobed arrangement containing webs. The greater the number of webs, and the closer the spacing, the smaller the surface lobes, and the more nearly a flat surface was simulated. Figure 1 illustrates pictorially this evolution of the cylinder toward a flat surface.

A number of years ago, a material called Airmat was invented which permitted the making of flat panels by replacing the multiple webs described above by a great number of closely spaced "drop threads". The carpet looms on which this material was woven were modified to permit increased drop-thread lengths (3 inches to 24 inches) and even variation in drop-thread length to be produced. The cloth woven

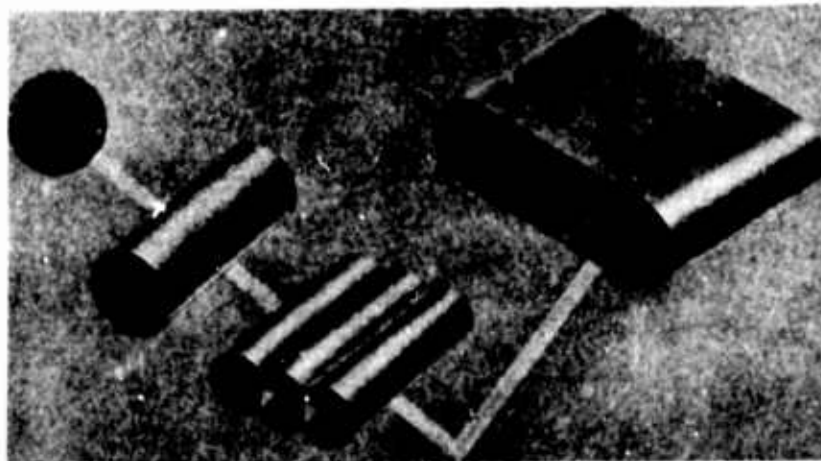


Figure 1. Expandable Structural Forms

on the looms was covered with neoprene to make it gas-tight, and these pressure vessels became some of the world's lightest structures. Airfoils were actually produced and in the mid-50's complete aircraft called Inflatoplanes were constructed and flown. Wing weights one-tenth of those previously possible by conventional construction were achieved. Figure 2 shows how variations in drop-thread length can define airfoil contours.



Figure 2. Airfoil Contours Defined by Variations in Drop Thread Length

The modified carpet looms used for this work had the advantage of high-speed production capability, but they lacked the versatility and quality control required for

aircraft applications envisioned. Goodyear Aerospace Corporation research and development programs, therefore, included the fabrication of a special pilot loom to permit the use of a wide variety of fibers at very precise weave arrangements. This loom was the forerunner of the giant Air Force loom just completed. This latter piece of equipment is all automatic, numerically controlled, and capable of making Airmat shapes large enough to be of interest to the balloon industry. When the pilot loom shown in Figure 3 was constructed, it was the largest of its type, being capable of weaving basic flat panels six inches thick and sixty inches wide with high precision. This piece of equipment was quite versatile and many of the fabrication techniques developed later were checked out on it. Figure 4 shows the larger loom developed by GAC for the Air Force. It is actually 17 feet high, 80 feet wide and 125 feet long and is capable of weaving Airmat in widths up to 21 feet.



Figure 3. Pilot Loom

The loom is so large it must be housed in a special high-bay area. It was designed to be able to make giant wings for space booster systems capable of flying back to earth through the high-heating re-entry corridors. It, therefore, is capable of handling high-temperature metal filaments such as stainless steel or Rene' 41, as well as other types of fibers. Drop-thread lengths or wing thicknesses of eight feet or bigger are possible. The coatings to achieve gas-tightness, of course, are then compatible with the fibers used and the environments to be encountered.

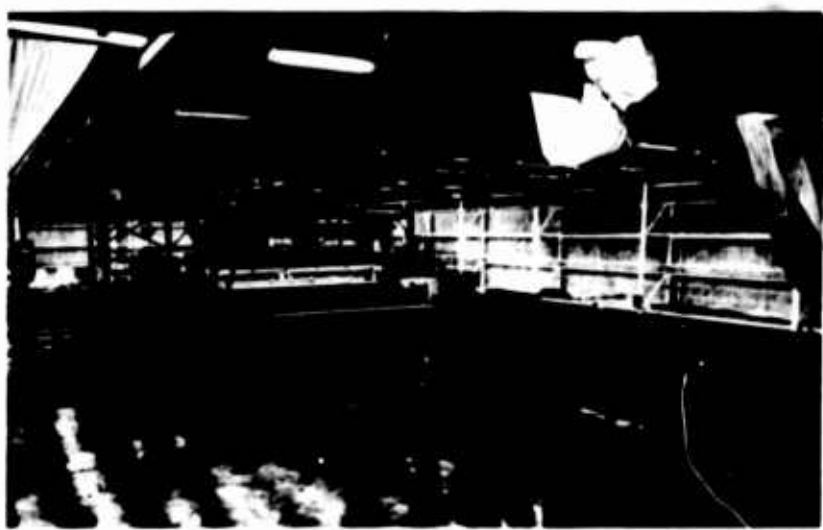


Figure 4. Air Force Loom

To the balloon designer, large sizes are most attractive because they mean large volumes and increased static-lift capability from the gas displacement of air. Now that Airmat structures of giant dimensions are possible, it is worthwhile to review possible applications and material choices to see if balloon-performance capabilities cannot be improved through the use of new materials.

### 3. APPLICATION

Perhaps the first place to look for a possible application would be the replacement of current structures using the web and lobe construction such as the tails of conventional barrage balloons or even the new high-lift, highly-stable Vee-Balloon, shown in Figures 5 and 6 respectively. Their aerodynamic performance can be improved by permitting the choice of good airfoils in place of simulated ones. Even the rigid tail surfaces of powered airships can be replaced by this structural technique. Studies show not only a possible weight savings, but also an improvement in safety because an overload on a pressurized tail surface can only result in a deflection and not a failure. (Current airship tail surfaces are already one of the most efficient aircraft structures ever made from a strength/weight standpoint, so meeting or beating this value is definitely a step forward.) Figure 7 illustrates the largest nonrigid airship built. It had a volume of 1,500,000 cubic feet and used tail surfaces which were fabric-covered metal framework that is typical of what could be readily replaced with the new structural material.

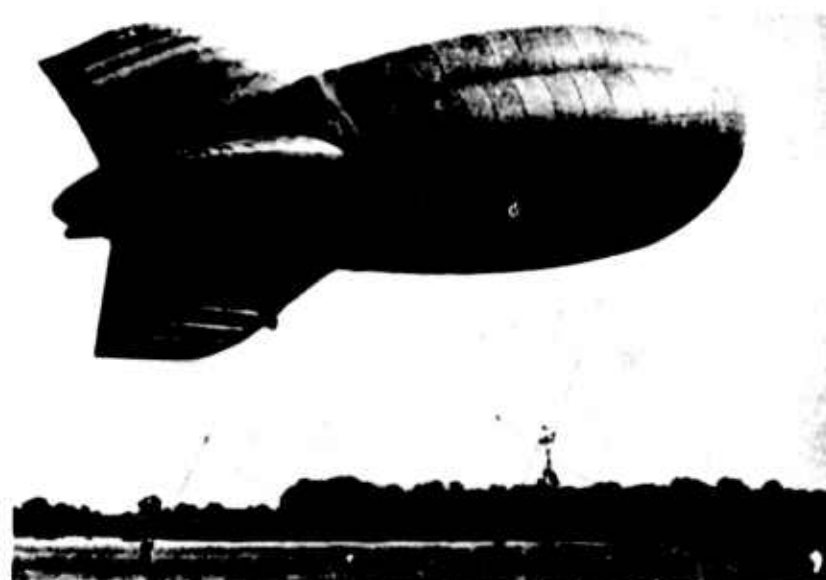


Figure 5. Conventional Barrage Balloon



Figure 6. Vee-Balloon



Figure 7. Nonrigid Airship with Volume of 1,500,000 Cubic Feet

In an attempt to determine where this structure might be employed in the future for applications not yet in existence, one might first examine the free balloon. It is not possible to improve much on the surface-to-volume ratio as far as the lifting gas is concerned. However, to improve the rate-of-climb of a free balloon, it might be advantageous to add tails for stability, and permit it to rise as a pressurized streamlined vehicle. Figure 8 illustrates graphically the size relationship between the spherical shape and a streamlined one of the same volume, while Figure 9 represents how a lobed tail could be replaced by a streamlined one for this application.

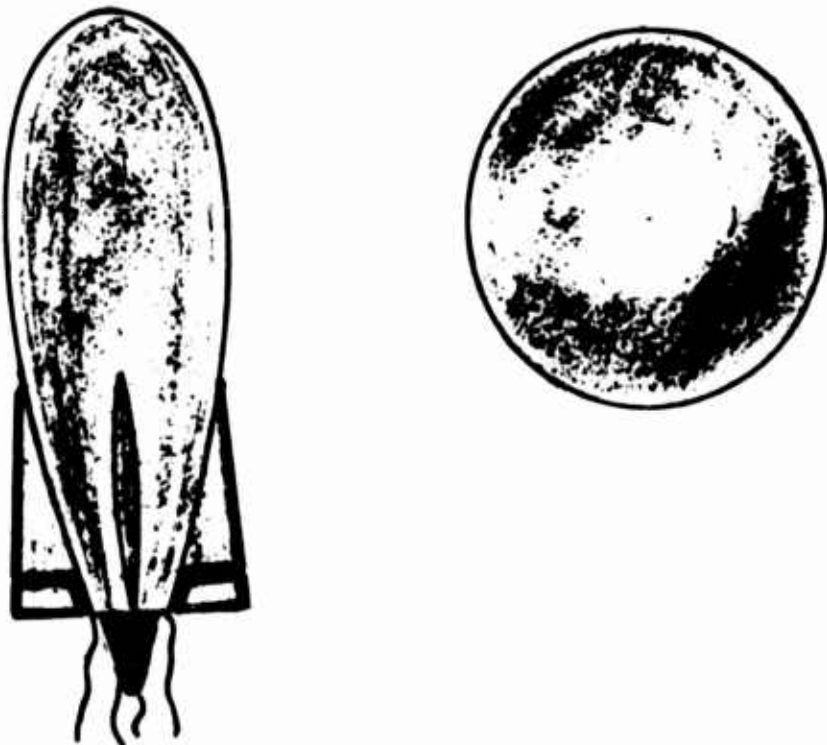


Figure 8. Aerostats of Equal Volumes

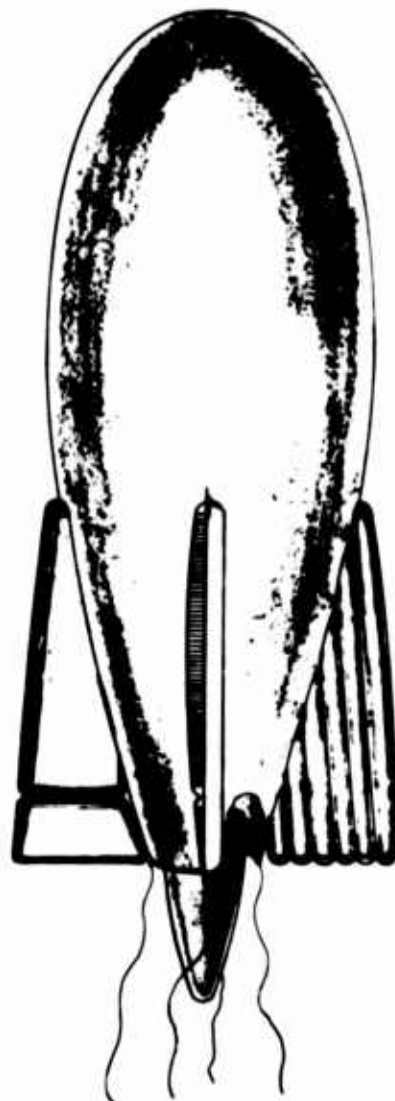


Figure 9. Streamlined Tail Replacing Lobed Tail

This approach will readily permit an increase in rate-of-rise of 4 to 1 for the same amount of excess lift, because of the reduction in drag of the new shape compared to a spherical pressure vessel. Obviously, the specific speeds and vehicle contours would depend upon the mission configuration. However, preliminary estimates of typical applications do not show 10 and 15 percent gains, but 350 and 450 percent increases, thus warranting further investigation regardless of the accuracy of detail features.

As mentioned earlier, the replacement of the multilobe control surface or stabilizer of tethered balloon tails by a new lightweight Airmat construction would permit better streamlining. This would not only result in improved aerodynamic performance from increased lift and reduced drag values, but it would also improve the structural integrity of the component, minimizing the regions of high stress, by distributing the load-carrying ability more effectively.

Because of the size potential now made practical by the giant Airmat loom, it is feasible to consider the extension of this tail construction concept to lifting surfaces beyond the tail alone. Applied to a tethered balloon in a wind or to a powered free balloon such as an airship, the increased lift possible by the application of high-lift surfaces will permit operations at altitudes not possible using the static lift of the gas alone. The effect of a lifting surface or increase in aspect ratio is readily illustrated by the large difference in dynamic lift shown by the Vee-Balloon when compared to a conventional single hull shape.

Studies have been made of ways to increase the payload or endurance of airships by means of the multilobe concept, and 40% improvement is readily possible. This same lift increase can be employed to drive an airship to heights greater than that attainable by static lift alone. With increase in span and aspect ratio, the resulting aerodynamic performance improvement again yields even higher altitude capabilities. In Figure 10, a plot of altitude vs velocity is used to illustrate qualitatively the increases possible as more and more of the required lift is handled dynamically by wing-type surfaces. In the past, vehicles for achieving these heights had to be of multilobed construction (see Figure 11) since great-depth Airmat was not yet feasible. Now, however, machinery large enough to fabricate giant wings is available and it needs only to be employed. The configuration, size, power source, range, and so forth, obviously are mission determined. But now new tools are available for vehicle design and construction.

#### 4. NEW MATERIAL POSSIBILITIES

Using the simplified formulas of Figure 12 it is possible to readily determine the magnitude of the forces and material weights required for any specific application. Although these do not take into account secondary loadings, which might be critical in a particular instance, at least an indication of the feasibility of utilizing the Airmat structural technique is presented. In the actual construction of a vehicle or component, such additional factors as deflection, gas permeability, environmental effects (humidity, temperature, ultraviolet exposure, and so on), scuff resistance, flexibility, and surface contour itself will be considered.

However, in order to obtain some idea of the strength and weight potentialities of lightweight Airmat, perhaps a sample calculation will illustrate the area for consideration. Assume, for instance, that an Airmat material is to be woven with top and bottom surfaces made of Dacron and weighing 1 oz/square yard each. Material of this weight has a tensile strength of approximately 30 to 40 pounds per inch. Being conservative, and using 30 in the equation given in Figure 12, and considering a section of a tail surface on a balloon with a wing loading of 1 pound per square foot, and a

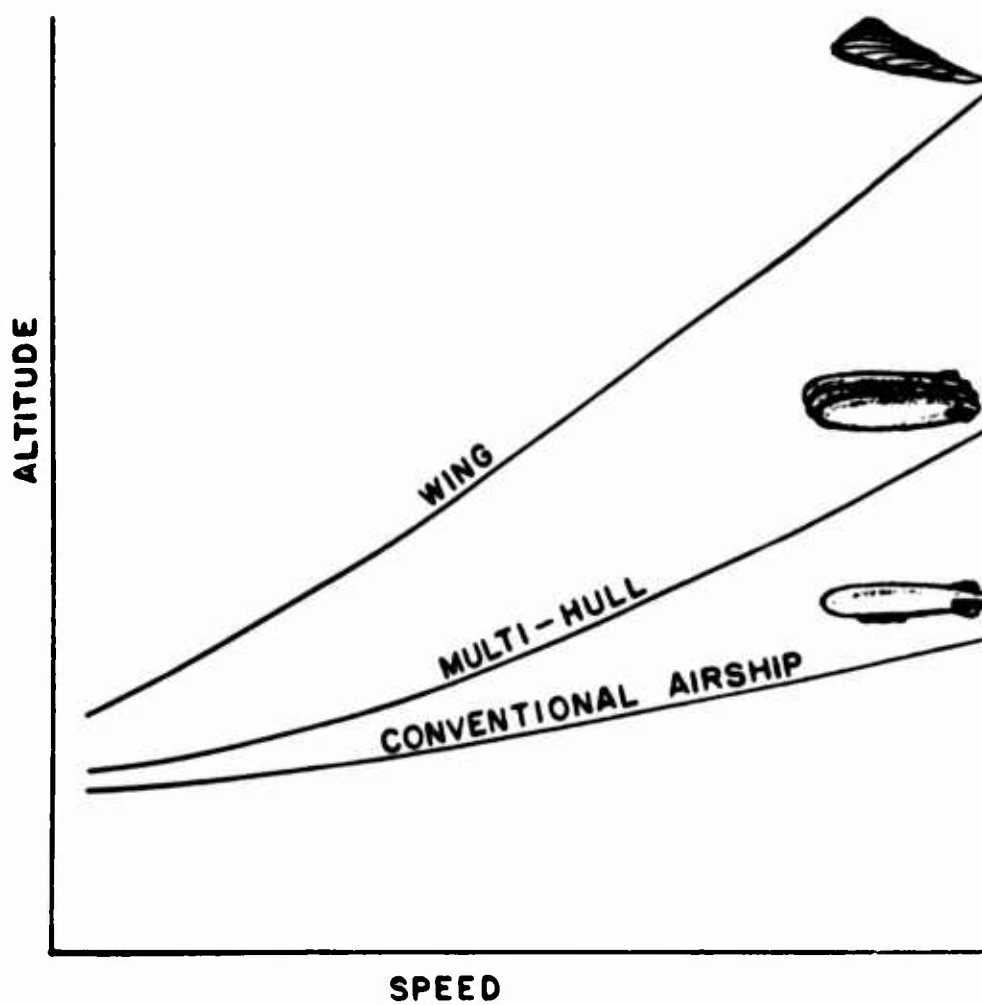


Figure 10. Improvement in Aerodynamic Performance Made Possible by the Use of Wing-Type Surfaces

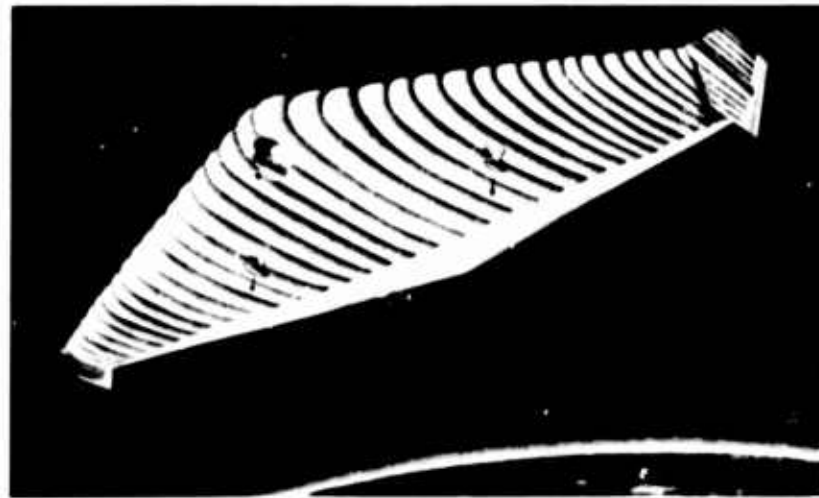
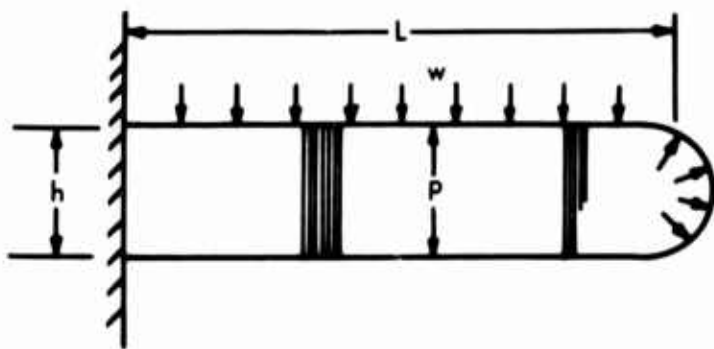


Figure 11. High-Altitude Aircraft-Multilobed Construction

Internal Pressure

$$p = \frac{2M}{h^2}$$

M = bend. mom./unit width

For uniform load on cantilever

$$M = \frac{wL^2}{2}$$

$$p = \frac{wL^2}{h^2}$$

Unit Skin Weight

$$W_s = p h n k$$

Drop-thread Weightper Unit Area

$$w_d = phnk_d$$

n = factor of safety against quick-break

k = weight/quick-break strength (ratio of the coated fabric @ 2:1 biaxial stress ratio)

$k_d$  = weight/quick-break loop strength (ratio of drop threads)

Figure 12. Formulas for Determination of Magnitude of Forces and Material Weights Required for Specific Applications

section span of 25 feet, with a wing thickness of 5 feet, it can be found that a pressure of only about 4-1/2 inches of water is necessary to support the load in a cantilever fashion. (This includes a safety factor of 3.)

If one were to similarly consider a wing loading of 10 pounds per square foot for the airplane-type vehicle, a unit skin weight of about one-half pound per square yard would be required. This is only about a tenth of a pound per square foot for total wing weight - far below that possible with any conventional structural technique. The pressure required to support this beam would be about 1-3/4 psi, again a very realistic value.

The two wing loadings examined and shown to be practical, above, 1 and 10 pounds per square foot, are extreme enough to illustrate the great potential of the concept. Specific mission configurations will probably fall well within these extremes. Materials such as Dacron, nylon and fiberglass can readily be considered as the strength-bearing fibers while fibers such as Mylar or even thin coatings of polyurethane might be used as the gas-retention barrier. Seaming techniques and attachment systems now employed in the balloon field will permit the assembly of components of the vehicle. However, the important fact to realize here is that the material made by the new weaving machinery is in itself an assembly of surfaces predetermined in shape and strength with no weight penalty for the fact that its strength members are each placed so that they are being loaded optimally.

Airmat material is already being employed in a great number of applications where its packageability features are used to advantage. It appears that this fabricating technique can now be considered for balloon applications where ultra-lightweight Airmat will permit the construction of efficient shapes for improved aerodynamic performance.

### XIII. Application of a Tethering System to a Specific Requirement

Michael S. Kretow  
Holloman Air Force Base  
New Mexico

It is hoped that before the end of 1965, an assault will be made on the moon with Surveyor, a squat three-legged derrick of piping and scientific equipment being built by Hughes Aircraft Company. Conversations about Surveyor usually begin with, "If you think Ranger was tricky . . ." and quickly point to the complexities of a "soft landing".

The Surveyor flight plan to the moon calls for a transit time of 60 hours. It includes firing a 10,000-pound-thrust retro-rocket to slow itself down, and delicately throttling three small vernier engines to complete braking and lock the legs in a down position. Surveyor is supposed to land on the moon with no more of a jolt than a parachutist feels on hitting the earth.

Among the less spectacular phases of this program, yet a very vital and necessary phase, was testing the impact characteristics of this vehicle. This involved retro-rocket and stabilization-hardware performance. So that a moon environment could be approximated a tethered balloon test bed was considered; this satisfied the basic philosophy which was to have a short drop with insufficient time for drag to build up. It also meant the balloon had to be precisely positioned 1200 feet above a fixed point to realize maximum optical coverage and a reasonable measure of safety for participating personnel. One could say that the tethered

balloon test bed provided the user with a tower having no structural impediments or with a hovering helicopter without vibration and atmospheric turbulence.

These Surveyor tests generated some rather special meteorological requirements. Approximately seven hours prior to drop, a layout direction for the drop must be provided, so that the winch-equipped vehicles can be positioned. This direction is based on the wind flow at the tethering altitude at sunrise. A balloon-layout direction must also be provided for the initial balloon release.

The seven-hour forecast for the sunrise direction is particularly tricky, because the winds are generally shifting from a nighttime to a daytime flow.

The surface-temperature inversion must also be carefully monitored, because a strong inversion will reduce the effective free lift of the balloon. Wind shear just above the inversion may sometimes generate an especially prohibitive barrier. Pibals are released at the launch site every 30 minutes, in order to facilitate forecasting of these parameters.

The Balloon R & D Test Branch located at Holloman AFB, New Mexico, currently employs a rather unique method for providing a stable and accurately-positioned platform for pre-flight and soft landing tests of the NASA Lunar Surveyor vehicle.

In order to achieve the aforementioned stable platform and to allow the Surveyor vehicle to be dropped free of any possible entanglement with tethering lines and to impact within 50 feet of ground zero, three winch-equipped trucks are employed. The tether lines form a triangle and are secured to the bottom end fitting of a balloon. The Surveyor vehicle is suspended beneath an open parachute that is also tied to the same bottom end fitting.

After the Surveyor vehicle pre-flight testing has been completed, the balloon with its payload is ready for release and reel-up. Following inflation and release from the roller arms, the balloon is restrained through the use of an explosive-type release device at the end of a crane boom. When the release is fired, the balloon rises to about one hundred feet and is then restrained by the three tether lines. At this time, the winch operators are given the command to begin reel-up.

As the balloon is being reeled-up, the problem is to contain the balloon vertically over ground zero; this is accomplished through a simple but precise positioning system. Two 20-power telescopes are gimbal-mounted, with one being located on a base line which goes through ground zero and the other on a line perpendicular to it. Electrical resolvers are mounted on the telescope axis. The telescopes are boresighted to ground zero for reference on both resolvers. The resolver output is fed into an analog computer that in turn drives the X Y pens of a plotting board. The X data are also presented on two 4-inch, zero-centered meters which are calibrated in ten-foot increments.

One meter represents East-West deviation from ground zero while the other meter represents North-South deviation from ground zero. The Y data are presented on a third meter which also reads altitude in increments of 10 feet.

Using this means of determining the X Y position of the test vehicle, the only other problem remaining is that of conveying the information to the winch operators. Each winch truck is equipped with a VHF/FM radio-telephone set. The Field Test Director observes the X Y meters and the plotting board and then directs the reeling operation.

With experienced crews operating the winches, it has been found that about twenty minutes are required to position the balloon at 1200 feet over ground zero. With the balloon finally positioned the operation is then turned over to the Surveyor Test Director or Project Manager.

After the vehicle has been dropped and the area cleared, the balloon is lowered for a repeat performance. At this time, the up-wind winch truck is driven toward ground zero until its tether line is slack enough to be placed in a sheave anchored in concrete at ground zero. After the truck is slowly backed to its original position, the reel-down continues until the balloon and its train can again be secured to the crane boom.

In summary, the balloon tether phase of Project Surveyor has proved to be relatively straightforward. This is but one specific requirement which was attacked through the use of a balloon envelope as a low altitude platform.

## XIV. Design Considerations for Soft Landing of Balloon Payloads

J. P. Jackson  
Vitro Laboratories  
Division of Vitro Corporation of America  
Silver Spring, Maryland

### I. METHODS OF ENERGY ABSORPTION

There are quite a number of techniques for absorbing the energy of a payload's impact with the earth or sea, and these methods can be grouped into the five following classes:

- a. Material Deformation
- b. Gas Compression
- c. Mass Acceleration
- d. Friction
- e. Chemical Energy

The differences in the choice of techniques within these classes are to be found chiefly in efficiency (under which heading I will include weight, cost, or whatever factor is of primary concern to the user) and in that technique's applicability to the limiting conditions of a particular case.

For example, some primary considerations in the selection of an energy absorption system would include:

Required energy dissipation capacity (defined as foot-pounds of energy absorbed per pound of device)

**Impact velocity****Deceleration, maximum and average**

**Deceleration - Onset rate** (As the name implies this is simply the rate at which the deceleration builds up to its peak value. Fairly limited data are available on the limits for man and equipment for this factor, but it should definitely be considered in manned systems.)

**Mechanical considerations****Weight****Size and Shape****Stroke****Stability****Landing terrain****Orientation of landing****Reliability**

Before getting into the specifics of ballooning, I would like to briefly cite some examples of each of the five classes of energy-absorption methods. Probably the most familiar to all of us are the Material-Deformation Systems.

From Figure 1 we can see that the chief use of paper honeycomb lies in the lower impact velocity range, although metal honeycomb can extend that range somewhat. One of the difficulties with honeycomb is in its directional properties, about which I will say more later.

Figure 2 shows another example of a material-deformation device. The foamed plastics and balsa wood can increase both the velocity range and the capacity of this class of methods.

The primary advantages of these systems are that they are simple, very reliable, and require no complex actuating devices. Not to be ignored is the fact that they are also relatively inexpensive.

Gas bags, depicted in Figure 3, offer the designer considerable flexibility in obtaining specific desired values of deceleration and deceleration-onset rate. Various methods can be used to control the gas pressure and each method has its own advantages and disadvantages. One of the chief disadvantages of gas bags, however, arises from this very flexibility. Once the bag has been designed to satisfy a specified set of conditions, it can tolerate very little deviation from those conditions without serious effects. At present gas bags are relatively expensive compared to material-deformation devices, and they too suffer from directional properties.

Under the heading of mass acceleration I have shown in Figure 4 aerial snatch and the impact spike. Naturally, an indispensable requirement in these techniques is auxiliary equipment in a proper location, or a prepared, or at least selected, landing surface.

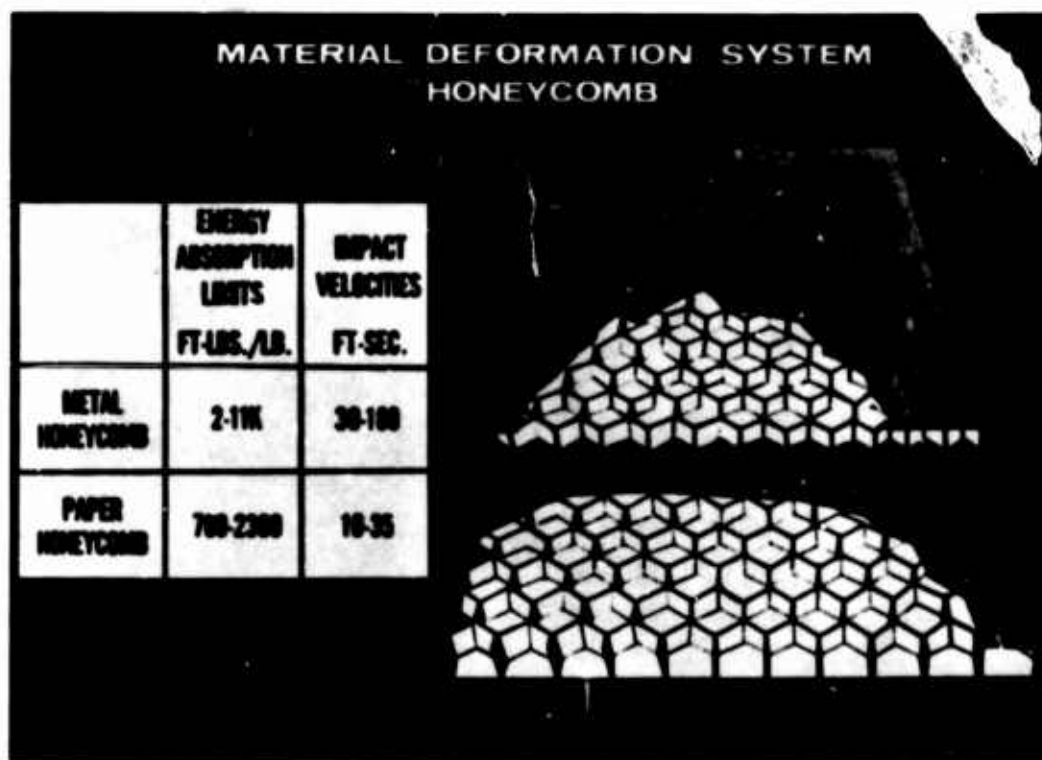


Figure 1. Material-Deformation System Honeycomb

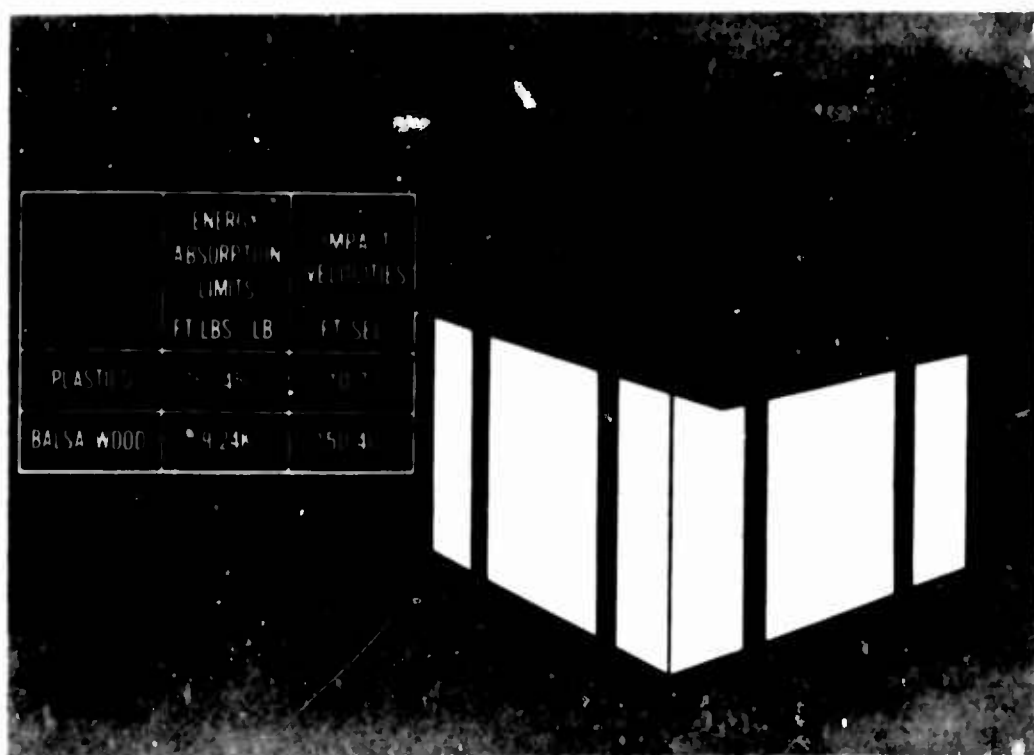


Figure 2. Material-Deformation System Foamed Plastic

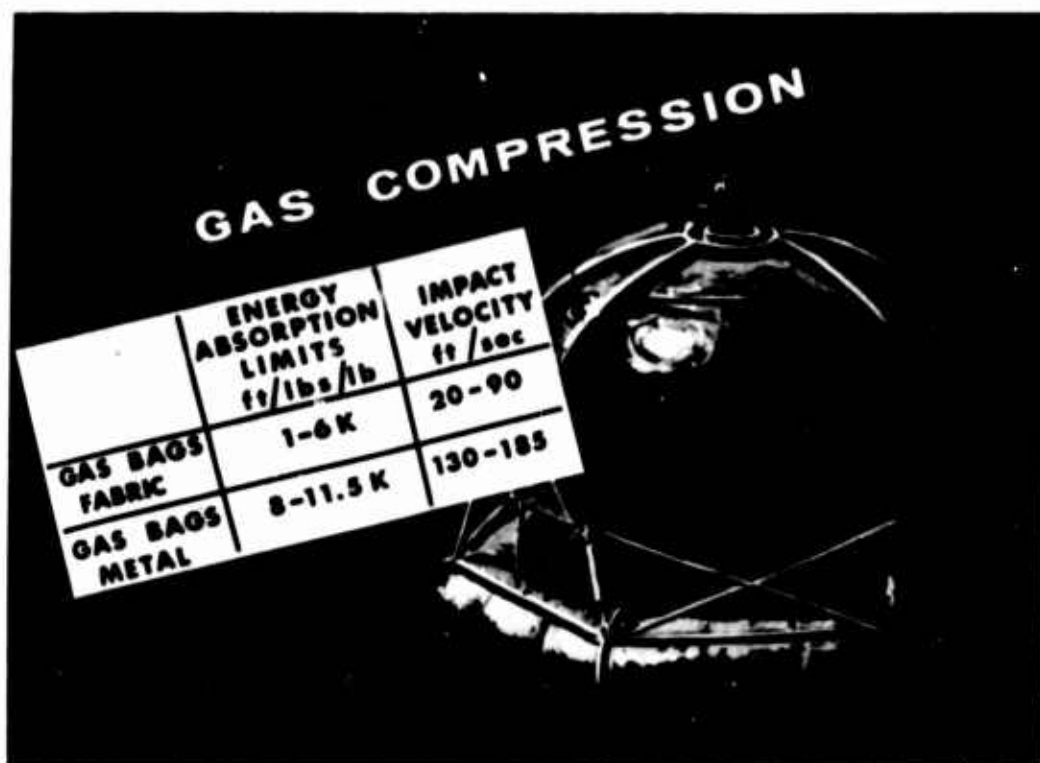


Figure 3. Gas Compression



Figure 4. Aerial Snatch, Spike

In the technique of absorbing energy by friction, exemplified in Figure 5 by a frangible tube, we have one of the most promising developments to come along in some time. This and other devices using similar principles offer a great increase in the range of energy-absorption capacity, and I believe we will be seeing more and more of these devices.

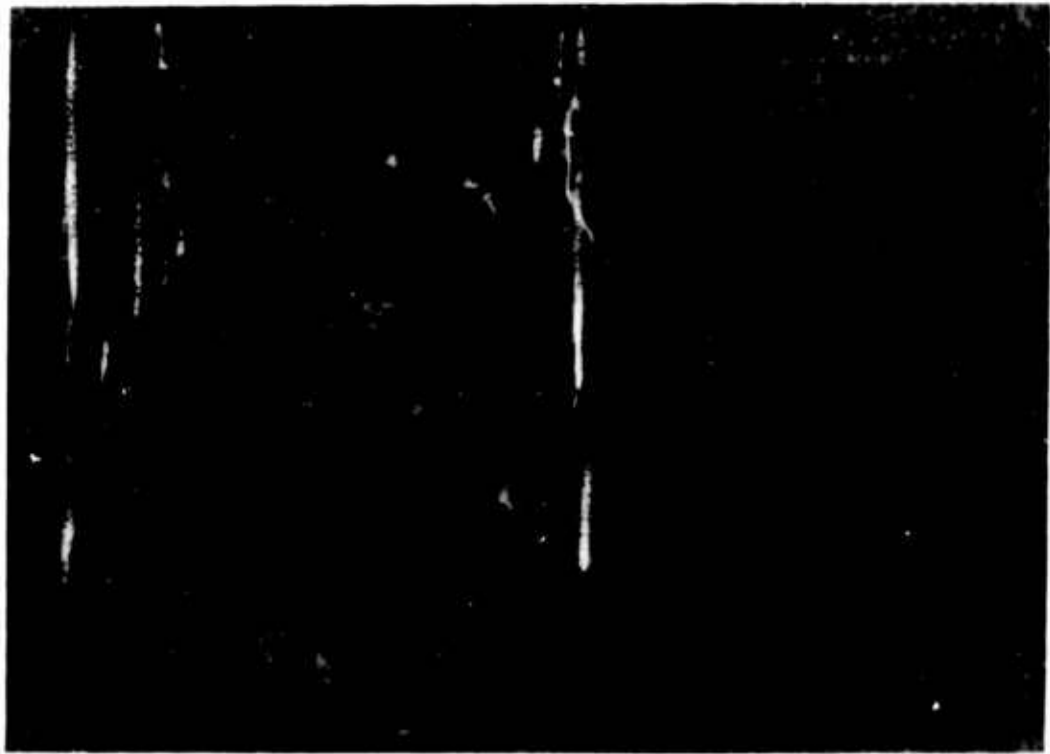


Figure 5. Frangible Tube System

Naturally, the chief advantages to the Retro Rocket shown in Figure 6 are that deceleration and deceleration-onset rate can be maintained at relatively low values, and the length of stroke is not a problem, as it is in all of the other systems considered. Retro rockets do, however, require careful timing and thrust control, and they are comparatively expensive.

Now for ballooning. For reasons of cost, reliability, simplicity and availability the majority of balloon users have selected material-deformation devices. In view of this I will direct the remainder of my discussion toward this method of energy absorption.

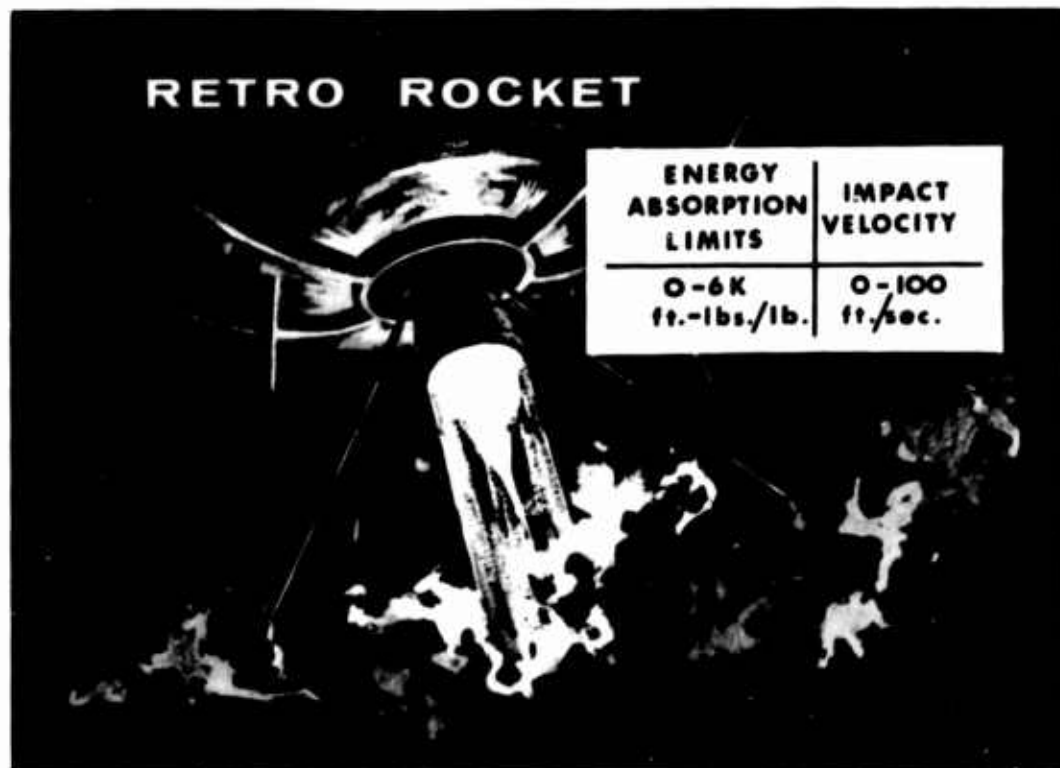


Figure 6. Retro Rocket

## 2. PHYSICAL PRINCIPLES OF MATERIAL-DEFORMATION SYSTEMS

It has been shown (and I am sure you will agree upon close examination) that the Stress-Strain curve is the single most useful device for examining the properties of a prospective energy-absorbing material. If you will now refer to Figure 7 you will note that the "Ideal" Stress-Strain characteristic implies a material which deforms at constant force, to zero final thickness. This "Ideal" material would therefore subject a payload to a constant deceleration and would possess no rebound energy. It also has an infinite deceleration-onset rate which isn't so "Ideal" from that point of view. But naturally, the "Actual" Stress-Strain curve depicted is more nearly the type encountered. Now using a typical stress-strain curve for paper honeycomb as shown in Figure 8 as an example, I would like to point out significant characteristics for the designer of a crash pad. The use of any given material depends upon the joint selection of two factors: first, the "footpad" area of the device which will determine the peak stress to be encountered (here stress in its classical definition is force per unit area, and is represented by  $S_m^1$  on the curve); and secondly, the strain, or percentage deflection, which determines the total energy capable of being absorbed in that deflection (represented by  $\epsilon_1$  on the curve). Most designers have found that the "optimum strain"  $\epsilon_o$  on the curve) is that point at which the stress

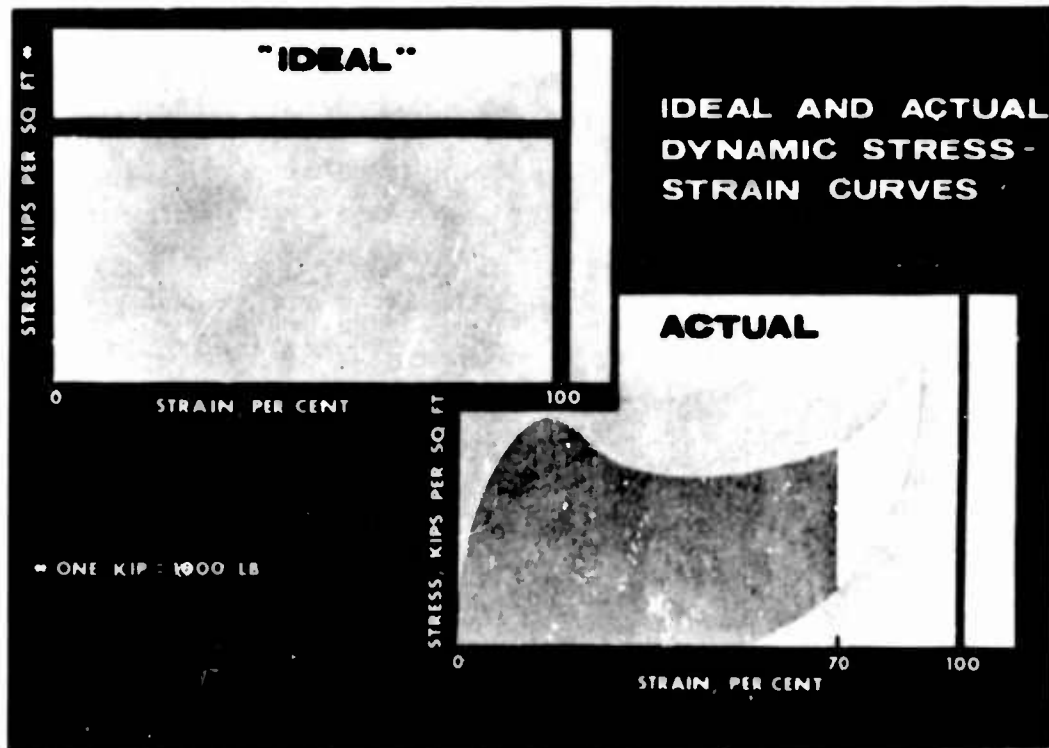


Figure 7. Ideal and Actual Dynamic Stress-Strain Curves

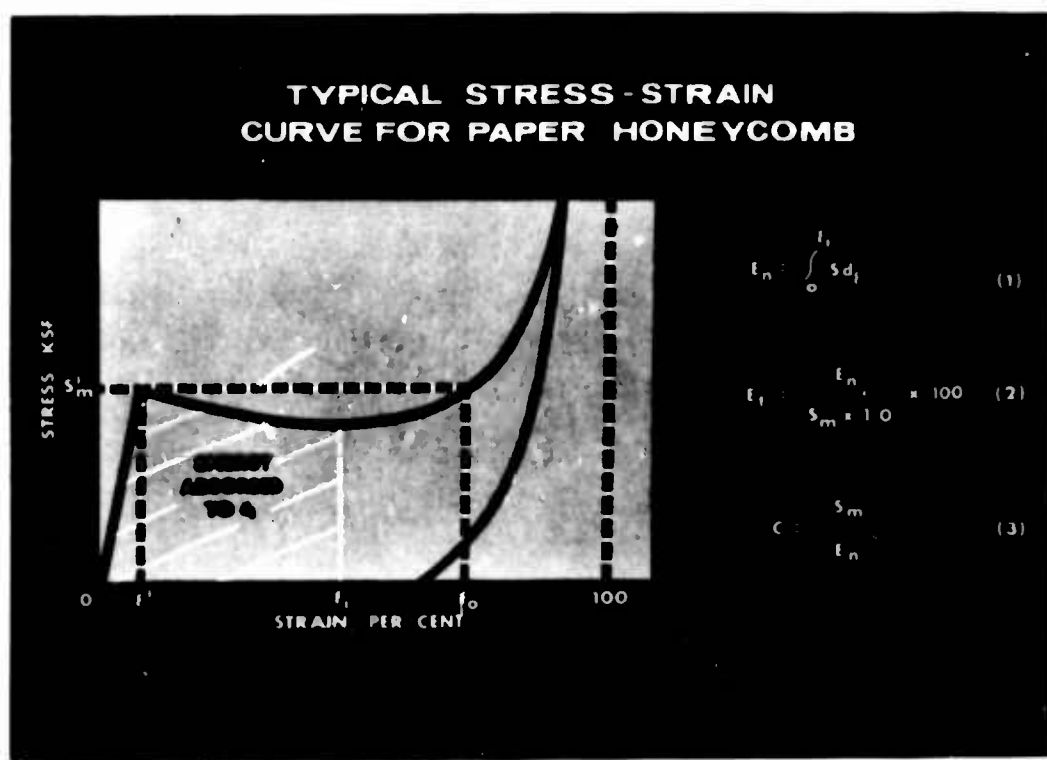


Figure 8. Typical Stress-Strain Curve for Paper Honeycomb

again equals the peak stress initially encountered. As you see from the curve, the rebound energy associated with the selected value of strain can also be determined by computing the area under the curve between the point of maximum strain, and the trailing end of the curve.

Now, still referring to Figure 8, let us consider for a moment the efficiency of our pad. Equation (1) defines the energy absorbed per unit volume. Then if we define 100-percent efficiency as represented by an "Ideal" material which crushes at constant stress (denoted by  $S_m$ ) to zero final thickness, Eq. (2) defines our "Thickness Efficiency." Some authors have found it convenient to define another term, the so-called "Cushion Factor" of a material, which as you can see from Eq. (3) is simply the reciprocal of "Thickness Efficiency",  $E_t$ . You can see from the equation that the lower the value of Cushion Factor, the lower the stress, and therefore the softer the material.

With that background we should now be ready to design a crash pad. We start with the parameters: the cushioning material, the payload weight, the peak allowable acceleration, and the expected impact velocity; and first determine the "footpad" area. Referring to Figure 9 you will notice that the area, A, the peak stress,  $S_m$ , and the allowable acceleration, G, may all be varied to suit the peculiarities of the problem. And naturally the peak stress establishes where you will have to work on the stress-strain curve. Next, we determine the necessary thickness of the pad by solving the basic-energy-conservation equation, where the total energy absorbed by the pad is equated to the kinetic energy of the system plus the work done in deforming the pad. Solving this equation for the thickness, t, gives the equations illustrated. I would like to point out in the first energy equation that if the equivalent drop height associated with the kinetic energy term is large (say ten times as large) compared to the distance of travel associated with the work term, the work term is usually ignored. Also, the expression for thickness of an "Ideal" pad is usable if your stress-strain curve is essentially rectangular, as most curves for paper honeycomb are.

### 3. MATERIAL-DEFORMATION DEVICES

Consider, now, two of the most common materials used for crash pads by the balloon industry.

Refer to Figure 10. Probably the most widely used material is paper honeycomb. It can be purchased in a variety of configuration, it has a respectable looking stress-strain curve (high efficiency and low rebound), it is reliable and mechanically simple to apply, and on top of this it is inexpensive. It does, however, possess certain limitations; for example, if the payload oscillates so that the longitudinal

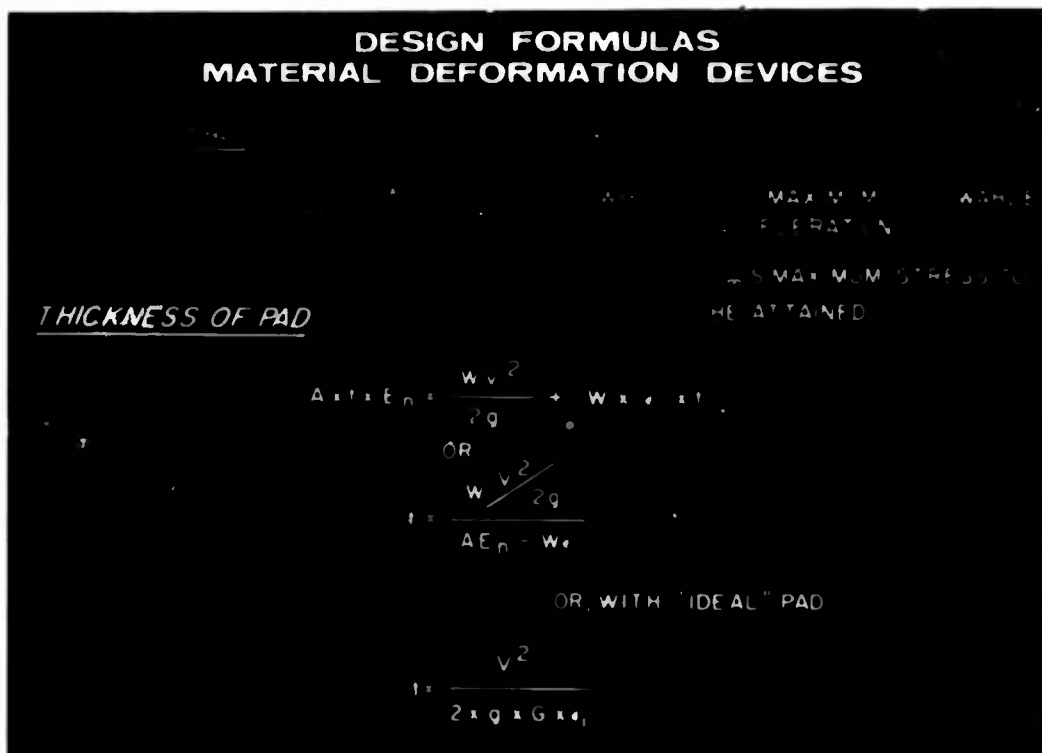


Figure 9. Design Formulas Material-Deformation Devices

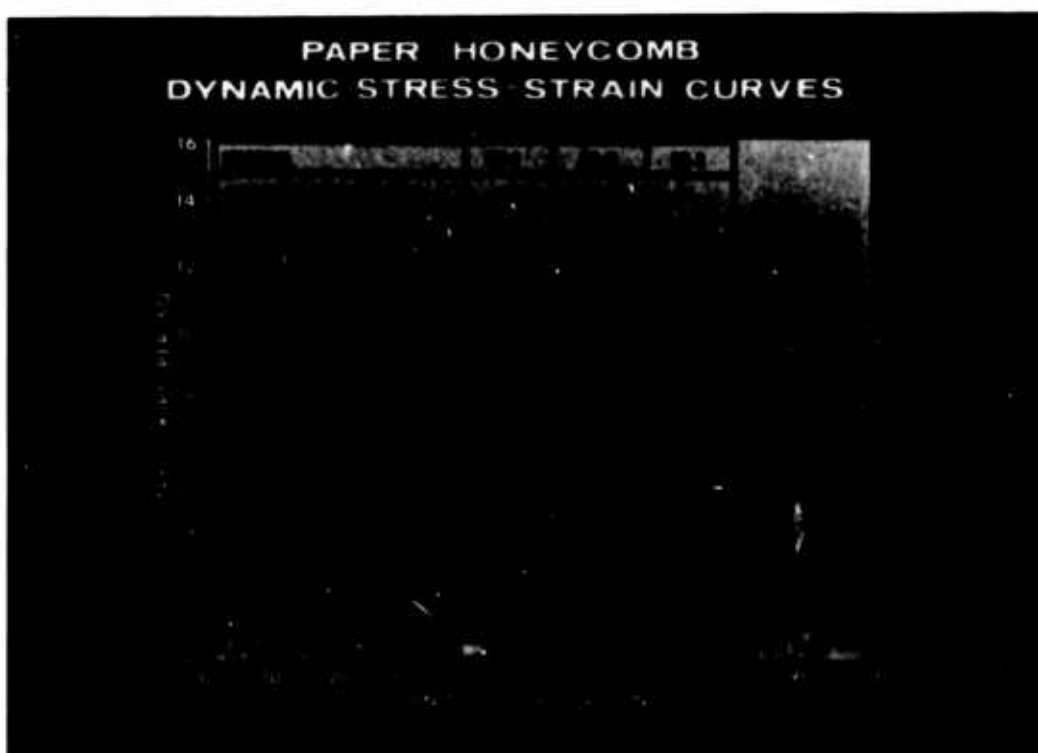


Figure 10. Paper Honeycomb Dynamic Stress-Strain Curves

axis of the cells is misaligned as much as 15 degrees from a perfectly vertical impact, the honeycomb may lose as much as 25 to 30 percent of its energy-absorbing capability. The simple "flat circular canopy" parachute has an advertised oscillation of up to  $> 25$  degrees. Another disadvantage, not often encountered in ballooning, is the limited energy-absorption range of paper honeycomb.

Now refer to Figure 11. Another material sometimes used is foamed plastic. Here, you can see, Styrofoam also possesses a good-looking stress-strain curve and has most of the same mechanical advantages found with honeycomb. I would rate the plastics slightly higher than honeycomb in their ability to accommodate a nonvertical landing, and you can usually find a higher range of energy-absorbing capability in plastics. The disadvantages of plastics should cause you to examine carefully the rebound energy and the shear strength of the specific material being considered. Also some plastics allow loss of their contained gas after long exposure to a hard vacuum and this could change their energy-absorbing characteristics.

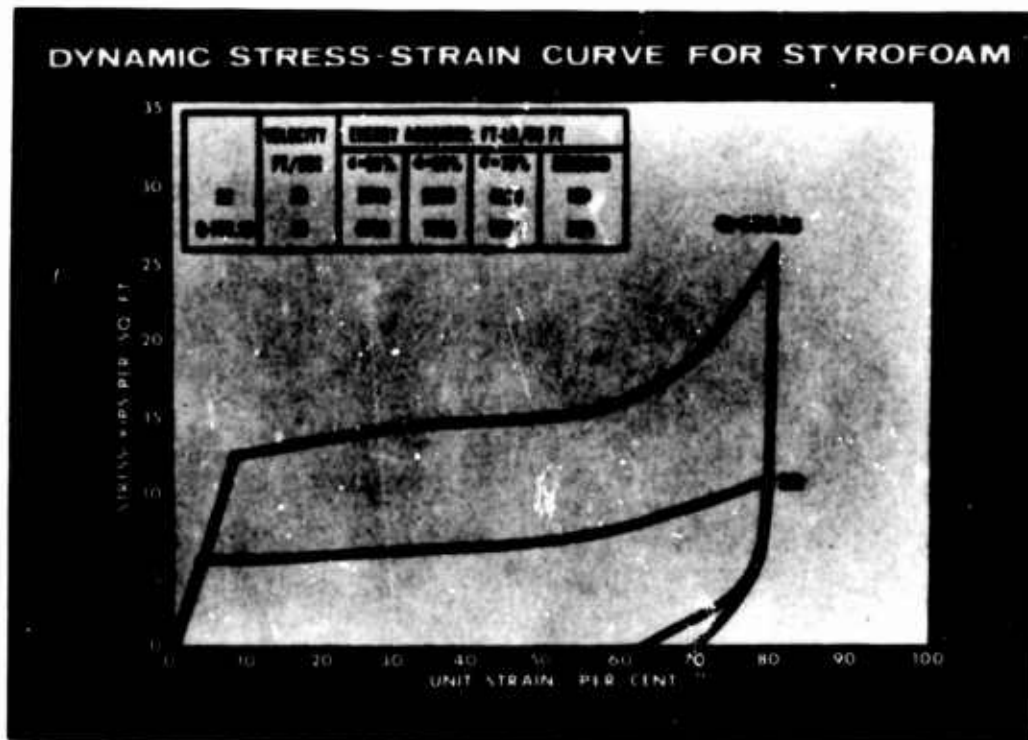


Figure 11. Dynamic Stress-Strain Curve for Styrofoam

Just for comparison, refer to Figure 12, which shows a typical stress-strain curve for Aluminum honeycomb. In general, within a comparable range, Aluminum offers no weight saving over paper; it has the same directional limitations for

orientation at impact, and is more expensive. It does improve the energy-capacity range somewhat, however.

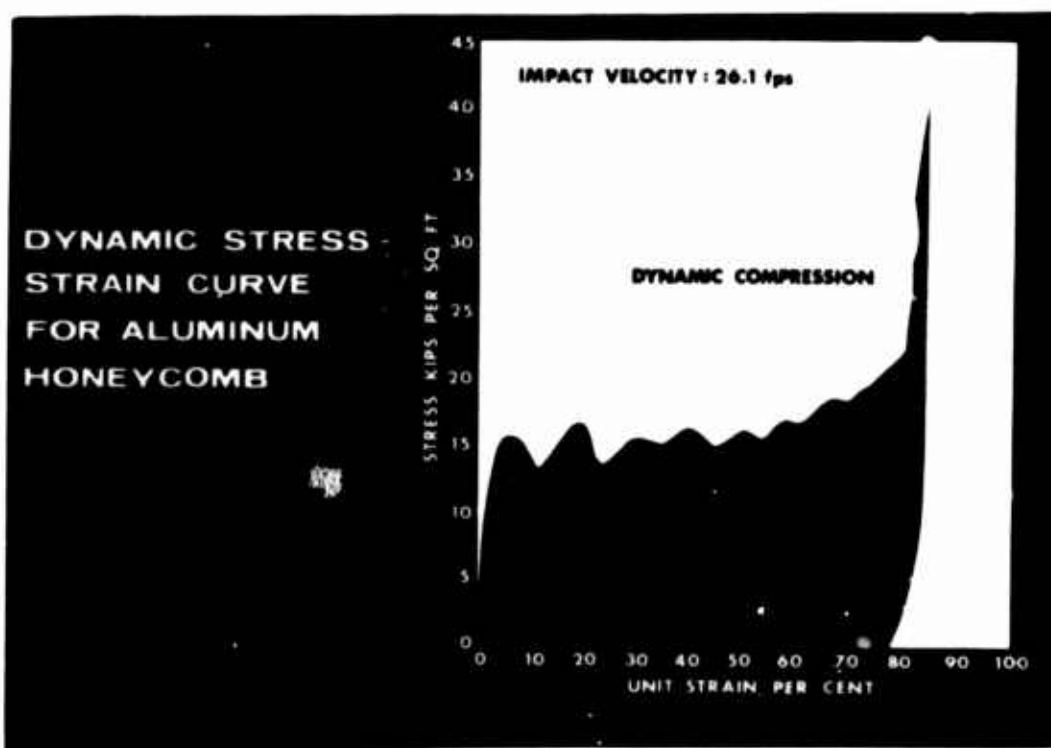


Figure 12. Dynamic Stress-Strain Curve for Aluminum Honeycomb

#### 4. STRATOSCOPE II CRASH PAD SYSTEM

Stratoscope II is at least one case where the mechanical configuration of the payload determined in large measure the final choice and design of the crash pad. Of course, weight has always been critical, and reliability was of utmost importance. By referring to Figure 13 you will see other considerations. First, the initial impact should be borne by the azimuth frame which is the "backbone" of the telescope. This means transferring the force across the "knuckle" about which the telescope pivots. The pad can employ no shifting mass which might upset the telescope's balance about this knuckle. A fairly low "G" factor of two or three was specified. The impact velocity might vary from 10 feet-per-second with a controlled valve, down to as much as 16 to 18 feet-per-second with the emergency parachutes. Landing can occur in the presence of surface winds as high as 20 knots, and with a variable amount of residual ballast.



Figure 13. Stratoscope II

Material-deformation devices were a fairly straightforward choice once the advantages and disadvantages of the other classes of devices were considered. We investigated both paper honeycomb and several plastics and chose a plastic because the honeycomb seemed to offer no significant weight or cost advantage, and suffered from the limits on nonvertical landings described before.

The Stratoscope II crash pad has evolved as a result of a series of changes in the payload weight. Initially conceived as 4500 pounds, it is now 7300 pounds. Our first crash pad tested was made of Styrofoam 22, and the test results showed that this material required a footpad area-to-thickness ratio somewhat too small to accommodate the buckling forces associated with the horizontal wind drift to be anticipated.

In our search for a plastic which would give us an acceptable area-to-thickness ratio as well as the low peak stress desired, it was decided to test Armalite.

This material is one of a variety of foamed plastics which were developed primarily as insulation materials. Tests with the Armalite were encouraging, so a new pad was designed of it, incorporating several innovations to help solve the problem of nonvertical landings. An idea suggested by our Program Technical Director, Dr. Schwarzschild, was to have the pad carry along its own sliding surface. In this way we hoped to absorb by friction some of the horizontal component of the

impact energy while giving the pad time to absorb the vertical component before buckling. Straps were placed around the pad to assist in containing any chunks of foam which might break off.

Figure 14 shows the present Stratoscope II Crash Pad. An aluminum sheet is inserted above the 4-inch-thick lower pad and provides the sliding surface just mentioned. The lower pad is held on by relatively weak bungee so that some motion of that pad is permitted. You will notice the center of the foam is cored out to give the desired footpad area.

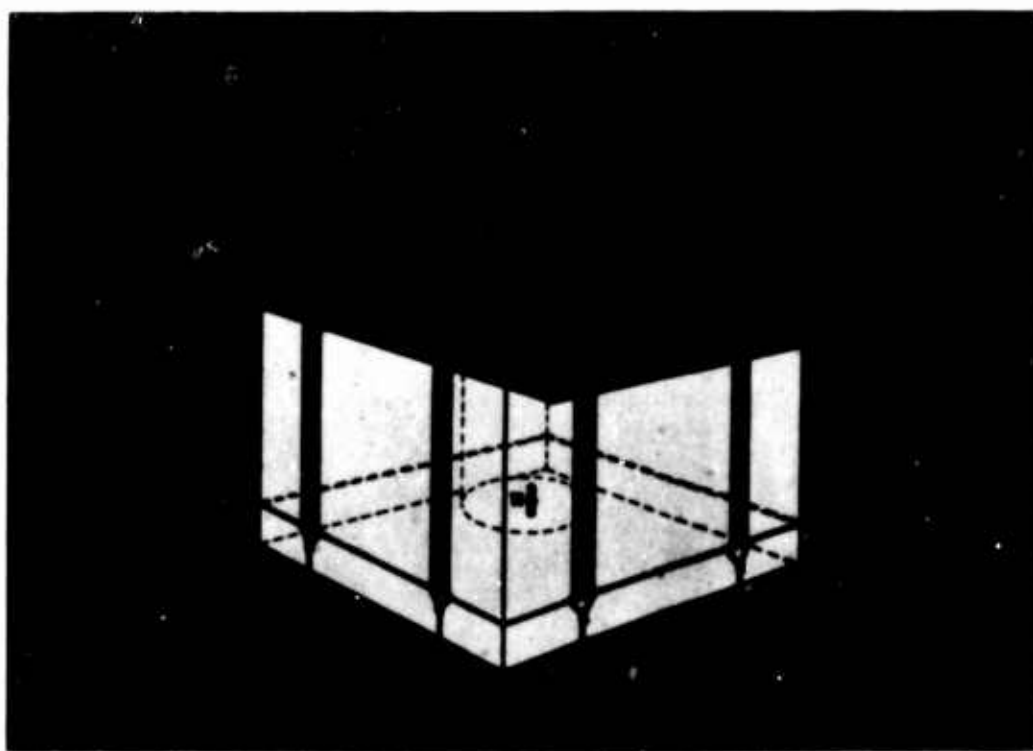


Figure 14. Stratoscope II Crash Pad

On the first scientific flight an 8000-pound load was landed on parachutes at an impact velocity of about 16 feet-per-second. Horizontal motion was negligible and Figure 15 shows the pad after impact. These artists' renditions, by the way, are based on the reassembled pieces of the pad after impact. The initial volume of this pad is about 16 feet<sup>3</sup>. The acceleration applied to the telescope was calculated in this case to be slightly less than 4 g's.

On the second scientific flight the 8000-pound payload was controlled to a landing at about 12 feet-per-second. There was very little horizontal motion but we landed on the side of a hill and in Figure 16 you can see the uneven compression.

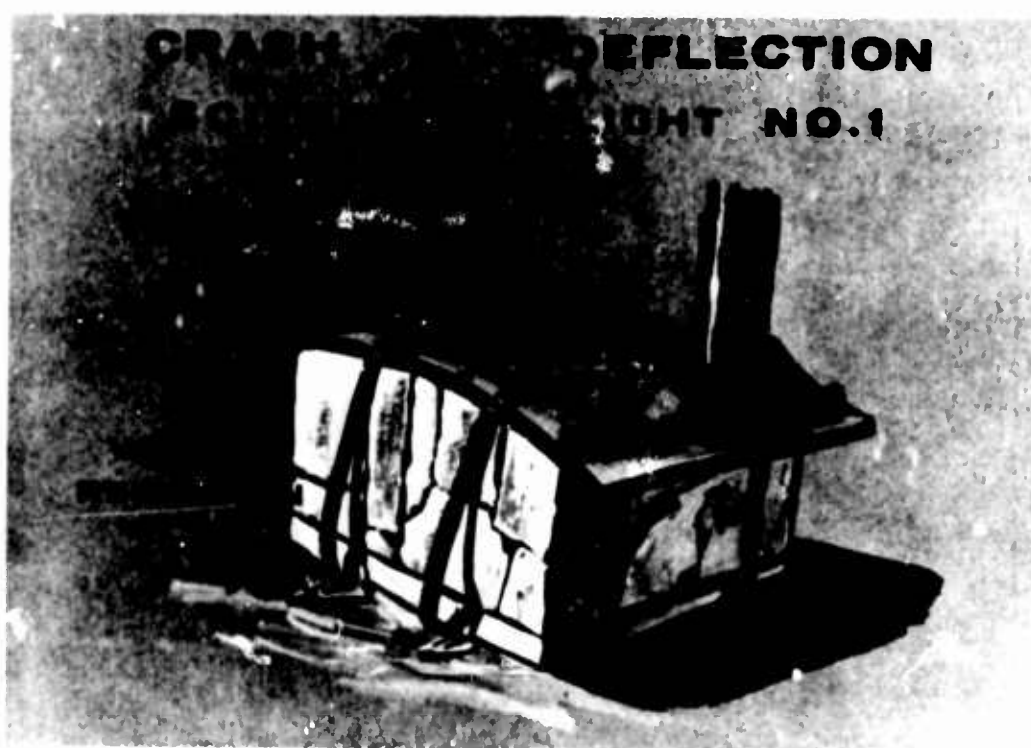


Figure 15. Crash Pad Deflection Scientific Flight No. 1

**CRASH PAD DEFLECTION  
SCIENTIFIC FLIGHT NO. 2**

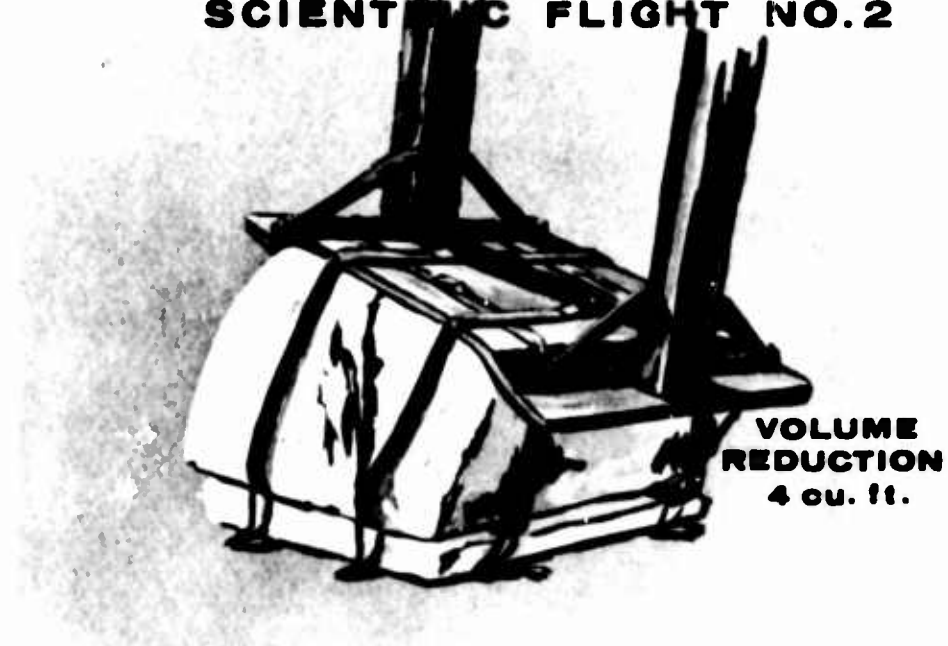


Figure 16. Crash Pad Deflection Scientific Flight No. 2

The initial volume was again 16 feet<sup>3</sup>, and acceleration to the telescope was calculated here to be slightly less than three g's.

One feature I would like to point out is the deformation of the metal floor of the crash pad. This is by design, since we wanted as much of the weight of the pad as possible to contribute to energy absorption. In this case the floor absorbed about half as much energy as the foam.

In closing I would like to say that the Stratoscope II Program would still be receptive to other materials which might offer advantages over Armalite, and we are looking with interest at the future development of friction devices.

## References

- Ali, A. (1957) Dynamic stress-strain characteristics of various materials, Cushioning for Air Drop, Part VIII, Structural Mechanics Laboratory, The University of Texas, Austin, Texas.
- Ali, A. and Benson, L. R. (1957) Bibliography of literature pertaining to the absorption of impact energy, Cushioning for Air Drop, Part IX, Structural Mechanics Research Laboratory, The University of Texas, Austin, Texas.
- Ali, A. and Benson, L. R. (1960) Energy Absorption Properties of Aluminum Honeycomb, Hexcel Products TSB-110, Hexcel Products, Inc., Berkeley, California.
- Esgar, J. B. (1962) Survey of Energy-Absorption Devices for Soft Landing of Space Vehicles, NASA TN D-1308.
- Fisher, L. J., Jr. (1961) Landing-Impact-Dissipation Systems, NASA TN D-975.
- Jones, R. E. and Hunzicker, D. L. (1954) Calculating Cushion Thickness by Analysis of Stress-Strain Curves, WADC Technical Report 53-334, Wright Air Development Center, Wright-Patterson Air Force Base, Ohio.
- Karnes, C. H., et al. (1959) Energy-Absorption characteristics of paper honeycomb, High-Velocity Impact Cushioning, Part V, Structural Mechanics Research Laboratory, The University of Texas, Austin, Texas.
- Kellicutt, K. (1952) Application of the Properties of Cushioning Materials in the Design of Cushions, Forest Products Laboratory Report No. R 1527, Madison, Wisconsin.
- Turnbow, J. W., et al. (1955) Cushioning for Air Drop, Part I, Structural Mechanics Research Laboratory, The University of Texas, Austin, Texas.
- Turnbow, J. W., et al. (1956) Characteristics of paper honeycomb under dynamic loading, Cushioning for Air Drop, Part III, Structural Mechanics Research Laboratory, The University of Texas, Austin, Texas.
- Turnbow, J. W. (1957) Characteristics of foamed plastics under dynamic loading, Cushioning for Air Drop, Part VII, Structural Mechanics Research Laboratory, The University of Texas, Austin, Texas.

## XV. Temperature Measurements from Floating Balloons

W. C. Wagner  
Air Force Cambridge Research Laboratories  
Bedford, Massachusetts

The main problems in the measurement of ambient air temperature from floating balloons are (1) the change in the air temperature caused by heat exchange with the balloon system and (2) the heat exchange of the sensor with the air and the radiation field.

The heat exchange of the balloon system with the air is dependent on the balloon dimensions, balloon movement, the balloon material and the radiation field. It can change the temperature field considerably. In Figure 1 is shown a scaled-down model of a balloon in a liquid where the Grashoff number is of the same order of magnitude as that of a balloon of medium size at high altitude. The temperature difference between the balloon and the air as in the model of Figure 1 corresponds to the condition of a mylar balloon at night. The temperature differences for polyethylene balloons are usually smaller due to the lower absorption coefficient of polyethylene in the infrared range. The balloon wake in this case is not so strong and breaks up at a shorter distance from the balloon. At daytime the balloon skin temperature is usually somewhat warmer than the air temperature. This will affect the area around the gondola when the balloon is slowly rising. The area around the gondola is therefore not a good place to measure the air temperature and a better place would be 2 to 3 balloon diameters below the balloon. The wind shear

**PRECEDING PAGE BLANK**



Figure 1. Wake of Balloon Model

is very often strong enough to carry the wake from the vertical line. Because the thickness of the boundary layer increases with the size of the object, one should keep the dimensions of any structure near the place of measurement as small as possible. As an example, Figure 2 shows a thermistor holder that is designed to be suspended on a long, thin cable. Acoustic thermometers have usually too large dimensions in the neighborhood of the measuring path and are therefore not very



Figure 2. Thermistor Holder

suitable for use with floating balloons. Radiative temperature measurements are not affected by the balloon wake, but expense, weight, and power consumption of the instrument are, up to now, prohibitive. In addition, the field of view is quite large at high altitudes. For these reasons immersion sensors have been used nearly always in floating balloon projects.

The heat exchange of the sensor with the air and the radiation field is described, for a bead thermistor, by the equation:

$$h S(T - T_a) + \frac{\pi d^3/2}{\pi h_w} (T - T_a + \frac{\sigma \alpha}{h_w}) h_w^{1/2} \lambda^{1/2} K - \alpha \sigma S_q + C \frac{dT}{dt} = 0 \quad (1)$$

- $h$  = Heat transfer coefficient for bead
- $h_w$  = Heat transfer coefficient for wire
- $T$  = Bead temperature
- $T_a$  = Air temperature
- $d$  = Lead diameter
- $\lambda$  = Thermal conductivity of the wire
- $S$  = Surface of bead
- $S_q$  = Axial cross section of bead
- $C$  = Heat capacity of bead
- $\sigma$  = Radiation intensity

- $\alpha$  = Effective absorptivity of bead surface  
 $K$  = Function of many parameters including binding post temperature, lead length, air pressure, and so on.

NB  $\cdot K \approx 1$  for  $\lambda \leq 31 \frac{\text{Watt}}{\text{C}^{\circ} \text{cm}}$ , and length  $\geq 0.5 \text{ cm}$ .

$t$  = Time.

The first term describes the convective heat exchange with the air; the second term, the heat exchange with the holding wires; the third, the radiative heat exchange; and the last term is caused by the lag of the sensor because of its heat capacity. For simplicity, the terms for the self-heating by the measuring current and the aerodynamic heating are left out. If Eq. (1) is rearranged to solve for  $(T - T_a)$ , which represents the error in measuring  $T_a$ , then it is clear that increase of the 3rd and 4th terms in Eq. (1) means increase of the error  $(T - T_a)$ . However, increase of the coefficient of  $(T - T_a)$  in the first and second terms in Eq. (1) means decrease of error. It is therefore desirable that the sensors have as high a heat transfer coefficient as possible. The fact that the second term can help to reduce the error, if the leads are not too short (that is,  $K > 0$ ), is often overlooked. The main source of error is the radiation described by the 3rd term in Eq. (1). This term is written in more detail in the following expression:

$$\alpha S_q \mathcal{F} = \alpha_s S_q \mathcal{F}_s + \alpha_i S \sigma (1/2 T_{\uparrow}^4 + 1/2 T_{\downarrow}^4 - T^4) .$$

Order of magnitude	$0.14 \frac{\text{Watt}}{\text{cm}^2}$	$0 \text{ to } 0.01 \frac{\text{Watt}}{\text{cm}^2}$	(2)
--------------------	--	--	-----

- $\mathcal{F}_s$  = Radiation intensity for visible range  
 $\alpha_s$  = Absorptivity for visible range  
 $\alpha_i$  = Absorptivity for intra-red range  
 $\sigma$  = Stephan Boltzmann constant  
 $T_{\uparrow}$  = Effective black-body radiation temperature of environment above sensor  
 $T_{\downarrow}$  = Effective black-body radiation temperature of environment below sensor.

The first term of Eq. (2) gives the absorption from the visible range of the solar radiation; the rest describes the infrared heat exchange. Because the value of  $S$  is about 4 times larger than  $S_q$ , the second term on the right side of the equation may be as large as 1/3 of the first term if  $\alpha_s = \alpha_i$ . It is therefore advisable to choose a coating the emissivity of which is small in the visible range as well as in the infrared range. Aluminum coating has a nearly uniform emissivity of 0.04 to 0.08 for freshly

deposited coatings. This will deteriorate with time when exposed to air and much more so if the air is humid and dusty. To take full advantage of the high reflectivity of the aluminum coating, it is therefore good practice to keep the element in a sealed, nitrogen-filled container until shortly before the launching.

The heat transfer is dependent on the ventilation velocity as long as we stay in the continuous flow region. The heat transfer coefficient shown in Figure 3 for ventilated and unventilated sensors was computed for the temperatures of the standard atmosphere. The effect of the ventilation decreases with decreasing pressure and can be neglected below 1 mb for sensors smaller than 5-mil diameter. In many considerations that follow, the ventilation velocity is assumed to be zero.

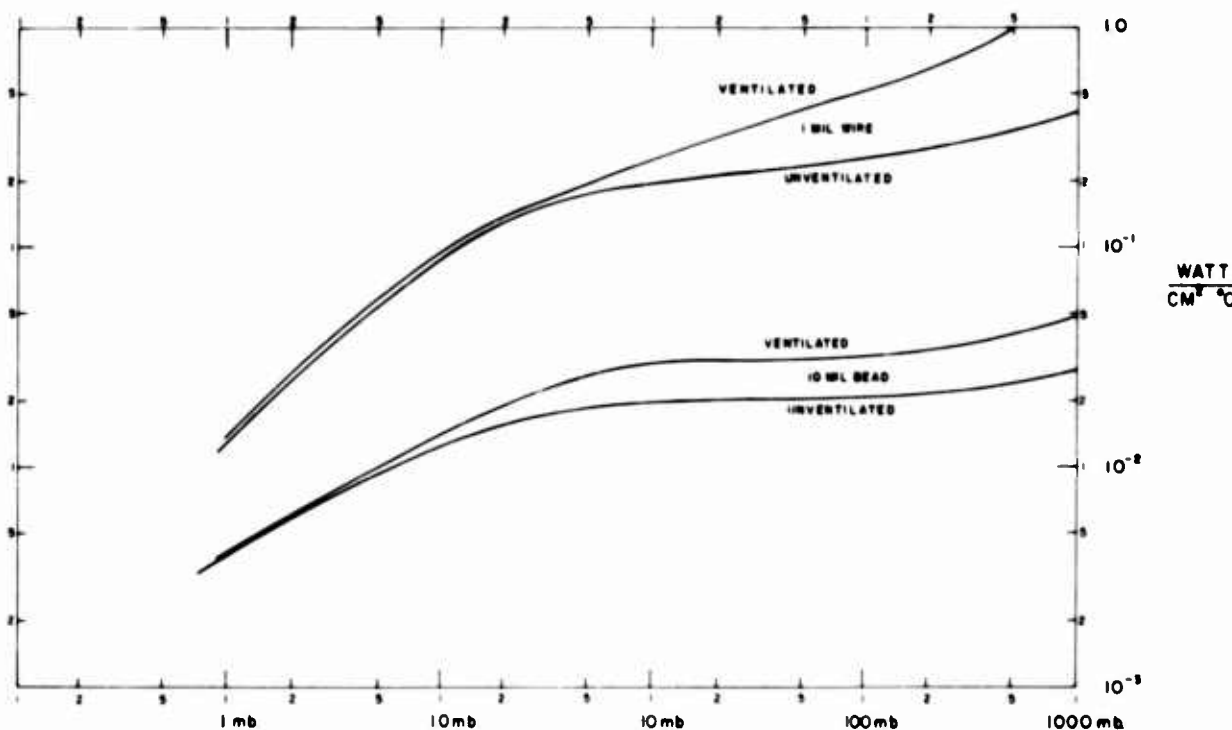


Figure 3. Heat Transfer Coefficient of Ventilated and Unventilated Thermistor Bead and Wire Thermometers

In Figure 4 are shown the heat transfer coefficients for three different sizes of bead thermistors. The increase of the heat transfer coefficient with decreasing size is obvious from the curves. Because the heat absorption from the radiative field is constant per unit surface area the radiation error will decrease with increasing heat transfer coefficient. The time constant decreases even more rapidly with bead size as may be seen in Figure 5. Here the reciprocals of the time constant for the same three beads are plotted versus pressure.

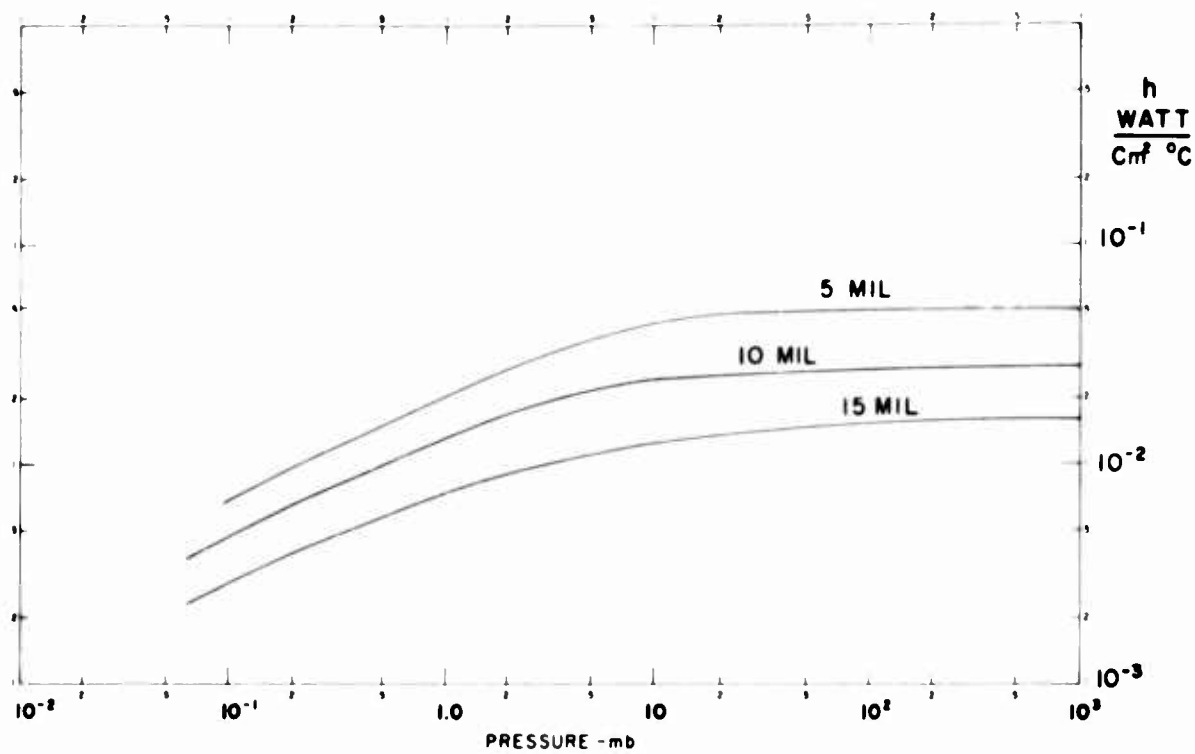


Figure 4. Heat Transfer Coefficient of Thermistor Beads vs Pressure

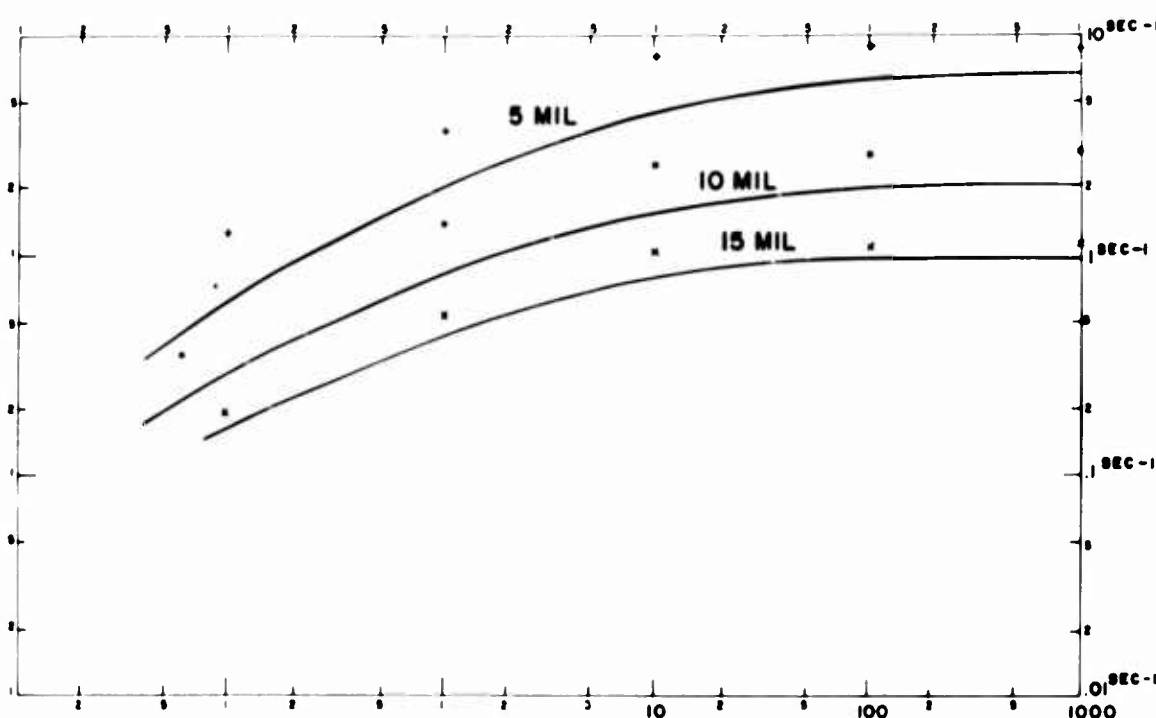


Figure 5 Reciprocal of Time Constants of Thermistor Beads vs Pressure

In Figure 6 are plotted the heat transfer coefficients of three different wire sizes. We see a relationship between size and transfer coefficient similar to that for bead thermistors but not so pronounced. Note that the heat transfer coefficient decreases rapidly at the low-pressure end of the scale as the wire size approaches the mean free path length of the air molecules.

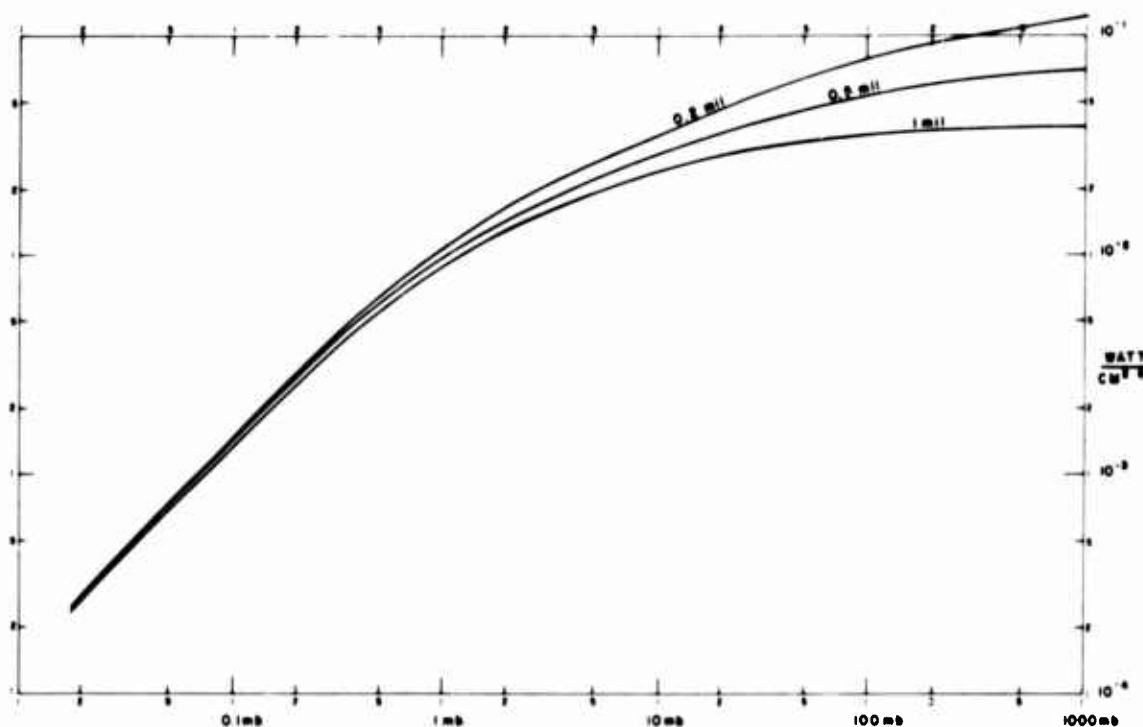


Figure 6. Heat Transfer Coefficient of Thin Wires

In the following discussion, the influence of the heat conducted through the leads on the overall heat transfer coefficient will be considered. Figure 7 shows the heat transfer coefficient for the 5- and 15-mil bead thermistor, and the heat transfer for the same beads where the heat flux into the wire has been subtracted. This is computed with the assumption that the length of the leads is at least 5 mm. In Figures 8 and 9 are shown the heat transfer coefficient and the reciprocal of the time constant, respectively, for a 15-mil bead with 4 leads, and with 2 leads. The lower curve of each set in Figure 8 gives the heat transfer coefficient for the bead without leads derived from the upper curve. That the two lower curves do not coincide is probably due to the interference of the leads close to the bead. It is obvious that the 4-lead bead has a better heat transfer characteristic and a shorter time constant than the 2-lead bead.

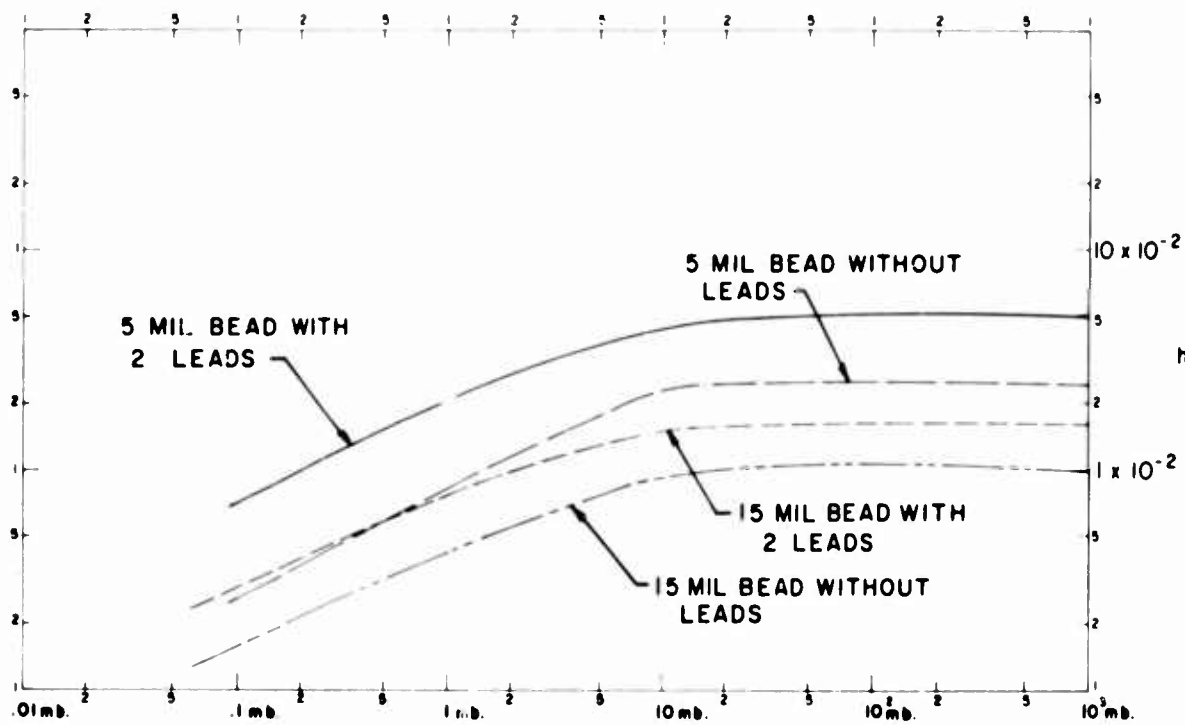


Figure 7. Heat Transfer Coefficient for 5 Mil and 15 Mil Beads with Two 1 Mil Leads

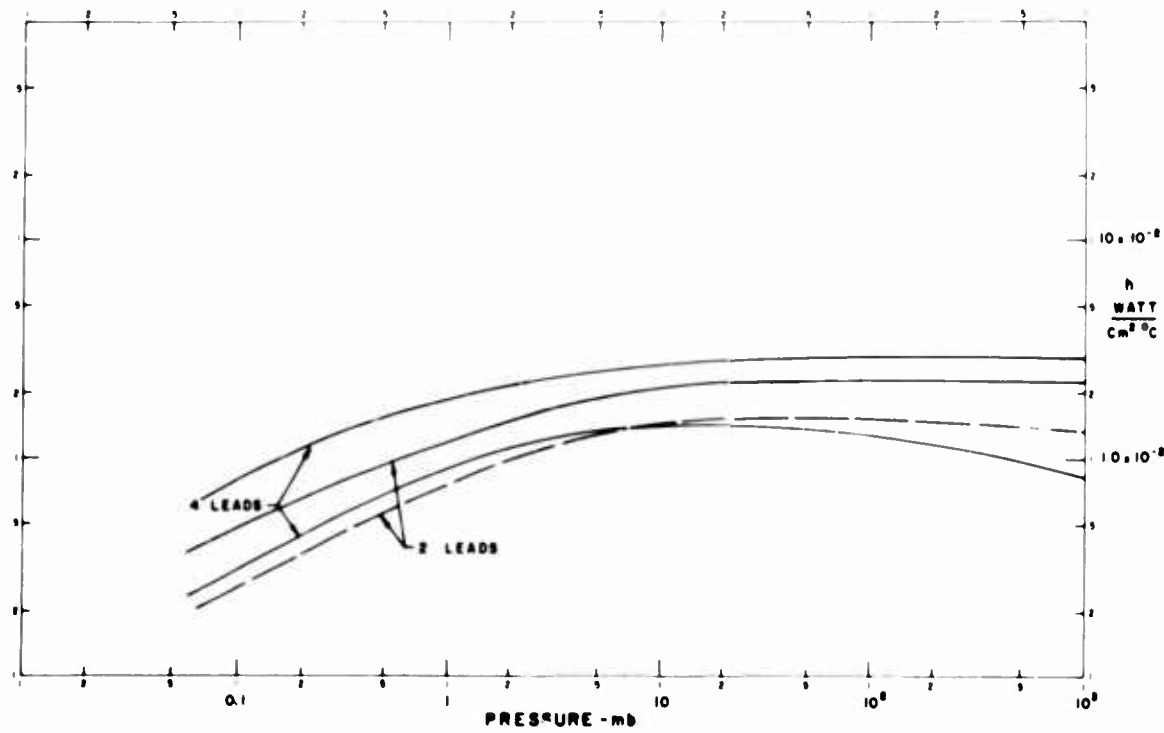


Figure 8. Heat Transfer Coefficient of 4 Lead Thermistor Bead vs Pressure

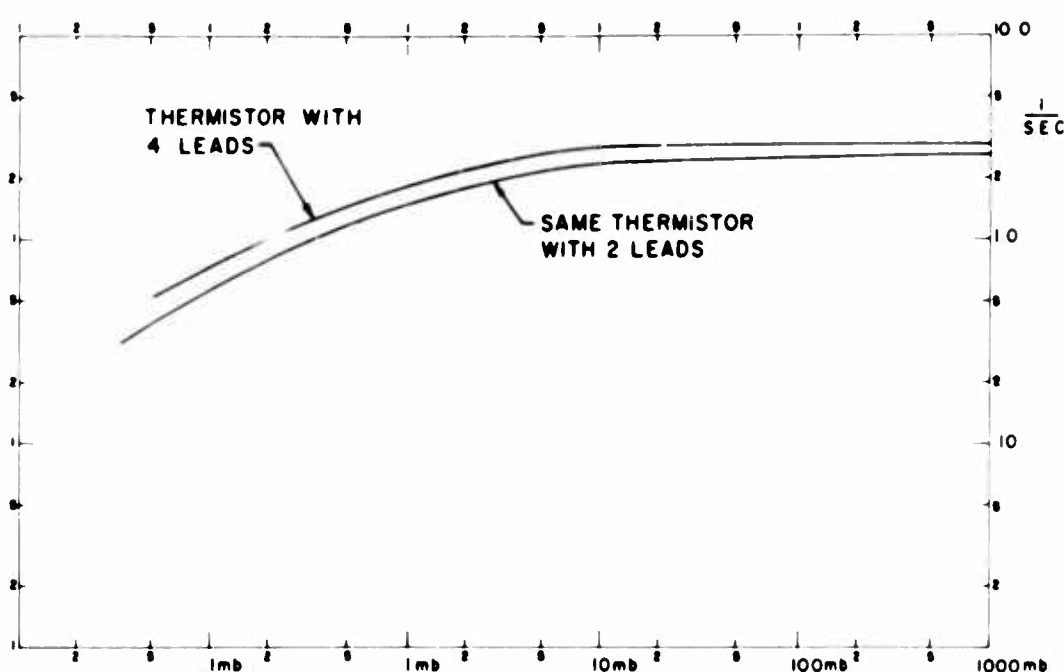


Figure 9. Reciprocal of the Time Constant of Thermistor Bead with 4 Leads vs Pressure

In Figures 10 and 11 are plotted the heat transfer coefficients and reciprocals of time constants respectively of two different beads, where the leads close to the bead are coated with silver for a length of 5 mm. The thickness of the coat is chosen so as to double the cross-sectional area of the lead wire. Because of the high thermal conductivity of silver the coated portions of the leads have practically the same temperature as the bead. This increases the effective heat transfer area and consequently the heat transfer coefficient when the total heat transfer is related to the bead surface only. Although the heat capacity is increased considerably by the coating, the time constant of the coated bead is shorter than that of the uncoated bead. The time constant of the 5-mil bead with coated leads approximates that of a 1.5-mil wire thermometer. Combining the advantage of the 4-lead bead and the high conduction leads, the heat transfer coefficient was computed for a 5-mil bead with 4 tungsten wires with 0.7 mil diameter and a lead length of 5 mm (Figure 12). The heat transfer coefficient was again computed as if the heat would be transferred through the bead surface only. If the heat transfer is divided, instead, by the combined surface of bead plus leads, the resultant heat transfer coefficient is, in fact, better than that of a 1-mil wire. One can expect that the time constant will also be somewhat better than that of such a wire. Further inquiries of Victory Engineering, Inc. have confirmed that the production of such beads seems feasible and may lead to even smaller bead sizes. The larger heat transfer coefficient allows also a lower measuring current, which is also important for many applications. The improved characteristics of the 4-lead transfer wire thermistor may bring highly desirable improvements in applications in radiosondes and dropsondes.

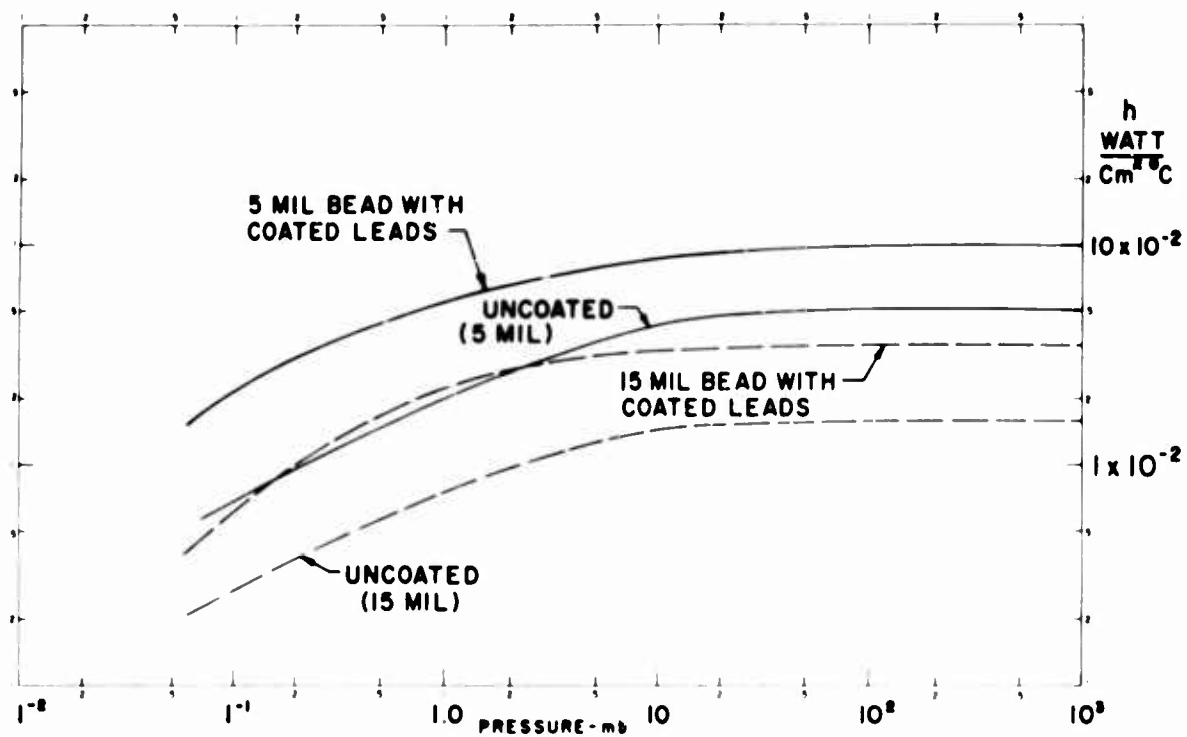


Figure 10. Heat Transfer Coefficient of Thermistor Beads with Partially Silver Coated Leads vs Pressure

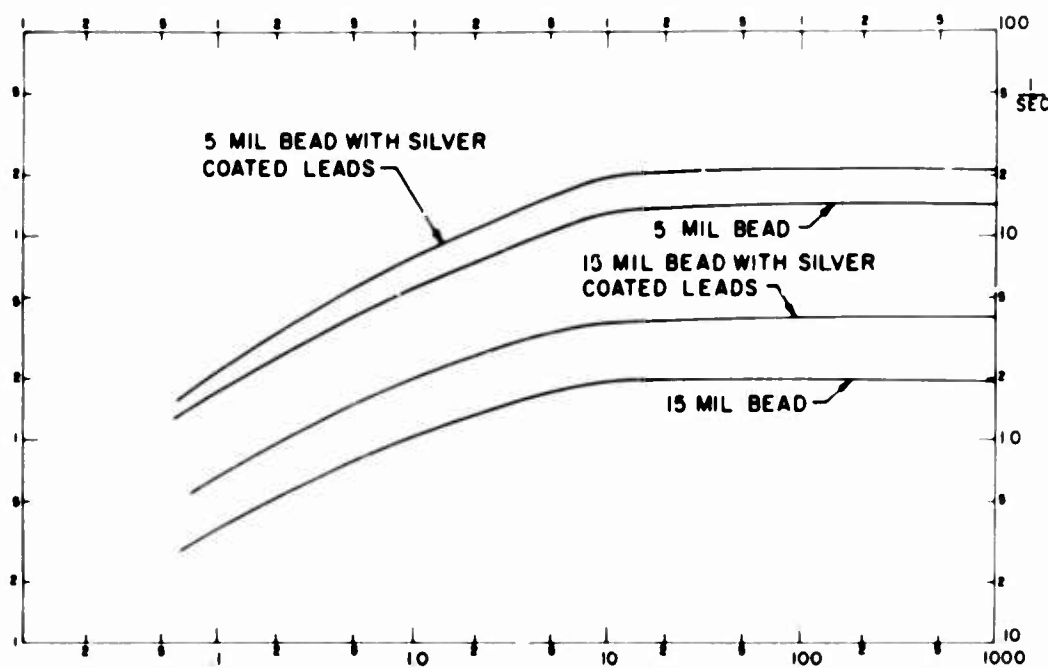


Figure 11. Reciprocal of the Time Constant of Thermistor Beads with Silver Coated Leads vs Pressure

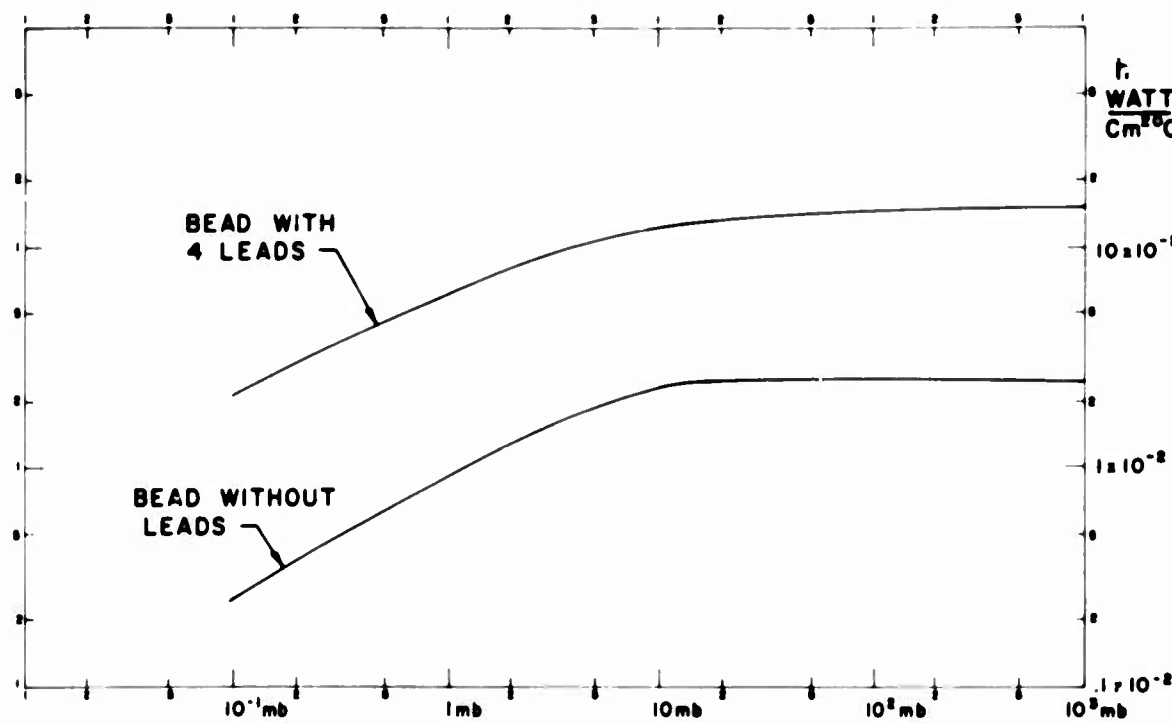


Figure 12. Heat Transfer Coefficient of 5 Mil Thermistor Bead with 4 Tungsten Wire Leads vs Pressure

To summarize our experience with immersion sensors for temperature measurements from floating balloons, some figures that may have useful applications are assembled in the table of Figure 13. As can be seen from the table it is not difficult to achieve an accuracy of  $1^\circ\text{C}$  over the whole altitude range of balloon operations. To improve the over-all accuracy to better than  $1/2^\circ\text{C}$  one has to be very careful, especially with the quality of the coating of the sensor and the dimensions of the holder. In any case, it is absolutely necessary to mount the sensor so that it is out of the balloon wake and out of the boundary layer of any structure.

	Power Limit Self Heating	Pulse Power Limit $\pm .2^\circ\text{C}$	Maximum Radia- tion Error at 10mb	Time Constant at 10mb	Accuracy of Measuring Equipment $\pm .2^\circ\text{C}$
Thermistor Bead 0.15" diameter Alum. coated	$5 \cdot 10^{-6}$ watt	$2.4 \cdot 10^{-5}$ watt sec	$0.28^\circ\text{C}$	1.2 sec	1 part in 250
Thermistor Bead 0.10" diameter Alum. coated	$2.5 \cdot 10^{-6}$	$1 \cdot 10^{-5}$ watt sec	$0.22^\circ\text{C}$	0.65 sec	1 part in 250
Thermistor Bead 0.05" diameter Alum. coated	$1 \cdot 10^{-6}$ watt	$2.5 \cdot 10^{-6}$ watt sec	$0.11^\circ\text{C}$	0.22 sec	1 part in 250
Thermistor Bead 0.05" diameter 4 Tungsten beads Alum. coated	$2.5 \cdot 10^{-6}$ watt	$2.5 \cdot 10^{-6}$ watt sec	$0.10^\circ\text{C}$	0.18 sec	1 part in 250
Thermistor Rod 0.10" diameter Alum. coated	$5 \cdot 10^{-5}$ watt inch	$8 \cdot 10^{-4}$ watt sec INCH	$2.3^\circ\text{C}$	6.5 sec	1 part in 250
Tungsten Wire $1 \cdot 10^{-3}$ " diam. Alum. coated	$7 \cdot 10^{-5}$ watt inch	$6.8 \cdot 10^{-6}$ watt sec inch	$0.22^\circ\text{C}$	0.12 sec	1 part in 2000

 $\Sigma = \text{error}$ 

• Computed Values

Figure 13. Temperature Elements

## XVI. Balloon Locating System

R. J. Cowie, Jr.  
Air Force Cambridge Research Laboratories  
Bedford, Massachusetts

It is my privilege to describe briefly a balloon-locating system that makes use of existing navigational aids. For years, investigations have been made to develop balloon-borne navigational devices and systems. These investigations, however, were oriented toward a system that would provide accurate position information on a global basis. Many possibilities have existed for using systems of limited coverage but the utility of such a system that would cover the continental United States, where most balloons are flown, was masked by the more ambitious concept. The system that appears to be optimum in terms of economy, accuracy and reliability and in compatibility with existing balloon equipment is VOR (VHF omnidirectional range). As you know, the VOR system is widely used by all types of commercial and military aircraft for navigational assistance within the United States and Canada. Moreover, the system is being continuously extended and improved. With slight modification, present VOR equipments can be adapted for balloon use with existing Air Force data-gathering and transmission facilities. The existing VOR network can provide position data easily interpreted without complex data reduction methods, and provide consistent accuracy with coverage superior to that of any balloon-locating system in use today. The approach undertaken by Zenith Radio Corporation and AFCRL has undergone limited flight testing on both balloons and aircraft to prove the feasibility

of such an approach and to study some of the basic problems concerned with system adaptation to high-altitude balloon work. Breadboard models suitable for flight testing have been constructed from available VOR equipments and made compatible with proven Air Force balloon-borne high-frequency command receivers and data transmitters. Position information is obtained on a preset schedule or by command, using a modified standard certified VHF VOR receiver on the balloon for receiving bearings from VOR ground stations. Bearing information obtained by the receiver will be converted to Morse code letter groups for retransmission to balloon data control and tracking stations. The accuracy of such a system should easily be five miles or better. A nominal system accuracy of one degree produces an error of less than five miles at a distance of 260 miles from a VOR station. The first VOR system dates back to 1928 and was called at that time "Very High Frequency Phase Comparison Radio Range". The initial investigation was by Bell Telephone Laboratories. The Civil Aeronautics Administration developed our present VOR system which is now operated and controlled by FAA. At present, there are approximately 900 VOR stations across the United States, as shown by Figure 1, operating on 600 channels in the 112- to 118-megacycle frequency band. New stations are being added periodically and constant improvements in station performance are being made by FAA to cope with the modern jet air age. The proposed balloon VOR system is composed of three major parts as indicated by Figure 2.



Figure 1. VOR Station Distribution in 1965. Source: Short Distance Radio Navigation. Prepared by U. S. Air Coordinating Committee

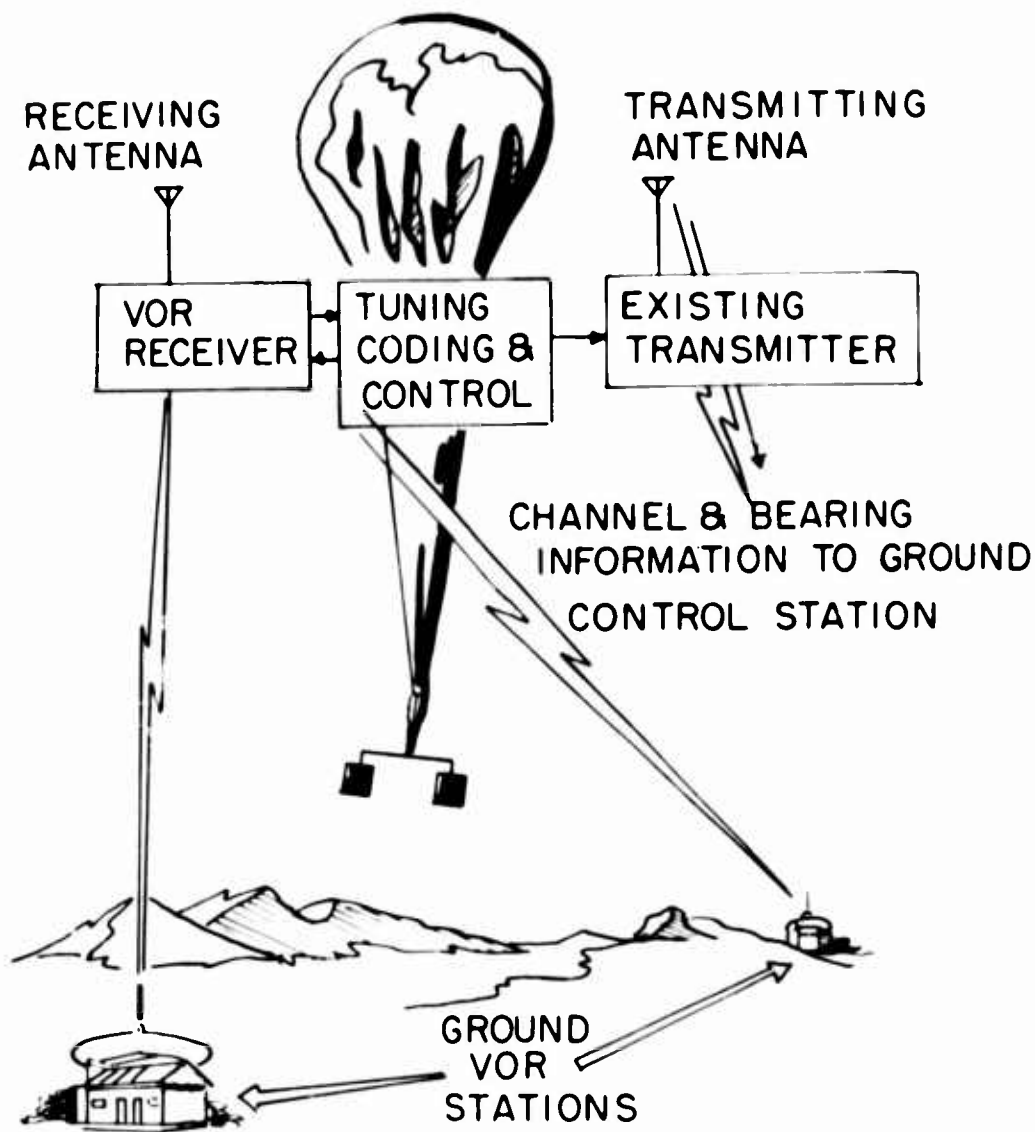


Figure 2. VOR Balloon Locating System

- 1) The ground VOR transmitter
- 2) The airborne VOR receiver and the data transmitter which is almost always present in balloon instrumentation systems.
- 3) Ground data monitoring and tracking stations - in our case, facilities at Chico, Holloman and potentially all FCC monitoring and tracking network stations.

The ground VOR transmitters are those now in operation by FAA. Our studies show that by utilizing only six different VOR channels or frequencies out of some 600 available, the entire United States can be adequately covered by considering only 260 nautical-mile-range circles about each available station on the frequencies selected. Figure 3 shows the very small area not fully covered by three possible



Figure 3. System Coverage of U.S.A. 80 K Feet, 260 N. Miles, Six Frequencies

bearing stations using six frequencies at 80,000 feet. These limited coverage areas can provide at least two bearing stations which would still be sufficient to provide adequate fix information. Figure 4 shows possible coverage using only three frequencies at 80,000 feet based upon 350 nautical-mile-range circles. The radiation from these stations is a vertical cone which can be received when the balloon-borne receiver is in the line-of-sight with the VOR transmitter. Stations are separated by a sufficient distance and radiation-controlled to minimize any interference between vertical cones. This interference and separation distance is established by altitude and transmitter power output. Power outputs range between 50 and 200 watts. Above certain altitudes and in specific areas as shown by Figure 5, limited confusion may exist on some channels but such interference is easily detected and the resulting anomaly will be discounted by the receiver and a new channel will be interrogated for bearing information. The airborne VOR system shown in Figure 6 resolves the complex radiated signal from the ground VOR station into a signal that is proportional to the magnetic bearing from the airborne unit to the ground station relative to magnetic north. The transmission principle of the omnirange is based on the creation of a phase difference between two radio signals as shown by Figure 7. One of these signals, called the reference phase, is omnidirectional and radiates from the station in a circular pattern.



Figure 4. System Coverage of U.S.A. 80 K Feet, 350 N. Miles, Three Frequencies

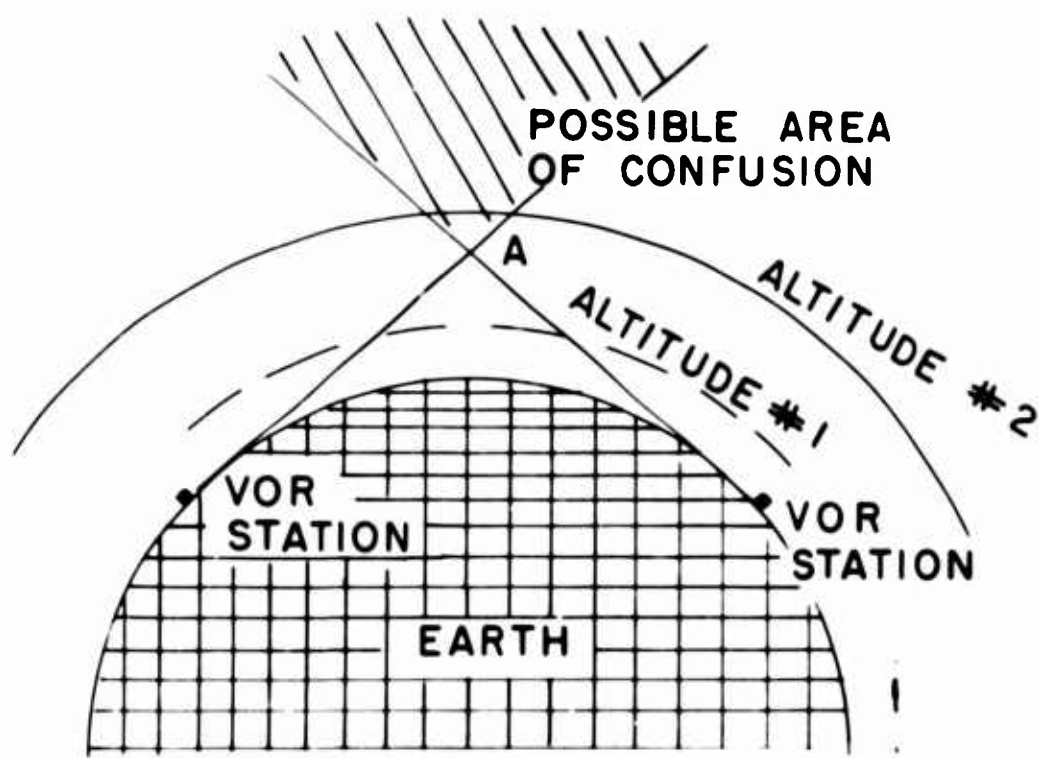


Figure 5. Confusion from Co-Channel Interference

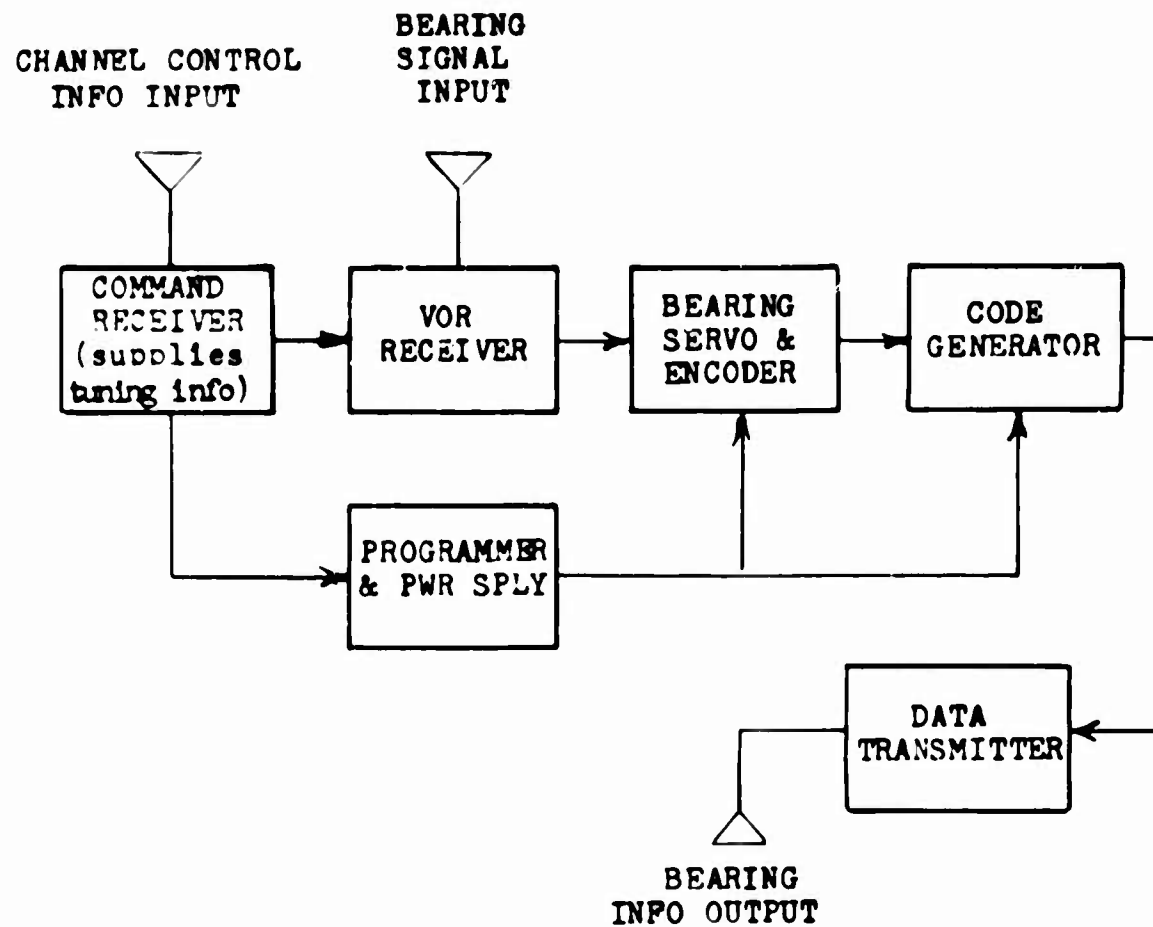


Figure 6. Balloon Locating System, Block Diagram

The phase of this signal is constant throughout its 360 degrees of azimuth. The other signal, called the variable phase is transmitted as a rotating field. This signal pattern rotates uniformly at 1800 RPM which causes the phase of the signal to vary at a constant rate. Therefore, there is a different phase of this signal at each separate point around the station. Magnetic north is used as the baseline for measuring the phase relationship between the reference and variable signals. The two signals are aligned so that at magnetic north they are exactly in phase. As you can see from Figure 7, a phase difference exists at any other point of azimuth around the station. The phase difference is measured electronically by the VOR receiver thus identifying its position in azimuth around the station. Each electrical degree of phase shift corresponds to a geographical degree around the station. The phase shift or bearing information interpreted by the receiver drives a phase-sensitive servo system which is coupled to a shaft-position encoder. Figure 8 shows the 9-bit Gray-code disk and Figure 9 shows the complete encoder and servo assembly. The encoder is used to switch a code-generating network of basic logic circuits to produce a unique combination of Morse code letters for every position of the shaft to which it is coupled.

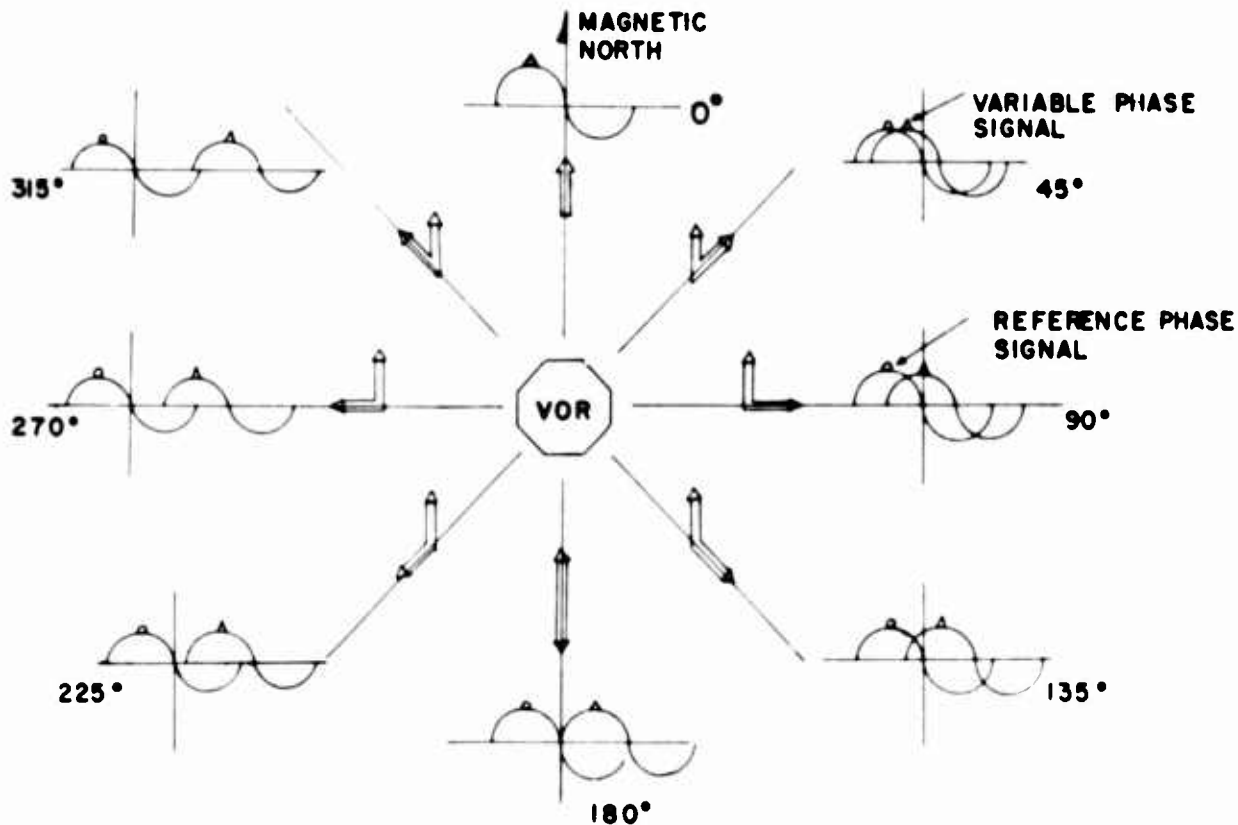


Figure 7. Signal Phase Angle Relationship

Resolution of this encoder is  $\pm 0.7$  degree with a total of 512 three-letter Morse code combinations available for 360 degrees of bearing information. The Morse code is used to key the data transmitter which relays the bearing and channel information to the ground-monitoring station via HF CW telemetry. Provision is made in the output circuit of the bearing-code generator to key out a frequency-identifying code originating in the receiver-tuning circuit with each bearing measurement. A dictionary containing all 512 code combinations is available so that ground-monitoring stations can obtain immediate bearing information merely by looking up the bearing when the Morse code is received. By using standard USAF operational navigation charts and knowing the frequency channels utilized for each measurement, unskilled personnel can accurately plot the position of the balloon upon receipt of the Morse code data from the balloon.

AFCRL conducted a test flight of the basic system in September from our Chico, California, launching facility utilizing a mock-up of a standard military VOR unit adapted for balloon work. Figure 10 shows the instrument rack assembly used for a first balloon-borne verification test. Figure 11 shows the block diagram of the instrument rack and Figure 12 shows the block diagram of the VOR receiver.

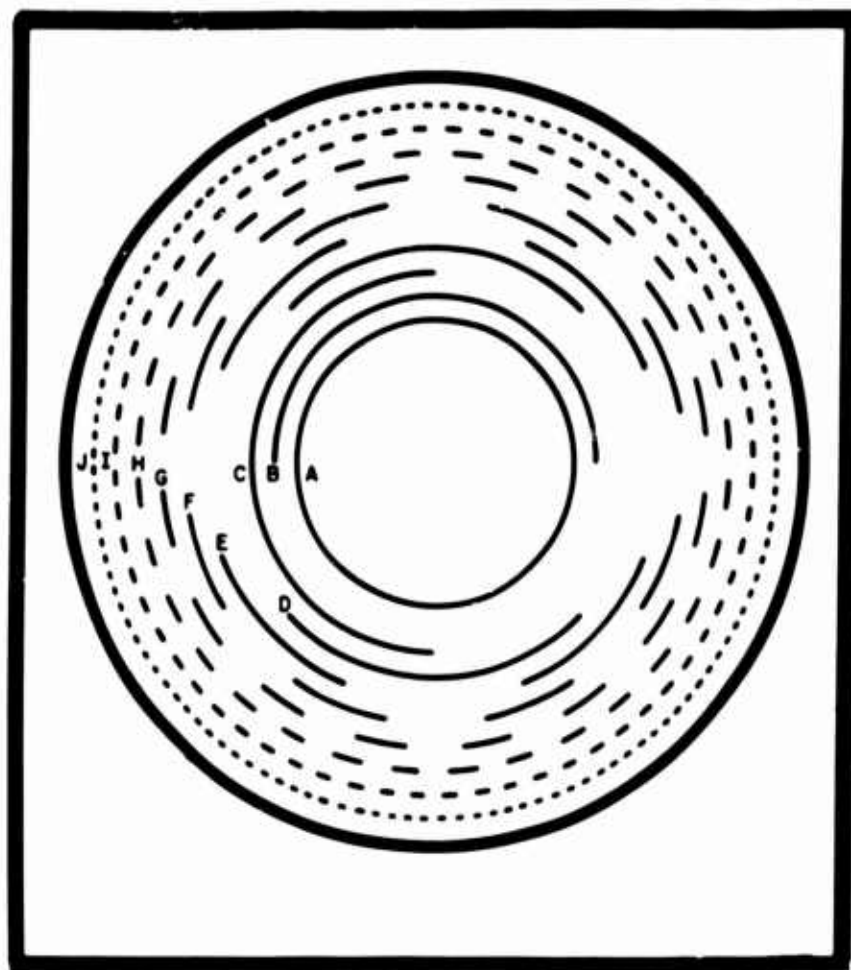


Figure 8. Shaft Position Encoder Code Disk

The Chico site as shown in Figure 13 was selected because it contains fewer VOR stations and these stations are suitable in frequency to investigate position accuracy and co-channel interference at high altitudes. All data from this flight were recorded photographically. Figure 14 shows a typical bearing-indicator reading as recorded photographically. The test results indicated that accuracy was better than five miles. Figure 15 shows a typical fix obtained from bearings received. No co-channel interference was observed during this test. A more sophisticated prototype model including the Morse-code-telemetry feature currently under development at Zenith - Chicago will be test-flown in January 1965. Figure 16 shows the VOR bench test setup for the prototype equipment. Figure 17 shows the all-transistorized VOR receiver unit, a modified Collins 51R-8. Figure 18 shows the bearing-encoder servo assembly and logic cards of the code generator. For those interested in specific project details, Mr. Henry Buschke, project leader at Zenith, will be pleased to assist me in answering your questions.

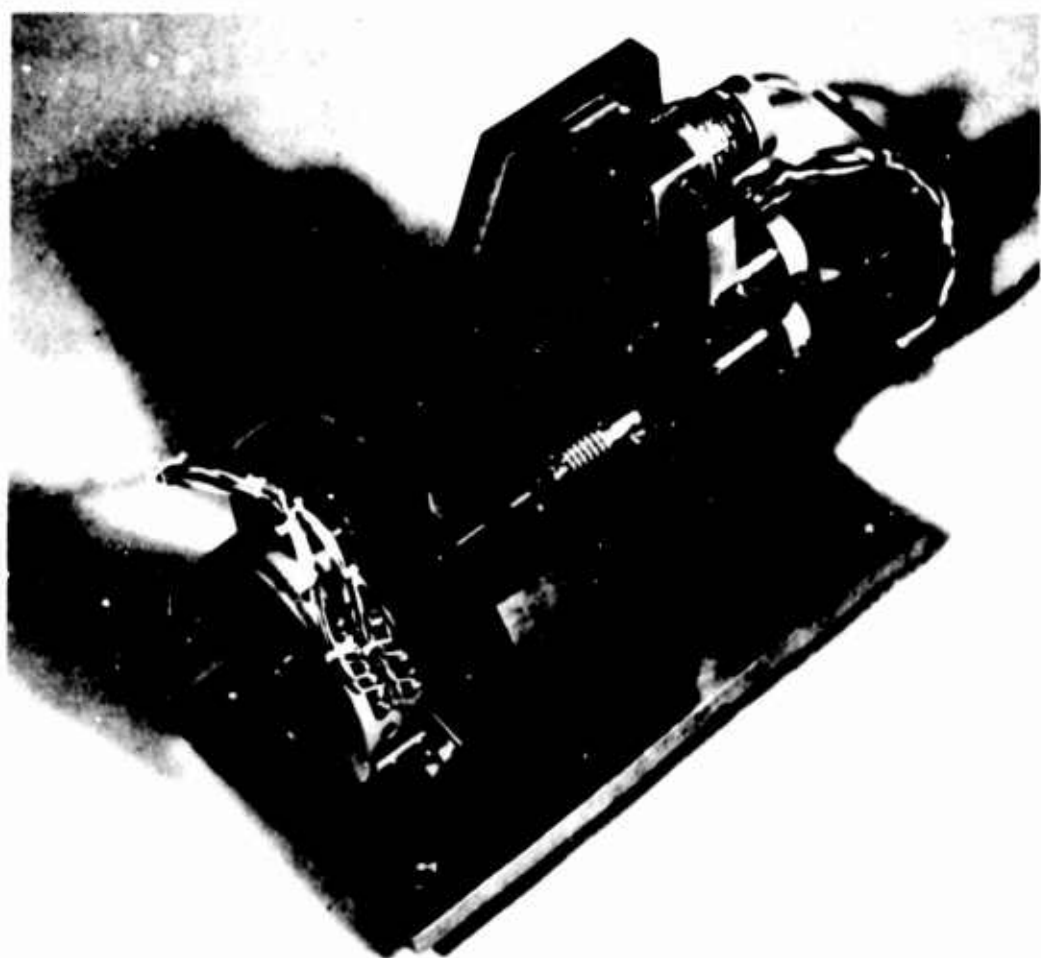


Figure 9. Complete Encoder and Servo Assembly

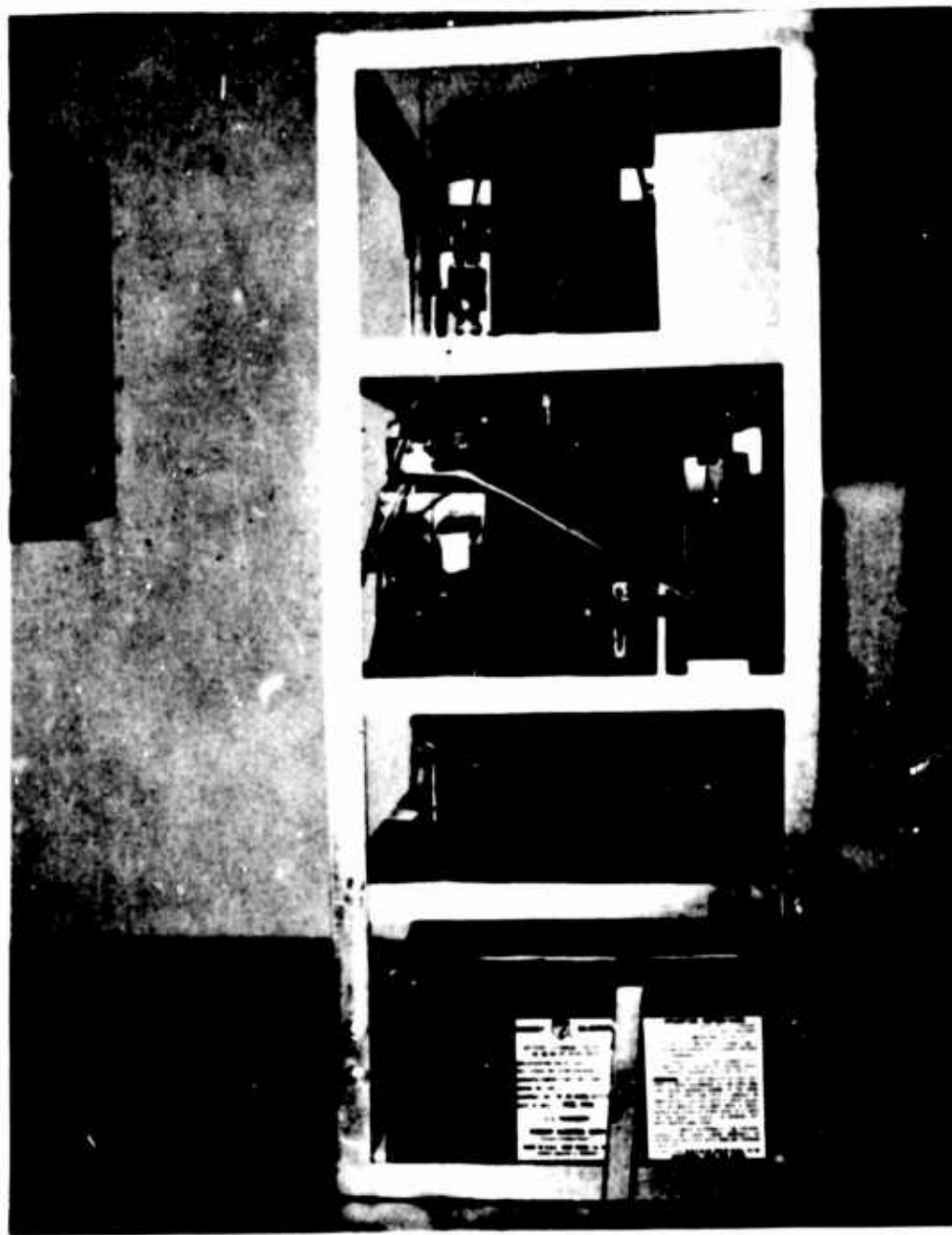


Figure 10. Instrument Rack Assembly

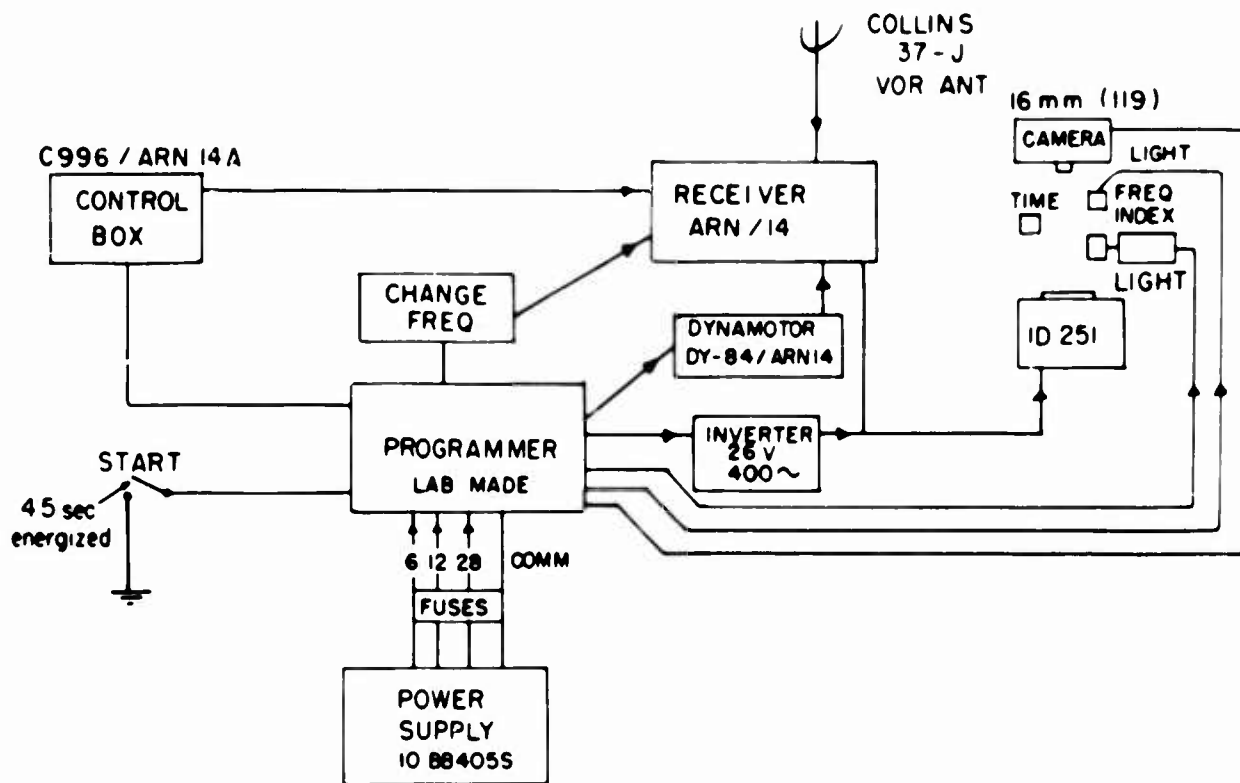


Figure 11. Experimental VOR Balloon Locating System

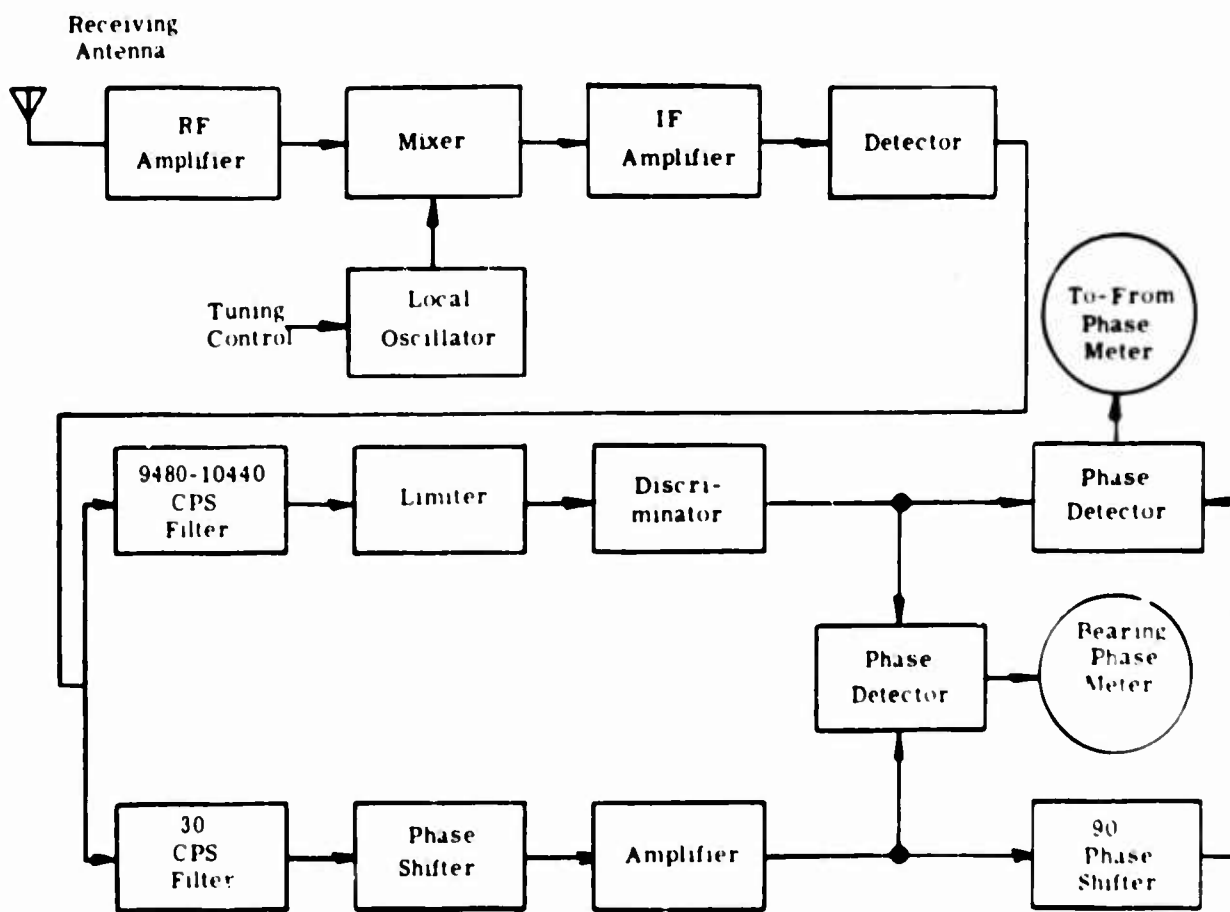


Figure 12. Typical VOR Receiver, Block Diagram

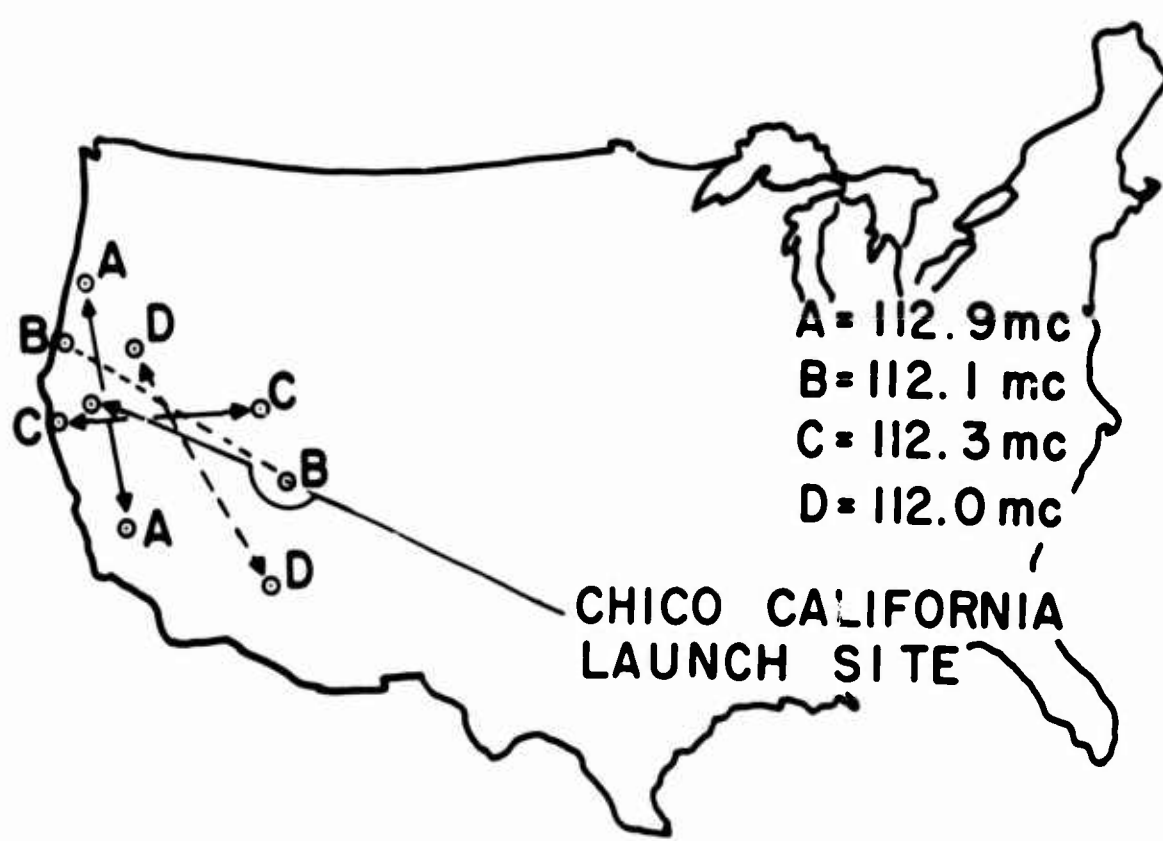


Figure 13. Co-Channel Interference Test Area



Figure 14. Bearing Indicator

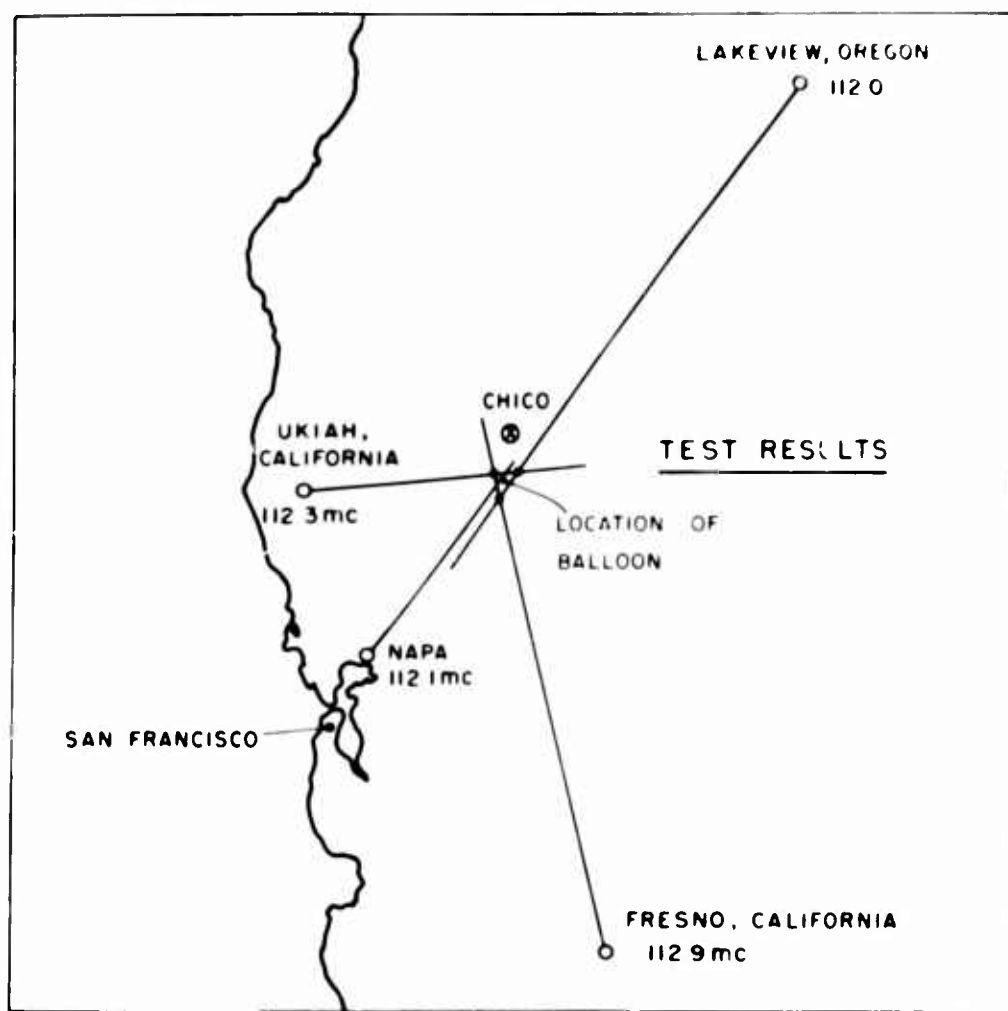


Figure 15. Test Results

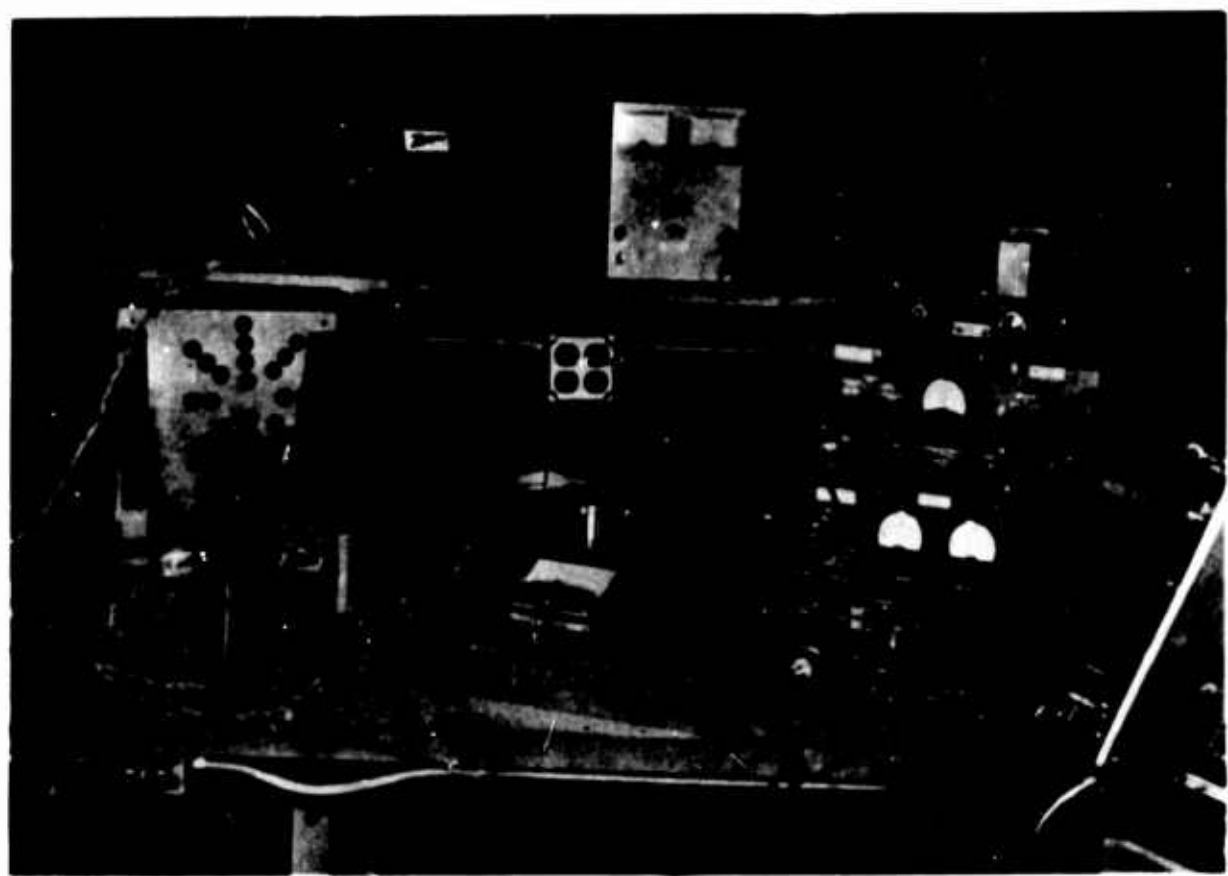


Figure 16. VOR Bench Test Setup

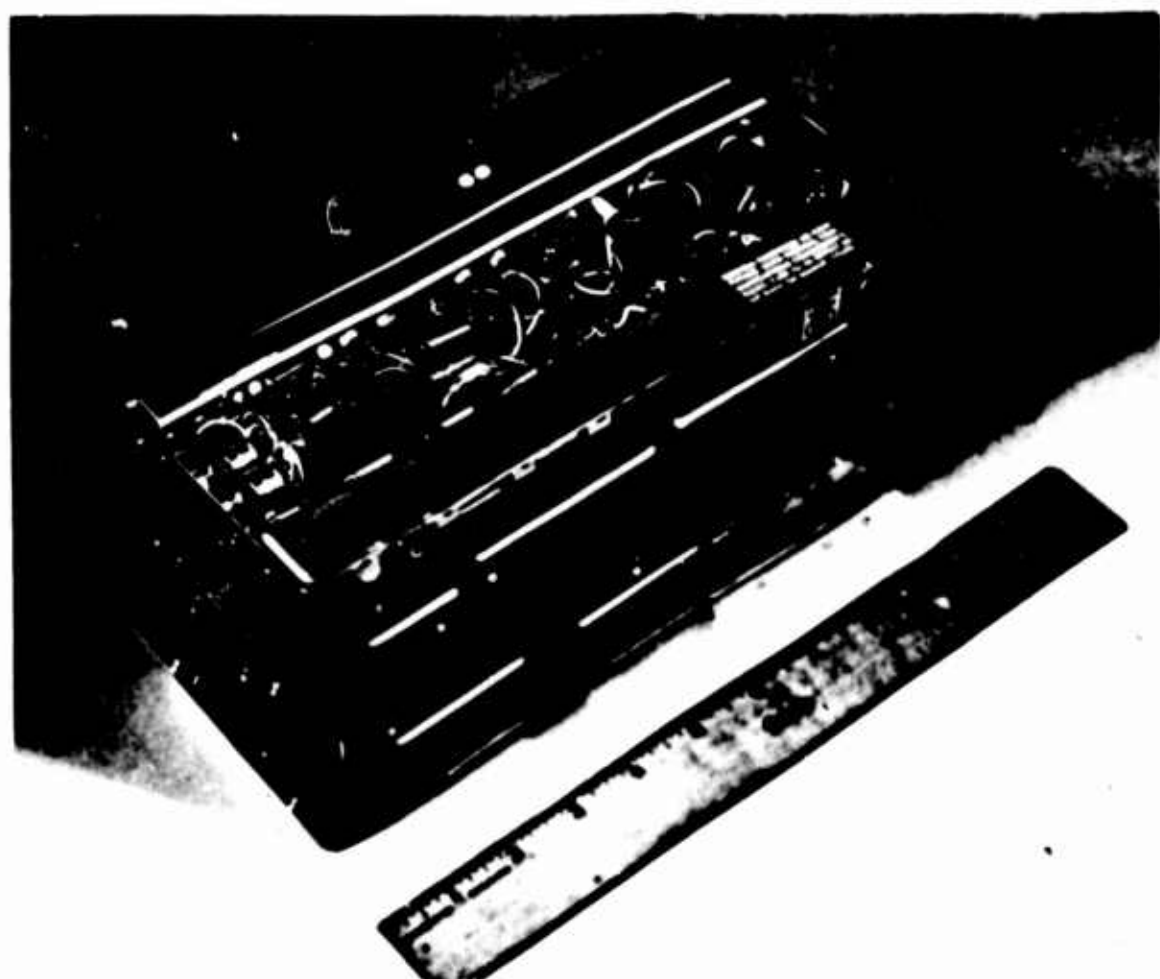


Figure 17. All-Transistorized VOR Receiver Unit

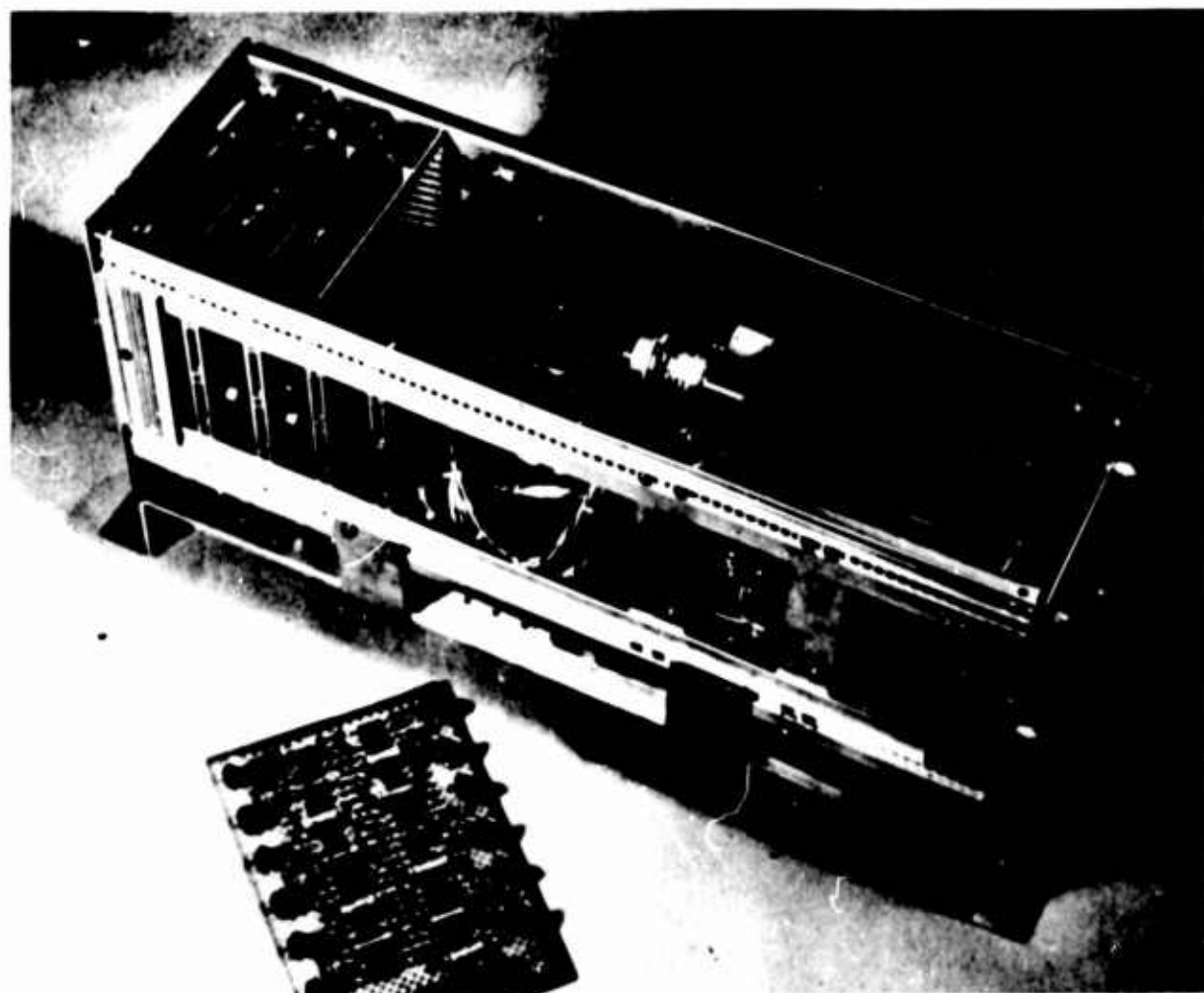


Figure 18. Bearing-Encoder Servo Assembly and Logic Cards of Code Generator

## XVII. Two New Special-Purpose Meteorological Balloons

Eric Nelson

Kaysam Corporation of America  
Paterson, New Jersey

Moses Sharenow

U. S. Army Electronic Research and Development Laboratory  
Fort Monmouth, New Jersey

The need has long existed for a balloon capable of reaching high altitudes during the tropical night and also during the arctic winter. The atmospheric conditions in these two locations actually present two different problems although they may both be classified generally as being in the low-temperature field. As can be seen from the temperature profiles shown in Figure 1, a balloon flown in the Temperate Zone is released at a relatively warm temperature which falls as the balloon ascends to levels in the order of  $-60^{\circ}\text{C}$  or  $213^{\circ}\text{K}$ , although temperatures as low as  $-70^{\circ}\text{C}$  or  $203^{\circ}\text{K}$  are encountered fairly frequently. This temperature is reached at an altitude of about 40,000 feet and it remains fairly constant until an altitude of close to 70,000 feet where a warming trend begins.

During the tropical night the balloon is normally somewhat warmer at release than in the Temperate Zone but the ambient temperature falls rapidly to about  $-85^{\circ}\text{C}$  or  $188^{\circ}\text{K}$  at approximately 50,000 feet. This is usually followed immediately by fairly rapid warming and the temperature at 100,000 feet is relatively close to that at the same altitude in the Temperate Zone.

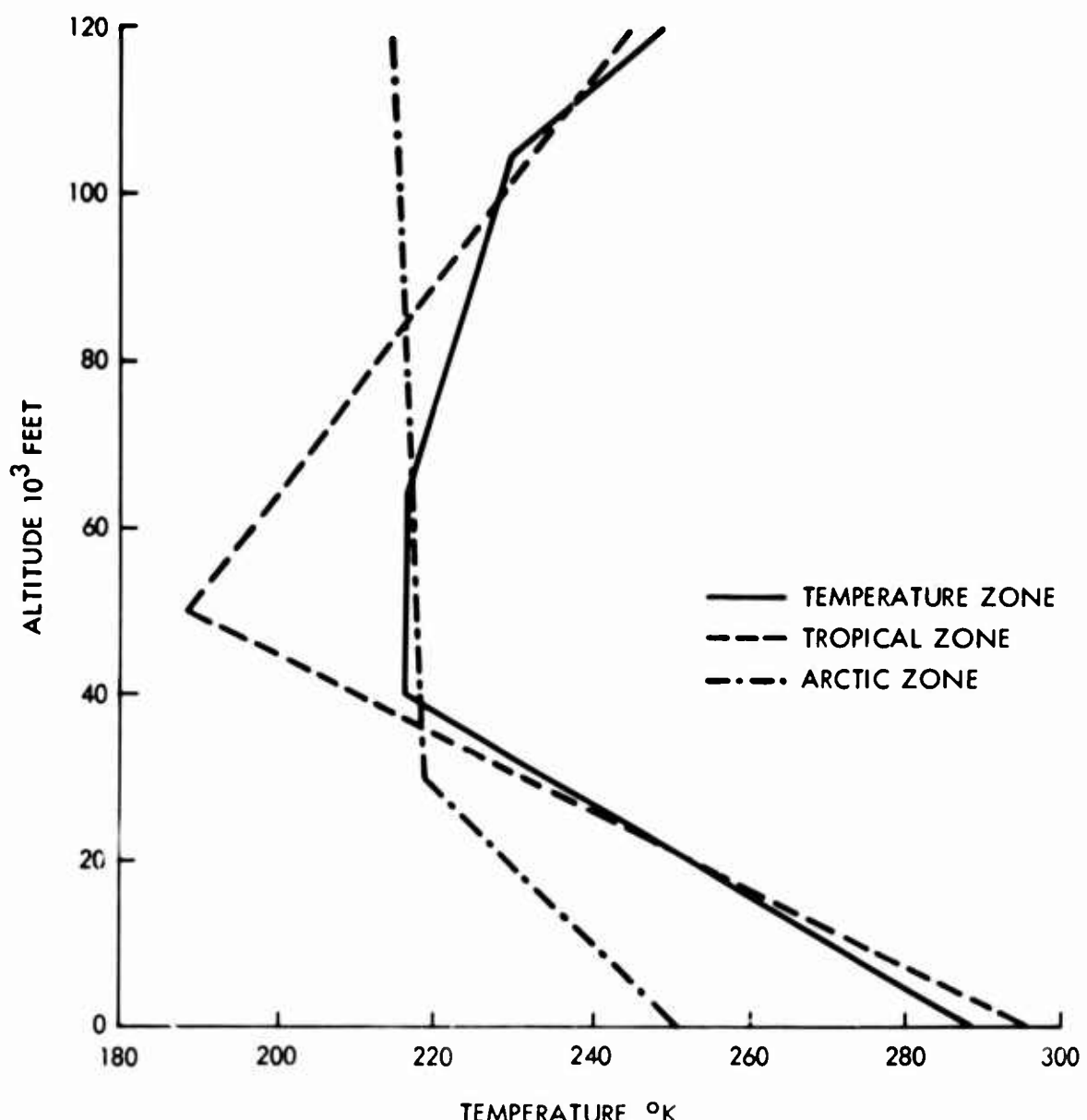


Figure 1. Standard Atmosphere Temperature Profiles

In the arctic winter the balloon is about 40°C colder at release than it is in the Temperate Zone and the temperature falls relatively slowly until a temperature in the order of -55°C is encountered at approximately 30,000 feet. The atmosphere then continues to cool slowly and the temperature at 100,000 feet is about -60°C.

The problem in developing this special-purpose balloon, therefore, was to design a compound with the following characteristics:

1. It must be capable of being cooled to a temperature of -85°C without freezing and becoming brittle.

2. It must be capable of continued exposure to temperatures in the order of -60°C without becoming leathery and losing its ability to stretch.
3. It must be capable of being handled and launched at the ground temperatures encountered in tropical areas in the daytime as well as at night since this will be used in a dual-purpose balloon.
4. It must retain sufficient elongation under the low-temperature conditions outlined to produce a balloon capable of ascending to 100,000 feet.

A series of compounds was evaluated and the physical characteristics, particularly the elongation, were determined at room temperature and at temperatures down to -85°C. For the compound selected, the elongation under various conditions is shown in Table 1. It can be seen that even if the balloon passes through a zone where the temperature is as low as -85°C it will not burst, providing that it is not expanded to an extent equivalent to a linear elongation of more than 300 percent. Since the balloon in question is only extended to an equivalent of 200 percent linear elongation at the altitude at which such low temperatures are encountered, it will successfully pass through this cold zone. As the temperature subsequently rises it will regain its ability to reach an elongation of 500 percent, for this reduction in elongation with temperature is a reversible phenomenon. Hence, the balloon will be capable of reaching the same altitude in the Tropical Zone as it does in the Temperate Zone.

Table 1. Low Temperature Elongation

Test Temp °C	Exposure Time	Elongation %
+20	10 Mins	805
-70	10 Mins	480
-70	30 Mins	520
-75	10 Mins	440
-75	30 Mins	470
-80	10 Mins	330
-80	30 Mins	400
-85	10 Mins	330
-85	30 Mins	410

It is also clear that prolonged exposure to low temperatures does not cause a progressive reduction in elongation. In fact in every case the elongation recorded

after maintaining the films at the designated temperature for thirty minutes is greater than that recorded after maintaining the films at the low temperature for only ten minutes. We presume that ten minutes is not long enough for the film to be completely chilled and that this sets up uneven stresses when the film is stretched and that these in turn result in premature breaks. Therefore, balloons flown during the arctic night can also be expected to ascend to altitudes equal to those reached in the Temperate Zone.

The validity of these arguments is demonstrated by the flight performance obtained, which is shown in Table 2. In all, thirty-one flights were successfully tracked to burst. Six of these were made at Fort Monmouth, New Jersey, twelve were made at Albrook Air Force Base in the Panama Canal Zone and thirteen were made at Fort Greeley, Alaska. The first three flights were made in the daytime and the remaining twenty-eight were all conducted during the hours of darkness.

Table 2. Flight Performance Kaysam 100 ATG Balloon

Flight No.	Location	Altitude	Rate of Rise	Min Temp
1	Ft. Monmouth	113,000	1048	
2	Ft. Monmouth	100,500	1077	
3	Ft. Monmouth	113,100	1075	
4	Ft. Monmouth	113,386	1072	
5	Ft. Monmouth	120,308	1039	
6	Ft. Monmouth	124,600	1124	
7	Ft. Monmouth	102,200	974	-79°C
8				
9	Albrook AFB	112,762	933	-79°C
10	Albrook AFB	116,110	1023	-79.5°C
11	Albrook AFB	101,100	958	-81.5°C
12	Albrook AFB	120,633	987	-78.8°C
13	Albrook AFB	109,850	1000	-80.5°C
14	Albrook AFB	115,420	1030	-79°C
15	Albrook AFB	108,770	989	-80°C
16	Albrook AFB	119,980	1025	-78°C
17	Albrook AFB	122,475	1033	-79°C
18				
19	Ft. Greeley	110,278	1090	-60.3°C
20	Ft. Greeley	114,380	1139	-58.2°C
21	Ft. Greeley	95,072	992	-58.3°C
22	Ft. Greeley	109,373	1090	-70.9°C
23	Ft. Greeley	101,322	1072	-69.2°C
24	Ft. Greeley	115,118	1083	-63.5°C
25	Ft. Greeley	107,812	1010	-63.7°C
26	Ft. Greeley	109,321	1069	-70.2°C
27	Ft. Greeley	103,432	1066	-69.8°C
28	Ft. Greeley	109,245	1042	-68°C
29	Ft. Greeley	98,543	1043	-69°C
30	Ft. Greeley	102,992	1058	-68.4°C
31	Ft. Greeley	112,700	1109	-66.7°C

Of the thirty-one flights completed, twenty-seven, or 87 percent, reached altitudes in excess of 100,000 feet. Eighty-three and one half percent of the tropical flights exceeded the 100,000-foot level as did 85 percent of the arctic flights. Some of the Tropical Zone balloons were a little slow in ascending but in general it is clear that a balloon capable of reaching an altitude of 100,000 feet by day or by night in any geographical location is now available. Whenever flights in the Tropics or the Arctic are planned, it would be wise to consider this balloon which will provide performance much superior to that obtained from the ML-537 balloon.

A need has also existed for a meteorological balloon capable of rapid ascents to 100,000 feet by both day and night. Prior to the development of the balloon to be described, no such vehicle was available. The ML-537 balloon is capable of reaching the required altitude, but it has an ascension rate of only 1,000 feet per minute. The ML-541 balloon rises at more than 1,700 feet per minute and, furthermore, it can only be used in the daytime. The fact that such a balloon exists might suggest that production of a balloon capable of reaching 100,000 feet at the same ascensional rate was a simple matter of extrapolation. This, however, is not the case, and a daytime altitude of 90,000 feet appeared to be maximum attainable by such means. The nighttime altitude was much lower, being in the order of only 60,000 feet.

The use of streamlined, nonexpanding plastic balloons with stabilizing fins has proved impractical. In order to reach an altitude of 100,000 feet an excessively large balloon and consequently very large volumes of hydrogen are required. In addition, expert rigging and alignment of the fins are necessary to produce the stability essential for rapid rates of ascent. Balloons of this type have been produced which performed satisfactorily but only to an altitude of 40,000 feet.

Large, thick-walled spherical balloons have proved to be erratic in performance and although a balloon can be designed which will meet the requirements set forth, it is heavy and requires a very high free lift. This again results in the need for excessive amounts of hydrogen or helium.

The balloon to be described involves a completely new concept and in order to understand the reasons for arriving at this design it is necessary to review some of the earlier theoretical work (Figure 2). The equation of motion for meteorological balloons is given by the formula  $L - D = \frac{mdV}{dt}$ .

where

L = Free Lift  
D = Drag  
V = Ascent Velocity

and

m = Mass of Equipment and Gas

$$L - D = m \frac{dv}{dr}$$

WHERE    L = FREE LIFT  
           D = DRAG  
           m = TOTAL MASS  
           v = RATE OF ASCENT  
           r = TIME

Figure 2. Equation of Motion for Meteorological Balloons

If a constant drag coefficient is assumed then the balloon will accelerate until it breaks. In practice, however, the drag coefficient is constantly changing and this fact coupled with a critical Reynolds-Number effect leads to the following conclusions:

1. A streamlined neoprene balloon, that is, a spherical balloon to which a roughly conical tail section has been attached, will accelerate rapidly to an altitude of about 50,000 feet. It then shows a rapid deceleration over the next 10,000 feet and thereafter accelerates very slowly.
2. Spherical thick-walled balloons designed for rapid rate of ascent also accelerate rapidly to between 50,000 feet and 60,000 feet. However, almost twice the lift is required to produce this acceleration as is necessary with a streamlined balloon. These balloons also show a sharp deceleration at 60,000 feet or thereabouts.
3. Large thin-walled balloons accelerate throughout the flight to burst, provided they do not reach the critical Reynolds Number. Their rate of ascent is, however, much slower below 50,000 feet than is the case for either of the other two balloons.

Figure 3 shows the relationship between drag coefficient and Reynolds Number for theoretical spherical and streamlined balloons. Balloons generally leave the ground as at the extreme right-hand side of the curve and follow it to the left as they ascend. When they reach the state near  $3 \times 10^5$  the drag coefficient rises sharply. If the balloon is sufficiently large and its ascent rate is high enough, it may not reach the critical number and will continue to accelerate to burst. This effect is more pronounced with fast-rising balloons than with slower 1,000 foot per minute balloons since other atmospheric parameters can cause ascent rate changes of the same magnitude as those encountered on the slower rising balloons.

Since a meteorological balloon does not behave as a perfect sphere or perfect ellipsoid due to deformation and distortion encountered during flight, the theoretical equations can only be applied in general terms. Nevertheless, the behavior of ML-537 and larger spherical balloons and that of the ML-541 streamlined balloon confirm the above theory.

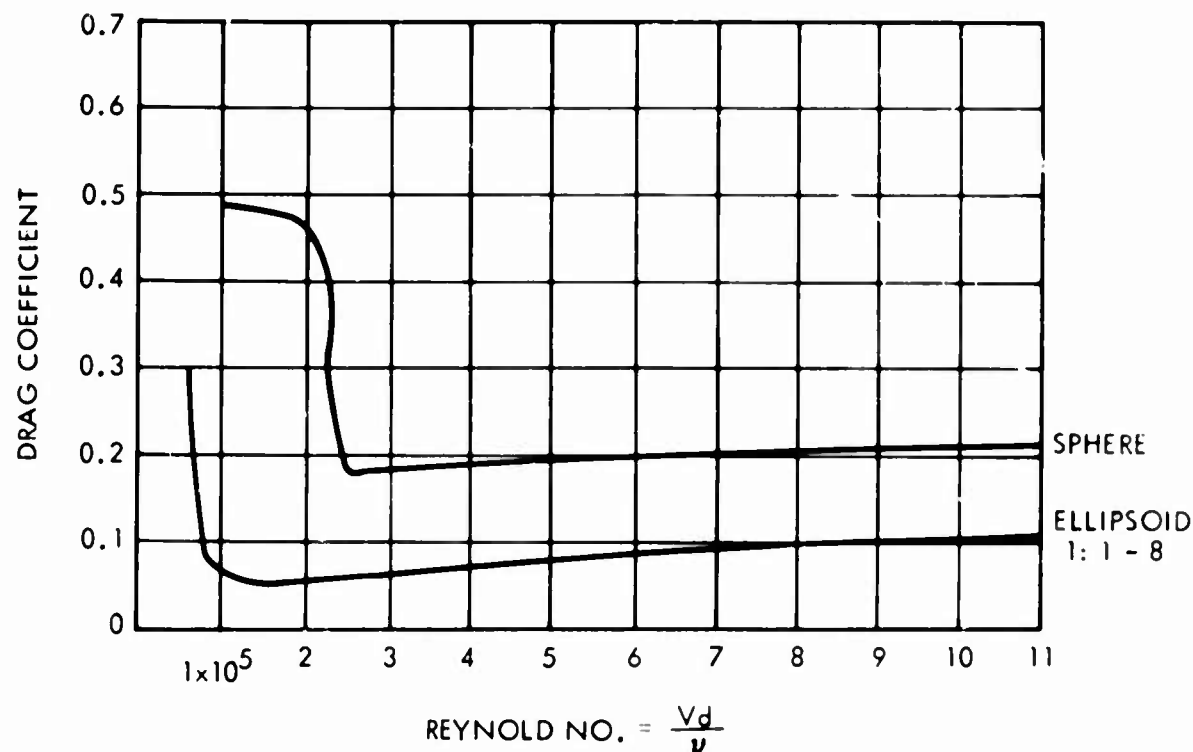


Figure 3. Drag of Rigid Sphere and Ellipsoid

It appeared to us, therefore, that in order to construct a balloon which is capable of reaching an altitude of 100,000 feet at 1,700 feet per minute, it is necessary to combine in some manner the characteristics of these two types of balloon. In other words, for the first half of the flight the balloon should be of the streamlined type and for the second part of the flight it should be a large, thin-walled spherical balloon. If we plot the rate of ascent against altitude for these two types of balloon we get the results shown in Figure 4. The upper graph is a typical plot of rate of ascent versus altitude for a thin-walled spherical high-altitude balloon. The lower graph is a typical plot for a streamlined balloon of the ML-541 type.

Figure 5 shows these two curves superimposed. It can be seen that at 60,000 feet both types of balloon have the same rate of ascent but whereas the streamlined balloon is decelerating, the spherical balloon is accelerating. If a combination balloon could be fabricated which consisted of a high-altitude spherical balloon enclosed in a streamlined balloon and the streamlined balloon could burst and fall away at about such an altitude, then the spherical high-altitude balloon will accelerate to the top of the flight. The graph of the rate of ascent versus altitude for such a combination balloon will appear as in Figure 6. Such a balloon would start out with a rate of ascent of about 1,400 feet per minute accelerating to 2,500 feet per minute (a conservative figure) at about 50,000 feet.

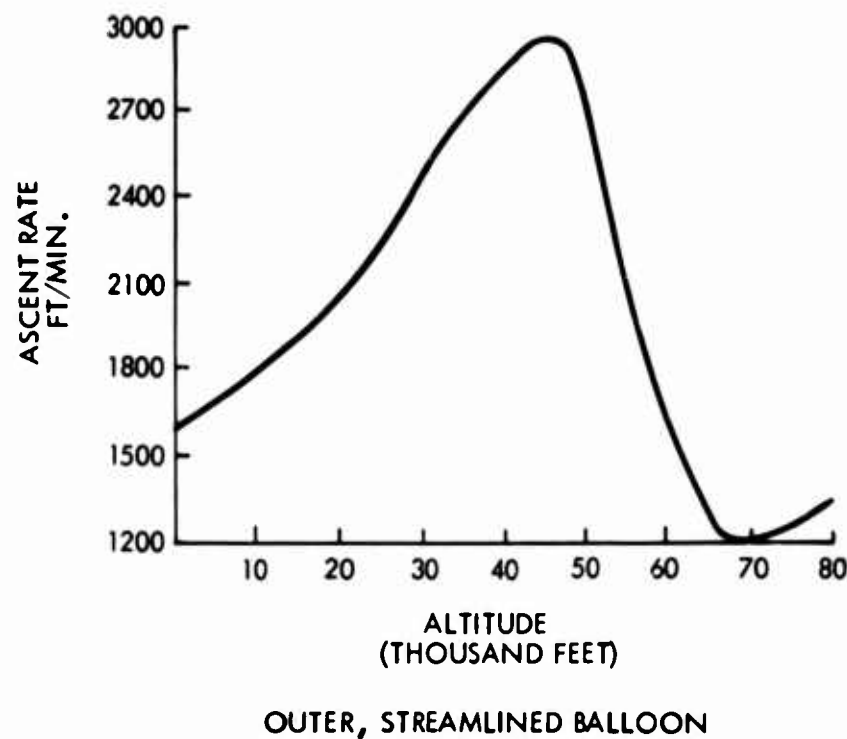
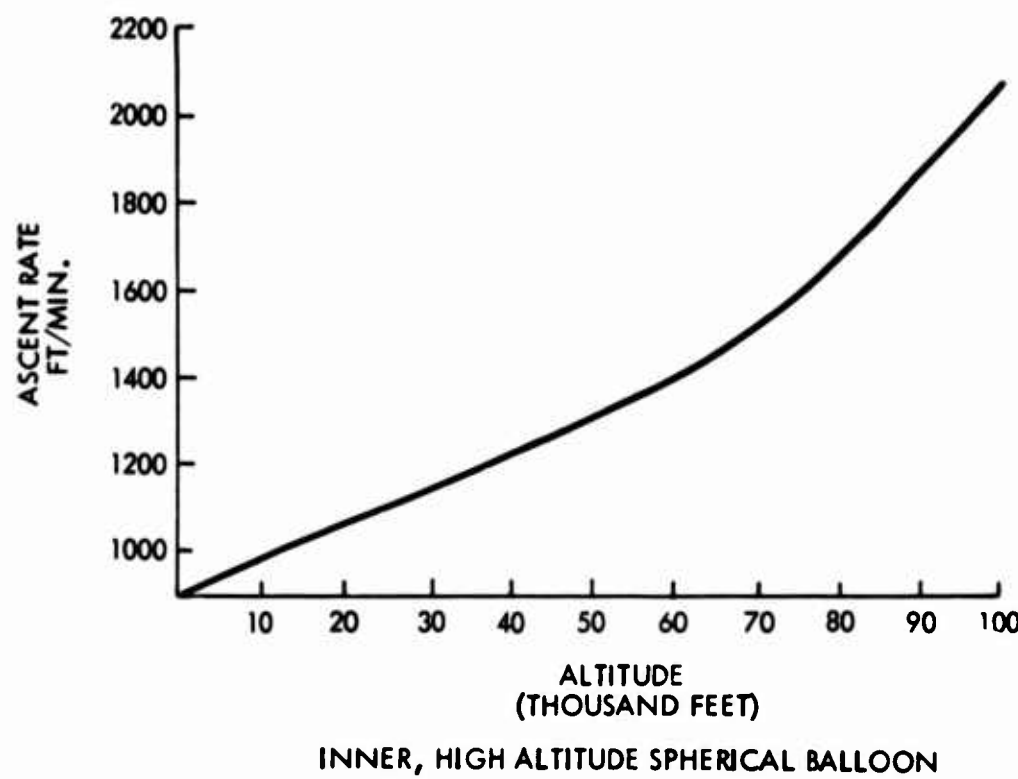


Figure 4. Ascent Rate vs Altitude

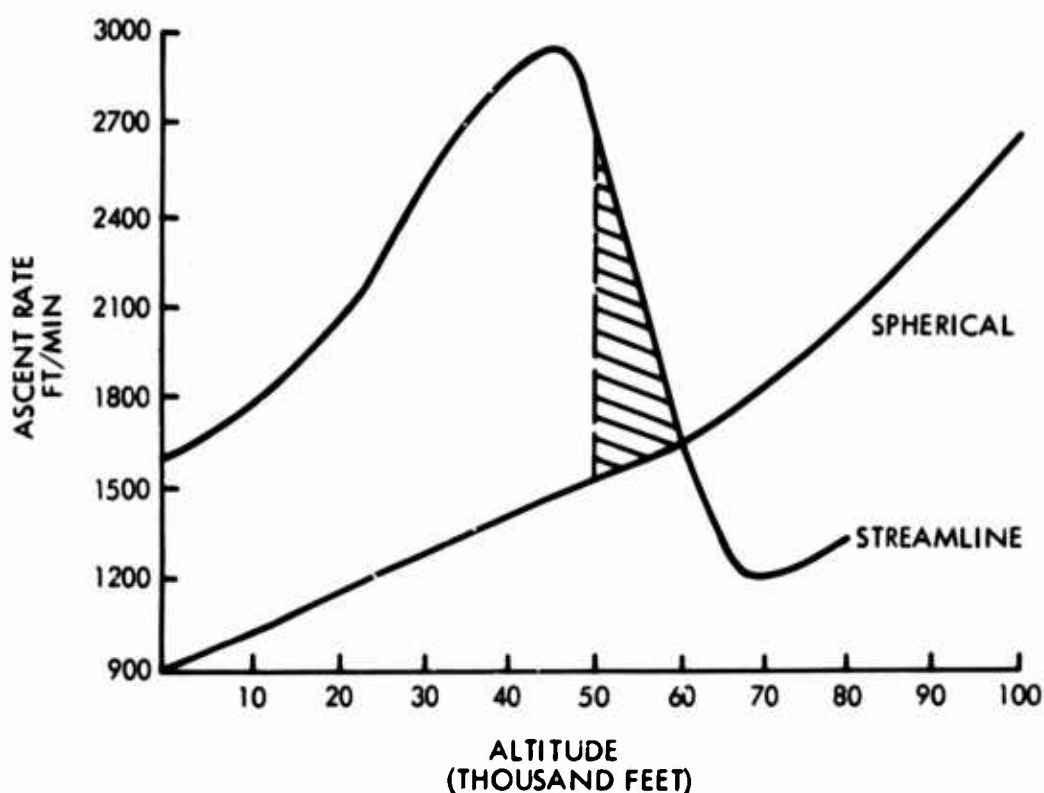


Figure 5. Combined Ascent Rates

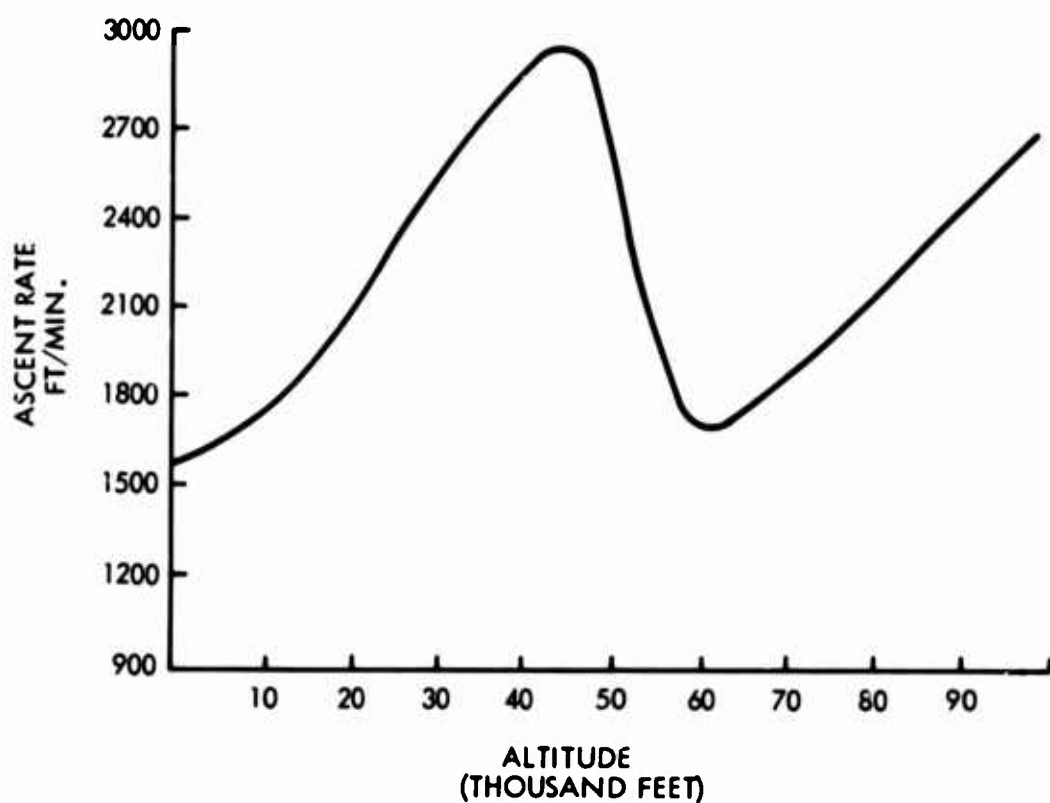


Figure 6. Actual Ascent Rate of Combination Balloon

Between 50,000 feet and 60,000 feet the streamlined balloon bursts and falls away and the inner spherical balloon, its free lift having been increased by an amount equal to the weight of the outer streamlined balloon which has fallen away, will now continue to accelerate until a rate of as high as 2,000 feet per minute is attained at 100,000 feet. The overall ascent rate for such a combination balloon would be more than 1,700 feet per minute.

It was, therefore, necessary to design two components (a) an inner balloon capable of reaching an altitude of 100,000 feet by day or night when flown with the necessary lift for the whole assembly and (b) an outer streamlined balloon capable of fast rate of ascent to 60,000 feet. It is important that this balloon does not substantially exceed this altitude for it is rapidly decelerating at this point and must be jettisoned so that the inner spherical balloon can begin to accelerate.

In order to produce the necessary lift for the type of assembly described, it was determined that a total lift of 9,500 grams would have to be employed. This is somewhat greater than twice the lift required for an ML-564 balloon to reach 120,000 feet when flown with a total lift of 4,600 grams. Hence, this 120,000-foot balloon when flown with the greater lift should be capable of reaching an altitude of at least 105,000 feet, which would be satisfactory. The inner balloon is essentially, therefore, an ML-564 although the weight was slightly increased to provide a somewhat thicker film and a more rugged balloon.

The outer balloon is a modified ML-541 balloon. This balloon is normally flown with a total lift of 5,950 grams and under these conditions will reach an altitude of 75,000 feet or better. If flown with a total lift of 9,500 grams this balloon would reach an altitude of about 65,000 feet, which is higher than is desirable. The length of this balloon was, therefore, reduced and the compound was modified to yield a slightly lower breaking elongation. By these means the bursting altitude of the outer balloon was reduced to between 50,000 feet and 60,000 feet. Because of the lower temperatures of the outer balloon at night the bursting elevation is reduced to about 40,000 feet, and this results in somewhat lower over-all ascent rates.

In addition, nighttime rates of ascent are generally lower than daytime rates of ascent for the same volume of gas for all balloons. This is due to the fact that solar radiation increases the free lift of a balloon in the daytime by raising the temperature of the gas in the balloon above the ambient temperature. The temperature of the gas in the balloon can be as much as 40°C warmer than the air outside the balloon from 50,000 feet to the bursting altitude. At night, on the other hand, the gas temperature is 5°C to 10°C cooler than the air temperature. The balloon at night, therefore, displaces a correspondingly smaller volume of air and has a lower free lift than does the balloon during the daytime.

In order to test the feasibility of breaking the outer balloon without damaging the inner balloon a comprehensive series of tests was conducted with small balloons in the factory. Assemblies consisting of three balloons of different sizes were then flown, the largest balloon being on the inside and the smallest balloon being on the outside. It was clearly demonstrated that the outer balloon breaks first, then the intermediate balloon ruptures and the inner balloon continues until it reaches the normal altitude for a balloon of that size flown with the amount of gas used. The slow ascent rate of this type of assembly during the early part of the flight unquestionably indicated that a streamlined outer assembly was necessary if over-all ascent rates of 1,700 feet per minute were to be achieved.

The final assembly is shown diagrammatically in Figure 7. In order to provide for easier inflation the tail is attached on a circle which is parallel to the circumference which passes through the neck of the head balloon. The dotted line indicates the high-altitude spherical balloon folded inside the streamlined balloon.

In attempts to ensure that the streamlined balloon with the tail falls away at break and does not hang below the radiosonde and constitute a drag, two types of release device were investigated. In the one case a small spherical balloon, weighing about 5 grams, was attached in the train-line between the tail and the radiosonde. This balloon was inflated with air to such a size that it would rupture at the same altitude as the head balloon. This would allow the tail and any of the head balloon still attached to it to fall away.

In the second type, a system of hooks which is illustrated on the left was also tried out. As long as the tail is intact and is carrying the weight of the radiosonde, the hook and eye remain engaged. As soon as the outer balloon breaks and the load is transferred to the line attached to the inner balloon the hook and eye will disengage allowing the tail section to fall clear.

A series of flights was conducted using both types of separation unit and comparing them with assemblies which contained no such device. There was apparently nothing to be gained by the use of either of these attachments. It can, therefore, be assumed that the streamlined balloon is shattering into a number of small pieces and that very little remains attached to the inner balloon during the remainder of the flight.

In order to eliminate the possibility of the two train-lines becoming entangled and preventing separation of the two balloons, the long slack string to the radiosonde was replaced by a shorter line which was attached to the other train-line just below the neck of the tail balloon.

The present model is illustrated in Figure 8 with the rigging in place. The instrument train is attached to the tail, using at least 75 feet of cord. The line running from the neck of the inner balloon to the tail is of sufficient length to ensure that it will not be in tight contact with the outer balloon at 60,000 feet.

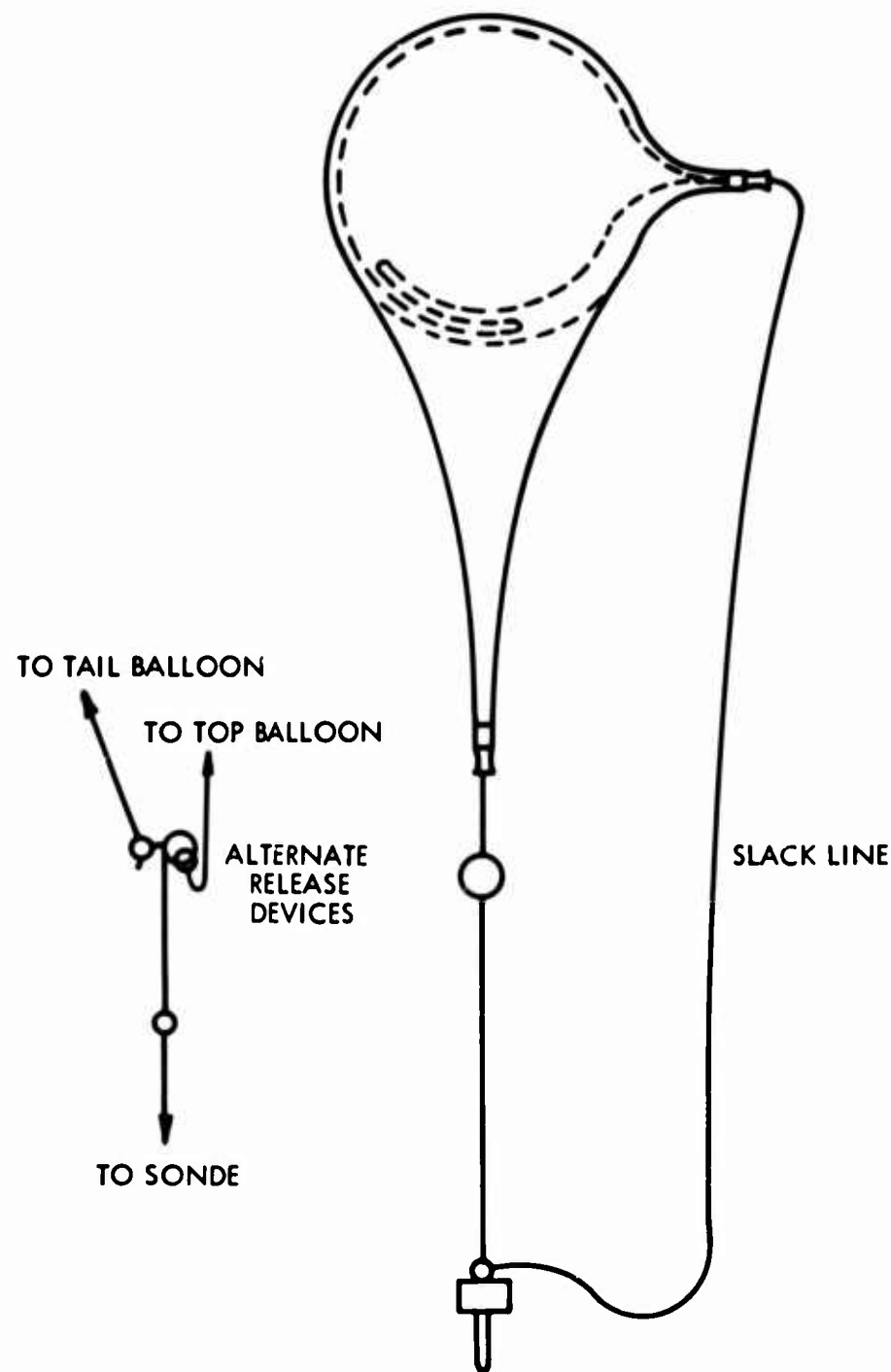


Figure 7. Combination Balloon

After the outer balloon assembly breaks in flight, the load is taken up by the inner balloon and the appearance now is as shown in Figure 9. The outer balloon has shattered and the bulk has fallen away and all that remains are the two neck sections, one of which is still attached to the neck of the inner balloon and the other to the train-line between the balloon and the radiosonde and much closer to the balloon.

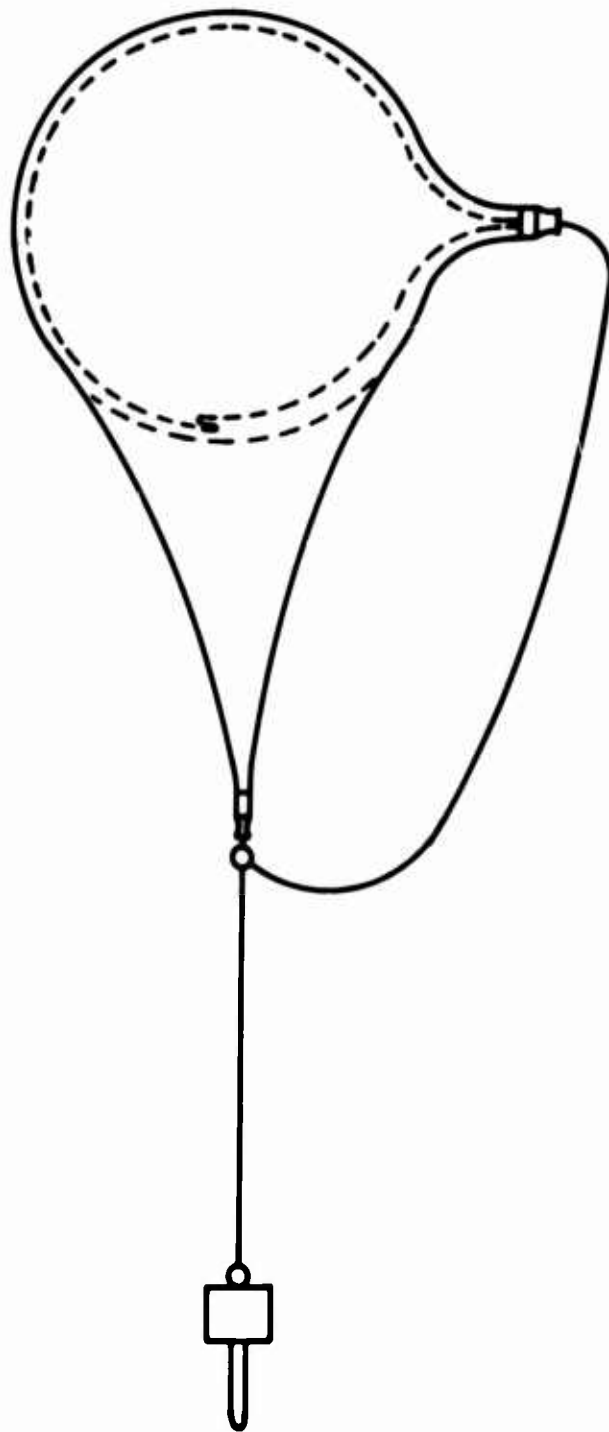


Figure 8. Combination Balloon at Release

This type of balloon reaches altitudes of 100,000 feet by day and by night. In the daytime it will rise at over 1,700 feet per minute with the majority of the ascent rate being more than 1,800 feet per minute and occasionally as high as 2,000 feet per minute. At night the balloons ascend at more than 1,600 feet per minute with approximately half the flights exceeding 1,700 feet per minute. The present

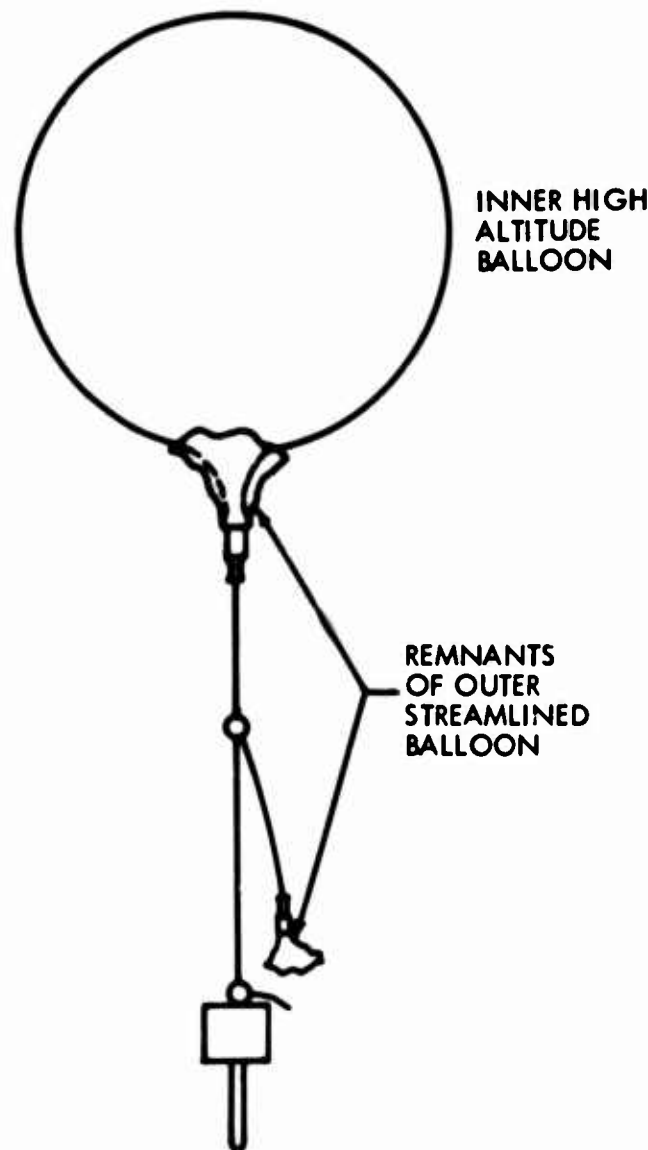


Figure 9. Combination Balloon Second Stage

reliability level is close to 80 percent and work is being continued to raise this to over 80 percent and to increase the nighttime ascent rate to 1,700 feet per minute.

To summarize, it may be said that two new balloon vehicles are now available. One of these, which is identified by Kaysam as the 100ATG balloon, will reach altitudes of 100,000 feet at 1,000 feet per minute in any geographical location by day or by night. This balloon will permit reliable high-altitude soundings during the tropical night and the arctic winter for the first time.

The other, which is identified by Kaysam as the 100GF balloon, is capable of reaching altitudes of 100,000 feet at 1,700 feet per minute during the daytime and 1,600 feet per minute at night. The advantages associated with the rapid rate of

ascent are obvious. The over-all time for making a sounding to 100,000 feet is reduced by about 30 minutes thus providing the required information that much sooner. In addition, the lateral drift is reduced and the observations are obtained much closer to the launch site. The possibilities of losing a balloon because of a low elevation angle are also lessened.

The 100ATG balloon requires a total lift of 4,200 grams when carrying a standard radiosonde and the 100GF balloon performs best when flown with a total lift of 9,500 grams. Both balloons can be inflated in conventional shelters and neither balloon presents any unusual problems as far as handling and launching are concerned.

### References

- Sharenow, M. (1950) Ascensional rate characteristics of large spherical balloons. Paper presented at a meeting of the American Meteorological Society, St. Louis, Missouri.
- Sharenow, M. (1956) Stream-line Neoprene Balloons, SCEL Technical Memorandum M-1776, Fort Monmouth, New Jersey.
- Sharenow, M. (1961) Stream-line neoprene balloons, Bulletin, American Meteorological Society, May 1961.
- Sharenow, M. and Nelson, E. (1963) Some recent advances in high-altitude balloon technology. Paper presented at a meeting of the American Meteorological Society, El Paso, Texas.

## XVIII. Superpressure Balloon Flights from Japan

Vincent E. Lally  
National Center for Atmospheric Research  
Boulder, Colorado

There has been much conversation about superpressure balloons for the last ten years but there have been very few flights. The only really outstanding flights have been performed by the Air Force Cambridge Research Laboratories, and these were with very large superpressure balloons, starting with 34-footers and moving up now to over 100 feet. One of the problems, of course, with these wonderful balloons is that Lou Grass here at Cambridge now has a marvelous balloon that will fly for some unknown long period but has no place to go. Our objective in going to Japan was to provide a little bit of room for ourselves to fly some very small superpressure balloons. The problem of flight with the superpressure balloon is a little more severe with small balloons than with large ones. We have more film area for a given volume, and flying at low altitudes increases the overpressure. Both of these effects mean that the problem of leakage in a balloon goes up inversely as the square of the diameter of the balloon: a 10-foot balloon would have about one-tenth the life of a 34-foot balloon, if both were made equally poorly.

We have made some tests in the United States on small balloons, and, of course, we ran out of grass. We moved to Japan to get a reasonably long fetch. Our second reason for flight from Japan was to test the navigating system which

**PRECEDING PAGE BLANK**

we could use for a much more ambitious test planned for next year. This navigating system was a very simple device. It consisted of a little bit of anodized aluminum, about one inch in diameter, with a thermistor pasted on the back. The thermistor was the controlling element in a resistance-controlled oscillator which was basically a clock which we used to generate a Morse code letter. Through use of a diode matrix we came out with any one of a number of simple codes. With a stop watch we could count how many "k's" the system was transmitting; in a minute, look it up against a calibration chart; find out what the resistance of the thermistor was; from this determine the temperature of the disc; and then determine sun angle. In the final flight program we used an empirical calibration system. Mr. Solot would tell us on the first day of the flight where our balloon was located. From these location points we would deduce the sun angle during the day and then use these angles as the actual calibration for the first day. Then for all future days we could use the same calibration. With a knowledge of sun angle at any time we have a line of position on the globe. With two sun angles which are spread apart by any reasonable period of time, we have something approaching a fix. We used 15.025 mc for our transmission, with the compliments of the Office of Naval Research. The frequency is only usable in daytime, but on this system we had no batteries; we had only solar cells, so that we could operate only during daytime hours. Our maximum output was approximately one watt in a simple center-fed antenna. The mass of the system was about 200 grams, most of this being styrofoam. We did carry in addition a timer, a cut-down timer, since we considered it unwise to fly into Europe. We set this from 6 to 10 days. The timer itself was a simple escapement from which we removed the spring and put on many turns of string (if we wanted a 300-hour flight, we could put 300 turns of string on). The escapement then moved away from the balloon system until all the string was gone and it fell off. The balloon then was too heavily overpressured and burst. These, by the way, were nine-foot balloons flying at 200 mb. The balloon itself weighed 2,000 grams.

The first objective on this trip was to try a cooperative international program. That was the first step toward our eventual international GHOST system. And it did work. It was a joint Japanese-American project. We had some difficulties although our sponsor was the Chief of the Japanese Meteorological Service. It turned out he was quite powerless to help us move our helium into Japan. The Japanese word for cylinder is "bomba" so these were helium bombas, and they are a little bit more dangerous than hydrogen bombas. It took us some three weeks to convince the authorities in Japan that these were not some desperate military weapons. We did use hydrogen on our first flights and eventually switched over to helium.

The second objective -- to test the navigator system -- was from our point of view wonderfully successful. We need this tracking system until we have a satellite to work with our balloon system. On all of the launches we released from a town north of Tokyo. One of our men, who knew when we were going to launch, was in Honolulu. In every case, in the thirteen flights that went up, he picked up our transmission immediately. On one of the flights we were picked up simultaneously from our own receiver in Japan, from Honolulu, and from an amateur who was helping us out in Milford, Massachusetts -- all of this with a power supply that weighed 15 grams with something approaching an infinite life. We are now convinced that we can operate test programs utilizing our simple transmitter and encoder, a very adequate telemetry and transmission system costing less than \$100, to test balloons and to test sensors.

Our third objective, of course, was to test balloons, and this didn't work out too well.

Table 1 is a summary of the flights. The names used were mostly those of children of the people who were over there. They also corresponded to the Morse code for the particular flight. We used hydrogen through the first seven flights. These just indicate the areas from which we picked up our signals: from Tateno, our Japanese site; from Hawaii, from Livermore, California; from Boulder, and later on from a man we put in Pittsburgh. Our Palestine people listened in a few times, too. We made no great effort to build up the network here because we were getting such good communication.

The first flight was on the evening when we finally got our equipment together. Unfortunately we did not know until after the fourth flight that we were having difficulties. The second flight moved to the north very rapidly. Sam Solot told us it was moving into Canada and we assumed we were not picking it up because it went too far north for our receivers, and it wasn't until later that we knew we were in trouble with our balloon.

We had made a number of test flights in Boulder before going to Japan. One of these tests got away from us -- the timer failed in a mountain wave -- and as far as we know it stayed up not less than 35 days. We were, therefore, quite confident that we would have no trouble on our 6- to 10-day flights, which was the time we figured it would take to reach the mid-Atlantic. The durations were very poor on our first flights. Table 1 lists the times we actually had signals; for example, for the flight of one-hour duration, we flew the balloon in the afternoon and after one hour it was sunset and we did not hear signals the next day. Presumably, that balloon flew for less than 24 hours. In general, the duration of the balloon flight was 12 hours to 2 days longer than indicated in the Table.

After the fourth flight, we decided that we did have a problem with our balloons. We thought the problem concerned the hydrogen because we couldn't

Table 1. Summary of Japan GHOST Flights, April 1964

BALLOON	TYPE	GAS	LAUNCHED GMT	LAST HEARD GMT	KNOWN DURATION DAYS TIMER SETTING (Days)	HEARD BY
1. Anna	S	Hy	4/3 0950	4/5 0220	1.7	6
2. Gertrude	S	Hy	4/4 0825	4/5 0442	0.8	6
3. Una	S	Hy	4/5 0815	4/10 0330	4.8	6
4. Wilma	S	Hy	4/6 0757	4/8 0408	1.8	6
5. Dawn	S	Hy	4/8 0846	Failed on ascent Low Ovcst-icing	6	
6. Rolane	S	Hy	4/11 0643	4/11 0742	1 hr.	8
7. Alice	R	Hy	4/14 2109	4/16 0612	1.4	10
8. Gwenn	R	He	4/16 2034	4/24 2014	8.0	10
9. Ursula	R	He	4/17 0839	4/19 0609	1.9	10
10. Thelma	R	He	4/19 0734	4/24 0636	5.0	10
11. Dianne	R	He	4/21 0723	5/2 1945	11.5	10
12. Ruth	R	He	4/22 1020	4/25 2309	3.5	10
13. Nancy	S	He	4/23 1017	4/24 0630	0.8	None
14. Kathy	S	He	4/23 1024	4/29 0025	5.6	None

T-Tateno, Japan  
H-Honolulu  
L-Livermore  
B-Boulder  
P-Palestine  
Pt-Pittsburgh

think of any other reason. As we analyze it now, I am sure use of hydrogen had nothing to do with it. We therefore delayed operations and then converted to helium as soon as we were able to get it released from Customs. We also switched to a balloon which at the time had not been proven out (as we thought the first type of balloon had). The second group of balloons flew much better, although not nearly as well as our tests had indicated they should.

Figure 1 shows the trajectories on some of the longer flights that we made.

The test was useful since it pointed out to us that what we considered a basically reliable balloon turned out to have leakage. How the balloons were damaged we are not sure. We made sample tests of balloons prior to shipping and had great confidence. We are convinced now that the only way to fly superpressure balloons is to make a leakage test on the balloon immediately prior to flight and from that point on never to deflate the balloon. You simply remove the excess gas and then fly it in that condition. We are not sure how much packaging will damage balloons, but certainly a double crease in a Mylar balloon can create a pinhole; and a pinhole with a diameter of 1/10 mil will bring one of these balloons down in one day.

Our next step is to build a device at Boulder which will permit us to make tests down to 0.01-percent leakage per day and in which the leakage tester will also serve as a launch shelter. We are going to be testing balloons all this winter. As a joint project with the U.S. Weather Bureau we plan to go to New Zealand next summer and start launching in the Southern Hemisphere with the approval of the World Meteorological Organization. It will be necessary to get specific approval from each of the forty nations we will overfly, but we have a general endorsement and apparently will have no great problems getting this approval.

We will build a similar test building at our Southern-Hemisphere launch area to permit test of any balloon prior to flight, and to check out its flight performance against its test performance. On this program we also will test out sensors. We are converting our navigation system into a 4-channel system. We will transmit sequentially 16 Morse code outputs from each of 4 data channels from each balloon. Our telemetry accuracy based on our Japanese experiments is much better than 1 percent. We hope during our Southern-Hemisphere venture to establish a climate in which superpressure balloons are flown without objections on a global basis.

Radiosondes are hazards but they are flown every day and people have come to accept them. We don't feel that our system will be a hazard but at the same time there are objections from the hazard point of view. We feel that by continuing to fly we can influence the international climate to accept the eventual system. In addition to the establishment of a better climate among nations, we are concerned with building up a climatology of the planetary circulation in the Southern Hemisphere which will be done by flying at 500, 200, and 30 mb. We plan initially 100 flights.

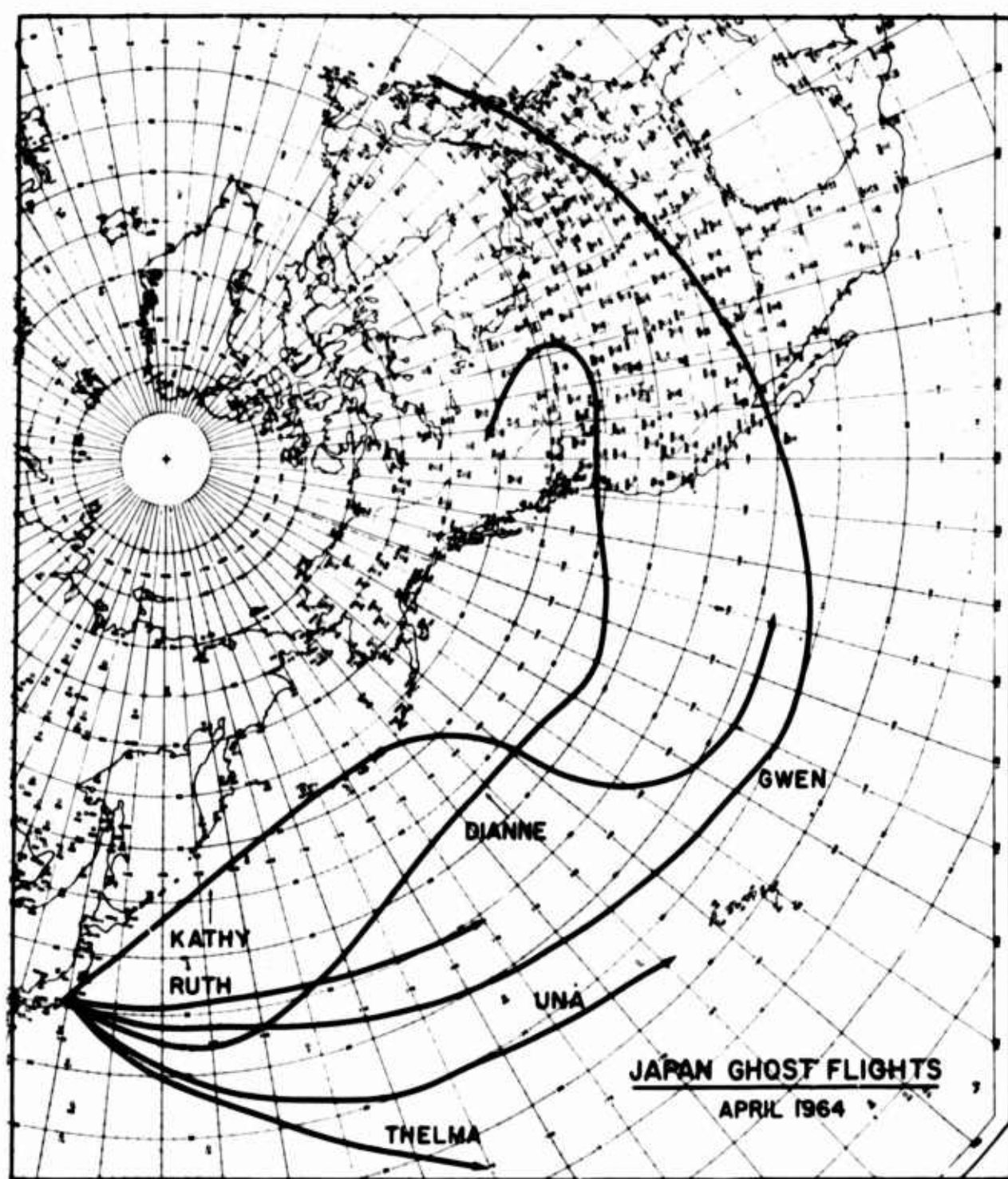


Figure 1.

During the flight program we should obtain answers to the questions of how much cross-equatorial flow we get, and what happens in terms of balloon clustering. Do the balloons tend to move together, or do they tend to stay reasonably randomly distributed? We hope also to be in position so that for the transition to the final GHOST system (the balloon-satellite system) we will have an available balloon capability ready for the satellite.

The data on the Japanese flights is being put together by Sam Solot. He has worked out a computer program in which he analyzed the entire sun-angle data for the day with all the noise inputs, and which provides not only the most probable position but even gives indications of the north-south and east-west components of balloon velocities. A paper will be published within the next few months which will provide complete information on exactly how our balloons flew during the Japanese experiment.

## XIX. Instability of Spherical Wind-Sensing Balloons

Daniel F. Reid, USAF

Aerospace Instrumentation Laboratory  
Air Force Cambridge Research Laboratories  
Bedford, Massachusetts

### Abstract

A description of the "ROSE" wind-sensing technique is presented. The problem of balloon instability as discovered during experiments at the Lakehurst Naval Air Station in the large airship dock is described with examples of balloon trajectories. Water analogy experiments being conducted at University of Southern California, Los Angeles (U.C.L.A) and their relationship to the balloon instability are discussed. A theory relating the instability to the balloon's wake is presented with possible solutions. Recent experimentation at Eglin Air Force Base, Florida, is described and the preliminary results presented. The optimum "quick fix" to the standard balloon and the recommended new design are presented.

### I. INTRODUCTION

Wind and wind variations influence the trajectory of all ascending vehicles. In the case of a boosted space craft or a military missile the gross effect of the wind

can often be corrected for through guidance instrumentation; however, small-scale wind fluctuations are of great concern since they cannot be corrected for and can excite elastic bending modes of the vehicle.

The "ROSE" system is designed to measure these small-scale wind variations in order to prevent both vehicle failure and over-design. The system provides winds and wind shears over altitude layers of one hundred feet, derived from the radar track of an ascending balloon. The "ROSE" balloon is a superpressured, metalized-mylar sphere. It is equipped with pressure-relief valves which vent gas during the ascent in order to maintain a rigid shape. The tracking radar is the high-precision AN/FPS-16.

## 2. BALLOON INSTABILITY

A major problem of spherical wind-sensing balloons was uncovered in an experimental program conducted by NASA Langley Research Center, and the U. S. Army Electronics Command at the Lakehurst Naval Air Station in the large airship dock (Murrow et al., 1964). Balloons that varied in size, weight, shape, material and surface roughness were released within the hanger under calm conditions and their trajectories recorded by phototheodolite and cameras. It was found that the balloons did not follow a vertical trajectory but rather indicated false winds. Figure 1 is an example of the typical trajectory of the 2-meter "ROSE" balloon. Surface roughness produced no apparent improvement in the "corkscrew" type instability. Investigation of operational "ROSE" data confirmed the existence of these horizontal oscillations, as shown in Figure 2, which is a plan view of the "ROSE" position at 0.10-second intervals. (This is the motion an observer sees looking down on the balloon as it rises toward him.) Such instability obviously yields erroneous wind data. The amplitude and wavelength of the oscillations determine the extent of the wind error.

## 3. U.C.L.A. EXPERIMENT

In order to investigate the phenomenon of horizontal oscillations of spheres, AFCRL funded an experimental program at U.C.L.A. (Shafrir, 1964). Spheres of various specific gravities and sizes were dropped in distilled water and the resulting trajectories photographed from two perpendicular directions. Figure 3 shows the type of oscillation observed. The spheres were released by a special mechanism such that no spin nor initial velocity was imparted to the body. A Reynolds-number range of approximately  $10^3$  to  $10^5$  was obtained. The maximum amplitude and the predominant frequency for each Reynolds number were determined. This experimental program showed that the amplitude of the oscillation increases with both

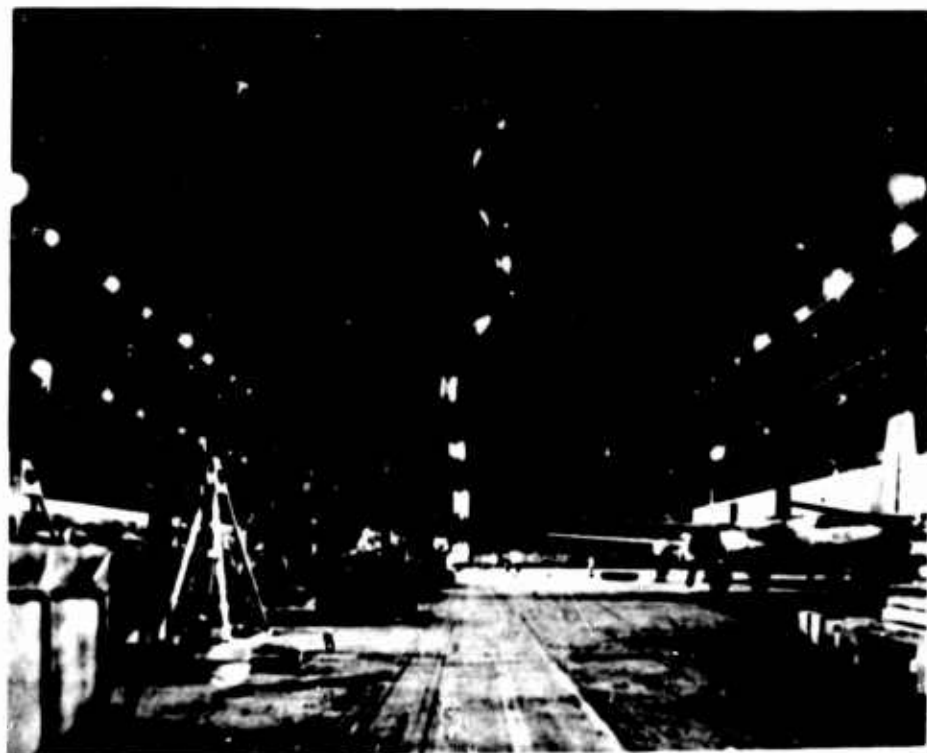


Figure 1. Intermittent Photograph of a Spherical Balloon Ascending in a Hangar

velocity and Reynolds number. Figure 4 shows the maximum peak-to-peak amplitude to be on the order of two to six times the radius of the sphere over the Reynolds-number range considered. The nondimensional frequency of the oscillations was shown to increase with increasing Reynolds number. Figure 5 shows this experimental data and the plotted curve

$$\frac{N_d}{\dot{Z}} = 0.0074 + 4.4 \times 10^{-6} e^{-\frac{\gamma}{1.6} R_e}$$

where  $\gamma$  is the density ratio of the sphere to the viscous medium (in this case water). It is seen that as the density of the sphere becomes large, the frequency becomes a constant (independent of Reynolds number in the experimental range). In applying this to a balloon rising in air, the inverse of the density ratio must be used such that a large ratio of air density to balloon density would yield a constant frequency of oscillation. Interpretation of these data proved that although the instability is present, the frequencies and amplitudes are such that the winds indicated by a spherical balloon under subcritical Reynolds number are valid.

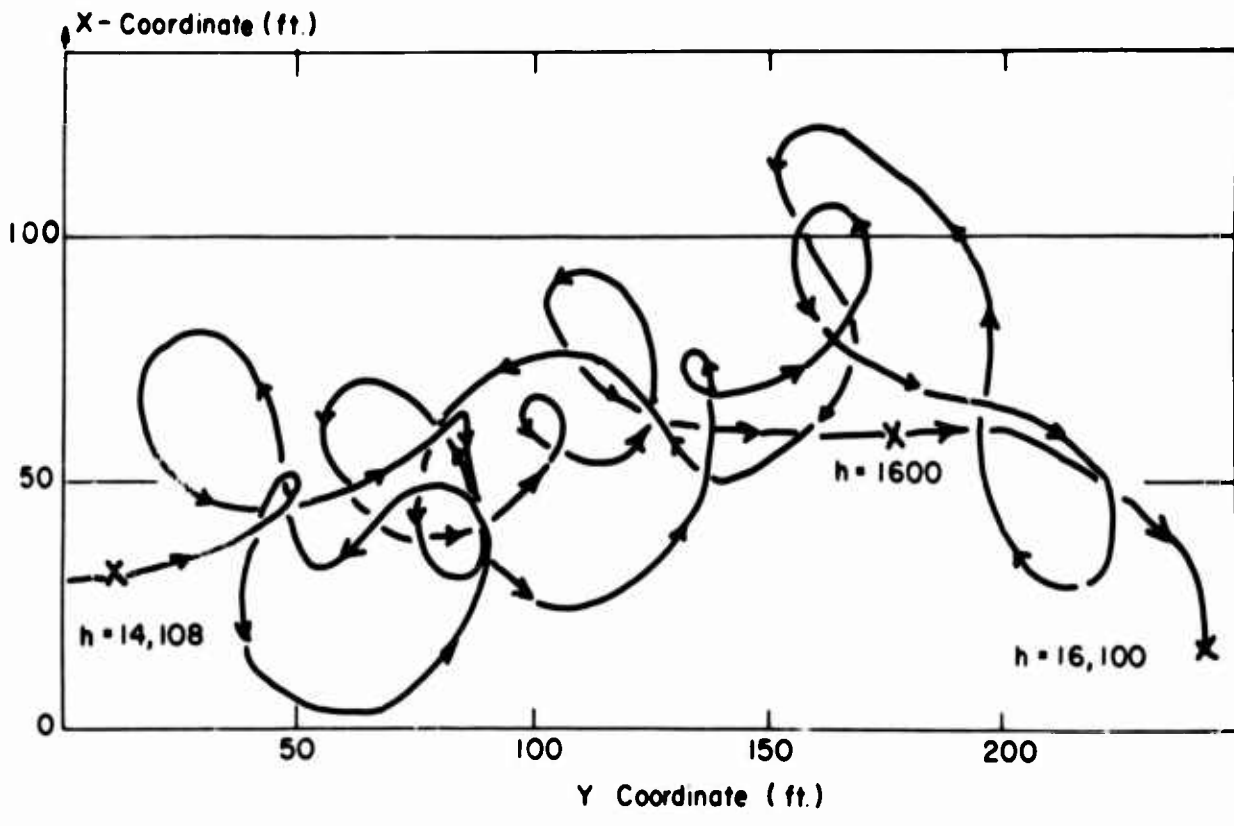
2-m Rose Supercritical  $Re \approx 8 \times 10^3$  X-Y Plot

Figure 2. Horizontal Position Plot of a Standard "ROSE" Balloon Flight

#### 4. CAUSE OF THE INSTABILITY

The cause of the horizontal oscillations found in freely rising and falling spheres has not been defined. Investigation of the "ROSE" instability has led to the following theory: the horizontal and vertical oscillations of spheres under subcritical Reynolds number are caused by the shedding of vortices. Under subcritical Reynolds number the boundary layer of the sphere is laminar with separation occurring somewhere near the equator. Vortex packages are alternately carried away by the outer flow causing the separation points to move back and forth so that the dimension of the dead area fluctuates. The sphere reacts with a spiral- or corkscrew-type motion. The frequency of the vortex shedding is related not only to the Reynolds number but also to the density ratio of the sphere to the fluid. The induced motion of spheres under supercritical Reynolds numbers is not caused by vortex shedding since the boundary layer is now turbulent. The wake separation point has moved downstream due to turbulent mixing and the dead area and drag coefficient are considerably decreased. The oscillations of the sphere are now caused by a varying line of separation on the surface of the sphere. The dimension of the dead area remains

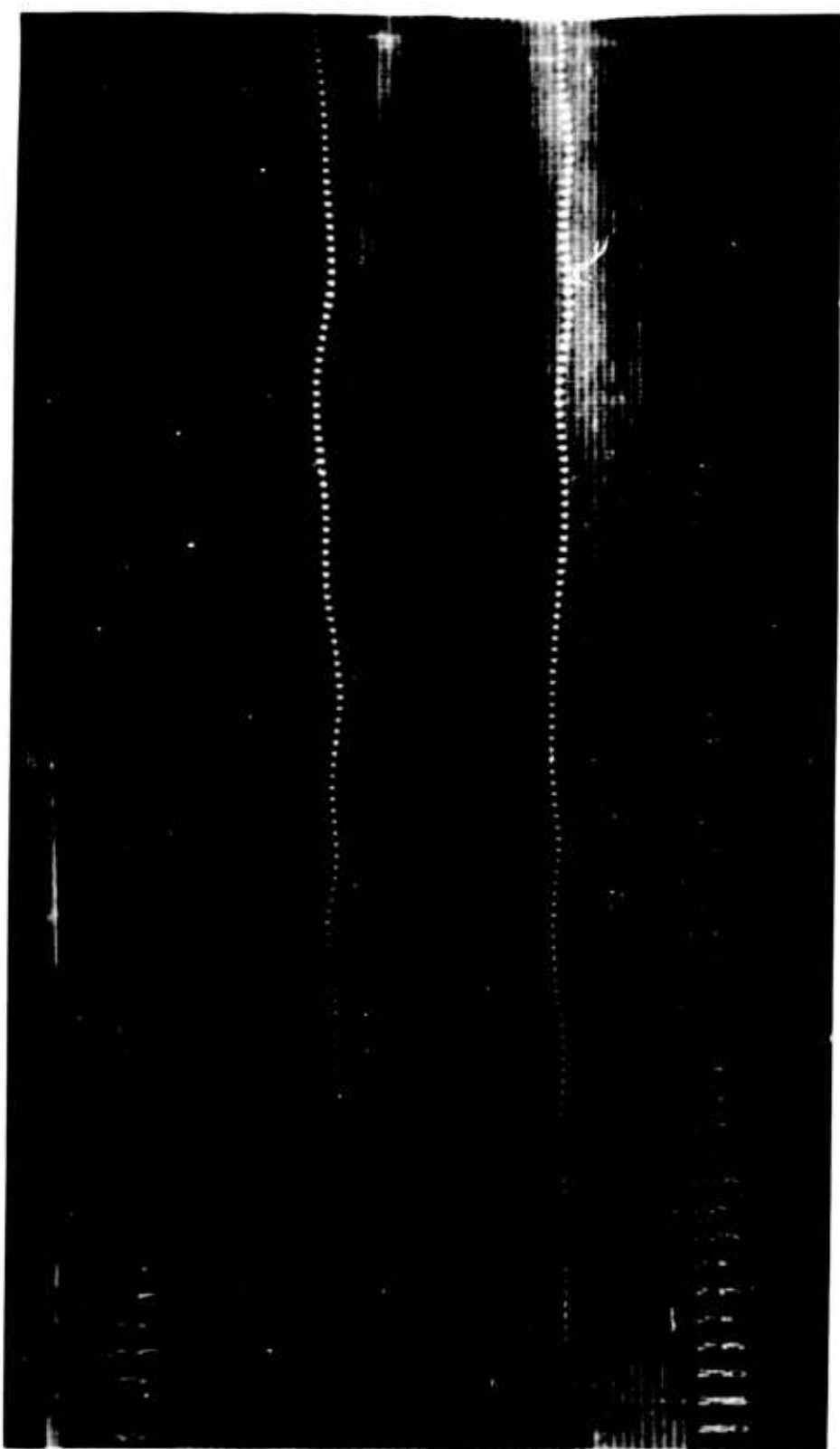


Figure 3. Intermittent Photograph of a Sphere Falling in Water

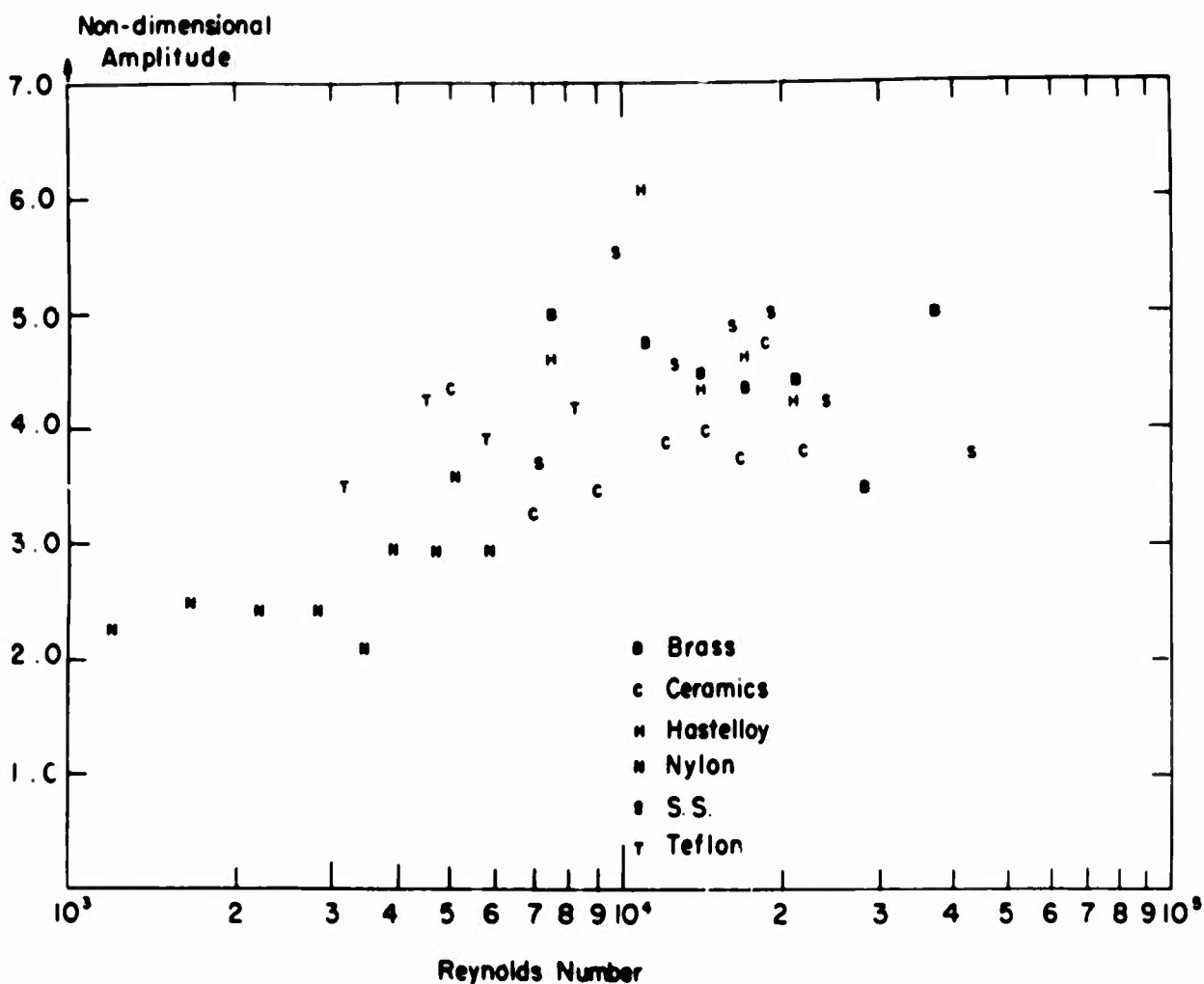


Figure 4. Nondimensional Amplitude of Oscillations of Spheres Falling in Water

constant but moves relative to the sphere. This is a wandering wake. The magnitude of the balloon motion induced by a wandering wake is considerably greater than that caused by vortex shedding.

### 5. SOLUTION

Based upon the conclusion that a subcritical type wake eliminates the instability problem, four possible techniques could be used to produce such a wake:

1. The first would be to control the separation so that it remains near the equator. This could be done by employing surface projections or bubble fences which produce separation (Scoggins, 1964). The projections would have to extend beyond the boundary layer to accomplish this, since surface roughness produces the undesired turbulent boundary layer.

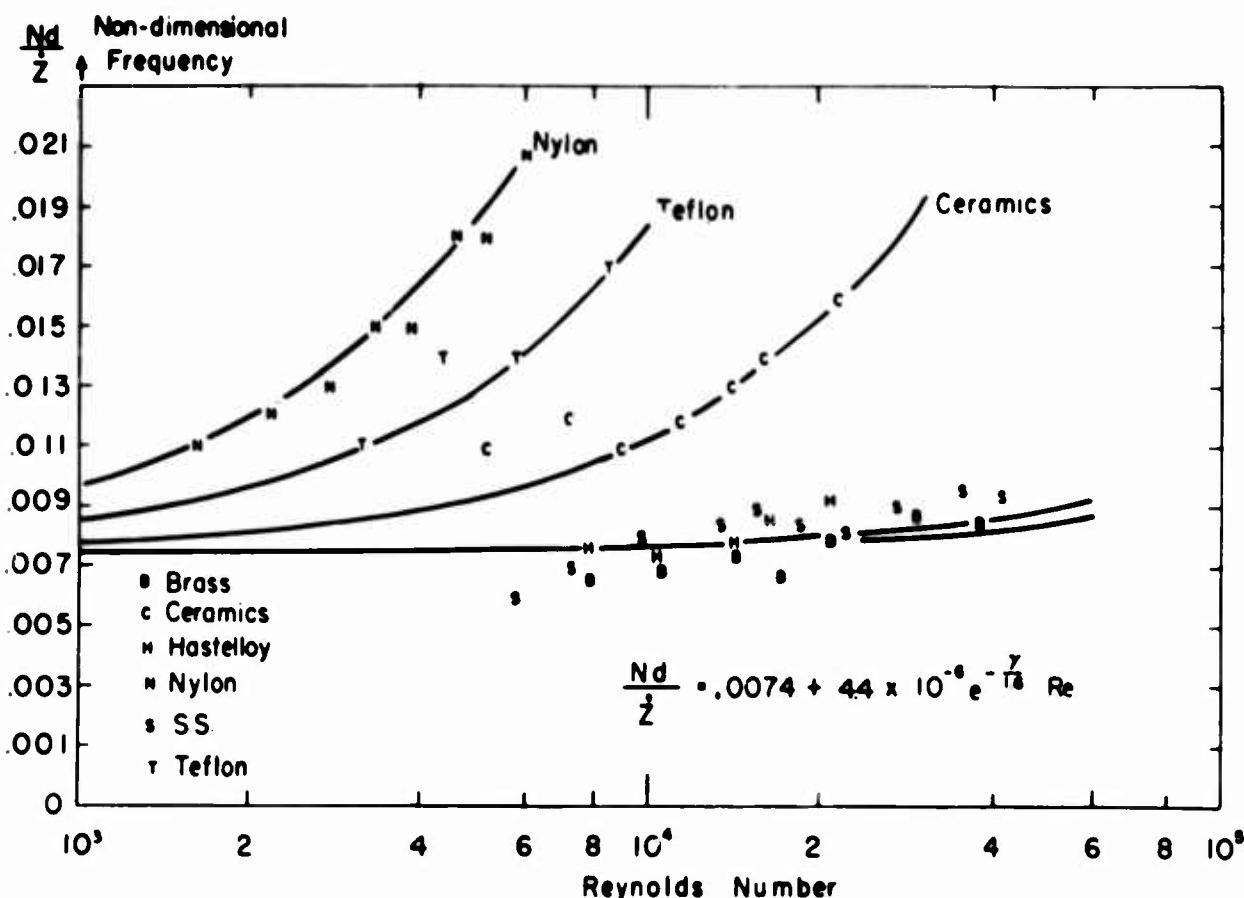


Figure 5. Nondimensional Frequency of Oscillations of Spheres Falling in Water

2. The second technique would be to maintain a laminar boundary layer. This could be accomplished by limiting the Reynolds number to subcritical values by reducing the size of the balloon.

3. The third technique would be to maintain a large dead area behind the sphere. This could be accomplished by using skirt-type devices.

4. The fourth technique would be a method of direct wake stabilization through the use of drag tails.

In making any modification to the balloon, consideration must be given to the effect upon its wind-sensing capabilities. Any added weight is undesirable as is an increased diameter due to the adverse effect on the wind response (Reid, 1964). At the same time, any objects put into the boundary layer will affect the apparent mass of the balloon. (The apparent mass may be thought of as that portion of air surrounding the balloon which must be accelerated as if it were a part of the balloon. It is approximately equal to one half the mass of the displaced air for the standard "ROSE".) Any modification which changes the shape of the balloon so that the drag area becomes a variable (a function of orientation) or which provides lifting surfaces is undesirable. Rotation of the balloon is undesirable in all cases because it tends to encourage a turbulent boundary layer.

## 6. EGLIN EXPERIMENTS

Over one hundred "ROSE" flights have been made at site D-3 of Eglin Air Force Base, Florida, using modifications which encompass the previously mentioned techniques. These experiments consisted of dual flights of standard and modified balloons launched within minutes of each other.

One group of modifications consisted of surface projections (conical and truncated conical paper cups) in varying size and number. Figure 6 shows a photograph of one of these balloons. The patterns were random with as few as 75 cups and as many as 300. The heights varied from 2.5 inches to 4.75 inches. Perpendicular belts of cups (one belt around the equator) were also used with variable-sized projections. This group of modifications attempted to control the separation point.



Figure 6. Photograph of "ROSE" Balloon Modified with 230 Surface Projections

Attempts to keep the boundary layer laminar included the use of small lightweight spheres which would be under subcritical Reynolds numbers for most of the flight.

Attempts to keep the dead area large consisted of providing the balloons with perpendicular belts of ribbons and loops made of polyethylene. These were to have acted as omnidirectional skirts.

Attempts to stabilize the balloon wake directly used balloons equipped with drag tails of various sizes, weights, and configurations.

As a first look at the performance of the modified balloons a comparison was made of the winds indicated by the paired flights. Figure 7 shows the winds indicated by a sphere with 230 truncated cups compared to the winds indicated by a standard sphere launched three minutes later. The modified balloon had approximately 4 ounces of added weight. Figure 8 shows a similar comparison of a standard and a small sphere. Since the instability appears as dispersion or noise in the winds, the standard deviation of the 100-foot winds from a 1000-foot average was computed. A large standard deviation is indicative of extreme instability. Figure 9 shows a plot of these standard deviations versus altitude for a standard and a modified flight. Note the reduction in the standard after critical Reynolds number is reached.

A comparison of the wind-vector variance was made for 5,000-foot layers. The percent reduction in variance was computed. Figure 10 shows this reduction versus altitude for a series of modifications.

## 5. EXPERIMENTAL RESULTS

The use of drag tails to stabilize the 2-meter spherical balloon is not effective. In some cases they add to the instability in the form of a very-high-frequency "fish-tail" type motion.

Surface projections will stabilize the 2-meter balloon if their height is considerably greater than that of the boundary layer. Conical projections are superior to truncated cones. In general the effectiveness of this modification increases with increasing number of projections to a point beyond which no advantage is gained. This point is dependent upon the size of the projections. Selected patterns of surface projections can be as effective as random placement. In particular an equatorial belt and a polar belt of surface projections are most effective if multi-edged projections are used. The effectiveness increases with increasing edges.

Omnidirectional skirts provide some stabilizing effect but not sufficient to offer a solution to the problem.

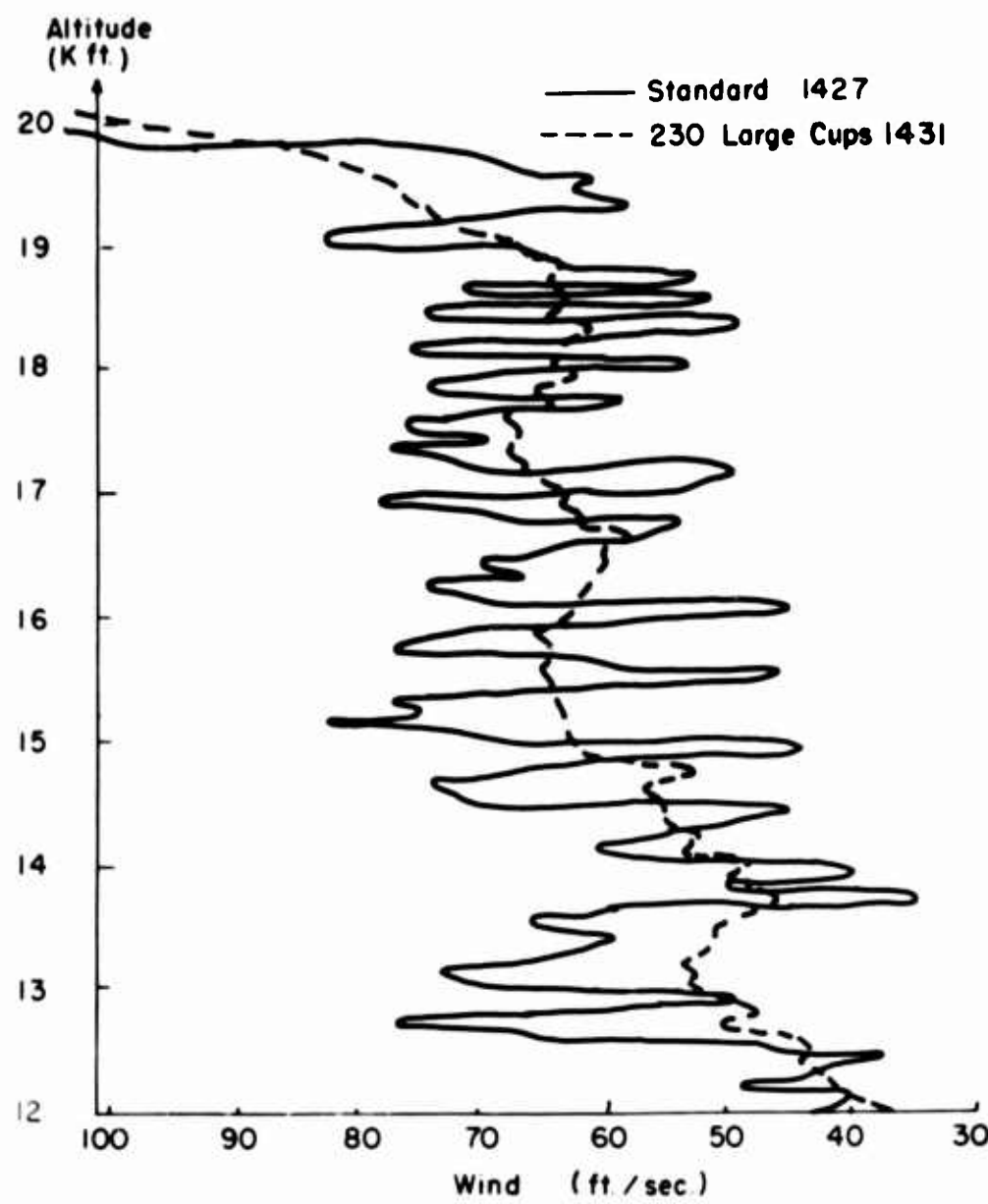


Figure 7. Comparison of Winds Indicated by a Modified and a Standard "ROSE" Balloon

The use of small lightweight spheres was found to be the most effective solution. The subcritical sphere is as stable as the best of the previously mentioned modified balloons. The use of 1/4-mil mylar balloons as wind sensors is practical, with no serious handling problems. "Weightless" valves (holes covered with a porous material, as designed by G. T. Schjeldahl Company) are effective and present no great problems provided they maintain sufficient balloon superpressure. Balloons equipped with these valves will rise more slowly initially than the standard balloon with a pop-out valve, and then more rapidly at higher altitudes. This is desirable in that the Reynolds number is lower at launch.

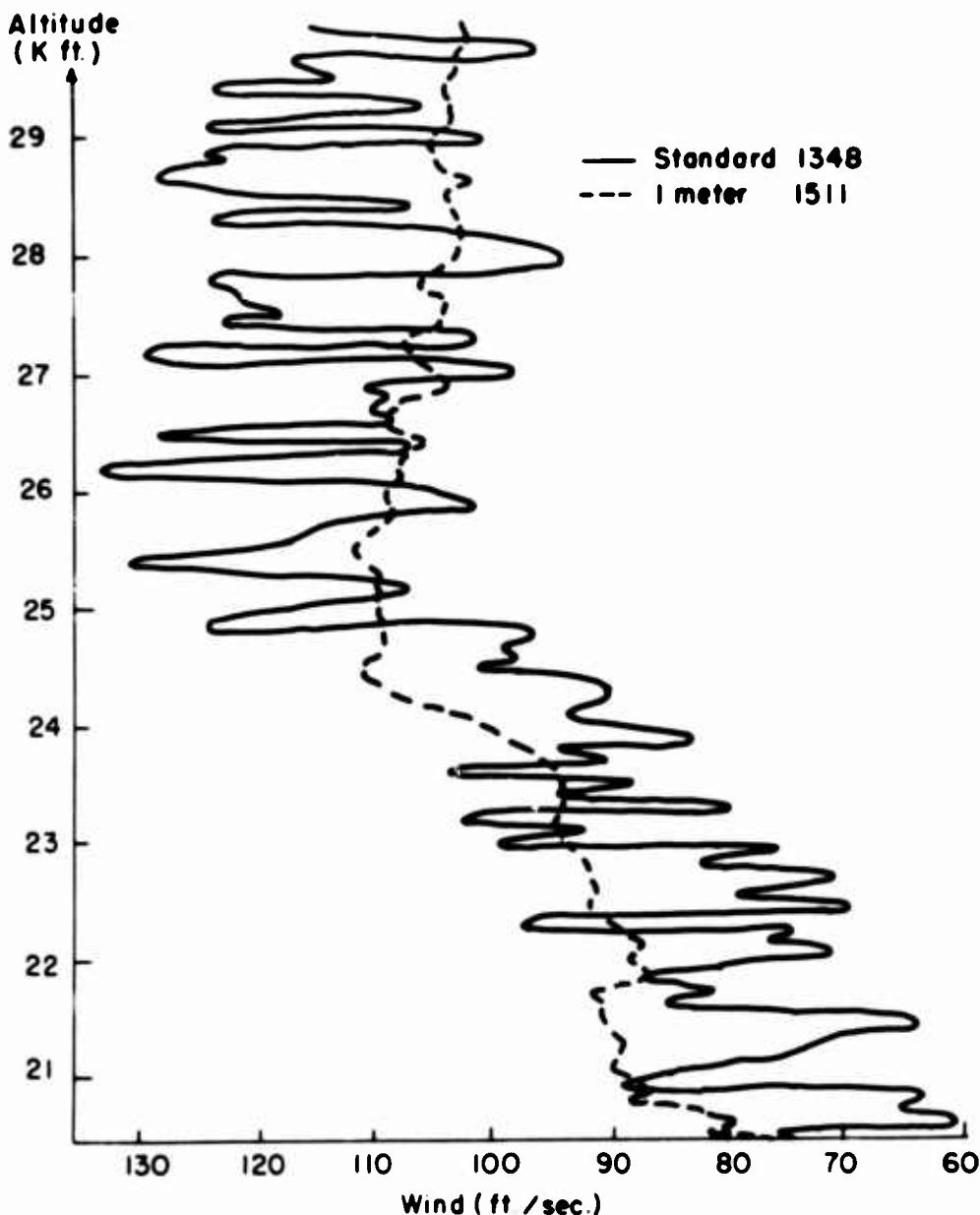


Figure 8. Comparison of Winds Indicated by a Modified and a Standard "ROSE" Balloon

Measured drag coefficients for the standard type "ROSE" balloons, with diameters of 36 inches, 40 inches, and 2 meters, were considerably different from the classical values. In general the measured drag coefficients reached peak values of approximately 1.0 near a Reynolds number of  $10^5$  and then decreased rapidly on each side of this point but remained greater than the classical values over the entire measured range.

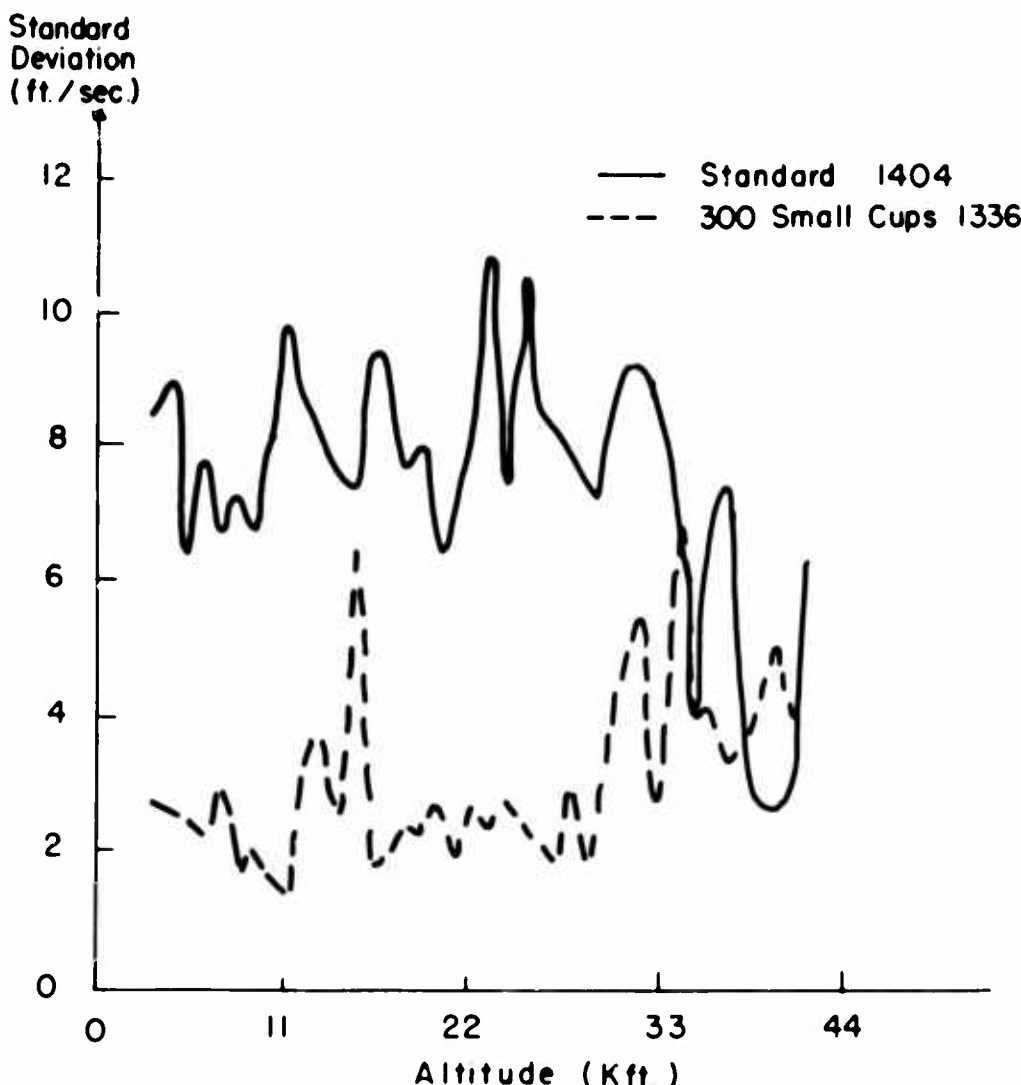


Figure 9. Standard Deviation of Winds Indicated by a Modified and a Standard "ROSE" Balloon

### 8. CONCLUSION

The optimum stabilizing modification to the 2-meter "ROSE" balloon is the addition of perpendicular belts each containing 96 conical paper cups (3.75 inches in height with a base diameter of 2.5 inches). The total added weight is 10 ounces.

The new design of the "ROSE" balloon is a metalized mylar sphere, 40 inches in diameter made of 1/4-mil material and equipped with the standard teflon relief valve. Maximum altitude is 56,000 feet with subcritical Reynolds number attained after the first few thousand feet. This balloon is considerably more responsive to the wind than the 2-meter size due to the reduction in the apparent mass.

Classical wind-tunnel drag coefficients are not applicable to the "ROSE" balloon and possibly not to any freely-rising spherical balloon.

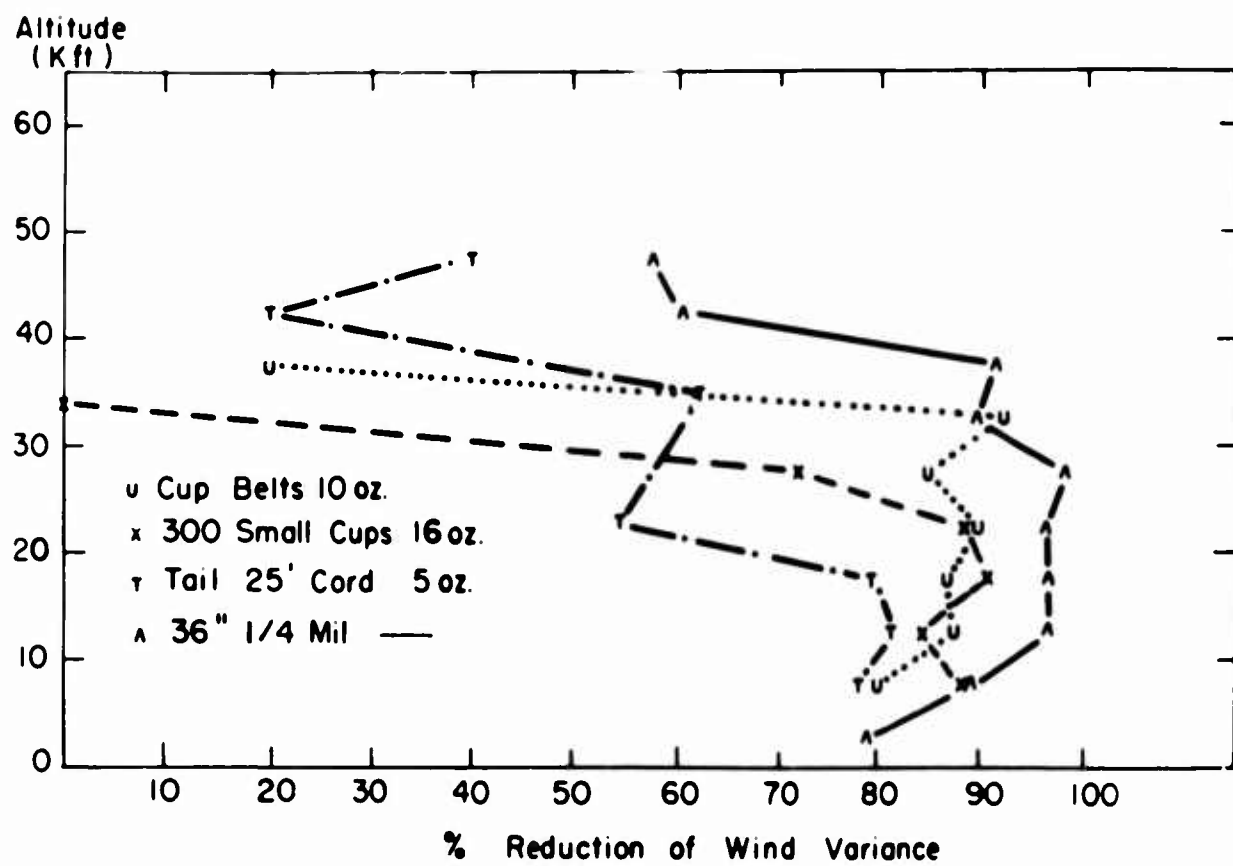


Figure 10. Percent Reduction in Wind Variance Produced by Balloon Modifications

## References

- Murrow, Harold N. and Henry, Robert M. (1964) Self-induced balloon motions and their effects on wind data. Paper presented at the AMS Fifth Conference on Applied Meteorology, Atlantic City, New Jersey.
- Reid, Daniel F. (1964) The Rose wind sensor. Paper presented at the AMS Fifth Conference on Applied Meteorology, Atlantic City, New Jersey.
- Scoggins, James R. (1964) Spherical balloon wind sensor behavior. Paper presented at the AMS Fifth Conference on Applied Meteorology, Atlantic City, New Jersey.
- Shafrir, Uri (1964) Horizontal Oscillations of Falling Spheres. Final report, Air Force Contract AF19(628)-3993.
- Wright, John B. (1964) The Robin and the Rose sphere. Paper presented at the 44th Annual AMS Meeting, Los Angeles, California.

**PRECEDING PAGE BLANK**

## **XX. A Preliminary Investigation of High Altitude Minimum Wind Fields \***

**George F. Nolan**

**Aerospace Instrumentation Laboratory  
Air Force Cambridge Research Laboratories  
Cambridge, Massachusetts**

### **Abstract**

During the summer months, a relatively stable layer of minimum winds exists in the lower stratosphere above the North American continent between latitudes 25°N and 65°N. Within the layer there are levels where the wind speed is close to zero. These phenomena can be utilized for balloon operations that require flights of long duration with minimum horizontal displacement from a fixed geographic location, and for high-altitude tethered-balloon operations that require float altitudes where dynamic pressure is minimum.

---

\*This talk was based on an AFCRL in-house report of the same title, AFCRL 64-843, by Mr. Nolan and Ralland A. Smith, published in October 1964. - Editor.

**PRECEDING PAGE BLANK**

## XXI. Toward Improved Measurements of Stratospheric Humidity with Balloon-Borne Frost-Point Hygrometers\*

J. G. Ballinger, L. E. Kochler, M. P. Fricke and R. D. Murphy  
Military Products Group Research Laboratory  
Honeywell, Inc.  
St. Paul, Minnesota

### Abstract

Efforts to increase the reliability of stratospheric frost-point measurements made with balloon-borne, automatic hygrometers are described. Two major problems limiting the accuracy of stratospheric data are examined quantitatively and shown to place very high requirements on the equipment used: (1) unsatisfactory instrument performance due to low mass-transfer rates of water vapor and (2) bias due to contamination of the moist-air sample by vapor desorbed from the instrument package and vehicle. General measures to improve the quality of future frost-point data from all sources are recommended, and specific techniques adopted by the Honeywell group are reviewed. Equipment for upcoming AFCRL vertical soundings and long-duration horizontal flights with Alpha Radiation Hygrometers is described.

---

\*Work performed for the Aerospace Instrumentation Laboratory, Air Force Cambridge Research Laboratories under contract numbers AF 19(604)-8418, AF 19(628)-3857, and AF 19(628)-4206.

## 1. INTRODUCTION

There is currently considerable interest in the water-vapor content of the stratosphere and in its variation with time. Meteorological interests include the development of stratospheric circulation theories; relevance to military technology includes the importance of water-vapor data to missile detection and tracking. Balloon soundings with automatic frost-point hygrometers offer a promising means to obtain continuous humidity information up to an altitude of about 100,000 feet.

Previous data obtained by this technique, however, have differed by more than two orders of magnitude in vapor-to-air mixing ratio. These data have been reviewed elsewhere (Mastenbrook, 1963, 1964; Gutnick and Salmela, 1963; Rohrbough and Ballinger, 1964) and can be divided roughly into two groups, those which show the upper stratosphere to be dry and stagnant and those which show it to be wet and variable in time.

Gutnick (1961) has suggested that this controversy over upper-stratospheric humidity cannot be settled by making measurements of no greater reliability than those made to date. We strongly support this point of view. The lack of reliability in frost-point data from automatic hygrometers stems from the fact that the quantity of water vapor present is extremely minute. This leads to two problems which will be discussed in some detail. First, the scarcity of water vapor makes the response time of automatic hygrometers so long that it may prove necessary to modify drastically current sampling techniques. Secondly, even the slightest amount of water-vapor contamination from the measuring system produces a very large fractional error. These problems pertain to all types of automatic frost-point hygrometers.

Our current activities include the preparation of instrument packages for an extensive stratospheric water-vapor study by AFCRL (Sissenwine, Grantham and Salmela, 1964). Based on our examination of the basic problems mentioned above, new techniques and equipment have been adopted for this study which are aimed at attaining unprecedented reliability. These are described in the remaining portion of this paper.

## 2. BASIC PROBLEMS

### 2.1 Frost-Layer Dynamics

In an automatic frost- (or dew-) point hygrometer, the temperature of the cooled surface is controlled by a servomechanism which strives to maintain a stable deposit of frost (or dew). The rates of buildup and sublimation of the frost

layer in this process determine not only the design parameters for optimum automatic control but the very feasibility of the device as a continuously monitoring instrument. Slow rates imply that, for a cooled-surface temperature far from the frost point, the frost deposit will take a long time to change enough to be detected and to cause a correction in the surface temperature. This can lead to intolerable response characteristics and gross errors in the frost-point determination if the instrument is used in an environment where the frost point changes in time (such as a stratospheric balloon flight).

We have estimated previously (Ballinger, Fricke and Murphy, 1964) this rate of deposit-thickness change for two typical geometrical cases: (1) flow of the moist-air sample over and parallel to a flat plate containing the condensate deposit, and (2) flow of the moist air through a narrow channel formed by two parallel walls, one of which contains the condensate layer. Changes in the bulk concentration of water vapor along the direction of flow (for example, a lowering of the concentration when the frost temperature is below the frost point) are neglected. Therefore, the estimated rates are valid only when they are small in magnitude and when the length of the deposit (along the direction of flow) is small; otherwise the magnitude of the calculated rate is larger than the actual value.

For either geometrical case, the rate of thickness change has the form

$$\frac{d\sigma}{dt} = \ell (\rho_A - \rho_F), \quad (1)$$

where  $\sigma$  is the thickness of the deposit in units of mass per unit area.

The partial densities of water vapor in the bulk flow and in a small boundary layer immediately above the condensate are  $\rho_A$  and  $\rho_F$  respectively.  $\rho_A$  can be taken to be the saturation vapor density corresponding to the frost point of the moist-air sample, and  $\rho_F$  that corresponding to the instantaneous temperature of the frost.

The mass-transfer coefficient  $\ell$  for the flat-plate geometry is given by

$$\ell = \frac{0.332V}{Re^{1/2} Sc^{2/3}}, \quad (2)$$

where  $V$  is the flow velocity,  $Re$  the Reynolds number, and  $Sc$  the Schmidt number. The latter are given by

$$Re = \frac{x\rho V}{\mu}$$

$$Sc = \frac{\mu}{\rho D},$$

where  $\rho$  is the (total) density of the ambient air,  $\mu$  is its coefficient of viscosity,  $D$  is the diffusion coefficient, and  $x$  is a characteristic distance from the leading edge of the flat plate to the point where  $\sigma$  is measured.

For the channel-flow geometry, the mass-transfer coefficient becomes

$$\lambda = \frac{3.75D}{b} , \quad (3)$$

where  $b$  is the distance between the walls of the channel. The apparent velocity-independence and indefinite increase with diminishing  $b$  hold only when the aforementioned assumption is valid, namely when the bulk water-vapor concentration varies little along the channel.

To examine experimentally these rates of mass transfer, an environmental chamber was constructed to reproduce typical values of humidity, pressure, temperature, and ventilation rates encountered by a hygrometer in stratospheric balloon-flight applications. An experimental study of other errors inherent in frost-point determinations, principally those due to thermal diffusion and the physical properties of thin layers of frost, is also contemplated.

This stratospheric-moisture simulator and associated instrumentation provide a continuous, nonrecirculating flow of air at a constant frost point. The test chamber uses a free-jet principle\* to allow a large working area within the test chamber without the necessity of providing a large humidity-controlled region. The chamber has a constant-humidity jet, conical in shape, and 1/2 inch in diameter by 2 inches long.

The simulator is specifically designed to provide frost points between -50°C and -100°C at equivalent pressure altitudes from 30,000 feet (300 mb) to 130,000 feet (3 mb) and flow velocities from 100 to 1000 ft/min. The air temperature in this particular version is not controlled but remains near typical free-air temperatures. Another heat exchanger, placed between the frost-point heat exchanger and the test cell, could be added to provide control of the air temperature.

The flow diagram is shown in Figure 1. Air from a pressure source is passed through the dryer and controlled by a mixing valve (A). This dry air is mixed, by an ejector and mixing tube, with humid room air to provide an air supply in the desired humidity range. The pressure equalization section allows this partially dry air to reach barometric pressure before entering the system inlet, providing a stable pressure source. The two metering valves (B and C), both of which operate as sonic orifices, establish the flow rate (velocity) and system pressure.

---

\*The following references establish the validity of using the free-jet principle.

1. Albertson, J.L., Dai, B., Jensen, R.A. and Rouse, "Diffusion of Submerged Jets", Transactions of American Society of Civil Engineers, Vol. 115, 1950.
2. Schlichting, H., Boundary Layer Theory, McGraw-Hill Book Co.
3. Amramovich, G.N., "Turbulent Jets Theory", Gasudarstvennoye Izdatel'stvo - Matematicheskoy Literatury 1960, Translation in ASTIA Document AD 283,858, August 1962.
4. Sato, H. "The Stability of a Two Dimensional Jet", Journal of Fluid Mechanics, Vol. 7, January 1962.
5. Heskestad, G. "Measurements in a Two-Dimensional Turbulent Jet", AFDSR 2456, April 1962.
6. Miller, D.R. and Comings, E.W., "Static Pressure Distribution in a Free Turbulent Jet", Journal of Fluid Mechanics, 3, 1957-8.
7. Foerthmann, E., "Turbulent Jet Expansion", NACA TM 789, 1936.
8. Tollmien, W., "Calculation of Turbulent Expansion Process", NACA TM 1085, 1945.
9. Crane, L.J., "Laminar and Turbulent Mixing of Jets of Compressible Fluid", Journal of Fluid Mechanics, Vol. 3, Part 1, October 1957.
10. v. Krzywoblocke, M., "Jets a Review of Literature", Jet Propulsion, Vol. 26, No. 9.
11. Corrsin, S. et al., "Spectra and Diffusion in a Round Turbulent Jet", NACA, Report 1040.
12. Betz, A., et al., "Application of the Theory of Free Jets", NACA TM 667, April 1932.
13. Donald, M.B., et al., "Entrainment in Turbulent Fluid Jets", Transactions Institute of Chemical Engineers, Vol. 37, No. 5, October 1959.

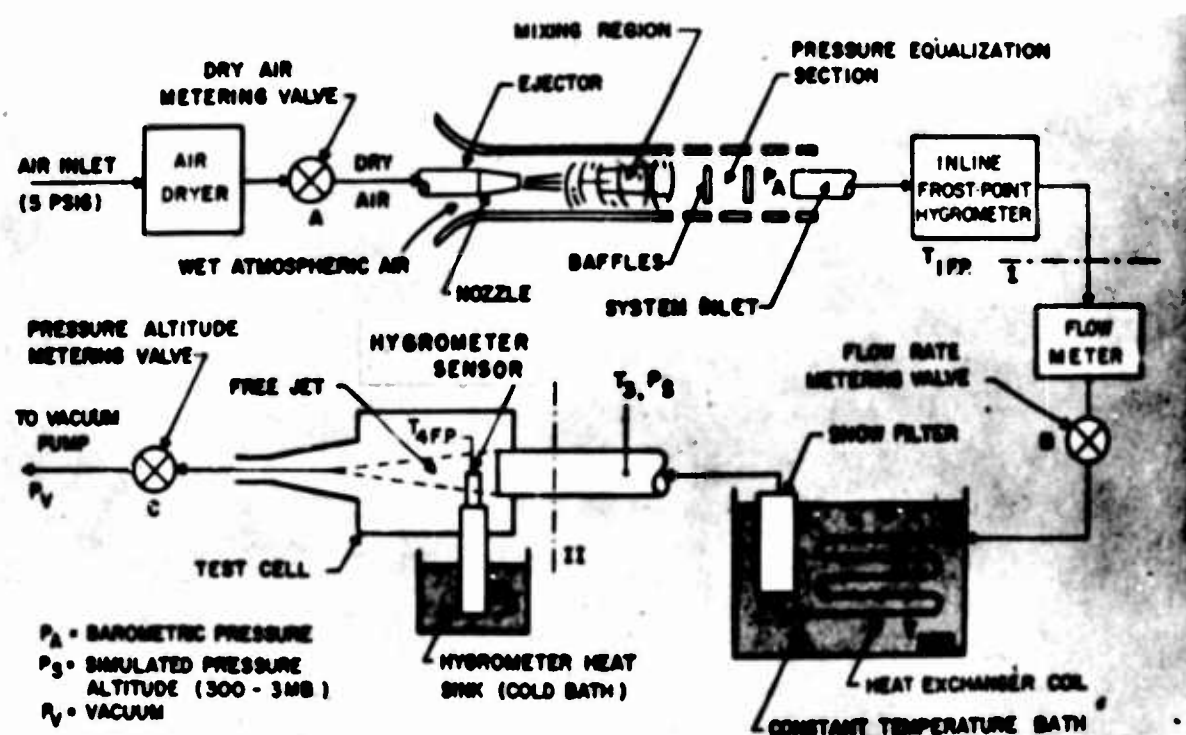


Figure 1. Stratospheric Moisture Simulator Flow Diagram

The hygrometer mounted upstream of valve B is used to establish the setting of valve A such that the air after expansion through valve B will have a frost point 5 to 10 degrees above the temperature of the control bath. The sole purpose of pre-drying the inlet air is to remove the major portion of the water ahead of the heat exchanger to avoid icing in the coils. This mixing process does not establish the operating points. The air is further cooled as it passes through the heat exchanger and comes into equilibrium with the constant-temperature bath which establishes the frost point. The use of constant-temperature baths (typical of these are mixtures of various substances and CO<sub>2</sub> snow which provide fixed temperatures in the range from -70 to -78.5°C) is a simple means of precisely controlling temperature for long periods of time.

The heat exchanger is designed to avoid any appreciable pressure drop across it. A snow filter consisting of stainless-steel wool is located at the downstream end to remove any airborne ice crystals.

Figure 2 shows a test fixture for the test cell. The components shown are a thermoelectric cooler mounted on a heat sink, and a fixture for positioning the frost-thickness sensor.

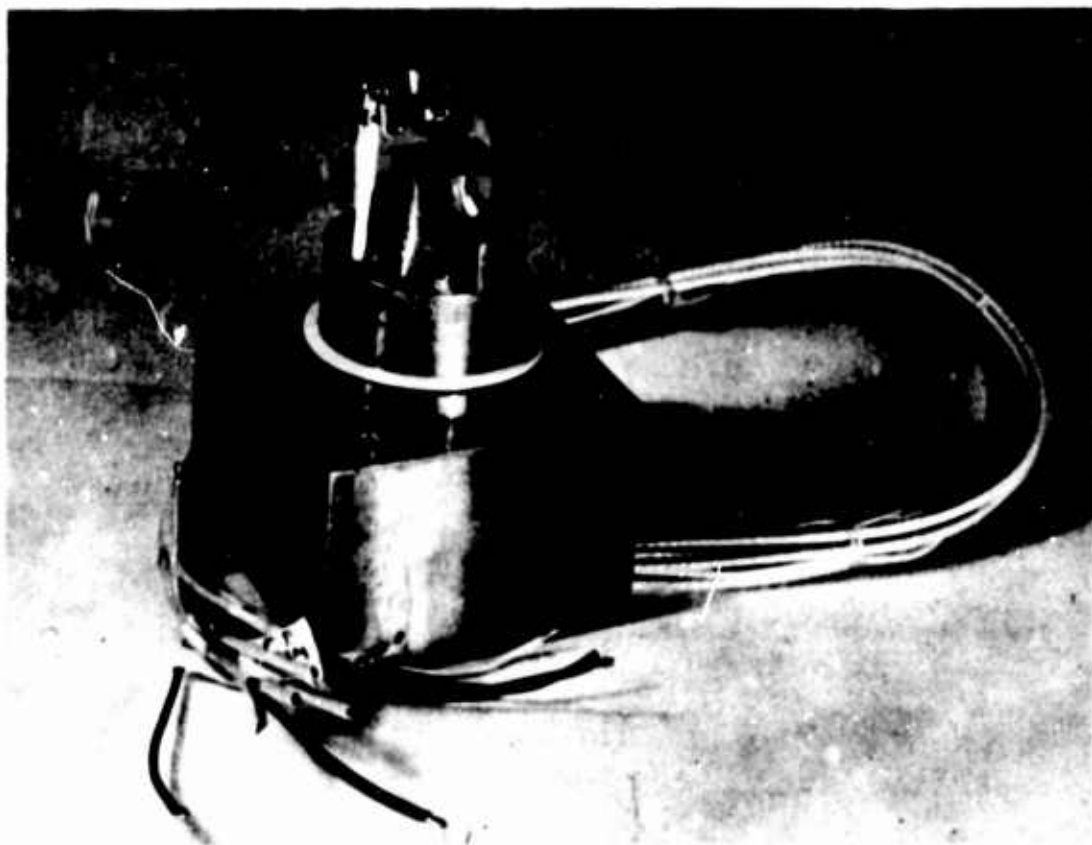


Figure 2. Thermoelectric Cooler and Alpha Particle Detector Mounted on Test Fixture

A preliminary experiment which was performed with this apparatus can be compared with the mass-transfer rate predicted above. Figure 3 shows the temperature readout of a hygrometer subjected to chamber conditions which correspond to stratospheric conditions at 70,000 feet and a ventilation rate of moist air through the unit of 400 ft/min. The instrument was initially operated in a full-heating mode to eliminate all condensate from the surface. The instrument, a Honeywell Alpha Radiation Hygrometer (Ballinger, 1964), was turned on at the time indicated  $t_A$  on Figure 3 (that is, the servo loop was closed), and a full-cooling mode resulted to re-establish a  $20 \mu\text{g}/\text{cm}^2$  layer of frost.\* This thickness was preset by adjusting the servo balance point with thin films of thickness known to about  $\pm 50$  percent. By the time denoted  $t_B$ , the  $20 \mu\text{g}/\text{cm}^2$  deposit had formed and thereafter the temperature began to cycle about the frost point in a usual manner to maintain this amount of deposit constant. The ragged variations seen in Figure 3 are superimposed on the slower cycling pattern and are due to the random nature of pulses received from the radiation detectors.

The time taken to form the  $20 \mu\text{g}/\text{cm}^2$  deposit  $(t_B - t_A) = 4 \pm 1$  minute, gives an estimate of the mass-transfer rate. Since the surface temperature and frost point were constant during this interval, we have

$$\left(\frac{d\sigma}{dt}\right)_{\text{exp}} = \frac{20 \pm 10 \mu\text{g}/\text{cm}^2}{4 \pm 1 \text{ min}} = 5^{+5}_{-3} \mu\text{g}/\text{cm}^2/\text{min}$$

$$= 0.08^{+0.08}_{-0.05} \mu\text{g}/\text{cm}^2/\text{sec}.$$

The sensor used in this experiment had very nearly flat-plate geometry. The frost point of the moist-air sample was maintained near  $-73^\circ\text{C}$ , and the calculated flat-plate value of  $l$  for the chamber conditions with a ventilation rate of 400 ft/min is, from Eq. (2),  $10.8 \text{ cm/sec}$ . As the surface temperature  $t_{AB}$  was  $-85^\circ\text{C}$ , the flat plate estimate for  $d\sigma/dt$  is, using Eq. (1),

$$\begin{aligned} \left(\frac{d\sigma}{dt}\right)_{\text{calc}} &= 10.8 \frac{\text{cm}}{\text{sec}} \left(0.001799 \frac{\mu\text{g}}{\text{cm}^3} - 0.000271 \frac{\mu\text{g}}{\text{cm}^3}\right) \\ &= 0.02 \mu\text{g}/\text{cm}^2/\text{sec}. \end{aligned}$$

\*This thickness is that of the control layer, the average amount about which the thickness varies during closed-loop operation, and is not to be confused with the sensitivity of the sensor which was less than  $1 \mu\text{g}/\text{cm}^2$  (30 monolayers).

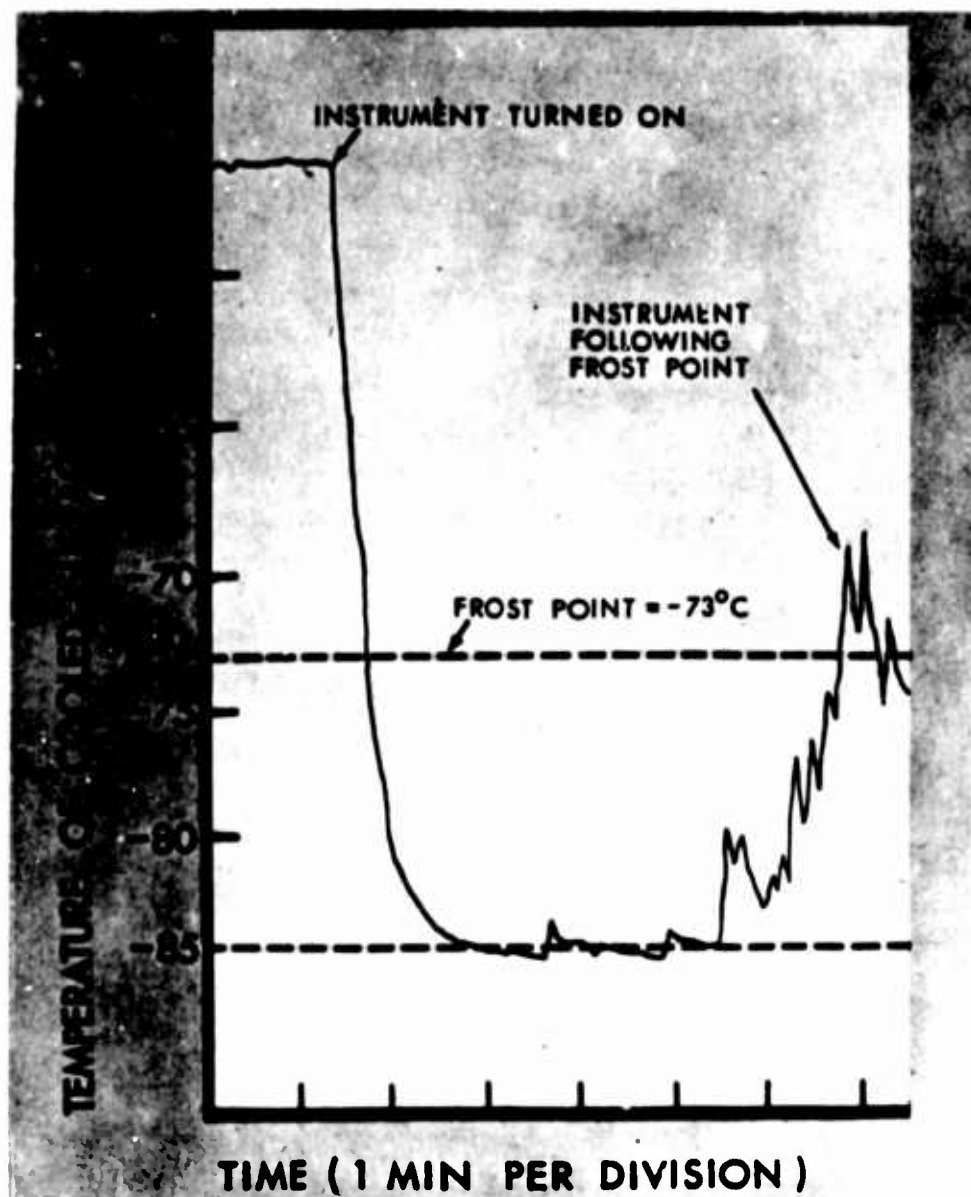


Figure 3. Hygrometer Readout During Formation of  $20 \mu\text{g}/\text{cm}^2$  Control Layer

In view of the experimental uncertainty in establishing a true fiat-plate flow, the estimated rate is considered to agree well with that observed.

We now consider the general limitation placed on any balloon-borne automatic frost-point hygrometer by the mass-transfer problem. Figure 4 shows typical "wet" and "dry" stratospheric frost-point data obtained with balloon-borne, automatic instruments (Mastenbrook, 1963, 1964; Gutnick and Salmela, 1963; Rohrbough and Ballinger, 1964), and Figures 5 and 6 show response times based on these data and the estimated rates of thickness change. The dry data corresponds to a constant mixing ratio of 0.003 g/kg above 50 thousand feet. The response

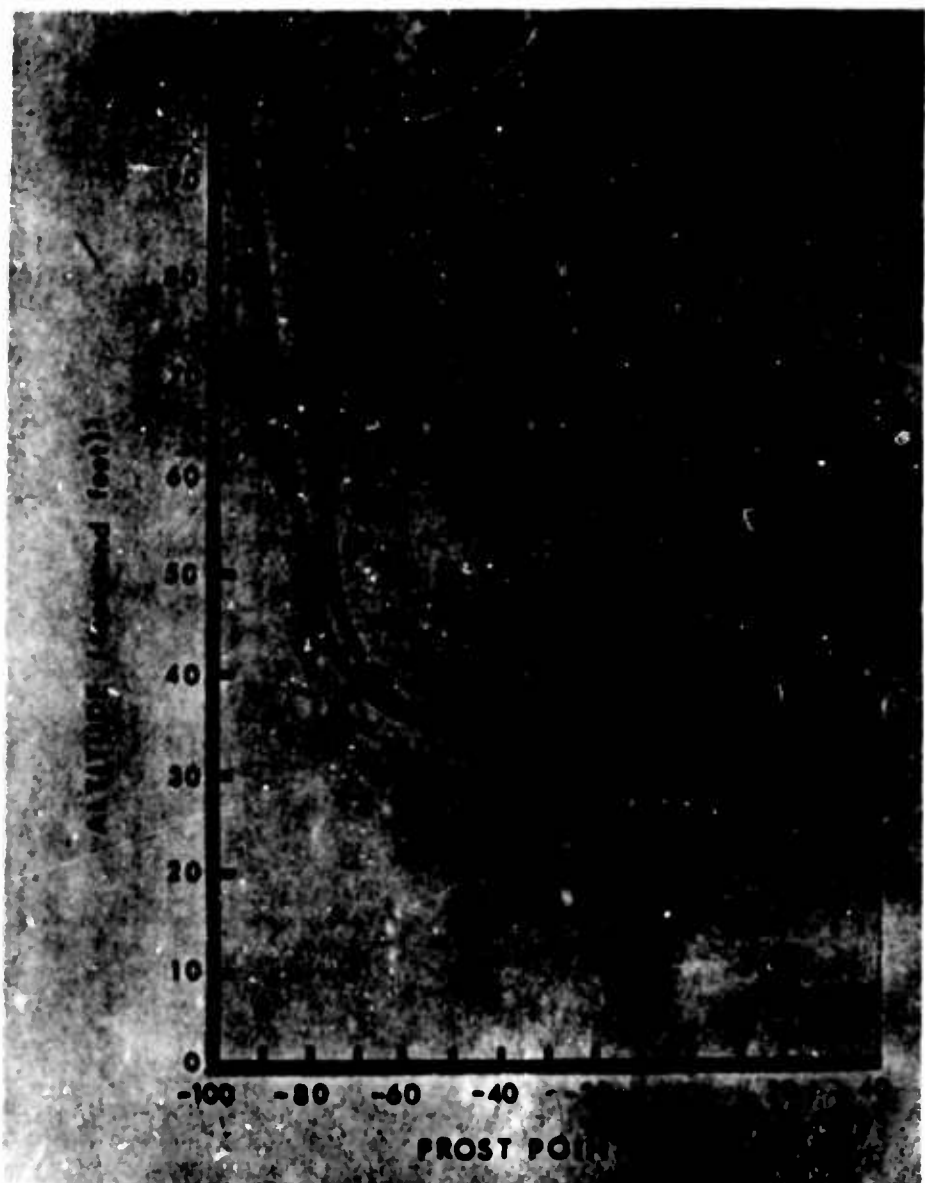


Figure 4. Typical Frost-Point Data

time given is the time required to increase the deposit thickness by 10 monolayers when the frost temperature is  $1^{\circ}\text{C}$  below the frost point of the air sample. This can be interpreted as the minimum time necessary for an instrument to respond to a  $1^{\circ}\text{C}$  change in ambient frost point if this instrument is capable of detecting a change in condensate thickness equal to 10 molecular diameters. If the instrument is not capable of detecting such a small increment in thickness, the response time is proportionately longer. The times given are also considered to be reasonably optimistic values for instruments of the optical type which employ a cooled surface with a temperature gradient and derive information from the area of the deposit as

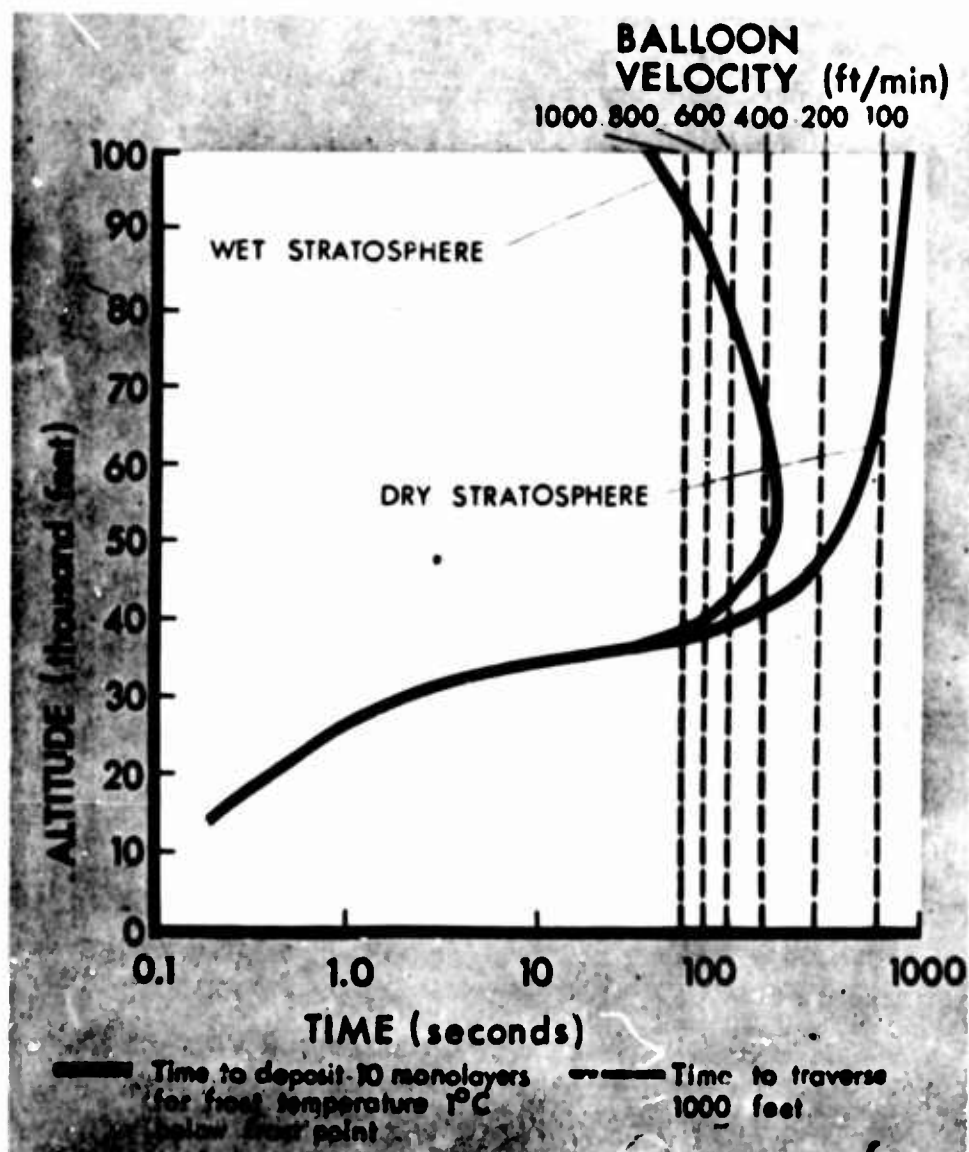


Figure 5. Response Times for Flat-Plate Geometry  
(Flow Velocity = 1000 ft/min, Characteristic Distance = 1 cm)

well as its thickness. In order to detect this change in area, a finite thickness of condensate must be formed or eliminated at the periphery of the deposit, and a reasonable lower limit for this minimum detectable thickness is a few molecular diameters. We note that this limit is determined by drift and noise in the instrument as well as by the theoretical limitation of the thickness sensor.

Also depicted in Figures 5 and 6 are the times necessary to traverse 1000 feet while ascending or descending on a balloon flight with various velocities. If "continuous" data is defined as that which can reflect a 1°C change in frost point over an interval no greater than 1000 feet, then acquisition of continuous data is possible so long as the response times are less than these traversal times.

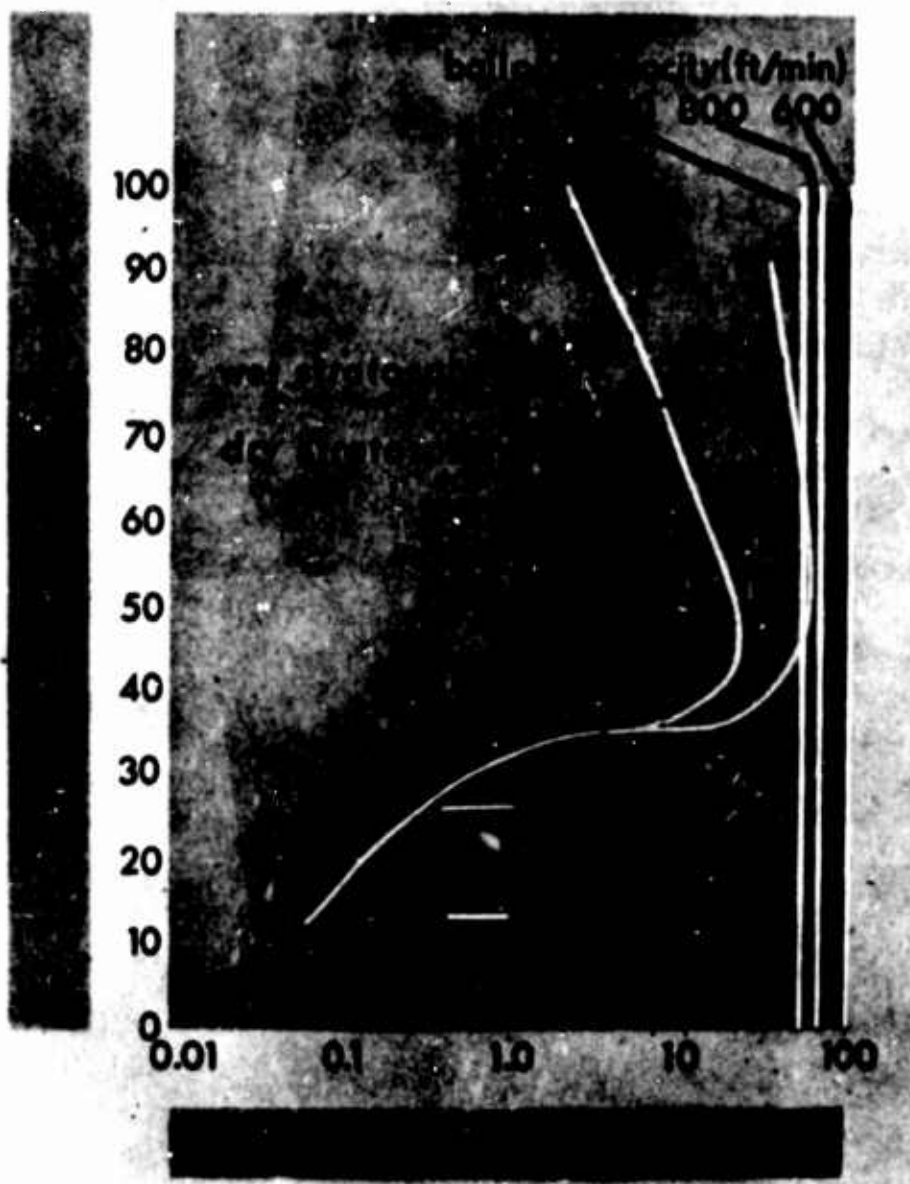


Figure 6. Response Times for Channel-Flow Geometry  
(0.030-Inch Channel)

As can be seen from Figure 5, a sensor with a flat-plate flow configuration, small frost-formation surface ( $x = 1$  cm), and a sizable flow rate ( $V = 1000$  ft/min) would not be expected to measure a dry stratosphere continuously unless the balloon velocity were less than 100 ft/min. Typical ascent and descent rates used in previous measurements, however, have been about 1000 ft/min.

Use of forced (high-velocity) flow through a narrow channel can improve matters considerably, as is seen in Figure 6. Because of the assumption of a constant bulk concentration, the times given above about 70,000 feet are valid for

the 0.030-inch channel and flow rate of 1000 ft/min only if the length of the deposit in the direction of flow is much less than 1 cm.

## 2.2 Contamination

From the point of launch to maximum altitude, the concentration of water vapor experienced by a balloon-borne hygrometer varies by a factor of  $10^5$ . Adsorption of water by the balloon and associated equipment at low altitudes and a subsequent desorption in the stratosphere, particularly under the influence of solar radiation, can introduce serious errors in the measurement of low frost points. The effect of such contamination can be seen (Figure 7) to be quite large at float and considerably less with sufficiently high balloon velocity.

Once desorbed from an exposed surface, a minute quantity of water vapor can produce a large elevation in the humidity of the surrounding air for a long period of time. Numerical estimates of the severity of this contamination problem have been obtained (Ballinger, Fricke and Murphy, 1964) by treating the one-dimensional diffusion problem, that is, by considering an equipment package to be a very large wall from which water molecules diffuse in the z-direction. The equation describing this situation is:

$$D \frac{\partial^2 n(z, t)}{\partial z^2} = \frac{\partial n(z, t)}{\partial t}$$

where

$n(z, t)$  = the excess concentration (particles per unit volume) of the water vapor  
 $z$  = the distance (one dimension)  
 $D$  = the mutual diffusion coefficient.

The concentration at the wall is taken to be constant in time and equal to the saturation concentration. The boundary conditions thus are:

$$n(0, t) = N = \text{Const.}$$

$$n(\infty, t) < \infty$$

$$n(z, 0) = 0, z > 0.$$

A solution meeting these boundary conditions is:

$$n(z, t) = N \left[ 1 - 2 \Phi \left( \sqrt{\frac{z}{2Dt}} \right) \right] \quad \Phi(\omega) = \frac{1}{\sqrt{2\pi}} \int_0^\omega e^{-\xi^2/2} d\xi .$$

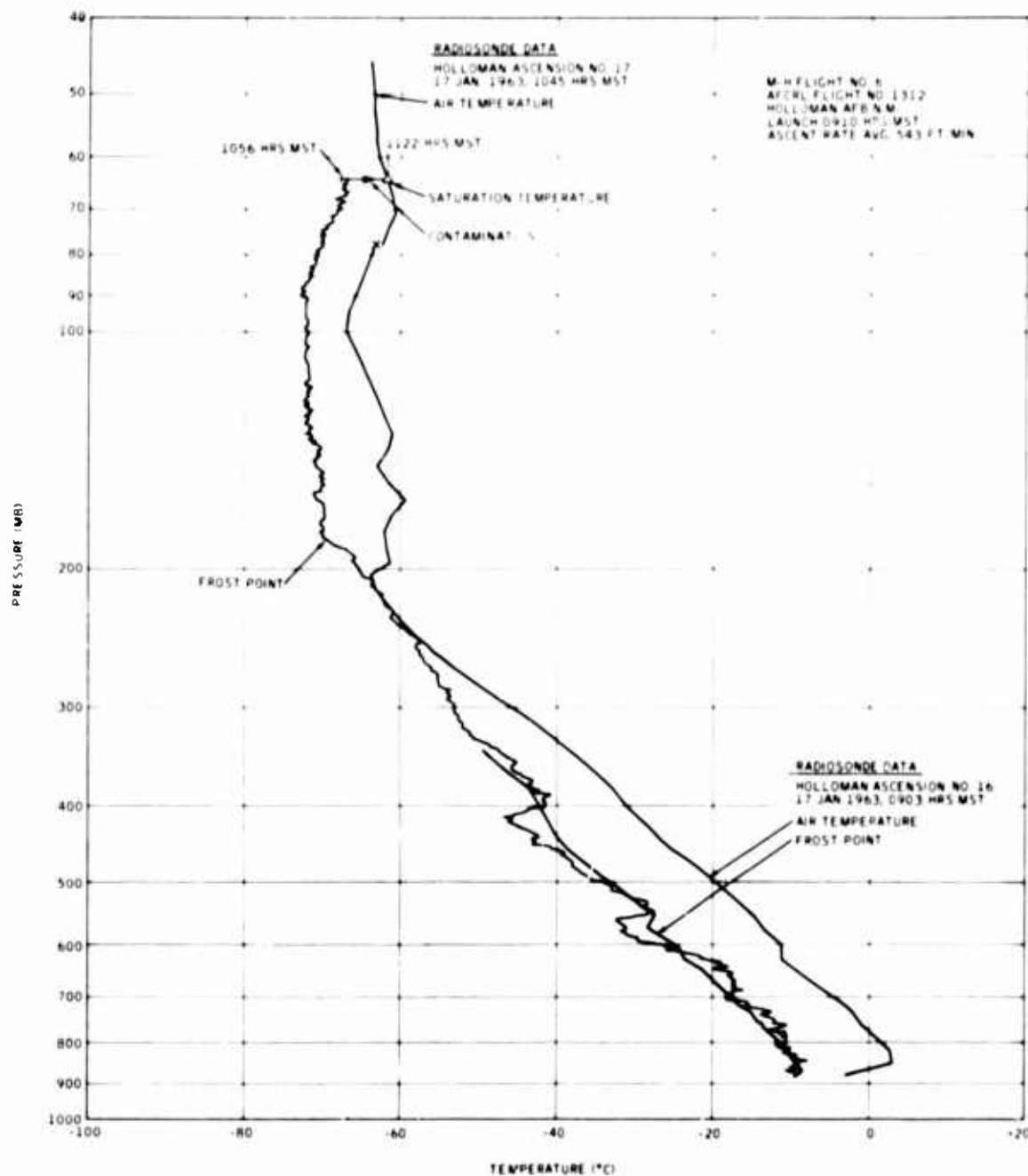


Figure 7. Frost-Point Profile, 17 January 1963 Flight

If a value of  $4.3 \text{ cm}^2/\text{sec}$  (appropriate to a height of about 80,000 feet) is used for the diffusion coefficient, numerical values for  $n(z,t)$  can be computed. Figures 8 and 9 illustrate two flights, one with the hygrometer located near the package and one with the hygrometer located farther from the package. It appears in both of these cases that the diffusive contamination hypothesis is an adequate explanation of the observed rise in measured frost point.

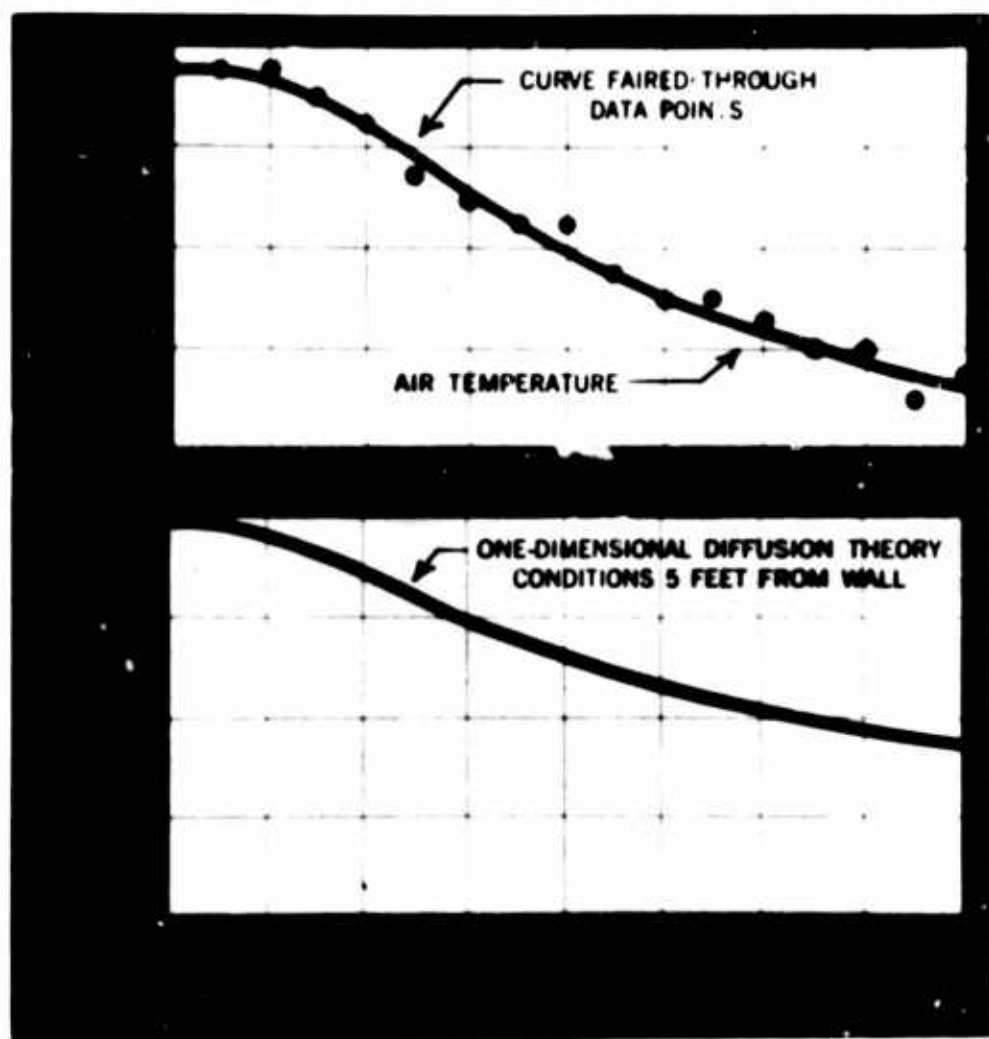


Figure 8. Contamination of Air Sample by Instrument Package M-H  
Flight No. 6, AFCRL Flight No. 1312 Holloman AFB N. M. 17 Jan. 1963  
Float Altitude 67 MB (61 Kilo Ft.) Hygrometer Located 5 Feet from  
Side of "Wet" Gondola

The severity of the contamination problem is emphasized by a calculation of the quantity  $M_T$ , which is defined as the total number of water molecules which leave a unit area of the wall in a time  $T$ . From Fick's diffusion law, it follows that:

$$M_T = -D \int_0^T \left[ \frac{\partial n(z,t)}{\partial z} \right] \Big|_{z=0} dt$$

$$= 2N \sqrt{\frac{DT}{\pi}} .$$

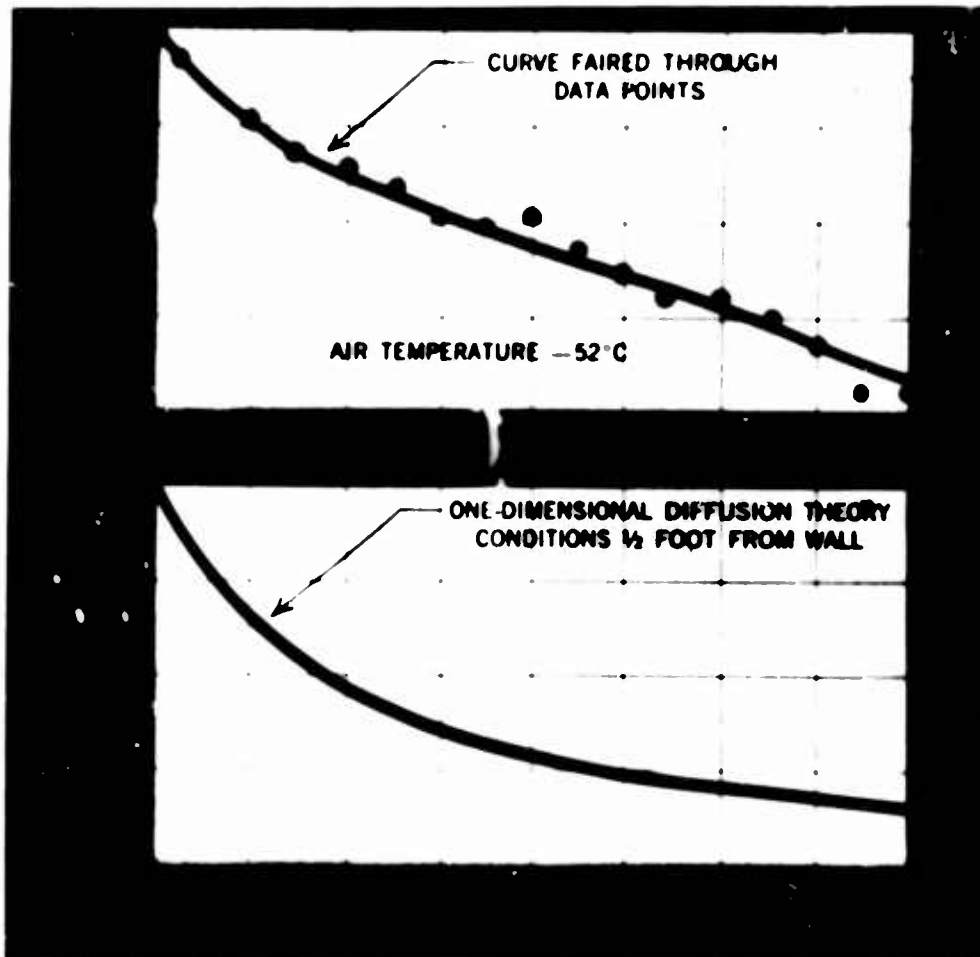


Figure 9. Contamination of Air Sample by Instrument Package M-H  
Flight No. 2, AFCRL Flight No. 1229 Holloman AFB N. M. 5 April 1962  
Float Altitude 24 MB (83 Kilo Ft.) Hygrometer Located 1/2 Foot from  
Side of "Wet" Gondola

Assuming  $N$  is the saturation concentration at  $-50^{\circ}\text{C}$  and a reasonable value for the free-air temperature in the stratosphere, we find for  $T = \text{one hour}$  that  $M_T$  represents a layer less than twenty molecules thick. Calculations from the expression for  $n(z,t)$  indicate that the effects of contamination will in one hour extend out to a distance of about one meter from the wall. Thus, a minute amount of adsorbed water will, because of the scarcity of stratospheric water vapor, cause a rather severe contamination problem for a long period of time.

To best avoid the problem of contamination, use of sample-inlet tubes extending past the boundary layer of the instrument package (on the descent portion of the flight) has been considered. However, the contamination introduced by the tube itself can be considerable.

The average partial density of water vapor  $\rho'$  at the outlet of a sampling tube of length  $l$  and uniform cross-sectional area  $A$  is

$$\rho' = \rho + \frac{1}{AV} \frac{dm}{dt} ,$$

where  $\rho$  is the partial water-vapor density of the incoming air sample,  $V$  is the flow velocity in the tube, and  $dm/dt$  is the total mass of water desorbed from the inner walls of the tube in unit time. If the desorption rate in mass per unit area per unit time is  $d\sigma/dt$ , then

$$\rho' = \rho + \frac{P\ell}{AV} \frac{d\sigma}{dt} ,$$

where  $P$  is the perimeter of the tube. For a cylindrical tube of radius  $R$ , which minimizes  $P/A$  in the above,

$$\rho' = \rho + \frac{2\ell}{RV} \frac{d\sigma}{dt} .$$

To minimize the contamination, then, a short cylindrical sampling tube with a large radius and a high flow velocity is desirable. However, should a constant volume blower or pump be used downstream from the tube to establish a high flow velocity, then the error is minimized by using a small radius (since in this instance one has the constraint  $R^2 V \approx \text{constant}$ ).

The desorption rate from stainless steel after one hour of pumping is about  $1.7 \times 10^{-7}$  torr-liters/sec-cm<sup>2</sup>, or  $1.7 \times 10^{-4}$   $\mu\text{g}/\text{cm}^2\text{-sec}$  (Dayton, 1962). Using this value for  $d\sigma/dt$ , a flow of 0.3 cfm, and a tube of length 1 foot and radius 1/8 inch (for which  $V = 447 \text{ cm/sec}$ ), we then have

$$\frac{2\ell}{RV} \frac{d\sigma}{dt} = 0.729 \times 10^{-4} \mu\text{g}/\text{cm}^3 .$$

If the air entering the tube were perfectly dry, the above corresponds to the partial density of water at the outlet and is equivalent to a frost point of -93°C. Moreover, this background would introduce an error of 1°C in the measurement of a frost point of -82°C.

More information on desorption rates occurring under conditions typical of stratospheric balloon flights is necessary to make firm conclusions about the use of sample-inlet tubes. However, the above example serves to illustrate the general severity of the contamination problem.

### 3. CURRENT EQUIPMENT AND TECHNIQUES

We will now describe briefly our present instrument packages and tentative plans for the flights on which they will be used. Some of the major design features

incorporated into these instrument packages to cope with the problems of low mass-transfer rates and sample contamination are described below.

### 3.1 Choice of Instrument

The type of instrument we use is the Honeywell Alpha Hygrometer (developed under Contract AF-19(604)-8418). The latest version is shown diagrammatically in Figure 10. It operates as an automatic frost-point (or dew-point) hygrometer; that is, the amount of frost deposited on a cooled surface is measured, and the deviation from some preset amount of deposit is used as an error signal in a closed servo loop. In this way, the instrument maintains the temperature of the surface at the point where the quantity of water on the surface remains constant--evaporation is balanced by condensation--and the surface temperature is thus at the frost or dew point.

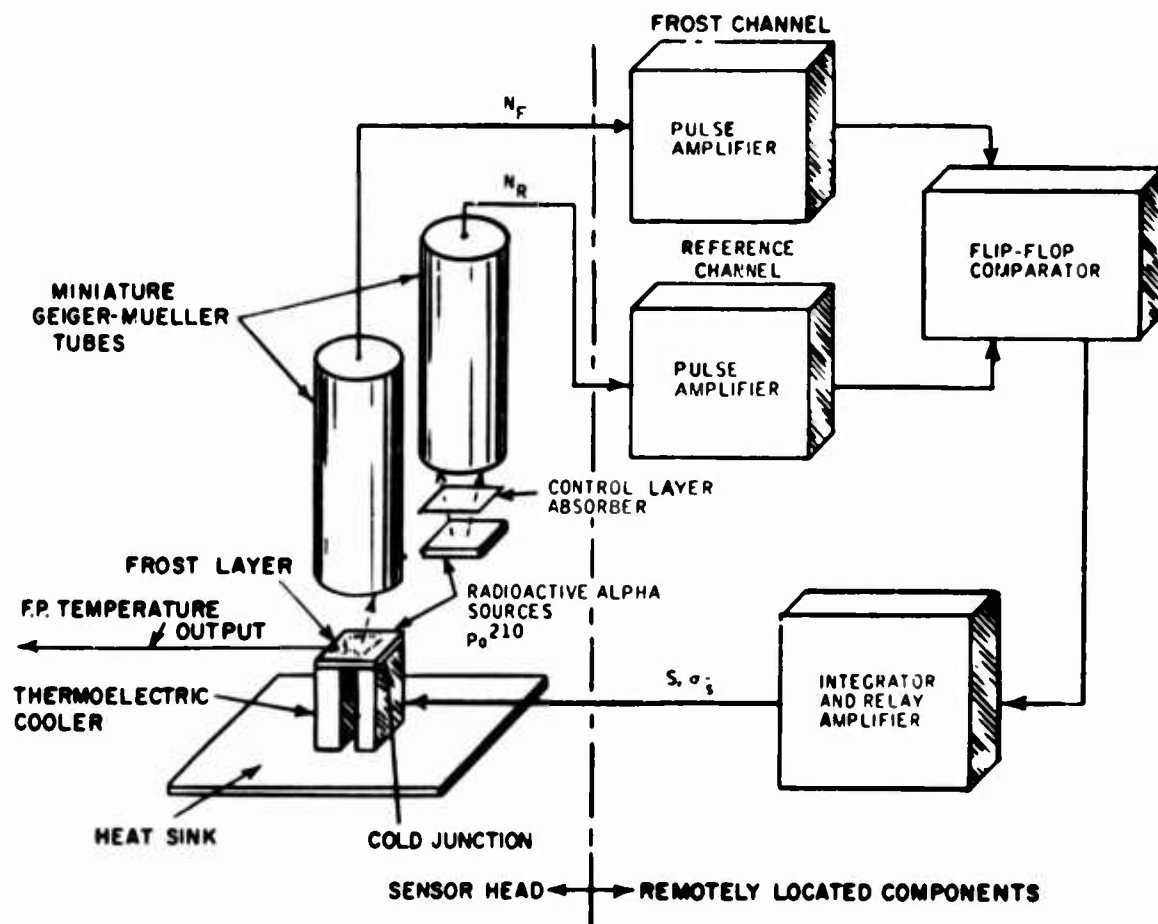


Figure 10. Alpha Radiation Hygrometer

Several versions of automatic frost-point hygrometers exist, usually employing optical techniques to determine the amount of frost on a cooled mirror. Honeywell's Alpha Hygrometer uses an  $\alpha$ -particle source in the cooled surface, and employs the technique of radioactive-thickness gauging to measure the deposit thickness. Two radioactive sources are used; one is cooled and the other is kept at a temperature well above the frost point and used to compensate for changes in air density. We refer to these as frost and reference channels. The preset deposit or control-layer thickness is determined by a thin absorber placed between the reference channel source and detector. (In actual practice, both channels have absorbers interposed so that the  $\alpha$ -particles have nearly reached the end of their range, the condition for which the thickness sensitivity is greatest. The control layer is set by using a slightly thicker absorber in the reference channel.) Output pulses from the frost- and reference-channel Geiger-Mueller tubes are fed into the two gates of a flip-flop, and the time spent in each state by the flip-flop depends on the number of pulses per second in each channel. The average number of pulses in the frost channel decreases as the frost thickness increases and the flip-flop output may be integrated to give a d-c signal proportional to frost thickness. This is the error signal, which is amplified and fed into a thermoelectric cooler to regulate the frost-channel source temperature.

Some advantages of the alpha gauging technique are as follows:

The sensitivity is high. Servo response is initiated by a change of less than  $10^{-6}$  cm (less than 30 molecular diameters) in the average condensate thickness.

The mass thickness of the deposit on the cooled surface is measured rather than its reflectivity which depends on the physical structure of the deposit.

The control-layer thickness can be precisely set by use of a calibrated absorber.

The cooled surface may be directly exposed to the atmosphere, since the detectors are not light-sensitive.

The radioactive source output is constant.

The thickness measurement depends solely on the number of pulses and virtually eliminates drift problems in detectors and electronics.

There is no critical mechanical alignment and no operational circuit adjustments are necessary.

### 3.2 Package Temperature Control

To insure against possible drift in batteries, power supplies, recorders, and so on, we control the interior temperature of the instrument package so that it remains above 10°C.

### 3.3 Heat Sink

The thermocooler establishes the cooled-surface temperature and this depends not only on the error signal (which, in turn, depends on frost thickness) but also on the temperature of the heat sink which serves as the thermocooler reference. If for some reason the heat-sink temperature changes, the cooled-surface temperature will follow this change until an error signal develops which can correct it. At the thermistor readout of the instrument one cannot distinguish whether the frost point has changed, or whether the heat-sink temperature is varying. This discourages the use of a heat-rejection fin, which will have variations due to changes in free-air temperature and solar heating. Similarly, the temperature of a boiling-liquid heat sink changes with altitude.

We have used a frozen liquid (such as ethyl alcohol) to provide a constant reference temperature, but the size of the sink required is unduly large. For this reason we use a heat sink consisting of a sealed container of dry ice with an absolute-pressure relief valve. This valve is set to about 300 millibars, and thus gives us a constant temperature above 30,000 feet. Below this altitude, the frost point (and mass-transfer rate) is high enough so that a slowly-varying sink temperature will not give rise to a significant measurement error.

### 3.4 Forced Ventilation and Channel-Flow Geometry

The low mass-transfer rates encountered in the stratosphere set the basic limitation on instrument performance, since this determines the ability of an automatic hygrometer to follow a changing frost point or, for that matter, to distinguish frost-point changes from internal and external sources of drift. We have shown, however, that these rates may be considerably enhanced by using the proper channel-flow geometry and a high ventilation rate. The flow channels in our hygrometer heads have a rectangular cross section 0.030 inch high by 0.30 inch wide, and we provide a flow velocity in excess of 3000 feet per minute. To achieve high flow velocities in this narrow channel, a miniature vane-type vacuum pump is connected to the outlet side of the hygrometer head. This is a positive-displacement pump which, when driven at constant speed, provides an essentially constant flow velocity over the entire altitude range covered.

### 3.5 Outside Container

The contents of the instrument package--vented wet-cell batteries, foam insulation with a large effective surface area and a frost-laden heat sink--represent a copious source of moisture. Since we prefer not to use a long sampling tube, for reasons previously given, it is necessary to seal these sources of contamination from the vicinity of the sample inlet. This is done by enclosing the components in a sealed stainless-steel container which is vented through a zeolite adsorber.

### 3.6 Long Load Lines

In order to sample air which is uncontaminated by the balloon, parachute, and other flight equipment, the hygrometer package should be located at a considerable distance from all other gear. Relatively small, lightweight instrument packages using inflight recording lend themselves readily to suspension far below other equipment. Packages which have enough battery and heat-sink capacity for long-duration flights, or which are not electrically independent, must be located within, say, thirty feet of the load bar. In this case, reliable data are assured only during descent or after floating long enough for clean-up to occur.

### 3.7 Sample Inlet Tubes

Since we cannot be assured that data obtained using long sampling tubes will be free from contamination errors, short inlet tubes are normally used. On the Contamination Study flights (Contract AF 19 (628)-3857) however, we plan to mount one hygrometer package on top of the balloon. To obtain a low center of gravity the package must be mounted immediately above the valve assembly. During ascent this package, which is in an aerodynamically unfavorable location, may be in contaminated surroundings. For this reason, air will be taken in through a ten-foot vertical sampling tube, and the possibility of contamination from the tube itself will be minimized by using small-diameter ( $\frac{3}{16}$  inch I.D.) tubing and a high flow velocity.

### 3.8 Performance Testing

In addition to life testing under simulated environmental conditions, each instrument is subjected to a performance check in the Stratospheric Moisture Simulator. For this purpose we use the setup pictured in Figure 11. The hygrometer head and fusion sink to be tested are enclosed in a bell jar, with the controlled-humidity jet entering through the baseplate. The inlet tube of the hygrometer samples air from within this jet, and we can make a performance check which includes calibration at a low frost point (the heat-exchanger coils attain a temperature of  $-7^{\circ}\text{C}$  with a dry-ice and alcohol bath).

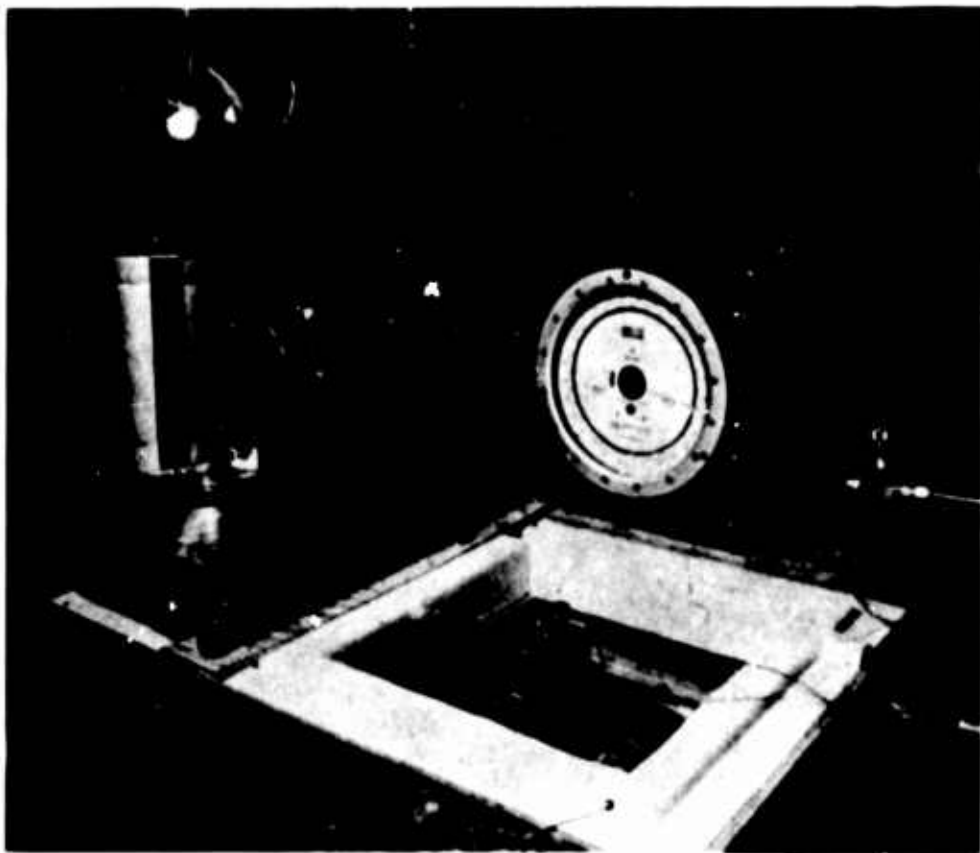


Figure 11. Hygrometer Test Fixture

### 3.9 Instrument Packages

Figure 12 depicts the flight train proposed for a forthcoming flight in the Contamination Study program. On top of the balloon is a package housed in an aluminum container and mounted on a six-foot diameter stabilizing platform. Figure 13, a photograph of this package with the cover removed, shows the hygrometer head, heat sink and relief valve, vacuum pump, hygrometer electronics, and battery power supply. The inlet is a ten-foot tripod-supported stainless-steel tube.

Suspended directly below the load bar is the main hygrometer package, shown in Figure 14. This package contains two hygrometers and associated equipment, and includes two in-flight recorders which monitor both hygrometer outputs, heat-sink temperature, interior temperature of the package, free-air temperature, and the hygrometer output and fusion-sink temperature from the top-mounted package. This main unit is housed in a stainless-steel container.

A third hygrometer package is lowered from a reel on a 2000-foot load line terminated with 30 feet of stainless-steel cable above the package. This unit is of the same design as the ones which will be used by AFCRL for vertical soundings in their Stratospheric Humidity program (Contract AF 19 (628)-4206). Figures 15 and 16 show the layout of components within the stainless-steel outer container.

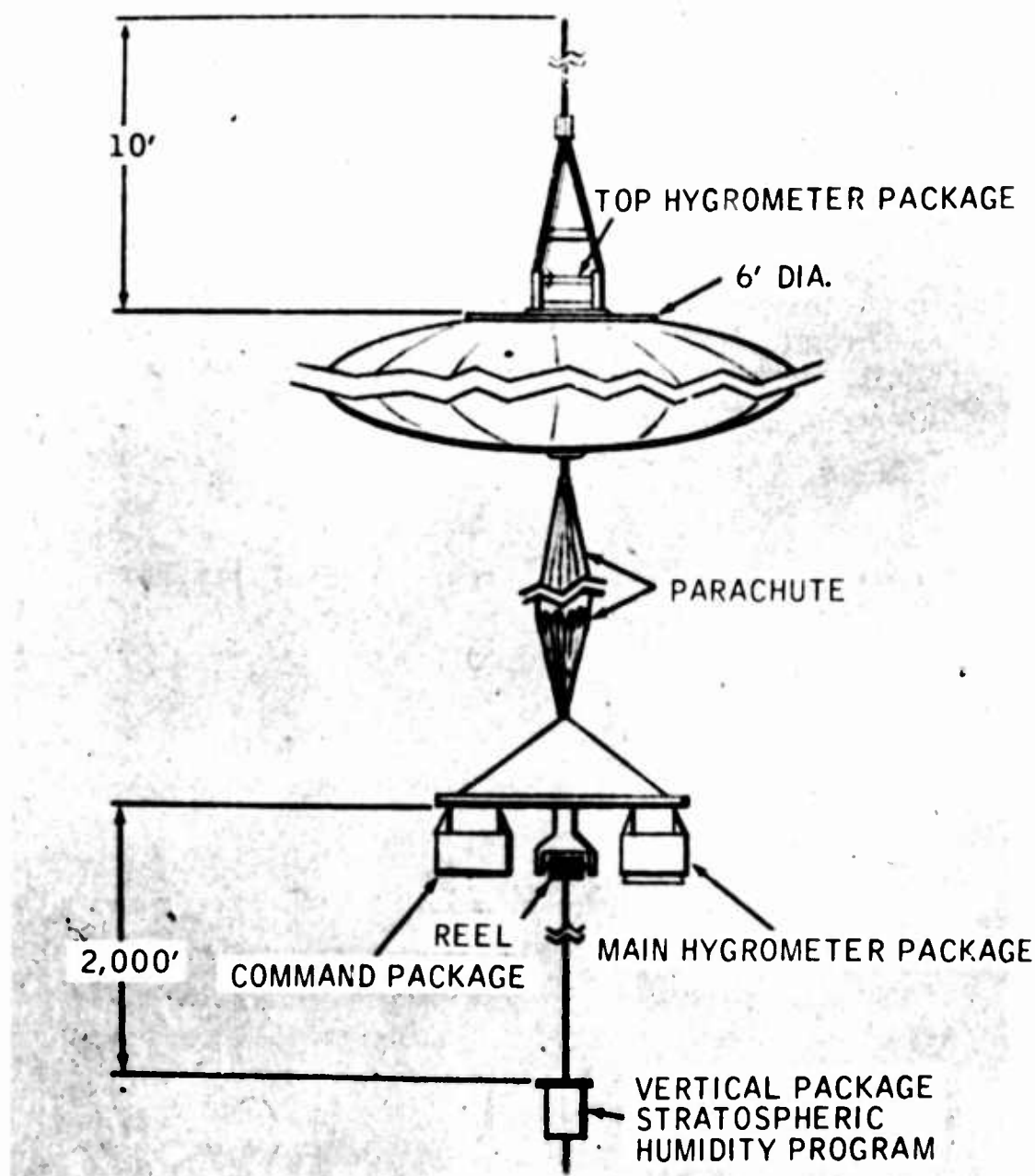


Figure 12. Proposed Flight Train for Contamination Study

A fourth instrument package incorporating the same general design features is shown in Figure 17. This package is designed for AFCRL for the horizontal flights in the Stratospheric Humidity program. Data will be transmitted for two minutes every two hours. Low mass-transfer rates, however, discourage us from operating the sensors intermittently because it may take nearly this long for a hygrometer to acquire a control layer and stabilize after turn-on. For this



Figure 13. Top Hygrometer Package, Mounted on Balloon Valve

reason, the instrument will run continuously during the flight (approximately ten days). The major difference between this and the other packages described is that heat-sink and battery-power capacities are considerably greater.

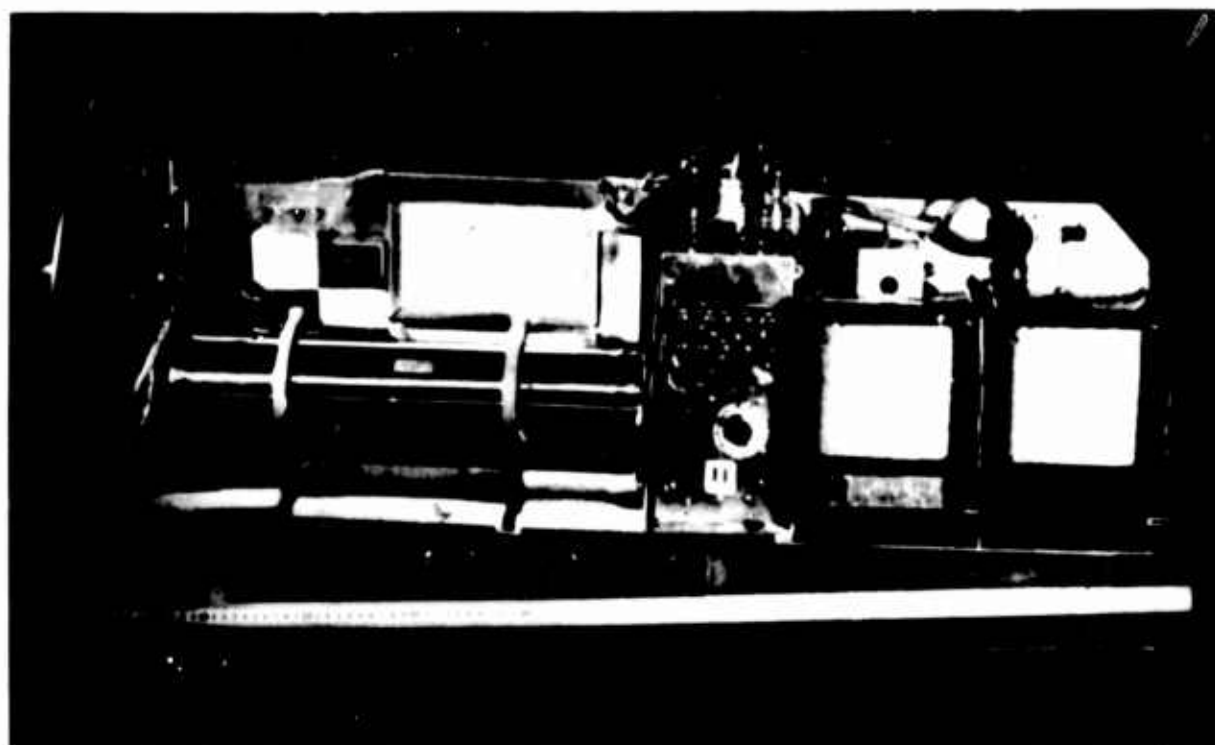


Figure 14. Main Hygrometer Package Mounted on Load Bar

#### 4. DISCUSSION

We believe that sufficient evidence now exists to cast serious doubt on the validity of virtually all previous stratospheric water-vapor measurements made with the balloon-borne automatic frost-point hygrometers. Both theory and experiment have been cited to show that the fundamental problems of low mass-transfer rates and contamination--both due to the scarcity of water vapor at high altitudes--are likely sources of the present controversy in stratospheric measurements.

One should note that efforts to avoid one of the two problems may aggravate the other. A rapid balloon descent velocity will, on one hand, eliminate the problem of contamination but may, on the other hand, lead to completely erroneous results because of the long response times inherent in stratospheric measurements. One finds that contamination, unless avoided by scrupulous packaging techniques, sets a lower limit to the velocity of the sampling vehicle; the response rates set an upper velocity limit, which is probably quite low. For a particular instrument system, it must be demonstrated that there exists an intermediate range of velocities which will adequately reduce both problems. For the upcoming AFCRL

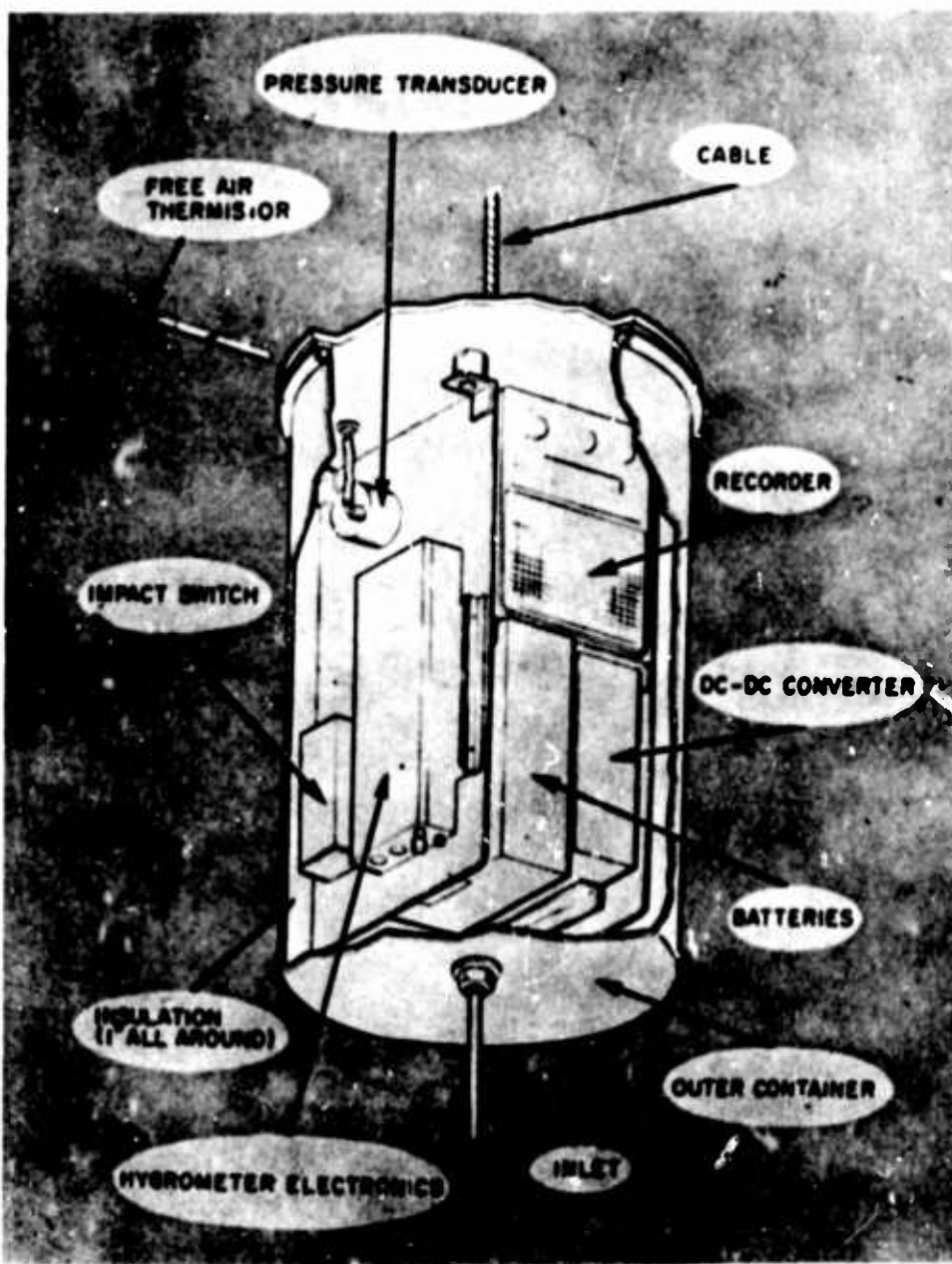


Figure 15. Vertical Flight Package

flights, the first of which are designed to measure contamination, the sensitivity of the Alpha Radiation Hygrometer should permit vertical balloon velocities of up to 400 ft/min in the region of poorest mass transfer.

The design features necessitated by these problems are not peculiar to our instruments; they are recommended as general measures to improve the quality of all future frost-point measurements.

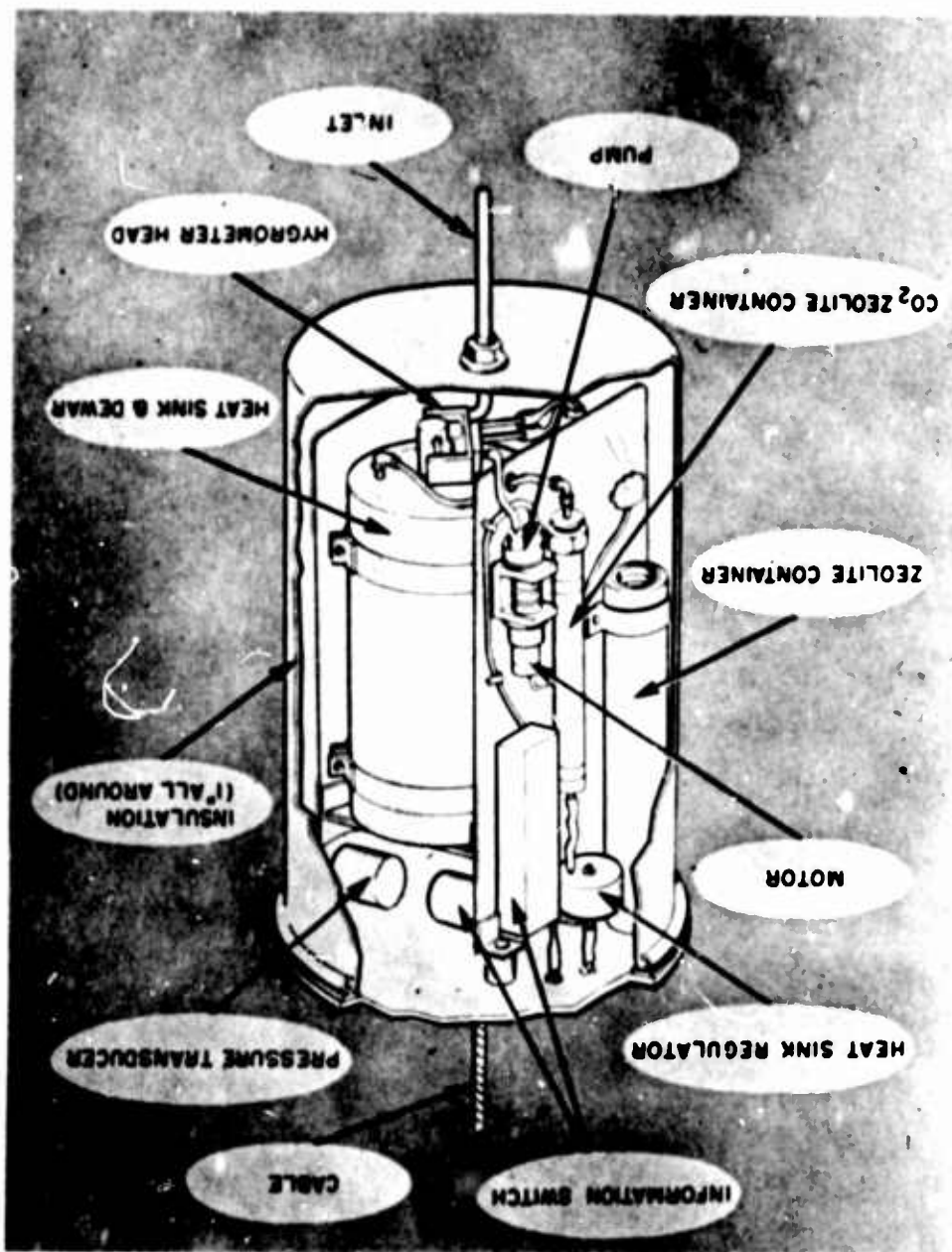


Figure 16. Vertical Flight Package

In summary, the instrument requirements which must be met to assure the validity of stratospheric frost-point data include:

The sensitivity and associated response time of the frost-thickness (or area) sensor must be optimized and compatible with the rate of sampling.

The hygrometer circuit drift must be virtually eliminated.

The heat-sink temperature should be held constant.

The flow-channel geometry of the sensor must be optimized.

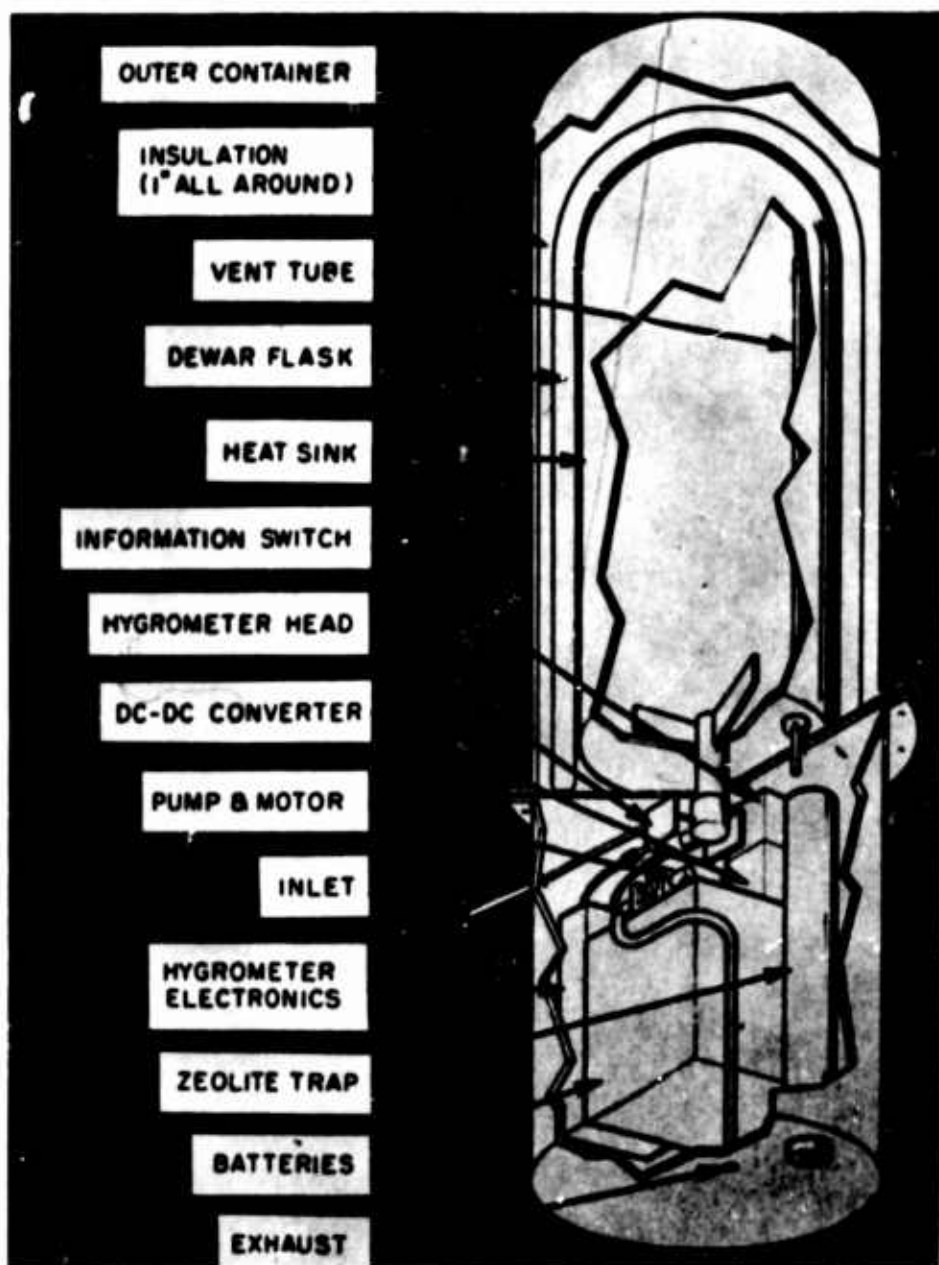


Figure 17. Horizontal Flight Package

High-velocity forced ventilation is desirable both to improve mass-transfer rates and to reduce sample contamination from the sample-inlet system.

The packages must be sealed to keep contamination away from the sample inlet area.

The sensor should be located far from the flight train.

In addition to these requirements, serious effort must be made to optimize the performance of the servo-control system as a whole if it is to be effective in the

regions of very low rates of mass transfer. Such considerations are worthy of a separate paper on the subject.

Although the contamination problem's existence (if not its severity) is well known, the dynamics problem has received little attention from investigators of stratospheric humidity using automatic frost-point hygrometers. This is unfortunate since mass-transfer difficulties may not be apparent, during application in an unknown environment, from the behavior of the recorded temperature or other easily-monitored instrument functions which depend upon the amount of condensate present. As a major criterion for the acceptability of future stratospheric data, it is therefore strongly recommended that thorough performance data be required for the instrument used. Cycling and response characteristics must be determined throughout the range of application; monitoring operation in a laboratory test facility with known and variable frost points should be a minimal requirement.

## References

- Ballinger, J.G., Fricke, M.P. and Murphy, R.D. (1964) Alpha Radiation Hygrometer. Current Problems in Stratospheric Water-Vapor Measurement Made With Automatic Frost-Point Hygrometers, AFCRL-64-600(III).
- Ballinger, J.G. (1964) An automatic frost-point hygrometer using radioactive detection, 1963 International Symposium on Humidity and Moisture, Washington, D.C. (Vol. I, Humidity and Moisture), Reinhold Pub. Co., New York.
- Dayton, B.B. (1962) (Vol. I, Transactions of the Eighth National Vacuum Symposium), Permagon Press, New York, pp. 42-57.
- Gutnick, M. and Salmela, M.A. (1963) Re-Evaluation of the Midlatitude Moisture Profiles, 1963 International Symposium on Humidity and Moisture, Washington, D.C., May 1963.
- Gutnick, M. (1961) How dry is the sky?, J. Geophys. Res. 66:2867.
- Mastenbrook, H.J. (1963) Frost-point hygrometer measurements in the stratosphere and the problem of moisture contamination, 1963 International Symposium on Humidity and Moisture, Washington, D.C.
- Mastenbrook, H.J. (1964) Water vapor observations in the stratosphere, Fifth Conference on Applied Meteorology, Am. Meteor. Soc., Atlantic City, N.J.
- Rohrbough, S.F. and Ballinger, J.G. (1964) Stratospheric frost-point measurements using the alpha radiation hygrometer, Atmospheric Biology Conference, University of Minnesota, Minneapolis, Minnesota.
- Sissenwine, N., Grantham, D.D., and Salmela, H.A. (1964) AFCRL Stratospheric Humidity Program, AFCRL Scientific Balloon Symposium, Wentworth By-the-Sea, Portsmouth, New Hampshire.

## XXII. AFCRL Stratospheric Humidity Program

D. Grantham, N. Sissenwine and H. Salmea  
Air Force Cambridge Research Laboratories  
Bedford, Massachusetts

### I. INTRODUCTION

Over the last decade there has been a growing interest in water vapor in the stratosphere, prompted in large part by those who are designing infrared detection systems for either the guidance or tracking of rockets (Sissenwine and Gutnick, 1960). Parallel scientific interests have developed from attempts to understand atmospheric circulation patterns and spectroscopic investigations of atmospheric composition of other planets from stratospheric balloon platforms for which assumptions of the overhead humidity are required (Bottema, Plummer and Strong, 1964).

With this growing interest, a controversy has evolved between two factions: one advocating a "dry and stagnant" stratosphere, and the second believing that the stratosphere is variable in both time and space, sometimes wet and sometimes dry (Gutnick, 1961).

Utilizing manually-controlled, aircraft-borne frostpointers, early British investigators usually observed frostpoints near  $-82^{\circ}\text{C}$  in the lower stratosphere up to 50,000 feet (Murgatroyd, Goldsmith and Hollings, 1957). These data supported a circulation theory, postulated by them, in which the stratosphere has a constant mixing ratio of about 2 mg/kg of dry air (Brewer, 1949; Dobson, 1956).

The condition of constant mixing ratio dictates continuously lowering frost point with increasing altitudes.

More recently, several American, Japanese and a few British investigators have observed mixing ratios of the order 80 to 120 mg/kg with continually increasing frost points up to 100,000 feet (Gutnick, 1962). Early Naval Research Laboratories measurements showed a relatively moist stratosphere, but these experiments are now being questioned. NRL now believes their recent dry soundings to be more representative of the truth and lean toward a 1- to 4- mg/kg mixing ratio (Masterbrook, 1964). The dot-dashed line in Figure 1 is an average of all frost-point data available, both dry and wet, which was prepared by Gutnick of AFCRL about two and a half years ago. The dashed curve on the left presents frost points associated with the British theory of constant mixing ratio above the tropopause. At 32 km, roughly 100,000 feet, the difference in the frost points, -70°C and -98°C, yields a 100-fold difference in water vapor density. An IR signal that would be attenuated in 100 miles, assuming the British dry profile, would be lost in one mile if average conditions were encountered.

As author of a chapter on the upper atmosphere for a forthcoming World Meteorological Organization publication, outstanding British meteorologist, R. G. Murgatroyd, one of the scientists responsible for the constant mixing ratio theory, now states: "...our knowledge of the distribution of water vapor above the lower stratosphere is very limited and there is urgent need for accurate measurements."

Recognizing the problem, AFCRL's Laboratory Director approved a special experimental program for resolving the stratospheric humidity controversy. The total AFCRL effort involves the development of a new humidity-measuring instrument, studying the problem of contamination due to outgassing during a flight, and an ambitious program of collecting humidity data during a one-year period.

## 2. SENSORS AND INSTRUMENTATION

Humidity measurements are very difficult to make in the lower stratosphere. Because of the extremely cold temperatures present, water-vapor density (the physical parameter that must be sensed to measure humidity) even for saturation, is five orders of magnitude lower than for cold winter surface conditions.

Sensors that have been used are the manually-controlled, optical dew pointer, automatically-controlled optical dew pointers, cold-trap and chemical-absorption-sampling devices, and infrared sun-seeking spectrometers.

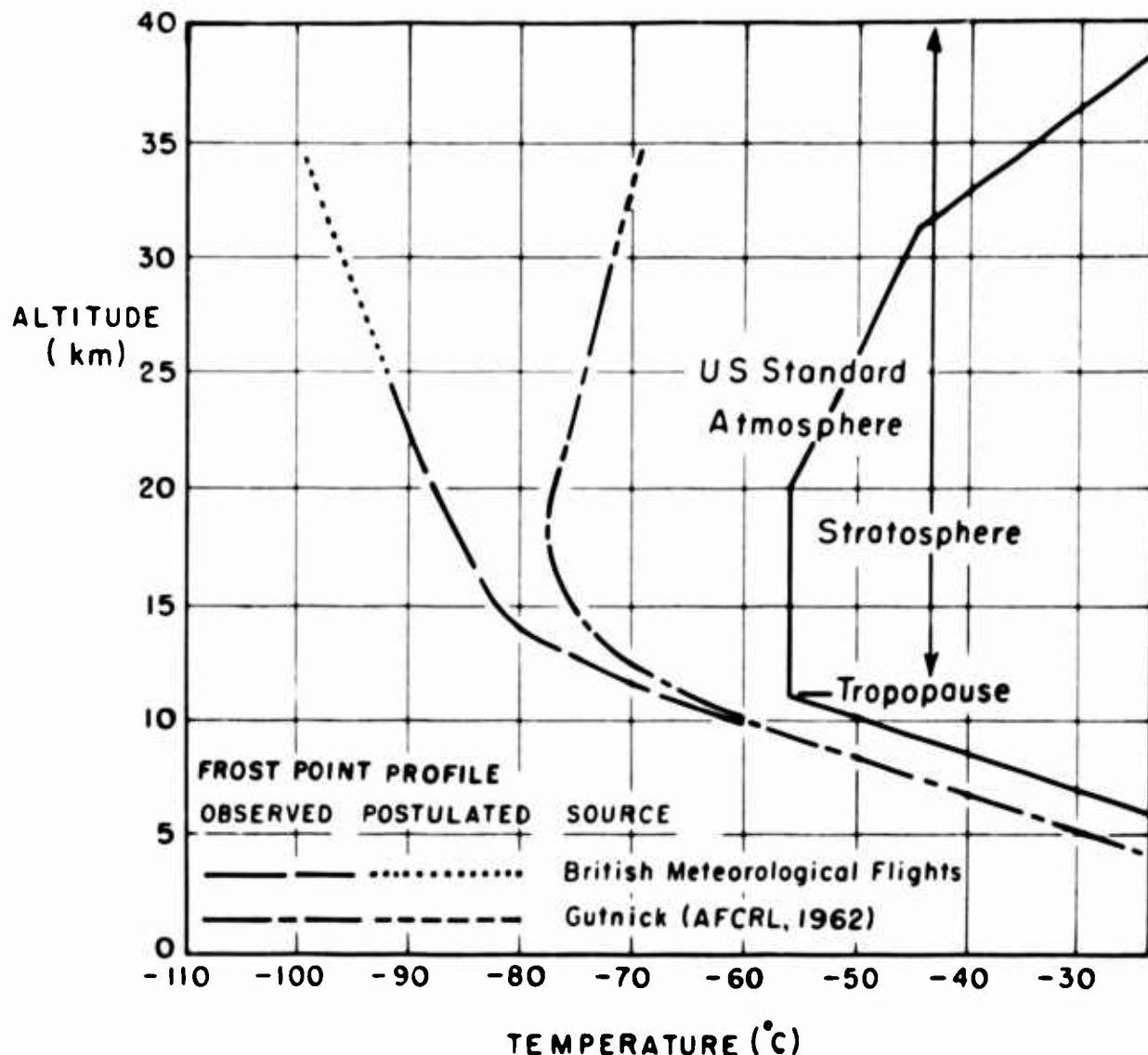


Figure 1. Controversy Concerning the Amount and Distribution of Stratospheric Humidity

Attempts to operate several types of instruments from the same balloon platform have been plagued by complexity of the experimental setup so that neither a real synoptic comparison of results of different instruments nor a real check of basic calibration at extremely low vapor pressures has been obtained. The logical solution would be to compare instruments under controlled conditions, but there have been no chambers available in which frost points of  $-80^{\circ}$  to  $-100^{\circ}\text{C}$  are reached and maintained.

Recently Honeywell, Inc., developed a chamber for testing and calibrating low-pressure, low-temperature frost-point hygrometers in support of their instrumentation effort. AFCRL is now in process of obtaining a similar chamber. Hopefully, we may soon have some valid comparisons of several types of instruments and be able to make a more careful assessment of their resulting observations.

The sensor that will be used in the AFCRL stratospheric humidity program is the alpha radiation frost-point hygrometer developed by Honeywell, under AFCRL contract (Ballinger, 1963; Ballinger, Koehler, Fricke and Murphy, 1964). This instrument operates on the principle of maintaining a predetermined thickness of water molecules on a polonium surface which is temperature-controlled at the frost point by monitoring the attenuation of alpha radiation. The mass-sensing technique of this hygrometer permits response to one microgram-per-square-centimeter change in water-layer thickness. The model being used in the AFCRL balloon program will have the capability of measuring frost points as low as -100°C.

### 3. RECENT DEVELOPMENTS

There have been several observations of stratospheric moisture since AFCRL's attempt to make sense of the data which led to Gutnick's now famous 1961 JGR article, "How Dry Is the Sky?". The results of six of the more recent flights are shown in Figure 2. The solid line curve on the right is Gutnick's Mean Annual Mid-Latitude Moisture Profile which was subjectively judged to be representative of all the available data in 1962.

It is clearly evident that all the recent observations have tended toward the dry (or colder) side. This could be due to greater precautions now being taken to reduce contamination effects that were undoubtedly present in some of the earlier soundings.

The three profiles shown were made with electronically-controlled optical dew pointers. The driest profile, on the left, was observed during descent at Kwajalein, M. I., November 1963, by Dr. Henry Mastenbrook, NRL. This is one of the driest soundings obtained in a series. Nearly the entire stratospheric portion is within NRL's now-postulated profile of constant 1- to 4-mg/kg mixing ratio.

Another NRL descent, obtained (January 1964) in Washington, D. C., is shown by the dash-dot line. Once again the profile is marked by the decreasing frost point with altitude; however, the sounding begins increasing in mixing ratio above 78,000 feet where Mastenbrook suspects that the contamination outweighs the actual moisture content above that altitude.

The dotted curve represents an Army Ballistic Research Laboratory ascent over Palestine, Texas, July 1964 (Mester, 1964). Instrument trouble precluded observations between 46,000 and 73,000 feet. When readings were resumed the dew point increased continually until near the top. At 73,000 feet the mixing ratio was 4 mg/kg, and increased to a maximum of 100 mg/kg at 94,000 feet nearly two orders of magnitude higher than for the NRL soundings.

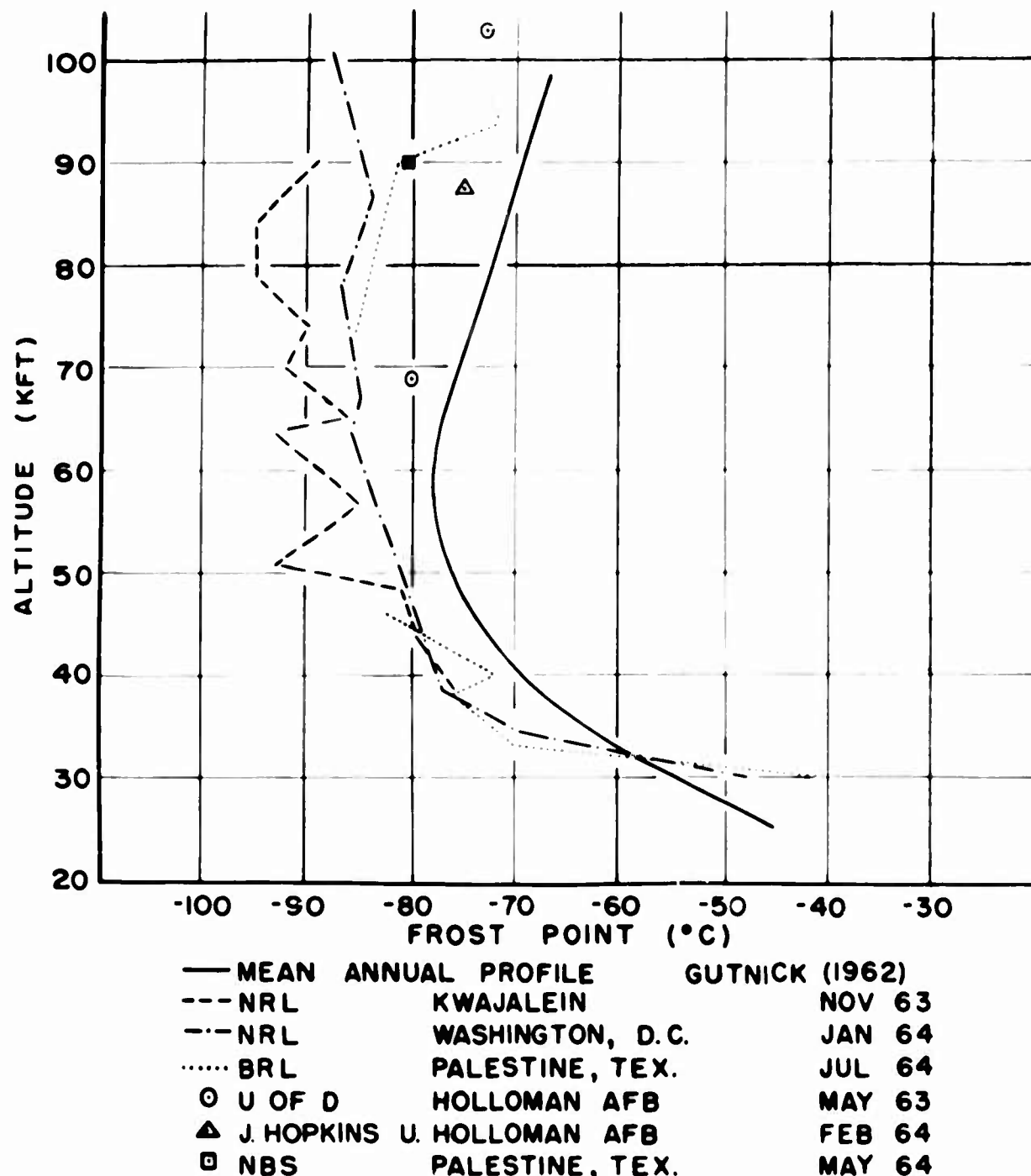


Figure 2. Frost Point ( $^{\circ}\text{C}$ ) and Information

The four "spot" observations were obtained by spectroscopic methods. Data obtained directly measure the total vapor in the sampled path rather than the vapor density where the sensor is immersed.

The two circled observations were Dr. David Murcray's (University of Denver) in May 1963, for Holloman AFB, N. M. (Murcray, 1964). The first, at an altitude of 69,000 feet was derived by making two observations approximately one km apart. The difference between the two readings can be assumed to be the water vapor present in the one-km layer. For such a determination, the effect of contamination becomes negligible. As long as the contamination is the same at both levels, the precipitable water, averaged for the layer, will be free of contamination.

Another of Murcray's observations was made at the top of the sounding, at float altitude, represented by the other circle at 103,000 feet. Such observations are very difficult to interpret. Contamination may be important and only the amount of moisture above the sensor is measured; there is no indication as to the distribution of this moisture. If the assumption is made that this water vapor is evenly distributed up to, say, 50 km where the total pressure is more than an order of magnitude lower, the total water content in terms of precipitable water can be converted into an average mixing ratio between the assumed pressure levels. This average mixing ratio can then be used to determine a "pseudo frost-point temperature" for a given altitude. Using this process, Murcray's observation of 10 microns of precipitable water above 103,000 feet produces a pseudo frost point of -73°C.

In an experiment to determine the amount of water vapor in atmosphere of Venus, Dr. John Strong, Johns Hopkins University, (AFCRL-supported) observed  $98\mu$  of precipitable water in the sampled path between his sensor and Venus. By using a Doppler-shift analysis between Venus and the sun,  $5\mu$  of this precipitable water was determined to be present in the earth's atmosphere above the sensor, positioned at 87,500 feet. This value reduces to a frost point of -75°C, at 87,500 feet, the triangular point in Figure 2.

In May 1964, Dr. David M. Gates, National Bureau of Standards, conducted stratospheric humidity soundings from Palestine, Texas, using a high-resolution infrared spectrometer (Gates, 1964). After analyzing the data, Dr. Gates thought the spectra were partially contaminated. He obtained  $3\mu$  of precipitable water above 90,000 feet, which reduces to a frost point of -80°C at that altitude, the boxed point in Figure 2.

The proponents of the dry sky theory have cited the quality of their instruments, the design of their packages and the care and skill in preventing moisture contamination during launch and flight. Since the amount of water vapor to be measured is so small, the spectre of moisture contamination is a real one. Poorly designed packages and sloppy operating procedures can very well yield measurements of outgassed moisture which was carried aloft by the balloon and package, instead of moisture present in the ambient air.

This contamination problem is now being examined through a special series of AFCRL flights designed to determine to what extent package design and flight

profiles contribute to moisture observed (Ballinger, Fricke and Murphy, 1964). Measurements of atmospheric moisture will be made from various balloon and instrumentation configurations. One instrument package will be placed above the balloon, another on the load-bar directly below the balloon and a third on a line 2,000 feet below the balloon. The first of these flights is scheduled for November of this year. The ultimate test will be a comparison of data from the three positions of the instrument packages flown simultaneously. These instruments will be calibrated in the stratospheric moisture simulator.

#### 4. AFCRL STRATOSPHERIC HUMIDITY EXPERIMENTS

The major AFCRL stratospheric humidity effort will consist of a series of 25 vertical and five horizontal balloon flights. These will be launched at Chico, California. Beginning in December 1964 two vertical soundings will be launched each month for a period of a year. Figure 3 presents the proposed flight profile. The vertical flights will use a 500,000-cubic-foot, 1.5-mil polyethylene, valving-controlled balloons to carry the payload of 450 pounds to 100,000 feet. Both ascent and descent rate will be less than 400 ft/min, with primary emphasis placed on the data obtained on descent. The slow ascent and descent rates are necessary to allow sufficient time for the instrument to respond to the very slow mass transfer rates of water vapor illustrated by Ballinger, Koehler, Fricke and Murphy. Tracking and recovery skill of the balloon technicians will be critical since the five sets of equipment will be reused to accomplish the 25 vertical flights. All data will be recorded on-board. Every effort will be carried out to minimize moisture contamination. (See Figure 4.) All components open to the atmosphere will be made of nonabsorbing materials. Ballast will be baked and sealed. Closed components, not necessary for sampling, will be hermetically sealed. Nylon rope will be used for reeling out a line which will lower the sensor package 2,000 feet below the balloon for the vertical soundings. Helium, used for inflating the balloon will be as contaminant-free as possible.

The effort will also include instrumented horizontal flights of several days' duration, a unique concept in sounding the stratosphere. The horizontal flight profile is shown in Figure 5. Horizontal flights of 500,000-cubic-foot, 2-mil, zero-pressure vehicles will carry a 1000-pound payload. They will carry the same type of sensor equipment as the vertical flights and will be floated for 10 to 12 days at a nominal altitude of 75,000 feet. Data will be gathered over thousands of miles while the platform passes over a spectrum of mid-latitude tropospheric weather systems. Observations will be telemetered every two hours through the FCC network. No payload recovery is anticipated. Observations of

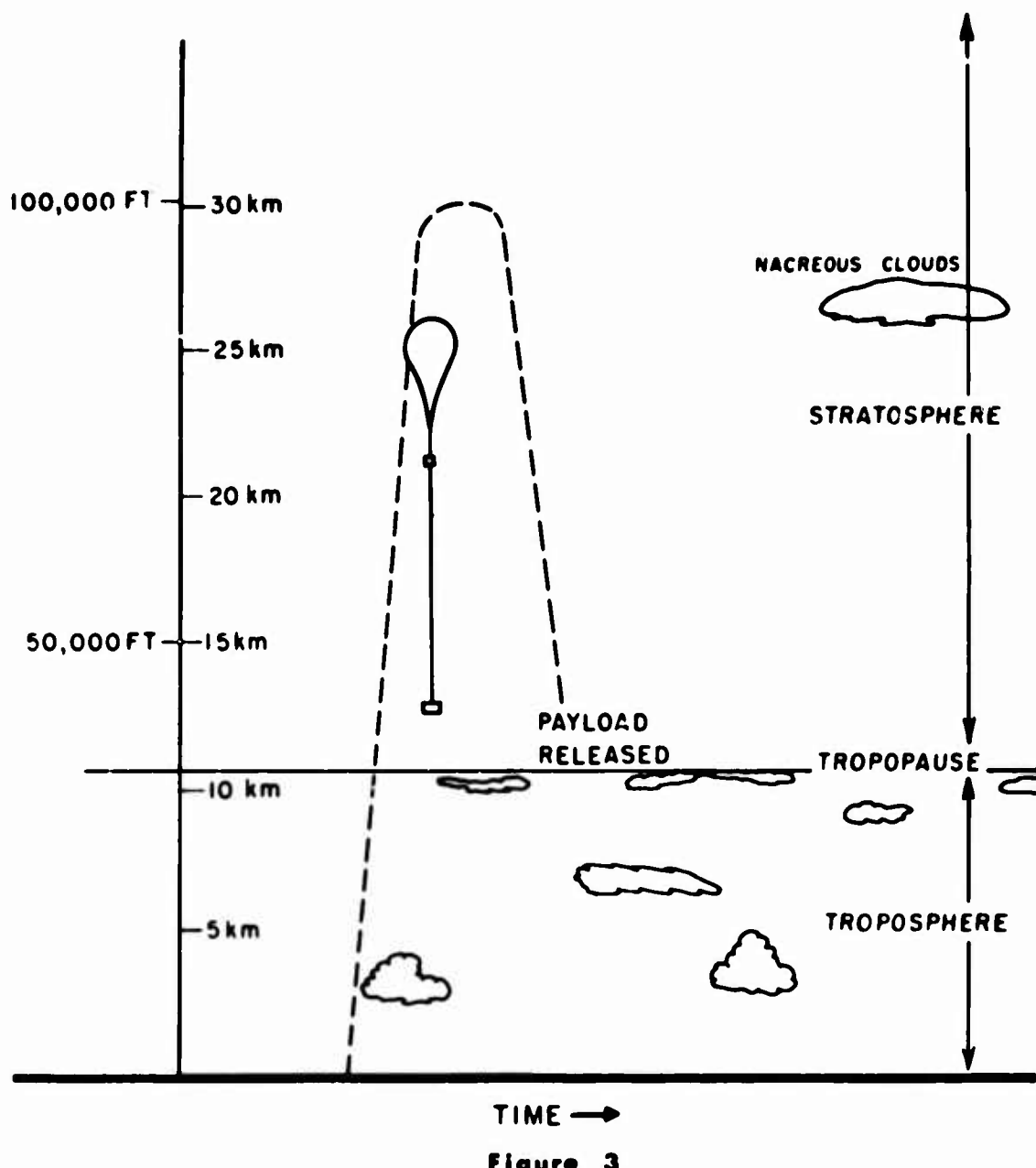


Figure 3

Figure 3. Vertical Soundings: 1. 25 Flights (Approx. 2 Per Month)  
2. Duration - 8 to 10 Hours Per Flight

contamination due to the emission of tropospheric-absorbed water vapor are anticipated for the first two to three days of flight but at least a week of uncontaminated data are expected to follow the drying-out period due to solar baking.

The objective of the AFCRL stratospheric humidity program is to determine vertical and horizontal distributions and seasonal variations of stratospheric humidity, and to correlate these moisture distributions with tropospheric weather systems. Through this program we hope to contribute toward answering the problem posed in 1961 by Murray Gutnik, in his article, "How Dry Is the Sky?".

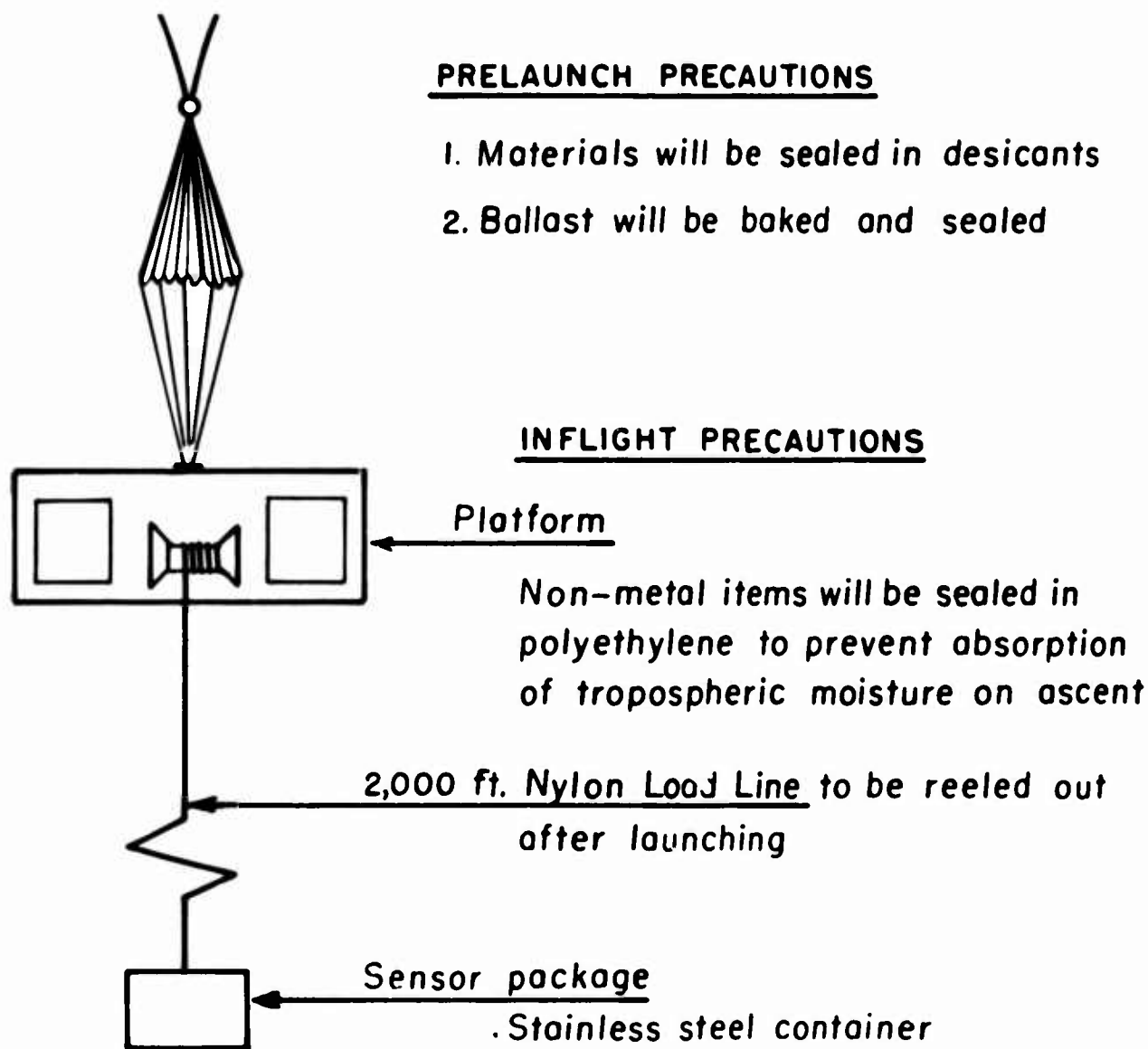


Figure 4. Precautions Against Water Vapor Contamination

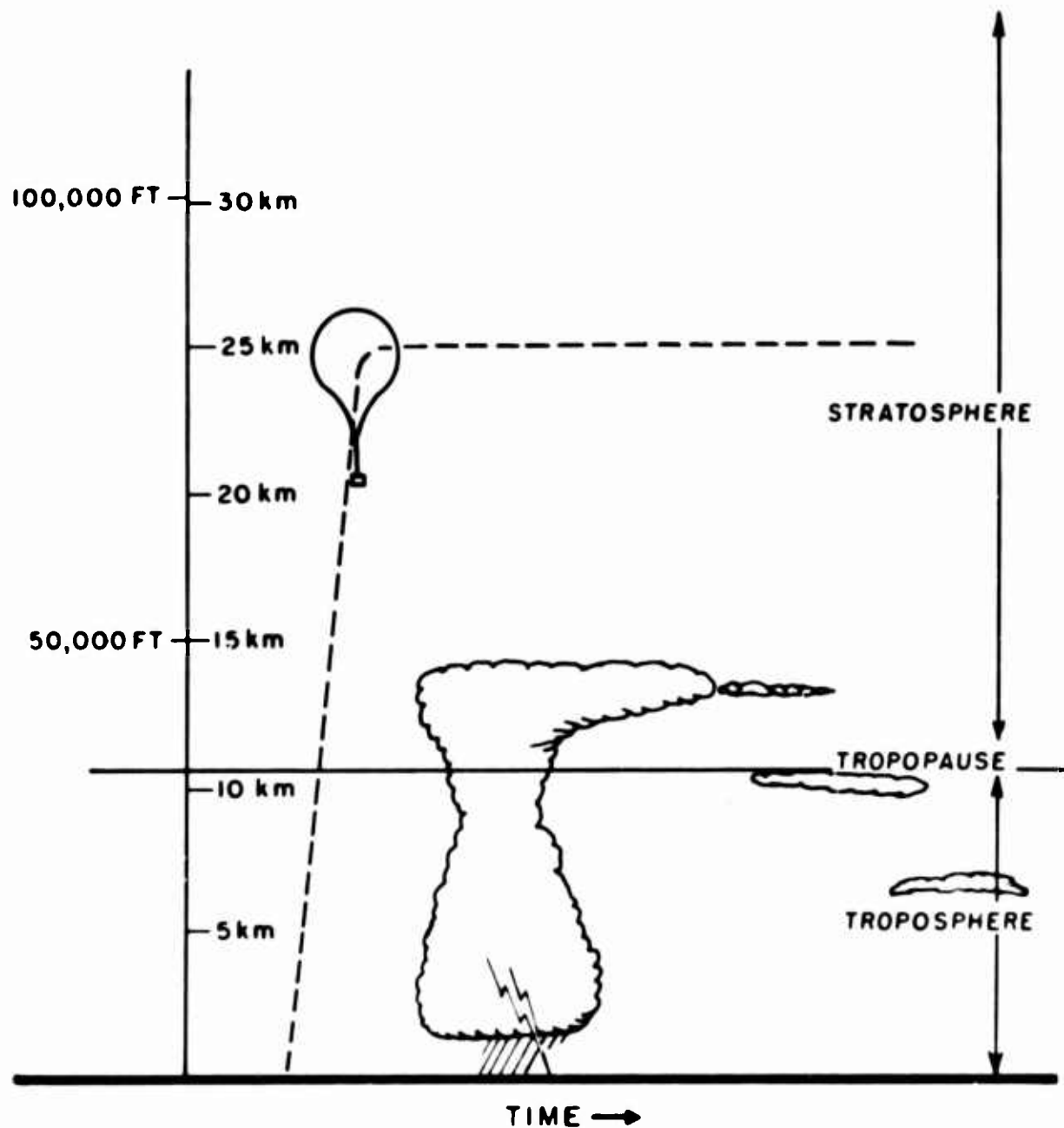


Figure 5. Horizontal Soundings: 1. 5 Flights (Spaced Over One Year)  
2. Duration - 10 to 12 Days Per Flight

## References

- Ballinger, J. G. (1963) An automatic frost-point hygrometer using radioactive detection, R-RD-6300, Honeywell, Inc., presented at the 1963 International Symposium on Humidity and Moisture.
- Ballinger, J. G., Koehler, L. E., Fricke, M. P., and Murphy, R. D. (1964) Toward improved measurements of stratospheric humidity with balloon-borne frost-point hygrometers, Paper presented at the AFCRL Scientific Balloon Symposium, Wentworth-by-the-Sea, Portsmouth, New Hampshire.
- Ballinger, J. G., Fricke, M. P., Murphy, R. D. (1964) Quarterly Report No. 1. for Geophysics Research Directorate, AFCRL, Contract AF 19(628)-3857.
- Bottema, M., Plummer, W., Strong, J. (1964) Water vapor in the atmosphere of Venus, The Astrophysical Journal, 139: No. 3.
- Brewer, A. W. (1949) Evidence for a world circulation provided by the measurements of helium and water vapor distribution in the stratosphere, Quart. J. Roy. Meteorol. Soc., 75:351.
- Dobson, G. (1956) Origin and distribution of the poly-atomic molecules in the atmosphere, Proc. Roy. Soc., London, 326 (1205) :187.
- Gates, D. M. (1964) National Bureau of Standards, Private Communication.
- Gutnick, M. (1961) How dry is the sky? J. Geophysics Research, 66:2867.
- Gutnick, M. (1962) Mean annual mid-latitude moisture profiles to 31 Km, Air Force Surveys in Geophysics No. 147.
- Mastenbrook, H. J. (1964) Water vapor observations in the stratosphere, Paper presented at the Fifth Conference on Applied Meteorology of the American Meteorological Society, Atlantic City, N. J.
- Mester, J. C. (1964) U. S. Army Ballistic Research Laboratories, Private Communication.
- Murcray, D. G. (1964) University of Denver, Private Communication.

Murgatroyd, R. J., Goldsmith, P., and Hollings, W. E. (1957) Some recent measurements of humidity from aircraft up to heights of about 50,000 feet over southern England, Quart. J. Roy. Meteorol. Soc., 81:533.

Murgatroyd, R. J., From a Draft Copy of Chapter 2 of a Forthcoming WMD Publication on the Atmosphere.

Sissenwine, N. and Gutnick, M. (1960) Precipitable water along high altitude ray paths, Proceedings of the Infrared Information Symposia, IRIS, 5, No. 3.

## XXIII. Balloon-Supported Platforms in Communications

Charles A. Strom, Jr. and Cleo N. Lawrence  
Rome Air Development Center  
Rome, New York

### Abstract

This paper considers some possible uses of balloons to enhance the line-of-sight distances over which microwave radio frequency communications can be used. Both tethered and free-floating balloons are discussed as supporting platforms for both active and passive radio repeater stations. The broad needs of microwave radio communications are outlined and the more serious problem areas of applying balloon techniques summarized.

### I. THE COMMUNICATIONS PROBLEM

The microwave communication problems in need of solution are several. To begin with, more bandwidth is needed. This is available only by going to higher radio frequencies. This in turn places a premium on line-of-sight type radio transmission. Second, there is a simultaneous need for less interference and more privacy. And of course there is a standing need for anti-jam capability. This suggests the use of highly-directional antennas and, from size and weight considerations, again points to the use of higher frequencies. Third, economy in

the use of communications is paramount. This suggests sharing facilities among several users and preferably serving several users simultaneously. This again calls for greater bandwidth and therefore higher frequencies.

Fourth, there is a standing need for circuit reliability. We cannot tolerate, for example, the dropouts on high-frequency radio circuits caused by magnetic storms and their associated high background noise. Line-of-sight networks should improve this situation. Fifth, improved survivability stands high on any list of communication needs. To reduce the number of stations in a line-of-sight network should numerically reduce the odds of system failure. Here we can easily go off the deep end, however, unless we remember a balloon is not as sturdy as a steel tower.

Sixth, any changes in the communications system should be readily adaptable to present plant. In this way growth can be realized by expansion of existing facilities. Seventh, the communications that we install now and plan for the future should be compatible with the Communication Master Plan of the Department of Defense. This means the ability to handle multichannel voice, low- and high-speed digital data, unusual modulation techniques like enciphered voice and video transmissions. Eighth, and perhaps to repeat in part, whatever communication facilities or approaches we use, they must possess suitable growth potential to adjust to changing requirements.

The requirements for greater bandwidth, hence higher frequencies, and for spanning greater line-of-sight distances places a premium on very-high-altitude platforms. Perhaps one of the simplest and most direct applications would be the use of a balloon to support an echo type passive repeater in the "scatter volume" zone of a tropospheric radio transmission link. This establishes a common line-of-sight point and transmission path computations indicate recovery of 70 percent of the 57-db loss normally attributed to the tropospheric scatter mode in comparison with free space. Based on  $d = \sqrt{2h}$ , where  $d$  is in miles and  $h$  in feet, it works out the smooth earth line-of-sight distance of a balloon tethered at 20,000 feet as 200 miles, that is, two tropospheric scatter radio stations separated 400 miles can be brought within effective line-of-sight. If a pseudo passive repeater consisting of an array of helical antennas and suitably biased tunnel diodes were used an additional 20 db can be realized above the passive configuration.

There are several other possible configurations as will be described briefly. One is a balloon-supported active repeater. Such a repeater can of course be narrow band or broad band. It can be located at midpoint between stations or directly over a central or command location. Such supporting balloons can be either tethered or free floating as best serves the operational requirement. A tethered balloon at 10,000 feet centrally located could provide line-of-sight coverage in an area of 130 mile radius about this center. By means of one of the

several random access, discreet address techniques now under consideration, user to user communications can be provided between all parties in this area of coverage.

Another application that appears attractive, referred to above as "narrow band", is extending the range of ground-to-aircraft command and control coverage by the use of a tethered or a free floating balloon. In the first case we are thinking of 10,000 feet; in the latter of 70 to 90,000 feet. If an aircraft under control were flying at 30,000 feet the maximum range of line-of-sight under optimum conditions would be of the order of 1,000 miles. Such a repeater could be launched from ground, from aircraft, or by means of a rocket, depending on position, time, operational requirement and acceptable cost.

Another application of airborne communications equipment is in the area of survivable communications and communications restoration. Here we are thinking of large manned platforms similar to the Navy dirigibles of World War II. This could include multiple frequency, broad band radio terminals, a switching and traffic routing capability and emergency Command Post facilities of the type adapted to limited war operations. Initially such a device operating as a flying laboratory would facilitate solution of many problems related to the use of balloons as communication platforms. A small, lightweight, well streamlined, "drone" version of such a dirigible capable of hovering in a specified zone for two or three days at 20 to 30,000 feet as a live-radio-repeater platform holds some interesting possibilities. Electric power derived from the propelling power plant would permit radio-frequency energy levels sufficient to assure reliable propagation over line-of-sight distances involved and perhaps without the use of highly-directional antennas required to compensate prime power restrictions of a tethered balloon platform.

## 2. GENERAL CONSIDERATIONS

As a point of philosophy it may be well to note that in the military, communications have virtually always the nature of a support function and receive secondary consideration with respect to weapons and weapon detection and neutralizing devices. On the other hand, without the cohesive aspect of a communication network, organization as such does not even exist, let alone function in the specialty for which it was conceived and established. It is customary therefore to take communications for granted to such an extent that any acceptable communication complex must function on a "no break" basis, 24 hours per day, 365 days per year.

There are other areas of general considerations that are more or less self explanatory. As in the case of any equipment considered for military use, certain basic criteria must be met. It must be technically feasible, economically

acceptable and operationally attractive or it doesn't have much chance of finding its way into inventory. By operationally attractive we mean easy to transport, handle, install and maintain and make a vital contribution to the assigned mission.

In addition to the availability and reliability of a balloon as a communication platform, radio communications must be designed with a fade margin. Here we must take into account at least propagation fade, equipment variation, and antenna misalignment. The need for a suitable high altitude platform to extend the line-of-sight coverage of microwave (broadband) radio dates from the inception of its use in the late 1930's. The fact that balloons are not in wide use for this purpose now, 25 years later, suggests major problems. It is realized that great strides are being made in balloon technology however, and we as communication engineers are making an effort to have at hand suitable ground and airborne communication gear by the time some of the problems in the use of balloons have been resolved.

An area in which circumstances might justify early use of balloons is jungle environment. Here we may find a double incentive; the fact that communications are generally nonexistent, and the need to get above the forest canopy to avoid the severe attenuation of radio signals being propagated through dense foliage at a low take-off angle. If we assume a canopy approximately 100 feet above ground and a balloon tethered 500 feet above the ground for smooth earth we can assume line-of-sight to a point of tangency 25 to 30 miles distant. Here we would still be faced with the problem of getting through the canopy at a thin angle at the remote end. If we use another balloon tethered at 500 feet the distance can be approximately doubled, but now we are faced with the problem of two balloons on a single link.

Some of the difficulties anticipated in the use of balloons in support of communications are summarized as follows: first, there is need of a suitable cleared area to avoid tether fouling. Improvement in ground handling facilities might ease this problem. Second, around-the-clock ground support for balloons is needed. An essentially unattended operation is desirable. Third, there is need for periodic "topping-off" of the balloon with buoyant gas. Again it would be desirable if this could be done on a demand basis without lowering the balloon. Fourth, it is necessary to make balloons less vulnerable to seasonal weather extremes. New fabrics and handling, bridling and tethering techniques may hold promise in this area. Fifth, balloons pose a hazard to friendly aircraft. This may necessitate the development of a specialized radio transponder or some new approach to assure aircraft safety. Sixth, balloons could provide fixed markers for enemy attack. This is an operational problem which can be solved in part by judicious deployment away from communication and command centers. Seventh, we currently lack suitable prime-power sources for use with active balloon-borne radio repeater equipments. Eighth, there is at present no equipment available to maintain orientation of a high-gain,

pencil-beam-type antenna on board a balloon. Antenna design improvements, application of tracking methods, and some stabilization of the airborne platform should help. Ninth, extremely lightweight electronic packages need to be assembled. Techniques are available, but packaging has yet to be done.

The picture really isn't all black however. For example, there are in various stages of progress at Rome Air Development Center (RADC) several balloon-related projects among which are:

- a. Development of a 100-watt butane-fired thermoelectric prime-power source for balloon use.
- b. Development of a balloon-borne UHF repeater which could extend ground-to-air control coverage to ultimate ranges of 500 to 1000 miles.
- c. Design and development, which is well along, of a pseudo-passive microwave repeater, the prime-power requirements for which is quite small.
- d. Exploration of the feasibility of transmitting primary power to balloons by beamed radio energy.
- e. As a result of work on another project, some microwave radio repeater hardware suitable for use in a balloon-borne complex should become available in about 18 months.
- f. A balloon-borne microwave transponder is currently being used as a bore-sighting target for radar antenna alignment. This could serve in part as a test bed for pseudo-passive circuit elements.
- g. A project is being initiated to examine the feasibility of transmitting primary power to balloons along a metallic tether with a "G String" type radio-frequency transmission.
- h. Similarly it is proposed that a project be initiated to consider the use of flat and partial spherical surfaces for reflecting directional microwave beamed energy from balloons toward selected terminal stations.

### 3. CONCLUSIONS

In the area of tethered balloons suitable for communications platforms much remains to be done. Ruggedness, long endurance, stability and suitable power sources head the list. Much in the way of simplification and automation needs to be worked out. In the area of free-floating balloons some attractive applications seem already within reach, the only remaining problem being to work out payloads.

What the future holds in the use of balloons for the solution of communications problems is not easy to foretell. Some day microwave radio repeaters, riding the natural currents of the thin upper reaches of the stratosphere and powered with solar cells, may bridge great distances, competing in a small way with orbiting

vehicles, and certainly at a fraction of the cost of many of the present globe-encircling networks. The possibilities are remarkable.

## XXIV. The Rotation of Balloons at Floating Altitude\*

A. E. Germeles  
Arthur D. Little, Inc.  
Cambridge, Massachusetts

### Abstract

The use of high-altitude balloons as stable platforms for meteorological and astronomical observatories necessitates an investigation of the dynamic behavior of balloons. This report deals with the azimuthal rotations of the balloon-gondola system. The aerodynamic damping and inertia of the system have been mathematically formulated and experimentally verified. The forcing torque, mostly aerodynamic in nature, has been described and its order of magnitude has been estimated for known balloon rotations.

These rotations have been alleviated in the past by control systems which orient the gondola by reaction torques applied to the balloon. The aerodynamic parameters which are evaluated in this report can be useful in the design of such a control system.

---

\*This talk was based on a research paper of the same title by Mr. Germeles and R. M. Lucas, of Arthur D. Little, Inc., and E. R. Benton of the National Center for Atmospheric Research, Boulder, Colorado. The report, dated December 1963, was prepared for the Office of Naval Research under Contract No. Nonr 3164(00). - Editor.

## XXV. A Balloon-Borne Microphone System

John W. Coffman  
U. S. Army Electronics Research and Development Activity  
Environmental Sciences Directorate  
White Sands Missile Range, New Mexico

### Abstract

This paper describes a balloon-borne microphone system developed at White Sands Missile Range, New Mexico, during the period from 1958 to 1961 (See References: Webb, Coffman and Clark, 1959). In a following paper, John Wescott describes the use of this system in the measurement of low-frequency background noise at high altitudes. The instrument was to have a frequency response of 0.1 cps to 100 cps, a dynamic range of 0.01 to 10 microbars, an expected lifetime of 12 hours, a weight of less than six pounds, and was to cost less than 100 dollars. Most of these goals were met, and the system which evolved incorporated several unique features.

#### I. BALLOON SYSTEM

The simplest component of the balloon-borne microphone system was the balloon. Two types of constant-level balloons were used: a polyethylene teardrop with an open vent at the base, and a neoprene sphere with a valve arrangement.

Figure 1 is a photograph of the polyethelene balloon during inflation. This balloon was small, roughly 30 feet in gore and 15 feet in diameter when fully distended, and was therefore easily released under most circumstances. Venting was accomplished by means of an opening adjacent to the load fitting in the bottom of the balloon. Ascent rates of between 600 and 800 feet per minute were obtained with a payload of six pounds and an initial inflation volume of 350 cubic feet of helium.



Figure 1. Polyethylene Balloon During Inflation

Figure 2 is a performance chart for the polyethylene balloon. Assuming a standard atmosphere, the altitude range is seen to be 87 to 68 thousand feet, corresponding to no load and six pounds of load respectively. In the actual operations, an effective method of selecting lower-level float altitude was evolved without increasing the load. The balloon was reduced in volume by the simple expedient of tying it off from the top. This was esthetically displeasing, but provided adequate results. With the temperature at the float altitude known, the balloon could be floated within a few thousand feet of the desired altitude.

The neoprene balloon, which was used to some extent, incorporated a unique arrangement for achieving constant-level performance. This float mechanism is schematically represented in Figure 3. The device consists of a ribbon wound around a reel which is fastened to a flapper valve at the base of the balloon. A second ribbon or tape is passed through an opening in the top of the balloon which

is sealed with a cork. Prior to release of the balloon, a predetermined amount of tape is pulled from the balloon - the amount depending upon the load and altitude desired. The cork is replaced, the balloon is released, and as it expands with altitude, the reel unwinds until its tape is fully extended, the flapper valve then vents gas, and the balloon stabilizes. A performance curve for this balloon, assuming the 1962 U. S. Standard Atmosphere and a six-pound payload, is shown in Figure 4.

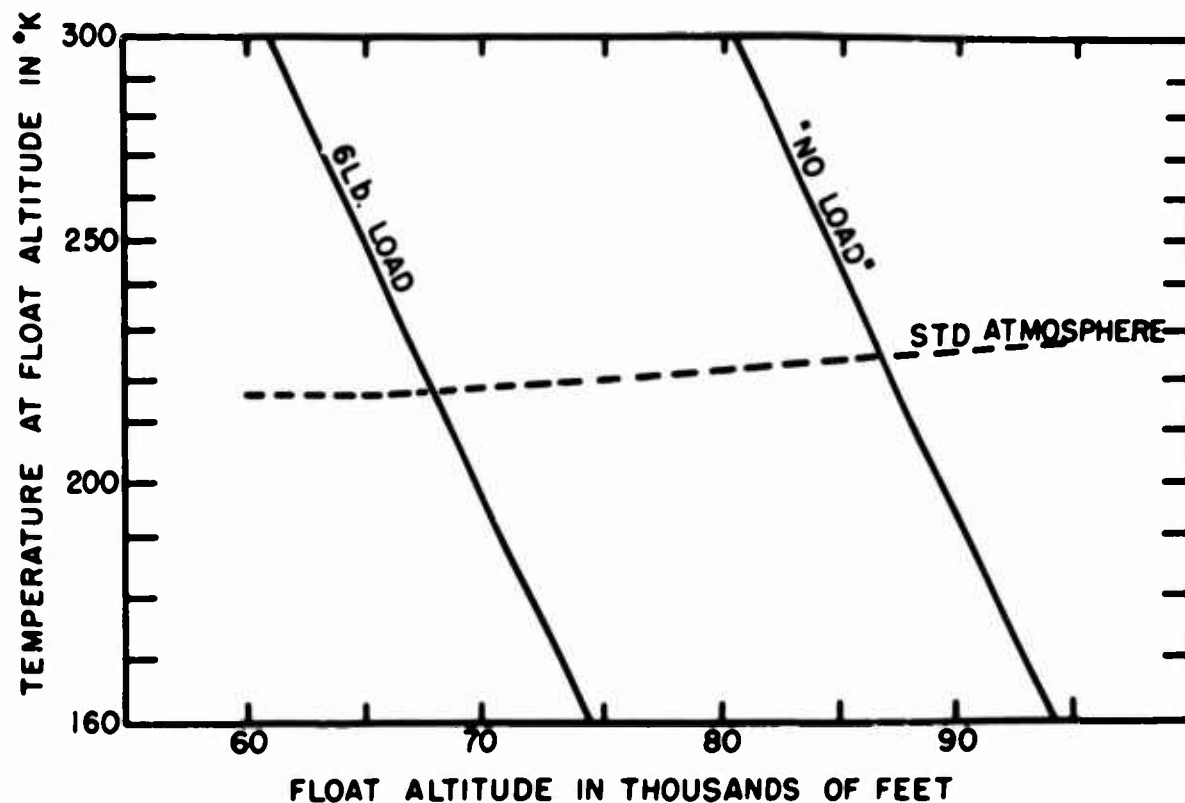


Figure 2. Polyethylene Balloon Performance

The final comment on the balloon system concerns a ballasting device (Figure 5) which was developed to alleviate the problem of the descent of the constant pressure balloons at sundown. A telescoping rod atop the bellows maintains a constant pressure on the ball valve as the balloon ascends. A slight backlash in the mechanism maintains the pressure while the balloon is at float altitude, but if the balloon descends, the bellows will contract, releasing the ball and thereby the fluid ballast. The device was designed to release ballast and stabilize the balloon through one sunset.

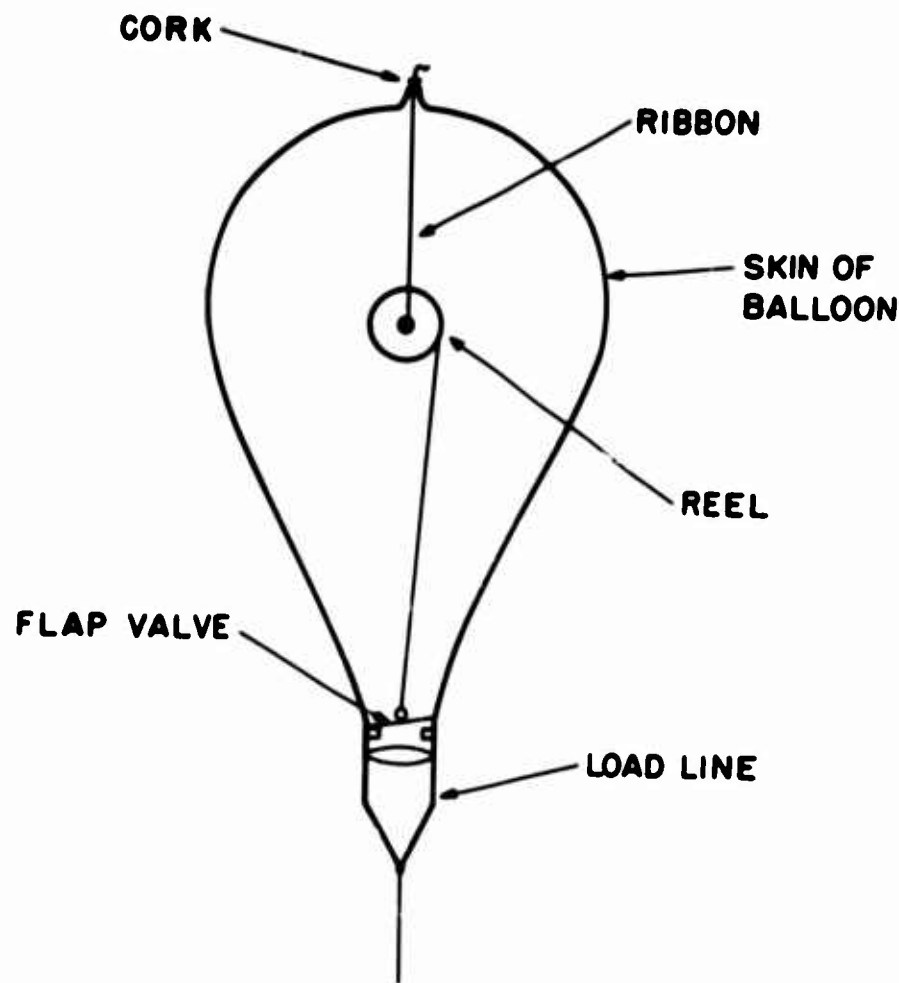


Figure 3. Float Mechanism of Neoprene Balloon

## 2. TELEMETRY SYSTEM

The telemetry scheme of the system was patterned after the radiosonde, due to the availability of the Rawin Set AN/GMD-1A, which uses a PDM-AM modulation (Clark, 1961). However, due to the broad bandwidth of the data, a pulse rate of 3000 pps was used instead of the 240 pps maximum of the radiosonde. A block diagram of the telemetry system is shown in Figure 6. The electrometer tube of the microphone was followed by one stage of gain and the modulation circuit, a voltage-controlled blocking oscillator. The output of the RF stage was thus pulse-modulated by the blocking oscillator at a rate proportional to the voltage of the microphone circuit.

A block diagram of the receiving system is shown in Figure 7. The output of this system was suitable for standard chart recorders. It was necessary to modify the GMD receiver due to the higher carrier rate. The overall frequency response

of the system is shown in Figure 8 with the 3-db points of the system at 0, 14 and 200 cps.

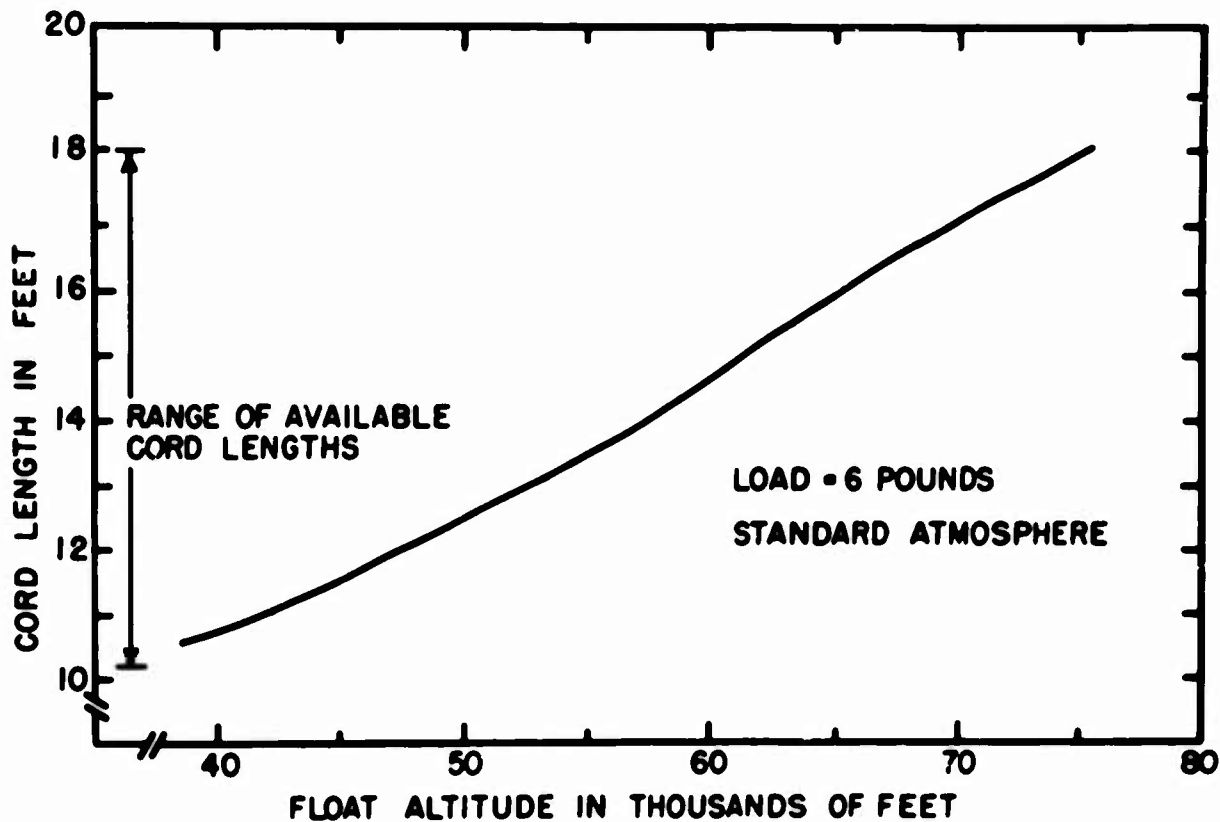


Figure 4. Float Altitude of Neoprene Balloon vs Valve Cord Length

The modulation characteristic of the entire system is shown in Figure 9. Quite large percentages of deviation of the subcarrier were tolerated without loss of linearity, hence a large range of pressure fluctuations was sensed with good fidelity.

### 3. FLIGHT INSTRUMENT

The configuration of the flight instrument is shown in Figure 10. The instrument was divided into three compartments containing the parachute, the battery, and the electronics. The upper compartment contained the battery, the lower half was occupied by the electronics, and the parachute was contained in the cell on the side.

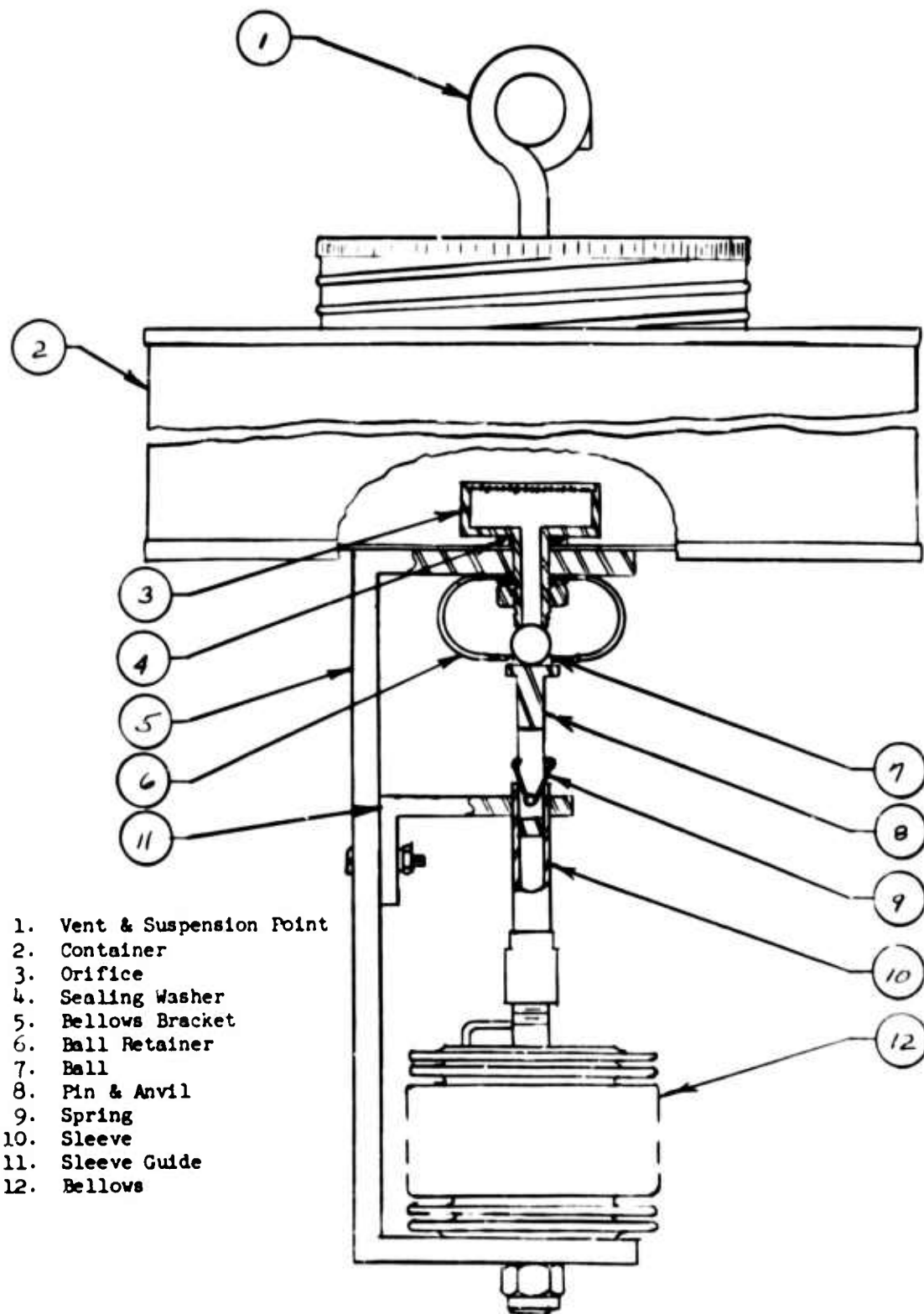


Figure 5. Sketch of Ballastor

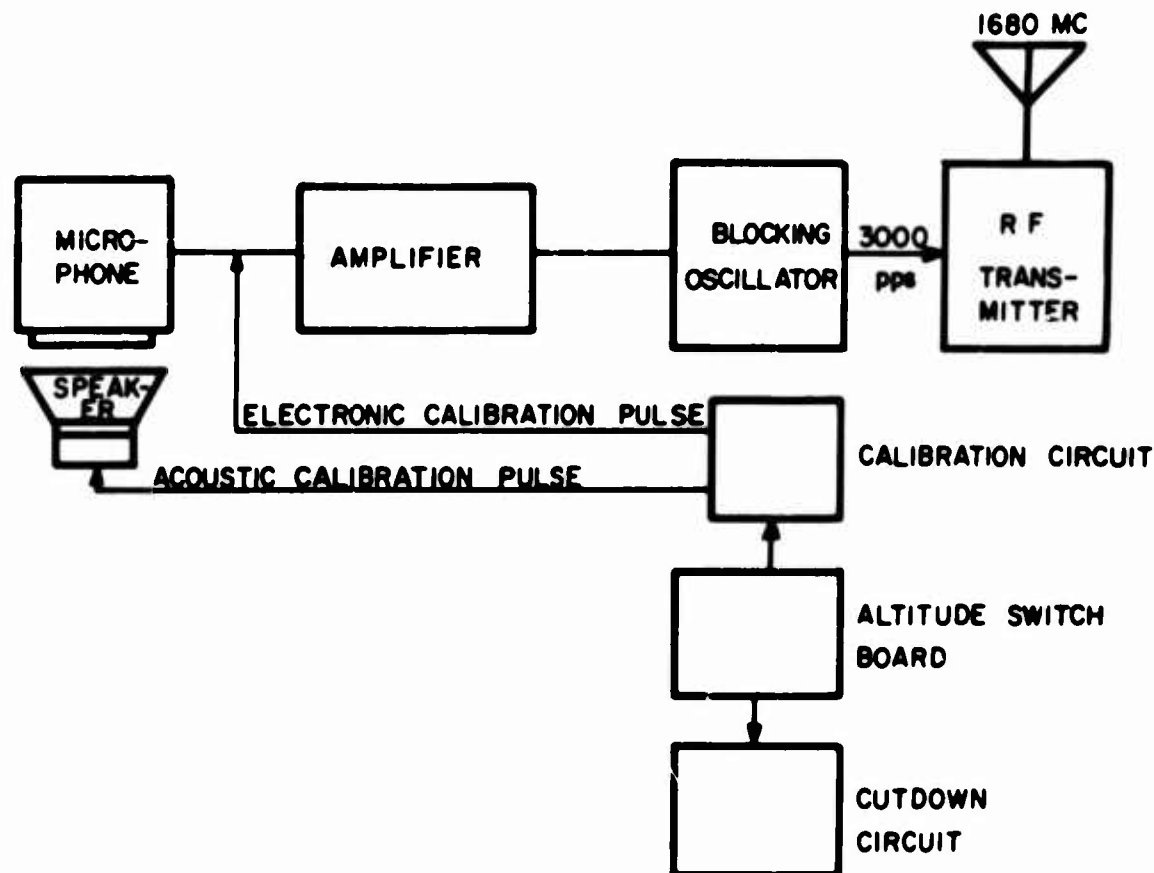


Figure 6. Block Diagram of Instrument

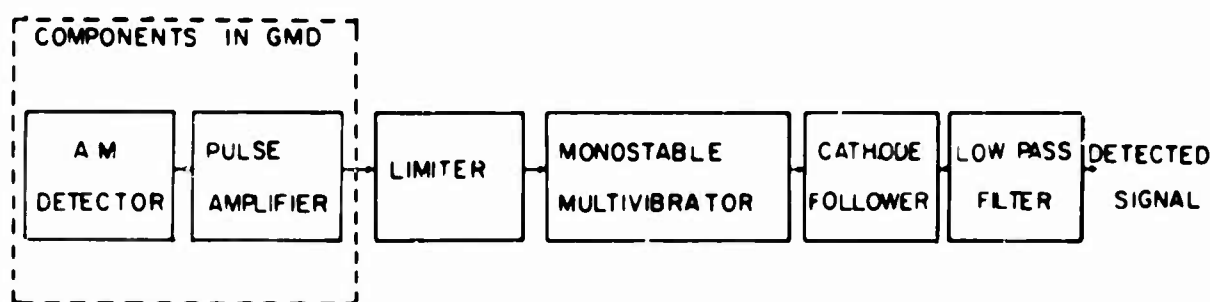


Figure 7. Receiving System - Block Diagram

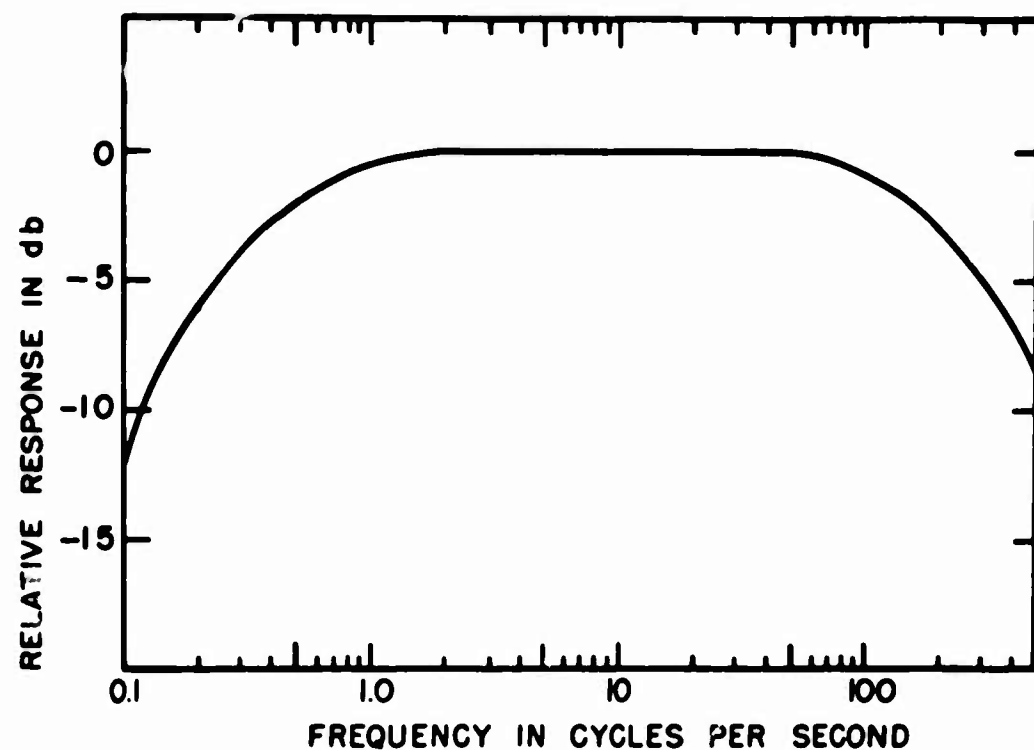


Figure 8. Overall Frequency Response of Pulsonde System

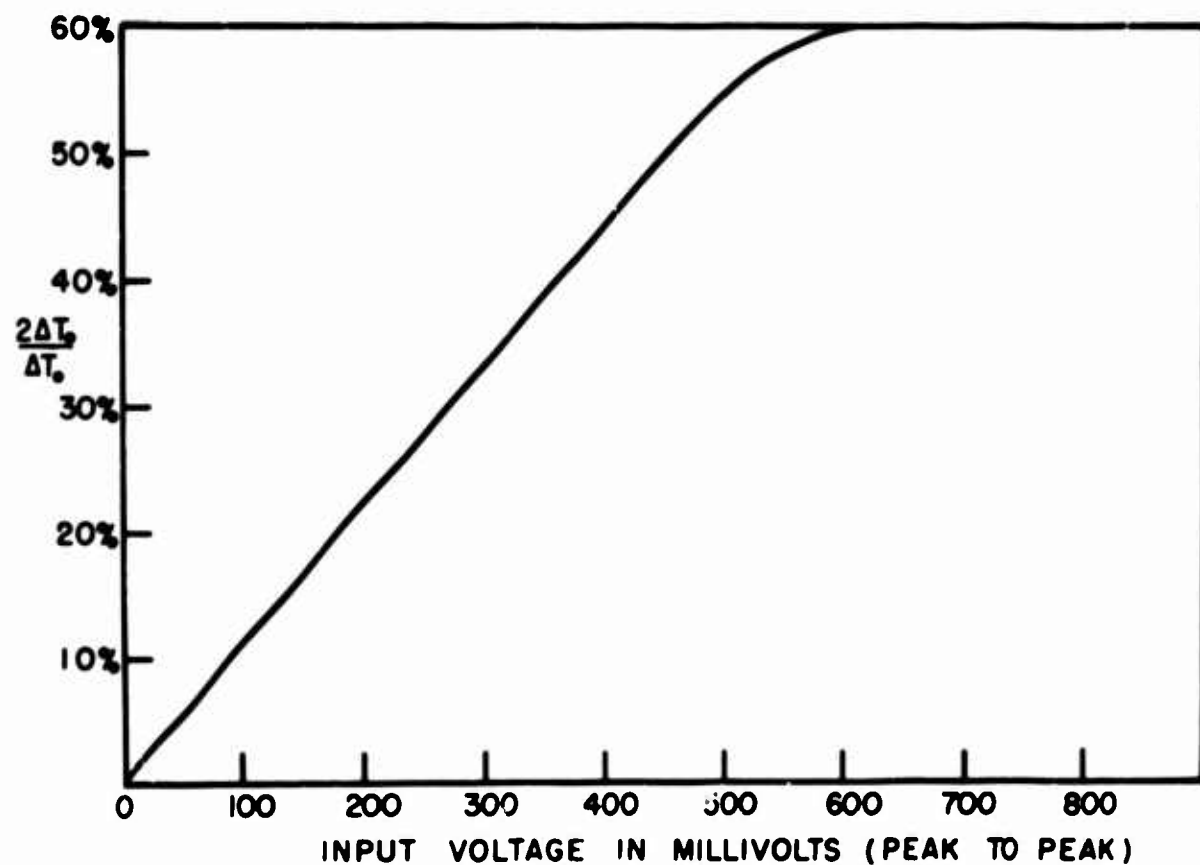


Figure 9. System Linearity



Figure 10. Cut-Away View of Pulsonde Acoustic Sensing Device

The heart of the instrument was a capacitor microphone with a coated mylar diaphragm and a large pressure-reference chamber. In Figure 11, the essential construction details of the microphone are shown. The separation between the diaphragm and the back plate was about 5 mils. The pressure-reference chamber had a volume of approximately  $150 \text{ cm}^3$ . The pressure leak of the chamber was constructed of a piece of stainless tubing, 20 mils inside diameter x 1 inch long, which gave the chamber a time constant of approximately two seconds.

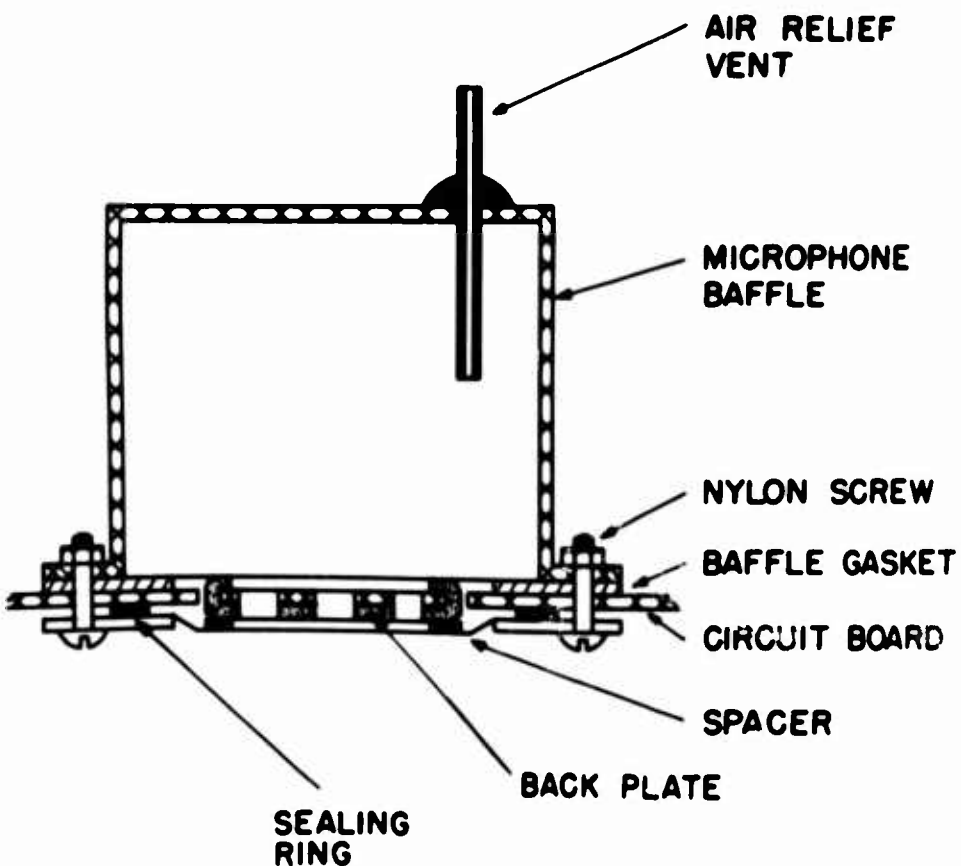


Figure 11. Capacitor Microphone

The microphone and its associated electrometer tube comprised a 0-db microphone, that is, one volt output for an input of one dyne/cm<sup>2</sup>. This high output was accomplished by means of the high-compliance diaphragm, and by using the electrometer as a stage of gain. In addition, the microphone had a large area,  $14 \text{ cm}^2$ , which lowered the electrical low-frequency cutoff of the microphone due to the increased capacity of the microphone.

The high sensitivity of the microphone was offset by two disadvantages: large pressure oscillations would cause the electrometer tube to bias itself to a cutoff condition, and the microphone sensitivity was a function of the ambient pressure because of the high compliance of the diaphragm (Izquierdo, 1961). The first difficulty was solved by the simple expedient shown in Figure 12. A neon bulb across the plate and grid of the electrometer is not normally conducting, but if the grid swings to cutoff, and therefore the plate reaches the supply voltage, the neon bulb will fire and restore the tube to a conducting condition.

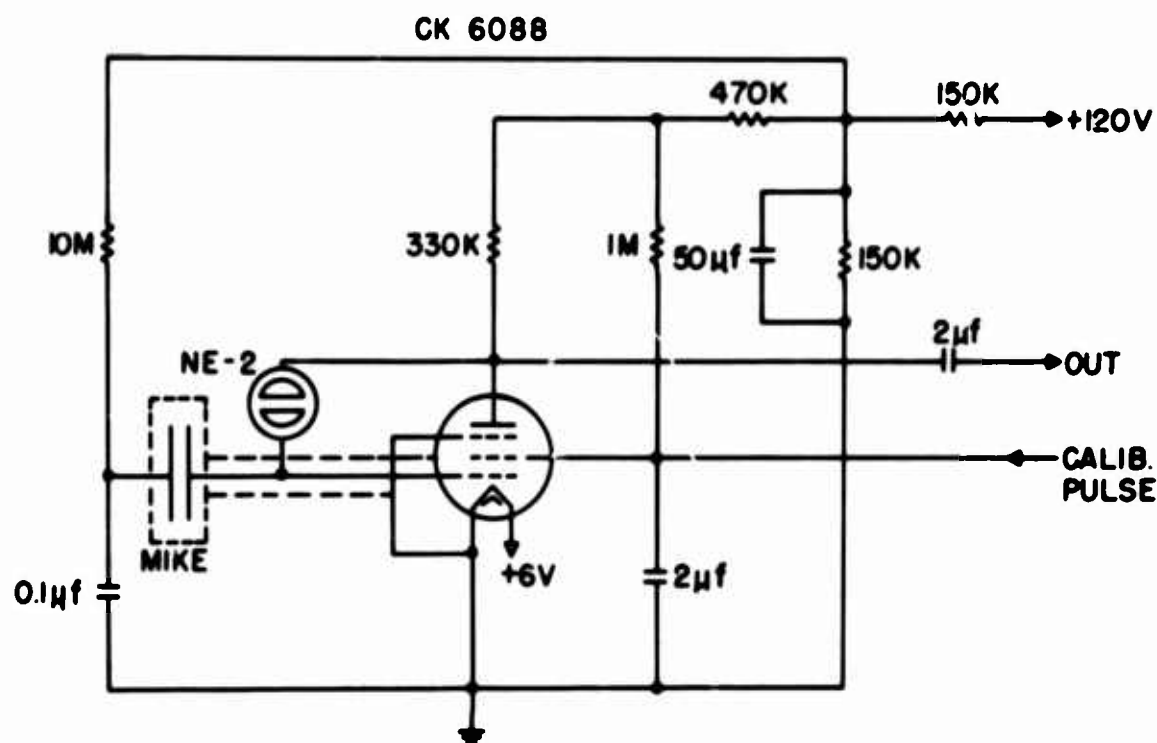


Figure 12. Microphone Electrometer Circuit

The other difficulty, the pressure sensitivity of the microphone, was solved by measuring in a vacuum chamber the change in response of the microphone with pressure. An electrical pulse was periodically injected into the screen grid of the electrometer tube to provide a continuous monitor of the electronic response of the instrument. During the development of the instrument, an electrostatic acoustic calibrator was tried and abandoned due to the stringent shielding requirement necessary for its use. Another calibration device which was included in the instrument was a small loudspeaker situated a short distance in front of the microphone and pulsed at intervals by a relaxation oscillator. The cone of this

loudspeaker had a large mass since roughly 100 grams of soft iron was glued to the cone to provide a transducer with a high Q and low resonant frequency. This device provided a highly-damped sinusoid at 90 cps, which was used primarily as a check upon the performance of the microphone. A baroswitch in the cut-down system was used to vary the time interval between the acoustic pulse and thus give a measure of the altitude of the instrument.

The cut-down system contained within the instrument incorporated a low-voltage relay to fire a guillotine squib device when the filament battery voltage fell below 4 volts, and an altitude cut-down which incorporated a baroswitch to energize the squib when the altitude of the instrument fell below 44 thousand feet.

In retrospect, the most severe constraint upon the immediate, successful design of the microphone system was the six-pound-weight limitation. The weight limitation precluded complex electronics, battery systems, environmental control devices and ground control.

The instrument was used successfully in the form described for many flights, and several modified forms were developed for specific tests. The instrument was easily adapted to measurement of variables other than pressure and is still occasionally flown in a form adapted to pressure measurements of shock waves.

## References

- Clark, G. Q. (1961) Pulsonde telemetry system, Proceedings of the Symposium on Atmospheric Acoustics, U. S. Army Signal Missile Support Agency, Vol. 1, p. 135.
- Izquierdo, M. (1961) Problems in the Construction of Infrasonic Microphones, Proceedings of the Symposium on Atmospheric Acoustics, U. S. Army Signal Missile Support Agency, Vol. 1, p. 131.
- Webb, W. L., Coffman, J. W., and Clark, G. Q. (1959) A High Altitude Acoustic Sensitivity System, U. S. Army Signal Missile Support Agency, White Sands Missile Range, Special Report No. 28.

## XXVI. Acoustic Detection of High- Altitude Turbulence \*

John W. Wescott  
MTI Radar Laboratory  
Institute of Science and Technology  
The University of Michigan

### Abstract

The causes of low-frequency acoustic background noise that was monitored from instrumented balloons floating at about 60,000 feet were investigated. Tape-recorded samples of the noise were analyzed. Spectrograms, signatures, cross-correlations and probability-density curves were obtained. Examples are shown. The results indicate that clear-air turbulence is one of the principal sources of infrasound in the upper air. A theory for the power spectrum of the far-field noise radiated from the turbulence is cited, and the predicted spectrum is compared to experimental results.

As the title of this paper implies, it is possible to detect the sound radiated by high-altitude turbulence--that is turbulence at jet-stream altitudes. Free-floating balloons and instruments described in the preceding paper were used to

\* The instrumented balloons and financial support for this work were provided by U. S. Army Electronics Research and Development Activity, White Sands Missile Range.

do this. Acoustic monitoring from free-floating balloons is nothing new. The use of the infrasonic frequency range to detect the far-field sound of atmospheric turbulence is new. The free-floating feature of balloons proved to be very useful to this investigation since it enabled the acoustic detectors to drift in unison with a local air mass. This feature reduced local wind noise to a minimum.

The central concern of this paper is to settle the questions of whether the energy detected is truly acoustic, and whether it is energy radiated from atmospheric turbulence. To answer these questions several different types of data analysis were employed. Spectrograms, signatures, cross-correlations and probability-density curves were produced from the data. These results were compared to a theoretical prediction for the acoustic power spectrum of turbulence. The evidence seems very strong that turbulence is the principal source of acoustic background noise at high altitudes.

The first data were recorded from a single balloon and microphone-transmitter. A detailed time-history of the acoustic spectrum was produced, and a typical segment from this analysis is shown in Figure 1. A complete spectrum analysis was made every two seconds in real time. The peak acoustic amplitude is about  $0.2 \text{ dynes/cm}^2$  at the low-frequency end of each frame in Figure 1. The frequency scale is 0 to 150 cps. The important things to note are the shape of the spectrum (its amplitude decreases with frequency at a rate of about 6 db/octave) and the time-steady nature of the spectrum.

Figure 2 shows a more qualitative type of spectrum analysis. In this figure the amplitude of the acoustic signal is roughly proportional to the darkness of the record, while frequency reads from left to right and time proceeds from top to bottom. By definition this is an acoustic signature since it shows the time-history of a frequency spectrum. This four-minute segment of data shows the Doppler effect that occurs whenever a piston-engine aircraft comes within acoustic range of a balloon-borne microphone, passes by and then recedes in the distance. Note the double trace for the main Doppler signal. The more steeply sloped portion shows the sound that propagated directly from aircraft to probe. The trace having less slope indicates a reflected path from aircraft to earth to probe. A faint Doppler curve at higher frequencies is at the second harmonic of the piston firing rate. This type of sound is rich in harmonics.

There are short horizontal traces occurring about once every 22 seconds in Figure 2. These were generated by an altitude-sensing device in the balloon-borne probe. As described in the preceding paper the repetition rate of this device was inversely proportional to altitude and, for the example shown, indicates an altitude of 60,000 feet. Finally, notice the time-steady nature of the spectrum below 30 cps, with most of the energy in this region at the very low frequencies. This is in agreement with Figure 1 and is the region of interest for studying turbulence.

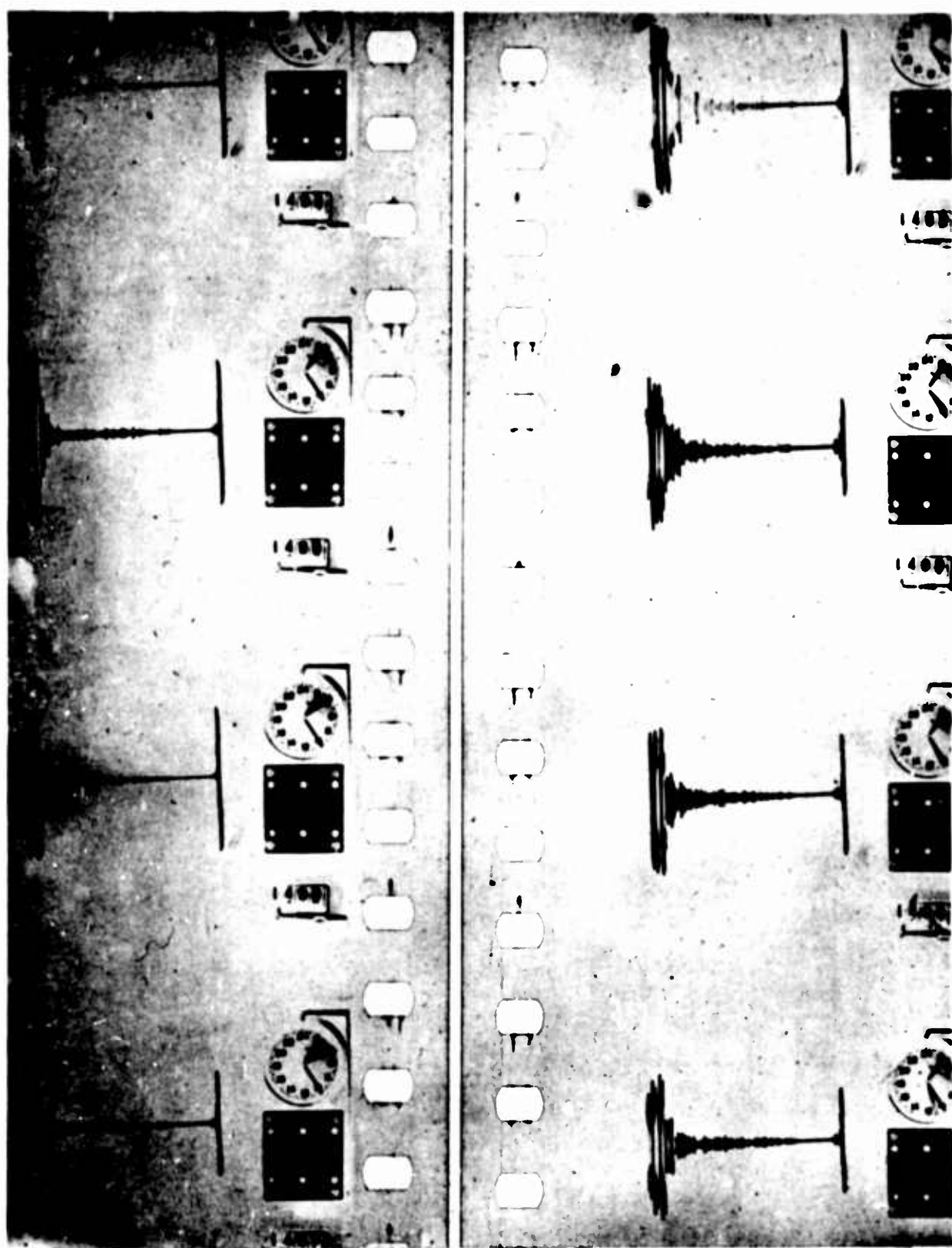
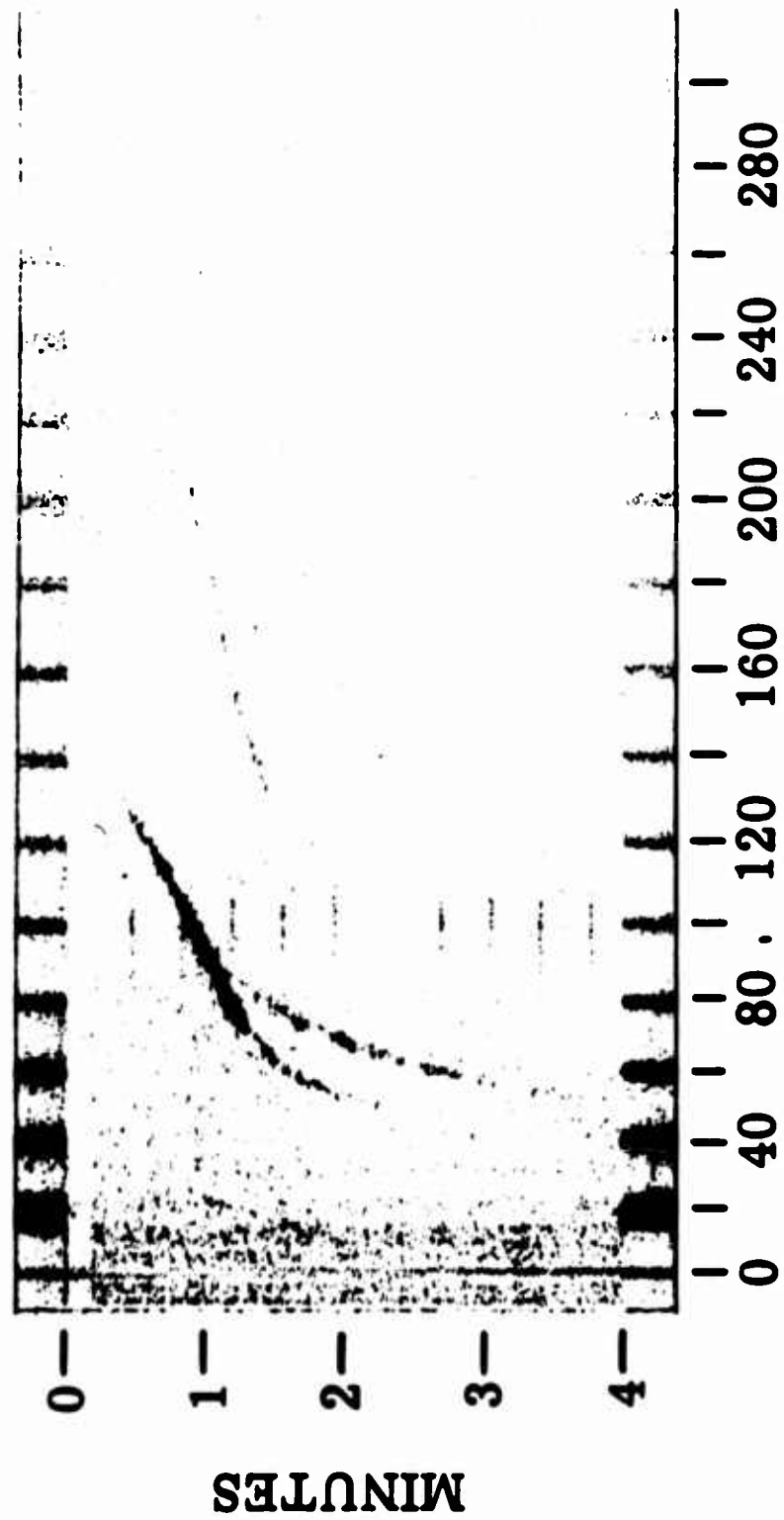


Figure 1. Time Series of Acoustic Spectra

**AIRPLANE DOPPLER ANALYSIS**

0-300 ~ Airplane from Flight 2420 25 August 1960 +6 db

Figure 2. Piston Aircraft Signature

It was decided to take advantage of the time-steady property of the lower frequency data. Accordingly, some tape loops were made and processed through an accurately-calibrated spectrum analyzer. Tape recordings from over 30 instrumented flights were analyzed. The highest, the lowest, and two typical intermediate levels of recorded background noise are shown in Figure 3. These curves show acoustic pressure level per cycle plotted against frequency. Note that each of these curves has a spectrum that falls off with frequency at about 6 db/octave. But the most dramatic point of Figure 3 is that it shows a 30-lb db diurnal variation in acoustic noise level. In the 1-cps region the diurnal variation in acoustic pressure is from 0.03 to 1 dyne/cm<sup>2</sup>. Assuming the noise was produced by turbulence, there must have been either large diurnal changes in nearby turbulent activity or large changes in distance between an acoustic probe and the turbulence detected.

Up to this point acoustic monitoring was done with a single, balloon-borne microphone and transmitter. The stability of an inexpensive, free-floating balloon at altitudes of 60,000 feet was questioned, and it was suggested that the microphone might be sensing air flowing past its diaphragm rather than a true acoustic signal. It was decided to settle this matter by launching two widely-separated acoustic probes on a single balloon system. If the same signal were detected by both probes it would mean that a legitimate acoustic signal was present. Noncorrelating signals, on the other hand, would indicate localized flow noise occurring independently at each microphone.

The approach was simply to use two of everything. As shown in Figure 4, two balloons were tied together to one of the payloads and were played out with several hundred feet of string. The second payload, tied to the bottom end of the string, was then released. The whole assemblage was supposed to rise gently from the earth and ascend to 60,000 feet. This became known as the worst method of launching. It never worked because the balloons drifted so far downwind that when the lower payload was released it swung to the ground and was destroyed. Subsequently, several attempted launches were made using the almost-as-bad method of standing 300 feet upwind with the balloons and one payload, while the final release man stood downwind on the rim of a deep gravel quarry with the other payload. The giant arc described by the lower payload at takeoff was almost as breathtaking as the involuntary descent into the quarry made by the final release man. Although two successful launches were made in this manner, the method was soon discarded in favor of a safer and more reliable technique.

Figures 5 and 6 show an inexpensive, commercially-available launching reel that was modified so that it would hold several hundred feet of number 18 braided Nylon cord. The reel, in its original form, is sometimes used for launching radiosondes in strong winds. It normally holds only 50 feet of string which deploys

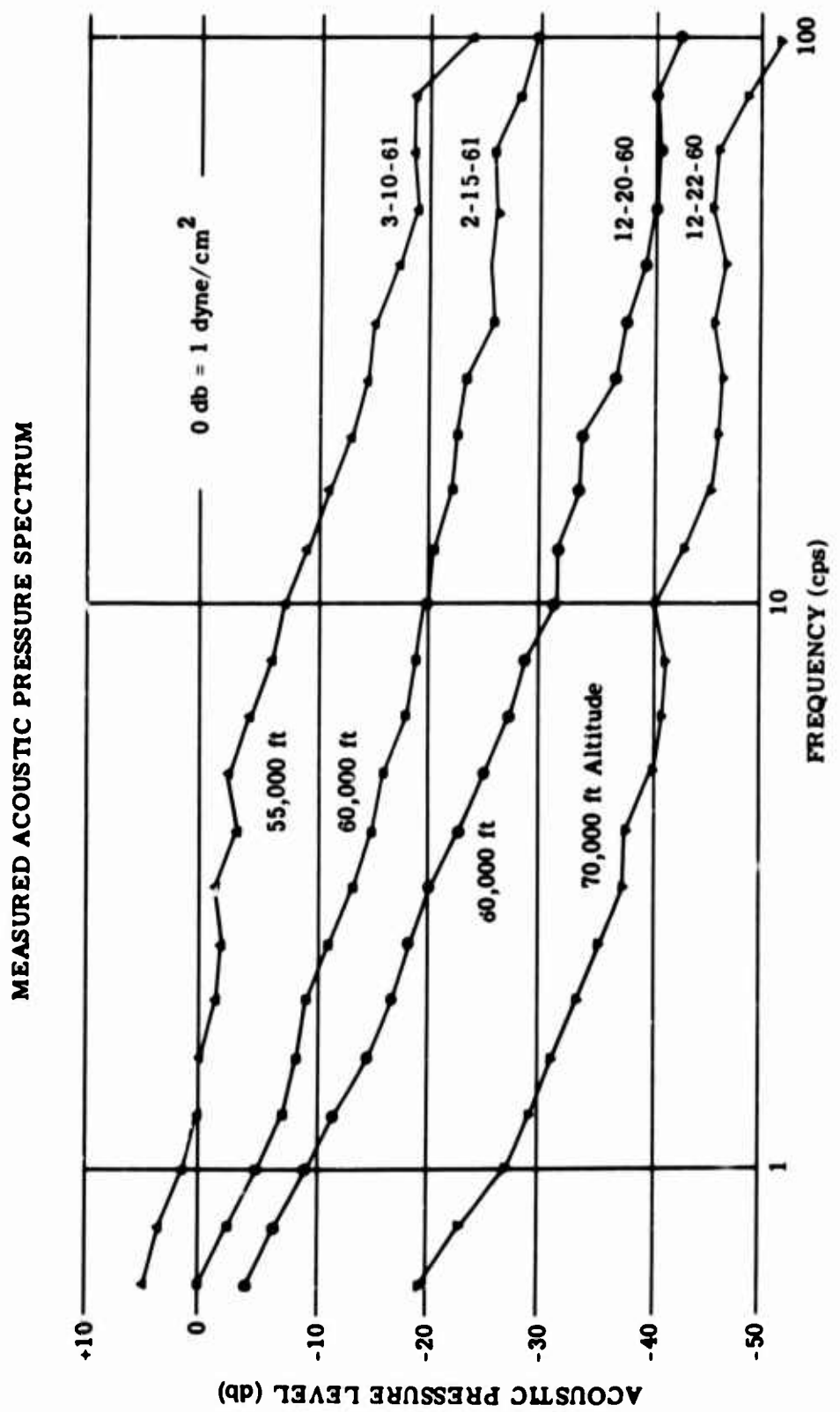


Figure 3. Acoustic Background Noise Levels

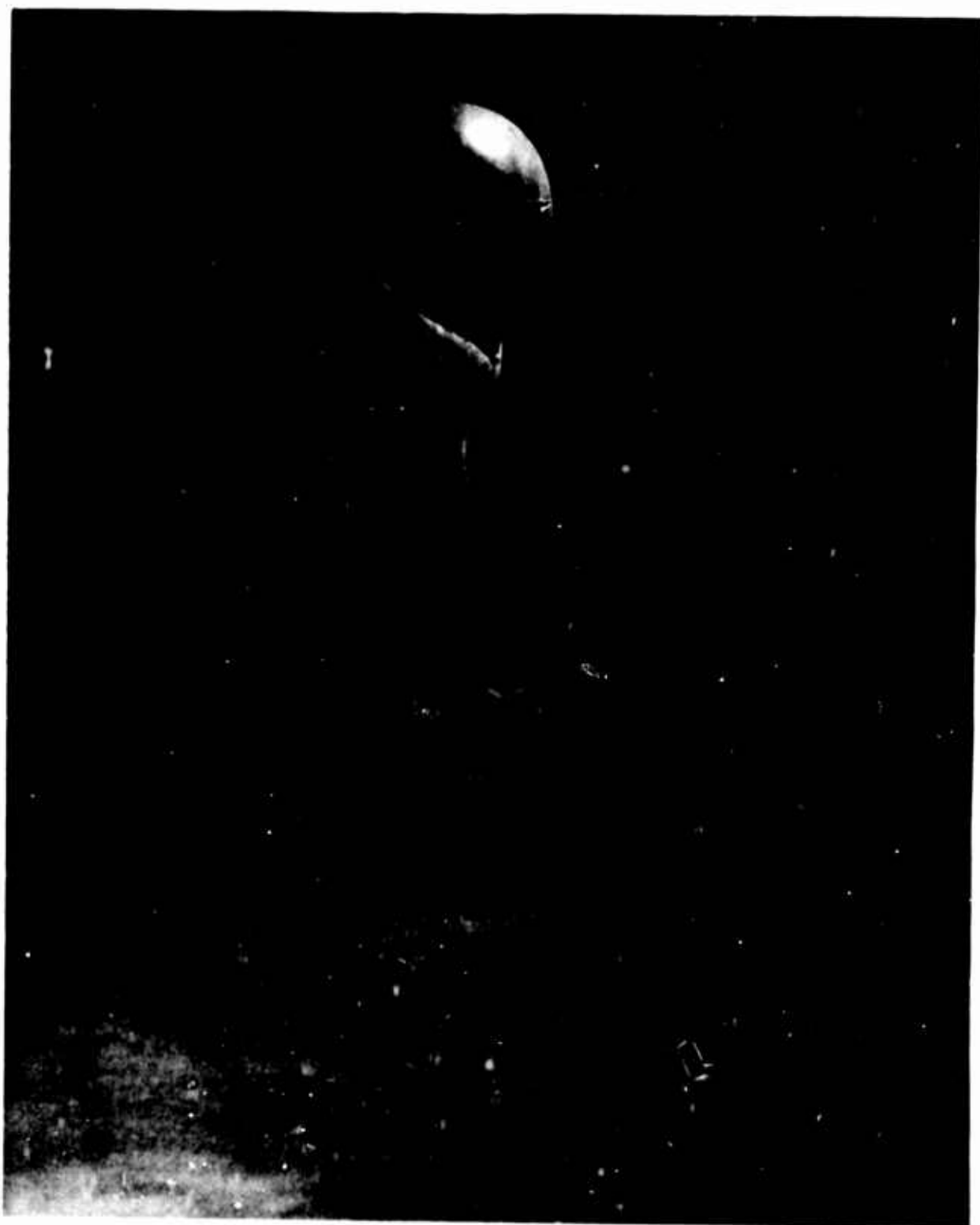


Figure 4. Double Probe Balloon Launch

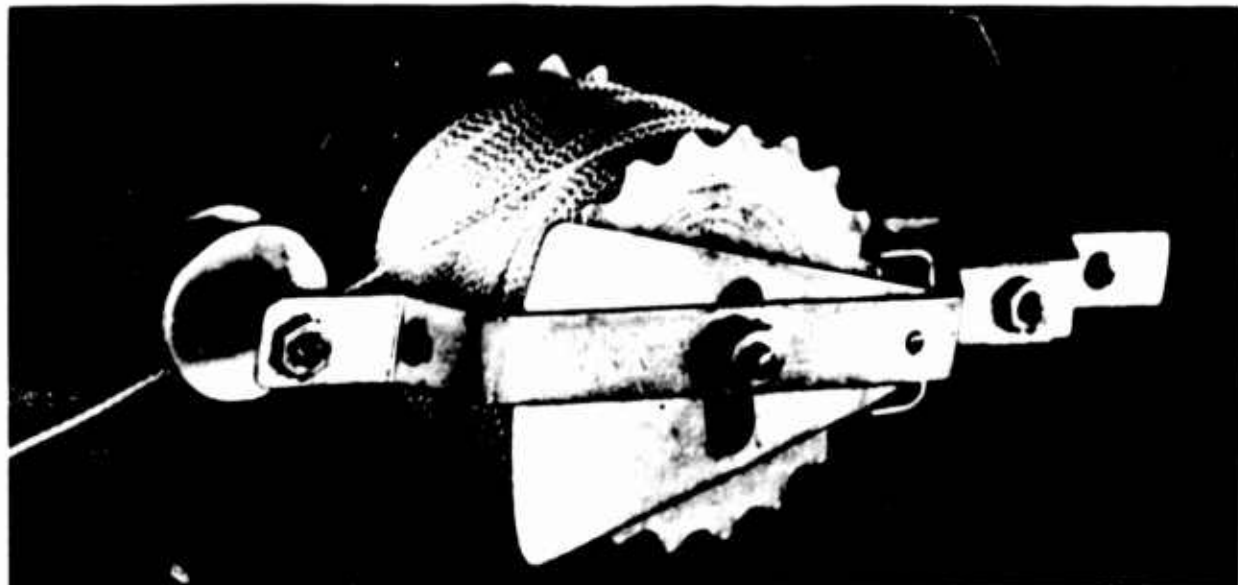


Figure 5. Launching Reel Escapement Action

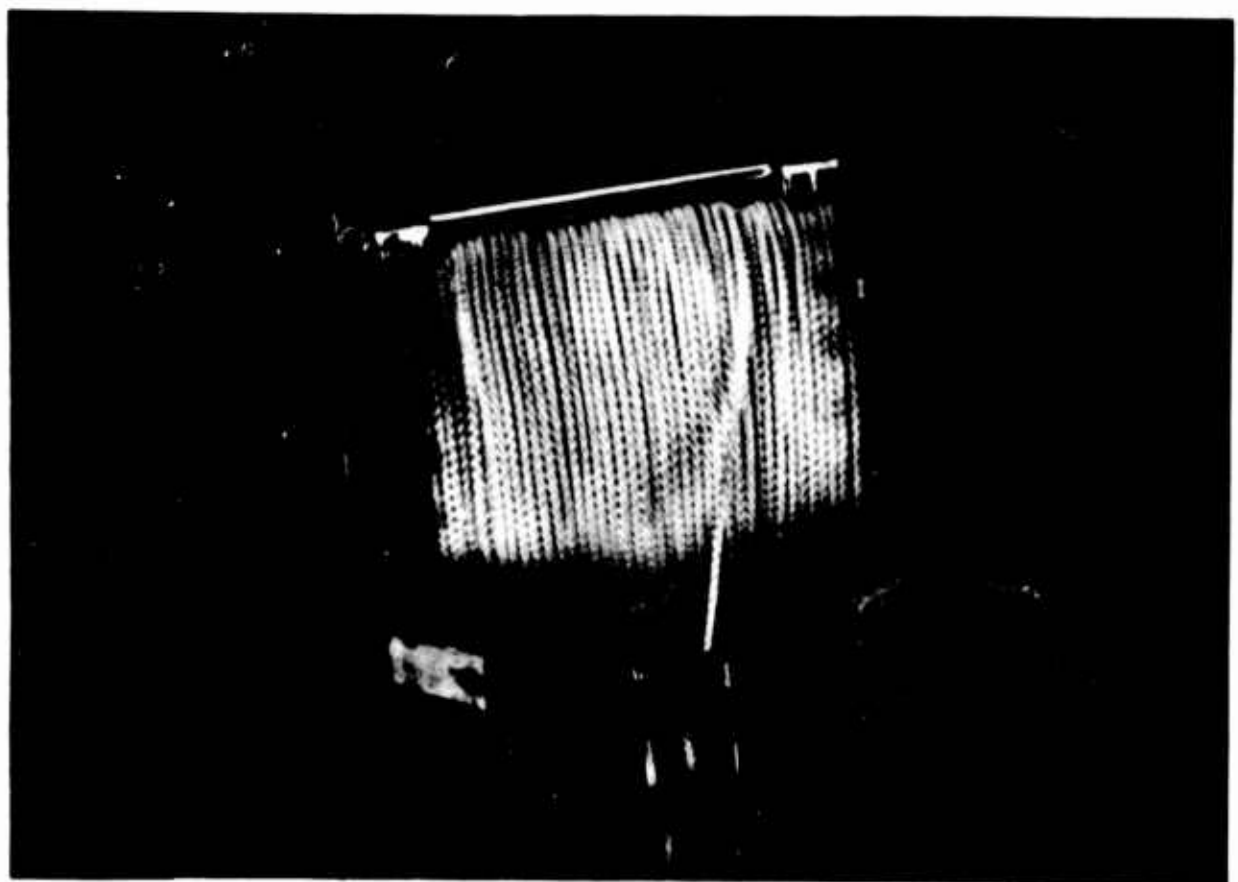


Figure 6. Launching Reel String Deployment

slowly after launching. Note the escapement mechanisms for controlling the rate at which the string unwinds. In the modified version shown here, two escapements from two reels are mounted on an extended hub. The unwinding string passes between two guide plates and loops once around a bakelite spacer which provides additional friction. This device will lower a nominal seven-pound payload 300 feet in about nine minutes. There are probably better or at least more sophisticated launching reels available. The virtue of this one is that the parts for it cost only \$1.26. By means of the device two acoustic probes were launched together with comparative ease, and separation to the required spacing occurred during balloon ascent.

The receiving station for data from the probes is housed in a tracking van shown in Figure 7. As was explained in the preceding paper, the whole data link is a modified version of an AN/GMD-1A Radiosonde Detector system, hence the familiar looking GMD antenna on the roof of the van. This servo-controlled antenna tracks automatically. Azimuth and elevation angles to the balloon are determined by antenna position and are displayed and recorded automatically in the van.



Figure 7. Tracking Van, Exterior View

Inside the van, as shown in Figure 8, tracking information is displayed and recorded by the equipment bay on the right. The second bay from the right contains a demodulator for acoustic data, and meteorological recording components used during standard Radiosonde flights. The third bay from the right contains a 7-channel FM tape recorder which preserves all acoustic data and voice commentary for later processing. The bay on the left contains a motor-drive amplifier for the tape recorder, and an oscilloscope for making circuit checks.

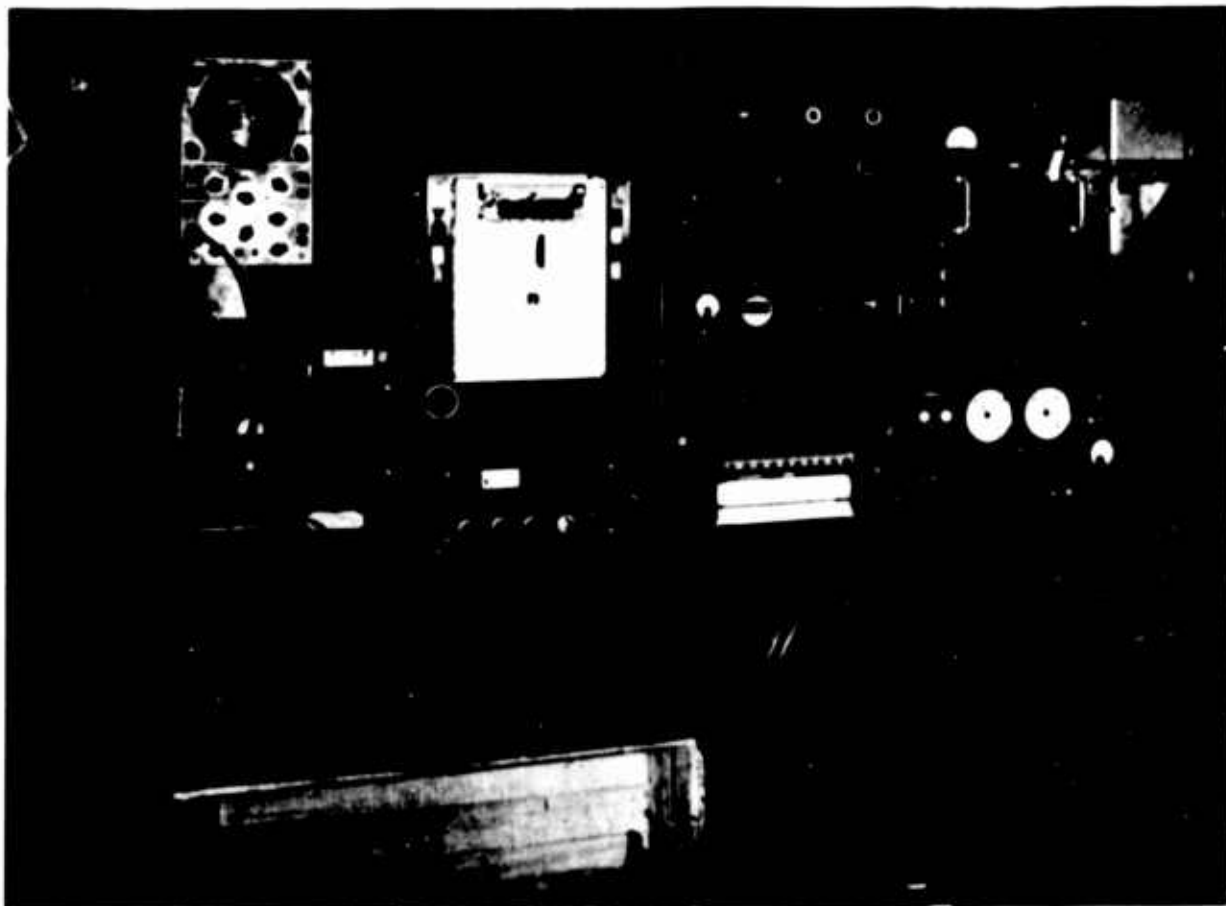


Figure 8. Tracking Van, Interior View

A block diagram of the two-channel receiving system (Figure 9) shows how it works. The feature of this system is that it requires only one high-gain, automatic-tracking antenna. Advantage is taken of the fact that two different IF frequencies will be developed by one local oscillator and mixer circuit by merely tuning the balloon-borne transmitters to slightly different frequencies. The frequencies chosen were 1680 and 1695 MC. Two standard GMD receivers were used in the van, with the local oscillator of the second receiver modified as indicated.

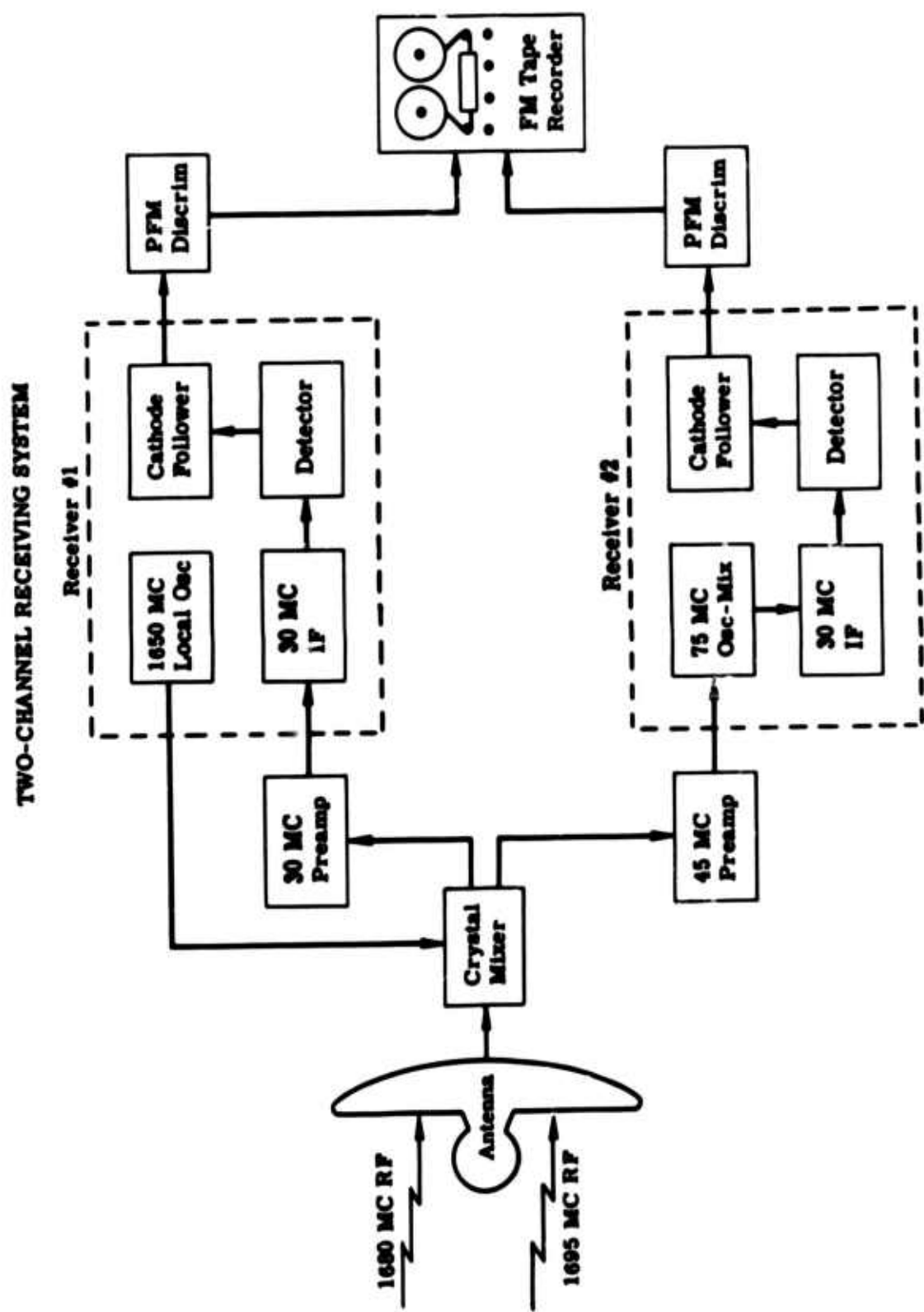


Figure 9. Block Diagram of Receiving System

Acoustic signatures from the double-probe flights (Figure 10) show the seemingly every-present Doppler curves from piston engine aircraft. Notice that both data channels show about the same background noise level and virtually identical aircraft Dopplers. This indicates that acoustic signals at the detectors were not being masked by hydrodynamic flow, and speaks well for the constant-altitude balloon as a quiet platform from which to make acoustic observations.

In another double-probe flight (Figure 11), jet aircraft as well as piston-engine aircraft were detected. Jet-aircraft detections appear as a temporary increase in broadband background noise level. Notice that in both Figures 10 and 11 the aircraft Dopplers do not extend to frequencies below about 30 cps.

A signature analysis restricted to frequencies below 30 cps confirms the absence of aircraft noise in this region (Figure 12). The record begins with the ascent of a double-probe ball on system and continues with a display of infrasonic events detected after the balloon reached equilibrium altitude. The dynamic range of the analyzer was set so that the record would fluctuate between black and white for a 12-db variation in signal level. Figure 12 shows this transition occurring in approximately 1 octave during the balloon ascent, thus indicating that the spectrum of nonacoustic flow noise has a negative 12 db/octave slope. This is twice the slope that was measured for true acoustic background as sampled from a stable balloon at equilibrium altitude.

A cross-correlation analysis was made of the acoustic data from one of the double-probe balloon flights. The object was to determine whether the background sampled at 60,000 feet was propagating sound or local flow noise. Propagating sound would cross-correlate; hydrodynamic noise would not. A data sample was chosen that was free of aircraft Dopplers, and only the frequency region below 30 cps was utilized. A tape recording of the data was played on a machine equipped with a special playback head shown in Figure 13. The individual pickups in this headstack can be moved along the tape in relation to one another so that any desired amount of time delay between channels can be obtained. For each time-delay setting the tape was played and the output signals were continuously multiplied together by an analog computer. The product of the signals was accumulated in an integrator and the result was displayed as a graph of normalized output from the integrator plotted against delay time settings. Figure 14 is a block diagram of the process. The bandwidth of the correlated data was from 0.2 to 30 cps. A 5-minute sample of data was used to allow ample integration time for the lowest frequencies present.

A pronounced correlation of 22 percent occurred for a time delay between channels of 0.105 seconds. Figure 15 shows the correlation curve. The vertical distance between acoustic probes happened to be 150 feet for this flight. The speed of sound was about 1000 fps at the altitudes considered. From the time

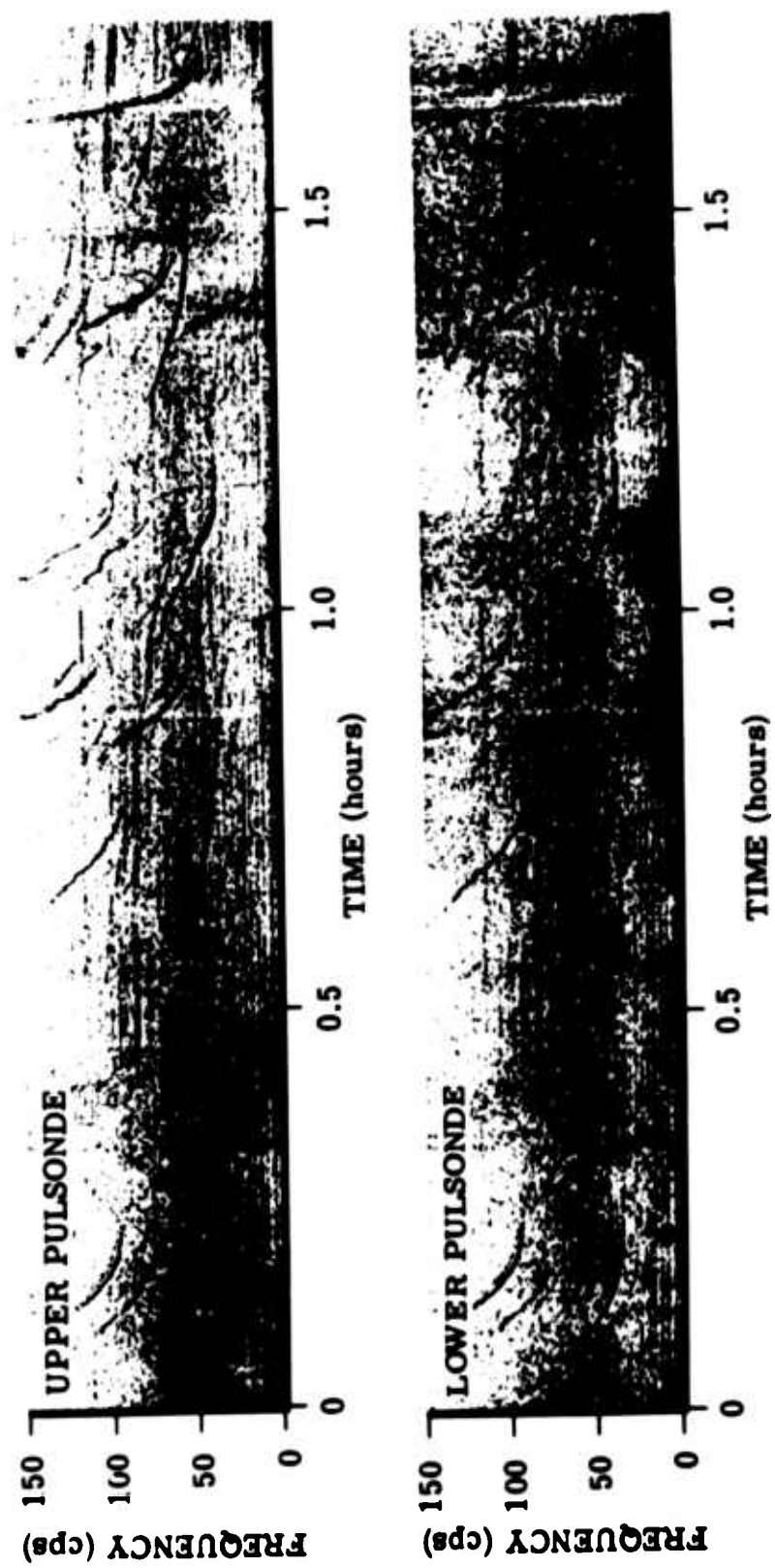


Figure 10. Aircraft Detections With 2-Probe System

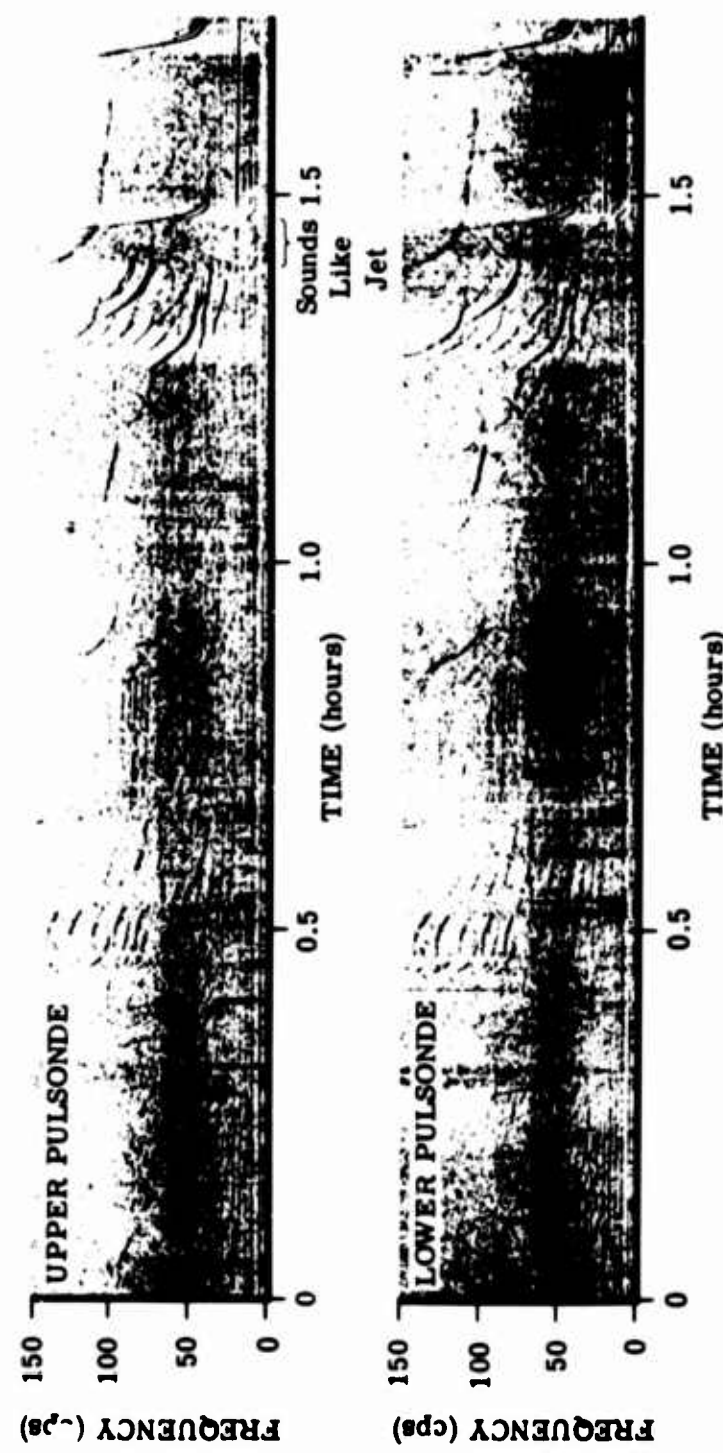


Figure 11. Piston and Jet Aircraft Detections

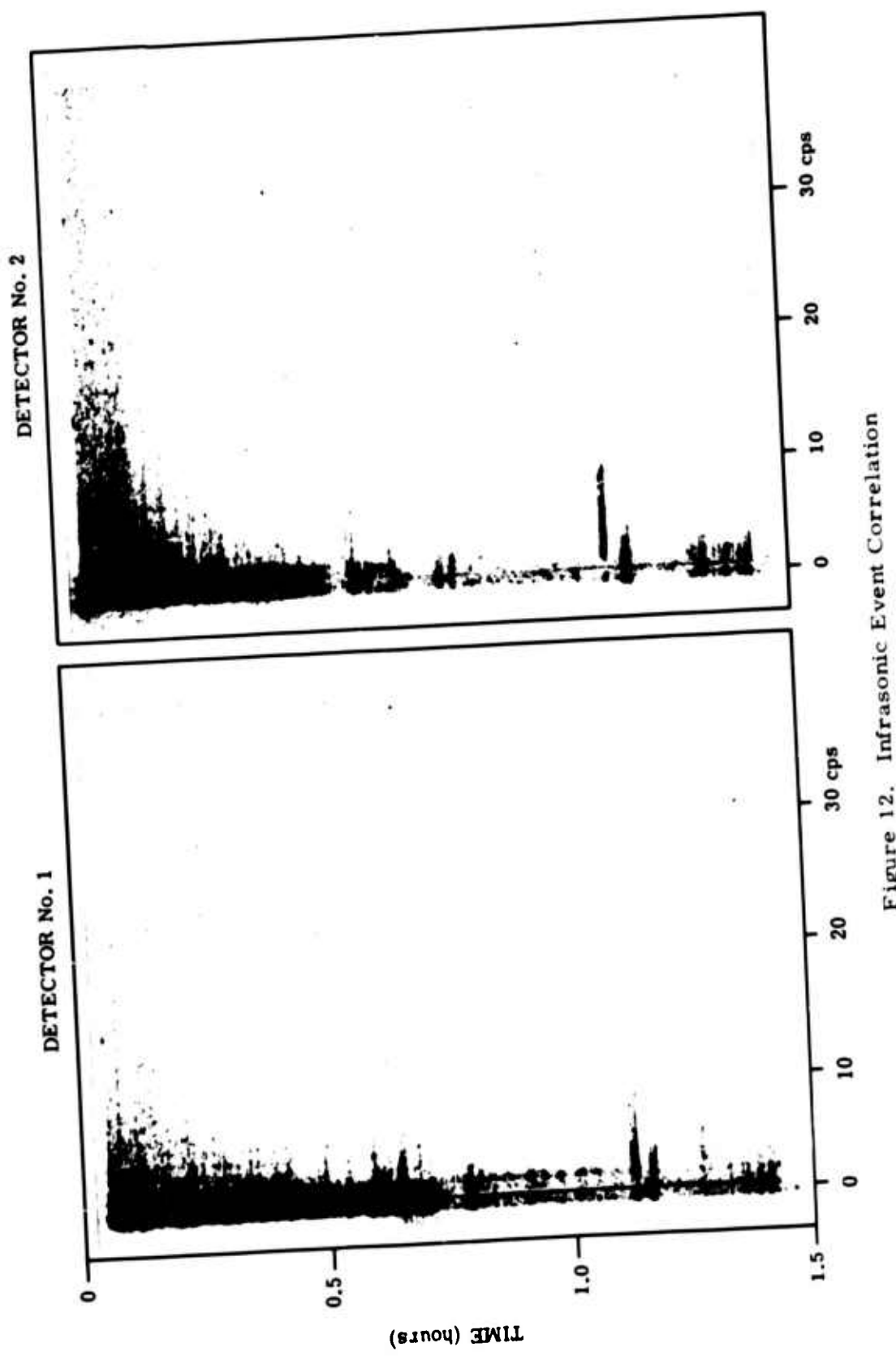


Figure 12. Infrasonic Event Correlation

delay, the probe spacing and the speed of sound one can calculate the apparent elevation angle at which correlating signals reached the microphones as 45 degrees, with no dependency on azimuth. This angle is just what would be measured if the sound were produced by a large volume or horizontal plane of statistically-independent noise sources such as the turbulent eddies in the atmosphere at jet stream altitudes. The value of delay time at which correlation occurred shows that the sound arrived first at the lower microphone, then at the upper one, and is proof that propagating sound rather than local flow noise was detected by the array.

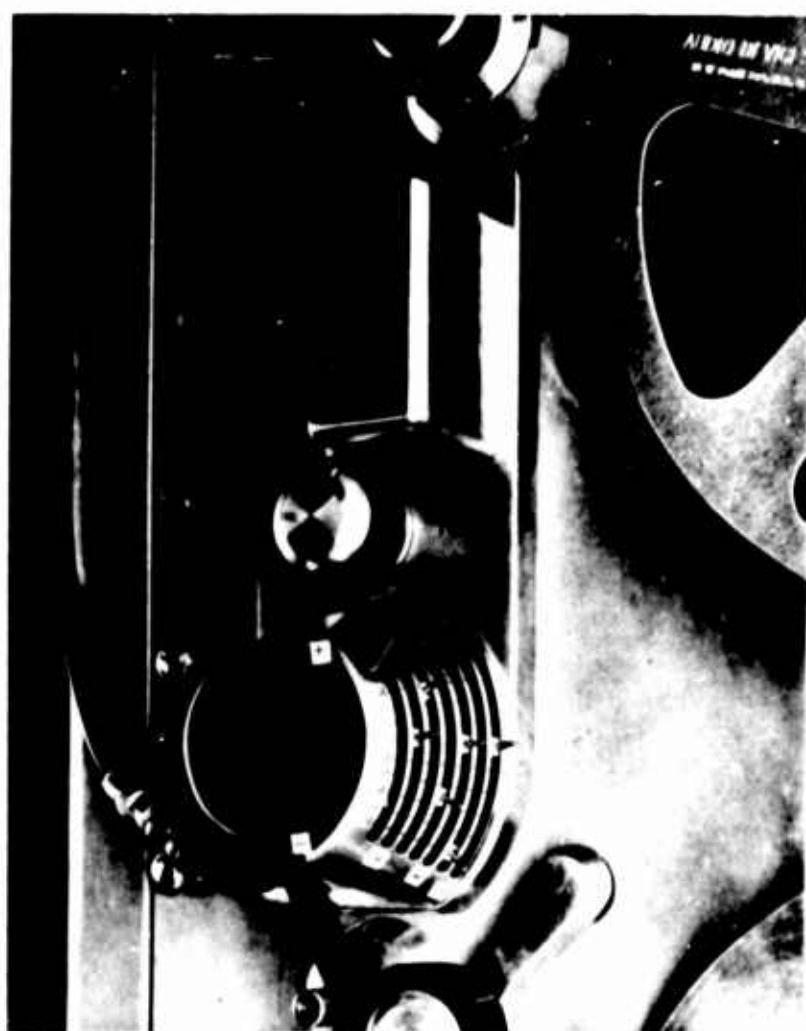


Figure 13. Moveable Playback Head

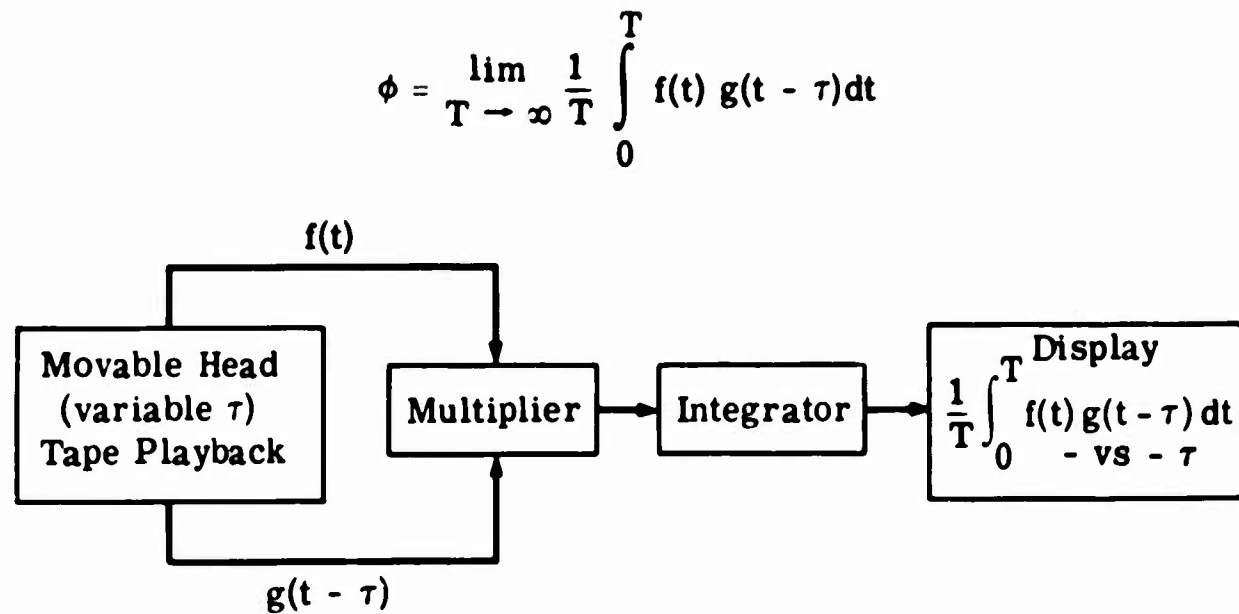


Figure 14. Cross Correlation Process

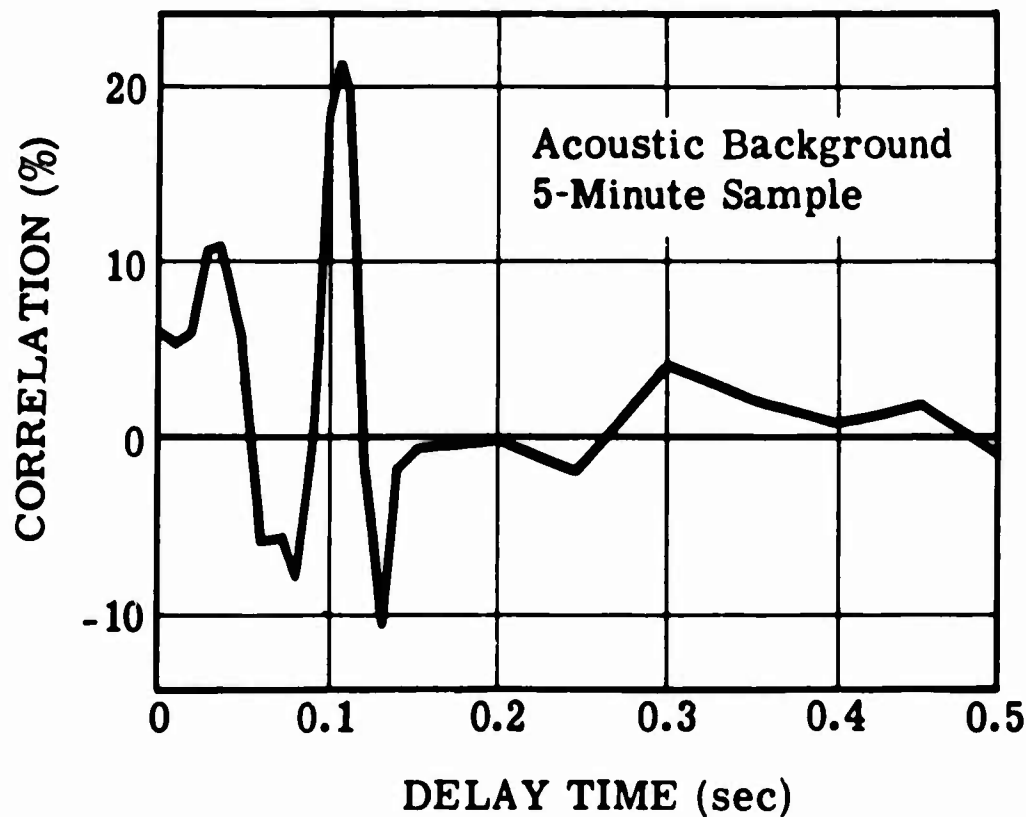


Figure 15. Correlation of 2-Probe Data

Another type of test was made on the data to determine whether or not the background sampled was acoustic or merely local flow noise. This was a probability-distribution test. Two well known types of probability distributions are Gaussian and sine wave. They are shown in Figure 16 merely to point out how dramatically different the probability distributions of various phenomena can be. A probability density curve can be determined empirically from an oscillogram of any complex waveform. Accordingly, oscillograms were made from samples of flow noise and high-altitude background noise. The sample of flow noise was obtained during the ascent phase of a balloon flight. The measured ascent rate was 700 fpm. The sample of acoustic background was obtained later on during the same flight, after the balloon had leveled off and was free-floating.

Probability-density curves were prepared from the oscillograms by measuring the percentage of total sample time that the waveform was at each amplitude level. The results (Figure 17) show that the probability-density curve for high-altitude acoustic background is practically Gaussian while the curve for flow noise is much steeper than Gaussian. These are very gratifying results when considered in the light of the source mechanisms involved.

The sound field radiating from atmospheric turbulence should be Gaussian because it is made up of contributions from a large number of randomly-distributed and statistically-independent sources--the turbulent eddies produced by wind shear. In hydrodynamic flow, on the other hand, it is known that the velocity fluctuations are Gaussian. This means that the corresponding pressure fluctuations are non-Gaussian because, by Bernoulli's principle, the pressure fluctuations are proportional to the square of the velocity fluctuations. The experimental results bear this out. Therefore it seems that one can identify the sound radiated from turbulence by using a single acoustic detector and observing the shape of the probability-density curve.

The various experimental results reported in this paper are in pretty good agreement with at least one theoretical prediction for the sound radiated from turbulence. To understand this, and to point the way to future work, one need only follow the conceptual outline of this theory.

In 1941 a Russian named Kolmogoroff published a fundamental paper on the local structure of turbulence utilizing the so-called cascade or similarity concept in which eddies generate eddies which generate eddies and so on. The bulk of experimental evidence from wind-tunnel, jet-exhaust, and meteorological measurements supports Kolmogoroff's theory.

Kolmogoroff supposes that there are three ranges of eddy sizes in a turbulent system. In the first range, energy is supplied to the turbulence by the generation of very large eddies. Such eddies would be generated in free atmosphere by wind-shear action around a jet stream core. In the second range, the large eddies

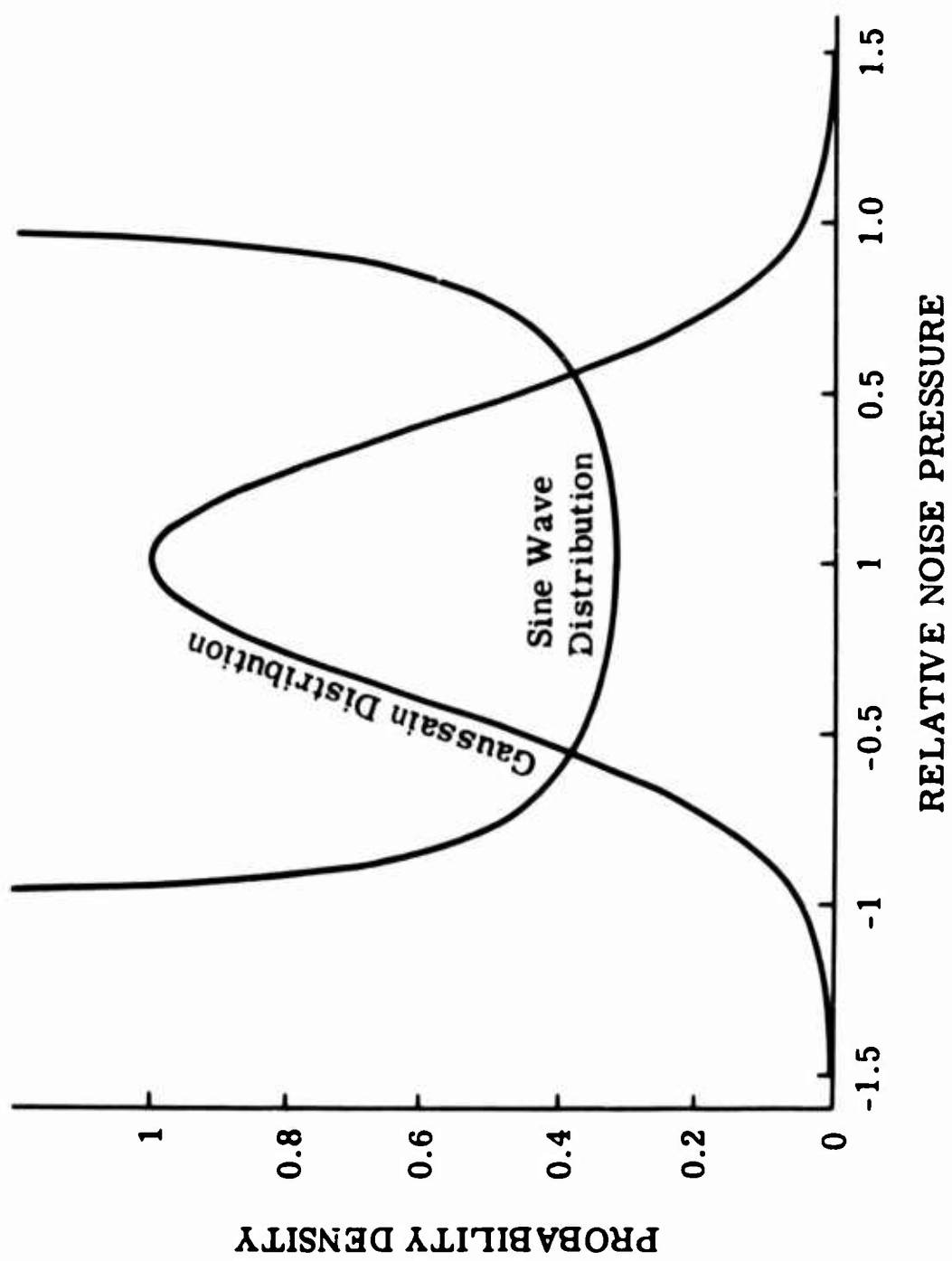


Figure 16. Gaussian and Sine Wave Distributions

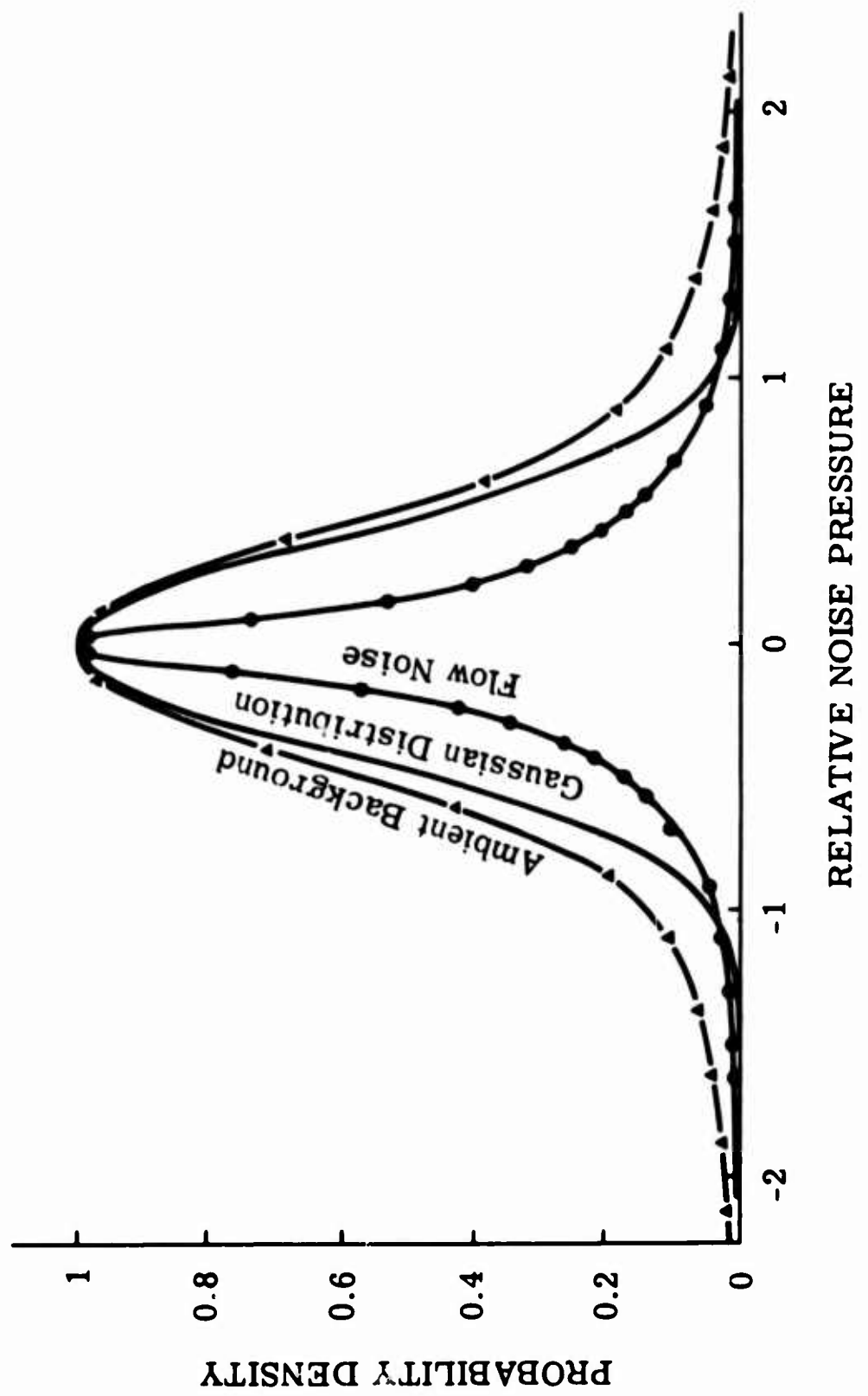


Figure 17. Acoustic Noise and Flow Noise Probability Curves

decay and in the process generate somewhat smaller eddies. In turn, these eddies decay while generating still smaller eddies. This cascading action produces a predictable energy spectrum in the second range, known as the inertial subrange of turbulence. It is in this range that the experimental acoustic measurements were made. In the third range of turbulence, eddy sizes are very small and fluctuations are so rapid that viscous effects in the medium quickly dissipate all remaining energy as heat.

Kolmogoroff's theory deals with the actual turbulent flow. More recently, two gentlemen named Meecham and Ford calculated the acoustic field that would be radiated from this type of flow. They calculated that the acoustic power spectrum in the first range, where the largest eddies are produced, will increase as the fourth power of frequency. For the inertial subrange they calculate that the spectrum will fall off as the  $7/2$  power of frequency. The expressions derived by Meecham and Ford are summarized in Figure 18.

#### Below Inertial Subrange:

$$P(\omega) \sim \rho_0 V c_0^2 M^3 \left( \frac{\omega L}{c_0} \right)^4$$

#### Inertial Subrange:

$$P(\omega) \sim \rho_0 V c_0^2 M^{\frac{21}{2}} \left( \frac{\omega L}{c_0} \right)^{-\frac{7}{2}}$$

#### Above Inertial Subrange:

Negligible noise radiated

$\rho_0$  = mean density

V = volume

$c_0$  = speed of sound

M = turbulence Mach number

L = size of largest eddies

Figure 18. Formulae for Acoustic Noise of Turbulence

From all of this one can now draw a simple graph for the overall power spectrum of sound radiated by turbulence (Figure 19). The slopes on the graph have been expressed in terms of db/octave for easier comparison with the experimental results. The acoustic measurements indicated a 6 db/octave slope in the inertial subrange as compared to the 10.7 db/octave slope shown on the theoretical curve.

The significance of this graph is that the curves for the first and second ranges of turbulence intersect at a frequency which, when determined, can be used to calculate the size of the largest eddies. Unfortunately, the only microphones available at the time this work was done, did not have enough low-frequency response to detect this peak in the energy spectrum. Various estimates place the frequency

of the peak between 0.2 and 0.02 cps, and, of course, its exact frequency will change from day to day. If any future work is done in this area, certainly the spectral peak, and hence the size of the largest turbulent eddies should be monitored with microphones or microbarographs that respond to the lowest frequencies involved.

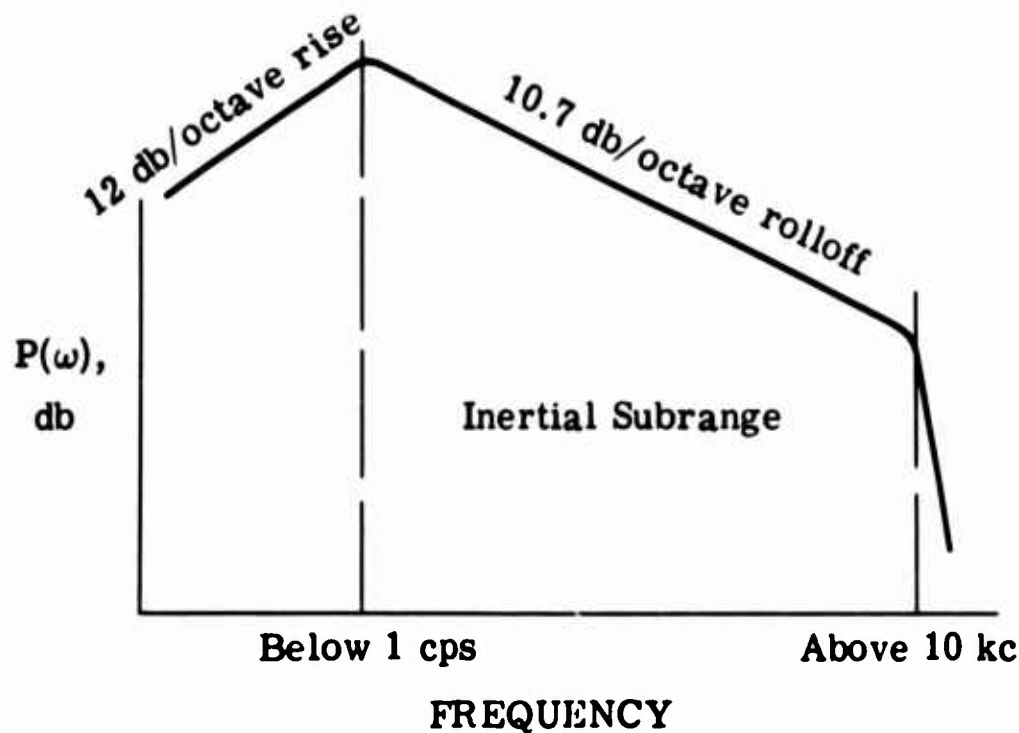


Figure 19. Theoretical Acoustic Spectrum of Turbulence

## XXVII. Quality Engineering of Scrim-Reinforced Balloons

T. W. Kelly and A. O. Korn  
Air Force Cambridge Research Laboratories  
Bedford, Massachusetts

L. Curtis and R. Moroney  
G. T. Schjeldahl Company  
Northfield, Minnesota

### Abstract

The scrim-reinforced Mylar balloon is a highly reliable carrier for heavy, expensive, scientific payloads but has been prohibitively expensive for general use. A 30 percent cost reduction has resulted from an 18-month program evaluating new films, fibers, and adhesives, refined lamination techniques, and balloon design simplification in combination with streamlined production procedures.

The successful flight test of a nonwoven scrim balloon, the development of a novel nonwoven scrim loom, as well as scheduled tests for balloon recovery and reuse, promise to further reduce the cost differential between supported and unsupported film balloons.

### I. INTRODUCTION

Ever since its introduction in 1945, the polyethylene balloon has been the workhorse of the balloon field. It has lifted scientific payloads of seemingly end-

less variety, been launched from the arctic to the tropics, in fair weather and foul, and has carried man practically to the top of the atmosphere for physiologic and environmental research. Although generally satisfactory, it has occasionally failed during ascent, especially when structural demands on the balloon vehicle have been too great.

During the fall of 1958, the National Science Foundation, Office of Naval Research, and Johns Hopkins University were engaged in a joint field test expedition in which two men were to fly a polyethylene balloon for astronomical observations. Shortly before scheduled take-off, failure of the balloon while it was still on the ground aborted the entire expedition. This experience provided dramatic motivation for developing a stronger, more reliable, balloon material whose safety factors were greater than obtainable with polyethylene. Further emphasis came from the stringencies of heavier payloads, an occasional need to launch under somewhat less than ideal conditions, and the advisability of greater protection of the costly investments in test equipment and flight operations.

Accordingly, a contract was initiated by ONR, under the terms of which the G. T. Schjeldahl Company was to produce a high-reliability balloon film from knowledge of the best of the current technology in plastic films and fibers. The contract resulted in a study of candidate materials and selection of the best available film-fabric combinations; several balloon flights clearly indicated that a strong, light material was feasible.

Tests were made during flights of the Stratoscope II telescope which, together with the flight instrumentation and ballast, made up a balloon payload of some 10,000 pounds. The first flight of this huge system took place at Hope, Arkansas, on 6 March 1962. Although not fully meeting the sponsor's requirements, the results of this flight were encouraging. The ensuing series of balloon flights has been beset by problems, as has any other complex pioneering system, but none of the scrim balloons has suffered catastrophic failure during ascent.

The Air Force Cambridge Research Laboratories first became interested in the scrim balloon during Project Stargazer. The mission required lifting a two-man, 4,000-pound gondola to an altitude of 80,000 feet for a one-day period but when flight tests with the reinforced polyethylene balloon designed for the task scored only 50 percent, a scrim-reinforced balloon was given a series of test flights. Several deficiencies previously unsuspected in such balloons were uncovered. These were corrected in cooperation with the G. T. Schjeldahl Company; and on 13 December 1962, under the overall direction of Major Thomas B. Spalding of AFCRL, a successful flight was made by Mr. William White and Major Joseph Kittinger, accompanied by a 5,200-pound payload of scientific instrumentation.

The story has been somewhat the same with other programs involving the flight of heavy payloads. Even though the cost has ranged from five to ten times

higher when scrim-reinforced Mylar balloons have been substituted for their polyethylene counterparts, the change to the more reliable scrim balloon has been justified by the results.

## 2. DEVELOPMENTAL PROGRAM

Early in 1963, AFCRL initiated a program to lower the cost of scrim-reinforced balloons by 30 percent within the year. Four areas were delineated for investigation. It appeared certain that basic balloon fabrics could be had for less money; scrim balloon designs could be both simplified and improved; production could be accelerated without sacrificing balloon quality; and launchings could be simplified to eliminate the need for a two-balloon launch system. The program was later expanded to include the recovery and re-use of scrim balloons.

### 2.1 Materials

The currently satisfactory Mylar-Dacron scrim is a clearly superior balloon fabric consisting of a plastic, gas-barrier film bonded to a network of reinforcing fibers by a thermoplastic adhesive. To find ways of reducing the cost of the basic balloon material without seriously compromising its good properties, a large number of films and lightweight fibers were obtained and tested. The more important characteristics of the better samples of scrims and films are summarized in Tables 1 and 2. Among the laminations tested were Dacron combined with polypropylene fibers, and polypropylene combined with Mylar film. Of the two adhesives used, the proprietary product of the Schjeldahl Company proved more suitable than the commercially available adhesive. Tests of nine different combinations of films, fibers, and adhesives gave the results summarized in Table 3. The balloon laminate used as the criterion for all the others was GT-11, a combination of Mylar and Dacron, 60 in. wide, costing \$.67 a lineal yard. In all cases, the polypropylene was rejected because of adhesive deficiencies, noted either during initial ply adhesion or during flex-testing, and production problems in the lamination. The most promising film was the M-1-MD, a Dacron-Mylar combination whose reinforcing fibers formed a nonwoven grid laid in three directions.

### 2.2 Design Simplifications

The design was simplified in two ways. First, the balloon valving duct was made rectangular instead of elliptic, thereby allowing machine rather than hand installation; the duct was also reinforced, which eliminated a structural discontinuity in the balloon wall without interfering with the mechanism for valving

excess lifting gas at the ceiling altitude of the balloon. Second, modifications in the balloon end fittings (Figure 1) reduced the installation time; the cost of the fittings dropped from \$3,500 to \$500. Changes in the valve wire and inflation tube installations appreciably simplified fabrication and resulted in a better end product as well.

### 2.3 Production Improvements

A cost analysis of earlier scrim balloons disclosed that fabrication labor accounts for approximately three-quarters of the total cost of a scrim balloon. Two procedures requiring many man hours of labor are gore-cutting and sealing. To determine the actual cost reduction afforded by the design simplifications and procedural changes evolving from our laboratory investigation, we fabricated two balloons.

First, all the gores for the test balloons were cut simultaneously, with a Wolfe cutter. Second, the gore-sealing speed was increased from eight to twenty feet per minute. The acceptability of both changes was supported by numerous preproduction tests. In addition, newly developed equipment for inspecting and splicing balloon material and for automatically dispensing material was used. Seal-tape splices and the use of larger rolls of sealing tape contributed to further reductions in production time. The net result of all of the improvements was a 30 percent reduction in the overall cost of a balloon exactly the same size (1.6 million cubic feet) as one manufactured just one year earlier.

Figure 2 shows the first of the two experimental scrim balloons during perhaps the most critical phase of a dynamic launching. This balloon was launched from the AFCRL R&D Test Facility, Holloman Air Force Base, New Mexico, and carried a payload of 4,000 pounds to an altitude of 74,000 feet. The performance was excellent.

## 3. RESULTS OF THE COST REDUCTION PROGRAM TO DATE

The curves in Figure 3 illustrate the cost reductions achieved, based on comparative costs of the 3.2 million-cubic-foot balloons first designed and procured for Project Stargazer at a cost of \$54,000 per balloon. The progression is downward to the AFCRL-sponsored Johns Hopkins University program, and subsequently to the Coronascope and US Weather Bureau programs, at a cost of \$33,000 each. In all of these balloons the scrim material used was the woven one designated GT-12. If the nonwoven GT-50 had been used, a further cost reduction of approximately two thousand dollars could have been expected. The broken line

indicates the most pessimistic cost outlook of the next phase in cost reduction: the use of a scrim layer.

#### 4. SCRIM LOOM

Aside from the actual cost reduction, perhaps the most important effect of the work described was the application of nonwoven scrim to balloon design. This opened the way not only to further cost reductions, but to significant improvements. Use of the nonwoven scrim was expedited by Korn's innovation of a simple loom. The first loom model was made inhouse, and a prototype (Figure 4) then manufactured under contract. This machine can best be described as a rotating-drum loom. It dispenses diagonal threads from the large rotating drum and longitudinal threads from a thread beam passing through the center of the drum. Notable advantages are: (1) elimination of the need for the flocking agent (Figure 5) used on nonwoven scrim material for thread stability during handling and shipping; (2) the thread layer permits tailoring threads to conform to the optimum gore reinforcement. For the first time the balloon designer will have an optimum material —one that has uniform longitudinal strength along the gore and can be varied in transverse strength as required.

Figure 6 illustrates three possible variations in thread pattern relative to the balloon gore that is finally cut from the basic scrim balloon fabric. Gores cut from the GT-12 rectangular-thread material lose numerous longitudinal threads. This requires changing the design to enlarge the width of the gores both top and bottom so as to ensure sufficient strength in the end sections. Gores cut from the GT-50 nonwoven thread material also lose many of the longitudinal threads. In the third version shown the longitudinal threads have been so tailored that a large end section is no longer necessary. Another innovation, not illustrated, has to do with spacing the diagonal threads from top to bottom of the gore to conform to the stress distribution in the balloon. The spacing of the longitudinal threads can easily be controlled by selective spacing of the longitudinal feeds. The speeds of the laminator and of the thread-dispensing drum, as well as the number of spools in the drum, can be controlled to produce desired variations in the spacing and angle of the diagonal threads. These features will be incorporated in the thread loom now under construction.

#### 5. BALLOON RECOVERY

The recovery and reuse of scrim balloons are being investigated as a possibility for further cost reduction. The most promising technique features the tandem

balloon, whose launching and recovery are respectively illustrated in Figures 7 and 8. Essentially, when the flight terminates the expensive lower balloon is ensleeved in a relatively heavy (2-oz/yd<sup>2</sup>) nylon material that fully protects the balloon during the landing and recovery phases of the flight operations.

In our single test to date—carrying a 4,000-pound payload to an altitude of 76,000 feet—the launching, ascent, and flight of the two-balloon system proceeded perfectly (Figure 9). During the descent, however, human error caused premature termination of the flight. No conclusion regarding the recovery technique is therefore presently possible, but our experiments with sleeve drop tests do indicate that balloon recovery is clearly feasible.

Recovery and reuse of scrim balloons on a routine basis will place scrim balloons in direct competition with the heavy-payload polyethylene balloons. Figure 10 illustrates the cost reduction possibilities of the tandem balloon recovery concept. Assuming a flight to 80,000 feet, the recovery and single reuse of a balloon would reduce the cost of the second flight to approximately 60 percent of the cost of the first. In this case, the system would be launched first as a tandem-balloon system and then, following recovery, as a single-balloon system (the top balloon having no essential function on a nonrecoverable system). The recovery and reuse of the main balloon twice (involving two expendable top balloons) would reduce the cost of the third flight to approximately 45 percent of the cost of the first. Projecting this to many reuses would probably lead to unrealistic figures although at some later date our experience might support such projections.

#### 6. SUMMARY

Scrim balloon costs have been reduced 30 percent, with no decrease in the quality of the product.

Nonwoven fibers have been successfully used for balloon reinforcement. In addition to reducing balloon costs, this development opens the way to a whole new technology for the balloon designer.

The scrim loom eliminates the need for using a flocking agent on the scrim material. In the long run, it will allow selection of the proper strength and weight parameters for a more nearly optimum balloon design. Incorporation of the gore-cutting feature will result in still further reduction of balloon costs.

Sleeve-drop tests to date clearly support the feasibility of recovering and reusing scrim balloons.

The dynamic launching of scrim balloons has been amply demonstrated to be feasible and should be used whenever the flight operation permits.

## 7. FUTURE WORK

The work on balloon shapes is being extended to determine optimum reinforcing scrim patterns. The results will be applied toward improving the nonwoven scrim loom design. The balloon recovery program will extend to testing several newly proposed techniques. The search for materials that are less expensive than Mylar and Dacron will continue. The results of these efforts will be applied as a total technology to the problem of creating a high-altitude medium-payload balloon at the earliest opportunity.

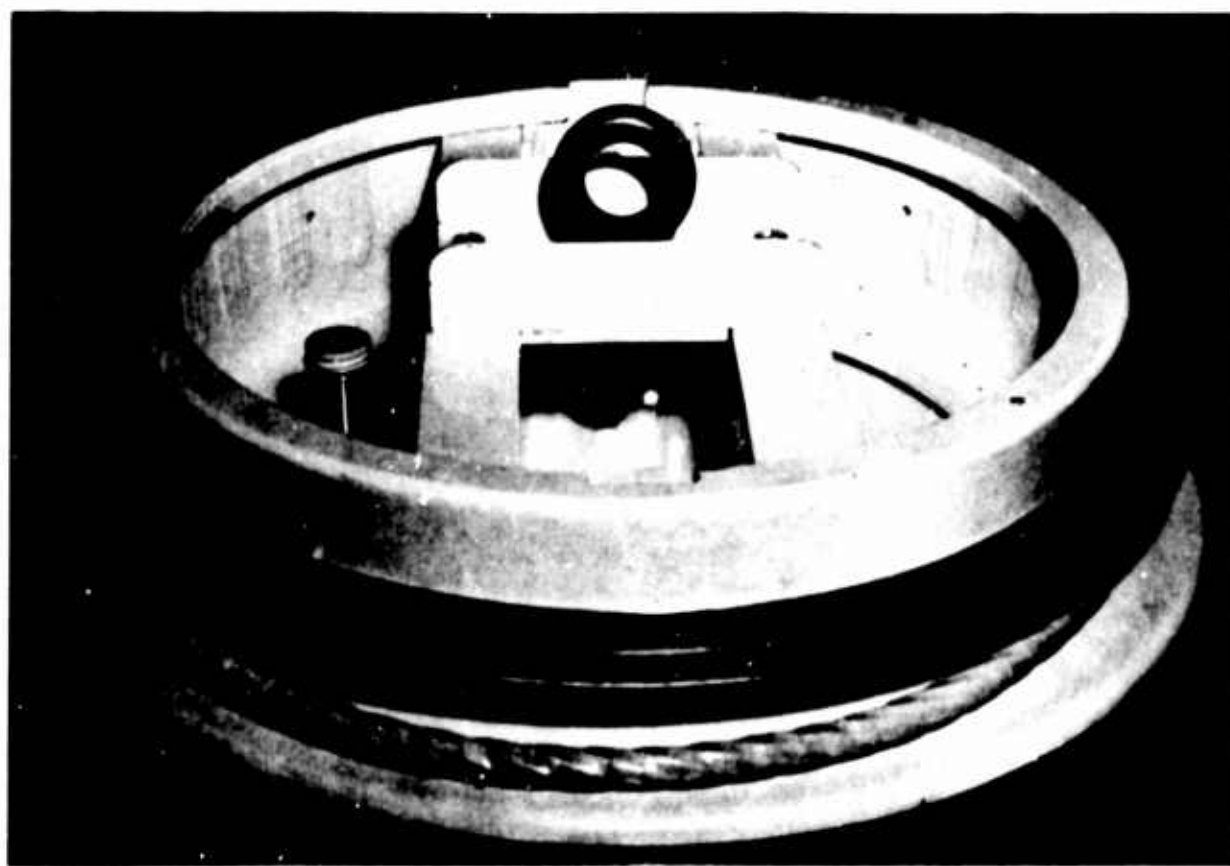


Figure 1. New End-Fitting Design



Figure 2. Launch of First Nonwoven Scrim Balloon (24 April 1964)

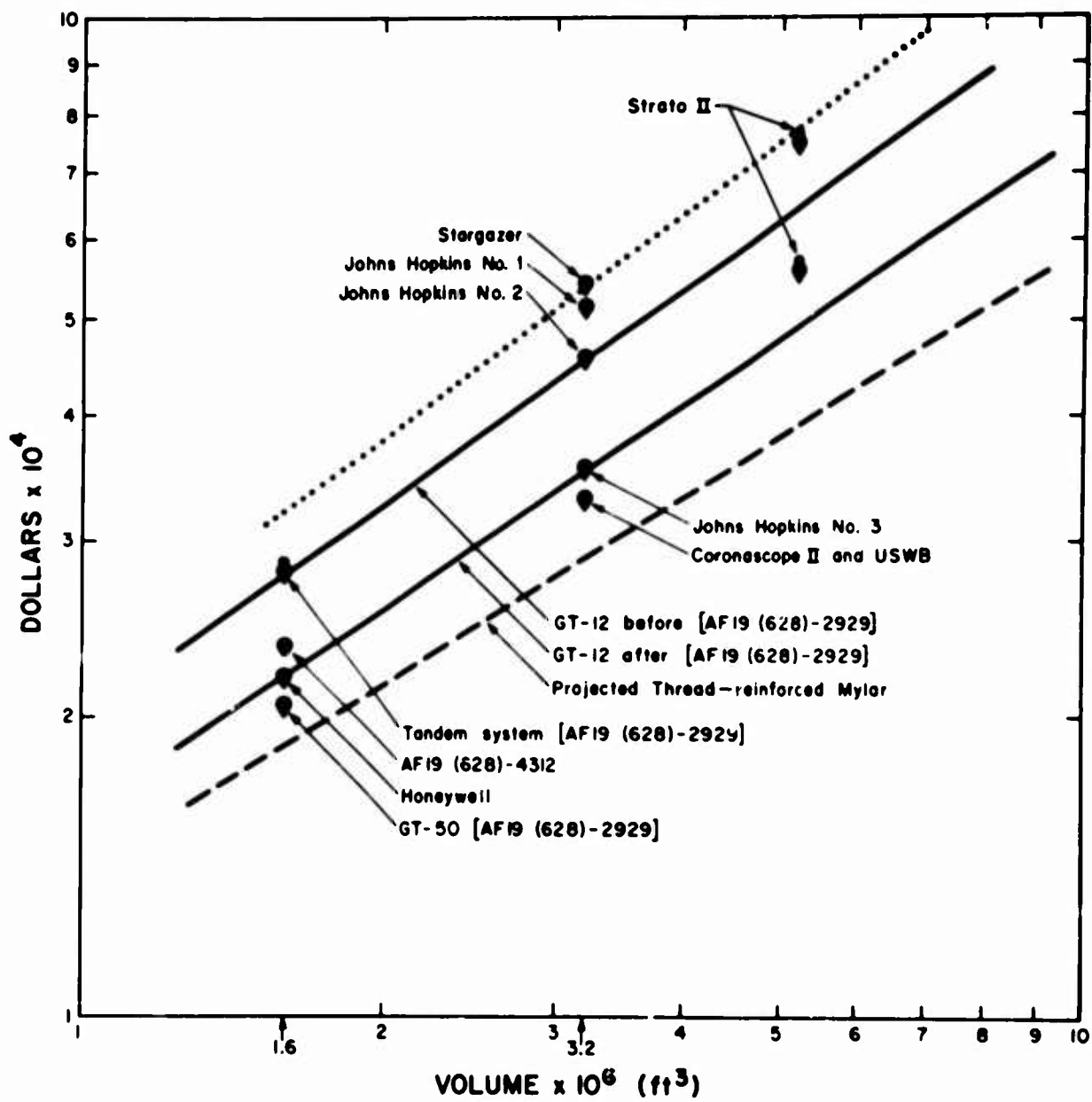


Figure 3. Comparative Costs of Heavy-Load Balloons

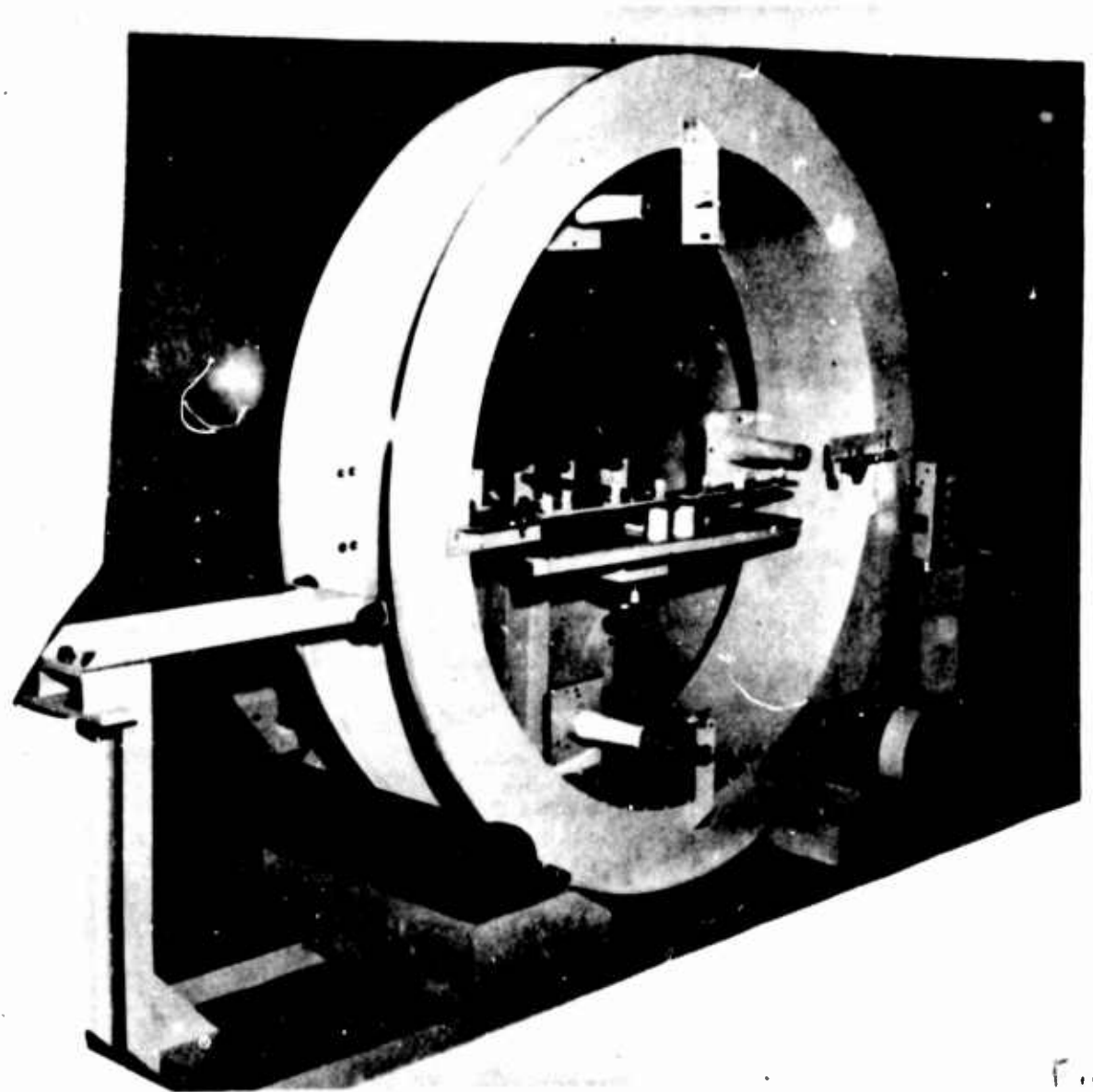


Figure 4. Model for Nonwoven Scrim-Layer

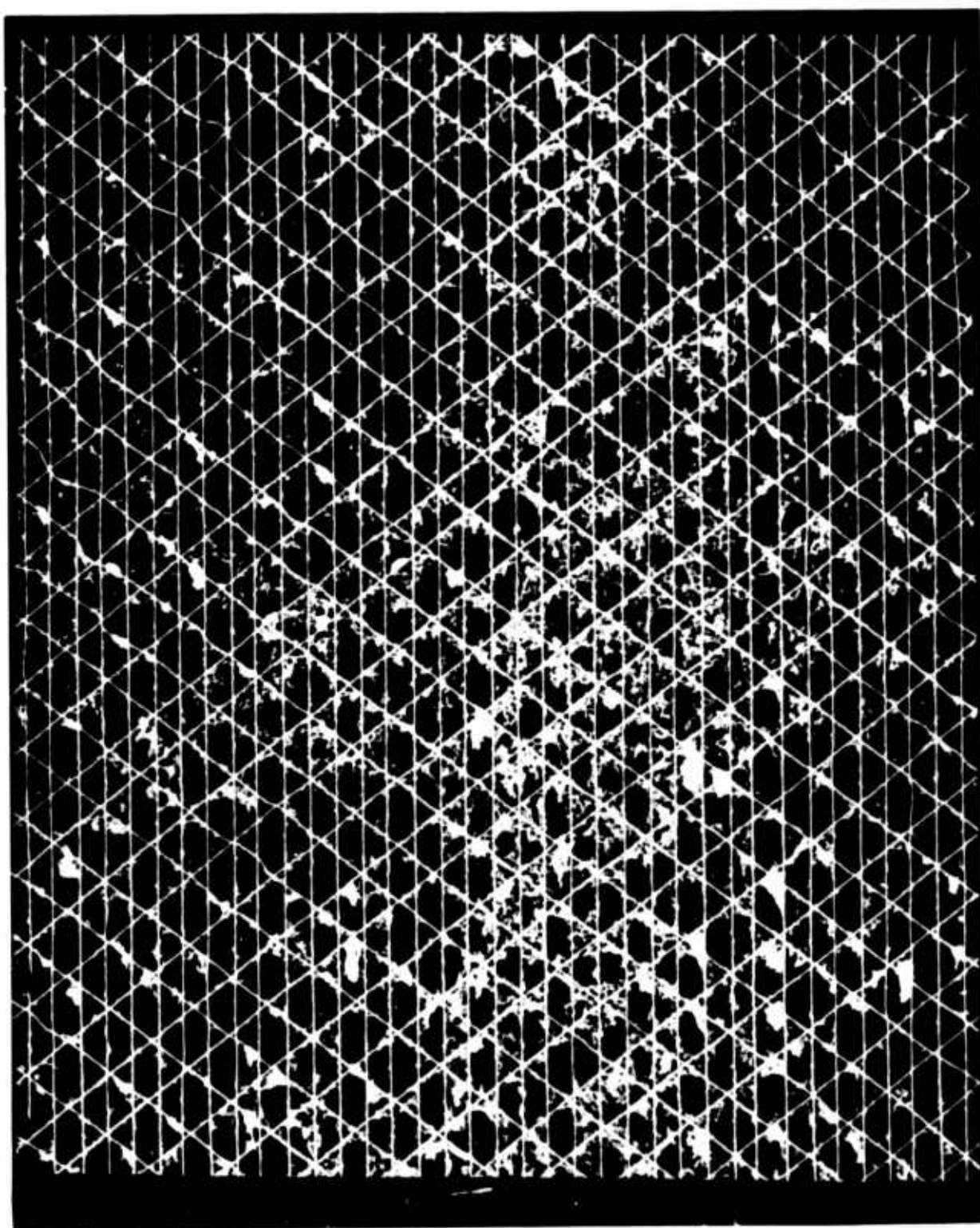


Figure 5. Toscony Nonwoven Scrim

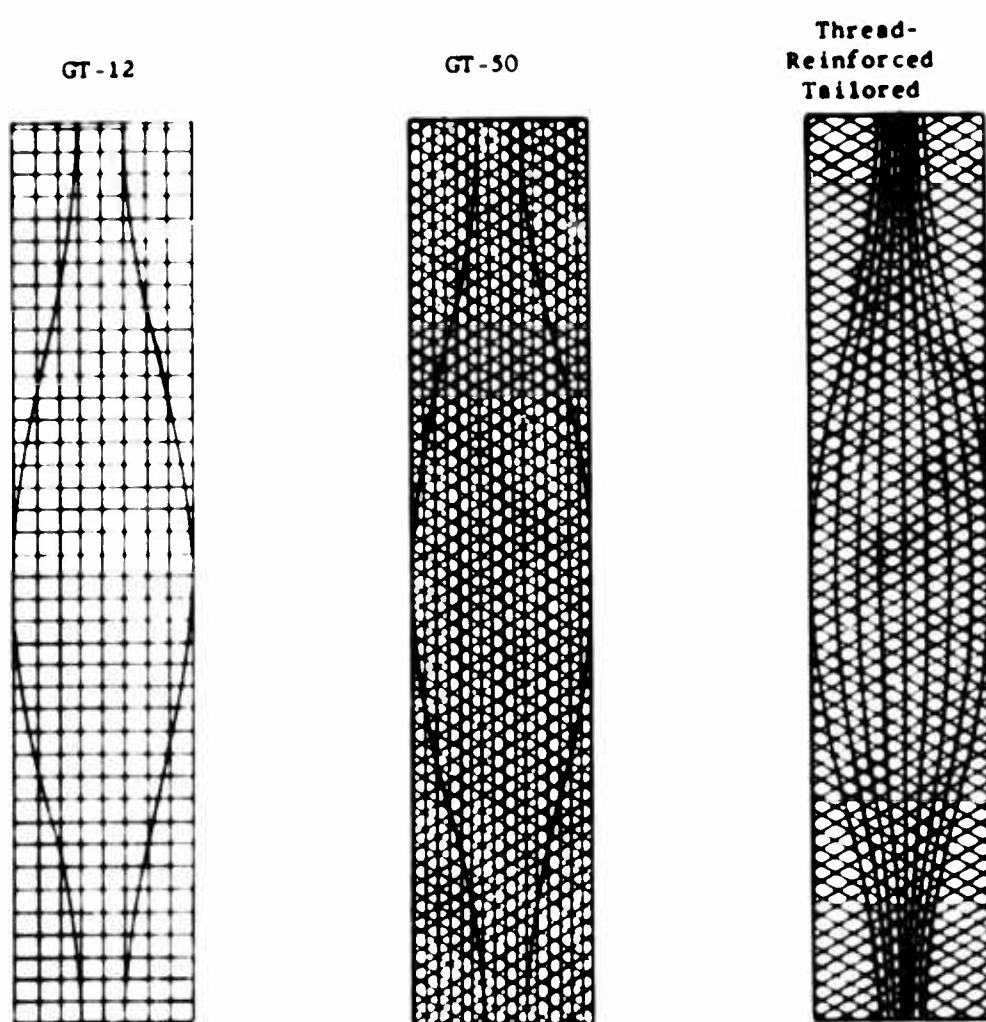


Figure 6. Gore Reinforcement Patterns

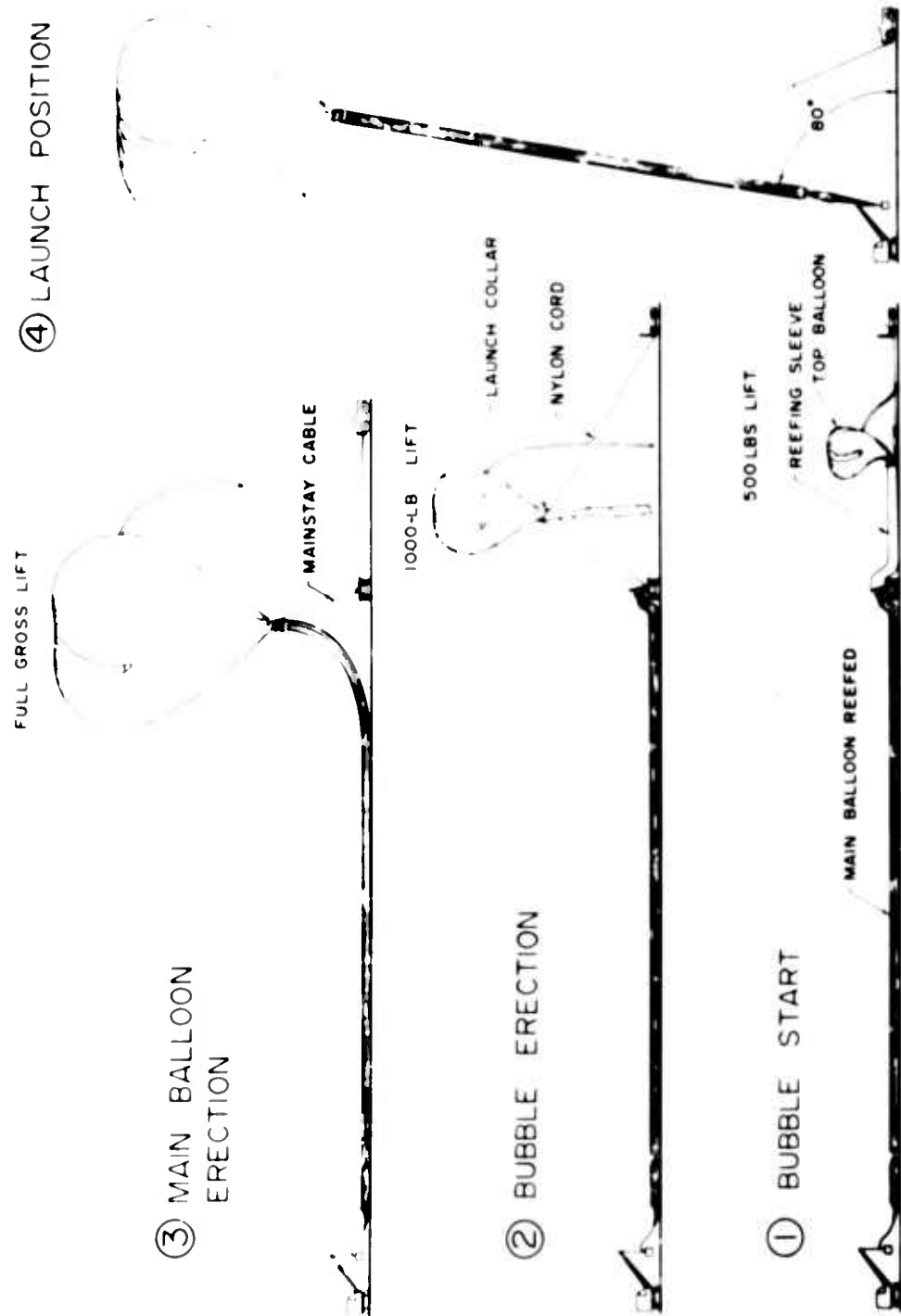


Figure 7. Launch Sequence 1.6 Tandem System [AF19(628)-2929]

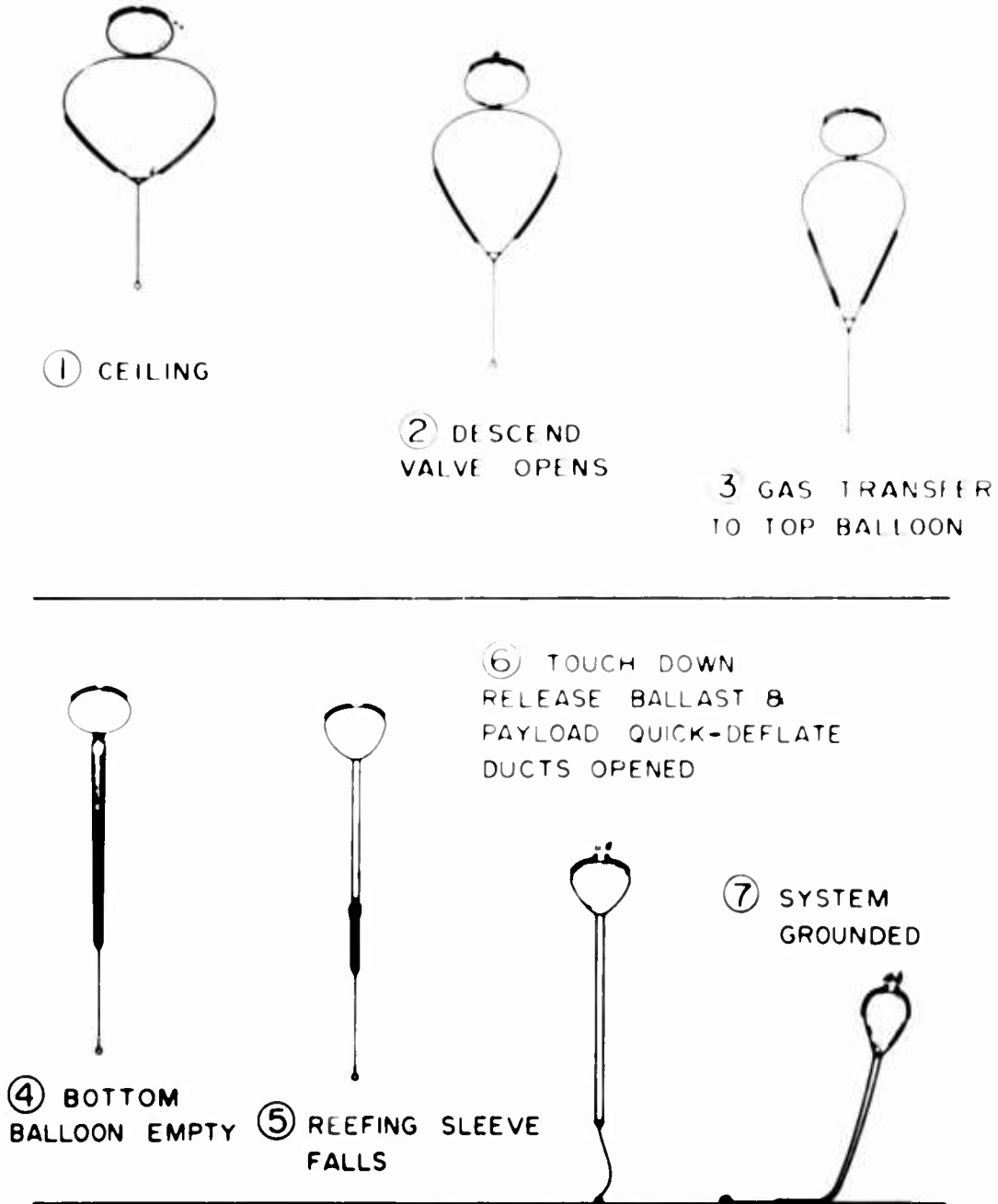


Figure 8. Tandem Balloon Recovery [AF19(628)-2929]



Figure 9. Tandem Balloon Reel-Up

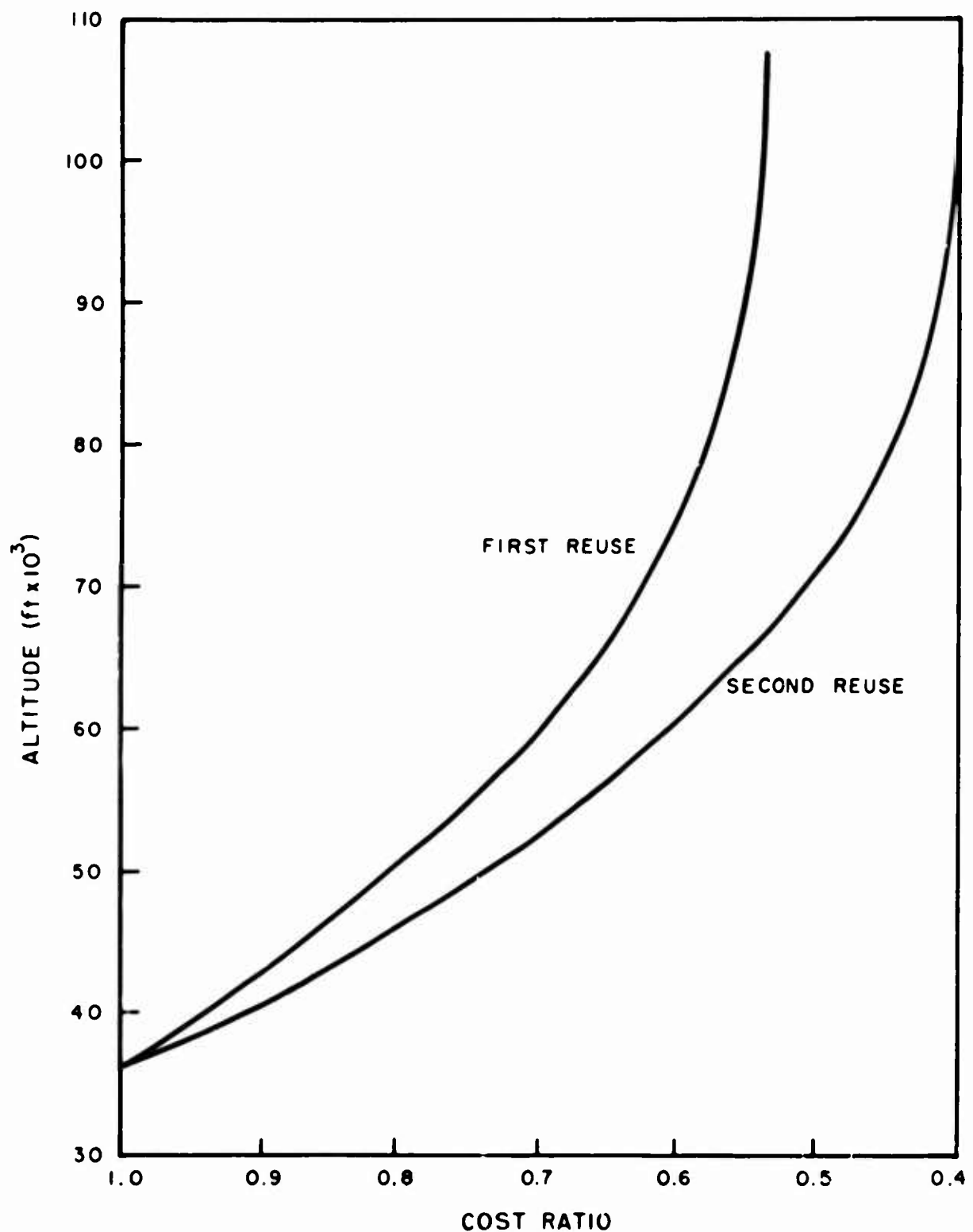


Figure 10. Flight Costs [assumes 100% recovery of main balloon (GT-11)]

Table 1. Characteristics of Reinforcing Materials

Material	Dacron*	Rayon	Polypropylene	Dacron, nonwoven
Weave	leno	leno	leno	three-ply, nonwoven
Weight (oz/yd <sup>2</sup> )	0.6	1.58	0.6	0.6
Width	60 in.	60 in.	60 in.	56 in.
Thread count	12 x 4	14 x 5	12 x 5	5 x 3 x 3
Yarns (denier)				
warp	220 2-ply	300 600	210 420	220 high-tenacity 220 rotoset
fill				
Tensile strength (lb)				
warp direction	25 16	27.7 26.4	30 27	25 15 (diagonal)
fill direction				
Price/running yard (for less than 100,000 yd 60 in. wide)	\$0.2475	\$0.175	\$0.1875	\$0.165

\*Scrim now used in GR-11 balloon material

Table 2. Characteristics of Selected Gas-Barrier Film Materials

	Designation	Maximum Width (in.)	Price per Pound	1-mil Film, Yield per Pound (in <sup>2</sup> )	$0.5\text{-mil Price/Yd}^2$	Approximate Tensile Strength (psi)	Notes
Mylar	Type C (50 ga)	84	\$ 2.50	20,000	0.075	20,000	standard material
polypropylene	Moplenane (50 ga)	36	0.84	31,000	0.018	15,000	adhesive problem
polypropylene	Udel (45 ga)	60	1.65	31,000	0.030	25,000	available also 0.6 mil
polypropylene	Hercules B-103 (50 ga)	72	1.40	31,000	0.031	30,000	corona-treated both sides
nylon	Capran 77C (50 ga)	40	2.50	24,000	0.070	7,000	dielectric-sealing possibility; high elongation

Table 3. Evaluation of Sample Laminates

Code	GT-11	P-1-D	M-1-P	P-1-P	M-1-MD
Film	1/3-mil Mylar	1/2-mil polypropylene	1/3-mil Mylar	1/2-mil polypropylene	1/3-mil Mylar
Reinforcement	Dacron	Dacron	polypropylene	polypropylene	nonwoven Dacron 5 x 3 x 3
Weight (gm/yd <sup>2</sup> )					
Warp tensile strength (ppi), & % elongation at room temperature	36.2	35.3	37.8	33.8	34.5
Warp tensile strength (ppi), & % elongation at -80°F	38.8, 12%	41.5, 14%	35, 56%	42, 67%	26, 11%
Fill tensile strength (ppi), & % elongation at -80°F	51.4, 13%	63.7, 14%	45, 33%	57, 35%	33, 9%
Ply adhesion (ppi) at -80°F	42.5, 16%	35.6, 13%	40, 40%	45, 42%	diagonal 20, 9%
Seal tensile strength (ppi) at -80°F	1.3	0.7	0.15	0.03	film tore; no delamination
Flex test	OK	OK	Fail (7)	Fail (8)	OK
Material cost per lineal yd	\$ .67	\$ .59	\$ .60	\$ .52	\$ .56

## XXVIII. Water in the Atmospheres of Planets

John Strong  
Laboratory of Astrophysics and Physical Meteorology  
The Johns Hopkins University  
Baltimore, Maryland

With an automatic daytime telescope of 30-cm aperture carried by balloon to 26.5 km we have made a determination of the amount of water vapor present above the reflective cloud layer on the planet Venus. Radiation was measured in the band at  $1.13 \mu$ , with a grating spectrometer of 2-Å resolving power. This portion of the spectrum was scanned once every ten seconds with a set of 21 exit slits arrayed to match 21  $H_2O$  absorption line groups. The radiation passing through was received by a chilled photomultiplier with S-1 surface, and its response was recorded on paper.

From 120 such records we have determined that the modulation produced by the water absorption, when the line groups were scanned, was  $(10.5 \pm 0.5)$  percent. By calibration, this modulation is the same as that produced by  $9.8 \times 10^{-3} g/cm^2$  of water vapor at atmospheric pressure.

Possible influence of water vapor in the earth's atmosphere above the balloon was assessed in two ways. Immediately after the observing period, and at the same altitude, radiation received from a piece of white cloth illuminated by the sun was analyzed. A much smaller modulation, resulting from water in the solar path, was measured.

We were also able to measure the influence of the Doppler shift on our recorded data. At one point in each scan cycle a mercury discharge spectral line at 11,287 Å was passed through one of the exit slits, and was recorded as a modulation in the reference-level spectrum. Measurements from this fiducial line to the Venus water dips, taken from 20 scans, exhibit a Doppler shift of  $(0.49 \pm 0.05)$  Å, in agreement with a shift of 0.495 Å calculated from the relative orbital motions of Venus and the earth. From this agreement also we see that telluric water vapor played a minor role in the 10.5-percent modulation.

Both assessments are in fair agreement with the accepted value of about  $0.7 \times 10^{-3}$  g/cm<sup>2</sup> of water above the altitude of the balloon. Thus only about 1/20 of the modulation measured while observing Venus may be attributed to water in the earth's atmosphere or in our apparatus.

At the time of our observation on 21 February 1964 the phase angle of Venus was 65 degrees. The effective slant path through the atmosphere of Venus is calculated to be 3.82 times the vertical path.

The interpretation of the measured absorption requires certain assumptions about the pressures to be expected at and above the Venus cloud top level, and the distribution of water vapor in this region. Pressure estimates reported by Sagan (1963) range from 90 mb to 600 mb at the cloud level. The amounts of water vapor calculated from our data for gravitational atmospheres at these base pressures are  $22.2 \times 10^{-3}$  g/cm<sup>2</sup> for the 90-mb case, and  $5.2 \times 10^{-3}$  g/cm<sup>2</sup> for the 600-mb case. The respective mixing ratios would be  $2.5 \times 10^{-4}$  and  $0.87 \times 10^{-5}$ . A choice between these values, or in this range, must await more knowledge about the actual pressures. It is interesting however to note that values reported for comparable levels in the earth's upper atmosphere (M. Gutnick, Air Force Surveys in Geophysics No. 147) represent the geometric mean of the extremes we have calculated for the planet Venus.

## Acknowledgments

The results reported in this paper were obtained with the support of the USAF Office of Aerospace Research, Air Force Cambridge Research Laboratories. In this experiment the telescope and spectrometer, developed under Office of Naval Research and National Science Foundation support and used in the 1959 Moore-Ross manned flight, were modified to make the system unmanned and automatic, under support of the Office of Aerospace Research.

## References

- Gutnick, M. (1962) Mean Annual Mid-latitude Moisture Profiles to 31 km, Air Force Surveys in Geophysics, No. 147, AFCRL-62-681.  
Sagan (1963) Ann. Rev. of Astron. and Astrophys., 1:235.

## XXIX. The Mars Balloon—Feasibility and Design

M. H. Davis and S. M. Greenfield  
The Rand Corporation  
Santa Monica, California

It is an intriguing idea that balloons might be used to probe the atmosphere of Mars and to give some mobility to instruments that have been transported to the planet. In principle no simpler method of transportation can be imagined. A floating balloon has the great advantages of simplicity and of requiring no motive power, although it suffers from the drawback that only flight duration and altitude are subject to control; the direction and distance of a particular flight are at the mercy of the wind. In the present paper we discuss the feasibility of Mars balloon operations. The paper to follow discusses how balloons might contribute significantly to the systematic exploration of the surface and atmosphere of the planet.

A detailed engineering study is required before the feasibility of the Mars balloon can be fully analyzed. Here, since we do not attempt to actually design the system, we can only outline some of the more important requirements and problems. Because of spacecraft limitations, feasibility will depend to a great extent on how much weight and volume must be expended in order to ultimately lift a useful payload into the Martian atmosphere. We will try to arrive at estimates of the weight and volume requirements for a balloon system, without attempting a detailed breakdown into components. An additional consideration, and one of primary importance, is the reliability of the system. It is essential to strive for simple and rugged subsystems and materials.

Before discussing weight and volume estimates, let us look in an over-all way at the suggested system. Two balloon types appear most fruitful for study. One is a balloon used to carry instruments from one point on the planet's surface to another point fairly nearby. We visualize hydrogen-filled balloons of the equal-pressure type for this job. The flight would be of fairly short duration, the objective being to lift the payload of instruments off the ground so that winds can move it to a new location. We must design the balloon to float at a density that is guaranteed to be off the ground, but need not be at a very high altitude. The other interesting balloon mission is to float at a fairly high altitude for long periods, carrying instruments designed to observe the atmosphere and surface. For this mission we might consider either a ballasted equal-pressure balloon (if flight duration is supposed to be longer than one day) or the superpressure balloon. The idea of carrying "dead" ballast to Mars or using some native material as ballast doesn't seem very sensible. However, it is perfectly reasonable to think of dropping instruments and other parts of the payload at the end of each day -- parts of the payload can act as droppable ballast for as long as there is any payload left. The superpressure balloon can, of course, have a duration of many days without ballast. However, it presents more critical problems with regard to material strength and reliability. As on earth, we might think of using balloons of extensible material to obtain vertical soundings of the atmosphere. This may certainly be done someday, but it seems less interesting for initial consideration since the probe that enters the planet's atmosphere and descends to soft-land on the surface can provide a vertical sounding.

It might conceivably be possible to launch balloons from the surface of the planet by encasing them in a protective structure while they are being filled. Such a procedure would, however, cost a great deal in weight and complexity. The balloons we are considering for use on Mars are 10 to 50 feet in radius -- unwieldy sizes to control in the winds that we suspect frequently occur on Mars. From observations of dust clouds it is known that winds up to 90 km/hr occur on the planet. Unless some very ingenious ideas are forthcoming, or present beliefs about the planet's atmosphere turn out to be wrong, the only practical way to launch balloons is in the atmosphere during entry.

Air-launch systems have already been developed and we suggest that this type of system be used for the Mars balloon. The balloon itself might be used as a parachute to slow the descent of its part of the instrument package during the time it is being filled with buoyant gas. The total payload would be split between a part that lands, and a part carried off by the balloon either a short distance or to drift for a prolonged time at altitude. It appears from what we know about the Mars atmosphere that ten minutes to half-an-hour could be available for balloon filling. This estimate of the time required to descend through the atmosphere at terminal velocity is derived in Appendix A.

The system in broad aspect, then, consists of the balloon with its packaging and release system, designed to be deployed as a parachute while it is being filled; its payload of instruments; a gas-generation apparatus capable of generating the required quantity of hydrogen in less than 30 minutes; spacecraft structure, heat shield, and so forth. At this stage we are primarily interested in estimating weights and volumes so as to form an opinion of whether the idea of a Mars balloon seems at all feasible. If it does, then more detailed studies will be warranted.

The total balloon-system mass,  $m_T$ , will be the sum of  $m_b$ , the mass of the balloon itself;  $m_p$ , the mass of the payload;  $m_t$ , the mass of the gas generation system (which includes the mass of the buoyant gas used) -- all multiplied by a factor,  $F$ , which allows for the auxiliary structure, heat-shield, and so on. Its total volume,  $V_T$ , will be the sum of  $V_k$ , the volume of the packed balloon;  $V_t$ , the volume of the gas generation system; and  $V_p$ , the volume of the payload -- multiplied by a factor  $F'$  to allow for structure, and so forth. (Using the experience of present spacecraft designs, the value 2 seems reasonable for both  $F$  and  $F'$ .) The efficiency ratios ( $m_p/m_T$ ) and ( $V_p/V_T$ ) then give an indication of the price we must pay to lift a given payload into the Mars atmosphere.

It is convenient to relate the mass and volume efficiency ratios to the quantity  $\zeta$  which we define to be the ratio of the payload mass to the sum of the masses of payload and balloon. Further define  $\beta = (\text{Molecular weight of atmospheric gases})/(\text{Molecular weight of buoyant gas})$ ;  $e_g = (\text{mass of buoyant gas generated})/(\text{total mass of gas generation equipment})$ . Then:

$$\frac{m_p}{m_T} = F \left[ \left( \frac{\beta}{\beta-1} \right) + \frac{1}{\beta} \left( \frac{1}{e_g} - 1 \right) \right]$$

Moreover, if we assume that the product of the packing efficiency of the balloon and the density of its material is about  $1.0 \text{ gm/cm}^3$  and that the density of the payload is also about  $1.0 \text{ gm/cm}^3$ , then

$$\frac{V_p}{V_T} = \frac{\zeta}{F' \left[ 1 + \left( \frac{V_t}{m_g} \right) \frac{1}{\beta} \right]}$$

(Balloon superheat has been ignored.)

The molecular weight of the Martian atmosphere has usually been assumed to be about 30, based on the idea that it is composed largely of nitrogen with a small

admixture of carbon dioxide and argon. Recent spectroscopic evidence (Kaplan, Münch and Spinrad (1964)) however, suggests that CO<sub>2</sub> may be a major constituent and that the molecular weight could be as great as 40. If hydrogen is the buoyant gas,  $15 < \beta < 20$ , but no significant error will be made if we assume for simplicity that  $1/\beta = 0.06$  and  $\beta/(\beta-1) = 1.05$  as typical values.

The characteristics of the gas-generation system depend upon what type of system we contemplate. In our previous report (Greenfield and Davis, 1963), we investigated three basic types of gas-transport and generation systems: transport under very high pressure in a steel pressure vessel with a simple transpiration valve; transport as liquid in an insulated cryogenic vessel together with a heater to evaporate the gas when needed; and transport as a hydrogenous chemical compound from which hydrogen can be extracted by heat or chemical reaction. For details see References (Greenfield and Davis, 1963). The conclusions expressed as mass and volume ratios, were:

for the high-pressure system:

$$e_g \sim 0.02 V_t/m_g \sim 60 \text{ (cm}^3/\text{gm)}$$

for the liquid-hydrogen employed to transport around 1 kg of H<sub>2</sub>:

$$e_g \sim 0.03 V_t/m_g \sim 400$$

for the best of the chemical systems:

$$e_g \sim 0.1 V_t/m_g \sim 20$$

The high-pressure system presents some engineering uncertainties, but seems attractive since it is conceptually simple and the gas is generated rapidly. The liquid hydrogen system is considerably more complex and suffers from requiring a proportionately large volume if only small quantities of gas are to be transported. (The efficiency ratios improve rapidly for amounts of gas in excess of 10 kg. The problem is two-fold -- liquid hydrogen has the very low density of 0.07, and considerable insulation is needed for storage during the spaceflight of 8 months to Mars.) There also may be a problem generating the gas at the rate required for balloon filling. The best chemical generation system appeared to be thermal decomposition of beryllium hydride -- a scheme that is certainly speculative since the properties of this compound are very uncertain. It appears that chemical

rnethods for gas generation merit careful investigation since they offer the advantage of easy long-term inert storage of the gas, although rapid gas generation may present a problem.

For the present analysis, we adopt a chemical gas generation system but derate the performance slightly from that of the BeH<sub>2</sub> system, taking as representative values  $e_g = 0.05$  and  $V_t/m_g = 50$ . Then, based on the various adopted values,

$$\frac{m_p}{m_T} \approx 0.1 \zeta$$

$$\frac{V_p}{V_T} \approx 0.1 \zeta$$

The remaining parameter that we must estimate is  $\zeta$ , the ratio of the payload mass to the total mass lifted by the balloon. A "natural-shaped" balloon -- one with vanishing circumferential stresses -- is characterized by the dimensionless parameter  $w$  which is defined

$$w = \frac{\delta}{m_p} \left( \frac{m_p}{b} \right)^{\frac{2}{3}}$$

where  $\delta$  is the area density of the balloon fabric (gm/cm<sup>2</sup>) and  $b$  is the density difference between the air outside the balloon at its buoyant altitude and the gas inside. See References (Smalley). (If  $\rho_a$  is the density of the air outside the balloon,

$$b = \rho_a \left( 1 - \frac{1}{\beta} \right) \approx \rho_a$$

ignoring balloon superheat.) For the natural-shaped balloon a relation can be derived between  $w$  and  $\zeta$ :

$$w \approx \frac{0.2 (1 - \zeta)}{\zeta^{1/3}} .$$

The superpressure balloon requires somewhat different treatment, since stresses in the fabric are much greater than in the equal-pressure case. The balloon is designed to maintain a positive pressure relative to the outside air during

the diurnal temperature cycle. If the change in effective balloon temperature is  $(\Delta T)$  during the one-day period, and we define

$$\gamma = \frac{R^* (\Delta T)}{4K_c M_a}$$

where  $R^*$  is the gas constant ( $8.3 \times 10^7$  cgs units),  $M_a$  is the molecular weight of the atmosphere, and  $K_c$  is the tensile strength of the material (dynes/cm<sup>2</sup>) divided by its density (gm/cm<sup>3</sup>), then we can write

approximately for the superpressure case:

$$w \approx \frac{0.2 (1 - \zeta - 10 \gamma)}{\zeta^{1/3}}.$$

It is difficult to estimate  $(\Delta T)$  for the Mars environment, since it depends on the radiative characteristics of the balloon film, and the ambient air temperature, as well as the day and night radiation environments. However, suppose that  $\Delta T$  is about  $20^\circ\text{C}$ . Then for  $K_c = 10^9$  cgs units,

$$w \approx \frac{0.2 (0.85 - \zeta)}{\zeta^{1/3}}.$$

The balloon volume is readily computed once  $\zeta$  is given, since

$$V_b = \frac{1}{\zeta} \left( \frac{m_p}{b} \right).$$

Our procedure will be to compute  $w$  for interesting combinations of payload and density, then using the above implicit relations, compute corresponding values for  $\zeta$ . Finally, using  $\zeta$ , we estimate the required balloon volume and the total mass and volume of the balloon system.

But first we must discuss balloon materials and the atmospheric densities we expect to find. We will assume that the balloon fabric has an area density of  $0.002 \text{ gm/cm}^2$  corresponding to 0.5-mil Mylar. Research into super-light film materials may reduce this value. But it should be kept in mind that the film used ultimately must be (1) of very high reliability, (2) unaffected by solar ultraviolet, (3) unaffected by the very low temperatures that may be encountered in the Mars atmosphere — as low as  $-150^\circ\text{C}$ , (4) capable of being positively sterilized —

preferably by dry heat at 135°C for 24 hours, (5) able to be stored in space for 8 months, (6) able to be unfolded rapidly and reliably without hanging-up.

At the time of writing "The Physics of Balloons and Their Feasibility as Exploration Vehicles on Mars" (Greenfield and Davis, 1963), it was thought that the atmospheric density near the surface of Mars would be found to be around  $8 \times 10^{-5}$  gm/cm<sup>3</sup> with temperatures around -70° to -20°C -- conditions resembling those at about 67,000 feet in the earth's atmosphere. However, the recent interpretation of spectroscopic data (Kaplan, Münch and Spinrad, 1964) suggests that the surface level density is probably closer to  $2 \times 10^{-5}$  gm/cm<sup>3</sup> -- corresponding to conditions at about 96,000 feet in the earth's atmosphere. For balloon operations we will consider three densities in the Mars atmosphere:  $8.0 \times 10^{-5}$  gm/cm<sup>3</sup>, which corresponds approximately to ground level under the old atmospheric estimates;  $2.0 \times 10^{-5}$  gm/cm<sup>3</sup>, which may be no higher than just off the ground; and  $1.0 \times 10^{-5}$  gm/cm<sup>3</sup>, which should occur no lower than about 10 km (33,000 feet) in the Martian atmosphere. (These densities correspond to 68,000 feet, 97,000 feet and 110,000 feet on earth.) It should be emphasized that our ideas about the atmosphere of Mars are very uncertain at present. However, even if balloons are used eventually as a part of the Mars exploration program, they will almost certainly not form a part of the first instrument package to land on the planet. Since the first package will have as one of its primary scientific missions the determination of the pressure and density in the Martian atmosphere, we can expect that a balloon designer will have this information available when he writes his final report. For the present, we must use the best information we have, uncertain as it is.

We will consider payloads of 1 kg for the superpressure balloon, and of 10 kg and 100 kg for the equal-pressure balloon at these three densities. Table 1 shows estimated values for  $m_T$ ,  $V_T$  and  $V_b$ .

Table 1.

Density (gm/cm <sup>3</sup> )	$m_p$	Superpressure		Equal-Pressure	
		1 kg	10 kg	100 kg	100 kg
$8 \times 10^{-5}$	$m_T$	11 kg	67 kg	550 kg	
	$V_T$	0.8 cu.ft.	4.6 cu.ft.	40 cu.ft.	
	$V_b$	$1 \times 10^3$ cu.ft.	$5.7 \times 10^3$ cu.ft.	$4.9 \times 10^4$ cu.ft.	

Table 1. (Cont)

Density (gm/cm <sup>3</sup> )	$m_p$	Superpressure		Equal-Pressure	
		1 kg	10 kg	100 kg	1000 kg
$2 \times 10^{-5}$	$m_T$	36 kg	100 kg	670 kg	4000 kg
	$V_T$	2.5 cu.ft.	7 cu.ft.	48 cu.ft.	270 cu.ft.
	$V_b$	$1.2 \times 10^4$ cu.ft.	$3.5 \times 10^4$ cu.ft.	$2.4 \times 10^5$ cu.ft.	$7 \times 10^5$ cu.ft.
$1 \times 10^{-5}$	$m_T$	100 kg	150 kg	830 kg	4600 kg
	$V_T$	7 cu.ft.	11 cu.ft.	58 cu.ft.	300 cu.ft.
	$V_b$	$7 \times 10^4$ cu.ft.	$1.1 \times 10^5$ cu.ft.	$5.8 \times 10^5$ cu.ft.	$2.7 \times 10^6$ cu.ft.

Although many difficult engineering problems remain, no calculations we have made so far invalidate the Mars balloon concept. It will not be an easy system to develop, particularly with the required high reliability, and as we have seen, it is expensive in weight and volume. However, balloons offer what appears to be a unique capability and so seem to us to have an important place in the Mars-exploration program as discussed in detail in the next paper.

## Appendix A

### Time Available for Balloon Filling

The time the balloon package will take to descend through the atmosphere using the balloon itself as a parachute can be estimated if we assume that the fall is at terminal velocity and that the drag coefficient has the approximate value 1.0. Then

$$\frac{1}{2} A \rho v^2 = mg.$$

The appropriate mass is  $m_T/F$ , since the structure and other parts accounted for by the factor  $F$  will be jettisoned. ( $A$  is the effective drag area.) Writing

$$v = \frac{dz}{dt} = - \frac{H}{\rho} \frac{dp}{dt}$$

where  $H$  is the atmospheric scale height (around 12 km on Mars) we obtain by integration of the above equation:

$$\Delta t = H \left( \frac{2 A \rho_0}{mg} \right)^{\frac{1}{2}} \left[ 1 - \sqrt{\frac{\rho_1}{\rho_0}} \right]$$

for the time to fall from density  $\rho_1$  to the surface (density  $\rho_0$ ). If  $\rho_1$  is considerably smaller than  $\rho_0$ ,

$$\Delta t \approx H \left( \frac{2 A \rho_0}{mg} \right)^{\frac{1}{2}} \approx 7 \sqrt{\frac{A}{m}} \text{ min.}$$

Taking our assumed parameter values,

$$\frac{A}{m} \approx 20 (1 - \zeta) \text{ cm}^2/\text{gm.}$$

Hence  $\Delta t$  will be in the range 10 minutes  $< \Delta t <$  30 minutes with the shorter times associated with the larger payloads.

Because of the exponential decrease of density with altitude, most of the time is spent falling through the last few kilometers. During filling, the balloon will gradually become buoyant, so the time estimates above are somewhat too small. At the end of the filling operation the gas-generation apparatus will be dropped.

### References

- Greenfield, S. M. and Davis, M. H. (1963) The Physics of Balloons and Their Feasibility as Exploration Vehicles on Mars, R-421-JPL, The Rand Corporation.
- Kaplan, L. D., Münch, G. and Spinrad, H. (1964) An analysis of the spectrum of Mars, Astrophys. J., 139:1.
- Smalley, Justin, H., Determining of the Shape of a Free Balloon, Report No. 2421, Contract No. AF19(628)-2783 Project No. 6665, Task 666501, General Mills, Inc., St. Paul, Minn.

## **XXX. Balloons for the Scientific Exploration of Mars**

**S. M. Greenfield and M. H. Davis  
The Rand Corporation  
Santa Monica, California**

### **I. INTRODUCTION**

The previous paper examined balloons as physical systems in a planetary atmosphere, and derived methods of assessing their feasibility. In this paper we shall attempt to answer the questions of how balloons can contribute to the exploration of a planet like Mars, and how their derived capability translates into a scientific utility.

In considering the usefulness of balloons for studying a planet, three modes in which such a vehicle can operate should be recognized. Each mode has its own utility.

The three modes of operation are:

- (a) The balloon used as a sensor. (The desired data are obtained by tracking the balloon itself and recording the motion.)
- (b) The balloon used as a platform. (The balloon supports instruments, which perform the measurements.)
- (c) The balloon used as a conveyance. (The balloon moves an object from one point to another.)

For each of these modes we can derive a possible set of experiments.

## 2. THE BALLOON AS A SENSOR

As we are well aware, a balloon that is neutrally buoyant in an atmosphere moves approximately with the air and its motion reveals the wind speed and direction at its floating altitude. Similarly, a balloon that rises until it bursts, if observed accurately enough, provides information on the vertical structure of the wind. In both cases, the balloon must be tracked quite accurately and almost continuously to provide other than rather grossly averaged winds. While we recognize the desirability of such information, we feel that it is, at present, considerably beyond our ability to obtain on Mars. This is particularly true in the case of the vertical balloon sensor, which to be useful must be launched frequently and over a wide area.

## 3. THE BALLOON AS A PLATFORM

Ignoring, for the purpose of this paper, any further consideration of the balloon as a sensor, we may move on to the second mode of operation which permits a broad choice of uses for a balloon on a remote planet. The balloon is a mobile platform. Any instrument small enough to be carried and reliable enough to be operated remotely is a candidate for use. A multitude of possibilities could be listed; no list would be exhaustive, but for illustration, a few specific examples can be cited.

The most familiar operation in this mode is the measurement of meteorological parameters. Using a single, extensible balloon that expands as it rises until it bursts, it is commonplace on Earth to send instruments aloft that measure pressure, temperature, radiant-heat flux, and other physical quantities as a function of altitude along a single, more-or-less vertical line. From such measurements can be derived the variation with altitude (over a single point) of such important parameters as density, water-vapor content, and radiation-flux divergence. On Mars, similar measurements would yield important information about the structure of the atmosphere, although the variation of many atmospheric parameters in space and time could not, of course, be predicted on the basis of one sounding (or even many soundings) over a single location.

However, a simple, single-point balloon ascent on Earth can provide many geophysical data beyond the usual meteorological measurements, and the same is true of Mars. As stated earlier, however, the true utility of a vertical rising balloon sensor is only realized through a multiplicity of launches distributed in space and time. Because of the added degree of complexity and the demands for serial reliability that such a requirement places on the balloon system, for the purposes of this paper we will not consider the vertical sounder further as a possible, currently useful Mars exploration tool.

Considerably more flexible in operation is a balloon that can float for a long period at a predetermined density level in the atmosphere. Such a vehicle becomes an observation platform of good stability that, depending on the winds, permits a variety of measurements to be made over a considerable distance and time.

From such a platform drifting across Mars, standard meteorological measurements could be made; the resulting data, when combined with measurements made by the capsule during entry, would begin to yield information on the structure and variability of the Martian atmosphere. To be sure, the balloon measurements would be made at a single density level in the atmosphere, or at most, at two or three levels, but these data could be supplemented by parachuting instruments in small packages from the "mother" balloon at regular intervals. Such a procedure would add another dimension to these data.

A platform suspended some distance below the balloon would permit instruments to look down or up at quite a large angular area of ground and sky. A radiation detector aimed downward could sense radiation emitted or reflected by ground, clouds, or haze. A more complex photographic or television camera could record surface-wind directions and speeds by observing dropped smoke bombs or flares, could scan surface features in detail, and could seek evidence of life. Data from infrared or microwave radiometers would permit estimation of the surface temperatures and the emissivities of relatively fine topographic features. A gamma-ray detector could provide evidence of the radioactivity of the surface.

A spectrometer and a polarimeter aimed upward at scattered visible sunlight would provide continuous data that, combined with knowledge of the look angle and the solar position, would provide information on scattering and polarization in the atmosphere, from which the nature of airborne particles might be inferred. Sensors could detect the presence of clouds and haze layers in the high atmosphere and thin horizontal distributions, either of which could then be studied more closely by other methods. Looking up in the ultraviolet absorption bands of ozone would lead to a determination of the vertical and the horizontal distribution of that gas.

A wind-carried platform would permit a wide variety of physical observations to be made at the floating level. The magnetic field could be monitored as the balloon drifts away from its launch point. Such data would be particularly useful if coupled with data from a continuously-recording magnetometer at the home base. There are other important physical quantities that could be measured: cosmic rays, atmospheric electric fields and field gradients, and electrical disturbances arising from such an atmospheric phenomenon as a dust storm.

Finally, although certainly not lastly, the search for life forms can be aided by balloon-carried instruments. As a part of this search, samples taken at the floating altitude of the balloon might be analyzed for the presence of spores and bacteria. In addition to the photographic or television survey already mentioned,

spectral measurements similar to those made by Sinton (1959) might produce data on the presence and distribution of plant life.

#### 4. THE BALLOON AS A CONVEYANCE

Used as a conveyance, a balloon can serve to move one or more devices, making it possible for (a) one package to operate successively at two or more locations, or (b) a number of devices to operate simultaneously at more than one location. By combining and pyramiding these two transportation functions, permutations can be evolved that are limited only by payload restrictions.

A balloon could be used to seed a number of similar experimental packages over a large area for simultaneous studies of selected parameters.

After the capsule has made its measurements at the landing location, it might also be desirable to move the entire instrument package to a new location having different environmental characteristics. The balloon would be launched and would rise to its floating altitude carrying the instrument package and noting the local albedo of the ground. It would continuously monitor the albedo of the planet's surface as it drifted with the wind at the equilibrium level. When the albedo was significantly different from the value at the original landing point it would descend. Obviously, any other measurable parameter could be used to trigger the descent of the balloon; the objective is for the balloon to descend where the "terrain" is different in kind, and repeat the measurements.

A variant on the operation just described would be to choose in advance two or more surface characteristics that would be of most interest. Then two or more balloon units would be included in the capsule. Regardless of the change environment at the landing point, the balloons would separately lift the units and would individually seek the two locations whose physical parameters corresponded to the preselected values (such as high and low surface radiativity or temperature), at which places surface studies would be made.

As a final interesting case, the balloon might be used to separate interfering parts of the same payload or parts that must be separated for the payload to function properly. Sensitive electronic and radiation-measuring equipment, for example, could be separated from a nuclear reactor. Explosive charges could be "seeded" by a balloon at various distances from a seismometer.

Having allowed our imagination to wander a bit, it might be interesting at this point to examine what experiments are actually being thought of for the exploration of Mars. It might also be well to examine how such a set of experiments meshes with derived balloon capabilities.

As part of the planning for the exploration of Mars, considerable work has been done by NASA and in particular by the Jet Propulsion Laboratory on the subject of the possible scientific experiments to be accomplished (Study of Mars and Venus Orbiter Missions Launched by the 3-Stage Saturn C-1B Vehicle, 1963). Basically, the desired objectives of such exploration are threefold, namely:

1. Exploration of the surface for evidence of life past or present, or precursors of future life.
2. Determination of the geological nature and history of the planet.
3. A continuation of interplanetary space-physics research.

Forgetting about the third objective which, for the present at least, is not connected with experiments that could be accomplished from the surface of the planet, let us examine what finally evolved out of a detailed consideration of the first two objectives. I should point out that the experiments that I shall mention are not necessarily those that will actually be done on early Mars missions, but rather they represent the conclusions to come after thoughtful consideration by the Jet Propulsion Laboratory group.

Under the first objective, the search for evidence of life, it was felt that there were three basic sub-objectives that determined the character of the desired experiments, and that these are:

1. The actual search for life (directly or indirectly), in the micro- or macro-environment of the planet, either presently existing or through biological residues, showing evidence of having existed. This objective is involved in the definition of what is life and involves searching visually for life forms, and such things as an examination of the metabolism and reproduction- and growth-rates of suspected life forms that are found.
2. Organic-chemical analysis of the planet because of its relevance to current ideas on biochemical evolution (once again a search for evidence of present or past life on the planet, as well as the possibilities for future life).
3. Ecological studies -- an examination of the environment (atmospheric, radiation, and so on), and its relationship to a possible biosphere. In this connection the environmental properties that appear to be most interesting are:
  - a. Prevailing temperature of lower atmosphere, soil surface, and immediate soil subsurface, and their diurnal variations.
  - b. The water content of the atmosphere and soil and its physical state within the soil.
  - c. The intensity and spectral distribution of the radiant energy at the surface.
  - d. The chemical composition and the surface pressure of the atmosphere.
  - e. The mechanical properties of the soil and the distribution of biologically significant ions.

Under the second objective, the sub-objectives are:

1. Topography -- the mapping of the geometry of the surface features (down to a scale of about a meter), and the division of the surface of Mars into units of homogeneous surface geometry, surface reflectivity (total and spectral), size, and shape, and so forth.
2. Surface photography to determine such information as crustal deformation, erosive and depositional processes, intensity and types of volcanic activity, sequence of formation of surface features, and consequent establishment of Martian time scale, and so on.
3. Internal structure and activity -- seismology.
4. Petrologic investigations -- the science of rocks in its broader aspects. Chemistry, crystallization, mineral assemblage, and so forth.
5. Surface and atmospheric environment -- atmospheric composition, surface radiation, temperature cycling, large eroding wind storms, and so on.
6. Shape of the planet.
7. Magnetic field.

These then are the objectives for the scientific exploration of Mars. Certainly they are ambitious, but one must remember that they represent an attempt to do on Mars what has already been done on Earth but at a much more accelerated pace. They are what ultimately must be done if we are serious about exploring Mars. With the recognition that some of these objectives can be met by orbiting vehicles (that is to say vehicles orbiting Mars), and that some are truly beyond our present capabilities, the following set was finally chosen as being within the capability of a single Mars lander:

1. A comprehensive biological survey by employing photography, microscopy, light scattering, radioisotope techniques and biological reactions for specific biochemical components; also growth detection over extended periods.
2. Color surface photography of resolution varying from 1 mm at 2-m distance to 5 cm at 100-m distance.
3. A total of approximately 500 surface pictures (both surface photography and microphotography).
4. Geological information through techniques of seismometry, x-ray diffraction, and petrological microscopy.
5. Composition and meteorology of the atmosphere by measurement of thermodynamic parameters, surface conditions, surface wind velocity and time variations of each of these.

From the very nature of these experiments, involving as they do measurements that require the instrument to be on the ground as well as those that do not carry this requirement, it is apparent that there are two basic ways that a balloon system

could be used to enhance the data acquisition. First, one might conceive of the entire package landing on the planet, and performing its assigned mission for a specific length of time. At the end of this period, a balloon is inflated and the package is carried to a second location to repeat its measurement cycle. Second, as an alternative mode one can visualize a sensor capable of making measurements while airborne being separated from the main capsule (which is landed on the planet), and being carried by balloon during its entire measurement cycle. Both of these possibilities offer obvious desirable advantages which have been mentioned previously; however, as may be imagined from the previous paper, both modes probably entail a considerable payload penalty. In the final analysis, it is this payload penalty which fixes the ultimate feasibility of the balloon system.

The degree of this payload penalty can be determined by attempting to estimate the payload masses involved in such a future space venture. The Jet Propulsion Laboratory people drawing on their considerable experience have already made this estimate (see References). The estimated masses that are attached to the various experiments attempting to accomplish the goals stated earlier are given in Table 1.

Table 1

Measurements	Instrument mass (kg)
Biology	13
Geology	15
Atmospheric	8
Surface Surveillance	9
Soil and Atmospheric Sampling	9
Sound	1
TOTAL	55

The instrumental masses are of course only the beginning in any analysis of payloads. In addition, one must include a sequencer, computer, data handler, transmitter, power supply, and so on, and doing so we very quickly convert the 55 kg to something of the order of 300 kg. If we then add the required structure to hold this package together, we finally arrive at a lander capsule with a mass of  $\sim 400$  kg. This approximately doubles to  $\sim 750$  kg as we go from the package landed, through a heat shield, and so forth, to the total entry vehicle which is separated from the orbiting capsule. This then is the determinant of the feasibility of a

balloon system to do the first job. In other words, if we are to move the entire package with its load of sophisticated experiments to a new location we are faced with the problem of lifting some 400 kg from the surface of the planet. It might be well to point out here that even if we were to further miniaturize our electronics and instruments, we are still left with a considerable mass involved in a power supply (convertor, batteries, isotope energy source, and so on) which may be much more difficult to reduce.

Moving to the second suggested mode, namely, choosing one sensor array to become a balloon-borne experiment, we can select the atmospheric package as the natural candidate. As indicated previously, the estimated atmospheric sensor mass is  $\sim 8$  kg.\* To this mass we must add as major components, a power supply, a sequencer, and a transmitter. In the case of the power supply, due to the fact that we have a considerable area available on the balloon, we can conceive of utilizing an array of solar cells and storage batteries rather than the much more massive isotope source and convertor. Applying the known efficiency and conversion factors (Study of Mars and Venus Orbiter Missions Launched by the 3-Stage Saturn C-1B Vehicle, 1963), we find that some 5 ft<sup>2</sup> of solar cells are capable of providing the instrumentation power requirements during the sunlit period plus an additional amount of power to be stored for use during the dark period. If we double this area and place four such areas equally spaced around the upper hemisphere of the balloon, they should cover a negligible fraction of the balloon's surface (of the order of 1 percent), and provide an adequate source of power despite its orientation. Once again taking into account the power needed and assuming a conservative battery capability (30 w-hr/lb), we arrive at an estimated power supply mass of 8 kg. We will arbitrarily add an additional 8-9 kg to account for a transmitter, a sequencer, and to increase the instrumentation power supply to handle the transmitter requirements. We therefore finally arrive at a value for the payload mass of 25 kg, recognizing that this figure has been artificially inflated to be conservative.\*\*

We recognize, as in the previous paper, that in all probability the required balloons are too large to be launched remotely from the surface. That is to say, it would probably increase the reliability of the balloon system if they were inflated while the capsule descends, thereby never permitting the package to reach the ground. In this case, it is obvious that we would have to provide two complete instrument packages for the first mode, one to be carried by the balloon to a different location, and one to descend immediately to the planet's surface. Taking all of these factors

\*This would include instruments to measure density, pressure, temperature, atmospheric composition (mass spectrometer, atmospheric gas chromatograph, and so on) and wind motion.

\*\*We have assumed that the determination of balloon location, data processing, transmission back to earth, and so forth, would be handled by the orbiting capsule.

into account, and utilizing the techniques presented in the previous paper, we can now calculate the total masses involved in attempting to accomplish the two suggested modes. The results of this calculation are presented in Table 2. These figures take into account both the "nitrogen atmosphere" of Mars based on an assumed surface pressure of 85 mb, and the "carbon dioxide atmosphere" based on the recent work of Kaplan, Münch and Spinrad (1964), indicating a possible surface pressure of  $\sim 20$  mb. It should be noted that for the 400-kg payload we have assumed and equal-pressure balloon (relatively short duration) and a density which allows it to just clear the ground ( $< 5$  km). In the case of the 25-kg payload we have assumed a super-pressure balloon (long duration) and a density to place the balloon at an altitude of about 10 km. Naturally these assumed atmospheres carry with them a considerable uncertainty, making any statement as to the actual altitude of these balloons somewhat meaningless.

Table 2

Payload (kg)	Density at Floating Altitude (gm/cm <sup>3</sup> )	Total Mass on Planet (kg)	Total Mass in Entry Capsule (kg)	Balloon Volume (ft <sup>3</sup> )
400 Equal-Pressure Balloon	"N <sub>2</sub> " Atmos- pheres	$8 \times 10^{-5}$	$\sim 1500$	$\sim 2550$
	"CO <sub>2</sub> " Atmos- pheres	$2 \times 10^{-5}$	$\sim 1700$	$\sim 2900$
25 Superpressure Balloon	"N <sub>2</sub> " Atmos- pheres	$6 \times 10^{-5}$	$\sim 100$	$2.2 \times 10^4$
	"CO <sub>2</sub> " Atmos- pheres	$1.5 \times 10^{-5}$	$\sim 170$	$1.3 \times 10^5$
Nonballoon Lander	—	$\sim 400$	$\sim 750$	—

It is apparent from Table 2 that in the case of the 400-kg payload, there is only a minor difference between the total masses required for the "CO<sub>2</sub>" and the "N<sub>2</sub>" atmospheres. This is because the balloon mass which is the component that undergoes

the major change as we change atmospheres is only a relatively small fraction of the total payload. In the case of the 25-kg payload, however, this is not true and the actual atmosphere that is encountered will play a considerable role in determining the feasibility of this system.

In general we may conclude that balloon payloads of the order of 400 kg, while very attractive from the standpoint of what they can accomplish, ultimately multiply back into too great a total load to be considered for Mars missions in the near future. This is apparently true even if we take into account the possible uncertainties inherent in this analysis. Examining the alternative second mode, we see that even if once again we take into account the potential uncertainties, in all probability we cannot do the original lander mission and also float a small package on a balloon. From our calculations, however, it is apparent that what may be feasible within the visualized Mars-mission capabilities in this decade is a floating experiment containing approximately 10 kg of sensors and a considerably reduced package on the ground (sensor mass of the order of 25 kg). Alternatively, one might consider a somewhat larger floating package, two or more smaller balloon-borne payloads, or, possibly most intriguing, a single small payload (10 kg) plus several small droppable sensors to be "seeded" during the total measurement cycle. In any case, balloons appear to offer a new dimension now and in the future to the exploration of a planet such as Mars, and certainly warrant further study in this connection.

### References

- Kaplan, L. D., Munch, G., and Spinrad, H. (1964) An analysis of spectrum of Mars, Astrophys. J., 139:1.
- Sinton, W. M. (1959) Further evidence of vegetation on Mars, Science, 130:1234.
- Study of Mars and Venus Orbiter Missions Launched by the 3-Stage Saturn C-1B Vehicle (1963) Jet Propulsion Laboratory, EPD-139, Vol. III.

## **XXXI. The Balloon as a Stepping-Stone to Space Flight**

**Otto C. Winzen  
Winzen Research Inc.  
Minneapolis, Minnesota**

### **Abstract**

The plastic balloon vehicle, native to the United States, is a valuable, proven test platform which could serve to fill the gap between earth-bound simulators and final space flight. Balloons operate at an altitude where the environment, both physically and psychologically, resembles closely that of space flight. The balloon vehicle is uniquely capable as a manned space station analog with the capability of long flight duration, at low cost and immediate availability. In the search to reduce the exorbitant cost of test programs leading to manned and unmanned space flight, we would be remiss not to explore its unique capabilities. The high confidence level achieved by seven successful major manned flights made by Winzen Research Inc. for the U.S. Navy and U.S. Air Force add to the attractiveness of the vehicle. The paper presents illustrations of these operations, illustrations of polyethylene balloon capabilities, and advanced concepts.

Seventeen years have passed since we flew the first plastic Skyhook balloon, sponsored by the Navy Office of Naval Research, then still the Office of Research and Inventions. The objective, then and now, was not so much to improve the art of ballooning as to develop a reliable and inexpensive research tool and test platform for science.

For this reason, then, ours is essentially a transportation company which designs and builds the vehicles and conducts the flight service. The scientific experiments are performed by civilian and government scientists. We try not to encroach on their territory.

Despite its apparently "built-in" ups and downs the industry has made steady progress as is evidenced at this fine meeting arranged by our hosts, the AFCRL. As a result, many new people have come in contact with our industry, and it may therefore be in order to review some of the accomplishments, and to point out some of the unique advantages of the plastic balloon vehicle as a test bed.

Those of us associated with the missionary work know that, while balloons may have become respectable and have gained in scientific stature, their capabilities need to be continuously expanded and adapted to the increasing and changing needs of science. While much has been accomplished, I, for one, feel that the most significant contributions the balloon vehicle can make still lie ahead. The fact that the balloon work has attracted so many competent workers, and continues to hold their interest, is evidence of its dynamic potential.

However, our industry will not grow by itself. If it is to support more than one or two companies, we must develop new applications, new materials, new instrumentation, and new equipment. A good example is the first Navy contract I mentioned at the beginning of this paper. It was not a contract to develop the balloons. Such a contract proved to be impossible to obtain. Instead, it was a contract to do a particular research job in which the balloon vehicle, yet to be developed, was used as a test platform.

One of our company's main interests has been the development and the application of the heavy-load balloon to test programs leading to manned space flight. We feel that in this area, one of our national goals, the balloon vehicle has a mission which may fill the wide gap between earth-bound simulators and space flight. In the effort to reduce the exorbitant cost and long lead-time of such test programs, we would be remiss not to explore and apply the unique capability of the balloon as a test bed operating in an environment which closely resembles that of orbital flight, within certain limits, of course. But then, all simulators have limits. A pilot knows that flying a Link-trainer is not the same as flying an airplane. The Link-trainer is on the ground and the pilot knows it.

To summarize, this substantial pool of experience offers the background for serious work in the test program leading to manned space flight. The vehicle offers:

1. Physical environment more closely resembling that of space than that achieved by any other simulator.
2. The psychologically correct stress environment.
3. A proven vehicle of high confidence factor.

4. The safety of three possible means of return to earth for pilots.
5. Relatively low cost.
6. Relatively short lead time.
7. Heavy load capability.
8. Extended flight duration capability.
9. Capability of carrying larger crew.

While we cannot presume to know all the problems involved in the space test work here are some the balloon vehicle may be able to solve.

1. Selection and training of astronauts in space craft.
2. Space equivalent testing of components and subsystems.
3. Preliminary run-through of manned space experiments.
4. Study of crew efficiency and performance in stress environment, in prolonged flight.
5. Test of life-support systems, including temperature control.
6. Test of air locks, possibly of docking procedures.
7. Test of space suits, under supervision of space surgeon.
8. Run-through of communications and telemetry methods and equipment.
9. The important study of man/machine relationships.
10. The study of the dust layers at high altitudes reported by all pilots on past flights.
11. Astronomical and astrophysical work in the study of planetary atmospheres and surfaces.

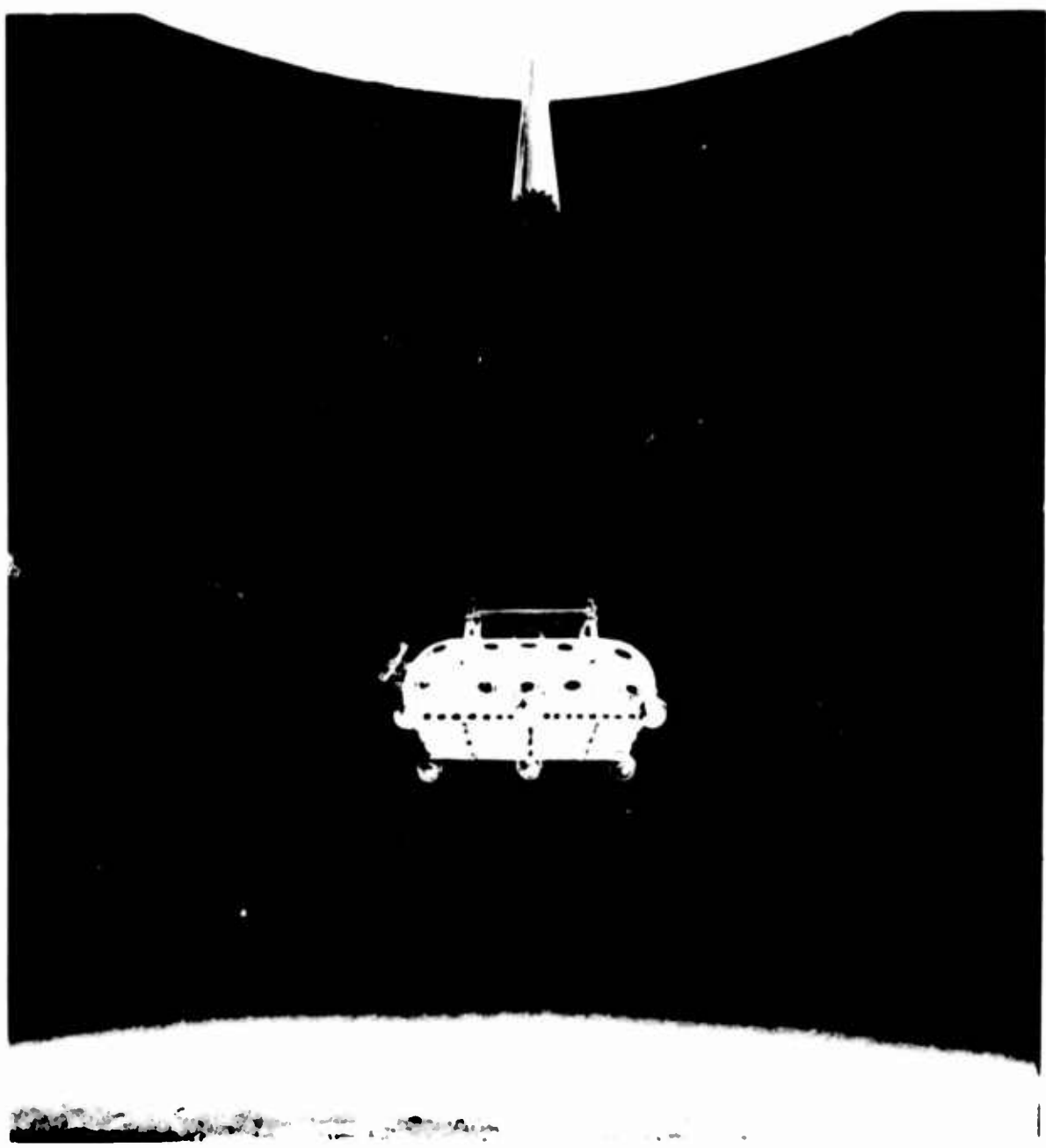


Figure 1. Artist's Drawing of Manned Balloon Capsule at Altitude, Showing Near-Space Environment: (1) Closely resembles visual environment of orbiting capsule. (2) Psychological stress environment is correct (no panic button is available). (3) Return to earth difficult and traumatic as in space capsule (however, there is the safety of three methods of return to earth, on the balloon, on the gondola parachute, on the personnel parachute at lower altitude). (4) High confidence level as a result of seven successful major flights. (5) Simulator which resembles space ship, no noise, vibration, and so on, as in airplane. (6) Above 99% of the earth's atmosphere, good enough for preliminary tests of manned space experiments with only the element of weightlessness missing

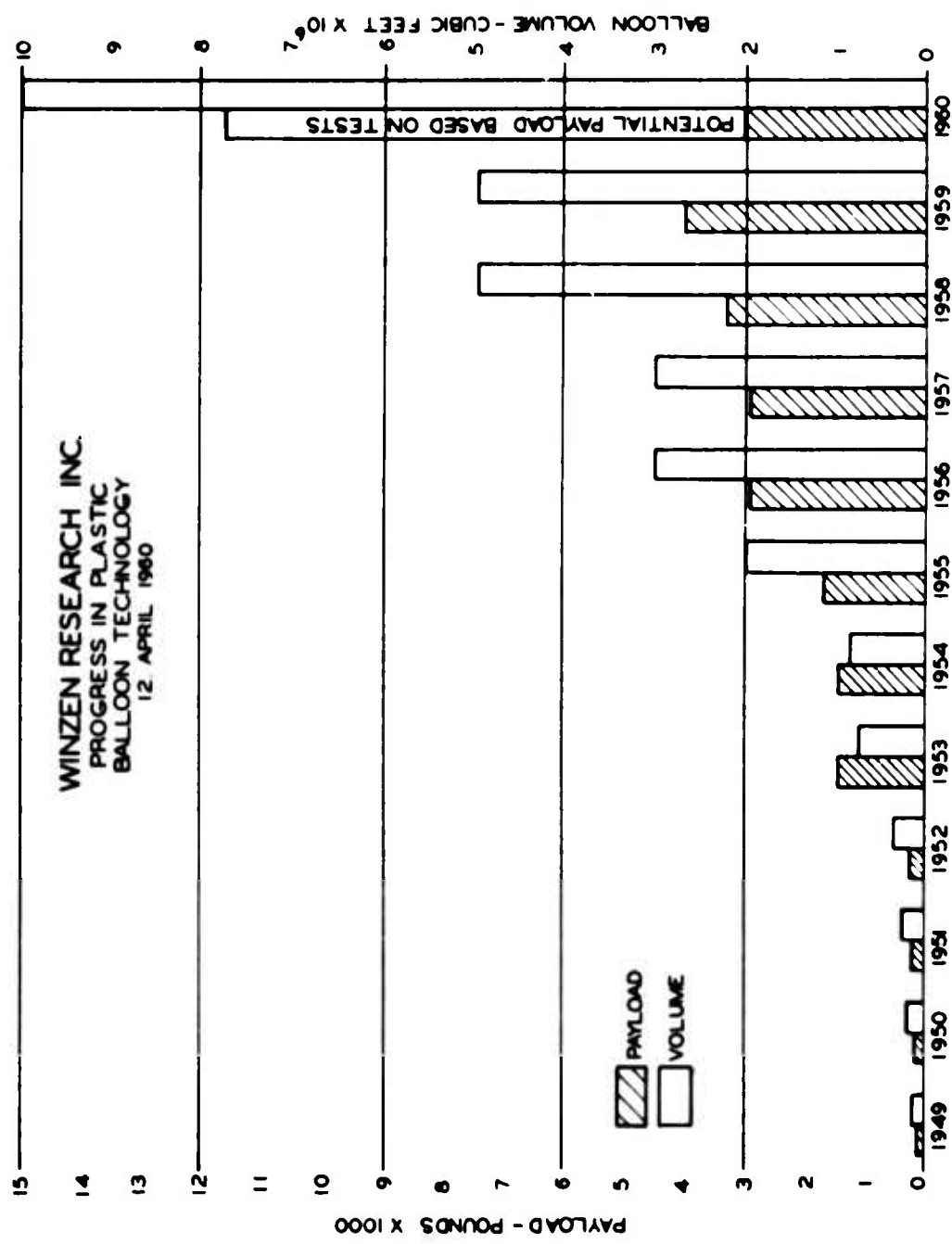


Figure 2. Graph of WRI Progress in Balloon Technology. Figure shows progress from original Skyhook balloon which carried 70 pounds to 100,000 feet on a 200,000-cubic-foot vehicle; steady progress in size of balloons and payloads. 1959 bars show 10,000,000-cubic-foot balloon inflated to a gross inflation of 15,000 pounds, this on a 1-mil capped polyethylene balloon; gross inflation is equivalent to a payload capability of 12,000 pounds.

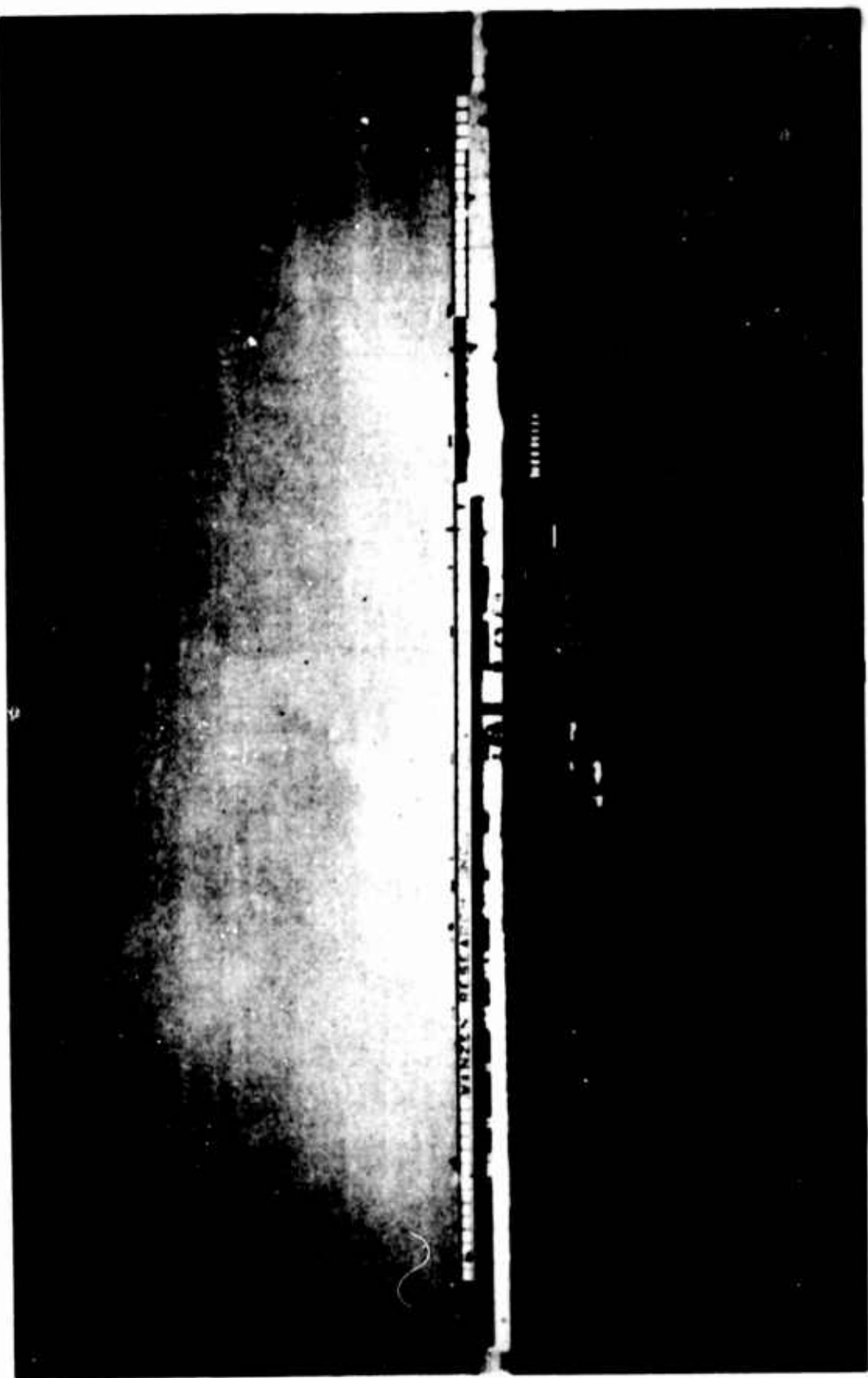


Figure 3. WRI Main Plant in Minneapolis, 455 Feet Long Emphasizes Requirement for Huge Balloon Lofts to Accommodate Balloon Assembly Tables up to 420 Feet Long. Balloon industry requires 10 times the floor space of the next comparable industry, the textile industry, per dollar of sales volume, explaining one of the overhead problems of the industry.

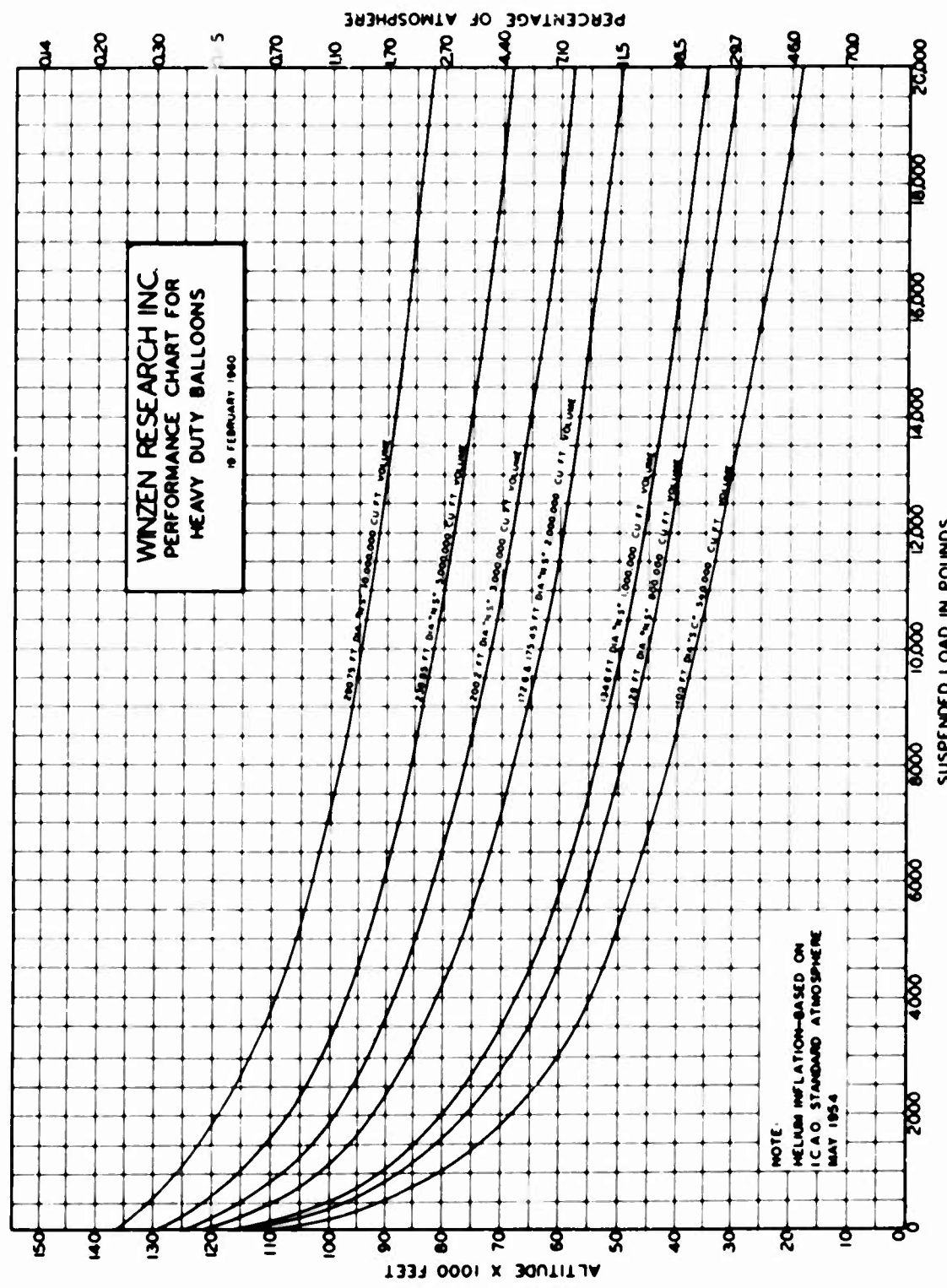


Figure 4. Heavy Duty Performance Curves Showing a Family of Some of the Larger WRI Balloons. Example, 10,000 pound payload to 95,000 foot altitude

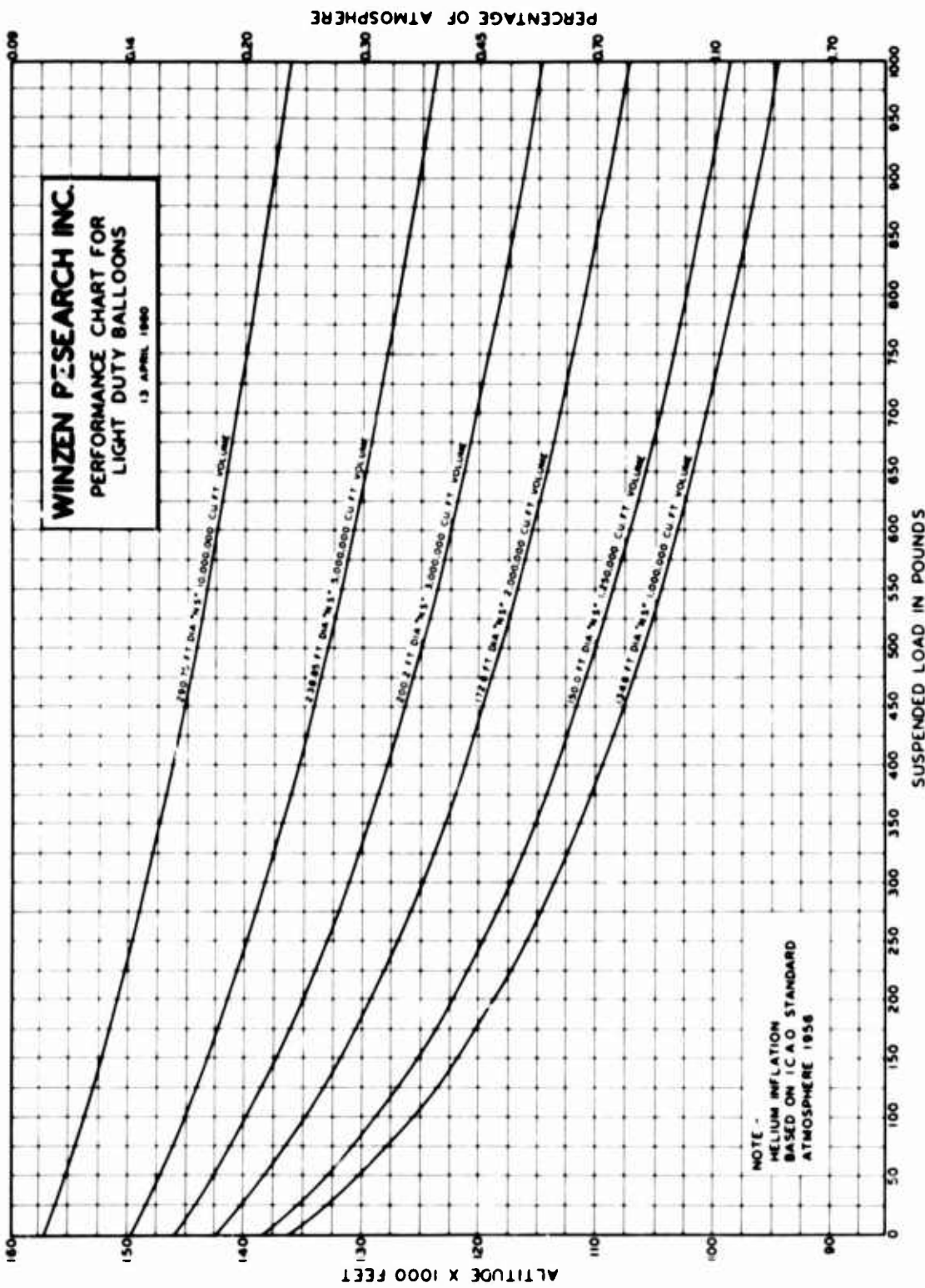


Figure 5. Light Duty Performance Curve. Example, 250 pound payload to 150,000 feet on WRI 10,000,000-cubic-foot balloon, light duty construction

Flight	Date	Pilot	Maximum Altitude	Duration
USAF MANHIGH I	2 June 1957	Capt. J. W. Kittinger	96,000'	7 hours
USAF MANHIGH II	19-20 August 1957	Major D. G. Simons	101,500'	32 hours
USN STRATO-LAB II	18 Oct. 1957	Lt. Cdr. M. D. Ross	86,000'	10 hours
USN STRATO-LAB III	26-27 July 1958	Lt. Cdr. M. D. Ross	82,000'	34-1/2 hours
USAF MANHIGH III	8 Oct. 1958	Lt. Cdr. M. L. Lewis	100,000'	12 hours
USN STRATO-LAB IV	28-29 Nov. 1959	Lt. Cdr. M. D. Ross Charles B. Moore	81,000'	28-1/4 hours
USN STRATO-LAB V	4 May 1961	Lt. Cdr. M. D. Ross Lt. Cdr. V. Prather	113,739'	9 hours
USN-BuWeps STRATO-LAB VII	IN PREPARATION			

Figure 6. List of Seven Major WRI Manned Flights, U.S. Navy Project StratoLab,  
U.S. Air Force Project Manhigh

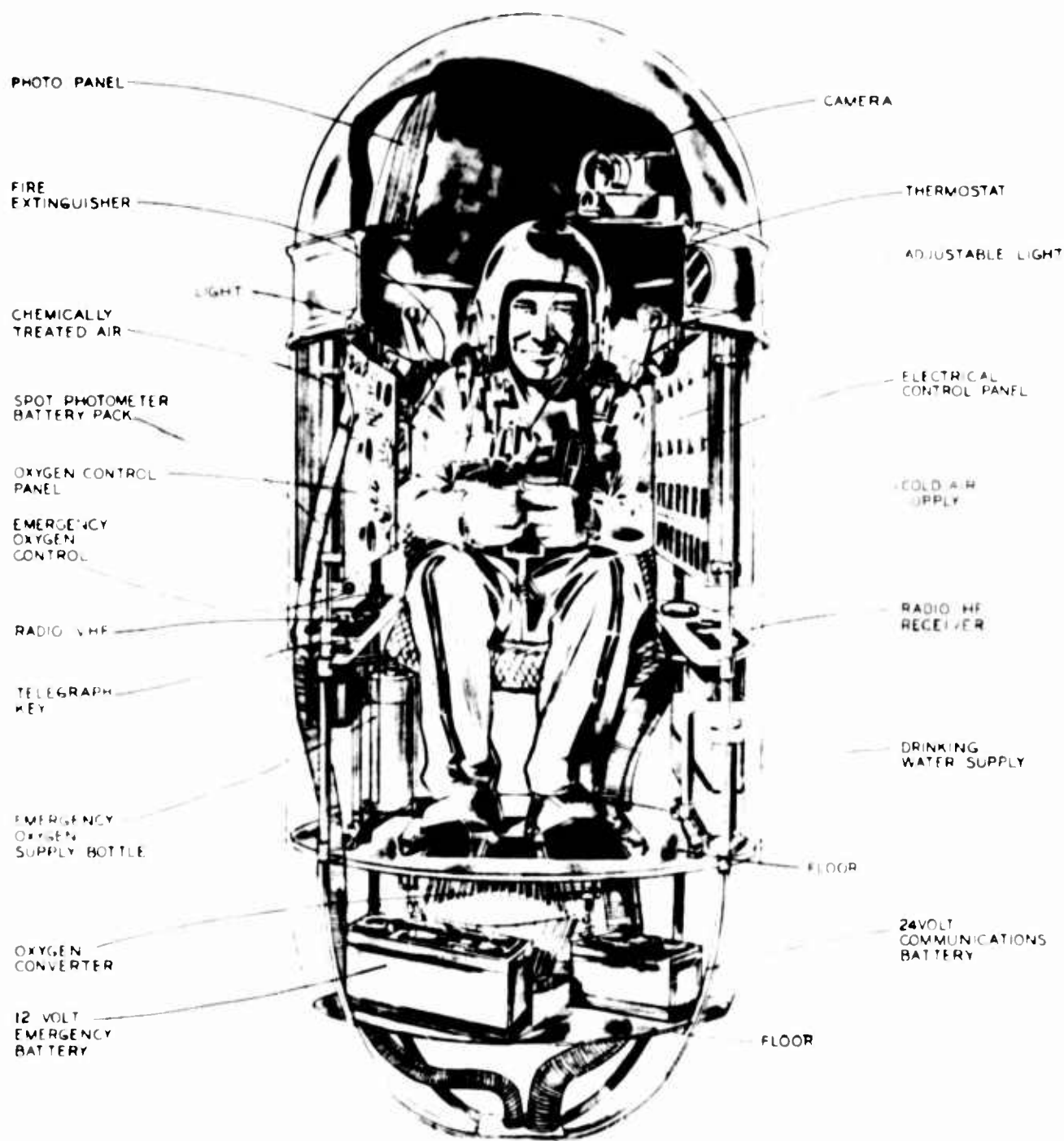


Figure 7. Artist's Drawing of Manhigh Gondola

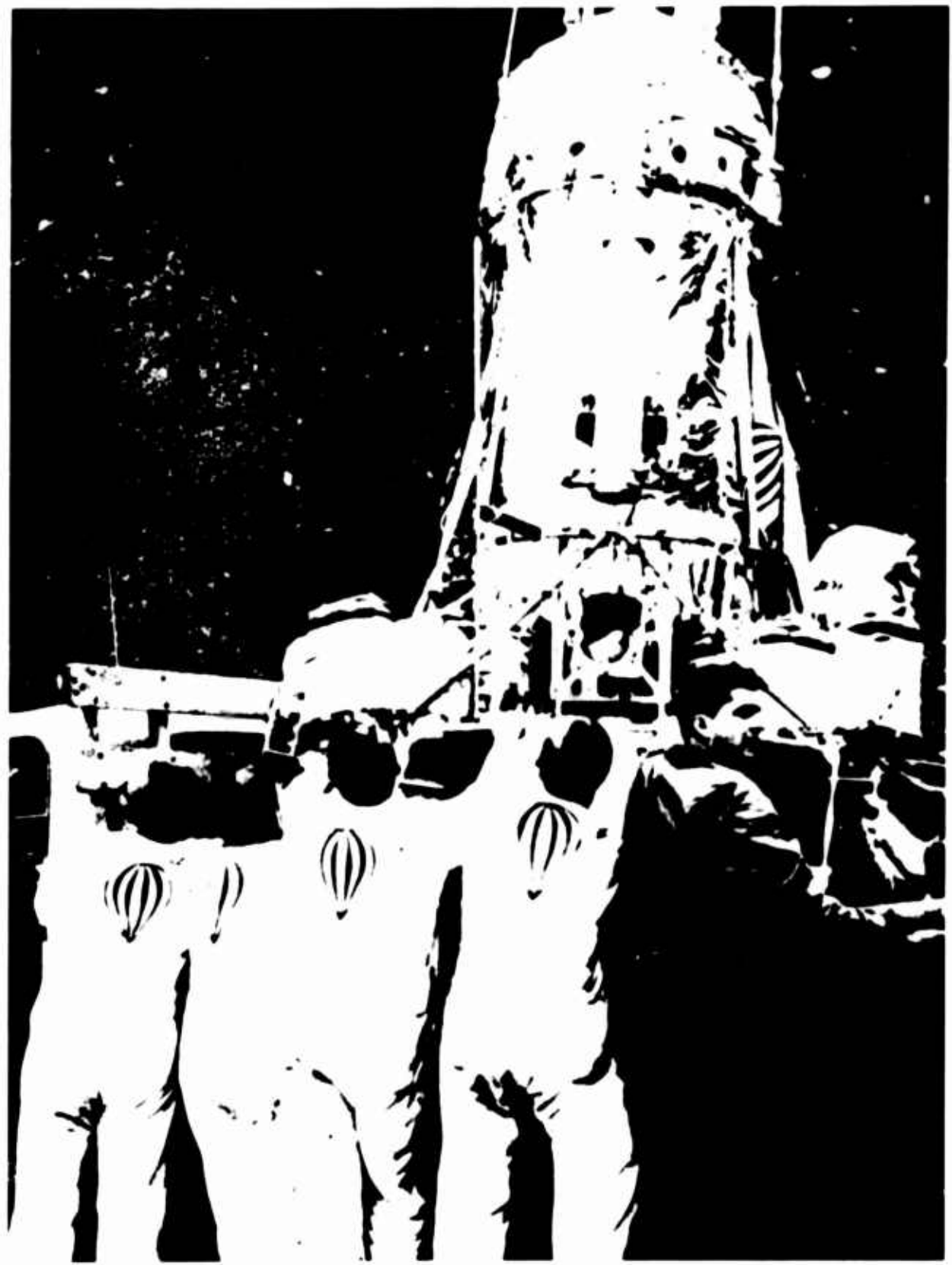


Figure 8. Manhigh II Gondola on Truck-Bed Prior to Launching from Open Pit Mine in Northern Minnesota. WRI crew of 10 men conducts launching.

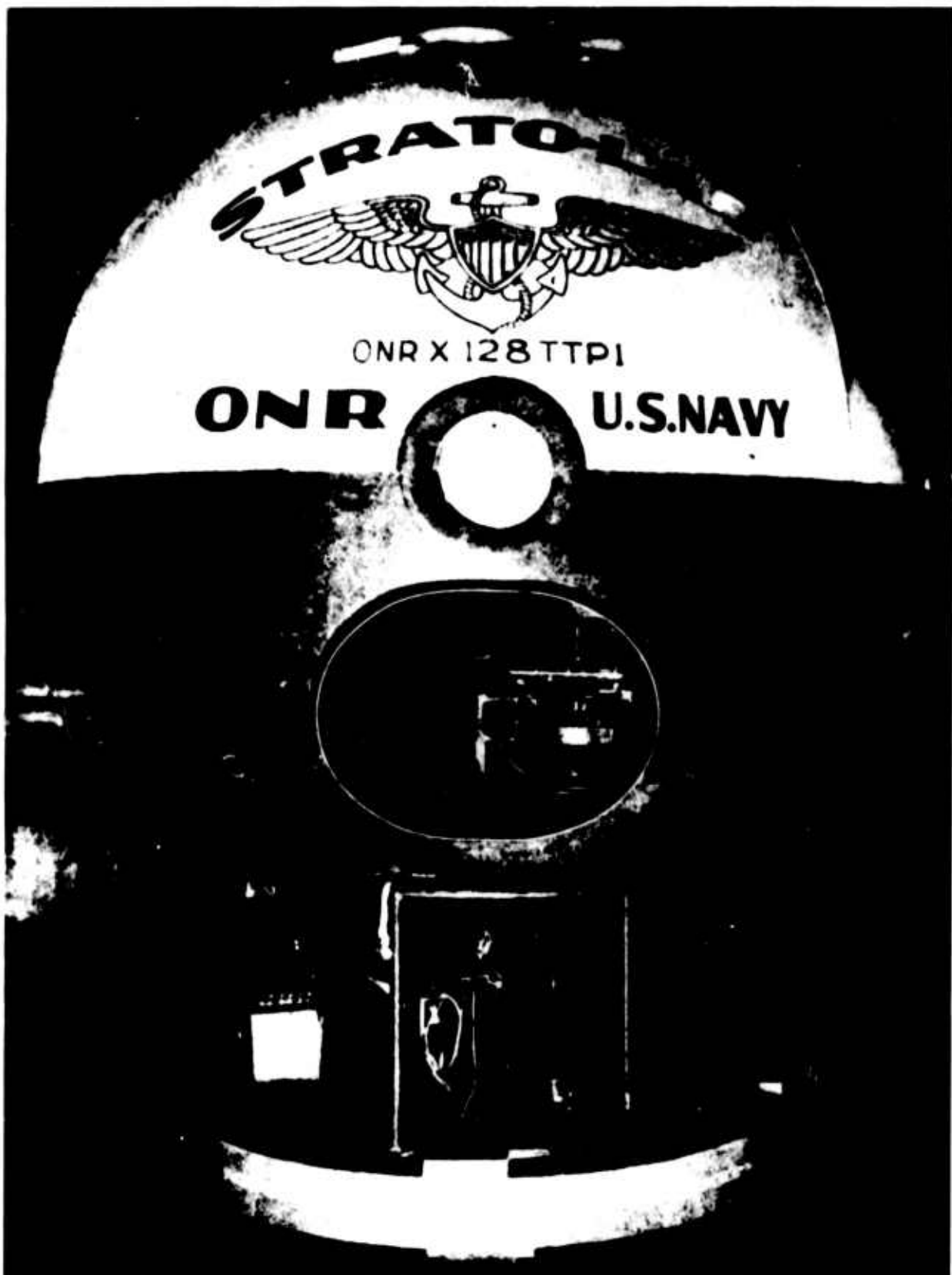


Figure 9. U.S. Navy StratoLab I and II Gondola for Daylight Flight Operations



Figure 10. U.S. Navy StratoLab IV Gondola with Johns-Hopkins Schmitt Telescope Prior to Launching From Strato Bowl South Dakota. First discovery of water vapor in atmosphere of planet Venus



Figure 11. WRI Balloon Launching From Open Pit Iron Mine in Northern Minnesota

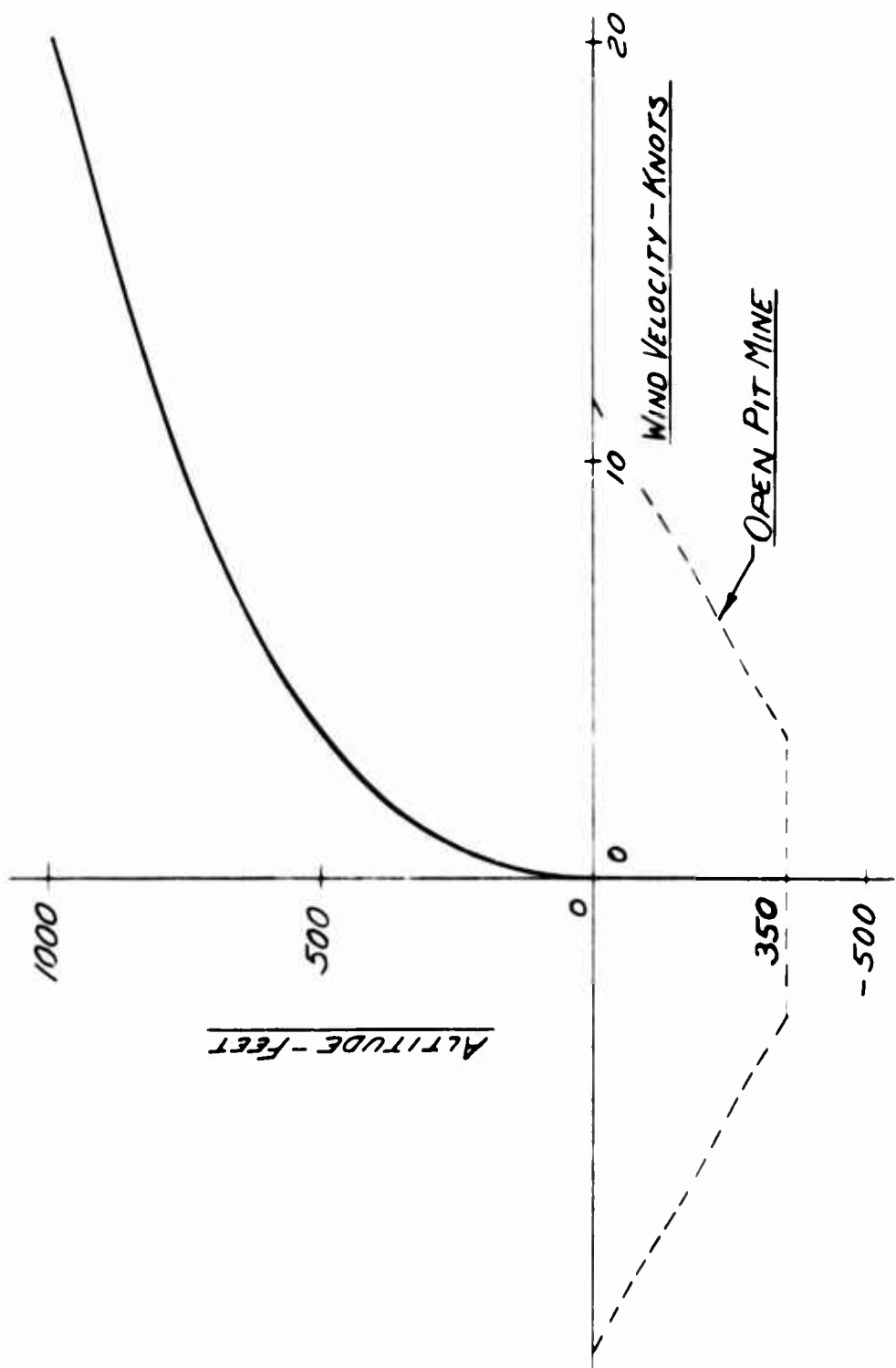


Figure 12. Diagram Showing Theory of Open Pit Launchings

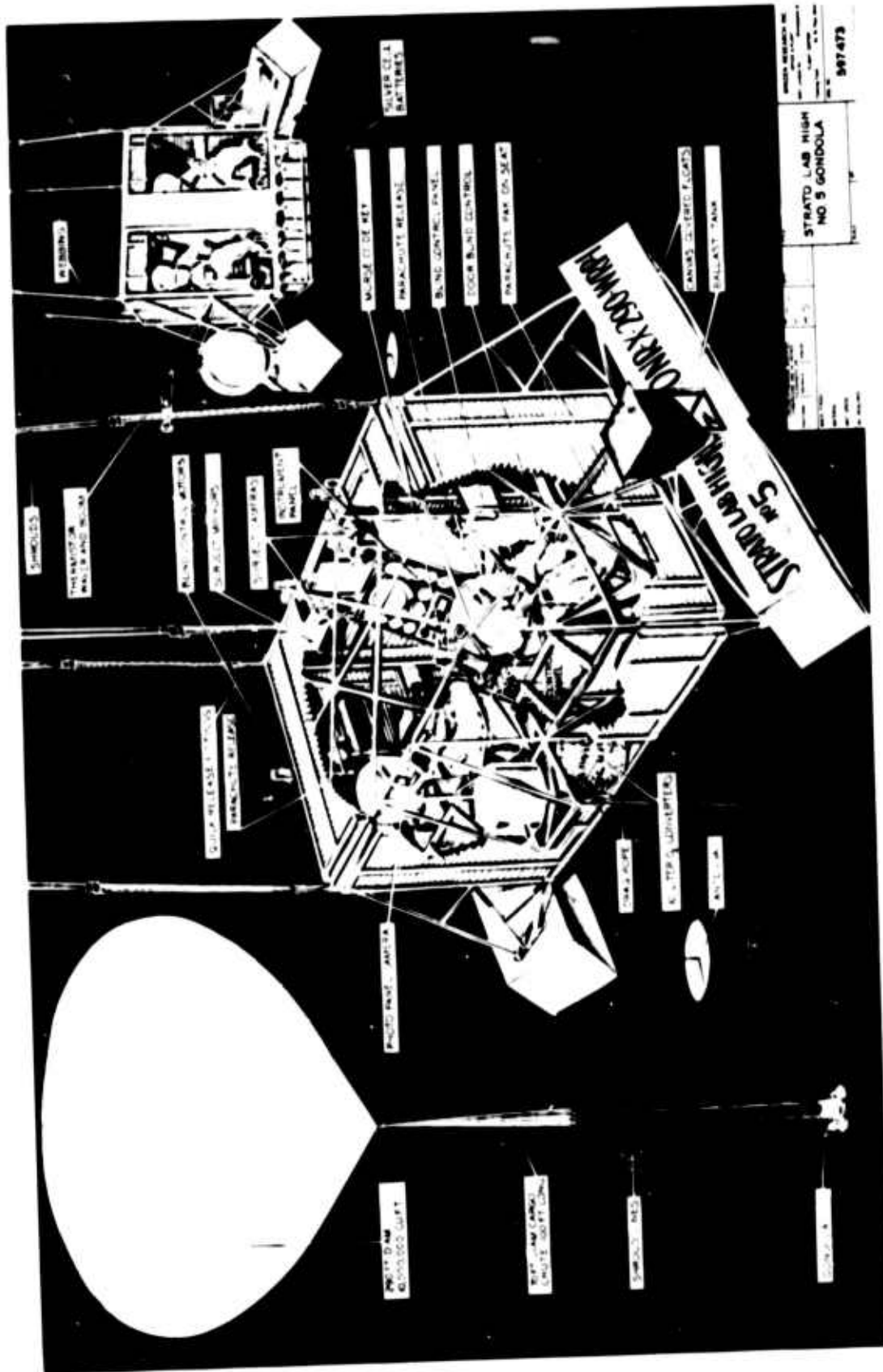


Figure 13. Artist's Drawing of StratoLab V Gondola

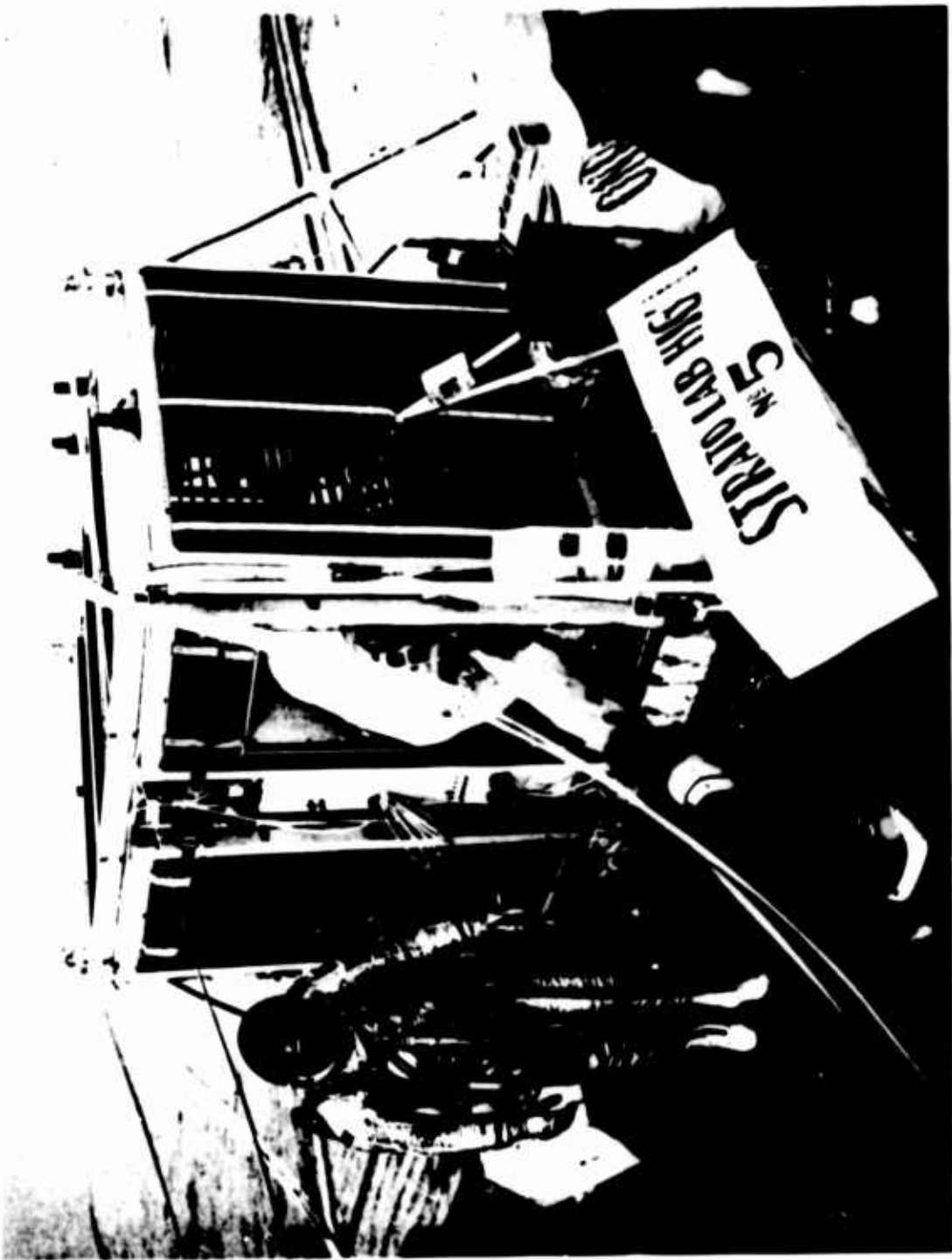


Figure 14. Stratolab V Gondola and Pilot Prior to Launching From U.S.S. Antietam; explanation of temperature control through electrically operated venetian blind system

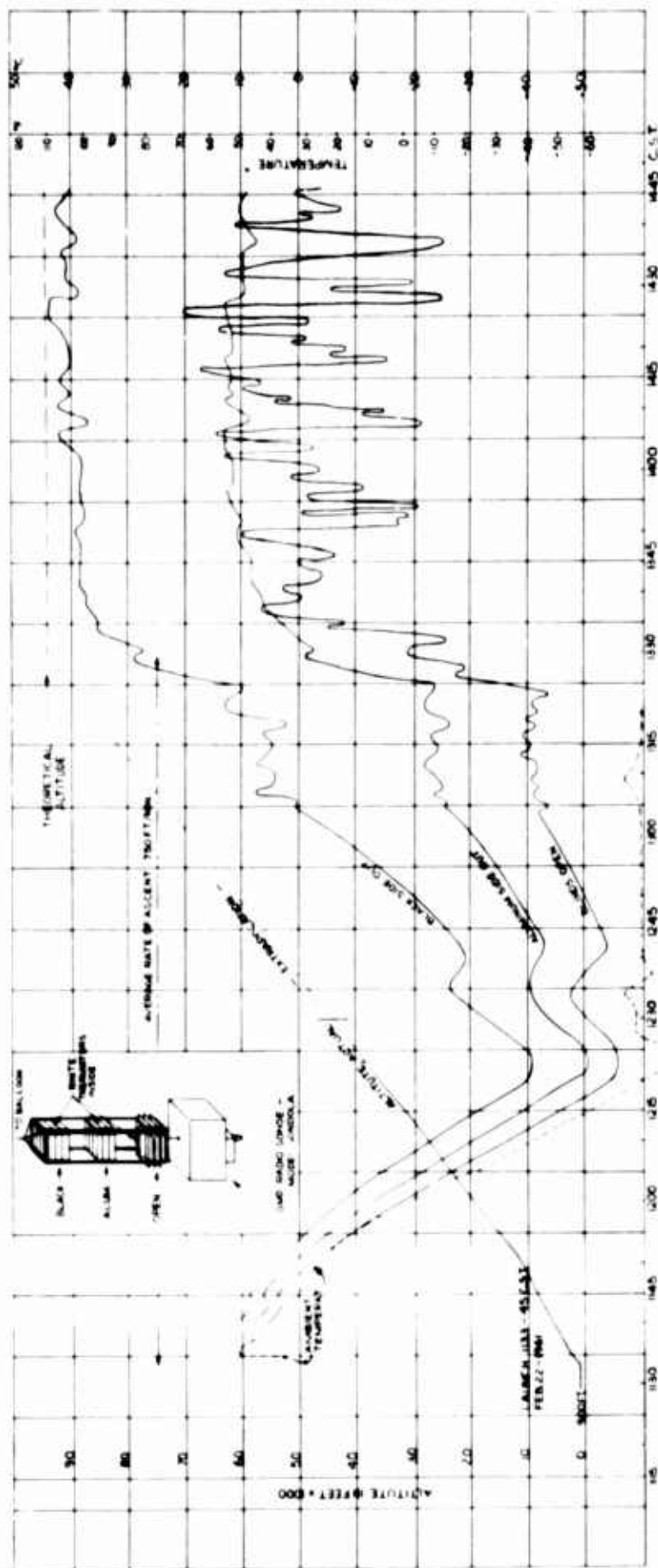




Figure 16. Stratolab V Gondola on the Carrier Deck During Preparation. Explanation of sealed capsule for transceiver.



Figure 17. Aerial View of U.S.S. Antietam with StratoLab V Aerostat Completely Erected Prior to Launching. Explanation of ideal nature of carrier launchings, tracking and recovery



Figure 18. StratoLab V Gondola. Pilots aboard pre-breathing oxygen, moments before launching



Figure 19. StratoLab V Test Gondola During Preparation for Training Launch on Deck  
of Carrier

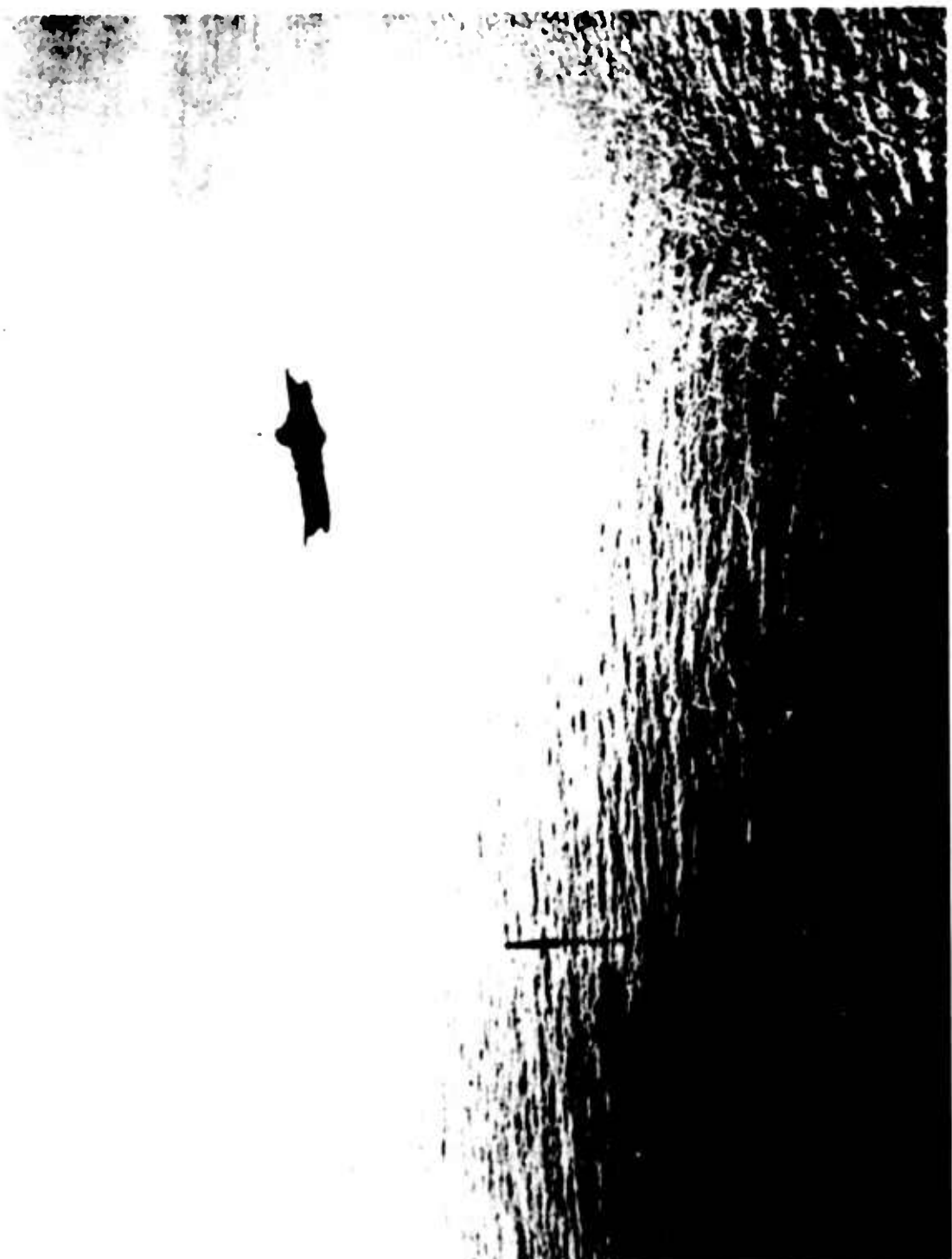


Figure 20. StratoLab V Gondola Floating at an Elevation of 150 Feet Above the Ocean,  
Carrier in Background

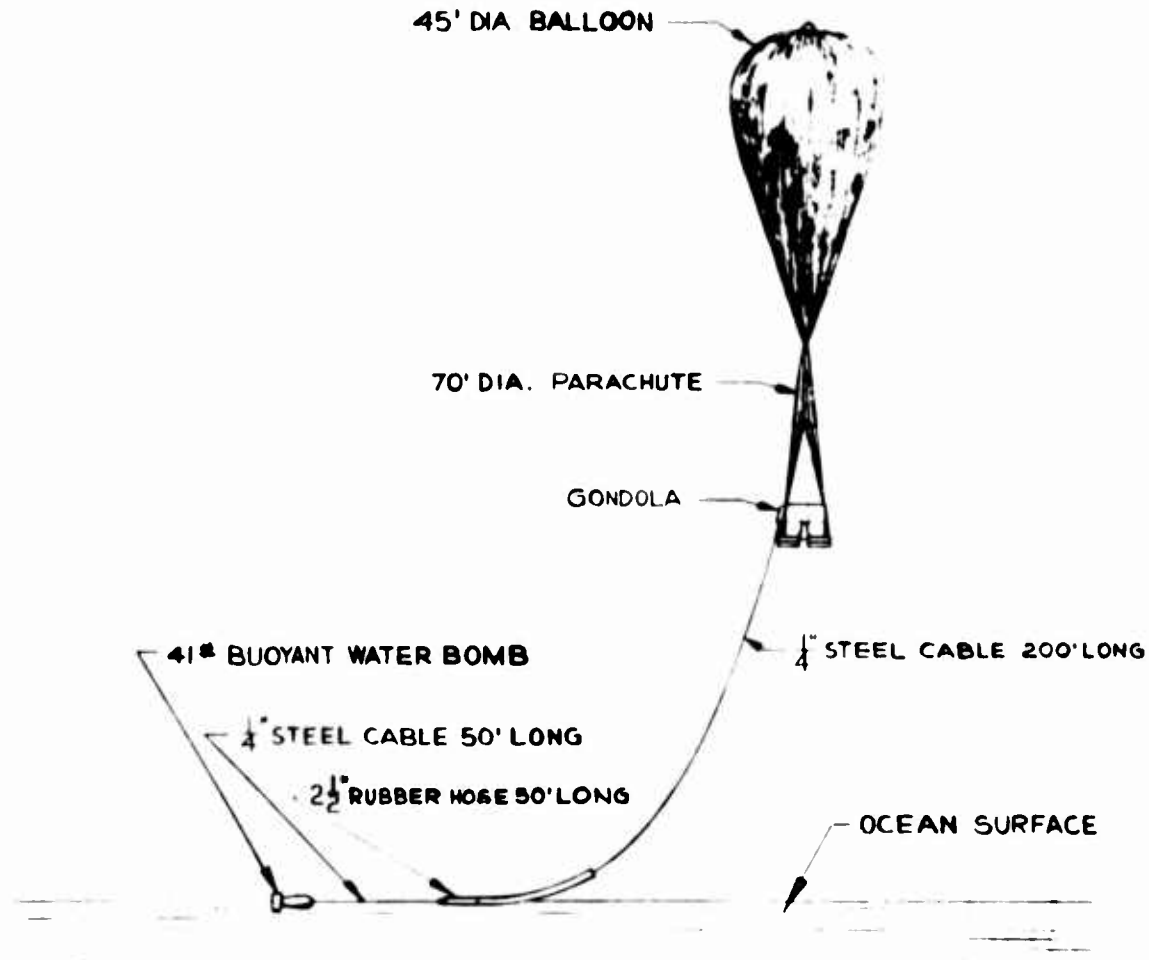


Figure 21. Diagram of Dry Recovery Method for Balloon Loads  
Applicable to Both Manned and Unmanned Balloon Flights

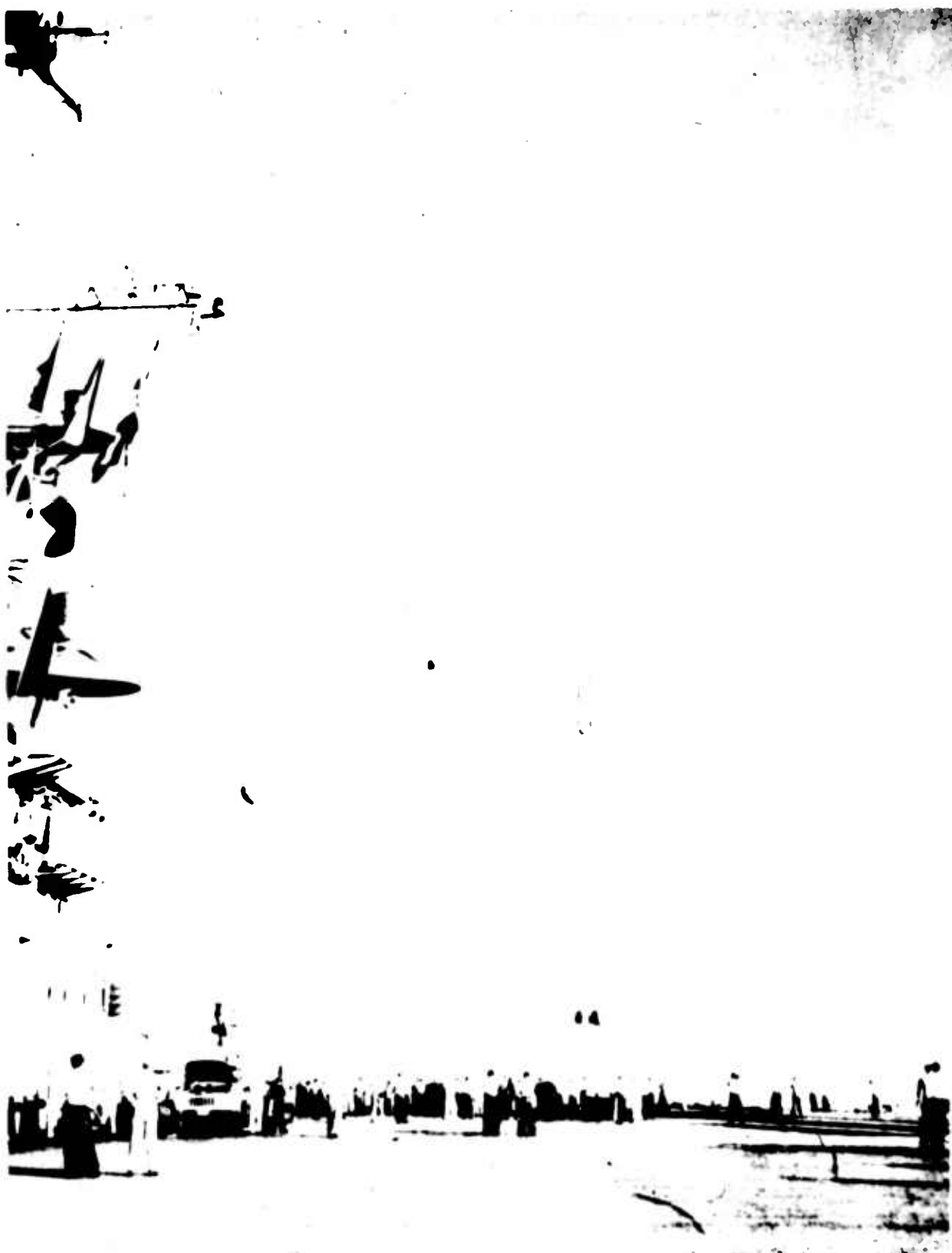


Figure 22. View of Stratolab V Test Gondola Being Hauled Down  
for Landing on After-Deck of Carrier

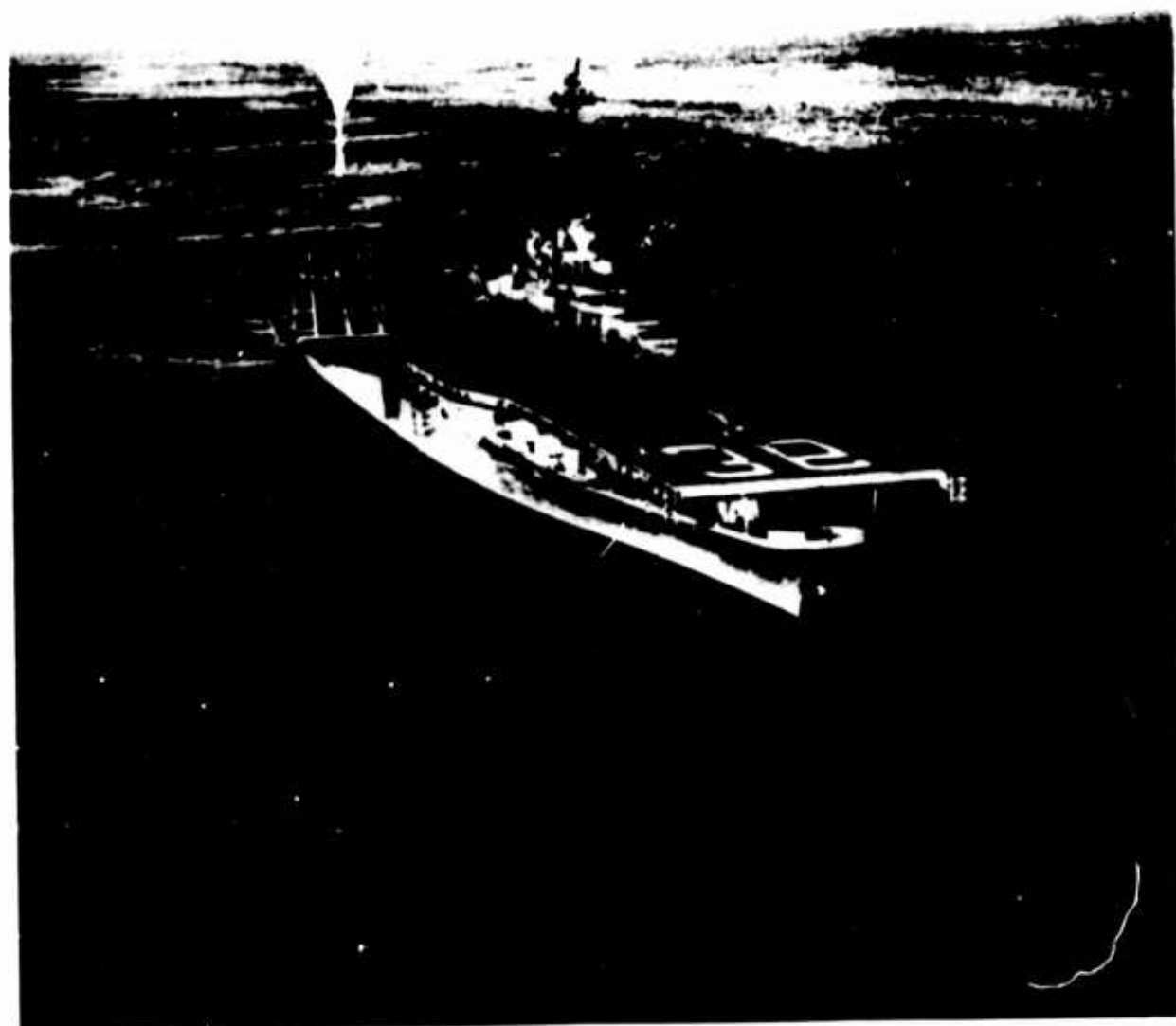


Figure 23. Side View of Carrier After Landing of Manned Test Gondola

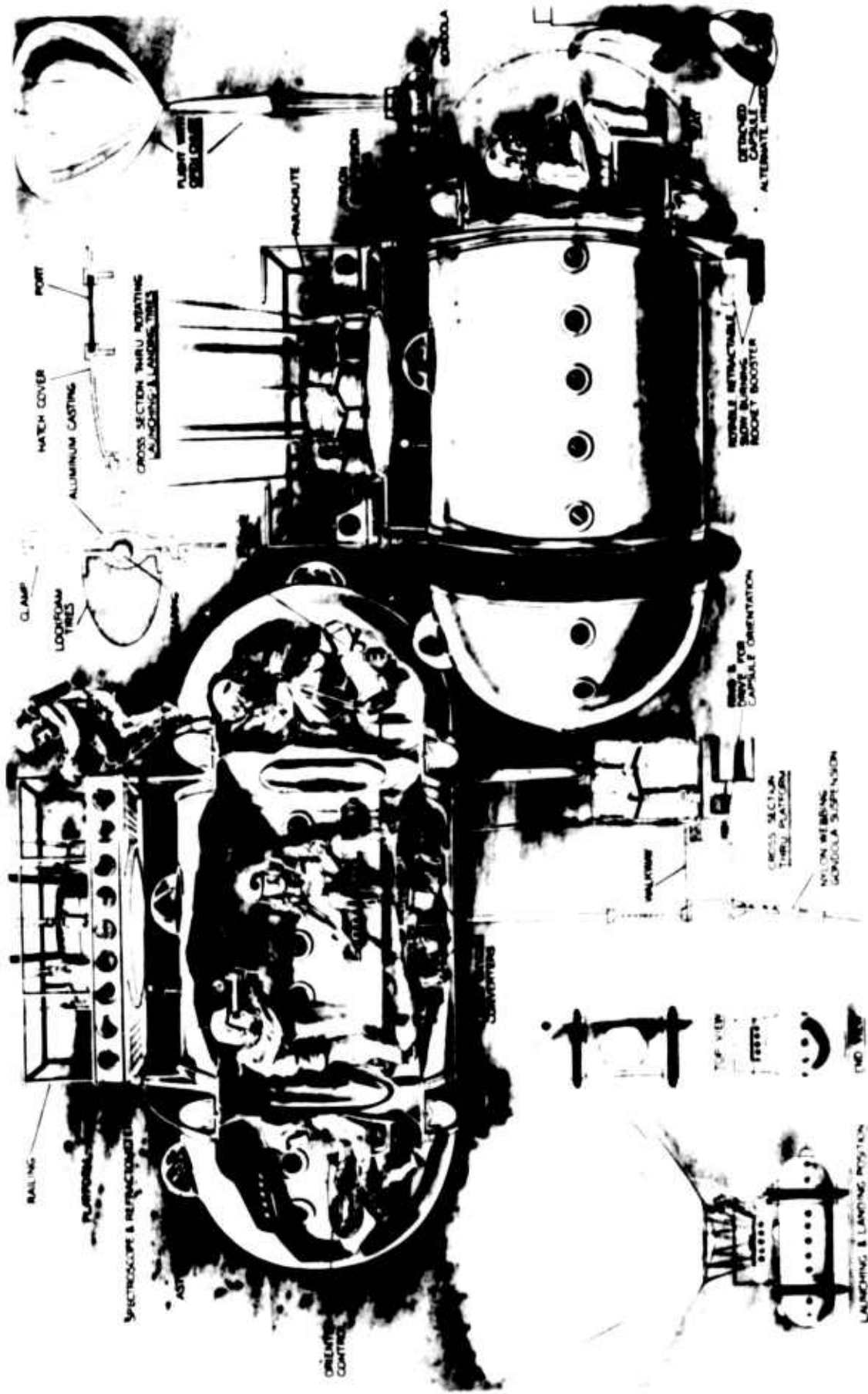


Figure 24. WRI Artist's Drawing for Proposal of Project SatelOrb Which Appears Like a Modern MOL Drawing but Was Prepared in 1957. Contract for this work which was to include flights of over one week duration with up to six persons aboard was cancelled when the Air Force Man-in-Space Program was halted at the end of 1958. The slide illustrates the various functions of the pilots and observers aboard, including a space surgeon. Other new concepts including those of a scientific panel at the control post on the ground were already part of this 1957 Project

## XXXII. Cosmic Ray Balloon Expedition to India, IQSY-EQEX

R. Kubara  
National Center for Atmospheric Research  
Boulder, Colorado

B. Stiller  
Nucleonics Division  
U. S. Naval Research Laboratory  
Washington, D. C.

Since early 1963, the United States Committee for the International Quiet Sun Year (IQSY) of the National Academy of Sciences has studied the feasibility of sending a balloon expedition to the vicinity of the equator during this IQSY period, to conduct research in the field of cosmic radiation. The committee held several meetings with interested experimenters and found that there was strong interest in such an expedition.

Informal discussions were held with Professor M. G. K. Menon, Director of the Cosmic Ray Laboratory, Tata Institute of Fundamental Research, Bombay, about the possibility of organizing a joint expedition. His group also expressed strong interest in such a venture and official sanction for the expedition was obtained from the Indian IQSY Committee.

The program thus became a joint Indo-American IQSY activity. A proposal for funding the expedition was submitted to the National Science Foundation and has been approved. The authors, Robert Kubara, National Center for Atmospheric Research, and Bertram Stiller, U. S. Naval Research Laboratory, are serving, respectively, as Project Manager and Scientific Coordinator.

Approximately 16 flights will be flown, all of them being planned to reach at least 120,000 feet and to stay at floating altitude for at least 8 hours. Table 1 is a table summarizing the experiments and the conditions necessary for successfully carrying them out. Two important scientific reasons for making these flights in India are:

1. To obtain cosmic-ray data near the earth's geomagnetic equator at altitudes much higher than previously attained.
2. To obtain these data during IQSY so as to permit comparison with data obtained at other latitudes during the same part of the solar cycle.

In addition, due to the development of new measuring techniques such as spark chambers and solid-state detectors, it will be possible for the first time for cosmic-ray physicists to intercompare data obtained by a large variety of detecting systems. This possibility is of special interest when analyzing data obtained near the geomagnetic equator because the earth's magnetic field permits mainly galactic cosmic radiation to reach the detectors. Such data can be used to study astrophysical problems connected with the origin of cosmic rays and with stellar evolution.

Two major problems faced the expedition in addition to the usual ones connected with diplomatic clearances, logistics and funding.

First, the location in India and the time of year had to meet the general requirements of long floating times and need for recovery. Although wind conditions are fairly well known up to about 100,000 feet for Central India where long duration flights are possible, essentially nothing is known about wind conditions above 120,000 feet. On the basis of a thorough operational analysis by Mr. Samuel Solot of the National Center for Atmospheric Research, using available data, it was decided to plan launching the flights in the period March-April 1965. During a recent survey trip to India for site location, discussions were held with Indian meteorologists which led to the same conclusions. Additional discussions with members of the balloon group at the Tata Institute of Fundamental Research, who have successfully flown and recovered 60 cosmic-ray experiments in Central India during the last several years, further strengthened our decision. The primary launch site will be Hyderabad, but two secondary sites, one on the east and the other on the west coast, were also selected to allow for strong easterly or westerly winds at floating altitude. In order to make trajectory forecasts, sounding balloons carrying hypsometers will be launched daily and tracked by our GMD-1 unit. This program will commence about two weeks before the cosmic-ray flights in order to provide current information about the wind conditions above 120,000 feet.

Second, the occurrence of tropopause temperatures as low as -80°C at these latitudes in the Spring could further aggravate the already-difficult problem of tropopause penetration by polyethylene balloons.

Table 1. Cosmic Ray Balloon Expedition to India-1965, IQSY-EQEX

Experimenter	Type of Apparatus	No. of Flights	Weight (lb)	Altitude (thousand ft)	Duration (hr)	Recovery
K. A. Anderson Univ. of Calif.	$\gamma$ + X-Ray Counters	3	40	130	$\geq 8$	Yes
J. G. Duthie U. Rochester	$\gamma$ - Ray Spark Chamber	2 day night	250	>120	15	Yes
J. T. A. Ely AFCRL	Charged Particle Counter Telescope	2	90	140	$\geq 10$	Yes
M. F. Kaplon U. Rochester	Solid State Detector Telescope	2 day night	220	140	12	Yes
S. A. Korff New York Univ.	Neutron Counters	2	100	140	$\geq 2$	Yes
K. G. McCracken SWCAR-Dallas	Counter Telescope	2	100	120	$\geq 8$	Yes
M. M. Shapiro NRL	Nuclear Emulsions	2	100	140	$\geq 12$	Yes
C. J. Waddington U. Minnesota	Nuclear Emulsions	1	120	140	$\geq 12$	Yes
J. R. Winkler U. Minnesota	Ionization Chambers	Several Hitchhikes	10	Any	Any	Yes
M. G. K. Menon Tata Institute	Emulsion Chamber	1	2000	100	30	Yes
M. G. K. Menon Tata Institute	Nuclear Emulsions	Several Hitchhikes	5	Any	Any	Yes

The use of mylar-scrim balloons was contemplated until it was shown that this material was not yet capable of being used for successful flights of large balloons. The introduction of Stratofilm by Winzen Research, Inc., gave us the opportunity to conduct a series of trial flights for the purpose of comparing this material with the "normal" polyethylene being used by other balloon manufacturers. Four, 3-million-cubic-foot, taped, 3/4-mil Stratofilm balloons were purchased from Winzen, and four similar but tapeless balloons of "normal" polyethylene were purchased from Raven Industries. All eight balloons were launched during OPERATION COLDTROP from Panama where low tropopause temperatures were expected. The launchings were carried out by NCAR personnel with the enthusiastic support of an observer from Winzen Research whose cooperation is gratefully acknowledged. Table 2 tabulates the results of these eight flights. Balloons made of "normal" polyethylene burst in 3 out of 4 flights and successfully penetrated the tropopause only once. The two Stratofilm balloons which were launched went into floating altitude successfully. Unfortunately, constructional defects in the other two Stratofilm balloons, discovered during inflation, forced us to abort these flights. As a result the already-limited statistical validity of our test program was drastically reduced. Our decision to use balloons made of Stratofilm on this expedition is therefore based primarily on the long history of "normal" polyethylene balloon bursts at the tropopause, including the three at Panama, and only secondarily on the 100%  $\pm$  70% success rate of the two Stratofilm balloons in Panama.

The flight operations will be conducted by Raven Industries and the anchor-line launch technique will be used for all flights, with the exception of the 2000-pound payload for the Tata Institute. This will be launched dynamically, using a launch arm mounted on a truck. All flights will be tracked by an aircraft which will also direct surface vehicles to the area of impact for recovery of payloads. If weather and other conditions permit, one flight will be launched every other day, so that approximately five weeks will be needed for all of them. The authors will be in the field for the duration of the expedition and will serve in their respective capacities in order to insure that optimum conditions exist from the point of view of each scientific group before a balloon flight is attempted.

Although the motivation for this expedition came from the cosmic-ray community, it is within the scope of the expedition to make exposures for other scientists. Questions concerning such exposures should be sent to either of the authors.

Table 2. Project Colddrop

Flight No.	Launch Date	Balloon Type	Balloon Weight (lb)	Gross Load (lb)	Free Lift (lb)	Ascent Rate (ft/min)	Flight Altitude (ft)	Remarks
1	8/5/64	Raven 3mm ft	456	781	88	1200	60,000	Balloon burst at 60,000 ft. Min. temp was -78°C @ 56,000 ft.
2	8/7/64	Winzen 2.94 NS	514	841.5	85	96.5	123,000	Successful flight. Trop. -76.3°C @ 53,000 ft.
3	8/8/64	Raven 3mm TT	444	767	61.5	930	126,000	Successful flight. Trop. -72.2°C @ 49,000 ft.
4	8/9/64	Winzen 2.94mm NS	520	845	68	88.5	123,000	Successful flight. Trop. -77.2°C @ 55,000 ft.
5	8/10/64	Raven 3mm TT	448.5	773.5	61.5	≈ 1000	51,000	Balloon burst at 51,000 ft. Temp. -71°C. Trop. -78°C @ 55,000 ft.
6	8/11/64	Winzen 2.94mm NS	566	891	80	0	0	Hole opened in balloon at top of 890 reinforcing tape 10 ft above inflation tube. 890 tape was attached directly to balloon without adequate reinforcement.
7	8/12/64	Winzen 2.94mm NS	559	884	79.5	0	0	Hole pulled in balloon at apex area starting at hoop and running out 18 in. Balloon not launched.
8	8/13/64	Raven 3mm TT	452	777	61.5	960	49,000	Balloon burst at 49,200 ft. Trop. was -75°C @ 49,000 ft.

### **XXXIII. The Technique of Clusters of Sounding Balloons**

**Audouin Dollfus**

**Section d'Astrophysique, Observatoire de Paris  
Meudon, Seine et Oise, France**

#### **I. THE TECHNIQUE OF CHAINS OF DILATABLE BALLOONS**

Dilatable sounding balloons with membranes of elastic latex or neoprene are currently used for lifting light payloads up to 100,000 feet. We developed a technique for linking many such balloons to carry heavy payloads.

Each balloon is manufactured with two necks, one at the bottom and the other diametrically opposite at the top. A vertical cable is passed through the two necks; the inferior neck is linked to the cable and carries the lift; the zenithal neck is gas-tight around the cable, but can slip along this cable to accommodate the balloon's increase in size with altitude (Figure 1).

By ropes and winches we were able to build up more than 30 such balloons one above the other, like a string of beads. The first balloon at the top has a single neck and is less inflated than the others in order to avoid a premature burst which might cause the cable and fragments to fall on top of the second balloon, and so on.

Preliminary experiments were conducted with French Delacoste 2,000-gram balloons, and with British Beritex 4,500-gram balloons carrying 16 pounds each at 85,000 feet. We finally used Dewey and Almy large 7,000-gram neoprene Darex balloons, each lifting 70 pounds at 100,000 feet.

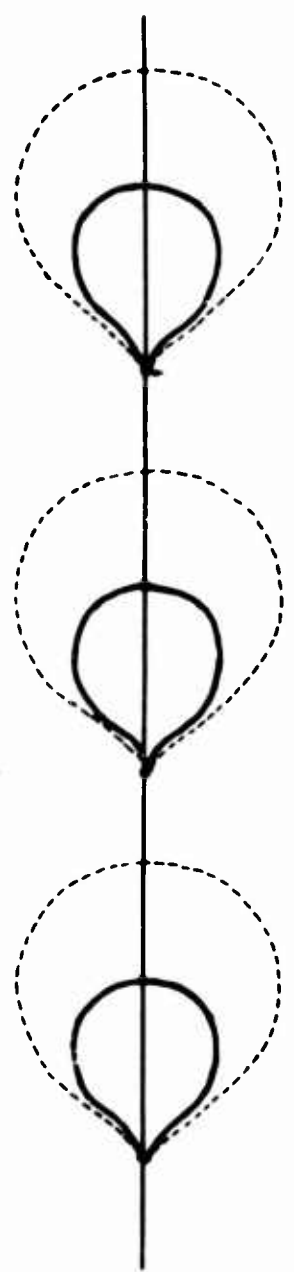


Figure 1. Schematic Drawing of a Chain of Dilatable Sounding Balloons

Some of these balloons were tested on the ground by inflating with compressed air to the bursting point. Balloons of different categories were studied also with increasing lifts and payloads to the limit of strength of the membrane around the inferior neck carrying the weight. The designs of the necks and load holders were improved and tested in flights; large Darex 7,000-gram single balloons were successfully launched with lifts as high as 90 pounds.

Aerodynamical drags on these balloons were studied. For the experiments on horizontal drags, the balloon or clusters of balloons were linked to a lorry moving with increasing speed against the wind. Deformations of the balloons were recorded, critical values were deduced above which expansion of the membrane in vail sharply increases the drag coefficients.

Vertical drags, with the change of aerodynamical type of flow for a critical value of the Reynolds Number and its reaction on the balloons, were studied in flight with high-sensitivity radar trackings.

Taking into account the information gained from these experiments on single balloons, we were able to proceed to the study of chains of 5 to 25 balloons, for flights with heavy payloads (Figures 2 and 3). Routine flights were launched with wind-velocity tolerance near the ground ranging up to 12 knots. Payloads of 500 pounds are lifted with rapid ascending rates of 1,500 feet per minute. Approaching the mean altitude of burst, some balloons burst, reducing the rate of ascent, and finally the whole equipment stabilizes at ceiling altitude, generally between 90,000 and 100,000 feet. Durations at floating altitude are difficult to predict if no ballasting is involved, but often range between 15 and 90 minutes.

Of particular interest is the versatility of the technique, and the safety of the design. The danger of failure of balloons, caused in large plastic balloons by defects in fabrics, is minimized by the great number of balloons. The technique is particularly safe for manned flights. The author experienced a night flight in a sealed cabin weighing 1500 pounds, with a five-hour duration at 43,000 feet, lifted by a chain of 104 Beritex balloons clustered according to a preliminary and less elaborate technique (successive stages of clusters of 3 balloons). A report of this flight is given by the author in the following paper.

## 2. APPLICATION OF CHAINS OF BALLOONS FOR THE STUDY OF WIND SHEAR STRUCTURES

Some of the instrumental payloads launched for unmanned flights include a vertical camera recording motions of the clusters of balloons. The motion of the great vertical chain of balloons seen from below is a very sensitive indicator of the wind shears in the earth's atmosphere. Figure 4 illustrates the successive

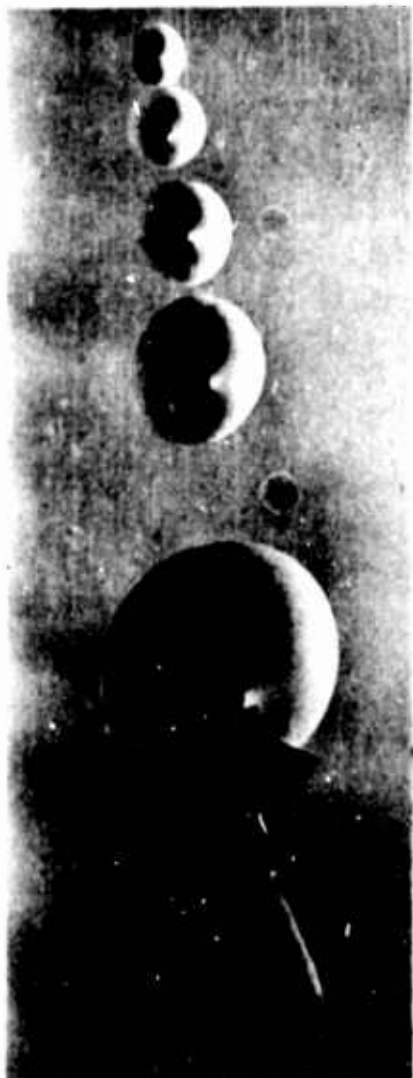


Figure 2. Chain of Balloons for Flights with Heavy Payloads

configurations of the cable when passing through a sharp layer of discontinuity of wind velocities. Figures 5 and 6 are selected photographs taken from films recorded in flight by the camera located in the gondola. Time intervals and differences of height (in meters) between each frame and the first one are reported.

From these illustrations one can deduce the successive configurations of the cable. These data are compared with the vertical shapes computed for different relative-wind velocities between two layers. Different thicknesses for the intermediate layer and the resulting vertical wind-velocity gradients in that layer are also investigated.

The films often disclosed very sharp discontinuities in wind velocities. The intermediate layer was often found to be very thin, the increase of wind velocities being localized in less than 40 meters only.

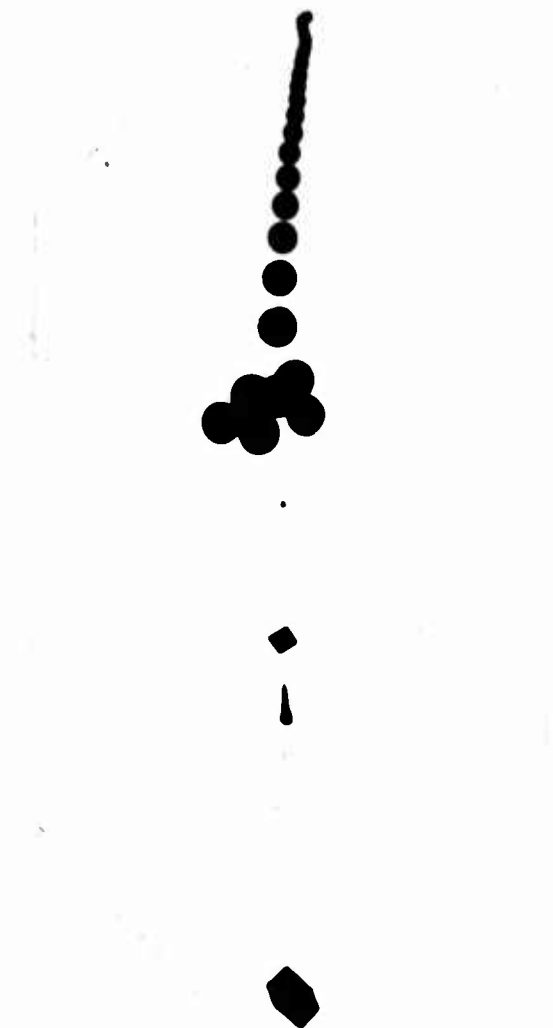


Figure 3. Chain of Balloons for Flights with Heavy Payloads

Resulting gradients as high as 0.2 or 0.4 meters per second for each meter of difference in height are indicated. These figures are larger than those resulting from the conventional technique of study of wind shears by accurate radar tracking of single sounding balloons. The layers of discontinuities are sharper than expected.

### 3. STUDIES OF SCINTILLATION OF STARS AND DISTURBANCES IN TELESCOPIC OBSERVATIONS

The wind-shear discontinuities are responsible for optical inhomogeneities in the earth's atmosphere. The turbulent layers generate disturbances in the propagation of beams of light; as a result, telescopic observations of stars and planets are blurred, and stars twinkle.

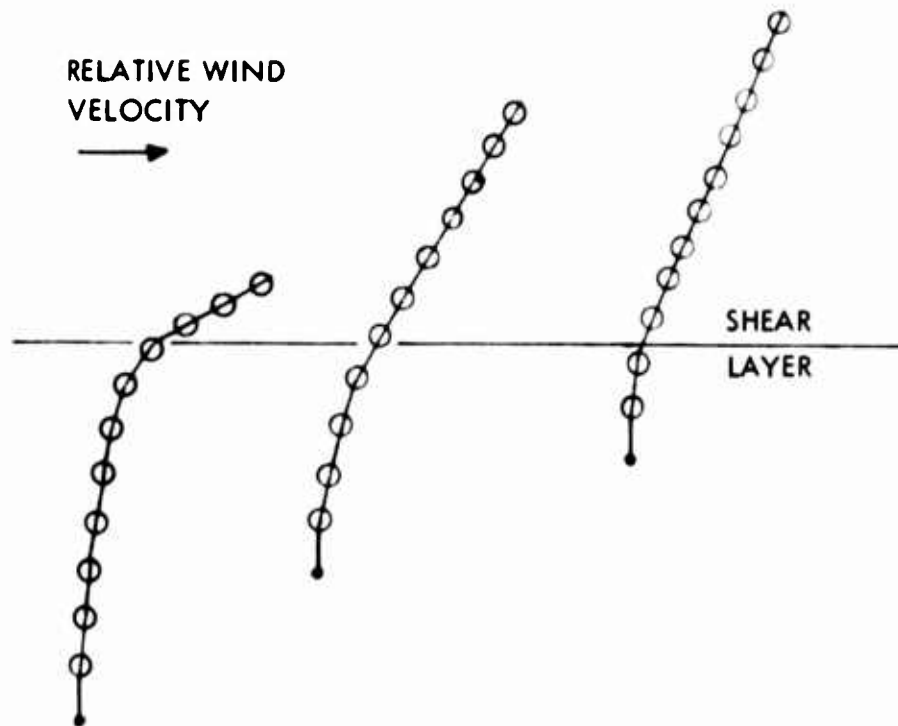


Figure 4. Configurations of a Chain of Balloons Passing Through a Shear of Negligible Thickness



Figure 5. Photographs of Chain of Balloons Taken in Flight by Camera in Gondola

C H A P E L E T D E 21 B A L L O N S.

30 MARS 1960 :  $t_0 = 0^{\circ}\text{C}$  TU.  $s_0 = 10,600 \text{ m.}$

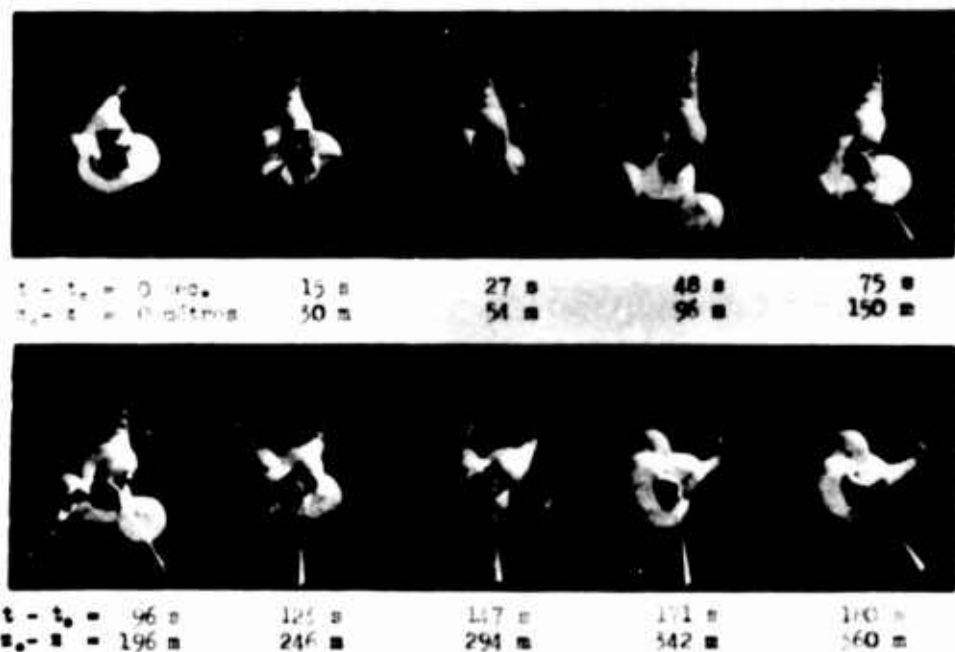


Figure 6. Photographs of Chain of Balloons Taken in Flight by Camera in Gondola

One purpose of our balloon observations was the study of these effects. On March 30, 1960, the temperature recorded by thermistors on board was respectively  $-53^{\circ}\text{C}$  and  $-58^{\circ}\text{C}$  above and below a sharp shear of  $0.2 \text{ second}^{-1}$ . The pressure was 240 mb and the resulting refractive indexes,  $n$ , were computed respectively to be  $77 \times 10^{-6}$  and  $79 \times 10^{-6}$ . The difference  $\Delta n$  amounted to  $2 \times 10^{-6}$ . A differential geometrical path of only  $L = 10 \text{ cm}$  generates a difference of optical path,  $\Delta n \cdot L$ , of 0.2 micron larger than the limit of tolerance of one quarter of a wavelength needed for perfect imaging of the telescope.

Very faint waves in the dioptric, with slopes of the order of only 20 inches, when the focal length is of the order of 10 km, make the light converge and diverge. They generate the rapid variations of brightness of stars called scintillation. Observations at different heights by the author during nighttime manned balloon flights showed that scintillation of stars appeared to be connected with the wind shears recorded by sounding balloons. Approaching a layer disturbed by shears the scintillation increases because the waves focusing light on the observer are of increasing slopes. Above the disturbed layer, the situation immediately improves.

Stellar scintillation and the blurring of the seeing through ground-based astronomical telescopes are clearly proved to be generated at least in part by shears in the motions of layers of air in our atmosphere.

**References**

Dollfus, A. (1962) C. R. Acad. Sci. 255:148.

## XXXIV. Detection of Water Vapor in the Atmospheres of Venus and Mars

Audouin Dollfus

Section d'Astrophysique, Observatoire de Paris  
Meudon, Seine et Oise, France

Since 1954 we have developed a program for spectroscopic detection of water vapor in the atmosphere of the planets Venus and Mars. The procedure consists of a photometric comparison of the intensities of the H<sub>2</sub>O infrared spectral absorption bands between the planets and the Moon (or the Sun). After reduction to the same paths in the atmosphere, and provided the spectral band is not saturated, the difference between the two signals delivered by the planet and the Moon (or the Sun) indicates the amount of water in the atmosphere of the planet.

High sensitivity requires selection of a strong spectral band, but these bands are desaturated only at high altitude in our atmosphere. Therefore, a balloon-borne telescope is particularly appropriate for our program.

To select the required wavelength range of spectrum centered on an absorption band of H<sub>2</sub>O, we used a birefringent filter of the type designed by B. Lyot. Figure 1 shows the principle of the modulation of the light by an absorption band. A periodic change in the orientation of the last polarizer in the birefringent filter gives alternately a transmission curve of Type 1 centered at the absorption band (Position 1), and of Type 2 with two maxima on the continuum on both sides of the absorption band (Position 2).

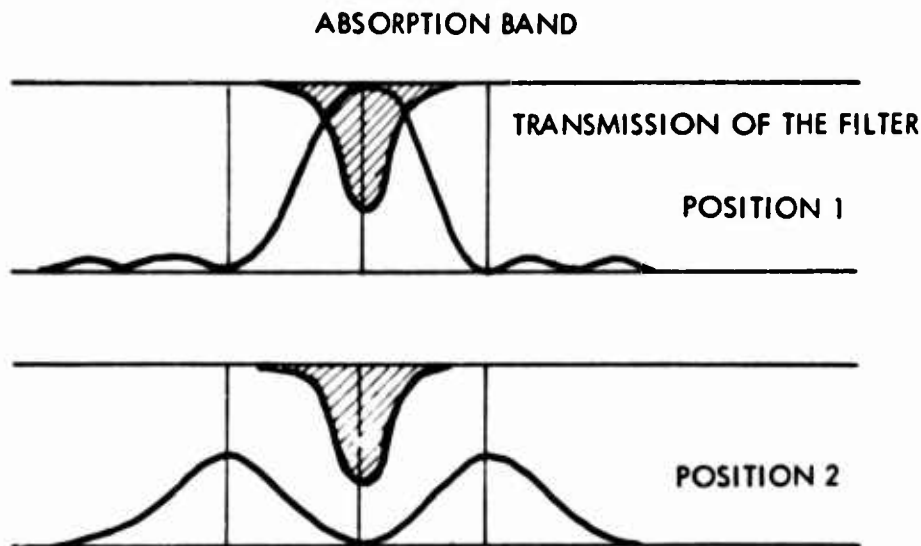


Figure 1. Modulation of Light by an Absorption Band

The main advantage of this technique is its large field. The filter has a surface of 1.5 inches  $\times$  1.5 inches, corresponding to a field of half a degree at the focal plane of the telescope (Figure 2). Such a large tolerance for the pointing of the telescope demands no accurate tracking and no elaborate image-stabilization device; manual control of the telescope by the observer, who looks at the field through the eyepiece of an auxiliary telescope, provides the required accuracy with no additional electronics. Figure 3 is a sketch of the balloon-borne telescope.

In order to test the feasibility of telescopic astronomical observations from a balloon, and to select the best spectral band for the detection of water in planetary atmospheres, we organized in 1954 a preliminary manned balloon flight.

A specially-designed azimuthal telescope equipped with an infrared spectrophotometer was flown to 23,000 feet during a seven-hour nighttime manned balloon flight - historically the first balloon flight instrumented for astronomical telescopic observations - (Figure 4). We observed Mars, the Moon and the Sun. Our observations showed the amount of water above 20,000 feet to be  $0.026 \text{ gr/cm}^2$ . We concluded from this flight that a balloon-borne gondola has enough stability for the operation of an astronomical telescope, and that the 1.4-micron band of  $\text{H}_2\text{O}$  is suitable, with the high sensitivity of the lead sulfide photocells, provided that the balloon observations are made at altitudes of at least 40,000 feet.

Since 1956 we have designed a very light sealed cabin, a sphere 72 inches in diameter and weighing 280 pounds. An azimuthal Cassegrain 20-inch telescope was attached above the gondola (Figure 5). Manual operation was from inside the cabin.

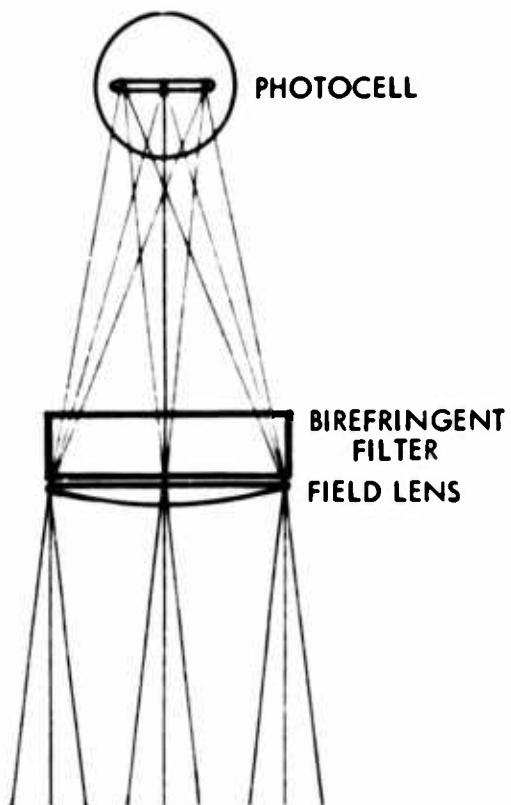


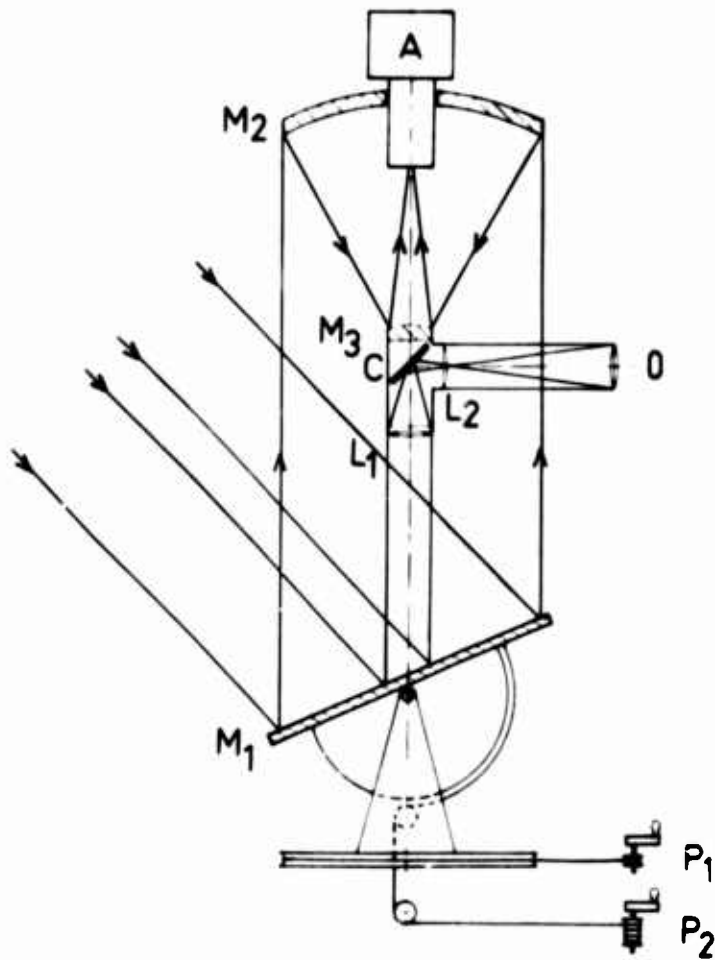
**Figure 2. Focal Plane of Telescope**

This stratospheric laboratory, weighing 1,500 pounds at launch including the observer and the ballast, was lifted by a cluster of 104 dilatable sounding balloons organized in 34 groups of three balloons, one above the other, along a vertical cable 1,400 feet long (Figure 6).

Launch was achieved at sunset on 22 April 1959 from Villacoublay Air Force Base near Paris (France). The five-hour night flight reached a long steady level at 43,000 feet. During the flight the author collected data on Venus and the Moon. The descent was operated by radio command on board, to an explosive switch releasing 18 balloons at the top of the cable. A landing in full night was followed by the pilot's phone call from the nearest village and a prompt recovery by the ground-tracking operation.

The operation of the telescope during the flight resulted in the following:

a) Information about the variations in the scintillation of stars with height, their close connection with the existence of atmospheric shears as observed by the tilt of the clusters of balloons, and their complete disappearance above the tropopause. These results are given in the conclusion of the first paper by the author given at this Symposium (XXXIII).



M<sub>1</sub> - FLAT MIRROR - AZIMUTHAL MOUNTING OPERATED BY P<sub>1</sub> AND P<sub>2</sub>  
 M<sub>2</sub> - PARABOLIC MIRROR OF 20". FOCAL LENGTH 60"

M<sub>3</sub> - CASSEGRAIN MIRROR

A - SPECTROPHOTOMETER WITH BIREFRINGENT FILTER

C - ADDITIONAL TELESCOPE FOR GUIDING

O - EYEPIECE

Figure 3. Balloon-Borne Telescope for Detection of Water Vapor in the Atmosphere of Planets



Figure 4. Balloon for Astronomical Observations Used for Flight of 30 May 1954 by Audouin Dollfus

b) A calibration of the IR spectrometer telescope for water-vapor measurements when the  $H_2O$  band at 1.4 microns is desaturated, and a measurement of the total amount of water vapor in the earth's stratosphere above 40,000 feet of at least  $0.005 \text{ gr/cm}^2$ . This high value assumes that, at the mean temperature of  $-60^\circ\text{C}$  of the stratosphere, the layers of air must be close to saturation in a large fraction of the stratosphere.

c) Preliminary measurements of the 1.4-micron band of water vapor on Venus; the result was marginal because an unexpected delay of half an hour at launch meant that the planet was not high enough above the horizon.



Figure 5. Stratospheric Sealed Gondola with 20-Inch Telescope

The careful study of the data collected during the flight enabled us to conclude that there were two ways to solve the problem of water vapor in the atmospheres of planets:

- a) By the same technique of stratospheric balloon flights. New flights may benefit by further improvements in the stabilization of the gondola, and by increase of the ceiling altitude.
- b) Alternately, by observations from high mountain sites with the same telescope calibrated from previous stratospheric flight, in exceptionally dry air at very low winter temperature, associated with a careful study of the amount of

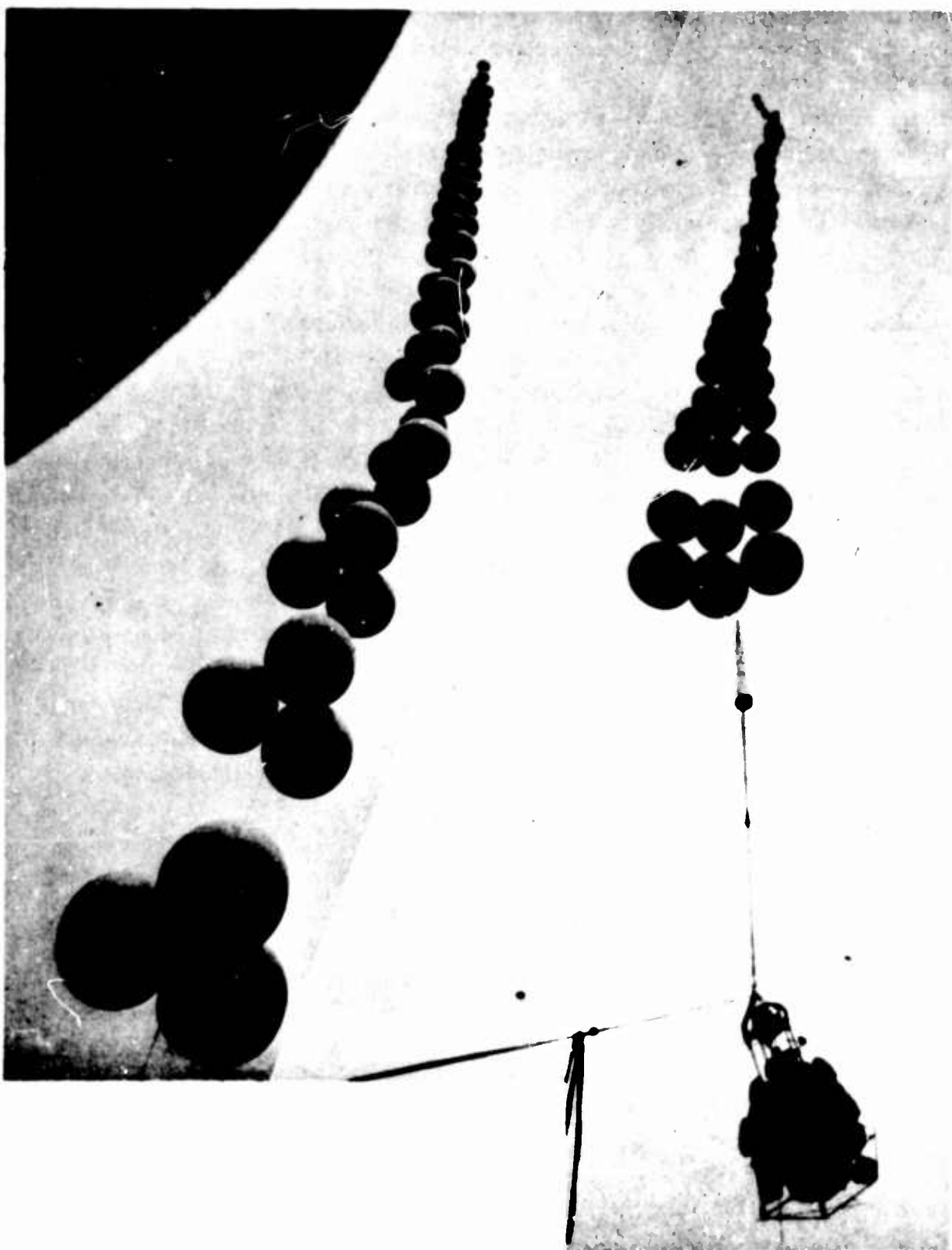


Figure 6. Chain of 104 Dilatable Sounding Balloons for the High Altitude Flight of 22 April 1959 by Audouin Dollfus

water in our atmosphere by nearest stars, the Moon or the Sun, to disentangle the faint signal delivered by the planet from the strong signal remaining from our atmosphere.

We went on simultaneously with both of these two ways, competitively.

During 1961 and 1962 several attempts were made to launch a new manned high-altitude balloon flight, from Orleans-Bricy and Villacoublay Air Force Bases. The improved lifting device was a chaplet-like cluster of 23 neoprene Darex 7,000-gram balloons, able to lift the strato-laboratory with the author on board up to 80,000 feet. This improved technique was described in detail in the first paper by the author at this Symposium. We were very unfortunate with weather conditions because required situations occurred always at new moon or during periods inappropriate for the positions of the planets in the sky.

Unexpected good weather conditions were finally reached for the high-mountain winter survey at the Jungfraujoch Scientific Station in Switzerland, in January, 1963. The altitude was 3.5 km, the temperature -35°C and the humidity below 15 percent during the best nights. One can compute that the remaining amount of water in the atmosphere above the station was low enough to desaturate the H<sub>2</sub>O band at 1.4 microns (saturation reached for 0.1 gr/cm<sup>2</sup>) in a vertical column above Jungfraujoch. Adequate studies of the very rapid variations of this amount with time, zenithal distance and azimuth were based mainly on observations on the Sun, the Moon and the star α Orionis. Direct measurements on Venus and Mars, and deduction of the contribution due to the earth's atmosphere enabled us to collect positive results about the amount of water in the atmosphere of these planets.

Reductions of these data, including several minor corrections and recalibrations, yielded the following values:

For Venus, about  $0.7 \times 10^{-2}$  gr/cm<sup>2</sup> of water above the cloud level for calibration at STP. This amount must be increased if the unknown atmospheric pressure at the cloud-top altitude is found to be small.

For Mars, about  $1.5 \times 10^{-2}$  gr/cm<sup>2</sup>. Possibly a reduction of this value may be investigated, depending on further tests on the expected Martian ground spectral reflectivity, still under completion at the Laboratory.

**References**

- Dollfus, A. (1954) C.R. Acad.Sci. 239:954.  
Dollfus, A. (1959) L'Astronomie 345:411 and 467.  
Dollfus, A. (1959) C.R. Acad.Sci. 249:2602.  
Dollfus, A. (1963) C.R. Acad.Sci. 256:3009 and 3250.  
Dollfus, A. (1964) L'Astronomie 41.

## **XXXV. The PARAVULCOON Recovery System — Aerial Deployment Feasibility Studies**

**A. J. Oberg  
Honeywell, Inc.  
Hopkins, Minnesota**

**R. A. Pohl  
Raven Industries, Inc.  
Sioux Falls, South Dakota**

**C. L. Pritchard  
Raven Industries, Inc.  
Sioux Falls, South Dakota**

### **Abstract**

The PARAVULCOON System is a terminal recovery scheme wherein the buoyancy of an aerially-deployed, inflated, and heated balloon filled with hot air is used to accomplish the atmospheric flotation and controlled descent to touchdown of the recovered body. The aerial-deployment phases of the system-activation sequence have not been previously demonstrated with practical sized systems, and furthermore are not amenable to analytical verification. Therefore, the program reported here was undertaken to experimentally demonstrate their feasibility.

The PARAVULCOON concept was originated by Raven Industries, Incorporated, and the overall system capabilities have been developed by Honeywell, Incorporated and Raven Industries, Incorporated. The feasibility studies reported here were conducted by Honeywell and Raven under the sponsorship of the National Aeronautics and Space Administration, Langley Research Center (NASA Contract NAS 1-3169). Mr. S. M. Burk of that facility was the NASA Technical Representative.

In this paper a brief description of the system concept and components is presented, and the experimental program objectives are defined. Then, the actual wind tunnel and free flight experimental studies are described and discussed.

## I. SYSTEM CONCEPT AND DESCRIPTION

The PARAVULCOON Recovery System utilizes an open-throat, low-permeability balloon filled with air as a drag and flotation device to accomplish the terminal deceleration and controlled touchdown of a given payload such as a reentry space vehicle or a spent rocket booster. Following aerial deployment and inflation of the balloon, the buoyancy for flotation is provided by heating the air in the envelope. Then, by controlling the temperature of this air, ascent, hover, or descent can be provided as desired.

The basic operational concept of this system is sketched in Figure 1 and consists of the following sequence of events:

- Initial stabilization and deceleration
- Balloon deployment
- Balloon inflation
- Initial heat addition
- Buoyant flotation and controlled descent.

Activation of the system proper begins with the payload stabilized by a primary deceleration system to descent at a subsonic velocity. At a predetermined altitude the PARAVULCOON deployment event is initiated; the balloon is extracted from its stowage and streamed behind the payload body. Then, as the system continues to descend, the envelope is inflated by ingesting air through its open throat. During this period and when fully inflated by the ram air pressure, the balloon acts as a trailing aerodynamic drag body to decelerate the system to the equilibrium descent velocity defined by the form drag of the inflated balloon and the total system weight. At this point, heat is added through the opening at the envelope base to initially heat the air in the balloon to the temperature required for buoyancy. Thus, as this buoyancy develops, the system is further decelerated until it reaches a condition of buoyant equilibrium.

Once this initial heating has been accomplished, the system may be controlled by the rate of heat addition to float at a chosen altitude or to descend to the earth for a controlled soft touchdown. Up to the maximum altitude defined by the maximum allowable envelope temperature, any float altitude may be chosen. During flotation, only sufficient heat input is required to replace the steady-state heat losses caused by convection and radiation from the envelope and ingested air. Hence, the duration of the float period before landing is solely a function of the amount of fuel which can be carried on board. It should be noted here that since the lifting capacity of a balloon is a function of its volume (diameter cubed) and heat loss is primarily a function of surface area (diameter squared), the float efficiency of the system increases with system size.

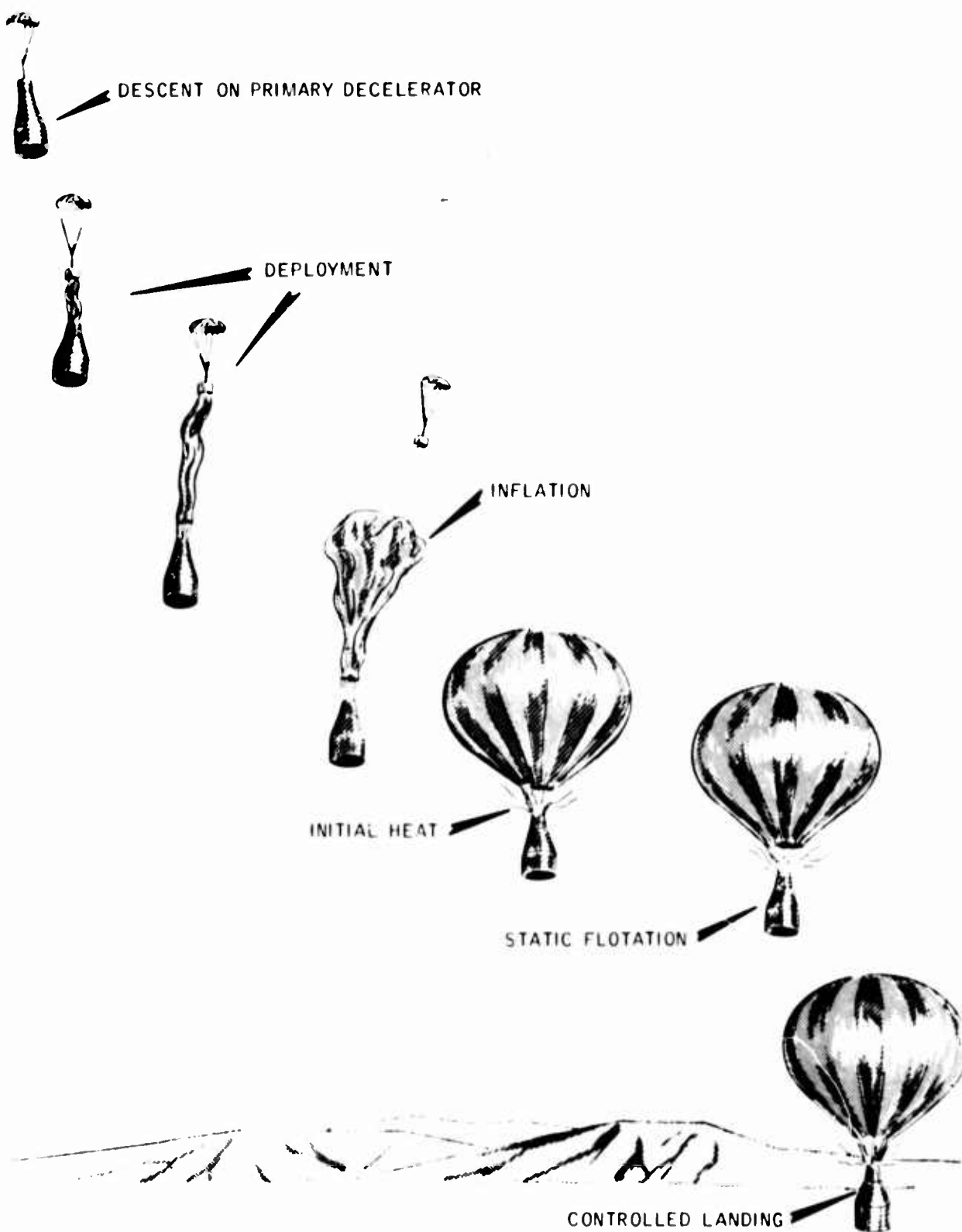


Figure 1. Overall PARAVULCOON System Sequence

The total system to accomplish this sequence therefore consists of the balloon envelope with its associated fittings and deployment mechanism, initial and sustaining heat generators with the necessary fuel tankage, and a control system which may include a radio control link if required.

Present hot gas balloons are made of rip-stop nylon, either with an acrylic coating or one which has been calendered to reduce permeability. However, laminated nylon and Dacron scrim have also been successfully used. All of these materials can be used at temperatures up to 300°F. Other materials under study may be usable at higher temperatures in the future. Furthermore, recent tests indicate that the temperature distribution inside the balloon will allow operation at higher average air temperatures than were heretofore expected without overheating the envelope fabric.

For the PARAVULCOON application the balloon envelope is of a "natural shape" or a variation of it. In this shape, theoretically, no circumferential stresses are developed in the fabric when the system is in buoyant equilibrium. All buoyant loads are carried through meridional load paths over the envelope and are transferred to the supported payload by a set of load lines. These lines leave the base of the envelope, which has a catenary load distribution structure, in a conical configuration and may be attached to the payload in a circular pattern or grouped at several hard points for load transfer. The base of the envelope is open to allow the aerial inflation of the envelope by the ram air and the subsequent heating of the air in the balloon by the heat generator. The diameter of this throat is 25 to 30 percent of the maximum envelope diameter. Prior to deployment, the envelope is packaged in a compactly folded condition. Several methods of aerial deployment have been considered; however, streaming from a deployment bag appears most promising and has been used in the experimental studies reported here.

To heat the air in the balloon and decelerate the system to buoyant flotation within a reasonable time, the initial heat generator must produce a high heat output for a short period (1 to 3 minutes). On the other hand, the sustaining heat generator must provide only about 1/10 of the heat-output rate of the former, but this output must be controllable and be available for prolonged periods (1 to 3 hours). For these purposes heat may be obtained by the use of a solid rocket fuel, burning a liquid hydrocarbon fuel such as propane or RP-1, or a system combining solid and liquid fuels, depending on the requirements of the particular application. In addition to the burner proper, fuel, tankage, and associated piping and valves are necessary for the complete heat-generator system. If the recovered payload is a spent liquid rocket booster with residual liquid fuel available, fuel and tankage weight and volume may be reduced by burning the residual fuel.

The control system is necessary to initiate the various events in the activation sequence and to control the heat generator for hover altitude and controlled letdown.

Preliminary studies indicate that such a system for the terminal recovery of the S-1C Saturn booster will weigh about 26,000 pounds. This is based on burning residual RP-1 from the booster for a 90- to 100-minute flotation period. For a longer float duration, an additional weight of 9,640 pounds for each extra hour of hover is estimated.

## 2. EXPERIMENTAL PROGRAM OBJECTIVES

Consideration of the PARAVULCOON System activation sequence suggests that the most critical phases with regard to concept feasibility are the aerial deployment and inflation of the balloon. To have a useful recovery system it must be possible to accomplish these events successfully at reasonable velocities and dynamic pressures. While it has been possible to establish the feasibility of some of the other sequence phases analytically, deployment and inflation have been found to be the least amenable to such methods. Rather, these phases consist of a combination of aerodynamic, dynamic, and mechanical actions which are more readily analyzed by experimental observation.

Therefore, under the sponsorship of the Langley Research Center of the National Aeronautics and Space Administration, a study program was undertaken to experimentally demonstrate the feasibility of the aerial deployment and inflation of a PARAVULCOON envelope capable of recovering a 1,000-pound payload. This program consisted of a relatively small number of cold-drop flight tests using 54-foot diameter balloons, preceded by a brief wind-tunnel study. The latter was intended to obtain a better understanding of the phenomena associated with the aerial deployment and inflation of PARAVULCOON envelopes and to provide a basis for the design of the larger-scale flight test equipment. Only cold-system drops were undertaken in this study as they could be performed using relatively simple flight test vehicles. To test the entire PARAVULCOON System sequence complete with heat addition would have required a program of larger scope. Such a program would have necessitated the design, fabrication, and preliminary testing of heat-generator and control systems for use in more complex and expensive test vehicles.

## 3. WIND TUNNEL MODEL STUDIES

It was realized that it is physically impossible to mechanically, dynamically, and aerodynamically scale the PARAVULCOON deployment and inflation sequence

in a wind-tunnel test situation. However, it was also felt that a brief wind-tunnel investigation would help to point out problem areas and give some physical insight into the phenomena before moving on to the full-scale free-flight tests.

### 3.1 Equipment and Methods

The Langley Research Center 20-foot Vertical Free-Spinning Wind Tunnel was made available for this study. This facility provides upward-directed velocities from 10 to 85 fps with infinite speed control. With this arrangement an unrestrained model of suitable weight and drag can be "floated" on the upward airstream to simulate vertical free descent. The model is thus free to accelerate and decelerate without restriction, thereby permitting observation of its dynamic characteristics. System drag can be measured by determining the velocity necessary to "float" the model. A mounting fixture of the more conventional wind-tunnel style was also available for tests with the model restrained in the airstream.

Naturally, to reduce scaling problems, as large a model as possible was desired. However, Langley Research Center personnel estimated that tunnel blockage limitations would not permit the use of larger than six-foot diameter model balloons in this tunnel. Furthermore, scaling studies indicated that even though complete scaling was not possible, the model envelope should be as light and flexible as possible. Therefore, all of the models were constructed in the natural shape with 12 gores and load lines in the 6-foot size. At the time of the study, fabric availability was limited, so the models were made of 1.1-oz-per-yd<sup>2</sup> and 0.8-oz-per-yd<sup>2</sup> nylon cloth, coated with acrylic. Since the 1.1-oz-per-yd<sup>2</sup> nylon material was also later used for the 54-foot diameter full-scale balloon, the model envelopes were obviously too heavy and stiff from the scaling standpoint. These models were made with 20-, 25-, 30-, and 40-percent throat openings, and various load-line arrangements were provided to allow variations of the throat-loadline-forebody geometry.

Streaming the envelope behind an open deployment bag that was being separated from the forebody by a drogue parachute was chosen as the most promising deployment scheme. Therefore, two wooden forebodies were provided which could model this scheme: a six-inch-diameter forebody in which a deployment bag with the envelope packed inside could be internally stored and a three-inch-diameter forebody from which a pseudo-deployment event could be accomplished with the deployment bag externally restrained behind the body. The smaller forebody was the properly-scaled version of the full-scale test vehicle; however, the model envelope was too bulky to be packed inside of it. Lead weights and shot were used to vary the forebody weight.

The 1.1-oz-per-yd<sup>2</sup> envelope with the 6-inch forebody is shown fully inflated in the Vertical Wind Tunnel in Figure 2.

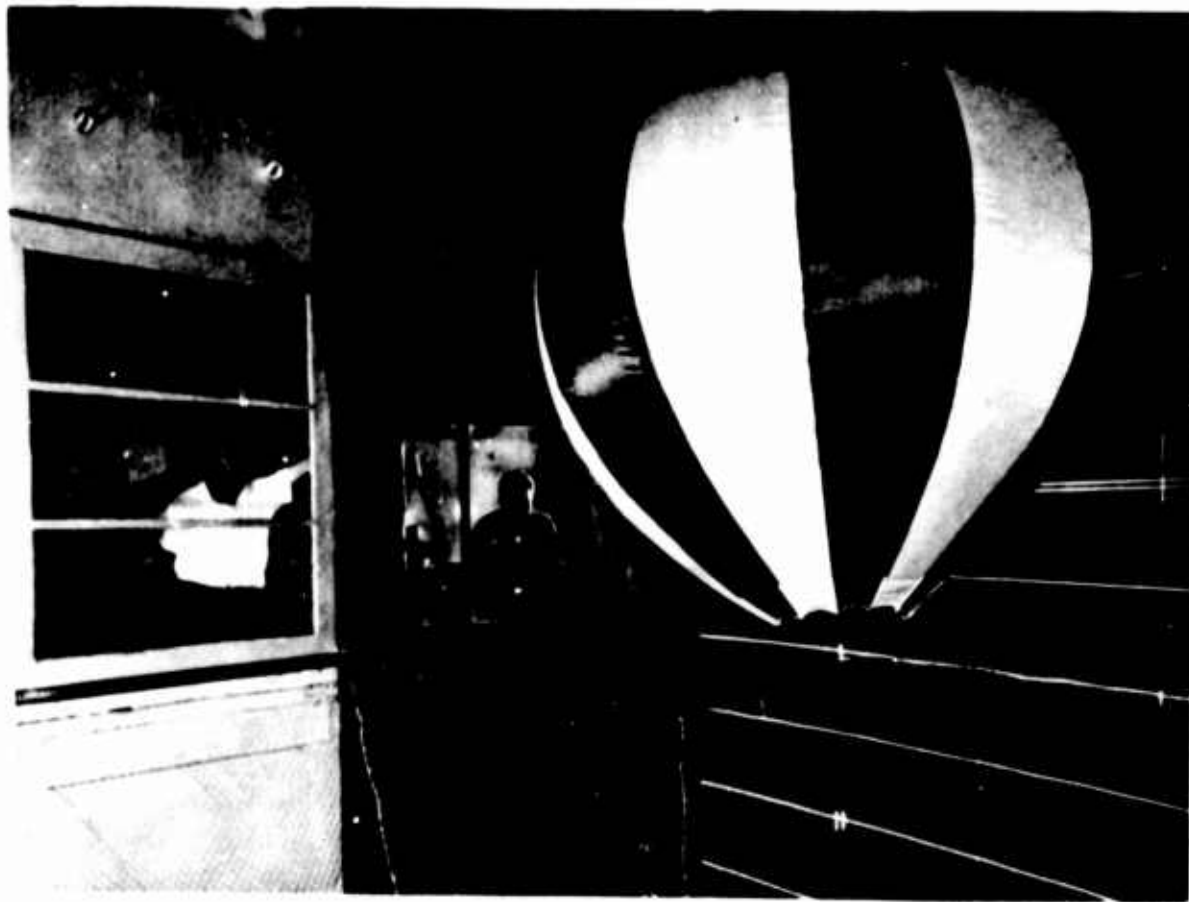


Figure 2. Inflated Model PARAVULCOON in 20-Foot Vertical Free Spinning Wind Tunnel

Deployment tests were conducted by supporting the model system in the tunnel airstream with a drogue parachute, releasing the deployment bag, and observing the ensuing deployment. Both free-floating and restrained tests were made. However, since the drag of the envelope was found to increase rapidly with a small amount of inflation, it was difficult to reduce the tunnel velocity fast enough to simulate the deceleration of a free-dropped system. As a result, in the dynamic tests the envelope tended to be blown into the screen at the top of the tunnel, and in the restrained tests the model was subjected to excessive buffeting. Hence, for the safety of the tunnel, deployment tests were held to a minimum.

Inflation characteristics, system stability, and the drag of the various model configurations were observed by hand-launching the system in a streamed configuration. For these tests the envelope from which the excess air had been removed was held in the airstream by the throat to prevent premature ingestion of air. Then, when the tunnel velocity had been adjusted to support the streamed system, the model was released.

To corroborate the wind-tunnel observations and be sure that there were no problems caused by the use of such a large model in the 20-foot tunnel, one of the model systems was free-dropped from a helicopter at about 2,000 feet.

### 3.2 Results

The performance of the wind-tunnel model system was considered in terms of deployment, inflation, system stability, and drag. However, due to the scaling limitations of the models, it was concluded that these results could only be extrapolated to larger systems in a qualitative rather than a quantitative manner.

The deployment scheme chosen operated well in every test. The envelope streamed smoothly from the deployment bag and immediately began to ingest air through the throat. Actual time from release until the deployment bag cleared the streamed envelope was less than one second, and there did not appear to be any significant opening shock transmitted to the forebody. Most of these runs were made at event velocities from 30 to 35 fps, but two tests were run at 62 and 82 fps, respectively.

In all the model variations tested, the envelope began to ingest air as soon as its throat was released. The drag immediately increased and quickly reached a value near that of the fully-inflated balloon. Thus, the inflation took place at a nearly constant velocity ranging from 8 to 18 fps with one heavy case at 27 fps. Although the motions of the envelope fabric appeared quite random with a continuous movement of the folds of material and some opening and closing of the throat area, the inflation time for a given configuration was surprisingly repeatable. Values ranged from 4 seconds with a rigid ring holding the throat open to over 40 seconds for the lightest configurations. During this period the system was completely stable. In general, inflation was found to be somewhat slow. However, when the rigid throat ring was used, the rapid inflation was so violent that it could not possibly be sustained in a large system. So while the desirability of a positive inflation aid was revealed, the need for a controlled gradual inflation was also indicated.

The major problem encountered in the wind-tunnel study was an instability exhibited by the system during the cold-descent period after the balloon was fully inflated. This occurred in the form of an indentation on the windward side of the balloon which resulted in a quasi-steady coning rotation of the system or system oscillations of varying degrees of intensity. Analysis indicated that this instability was the result of having to operate the model envelopes in the laminar-to-turbulent transition flow regime. It was further shown that in this regime unsteady asymmetric separation of the boundary layer from the balloon can exert large pitching moments. Since the full-scale test balloons operated at a much larger Reynolds number, well

into the turbulent regime, the instability problem was not expected to occur with them. This conclusion was partially verified by a simple free drop of a 40-foot-diameter hot-gas balloon in the streamed configuration. Also, it was found that the instability of the six-foot model could be "fixed" by the addition of a skirt-like fence around the balloon near its equator to provide a uniform flow-separation line.

Due to the instability problem, it was not possible to obtain valid drag measurements for the model system in the fully-inflated configuration. However, drag measurements for the envelope in the streamed configuration were obtained.

The free-flight drop of the model system from the helicopter with a deployment-event velocity between 90 and 100 fps verified the observations and conclusions of the Vertical-Wind-Tunnel tests.

In general, the wind-tunnel observations and associated studies indicated that the overall mechanization of the PARAVULCOON deployment and inflation was feasible. No problems or phenomena were encountered which tended to disprove the feasibility of the system concept or were expected to interfere with the orderly accomplishment of the full-scale flight tests.

#### 4. FULL SCALE FREE FLIGHT STUDIES

The principal means of attaining the program objectives were the four free-flight cold-drop tests of a large PARAVULCOON System. Since it was desired to observe the performance of a larger balloon, the simulated recovery of a 1,000-pound-payload size was chosen as it required a fairly large balloon (50 to 60 feet) but still was not so heavy as to create test inconvenience. These flights were conducted at the U.S. Department of Defense, Joint Parachute Test Facility, El Centro, California, with the technical support of the U.S. Air Force, 6511th Test Group (Parachute).

##### 4.1 Equipment and Methods

As noted above, the deployment-bag method was used to deploy the PARAVULCOON envelope. It was decided that the simplest means of creating the desired-event conditions was to suspend the test system from a drogue parachute sized to provide the desired-event velocity in equilibrium vertical descent at the chosen altitude. Then the same parachute was used to extract the deployment bag and stream the envelope. This sequence is illustrated in Figure 3.

In order to produce this situation, the flight-test vehicle was dropped on a wooden skid from a C-130 transport aircraft. As the skid fell away from the aircraft, static lines actuated cutters to release the vehicle from the skid and streamed the skid-recovery parachute. The streaming of this parachute deployed the vehicle

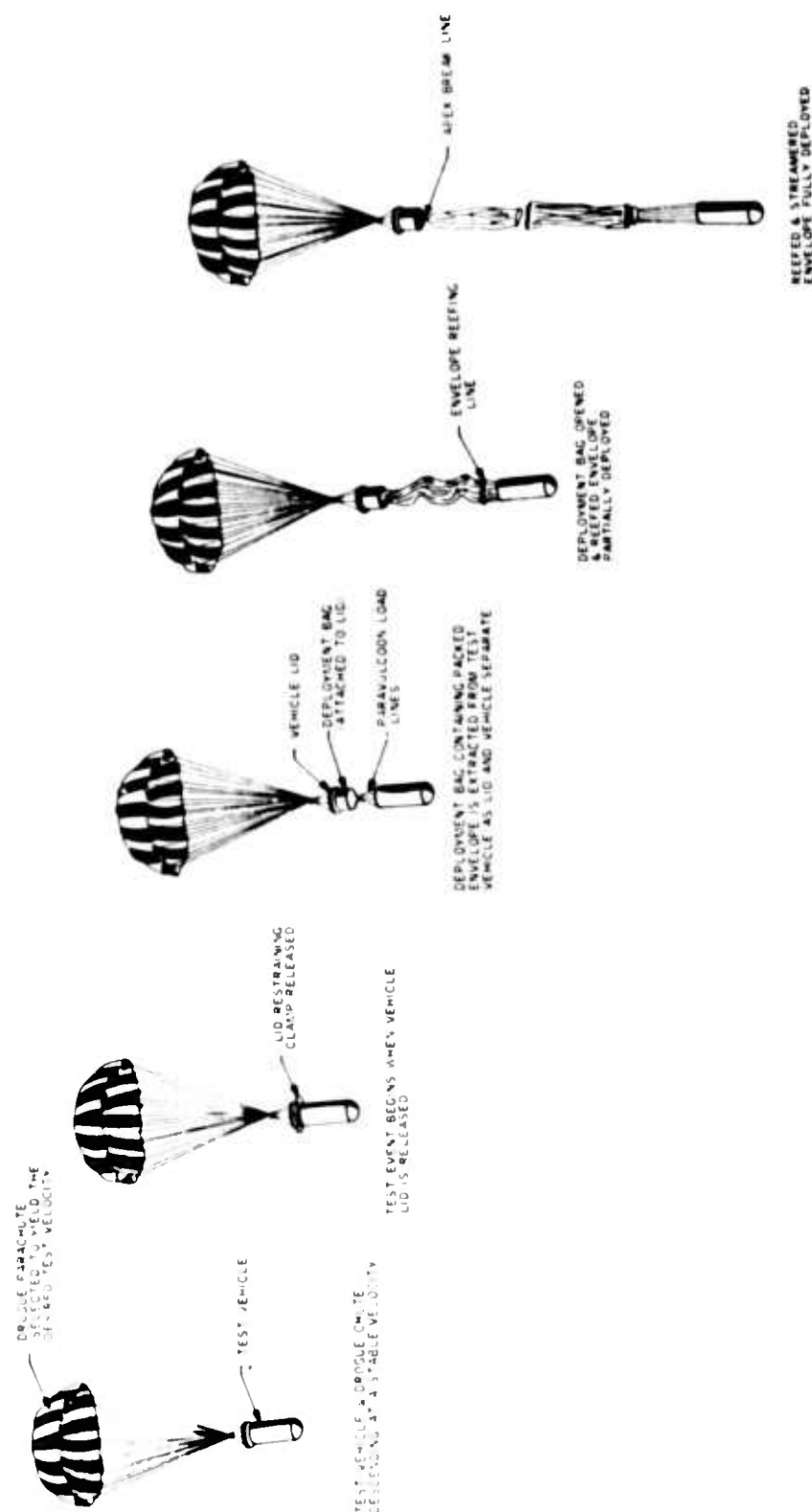


Figure 3. Envelope Development Sequence

drogue chute by a static line, and the actual flight test was underway 1.5 to 3.0 seconds following the extraction of the skid from the aircraft. The deployment event was initiated by preset mechanical timers which were started by pull lanyards as the flight-test vehicle and its launch skid separated. Drogue parachute sizes and timer settings were determined from trajectory studies to give a long enough drop to ensure near-vertical, oscillation-free descent at the time of the deployment event. This aerial-drop system performed satisfactorily and without problems in all four flight tests.

Range instrumentation for these tests consisted of space-time data from a cinetheodolite tracking system and high-speed motion pictures including air-to-air coverage from chase aircraft and ground-to-air coverage with telescopic lenses.

The actual PARAVULCOON flight-test system consisted of the balloon proper, the flight-test vehicle, and the deployment system.

System studies indicated that a PARAVULCOON envelope to simulate the recovery of a 1,000-pound payload should be 54 feet in diameter. Thus, a "natural shape" design in this size was developed. Stress considerations for this design were based on the predicted deployment and inflation environment and static and dynamic tests conducted on several of the features of the design. This test envelope consisted of 20 gores of acrylic-coated 1.1-oz-per-yd<sup>2</sup> rip-stop nylon with a 16.2-foot diameter, 30-percent throat opening. Twenty load lines of nylon-covered steel aircraft cable were connected to 20 load-distributing catenaries around the throat. The basic characteristics of this balloon design are listed in Table 1.

Table 1. X-54 PARAVULCOON Characteristics

Diameter	5.4 feet
Volume	76,842 feet <sup>3</sup>
Surface Area	8,754 feet <sup>2</sup>
Inflated Height	56.1 feet
Gore Length	85.1 feet
Number of Gores	20
Weight (approximate)	110 pounds
Packed Volume (approximate)	6.0 feet <sup>3</sup>

As deployment loads in the envelope crown were anticipated to be severe, the original design had a reinforcing nylon cap in this region. However, after one flight it was found that this cap caused stress concentrations which resulted in a terminal descent failure, and a redesign was necessary. Since all of the envelope loads are

brought to a theoretical confluence at the envelope apex, the structure in this area must be reinforced without creating load-path discontinuities. To do this, the redesigned envelope incorporated a method of construction, developed by Raven Industries, Inc., designated as Simulated Variable Thickness (SVT). Its purpose was to better carry the meridional load on each gore across the envelope apex to its diametrically-opposite gore without abrupt changes in fabric thickness. This is achieved as is shown in Figure 4 by shaping each gore with a minimum constant width at its upper end, overlapping the excess material progressively and thus creating the equivalent of a gradual buildup of fabric thickness toward the apex of the envelope.

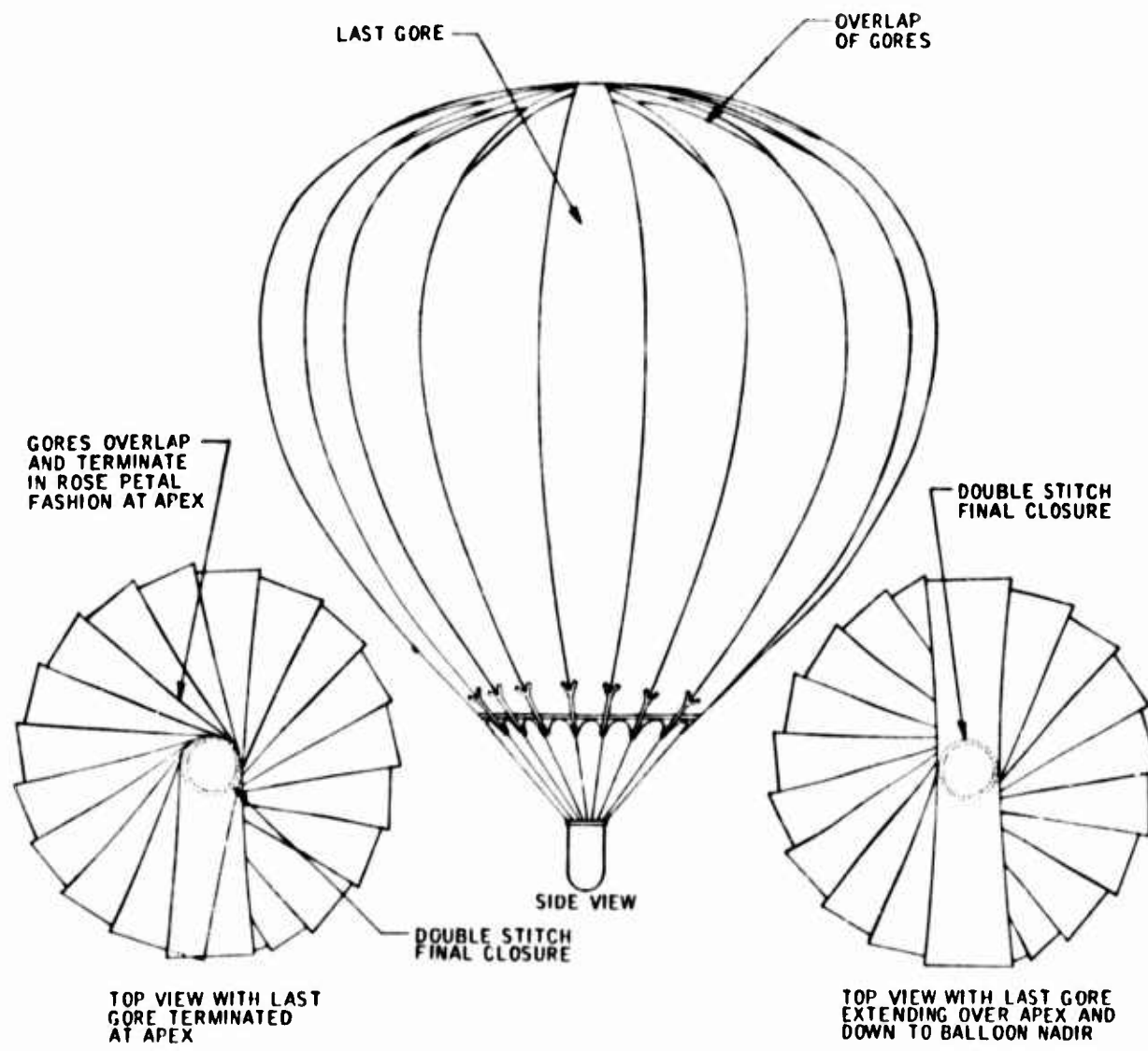


Figure 4. Envelope Configuration with Simulated Variable Thickness Top

In addition to simulating a payload, the flight-test vehicle made possible the necessary test mechanics to accomplish the basic program objectives. The vehicle used was a 30-inch-diameter by 60-inch hemisphere cylinder of 1/4-inch steel. Prior to event, the deployment bag was stowed in the smooth cylindrical aft section of the vehicle, and the balloon load lines were attached around an external load ring at the aft edge. This compartment was closed by a rear closure plate to which the drogue parachute was attached. A pair of semicircular clamp bands which fit over the matching beveled edges of the closure plate and the aft ring were used to hold the rear closure plate in position and transmit the drogue parachute loads to the vehicle. The bands were in turn secured by a pair of explosive bolts. The deployment bag was attached to the underside of the closure plate. Hence, to produce the deployment event, the explosive bolts were fired, the clamp bands parted and released the rear closure plate, and the drogue parachute lifted the then-freed closure plate away from the vehicle and thus extracted the attached deployment bag. This design provided a jerk-free transfer of the drogue parachute suspension loads from the flight test vehicle to the bag. Static tests demonstrated that if either of the explosive bolts fired, the rear closure plate could not fail to separate.

In this deployment scheme, as shown in Figure 3, the deployment bag must lift the packed envelope from the vehicle; and then in turn, as it separates from the vehicle, must open to allow the envelope to stream freely to its full length. Since this action is so crucial to deployment success, considerable design and experimental attention was given to the deployment bag design. The final design is shown in Figure 5, suspended from the rear closure plate in the extracted position above the flight test vehicle just prior to the opening of the bottom of the bag. The design consisted of a clamp arrangement to attach the 2.2-oz-per-yd<sup>2</sup> nylon fabric bag reinforced by a 1-1/2-inch nylon webbing to the bottom of the closure plate. This bag was actually an overlength tapered cylinder lined with Teflon-coated gloss fabric whose excess length formed the bottom of the bag when it was closed. A four-piece aluminum breakaway spool locked by a nylon strap and pull pin was used to close the base of the bag. After the bag and the vehicle had separated about six feet, the pull pin was extracted by a steel cable attached to one of the load lines. Since the bag was designed overlong, the breakaway spool quadrants ended up on the outside of the bag after opening. This provided a completely smooth passage for the streaming envelope to leave the bag.

In addition to the timers and circuitry to initiate the explosive bolts, on-board equipment on the vehicle included an accelerometer and telemetry system to measure axial loads on the vehicle, and an "up camera".

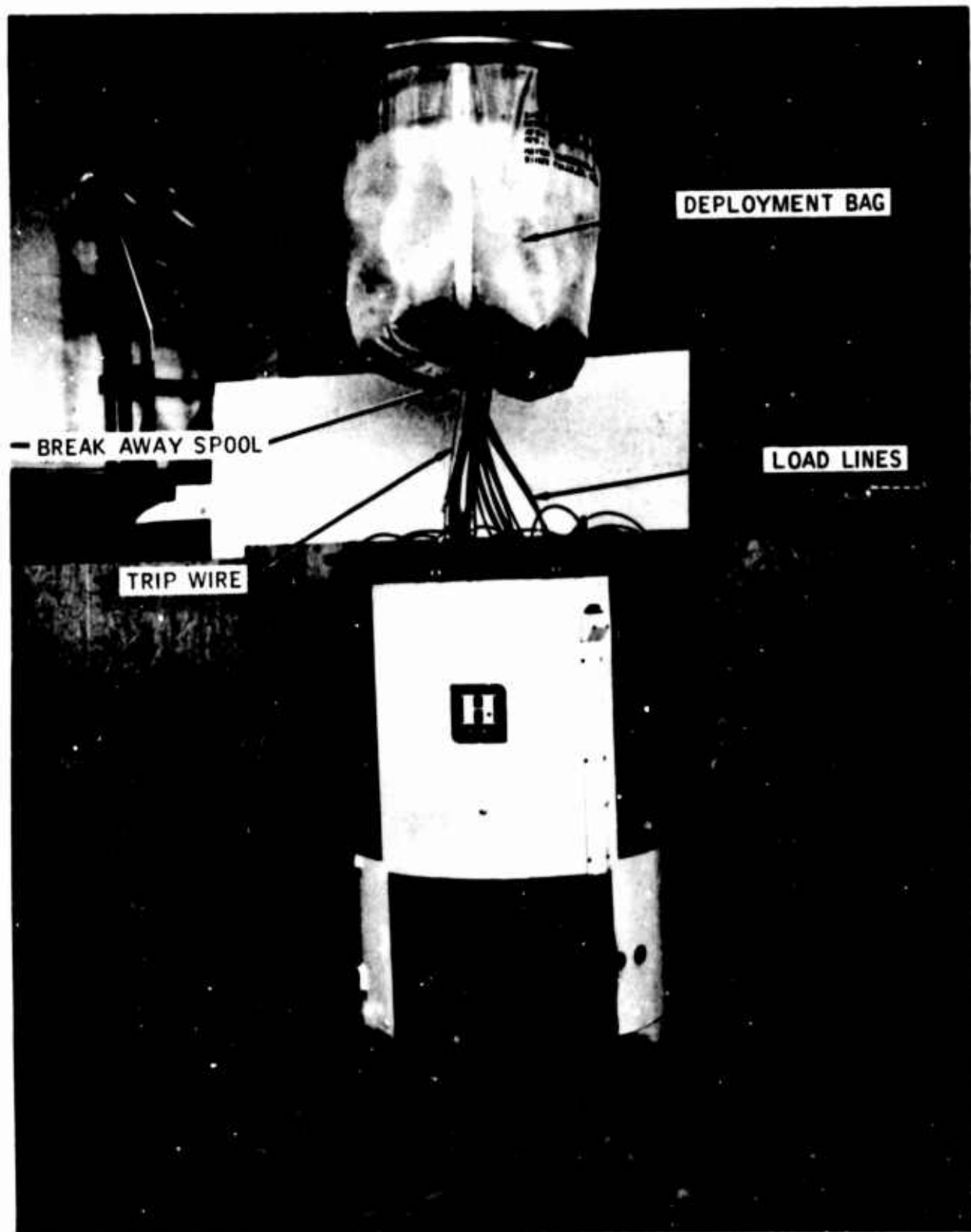


Figure 5. PARAVULCOON Flight Test Vehicle and Deployment Bag  
(Position Just Prior to Release of Breakaway Spool)

### 4.2 Results

Two of the four flight tests were conducted at nominal deployment-event velocities of 100 fps and two at 200 fps. With this small number of drops it was decided to initiate all the events at the nominal altitude of 15,000 feet. This height was good for ground-to-air and air-to-air photographic coverage and still provided plenty of total altitude to observe all phases of the sequence.

The overall test conditions and results are summarized in Table II.

Table 2. Summary of Full-Scale Free-Flight Tests

Drop Test Number	1	2	3	4
<u>Event Conditions</u>				
Altitude (ft)	15,300	15,107	15,494	16,690
Velocity (fps)	111	105	176	204
Dynamic Pressure (psf) (Actual from flight data)	10.0	8.1	22.8	29.3
Weight Suspended from P.V. (pounds)	1,005	1,015	1,015	1,020
Deployment Time (sec.)	~1.3	~1.5	--	~1.0
<u>Complete Envelope Inflation</u>				
Time (sec.) Distance (ft.) } from event	93.5	95	--	99.5
Terminal Equiv. S.L. Rate of Descent (fps)	25.2	27.8	--	21.7
<u>Performance</u>				
Deployment	Good	Good	Failed	Good
Inflation	Stable but long with violent envelope motions.	Stable, less violent envelope motions.	--	Stable, less violent envelope motions.
Terminal Cold Descent	Stable, failed at 1,610 feet.	Stable.	--	Stable.

The deployment of the envelope was in general satisfactory as planned and quite similar to the wind-tunnel model tests. At the lower speed (dynamic pressure - 10 psf) no problems were encountered, but the throat immediately ingested air which resulted in the formation of a flared-out bubble of balloon fabric which followed the moving deployment bag the full length of the streaming envelope. This is shown in Figure 6. However, at the higher speed with a dynamic pressure over

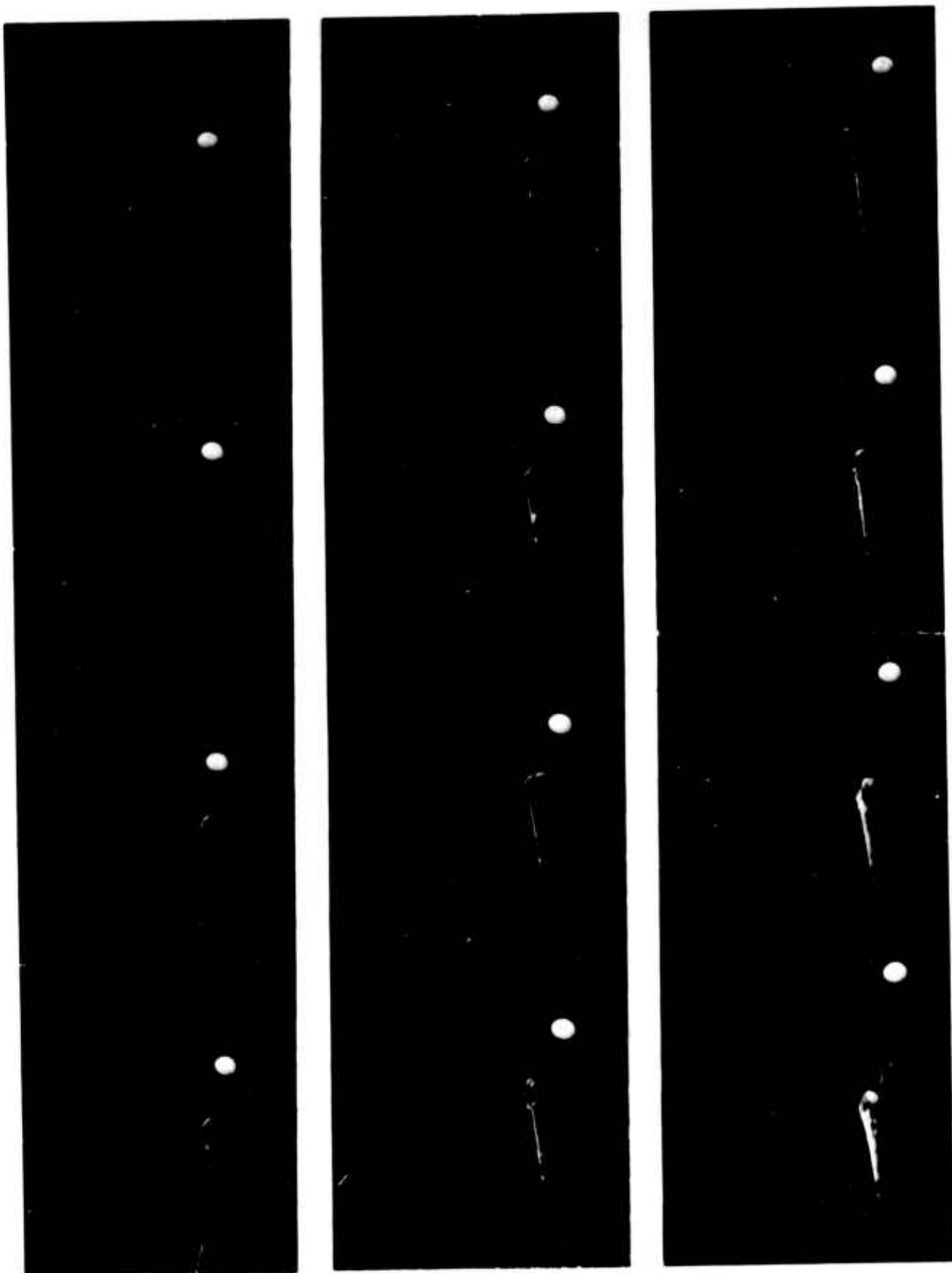


Figure 6. Test PARAVULCOON Deployment Sequence

20 psf this bubble was much larger and caused the envelope to fail before deployment was completed. This problem was completely rectified by temporarily reefing the envelope throat closed to prevent the ingestion of air until the balloon was fully streamed. As shown in Figures 7 and 8, this provided a smooth deployment and a more gradual start to inflation. Therefore, the feasibility of PARAVUL-COON envelope deployment at these speeds and dynamic pressures was completely demonstrated provided that a temporary throat reefing is used.

Inflation of the envelope began immediately and was completed within a reasonable distance. Also, the system was stable during this period and its drag quickly increased to nearly the fully inflated value. However, due to the tendency of the balloon throat to close off and prevent ram pressure ingestion a large percentage of the time, the resulting envelope distortions subjected the fabric to some rather violent motions. This was particularly true after inflation was 40-to 50-percent complete when enough air had been ingested to extend the envelope to nearly its full diameter, but the bubble inside was not large enough to keep the envelope fully extended and prevent fabric flapping and breathing in and out. Some of these motions are pictured in Figures 9 and 10. These motions were particularly severe in the first test and were judged to have weakened the envelope and thus caused the eventual failure of the balloon during its cold-terminal descent at an altitude of 1,610 feet. With the revised balloon design these motions were somewhat less severe and the problem partially alleviated.

Envelope inflation was found to be consistent and positive and thus completely feasible. Starting from a dynamic pressure of about 20 psf (approximately the terminal descent of this system with the envelope streamed), 95 to 1000 seconds and 4,000 to 5,000 feet of descent were required to complete inflation. Since the system decelerated to velocities below 70 fps during the first 10 seconds of flight (including deployment), the velocity at the beginning of inflation does not appear to have a significant effect on the inflation time or distance. However, although the system was completely stable during this period, the motions of the envelope fabric were more severe than would be desired from the standpoint of stresses in the envelope. Thus it appears that the inflation performance could be greatly improved by the use of a positive inflation control during the middle portion of this sequence (from about 30 to 85 percent inflated). One such system would positively hold the throat open, first at a reduced diameter to preclude too sudden inflation and then at successively larger diameters to prevent the choking off of the throat and aid in more rapid and less violent inflation. Peripheral inflation scoops might also be useful to speed inflation without overloading the envelope.

Once a temporary reefing scheme and a positive inflation control have been perfected, there does not appear to be any further obstacle to the development of the deployment and inflation of larger balloons at moderate speeds or the deployment of 50- to 60-foot balloons at higher dynamic pressures.

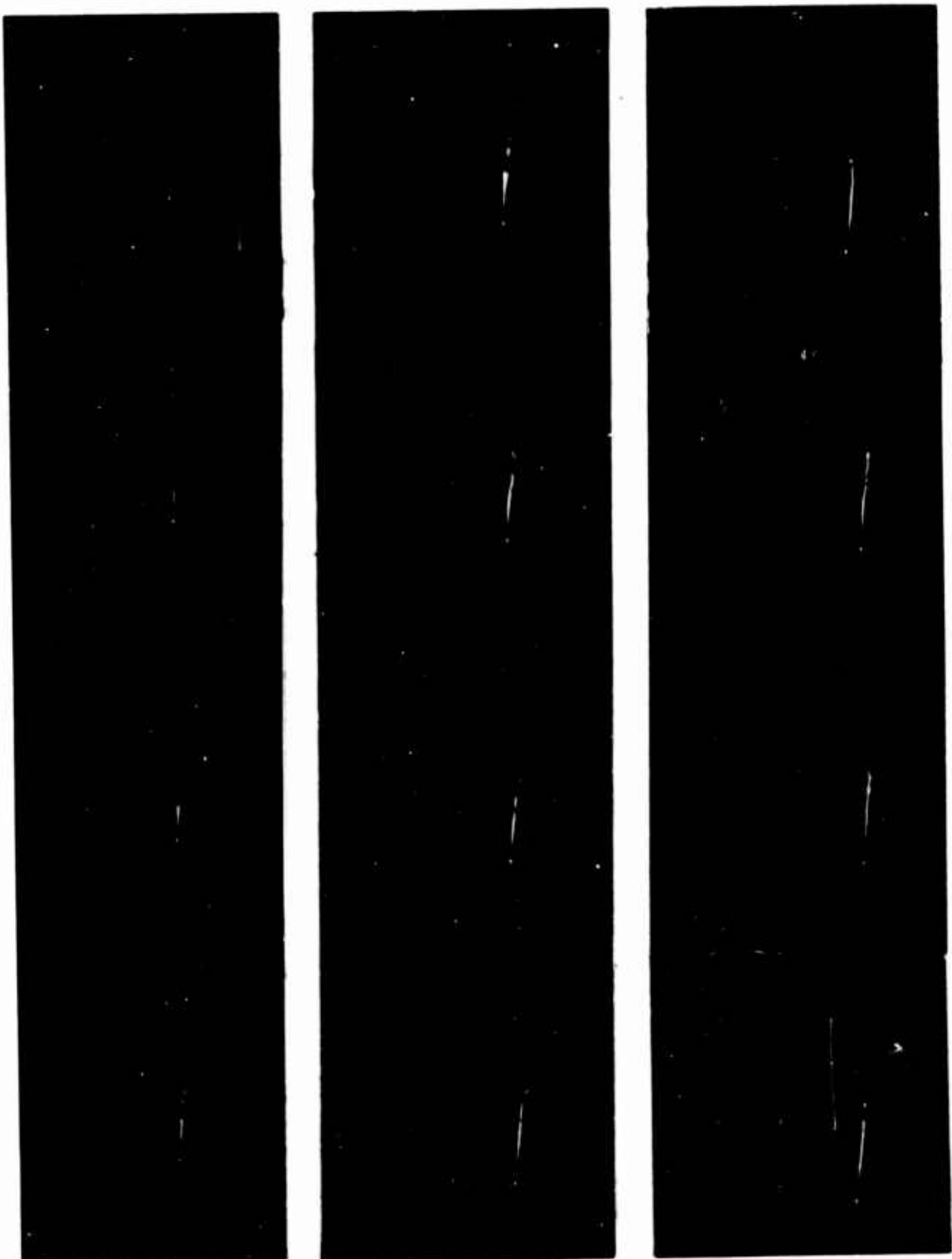


Figure 7. Deployment of Temporarily Reefed PARAVULCOON Envelope

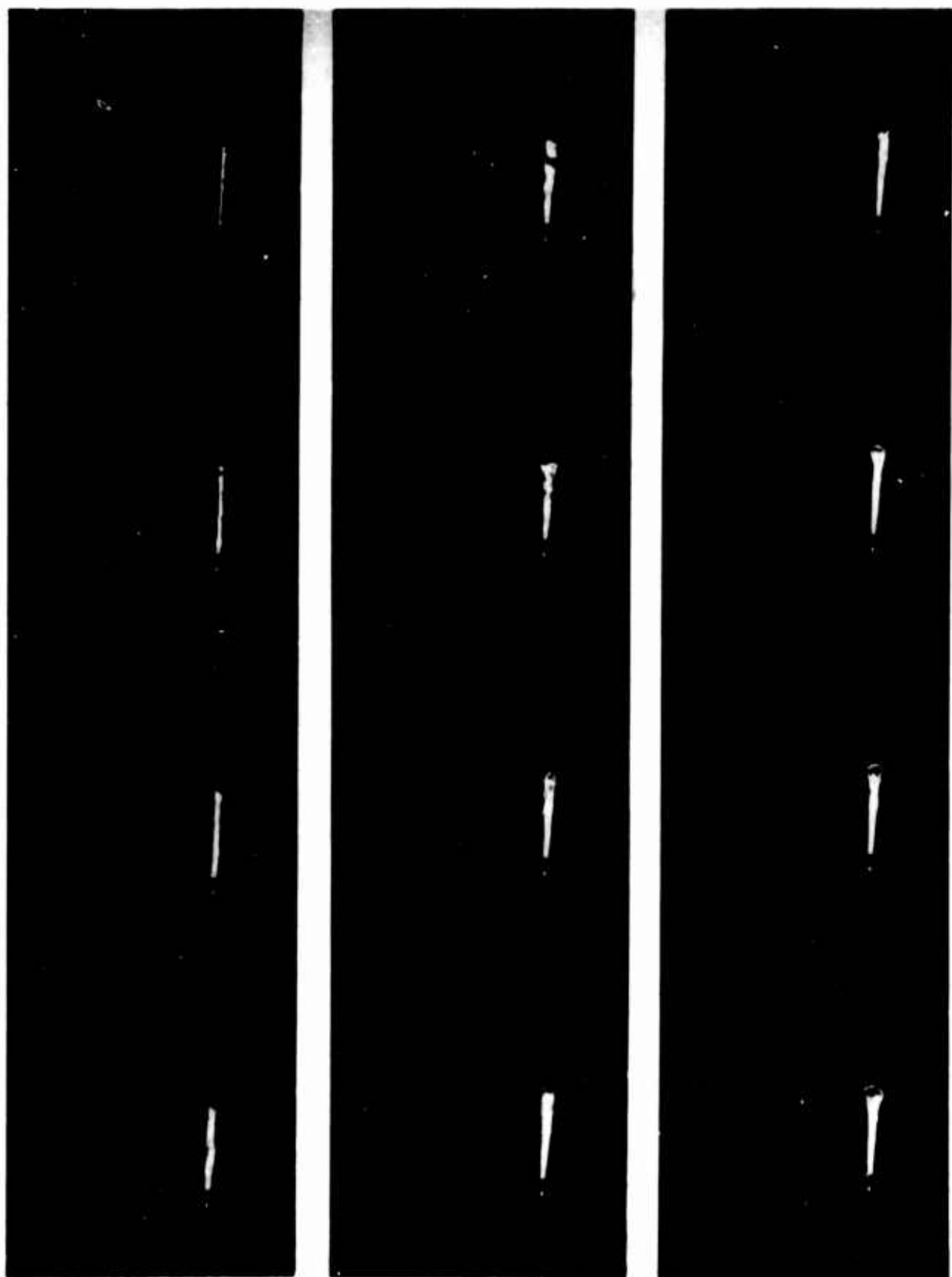


Figure 8. Deployment of Temporarily Reefed PARAVULCOON Envelope  
(Beginning at Instant of Disreef)

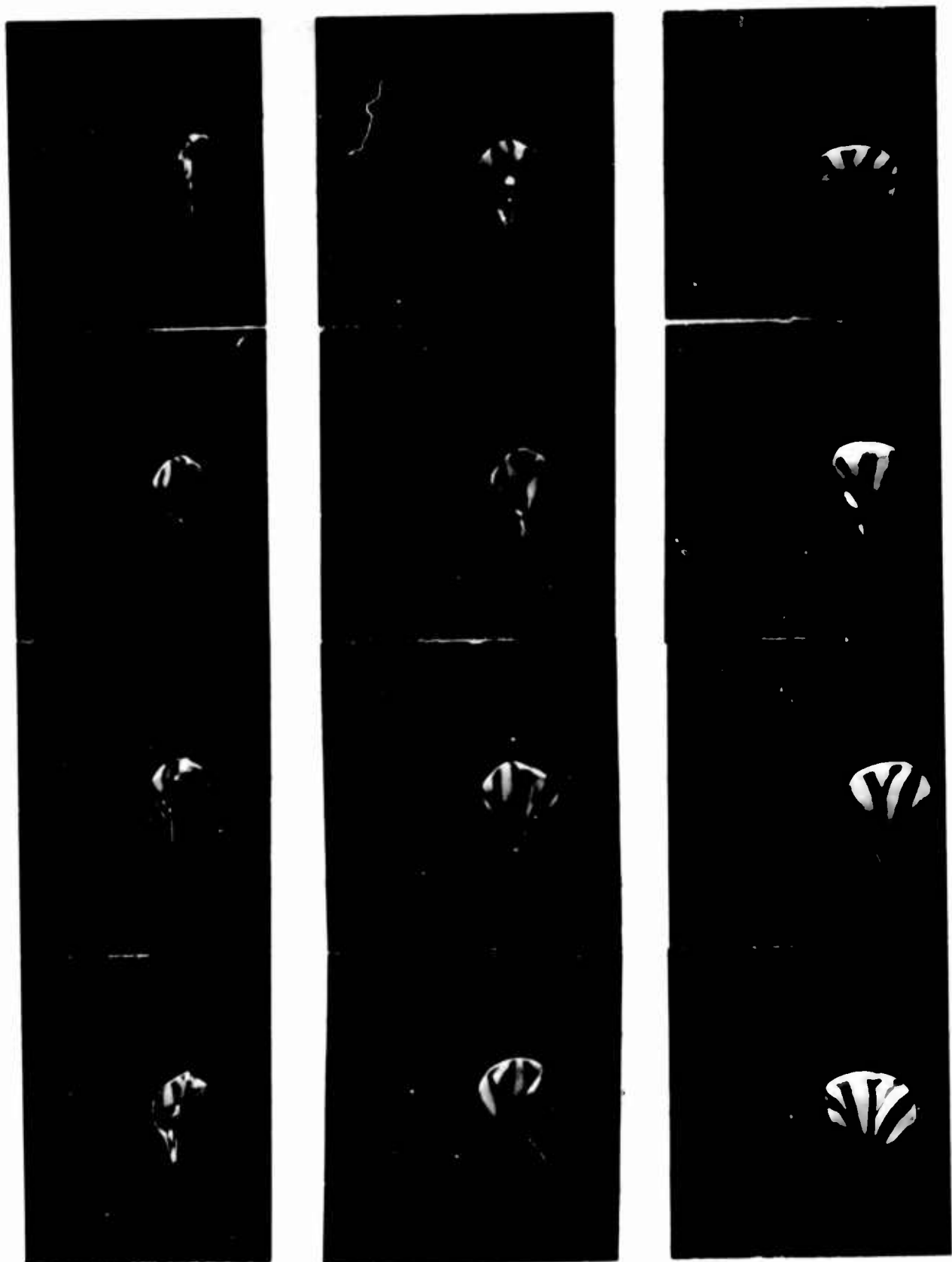


Figure 9. PARAVULCOON Inflation Sequence I

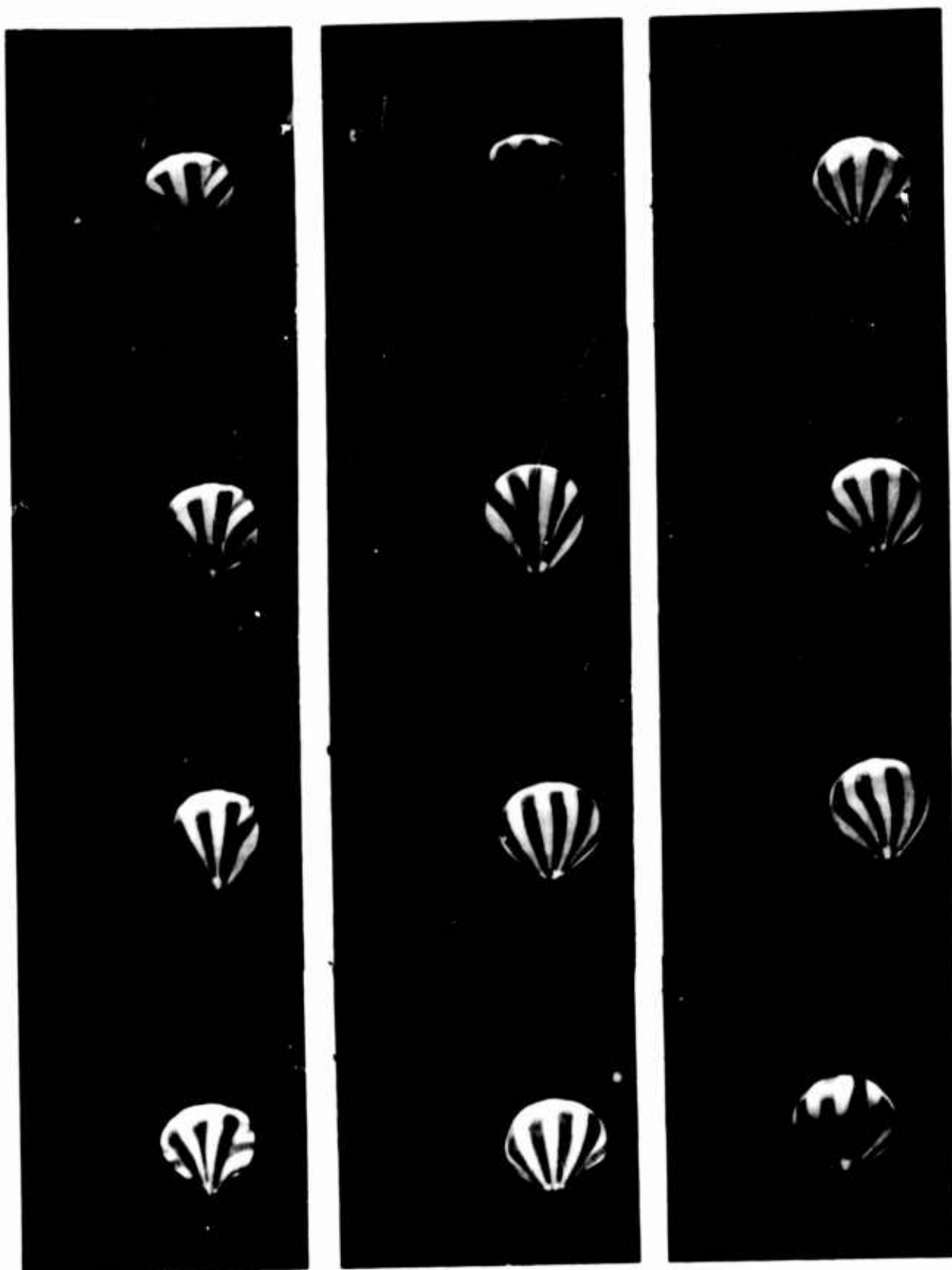


Figure 10. PARAVULCOON Inflation Sequence II

During terminal descent of the fully inflated cold balloon, some slight dimples and indentations were observed similar to those in the model tests. Also, some slow, damped rotation occurred. However, in general, these motions were judged to be so moderate as not to warrant the application of a mechanical "fix" to the large balloon. An average drag coefficient of about 0.5 based on the horizontal cross-sectional area of the balloon was observed for this mode. This was considerably higher than had been previously estimated.

## 5. CONCLUSIONS

The principal objective of these studies was achieved. Namely, the basic feasibility of the concept of aerially deploying and inflating PARAVULCOON envelopes has been experimentally demonstrated in both wind-tunnel model tests of 6-foot diameter models and free-flight tests of 54-foot-diameter balloons with a 1,000-pound simulated payload.

The following general conclusions have been drawn from this study:

Deployment of the envelope by streaming it out of a deployment package was found to be simple, practical, and reliable in both the model and full-scale systems at velocities up to 204 ips and dynamic pressures up to 29 psf. However, for dynamic pressures above 10 psf the PARAVULCOON envelope throat must be reefed until the envelope is fully extended.

The inflation of the PARAVULCOON envelope by ingestion of air through the throat opening in its base is feasible. The time and distance required for inflation is consistent and repeatable. Since this time is relatively long due to the tendency of the balloon throat to close off a large percentage of the time, a more practical system can be attained by providing a positive control of inflation. This will reduce the time required for inflation and thus reduce the severity and duration of the envelope motions and the accompanying stresses in the balloon fabric during the inflation period.

Although a terminal instability problem was encountered with the small models, the full-scale system was found to be completely stable during the development and inflation phases of its activation sequence. During the cold-descent phase, the slow rotations observed did not present any problems.

An average system drag coefficient of about 0.5 was found for the equilibrium cold descent of the system. Almost as large a value was observed during most of the inflation phase.

Once deployment has been accomplished, the inflation phase and thus the remainder of the activation sequence are relatively independent of the deployment environment.

During this program no factors were encountered which would be expected to hamper the reasonable extension of system capabilities with regard to balloon size and the severity of deployment-event conditions or to prevent the orderly development of a practical system.

## AIR FORCE SURVEYS IN GEOPHYSICS

- No.100. A Phenomenological Theory of the Scaling of Fireball Minimum Radiant Intensity with Yield and Altitude (U), H. K. Sen, Apr 1958. (*SECRET Report*)
- No.101. Evaluation of Satellite Observing Network for Project "Space Track", G. R. Miczaika and H. O. Curtis, Jun 1958.
- No.102. An Operational System to Measure, Compute, and Present Approach Visibility Information, T. O. Haig and W. C. Morton, III, Jun 1958.
- No.103. Hazards of Lightning Discharge to Aircraft, G. A. Faucher and H. O. Curtis, Aug 1958.
- No.104. Contrail Prediction and Prevention (U), C. S. Downie, C. E. Anderson, S. J. Birstein and B. A. Silverman, Aug 1958. (*SECRET Report*)
- No.105. Methods of Artificial Fog Dispersal and Their Evaluation, C. E. Junge, Sep 1958.
- No.106. Thermal Techniques for Dissipating Fog From Aircraft Runways, C. S. Downie and R. B. Smith, Sep 1958.
- No.107. Accuracy of RDF Position Fixes in Tracking Constant-Level Balloons, K. C. Giles and R. E. Peterson, edited by W. K. Widger, Jr., Oct 1958.
- No.108. The Effect of Wind Errors on SAGE-Guided Intercepts (U), E. M. Darling, Jr. and C. D. Kern, Oct 1958 (*CONFIDENTIAL Report*)
- No.109. Behavior of Atmospheric Density Profiles, N. Sissenwine, W. S. Ripley and A. E. Cole, Dec 1958.
- No.110. Magnetic Determination of Space Vehicle Attitude (U), J. F. McClay and P. F. Fougere, Mar 1959. (*SECRET Report*)
- No.111. Final Report on Exhaust Trail Physics: Project 7630, Task 76308 (U), M. H. McKenna, and H. O. Curtis, Jul 1959. (*SECRET Report*)
- No.112. Accuracy of Mean Monthly Geostrophic Wind Vectors as a Function of Station Network Density, H. A. Salmela, Jun 1959.
- No.113. An Estimate of the Strength of the Acoustic Signal Generated by an ICBM Nose Cone Reentry (U), N. A. Haskell, Aug 1959. (*CONFIDENTIAL Report*)
- No.114. The Role of Radiation in Shock Propagation with Applications to Altitude and Yield Scaling of Nuclear Fireballs (U), H. K. Sen and A. W. Guess, Sep 1959. (*SECRET/RESTRICTED DATA Report*)
- No.115. ARDC Model Atmosphere, 1959, R. A. Minzner, K. S. W. Champion and H. L. Pond, Aug 1959.
- No.116. Refinements in Utilization of Contour Charts for Climatically Specified Wind Profiles, A. E. Cole, Oct 1959.
- No.117. Design Wind Profiles From Japanese Relay Sounding Data, N. Sissenwine, M. T. Mulkern, and H. A. Salmela, Dec 1959.
- No.118. Military Applications of Supercooled Cloud and Fog Dissipation, C. S. Downie, and B. A. Silverman, Dec 1959.
- No.119. Factor Analysis and Stepwise Regression Applied to the 24-Hour Prediction of 500-mb Winds, Temperatures, and Heights Over a Silent Area (U), E. J. Aubert, I. A. Lund, A. Thomaseli, Jr., and J. J. Pazniokas, Feb 1960. (*CONFIDENTIAL Report*)
- No.120. An Estimate of Precipitable Water Along High-Altitude Ray Paths, Murray Gutnick, Mar 1960.
- No.121. Analyzing and Forecasting Meteorological Conditions in the Upper Troposphere and Lower Stratosphere, R. M. Endlich and G. S. McLean, Apr 1960.
- No.122. Analysis and Prediction of the 500-mb Surface in a Silent Area, (U), E. A. Aubert, May 1960. (*CONFIDENTIAL Report*).
- No.123. A Diffusion-Deposition Model for In-Flight Release of Fission Fragments, M. L. Barad, D. A. Haugen, and J. J. Fuquay, Jun 1960.
- No.124. Research and Development in the Field of Geodetic Science, C. E. Ewing, Aug 1960.
- No.125. Extreme Value Statistics -- A Method of Application, I. I. Gringorten, Jun 1960.
- No.126. Notes on the Meteorology of the Tropical Pacific and Southeast Asia, W. D. Mount, Jun 1960.
- No.127. Investigations of Ice-Free Sites for Aircraft Landings in East Greenland, 1959, J. H. Hartshorn, G. E. Stoertz, A. N. Kover, and S. N. Davis, Sep 1961.

## AIR FORCE SURVEYS IN GEOPHYSICS (Continued)

- No. 128. Guide for Computation of Horizontal Geodetic Surveys, *H. R. Kahler and N. A. Roy*, Dec 1960.
- No. 129. An Investigation of a Perennially Frozen Lake, *D. F. Barnes*, Dec 1960.
- No. 130. Analytic Specification of Magnetic Fields, *P. F. Fougere*, Dec 1960. (*CONFIDENTIAL Report*)
- No. 131. An Investigation of Symbol Coding for Weather Data Transmission, *P. J. Hershberg*, Dec 1960.
- No. 132. Evaluation of an Arctic Ice-Free Land Site and Results of C-130 Aircraft Test Landings - Polaris Promontory, No. Greenland, 1958-1959, *S. Needleman, L. Klick, C. E. Molineux*, Mar 1961.
- No. 133. Effectiveness of the SAGE System in Relation to Wind Forecast Capability (U), *E. M. Darling, Jr., and Capt. C. D. Kern*, May 1961. (*CONFIDENTIAL Report*)
- No. 134 Area-Dosage Relationships and Time of Tracer Arrival in the Green Glow Program, *W. P. Elliott, R. J. Engelmann, P. W. Nickola*, May 1961.
- No. 135 Evaluation of Arctic Ice-Free Land Sites - Kronprins Christian Land and Peary Land, North Greenland, 1960, *W. E. Davies and D. B. Krinsley*, May 1961.
- No. 136 Missile Borne Radiometer Measurements of the Thermal Emission Characteristics of ICBM Plumes (U), *R. E. Hunter and L. P. Marcotte*, Jul 1961. (*SECRET Report*)
- No. 137 Infrared Studies of ICBM Plumes Using Missile - Borne Spectrometers (U), *R. E. Hunter and L. P. Marcotte*, Sep 1961. (*SECRET Report*).
- No. 138 Arctic Terrain Investigations Centrum Lake, N E Greenland, 1960, *S. M. Needleman* Jul 1962.
- No. 139 Space and Planetary Environments, *S. I. Valley, Editor*, Jan 1962
- No. 140 Proceedings of National Symposium on Winds for Aerospace Vehicle Design, *N. Sissenwine and H. G. Kasten, Co-Chairmen*, Mar 1962.
- No. 141 Atlas of Monthly Mean Stratosphere Charts, 1955-1959, Vol. I, January to June, *H. S. Muench* May 1962.
- No. 142 Infrared Atmospheric Transmissions: Some Papers on the Solar Spectrum from 3 to 15 Microns, *J. N. Howard and J. S. Garing*, Dec 1961.
- No. 143 AFCRL Ballistic Missile Infrared Measurements, IRMP 59/60, *T. P. Condron, J. J. Lovett and R. L. Morgan*, June 1962.
- No. 144 Effective Transmission of Thermal Radiation from Nuclear Detonations in Real Atmospheres, *J. P. Cahill, H. P. Gauvin and J. C. Johnson*, June 1962.
- No. 145 Summary Report - Project ICEWAY, *W. D. Kingery, Editor*, May 1962.
- No. 146 Silent Area Wind for USAF Manned Bombers (U), *E. M. Darling, Jr., I. A. Lund*, Jul 1962 (*SECRET Report*).
- No. 147 Mean Annual Mid-Latitude Moisture Profiles to 31 Km, *M. Gutnick*, Jul 1962.
- No. 148 Spectral and Spatial Measurements of Infrared Radiation (U), *L. C. Block, L. P. Marcotte and C. C. Ferriso*, May 1962 (*SECRET Report*).
- No. 149 Infrared Celestial Backgrounds, *R. G. Walker*, Jul 1962.
- No. 150 Transmission of the Atmosphere in the Infrared, A Review, *J. N. Howard and J. S. Garing*, Jul 1962.
- No. 151 Density Distribution, Interlevel Correlations and Variation With Wind, *Allen E. Cole and Arnold Court*, Jul 1962.
- No. 152 The Development of an Operational Contrail Suppression System (U), *Seymour J. Birstein*, Aug 1962 (*CONFIDENTIAL Report*).
- No. 153 Air Force Interim Supplemental Atmospheres to 90 Kilometers, *Allen E. Cole and Arthur J. Kantor*, Dec. 1963.
- No. 154 Proceedings of the AFCRL Scientific Balloon Symposium, Dec. 1963.
- No. 155(I) Celestial Background Radiation. Vol. I, A Revised Scale of Bolometric Corrections, *Russell G. Walker*, March 1964.

AIR FORCE SURVEYS IN GEOPHYSICS (Continued)

- No. 156. Operational Prediction of Diffusion Downwind From Line Sources, *William P. Elliot and Morton L. Barad*, March 1964.
- No. 157. Horizontal and Vertical Distributions of Atmospheric Density, Up to 90 km, *Allen E. Cole and Arthur J. Kantor*, June 1964.
- No. 158. Radar in Tropical Meteorology, *R.J. Donaldson, Jr., and David Atlas*, September 1964 (REPRINT).
- No. 159. Electron and Proton Fluxes in the Trapped Radiation Belts Originating From an Orbiting Nuclear Reactor, *John C. Ringle, Ludwig Katz, and Don F. Smart*, October 1964.
- No. 160. Correlations of Temperature, Pressure, and Density, to 30 Kilometers, *A.E. Cole and P.F. Nee*, January 1965.
- No. 161. Zonal and Meridional Winds to 120 Kilometers, *A.J. Kantor and A.E. Cole*, February 1965 (REPRINT).
- No. 162. The Equatorial Airglow, *S.M. Silverman*, April 1965.
- No. 163. Studies of Detonations at Ionospheric Altitudes Under Project Red Lamp, *N.W. Rosenberg, T.D. Conley, S.R. Curley, and A.H. Lorentzen*, May 1965.
- No. 164. Mean Atmospheric Properties in the Range 30 to 300 km, *K.S.W. Champion*, June 1965.
- No. 165. Specification and Prediction of Pressure, Temperature, and Density in a Silent Area, *Iver A. Lund and Eugene A. Bertoni*, June 1965.
- No. 166. The Constancy of the Winds in the Lower Stratosphere and Constant-Level Balloon Flight Planning, *George F. Nolan*, June 1965.
- No. 167. Proceedings, 1964 AFCRL Scientific Balloon Symposium, *Arthur O. Kom*, Editor, July 1965.